CARDIAC DEVELOPMENT

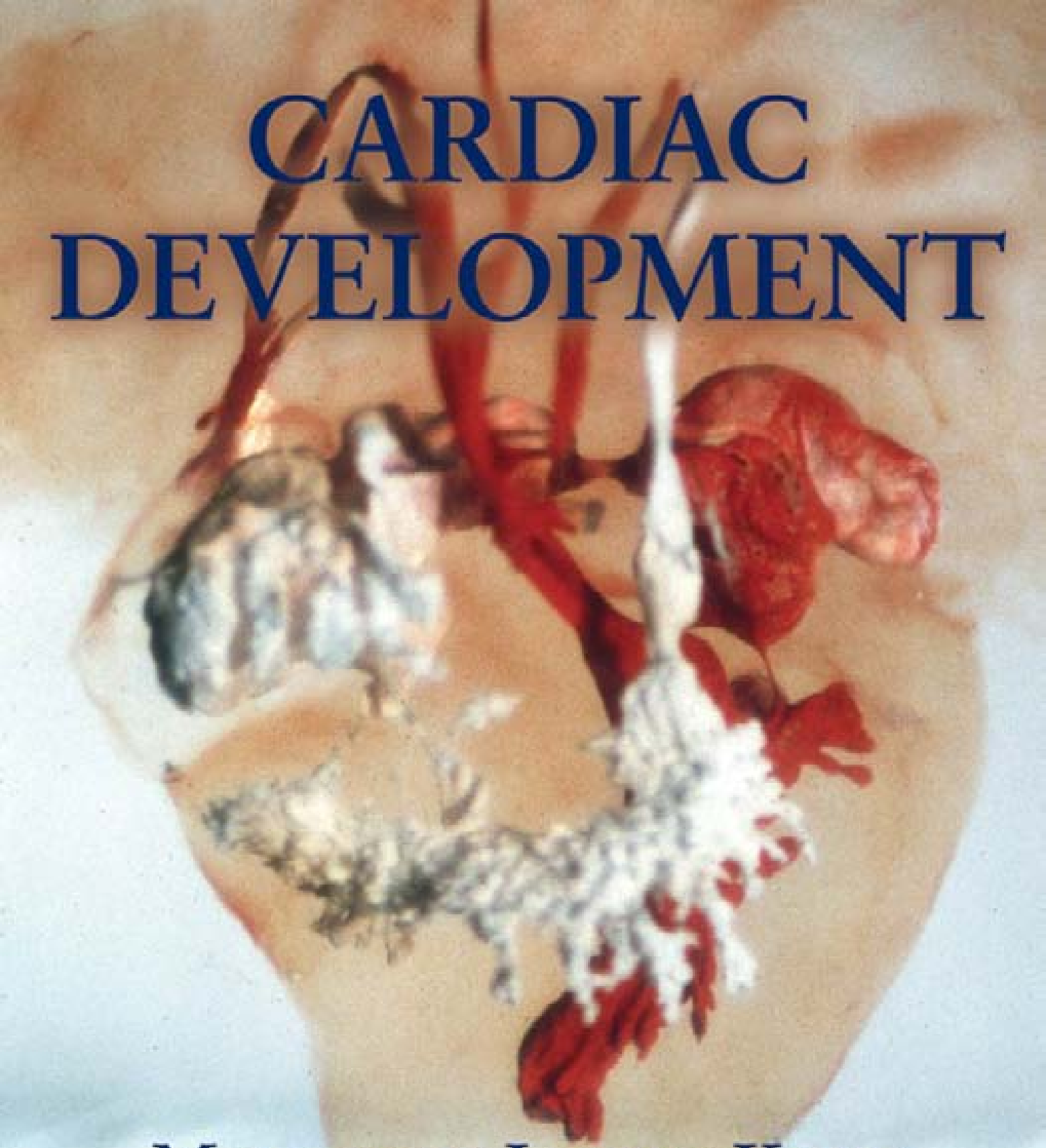

MARGARET LOEWY KIRBY

with illustrations by

KAREN WALDO

Cardiac Development

This page intentionally left blank

Cardiac Development

Margaret Loewy Kirby, PhD
Professor of Pediatrics, Cell Biology and Biology
Duke University

Regents' Professor Emeritus
Medical College of Georgia

OXFORD
UNIVERSITY PRESS

2007

OXFORD
UNIVERSITY PRESS

Oxford University Press, Inc., publishes works that further
Oxford University's objective of excellence
in research, scholarship, and education.

Oxford New York
Auckland Cape Town Dar es Salaam Hong Kong Karachi
Kuala Lumpur Madrid Melbourne Mexico City Nairobi
New Delhi Shanghai Taipei Toronto

With offices in
Argentina Austria Brazil Chile Czech Republic France Greece
Guatemala Hungary Italy Japan Poland Portugal Singapore
South Korea Switzerland Thailand Turkey Ukraine Vietnam

Published by Oxford University Press, Inc.
198 Madison Avenue, New York, New York 10016

www.oup.com

Oxford is a registered trademark of Oxford University Press.

Library of Congress Cataloging-in-Publication Data
Kirby, Margaret L.
Cardiac development/Margaret Loewy Kirby.
p. cm. Includes bibliographic references.

ISBN-13: 978-0-19-517819-7
ISBN-10: 0-19-517819-X

1. Heart–Growth. I. Title.
[DNLM: 1. Heart–embryology. 2. Heart–growth & development.
3. Heart–innervation. 4. Heart Conduction System–embryology.
5. Myocardium. WG 201 K58c 2006]
QP111.4.K57 2006
612.1′7–dc22 2006003811

9 8 7 6 5 4 3 2 1
Printed in China
on acid-free paper

To my mother, Margaret Vaile Loewy,
who gave me an abiding love of books,
To my father, Henry Loewy, who always knew I was a scientist
even though I thought I was a humanist and
To my best friend, Elsebet Jegstrup, the philosopher
who knew I had a book in me long before I did ...did I?

This page intentionally left blank

Preface

It is perhaps wise to begin by asking whether a new book on heart development is necessary, but I have found that previous works on this subject lacked a holistic perspective that I have always found helpful in learning and teaching. When I was learning about heart development and ever since I began to teach this subject, there has not been a book that covers all aspects of heart development evenly, so that a person new to the field can acquire something of a holistic understanding of the subject. A holistic approach to the subject of heart development has always been the perspective from which I think this subject is best understood.

What brought about this effort of a book on cardiac development started a long time ago when a major aporia in my life changed the course of my research. My technician had placed a flat tray of slides on my desk that had sections of chick embryos with neural crest ablations. Even though I was a budding neuroscientist at the time, I realized from across the desk, without a microscope, that there was something very wrong with the heart. Like many others of my generation, I had been given the quick version of heart development in medical embryology by someone who did not fully understand it himself and I had taken away only the certainty that I never wanted to be intimately involved with heart development because it was entirely too complicated and three-dimensional for a human mind to comprehend. Now, faced with my daunting slides, I was confounded by the fact that I would have to abandon a truly interesting discovery—that neural crest is somehow involved in normal heart development—or bite the bullet and learn about heart development. The subject itself is hard enough but add to that the fact that different nomenclature was used by different labs, and the disagreements over almost all aspects of nomenclature and how malformations occur was enough to turn away even the most assiduous student. Fortunately, because many of the experts in heart development were kindhearted and willing to take a novice into the fold, I was able over many years to learn enough about the heart to hold my own with colleagues. It has taken a long time and I am still learning. Hence, this book is my effort to make heart development approachable and inclusive for beginners. One of the major goals was to cover all aspects of heart development evenly. I have tried not to make the neural crest chapter (my primary expertise) more complicated than the others and yes, neural crest is indeed an important part of normal heart development. I am by no means an expert in everything I have written about. For this, I hope that my colleagues who are experts will forgive me.

It is my great pleasure to introduce you to heart development from my perspective, which may be somewhat different from the mainstream. However, I encourage all of us, especially those new to heart development, to keep thinking outside the box, for that is the only way we will truly begin to understand how this amazing organ develops. Let us not forget that progress and a deeper understanding of things only happen when there is thinking outside the box (Thomas Kuhn. 1962. The Structure of Scientific Revolutions. University of Chicago Press: Chicago).

This book contains an extensive glossary and the first usage of a word in the glossary is in small capital letters. Italics have been used for genes with human genes capitalized and italicized. References to RNA messengers and proteins have only the first letter capitalized.

This page intentionally left blank

Acknowledgments

This book would never have existed without enormous help from many people. I am grateful to Harriett Stadt, Ping Zhang, Kelly Nembhard, Adrian Grimes, and Asako Sato for keeping our lab together all these months while the book developed and my brother Ray Loewy, the lab computer guru, without whose help the mysteries of computers would have overwhelmed us all. Joyce Newton, our lab secretary, bookkeeper, and histologist, obtained permissions for reprinting the figures in between all her other duties. Many others have contributed to the intellectual development of the book: Radwan Abu-Issa started us all thinking about cardiogenic fields and we have all benefited from his insightful views and numerous discussions of heart field and early heart development; Mary Hutson, my longtime associate whose incisive comments on many of the chapters made them ultimately readable; Laura Barbosky, the comma police, who slogged through all of the early chapters with question marks showing me where I had become particularly obscure. My thanks to Rob Gourdie, Brian Hall, Page Anderson, and Vicki Bausch who took the time to read and correct various chapters. I would also like to thank Tony Creazzo, who contributed Chapter 5, for his warm friendship and collaboration over many years and Fred Schachat for his wonderful insight into the evolutionary developmental biology of the heart for Chapter 14. Finally, several of the early chapters have undergone "beta" testing by members of the Department of Pediatrics (Cardiology) at Duke, who have provided good suggestions for revision and correction.

I owe special thanks to Shirley Ann Gilmore who provided a wonderful role model of what a scientist could and should be.

This page intentionally left blank

Contents

Contributors *xiii*

Chapter 1
An Overview of Cardiac Morphogenesis: Getting from a Muscle-Covered Tube to a Four-Chambered Pump *3*

Chapter 2
Vascular Development *9*

Chapter 3
Cardiogenic Fields and Heart Tube Formation *21*

Chapter 4
Induction and Differentiation of the Myocardium *35*

Chapter 5
Functional Developmental Biology of the Myocardium (By Tony L. Creazzo) *53*

Chapter 6
Development of the Poles of the Heart *69*

Chapter 7
Molecular Control of Looping *87*

Chapter 8
Chamber Specification and Ventricular Septation *103*

Chapter 9
Endocardium, Cardiac Cushions, and Valve Development *119*

Chapter 10
Epicardium and Coronary Vessel Development *133*

Chapter 11
Neural Crest, Great Arteries, and Outflow Septation *143*

Chapter 12
Development of the Cardiac Pacemaking and Conduction System *161*

Chapter 13
Innervation of the Developing Heart *179*

Chapter 14
Evolutionary Developmental Biology of the Heart (Co-authored with Fred Schachat) *199*

Chapter 15
Some New Insights into the Embryogenesis of Heart Malformations in the Context of Syndromes *215*

Chapter 16
Myocardial Stem Cells *233*

Appendix *245*

Glossary *247*

Index *265*

This page intentionally left blank

Contributors

With illustrations by

Karen Waldo, MS

Chapter 5 contributed by

Tony L. Creazzo, PhD
Associate Professor of Pediatrics and Cell Biology
Department of Pediatrics (Neonatology)
Neonatal-Perinatal Research Institute
Duke University Medical Center

Chapter 14 coauthored by

Fred Schachat, PhD
Associate Professor of Cell Biology
Department of Cell Biology
Duke University Medical Center

This page intentionally left blank

Cardiac Development

This page intentionally left blank

1

An Overview of Cardiac Morphogenesis: Getting from a Muscle-Covered Tube to a Four-Chambered Pump

The heart is a mystery. If you've seen your own heart on a video screen, as millions by now have done, convulsing and opening rhythmically, you may have wondered why this persistent muscle is so faithful in its function from the uterus to the last breath. This rhythmic gripping and relaxing blindly goes on. Why? How?—Saul Bellow, Ravelstein, Penguin Putnam, New York, 2000, pp. 146–147

The heart is the first organ to function during embryonic development, and until recent times, cessation of heart function constituted death. Heart development in all vertebrates from fish to humans follows the same general pattern: fusion of myocardium and endocardium in the ventral midline to form a simple tubular heart; onset of function, looping to the right side; chamber specification and formation; and finally, development of specialized conduction tissue, coronary circulation, innervation, and mature valves. The variation on this theme involves expansion and remodeling of the heart tube followed by septation to form two-, three-, or four-chambered hearts. The fish heart has undivided pulmonary and systemic circulations and uses chambers pumping in series, so virtually no septa form, whereas all warm-blooded animals have divided pulmonary and systemic circulations that function serially, but in parallel, requiring complex septation of the heart (Fig. 1.1).

The earliest PROGENITORS of the heart are located in bilaterally paired CARDIOGENIC FIELDS in the splanchnic layer of anterior lateral plate mesoderm (Fig. 1.2). The first morphological sign of heart development begins when two bilateral troughs of MYOCARDIUM cradling ENDOCARDIAL TUBES are brought to the ventral midline during closure of the ventral foregut (Fig. 1.3). The cranial borders of the cardiogenic fields form myocardial troughs that are brought into apposition to fuse at the ventral midline, forming the future outer curvature.

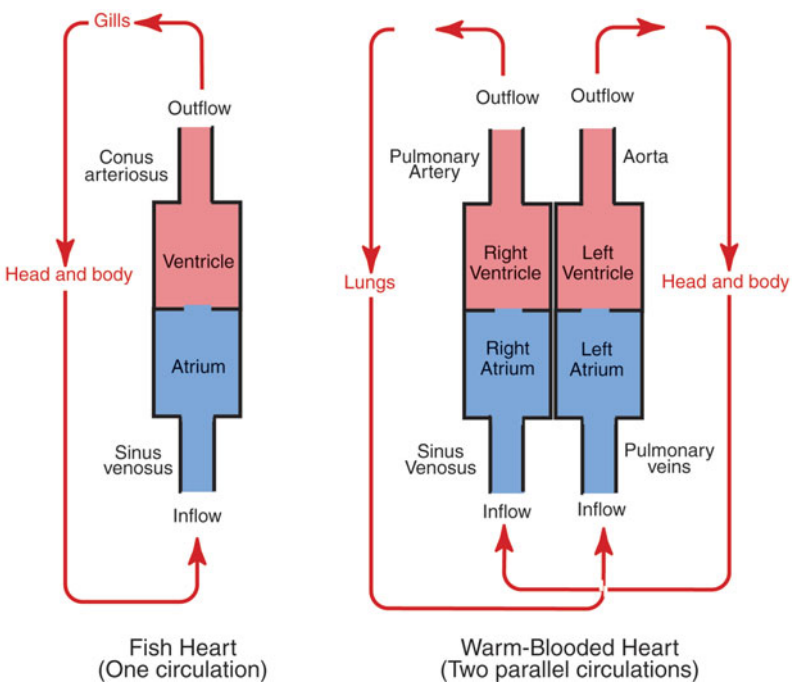

Figure 1.1. Diagrams comparing serial circulation found in animals that exchange oxygen via gills, such as the zebrafish, with the completely separated parallel circulations found in warm-blooded, lunged animals represented by avian and mammalian species.

The lateral borders of the myocardial troughs remain attached to the ventral foregut, forming a W-shaped myocardium open to the foregut. It is only after fusion of the endocardial tubes that the arms of the W-shaped myocardium fuse just beneath the foregut to form the dorsal midline seam of myocardium that will become the inner curvature and dorsal mesocardium, thus creating the primary cardiac tube. All through this process, the myocardium secretes a thick acellular matrix called CARDIAC JELLY that forms a layer separating the myocardium and the endocardium. During the next phase of development, the heart tube narrows and lengthens by accretion of cells at each end and, concurrently, loops to the right. LOOPING allows the caudal, inflow end of the tube to be brought into approximation with the cranial, outflow end of the tube in a process called CONVERGENCE (Fig. 1.4). During looping, the cardiac tube is lengthened by addition of myocardium from the SECONDARY HEART FIELD and endocardium to the OUTFLOW POLE (Fig. 1.5). At the end of this process, the heart contains all of the myocardium that forms the named segments of the tubular heart from inflow to outflow, called SINUS VENOSUS, COMMON ATRIAL CHAMBER, ATRIOVENTRICULAR CANAL, PRESUMPTIVE LEFT AND RIGHT VENTRICLES, and CONOTRUNCUS or definitive OUTFLOW TRACT (Fig. 1.6). Looping creates a broad OUTER CURVATURE and a narrow INNER CURVATURE. The cavities of the definitive CHAMBERS are formed primarily by growth of the outer curvature. The endocardium

Figure 1.2. Diagram of the location of the bilaterally paired cardiogenic fields in a stage 5 chick embryo. The cardiogenic fields form the initial heart tube.

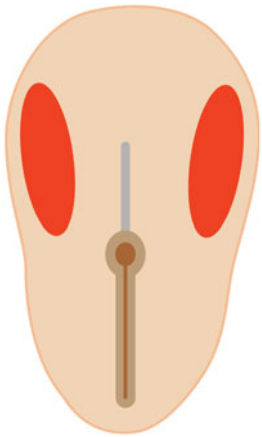

Figure 1.3. Diagrams showing the steps in development of the bilateral cardiogenic fields in the splanchnic mesoderm into a single midline heart tube (*A–D*). Formation of the midline heart tube depends on formation of the foregut pocket that forms the pharynx. The myocardial trough (*C* and *D*) already shows three layers: cellular endocardial and myocardial layers with an acellular layer of cardiac jelly in between.

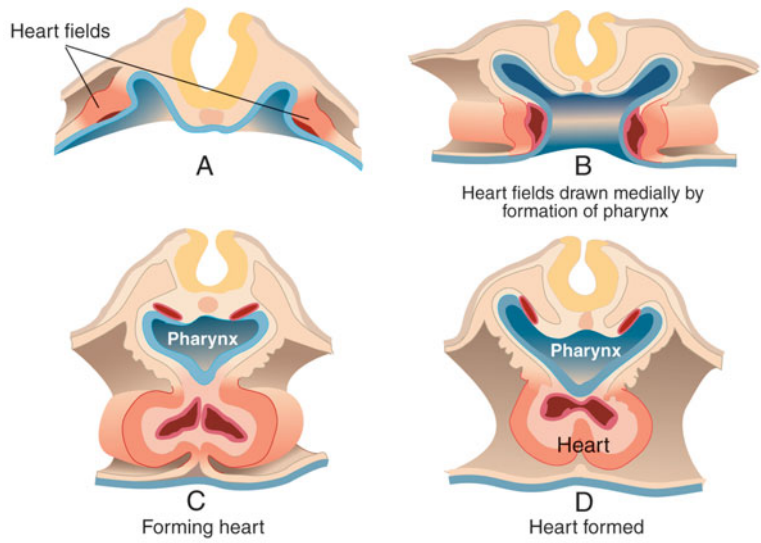

Figure 1.4. The heart tube begins as a straight midline tube with blood entering caudally via the inflow and exiting cranially via the outflow tract. Under normal circumstances the tube loops to the right, creating an inflow limb (*blue*) and an outflow limb (*red*). The distal extremities of the inflow and outflow limbs grow toward each other in a process of convergence that is necessary before septation can create a four-chambered heart.

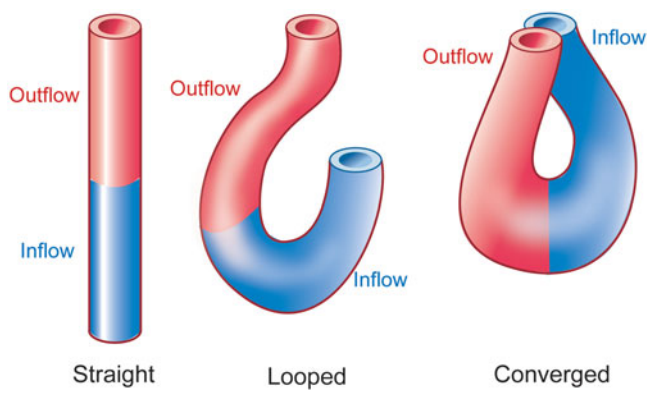

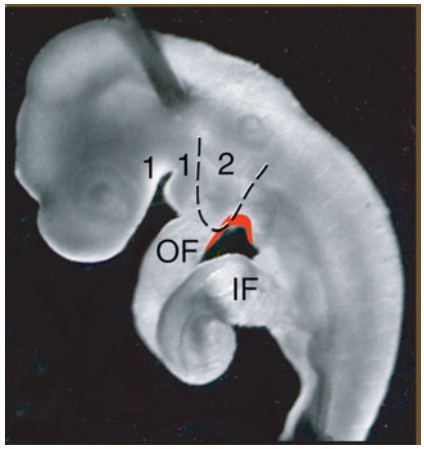

Figure 1.5. Stage 14 chick embryo. Correct looping depends on addition of myocardium to the outflow limb from cardiogenic mesoderm behind the outflow tract (OF) shown in red. IF, Inflow limb.

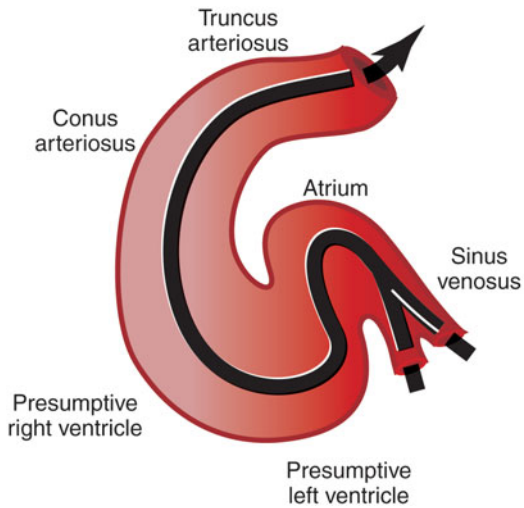

Figure 1.6. Traditional view of the named segments of the looped heart tube.

of the atrioventricular canal and outflow tract generates cells that populate the cardiac jelly with MESENCHYME in these regions. The regions where cells begin to populate the cardiac jelly bulge into the LUMEN and are called CARDIAC CUSHIONS. At the same time, the myocardium of the atrial and ventricular chambers begins to develop TRABECULATIONS or ridges of endocardially covered myocardium that extend into the lumen.

Three populations of cells located outside the heart called EXTRACARDIAC CELLS invade the heart: PROEPICARDIUM, VESTIBULAR SPINE (SPINA VESTIBULI), and NEURAL CREST to form the EPICARDIUM, part of the PRIMARY ATRIAL SEPTUM and OUTFLOW SEPTUM, respectively.

Because the heart begins to beat while it is a myocardium covered tube, functional development of the myocardium is a critical step. This involves development of appropriate CHANNELS to allow electrical currents to be propagated through the myocardium. In addition, the molecular substrates of EXCITATION-CONTRACTION COUPLING develop to couple electrical currents with the developing CONTRACTILE APPARATUS.

With the inflow and outflow ends of the tubular heart now in proximity, and the chambers specified and functional, cardiac septation can begin. All of the septa fuse ultimately with the ATRIOVENTRICULAR CUSHIONS. These cushions form the ATRIOVENTRICULAR SEPTUM that divides the atrioventricular canal into right and left canals. The right atrioventricular canal expands to the right, as does the right ventricle, allowing incoming blood from the sinus venosus to pass directly from the presumptive right atrium to the presumptive right ventricle without passing through the presumptive left atrium and left ventricle. The atrial septum in mammals has two components; one is a true septum, the primary atrial septum, while the SECONDARY ATRIAL SEPTUM is actually a fold of atrial myocardium that forms to the right of the primary septum and appears late in development. The primary septum forms from mesenchyme of the DORSAL MESOCARDIUM that extends into the heart (Fig. 1.7). The vestibular spine, a controversial structure that was identified as a mesenchymal condensation, also has its origin outside of the heart. This mesenchyme borders the lower edge of the primary septum although a newly identified population of cells

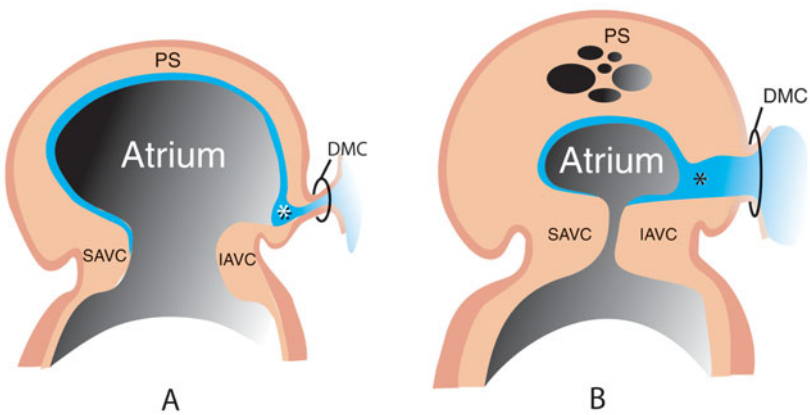

Figure 1.7. Atrial septation involves the formation of a primary atrial septum (PS) which becomes perforated prior to fusion of its free edge with the superior (ventral) and inferior (dorsal) atrioventricular cardiac cushions (SAVC and IAVC, respectively). The dorsal mesocardium (DMC) harbors a mesenchymal band (*blue*) that extends from the splanchnic mesoderm near the pulmonary mesenchyme to the free edge of the primary atrial septum. This band is called the vestibular spine or "spina vestibuli."

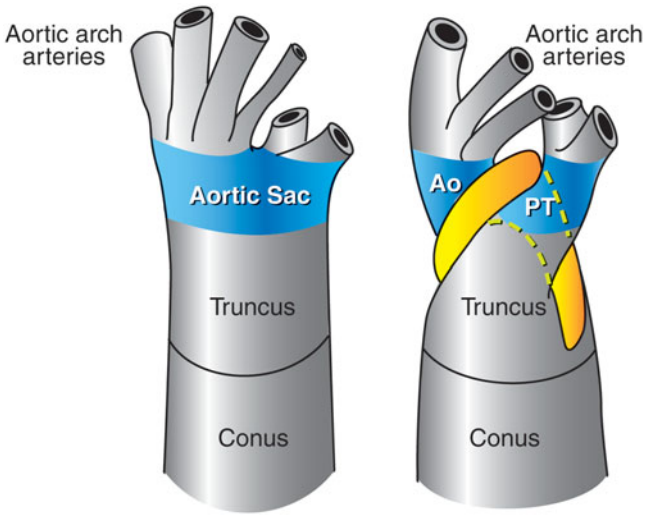

Figure 1.8. The aortic arch arteries are bilaterally paired arteries that originate from the aortic sac and receive all of the cardiac output during early development. Division of the outflow tract by the aorticopulmonary septum (APS) begins in the aortic sac between the fourth (systemic) and sixth (pulmonary) aortic arch arteries to form the base of the aorta and pulmonary trunk. Septation proceeds into the truncus and then conus. The divided truncus is the region where the aortic and pulmonary semilunar valves form. The conus is incorporated into the right and left ventricular outlets as the infundibulum and vestibule, respectively.

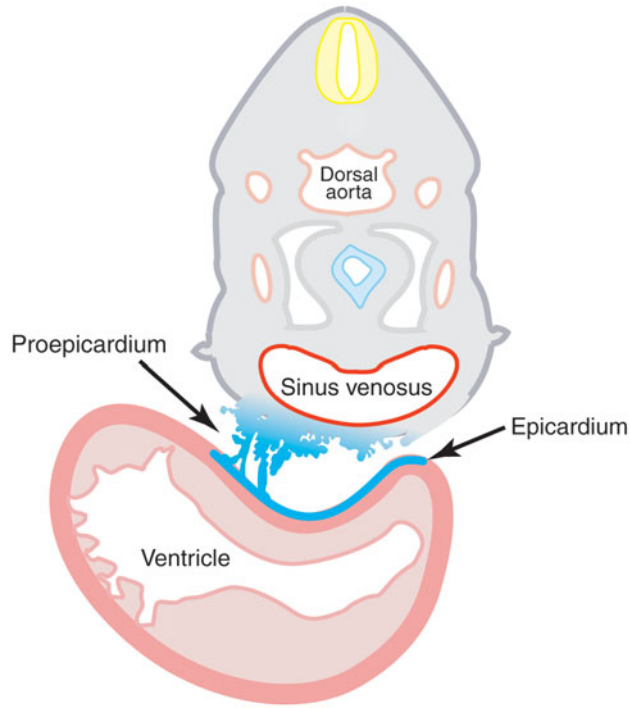

Figure 1.9. The epicardium develops from the proepicardium that originates from the mesenchyme near or in the liver. It is added after myocardial chamber specification and provides all of the cells needed to form the coronary vessels and the connective tissue of the heart.

generated by EPITHELIAL-MESENCHYMAL TRANSFORMATION from ENDOCARDIUM may play a more important role than the vestibular spine in fusion of the primary septum with the endocardial cushions. The ventricular septum arises from the deepest convexity of the loop and grows toward the atrioventricular septum but does not fuse with it. The outflow septum begins in the AORTIC SAC, a vessel located just distal to the myocardium of the cardiac outflow tract proper (Fig. 1.8). The distal portion of the septum, which divides the base of the AORTA from that of the PULMONARY TRUNK, begins as a shelf between the exit of the fourth (systemic circulation) and sixth (pulmonary circulation) AORTIC ARCH ARTERIES from the sac. The shelf is directed into the DISTAL OUTFLOW TRACT (TRUNCUS) by two arms or prongs that extend in the outflow cushions toward the PROXIMAL OUTFLOW TRACT (CONUS). The shelf elongates in the direction of the prongs, separating the region where the semilunar valves will form. The proximal outflow tract, in contrast to the distal, is divided by apposition of the outflow cushions. The cushions bulge and touch as myocardial cells invade the mesenchyme beneath them. They fuse at these sites and finally, most proximally, fuse with the atrioventricular cushion tissue. As the outflow septum forms, the proximal outflow tract (conus) is incorporated into the right ventricle.

The central and peripheral portions of the cardiac PACEMAKING AND CONDUCTION SYSTEM form in conjunction with the developing CORONARY VASCULATURE from regions of specialized myocardium that are set aside from working myocardium.

The epicardium invests the developing heart after it is a looped tube. Most of the epicardium, with the exception of that over the distal outflow tract, is derived from an epicardial PRIMORDIUM called the proepicardium that grows from the mesenchyme of the SEPTUM TRANSVERSUM or liver, at the venous end of the tube (Fig. 1.9). The epicardium migrates over the surface of the heart until it has completely covered the organ, with the outflow tract being the last structure covered. Endothelial and smooth muscle cells of the coronary vasculature, as well as connective tissue, are formed by epithelial-mesenchymal transformation of the epicardium. Innervation of the heart is from PARASYMPATHETIC INTRINSIC GANGLIA and SYMPATHETIC PARAVERTEBRAL GANGLIA. The innervation to the heart begins to function late with respect to cardiac function. As can be appreciated, cells from many different sources are important in building a functional heart (Fig. 1.10).

The last step in morphological heart development is sculpting of the ENDOCARDIAL CUSHIONS at the atrioventricular and VENTRICULOARTERIAL JUNCTIONS to form VALVE LEAFLETS. In the case of the atrioventricular valve leaflets, the leaflets are formed by cavitation of the mesenchyme at the atrioventricular junction. Undermining the layer of cells just under the luminal cells frees the body of the leaflets while leaving their

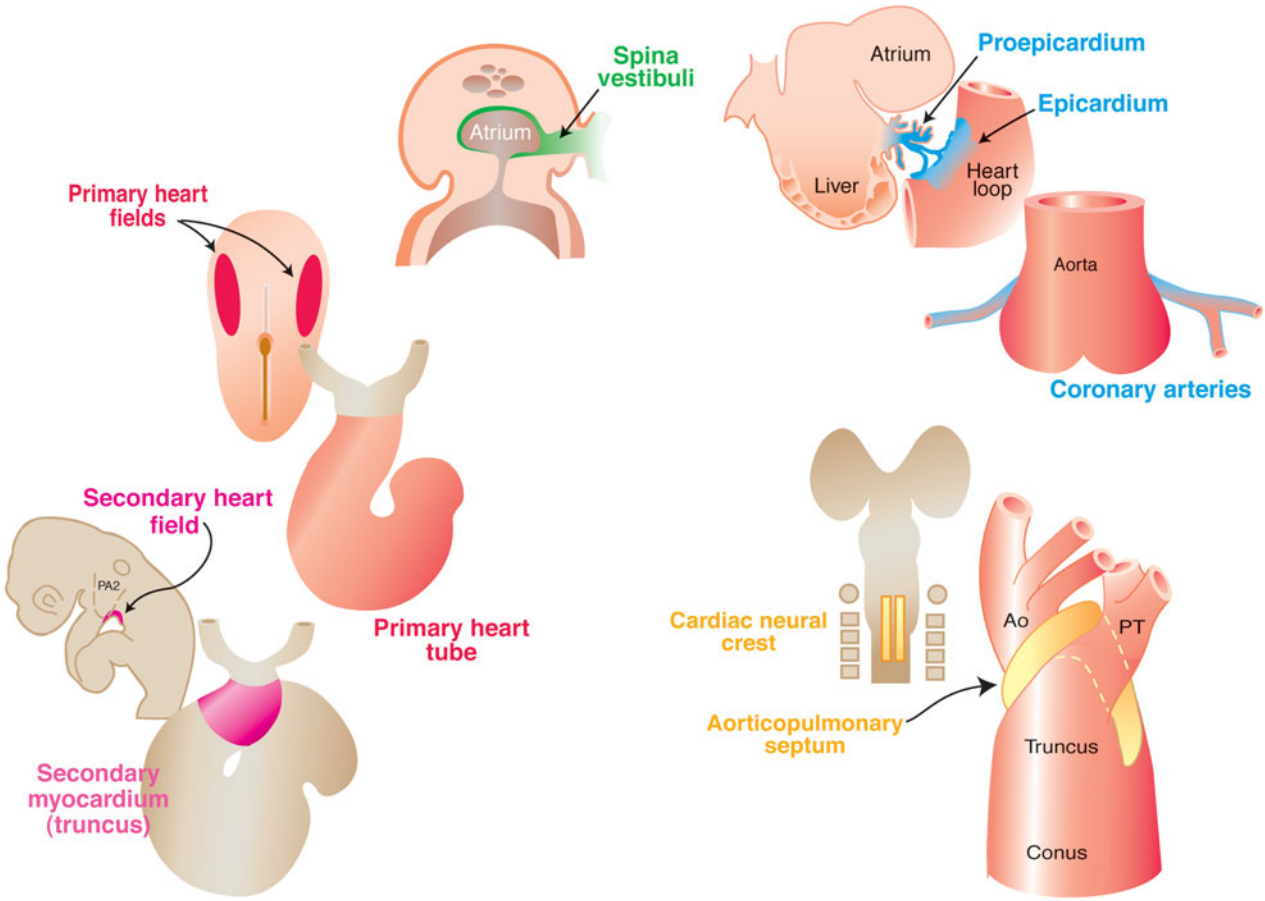

Figure 1.10. Summary of the tissues that are needed for heart development and their roles.

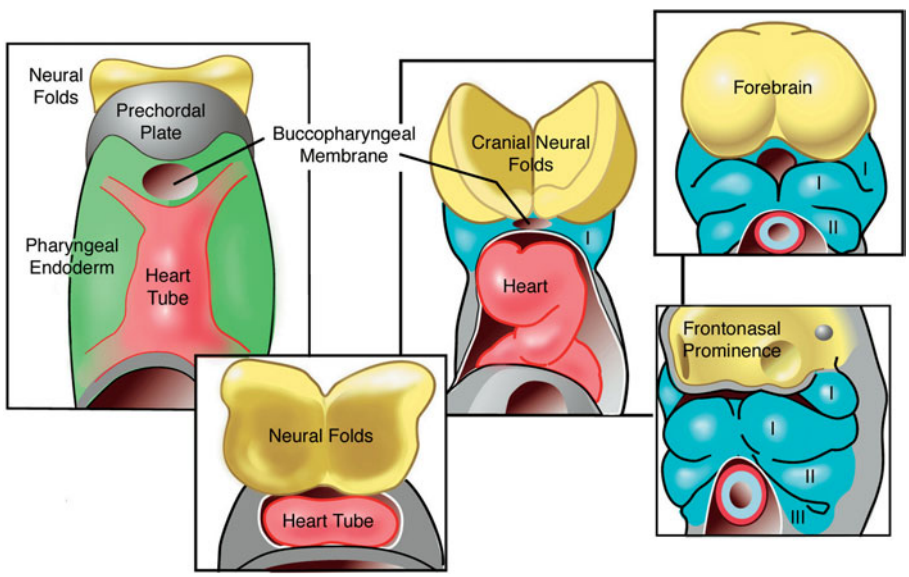

Figure 1.11. Schematic representation of the cardiocraniofacial morphogenetic field or module. Early in FOREGUT POCKET formation (*left*), the CRANIAL NEURAL PLATE (*yellow*), PRECHORDAL PLATE (*gray*) and fused midline heart tube (*pink*) are in close apposition with the ventral pharyngeal endoderm (*green*) in the region in which the face will develop. As development proceeds, the CRANIAL NEURAL FOLDS grow forward forming the forebrain, and the heart is pushed ventrally. Interposition of the PHARYNGEAL ARCHES (*blue*) and formation of the FRONTONASAL PROMINENCE push the heart farther caudally and establish the elements that will form the face. The second panel represents a mouse heart which develops somewhat differently from chick and human hearts because of the shortened distance between the forebrain and the anterior intestinal portal. However, it illustrates the close relationships in the cardiocraniofacial morphogenetic field.

distal edges attached to myocardium. The myocardium forms PAPILLARY MUSCLES that remain attached to the valve leaflets by CHORDAE TENDINEA. At the ventriculoarterial junction, the sculpting is distal to the cushion and forms the AORTIC AND PULMONARY SINUSES.

Finally, because the heart develops in an integral relationship with the forebrain, face, and ventral neck, as part of a CARDIOCRANIOFACIAL FIELD (Fig. 1.11), it is important to understand heart development in the context of this field. It is only after the elements that will form the adult heart have accumulated in the developing heart that it is displaced into the chest cavity. Insight into uniquely occurring heart defects and those that occur as part of sequences of malformations is gained when the heart is viewed from this perspective.

2

Vascular Development

The vascular system in vertebrates is patterned via two major processes called VASCULOGENESIS and ANGIOGENESIS, which generate blood vessels required for the formation of the arteriovenous vasculature and heart development. All of the earliest development is via vasculogenesis, in which vesicles of angioblasts form de novo and coalesce to form tubes or SINUSOIDS. Later development is via both vasculogenesis and angiogenesis. In angiogenesis, new vessels sprout from endothelial cells in pre-existing vessels. Once flow commences, the primary capillary plexus is remodeled into a hierarchical system of large to small blood vessels by angiogenesis of new vessels and regression of existing channels. These vessels are stabilized by PERIVASCULAR CELLS attracted during the period of remodeling. The stabilized vessels recruit investing cells that will be organized into the tunics of the mature vessels, or pericytes in the case of capillaries.

Endothelial Precursors

Precursors for ANGIOBLASTS are thought to form as early as gastrulation, although very little is known about their developmental history before the expression of definitive markers. Beginning at the time they are formed, these cells are migratory and invasive, and are quickly distributed widely throughout the intraembryonic and extraembryonic mesenchyme (Fig. 2.1). Endothelial cells arise from all levels of the primitive streak during gastrulation (Garcia-Martinez and Schoenwolf, 1993).

Development of the vascular system begins extraembryonically in the YOLK SAC. In the yolk sac, angioblasts are generated from bipotential HEMANGIOBLASTS that can give rise to both hematoblasts that form blood cells and angioblasts that form blood vessels. Hemangioblasts form BLOOD ISLANDS in the yolk sac that begin producing blood cells while the angioblasts form an extraembryonic capillary network that will later become part of the placenta. Vascular development is initiated in the embryo soon after it begins in the yolk sac. Intraembryonic blood vessels arise from intraembryonic angioblasts; however, circulating blood island-derived cells from the yolk sac can contribute to the intraembryonic blood vessels (LaRue et al., 2003).

The driving force for vascular development is multifactorial. Vasculogenesis occurs by coalescence and lumenization of endothelial precursor cells that are laid down in a prepattern, while angiogenesis is driven by both patterning instructions and metabolic requirements. In early development, metabolic needs are satisfied by diffusion, during which time the prepattern for the early vasculature is formed by strands of angioblasts that are guided by molecular patterning cues. These cues involve cell–cell and cell–matrix interactions. It is only later that growth of the vasculature is driven by metabolic requirements. Hypoxia appears to be a major factor driving growth of the vascular network. Repatterning from an initial bilateral plexus of loosely organized vessels to the adult configuration as occurs in the GREAT ARTERIES and CENTRAL VEINS is likely dependent on molecular cues, hemodynamics, and metabolic requirements (Kirby et al., 1997).

Endothelial Differentiation

VASCULAR ENDOTHELIAL GROWTH FACTOR (VEGF) signaling is essential for the DIFFERENTIATION, PROLIFERATION, and MIGRATION of angioblasts. FLK1 (Vegf receptor 2, VEGFR2), A RECEPTOR TYROSINE KINASE that mediates VEGF signaling is required along with Scl, A BASIC HELIX–LOOP–HELIX (BHLH) TRANSCRIPTION FACTOR, during the initial stages of hematopoietic and endothelial cell lineage differentiation (Fig. 2.2). In mice, Flk1 expression is detected in blood island progenitors in the mouse yolk sac on embryonic day (E)7 (Dumont et al., 1995; Yamaguchi et al., 1993). *Flk1*-deficient mice fail to form blood

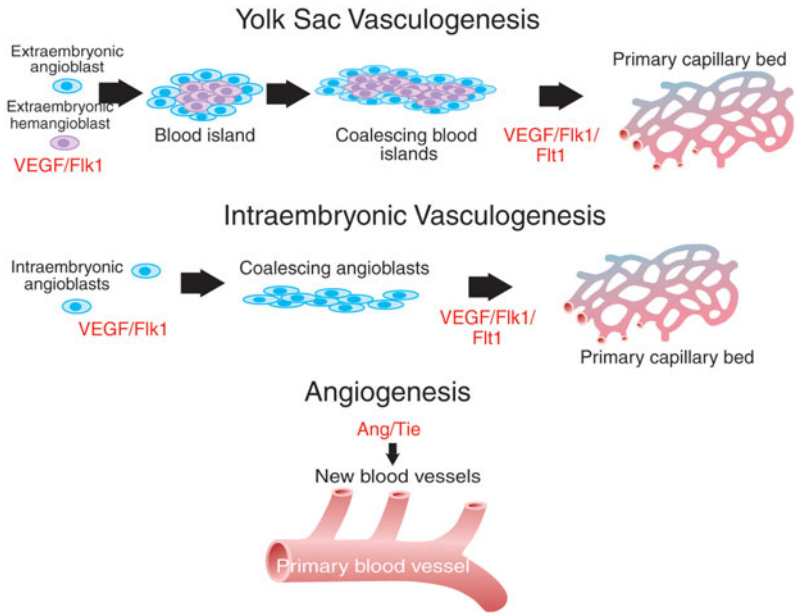

Figure 2.1. Vasculogenesis begins in the extraembryonic yolk sac where blood islands form that coalesce into capillary beds. Angioblasts in the embryo (intraembryonic) also form capillary beds by vasculogenesis. These original vascular networks sprout via angiogenesis or growth of new vessels from pre-existing ones.

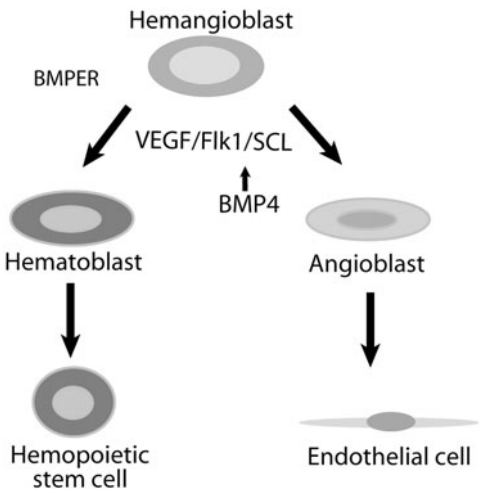

Figure 2.2. Differentiation of the hemangioblast into hematoblasts that give rise to hematopoietic stem cells and angioblasts that give rise to endothelial cells.

islands and die between E8.5 and E9.5 (Shalaby et al., 1995). *Flk1*-null ES cells cannot participate in endothelial tube formation or contribute to hematopoiesis in wild-type embryos (Shalaby et al., 1995). *Scl*-deficient mice also fail to establish normal hematopoietic and endothelial cell lineages. They die around E10.5 as a result of failure to form a primary vascular plexus in the yolk sac (Visvader et al., 1998). BONE MORPHOGENETIC PROTEIN (BMP)4 signaling is required for Flk1 and Scl expression by the hemangioblasts, and Vegf signaling through Flk1 causes proliferation of both hematopoietic and endothelial cell progenitors. Proliferation of Scl-positive cells is inhibited by TRANSFORMING GROWTH FACTOR (TGF)β1, independent of Vegf/Flk1 signaling (Park et al., 2004).

Bone morphogenetic protein-binding endothelial cell precursor-derived regulator (Bmper) is specifically expressed in Flk1-positive cells (Moser et al., 2003). Bmper interacts with Bmp2, -4, and -5, antagonizes Bmp4 signaling, and can antagonize differentiation of endothelial cells, thus functioning to limit the differentiation of hemangioblast cells along the endothelial lineage. The existence of this an anti-endothelial pathway suggests a tightly controlled generation of endothelial cells from hemangioblast progenitors.

Patterning the Vasculature

While considerable variation exists in the vascular patterning, arteries and veins are generally identifiable by their location from one vertebrate species to another and from individual to individual, indicating that the basic vertebrate plan of the vasculature is remarkably stable. The earliest embryonic vascular pattern is bilaterally symmetrical, and this symmetry is maintained in the head and limbs, but the central vessels undergo extensive remodeling during organogenesis and the pattern of both veins and arteries in the trunk becomes asymmetrical (Fig. 2.3). The bilateral aortic arch arteries, which will become the definitive great arteries of the thorax, form from endothelial strands that are located approximately segmentally along the ventral pharynx in a pattern reminiscent of the arch arteries (de Ruiter et al., 1993). As the pharyngeal arches form, the endothelial strands are lifted away from the ventral pharyngeal endoderm and begin to open at their origin from the aortic sac and their termination at the DORSAL AORTAS (Waldo et al., 1996). The central portion of the aortic arch artery is the last to become patent. Thus it appears, incorrectly, that the arch arteries are sprouting from the aortic sac and dorsal aorta and

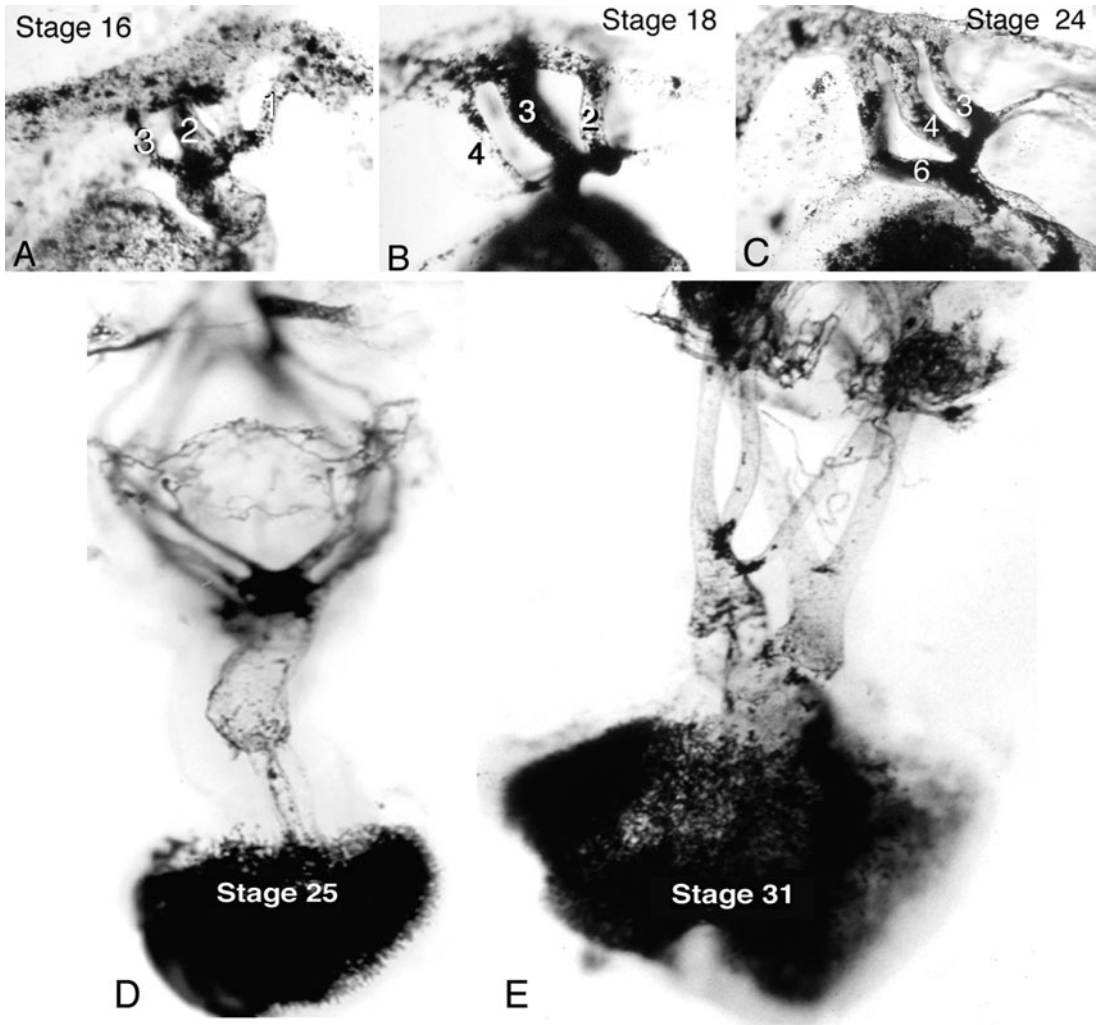

Figure 2.3. Formation and remodeling of the aortic arch arteries in ink injected chick embryos. (*A–C*) Sagittal views showing progressive development and regression of the aortic arch arteries. (*D* and *E*) Frontal views showing the relationship of the aortic arch arteries as they develop from bilaterally symmetrical pattern (*D*) to asymmetric (*E*) during outflow septation.

meeting in the middle, when in reality, the vessel primordium is becoming lumenized. The cranial two aortic arch arteries (1 and 2) regress into capillary beds while aortic arch arteries 3, 4, and 6 persist. This leaves a bilaterally symmetrical pattern of arteries that is subsequently remodeled by regression of some arteries and growth of others to result in the great arteries—aorta, carotids, brachiocephalic, subclavian, and ductus arteriosus (Fig. 2.4).

The central venous system is also remodeled extensively. Three sets of bilaterally symmetrical venous systems, the vitelline, umbilical, and cardinal veins drain to the heart. As venous drainage is shifted to the right atrium, veins of the left side involute or form anastomotic connections with veins on the right side. The inferior vena cava is composed of elements of four separate systems. The head and neck veins form from the anterior cardinal veins. The left anterior cardinal vein that drains the left side of the head and neck and left arm involutes and an anastomotic channel connects the left with the persisting right anterior cardinal vein. The right anterior cardinal becomes the superior vena cava.

Part of the remodeling process involves a transition from bilateral symmetry to a distinctly asymmetrical pattern that adheres to strict left–right axis instructions. The venous system in the trunk behaves in a similar manner in that a bilaterally symmetrical venous vasculature is laid down and then extensively remodeled into an asymmetrical venous system.

Little is known about how the initial vascular patterns are generated in the embryo. Because the endothelial cells seem to adhere to a prepattern, at least reminiscent of the pattern they will have after circulation begins, it is likely that they follow a pattern established by their nonendothelial neighbors. Recently, the neural tube has been shown to act as a vascular patterning center, probably via production of Vegf. This suggests that embryonic structures with little or no capacity to

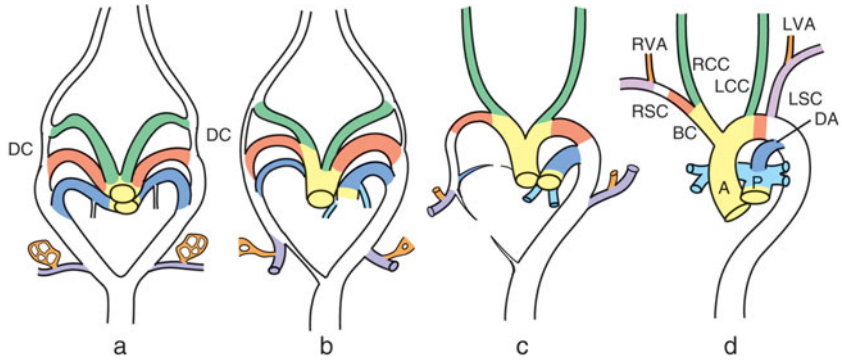

Figure 2.4. Diagram of the bilaterally symmetrical aortic arch arteries that carry the early cardiac output to the dorsal aorta which then distributes blood to the mouse or human embryo. The early symmetry is lost when these vessels are remodeled to be the adult great arteries of the thorax. *Green*, aortic arch artery 3; *red*, aortic arch artery 4; *blue*, aortic arch artery 6; DC, ductus caroticus; RVA and LVA, right and left vertebral arteries; RSC and LSC, right and left subclavian arteries; BC, brachiocephalic artery; RCC and LCC, right and left common carotid arteries; DA, ductus arteriosus; A, aorta; P, pulmonary trunk.

generate angioblasts themselves act as a nexus for vessel patterning (Hogan and Bautch, 2004).

Endothelial cells interact with their surrounding MATRIX and with each other in order to migrate and to form VESICLES and finally tubes. INTEGRIN-mediated cell adhesion is necessary for normal endothelial tube formation (Francis et al., 2002). After vascular tube formation, interendothelial tight junctions regulate intercellular permeability and maintain endothelial cell polarity.

The first recognizable vessels in the embryo are the bilaterally paired dorsal aortae. While most organs support a combination of vasculogenesis and angiogenesis, some organs—lung, pancreas, spleen, and stomach—also contain many of their own endothelial precursors, which self-assemble by vasculogenesis. Other organs, such as the brain, kidney, thymus, and limb bud, are almost completely vascularized by angiogenic ingrowth from pre-existing vessels (Risau, 1986; Sariola et al., 1983; Stewart and Wiley, 1981). Many organs, including the heart, acquire their early vessels by vasculogenesis followed by angiogenesis within the organ. Angiogenic growth of vessels from this intraorgan network results in arterial and venous connection with the established vasculature and the onset of a functional circulation to the organ (Robert et al., 1998). Interestingly, there is no difference in endothelial cell size between small- and large-diameter vessels (LaRue et al., 2003).

Some of the bilaterally symmetrical patterns that are established early are maintained. For example, the vasculature of the somite derivatives and spinal cord has an extremely regular pattern. The INTERSEGMENTAL ARTERIES AND VEINS originate from the dorsal aorta and cardinal veins and run between each pair of somites (Childs et al., 2002).

Signaling and Early Vascular Development

Understanding signaling networks is essential to understanding both vasculogenesis and angiogenesis. Many signaling factors are used and reused during early differentiation of the endothelial cells, formation of vesicles and tubes, and remodeling. One of the most important signaling pathways in vascular development is Vegf. The initial step in differentiation of endothelial cells is expression of the Vegf receptors. The first receptor expressed is Flk1 (Vegfr2) followed later by FLT1 (Vegfr1) (Millauer et al., 1993).

VEGF acts as a vascular morphogen by stimulating protrusive (exploratory) activity that leads to endothelial cell migration. Protrusive activity and migration lead to organization of a primary vascular pattern. Vegf is secreted by cells in four isoforms that have somewhat different functions. Localized sources of Vegf play a role in patterning the primary capillary plexus. Treatment with exogenous Vegf results in a massive "fusion" of vessels, while endothelial cells of embryos injected with Vegf antibody before the onset of circulation fail to form the elongated processes necessary for vessel morphogenesis (Drake et al., 1998). In addition, null mutation of one allele of *Vegf* is HAPLOINSUFFICIENT, leading to death early in gestation with a reduction in the size and diameter of blood vessels (Carmeliet et al., 1996; Ferrara et al., 1996). Furthermore, loss of *Flk1* leads to failure in development of angioblasts. On the other hand, embryos without *Flt1* have a disorganized primary capillary plexus with an overgrowth of endothelial cells (Fong et al., 1995, 1999, Kearney et al., 2002). Flt1 appears to negatively regulate Vegf signaling by modulating the phosphorylation of Flk1 (Roberts et al., 2004).

Vegf continues to play a role in promoting growth of blood vessels in later development and supports vascularization of developing organs. The different ISOFORMS of Vegf are important because isoform-specific knockout causes abnormal myocardial angiogenesis and abnormal vascular patterning in other organs (Carmeliet, 1999; Stalmans, 2005).

It is not clear how endothelial cells find their pathways, but it is clear that they share some of their pathfinding machinery with axon pathfinding. TRANSGENIC zebrafish embryos with an endothelial cell-specific promoter driving expression of green fluorescent protein show that endothelial cells undergoing angiogenesis have FILOPODIAL activity and pathfinding behavior similar to neuronal growth cones (Lawson and Weinstein,

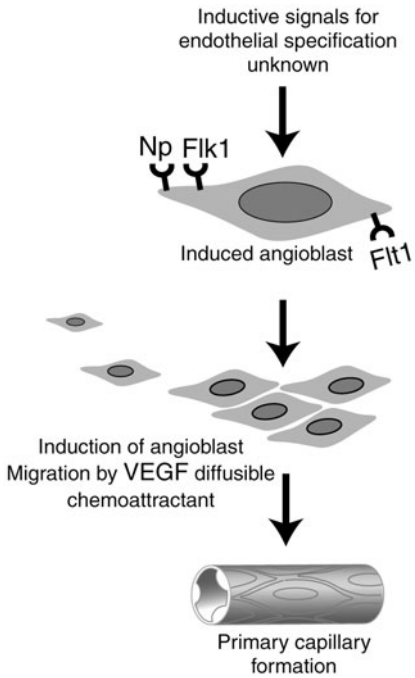

Figure 2.5. Some of the signaling pathways involved in establishing the vascular network.

2002). Both axons and endothelial cells are guided by factors that promote and inhibit their migration. Pathfinding activity is regulated by NEUROPILINS (NP) (Fig. 2.5), which are transmembrane proteins. In endothelial cells, Nps act as coreceptors for Flk1-mediated Vegf signaling and function to enhance Vegf binding to promote migration (Neufeld et al., 2002; Takashima et al., 2002).

SLIT ligands are a major class of neuronal guidance molecules. Three Slit ligands have been identified that provide chemorepulsive signals for axons. The Slit ligands interact with members of the *ROUNDABOUT* (*ROBO*) receptor gene family. Robo4 is expressed in endothelial cells. Binding of Slit to *Robo4* inhibits cellular migration and may provide a repulsive cue to endothelial cells (Park et al., 2003). Netrins are laminin-related secreted guidance cues for axons. Some netrins attract and others repel. The repulsive netrin receptor Unc5B is expressed by endothelial cells and appears to function as a repulsive signal for endothelial cells. *Unc5b*-null mice, or disruption of *Unc5b* or *Netrin-1a* expression in zebrafish, leads to abnormal filopodia extension by endothelial cells, excessive vessel branching, and abnormal migration (Lu et al., 2004). EPHRIN signaling was first recognized in axon pathfinding and neural crest cell migration, and it is also required for vessel remodeling. EPH receptors are tyrosine kinases that bind several ephrin ligands. Some ephrin ligands are soluble, but the most numerous class is membrane-attached cell-surface molecules (Adams and Klein, 2000). This means that ephrins have the potential to signal bidirectionally: to the cell that expresses them and to the cell expressing an Eph receptor (Bruckner and Klein, 1998). EphrinA ligands are CHEMOATTRACTANTS for migrating endothelial cells and are found at sites of remodeling (Daniel et al., 1996; Flenniken et al., 1996; McBride and Ruiz, 1998).

EphrinB ligands and EphB receptors can function as chemorepellants. Disrupted interactions between EphB4 expressed by intersomitic endothelial cells and ephrinB ligands on somitic mesodermal cells lead to disordered patterning of these usually very regular segmental vessels because the endothelial cells are unable to recognize the somite boundaries in the absence of normal ephrin signaling (Helbling et al., 1999; Oike et al., 2002).

Angiogenesis and Remodeling

Remodeling of blood vessels involves formation of new vessels by branching, fusion of endothelial tubes to form larger vessels and pruning of excess branches. Several growth factor families are involved in these steps. ANGIOPOIETIN (ANG) and its receptors TIE1 and Tie2 contribute to vascular remodeling and vessel stabilization (Fig. 2.6) (Dumont et al., 1992; Korhonen et al., 1994; Sato et al., 1993; Schnurch and Risau, 1993). Little is known about Ang signaling through the Tie1 receptor. More is known about the Tie2 receptor, which is a receptor tyrosine kinase. After binding the Ang ligand, Tie2 forms AUTOPHOSPHORYLATED HOMODIMERS (Jones et al., 1999). Null mutation of *Tie2* or *Ang1* causes embryonic death in mid-gestation because of the inability of blood vessels to remodel and stabilize (Dumont et al., 1994; Sato et al., 1995). Ang2 overexpression leads to a phenotype similar to the null phenotype of Tie2 or Ang1, indicating that it acts as an antagonist of Ang1/Tie2 signaling (Fig. 2.7) (Maisonpierre et al., 1997). Because Ang2 is expressed at sites of remodeling and branching, it is thought to act locally to block Ang1 signaling, which leads to vessel destabilization, an important step in initiating remodeling (Maisonpierre et al., 1997). If Vegf is present, the vessel remodels at sites of destabilization. In the absence of Vegf, the destabilized endothelial cells undergo apoptosis and the vessel regresses (Loughna and Sato, 2001).

As mentioned previously, the primary capillary plexus is symmetrical when it first forms and becomes asymmetrical during remodeling. The presence of left–right axis asymmetry is indicated molecularly in the primary capillary plexus. The sinus venosus is the major collecting point for all of the blood returning to the heart. When it is first formed, it is bilaterally symmetrical but quickly shows asymmetrical repatterning and is largely incorporated into the right atrium. Tie1 is expressed symmetrically in the sinus venosus, while Ang1 is expressed only in the right side before the vasculature shows any morphological asymmetry. This suggests that there is a distinct genetic program for establishing right versus left side vascular networks well before any asymmetry is morphologically discernible (Loughna and Sato, 2001). Null mutation shows that Ang1/Tie1 signaling is necessary for the development of the right-sided venous system while it is dispensable for the left-sided venous system.

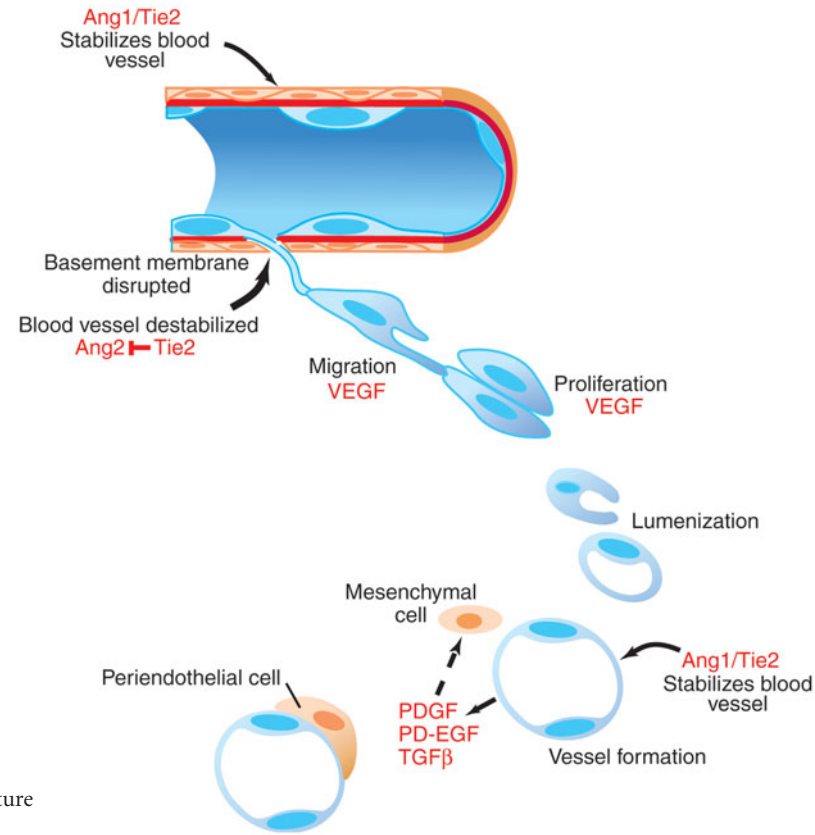

Figure 2.6. Factors involved in remodeling the vasculature and branching.

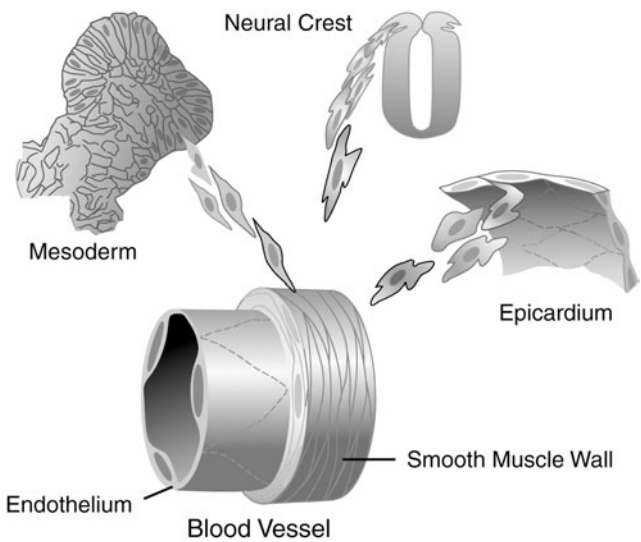

Figure 2.7. Diagram showing the three sources of vascular smooth muscle: mesoderm, epicardium, and neural crest. These cells are recruited by the endothelium to form the blood vessel wall.

Unlike Vegf, the Ang/Tie2 signaling system does not appear to function until circulation begins. Ang1 promotes signaling through the Tie2 receptor; however, Ang2 inhibits Tie2-mediated signaling by blocking Ang1. If embryos are injected with Ang2 they display malformed endocardial tubes, which appear perforated and discontinuous. Instead of large vessels with a single lumen, Ang2-treated aortic primordia resemble a small plexus of microvessels (Drake and Little, 1999). This suggests that Ang1 may help to stabilize vessels while Ang2 destabilizes vessels, a step that is required for both sprouting of new vessels and regression of nonpersisting vessels.

Stabilization of the Vessel Wall

Once the vascular pattern has been established after remodeling, stabilization of the vessel wall is critical for continued growth and stability of the vascular pattern. Stabilization of the vessel wall by recruitment of mural cells relies on short-range mesenchymal-to-endothelial signaling (Lindahl et al., 1998). Vascular MURAL cells are derived from several sources: mesoderm, neural crest, and epicardium (Fig. 2.7). These cells migrate to associate with endothelial cells and form the vessel wall (Fig. 2.8). There is some evidence that endothelial cells have the potential to give rise to vascular smooth muscle cells in that Flk1-positive embryonic stem cells can differentiate into both endothelial and mural cell lineages in vitro and in vivo (Yamashita et al., 2000). However, most mural cells are recruited from the surrounding nonendothelial mesenchyme.

Recruitment of vascular smooth muscle has been studied extensively along the dorsal aorta. The first mesodermally derived cells to associate with the dorsal aorta do so at the ventral surface. Recruitment of these cells proceeds in a

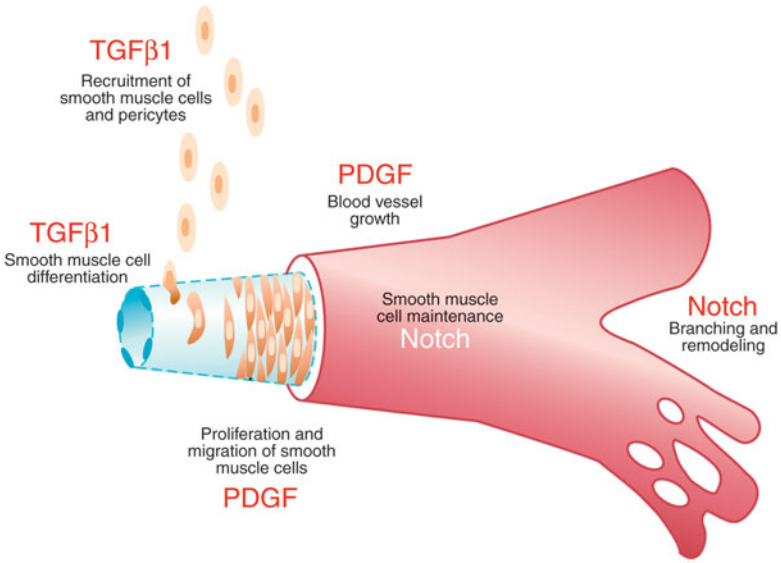

Figure 2.8. Growth factors and their roles in angiogenesis and remodeling.

ventral to dorsal direction along the aorta and in a radial direction from the endothelium. Differential expression of extracellular matrix components is an important step after the mural cells have been recruited. FIBULIN-1 is expressed by the earliest mural cells recruited and ELASTIN is subsequently expressed by cells added later to the vessel wall. This differential expression suggests that there may be early diversity among embryonic vascular smooth muscle cells (Hungerford et al., 1997). Vascular smooth muscle cells can be thought of as existing along a continuum of phenotypes. This spectrum varies from mainly matrix-producing cells to primarily contractile cells; thus no one cell type typifies vascular smooth muscle (Drake et al., 1998).

MYOCARDIN, PLATELET-DERIVED GROWTH FACTOR (PDGF)B, Pdgf receptor (Pdgfr)β, ang1, and *tie2* knockout mice all show deficient development of perivascular cells. Myocardin is a smooth muscle transcriptional coactivator of serum response factor that is essential for smooth muscle differentiation (Hauschka, 2001; Wang et al., 2001). Myocardin is a nuclear protein that activates cardiac muscle promoters by associating with SERUM RESPONSE FACTOR (SRF). When expressed ECTOPICally in non-muscle cells, myocardin induces smooth muscle differentiation (Du et al., 2003). Mouse embryos HOMOZYGOUS for a myocardin loss-of-function mutation show no evidence of smooth muscle cell differentiation, suggesting that myocardin is a master regulator of smooth muscle cell lineage similar to the role of MYOD in skeletal muscle (Li et al., 2003). Pdgf signaling is critical for proliferation and migration of smooth muscle cells and pericytes to support the endothelial cell wall (Lindahl et al., 1998). This process involves reciprocal interactions of endothelial and smooth muscle cells (Drake et al., 1998). Endothelial cells express the Pdgf LIGAND while smooth muscle cells express the Pdgfrβ receptor (Betsholtz, 1995). Mutation of the *Pdgfβ* gene for Pdgfβ ligand results in failure of recruitment of pericytes (Lindahl et al., 1998). Smooth muscle cells and pericytes initially form around endothelial vessels but cells lacking Pdgf signaling cannot proliferate and migrate as the vessels sprout and enlarge (Hellstrom et al., 1999).

The Notch signaling pathway was first recognized in *Drosophila* for its role in cell–cell signaling that regulates cell fate decisions. Notch proteins are transmembrane receptors that receive a variety of membrane-bound ligands including delta-like (Dll), serrate, and jagged (Fig. 2.9) (Schroeter et al., 1998; Struhl and Adachi, 1998). When the ligand binds the Notch receptor, its intracellular domain is cleaved by a γ-secretase complex that releases it from the cell membrane. The cytoplasmic tail then binds to the transcription factor RBPJκ, and the complex enters the nucleus, where it activates gene transcription; (Artavanis-Tsakonas et al., 1999; Fortini and Artavanis-Tsakonas, 1994). Targets of Notch signaling include the *HES* (Hairy/Enhancer of Split) gene, which is a bHLH transcription factor. *Hes* represses transcription to suppress specific cell fates in the signaled cell (Cau et al., 2000). Notch signaling is needed for branching and maintenance of the vascular smooth muscle coat in addition to its function in establishing arteries and veins from endothelial progenitors (discussed later). Notch3 is localized to smooth muscle cells surrounding arteries and Dll1 is expressed by endothelial cells (Shutter et al., 2000; Uyttendaele et al., 1996, 2000). Since there may be a common endothelial–smooth muscle lineage, it is possible that Notch signaling could play a role in determining the ratio of endothelial to smooth muscle cells (Yamashita et al., 2000). *Notch1*-deficient and *Jagged1* mutant embryos have defects in vascular remodeling and show poor branching (Krebs et al., 2000; Xue et al., 1999).

Tgfβ1 signaling is needed for vascular smooth muscle cell differentiation and recruitment (Larsson et al., 2001; Pepper, 1997). Tgfβ1 binds to the Tgfβ type II receptor (TbrII). In endothelial cells, TβrII recruits and phosphorylates type I receptors, known as activin-like kinase (Alk) receptors (Hoodless and Wrana, 1998). The heterodimer of TβrII–Alk then initiates

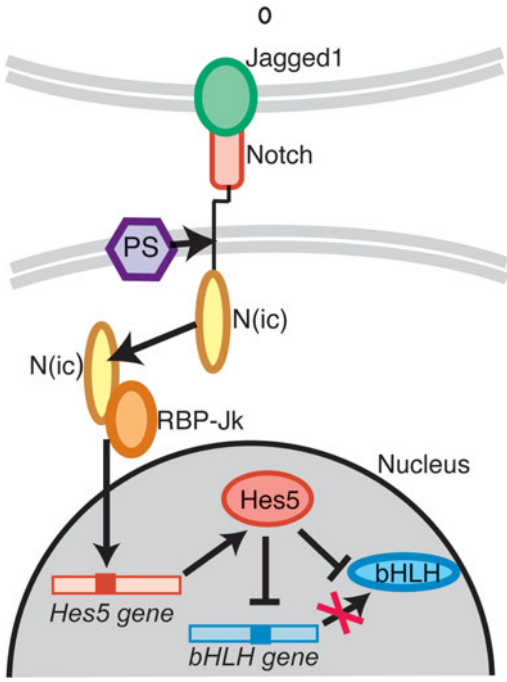

Figure 2.9. Notch signaling pathway. The Jagged ligand initiates Notch signaling by activating presenilin secretase (PS), an enzyme that cleaves the intracellular domain of the Notch receptor (Nic) which couples with RBPJκ. The complex translocates to the nucleus where it activates (*Hes5*) and/or represses (bHLH-containing transcription factors) expression of downstream targets.

a phosphorylation cascade that terminates in the nucleus where target gene transcription is initiated. Endothelial cells express a type II co-receptor called ENDOGLIN, which reduces the Tgf signaling response (Barbara et al., 1999; Letamendia et al., 1998). Embryos deficient for Alk5 die at E10.5–11.5 with vascular defects similar to Tgfβ1 and TβrII mutants in that they have HYPOPLASTIC smooth muscle walls (Oh et al., 2000).

Establishing the Identity of Arteries and Veins

Artery versus vein identity is programmed developmentally rather than differentiating as a functional characteristic (Fig. 2.10). A signaling cascade has been recognized that establishes artery versus vein identity. Both Vegf and its receptor Flk1 are expressed in arteries and veins but Vegf signaling gains specificity for artery versus vein differentiation by the expression of its co-receptor Nps. Np1 is artery-specific, while Np2 is restricted to the venous endothelium (Herzog et al., 2001). Tgfβ activation of Alk1 signaling is also involved in establishing artery versus vein identity (Urness et al., 2000). Alk1-null mutation in mice leads to formation of abnormal SHUNTS between the dorsal aorta and cardinal veins. Mutations in the human *ALK1* and *ENDOGLIN* genes are associated with HEREDITARY HEMORRHAGIC TELANGIECTASIA (discussed later),

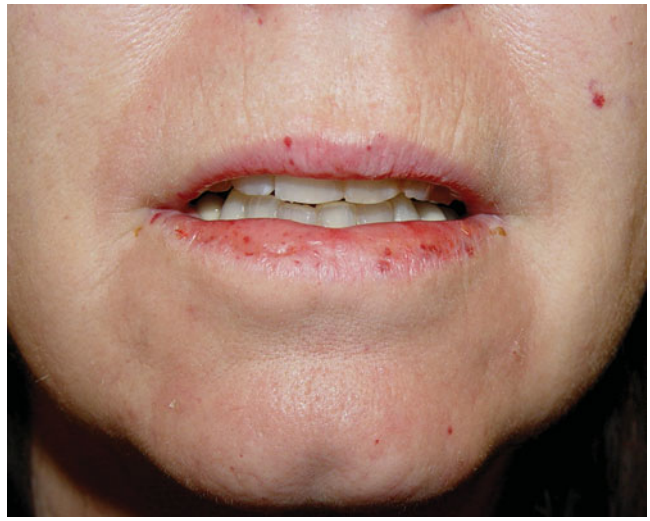

Figure 2.10. A 46-year-old woman with hereditary hemorrhagic telangiectasia that appear as multiple widespread 2–5 mm blanching red macules and partially blanching papules on the face and lips. (From DermAtlas, Johns Hopkins University; 2000–2005 Bernard A. Cohen, MD, Christoph U. Lehmann, MD, with permission.)

a disorder that results in arteriovenous shunts (Azuma, 2000; Urness et al., 2000). Indeed, mice lacking endoglin develop arteriovenous malformations (Sorensen et al., 2003).

Notch and ephrins are differentially expressed on arterial versus venous endothelial cells. Tgfβ/Alk1 signaling may activate both ephrin and Notch signaling, which suppresses venous fate. In mice with *Alk1*-null mutation, the dorsal aorta and arteries fails to express ephrinB2, which is specific for arterial endothelium (Urness et al., 2000). The cognate receptor for ephrinB2, EphB4, is expressed in venous endothelial cells (Wang et al., 1998). An ephrinB2–EphB4 interaction is probably necessary to establish the arterial–venous boundary (Adams and Klein, 2000; Adams et al., 1999). Venous endothelial cells coexpress high levels of EphB3 and EphB4 receptors and the ephrinB1 ligand, while both ephrinB1 and -B2 are expressed with low levels of EphB3 and B4 in the arterial endothelium (Adams et al., 1999; Gerety et al., 1999). However, other factors must be involved, as loss of ephrin signaling does not lead to mixing of arterial and venous endothelial cells (Gerety et al., 1999; Wang et al., 1998).

Notch1, Notch4, Delta4, Jagged1, and Jagged2 are expressed in the arterial endothelium (Shirayoshi et al., 1997). Jagged1 and Notch2 are colocalized and required for renal glomerular differentiation and patterning. *Notch2*-null homozygotes also display myocardial hypoplasia, edema, and hyperplasia of cells associated with some of the vasculature of the eye (McCright et al., 2001). Angioblast precursors for the dorsal aorta and posterior cardinal vein are spatially mixed in the lateral posterior mesoderm and Notch signaling is important for proper assignment of arterial versus venous fate to these cells (Lawson et al., 2002). In zebrafish, progeny of each angioblast are restricted to one of the vessels by GRIDLOCK

(*grl*), a downstream target of Notch signaling that is expressed only in arterial endothelium in the lateral posterior mesoderm (Zhong et al., 2000). Graded reduction of *grl* expression, by mutation or morpholino antisense, progressively reduces the artery and expands contiguous regions of the vein. This suggests that Grl normally suppresses venous endothelial fate. Expansion of the vein is preceded by an increase in expression of the venous marker, EphB4 receptor, and diminution of expression of the arterial marker ephrinB2. Interference with Notch signaling by blocking SUPPRESSOR OF HAIRLESS (SuH), a cofactor needed for Notch transcriptional activity, similarly reduces the arterial fate at the same time expanding venous endothelial cells. Thus, a Notch–grl pathway controls assembly of dorsal aorta and posterior cardinal veins by adjudicating an arterial versus venous cell fate decision (Zhong et al., 2000).

Some Arterial and Venous Malformations

Hereditary Hemorrhagic Telangiectasia (Rendu–Olser–Webber Disease)

Hereditary hemorrhagic TELANGIECTASIA (HHT) is an autosomal dominant disorder characterized by vascular dysplasia and hemorrhage (Fig. 2.10). Pulmonary arteriovenous malformations have a variable incidence rate ranging between 15% and 33%. Hemorrhages from the gastrointestinal tract occur in 10%–40% of patients with HHT localized in the duodenum. The prevalence of cerebrovascular malformations in HHT patients is 5%–27%, and several types are described including telangiectasias, CAVERNOUS ANGIOMAS, arteriovenous malformations, and ANEURYSMS. The most common symptom in HHT patients is nasal hemorrhage. Nosebleeds begin before 10 years of age and become more severe in later decades (Fiorella et al., 2004). HHT is a genetically heterogeneous disease associated with mutations in components of the Tgfβ family signaling pathway. Some of the identified mutations are in *ENDOGLIN*, located on chromosome 9q3 and *ALK1* (Cole et al., 2005; McAllister et al., 1994; Vincent et al., 1995). In addition, patients have been identified with HTT-JUVENILE POLYPOSIS overlap syndrome due to Smad4 mutations (Cole et al., 2005).

Interrupted Aortic Arch

Several experimental models of INTERRUPTED ARCH exist and many genes have been identified that are required for development of the normal pattern of great arteries. However, little is known about the mechanism of aortic arch artery formation or repatterning. Repatterning the initially bilaterally symmetrical aortic arch arteries into the great arteries requires an intact neural crest (Kirby et al., 1997; Waldo et al., 1996). One of the factors needed for normal repatterning includes MESENCHYME FORK HEAD1 (MFH1), transcription factor defined by a conserved winged helix DNA-binding domain. Mfh1 is expressed in cephalic neural crest and mesenchymal cells in the prechordal region of early embryos. Subsequently strong expression appears in the dorsal aortas. *Mfh1*-deficient mice have isolated interrupted aortic arch (Iida et al., 1997). FIBROBLAST GROWTH FACTOR (FGF)8 expressed in the ectoderm overlying pharyngeal arches 3–6 is required for formation of aortic arch 4. The left arch 4 artery is repatterned to the arch of the aorta. Specific deletion of Fgf8 expression specifically from the ectoderm leads to interrupted arch (Macatee et al., 2003).

Alagille Syndrome

Mutations in *JAGGED1* and *NOTCH3* are associated with human diseases that have significant arteriovenous shunting vascular malformations called Alagille syndrome. The Alagille syndrome (AGS) is a dominantly inherited disease characterized by abnormalities in the liver, heart, face, vertebrae, and eyes. The responsible gene has been recently identified as the human *JAGGED1* (*JAG1*) gene, which encodes a ligand for the Notch receptor (Krantz et al., 1998; Oda et al., 1997; Yuan et al., 1998).

CADASIL

CADASIL is an acronym for *C*erebral *A*utosomal *D*ominant *A*rteriopathy with *S*ubcortical *I*nfarcts and *L*eukoencephalopathy. The disease is a progressive vascular disorder that appears by age 60. The symptoms include migraines with or without an aura, mood disturbances, focal neurologic deficits, strokes, and dementia. The symptoms are underlain by recurrent subcortical ischemic events that cause permanent deficits in many patients. Mutations in the *NOTCH3* gene on chromosome 19 are linked with the phenotype (Milunsky et al., 2005; Peters et al., 2005).

REFERENCES

Adams, R. H., and R. Klein. 2000. Eph receptors and ephrin ligands. Essential mediators of vascular development. Trends Cardiovasc. Med. 10:183–188.

Adams, R. H., G. A. Wilkinson, C. Weiss, F. Diella, N. W. Gale, U. Deutsch, W. Risau, and R. Klein. 1999. Roles of ephrinB ligands and EphB receptors in cardiovascular development: demarcation of arterial/venous domains, vascular morphogenesis, and sprouting angiogenesis. Genes Dev. 13:295–306.

Artavanis-Tsakonas, S., M. D. Rand, and R. J. Lake. 1999. Notch signaling: cell fate control and signal integration in development. Science 284:770–776.

Azuma, H. 2000. Genetic and molecular pathogenesis of hereditary hemorrhagic telangiectasia. J. Med. Invest. 47:81–90.

Barbara, N. P., J. L. Wrana, and M. Letarte. 1999. Endoglin is an accessory protein that interacts with the signaling receptor complex of multiple members of the transforming growth factor-a superfamily. J. Biol. Chem. 274:584–594.

Betsholtz, C. 1995. Role of platelet-derived growth factors in mouse development. Int. J. Dev. Biol. 39:817–825.

Bruckner, K., and R. Klein. 1998. Signaling by Eph receptors and their ephrin ligands. Curr. Opin. Neurobiol. 8:375–382.

Carmeliet, P. 1999. Basic concepts of (myocardial) angiogenesis: role of vascular endothelial growth factor and angiopoietin. Curr. Interv. Cardiol. Rep. 1:322–335.

Carmeliet, P., V. Ferreira, G. Brier, S. Pollefeyt, L. Kieckens, M. Gertsenstein, M. Fahrig, A. Vandenhoeck, K. Harpal, C. Eberhardt, C. Declercq, J. Pawling, L. Moon, D. Collen, W. Rissau, and A. Nagy. 1996. Abnormal blood vessel development and lethality in embryos lacking a single VEGF allele. Nature 380:435–439.

Cau, E., G. Gradwohl, S. Casarosa, R. Kageyama, and F. Guillemot. 2000. Hes genes regulate sequential stages of neurogenesis in the olfactory epithelium. Development 127:2323–2332.

Childs, S., J. N. Chen, D. M. Garrity, and M. C. Fishman. 2002. Patterning of angiogenesis in the zebrafish embryo. Development 129:973–982.

Cole, S. G., M. E. Begbie, G. M. Wallace, and C. L. Shovlin. 2005. A new locus for hereditary haemorrhagic telangiectasia (HHT3) maps to chromosome 5. J. Med. Genet. 42:577–582.

Daniel, T. O., E. Stein, D. P. Cerretti, P. L. St John, B. Robert, and D. R. Abrahamson. 1996. ELK and LERK-2 in developing kidney and microvascular endothelial assembly. Kidney Int. Suppl. 57:S73–81.

de Ruiter, M. C., A. C. Gittenberger-de Groot, R. E. Poelmann, L. Vaniperen, and M. M. T. Mentink. 1993. Development of the pharyngeal arch system related to the pulmonary and bronchial vessels in the avian embryo: with a concept on systemic-pulmonary collateral artery formation. Circulation 87:1306–1319.

Drake, C. J., J. E. Hungerford, and C. D. Little. 1998. Morphogenesis of the first blood vessels. Ann. NY Acad. Sci. 857:155–179.

Drake, C. J., and C. D. Little. 1999. VEGF and vascular fusion: implications for normal and pathological vessels. J. Histochem. Cytochem. 47:1351–1356.

Du, A., J. M. Sanger, K. K. Linask, and J. W. Sanger. 2003. Myofibrillogenesis in the first cardiomyocytes formed from isolated quail precardiac mesoderm. Dev. Biol. 257:382–394.

Dumont, D. J., F.-H. Fong, M. C. Puri, G. Gradwohl, K. Alitalo, and M. L. Breitman. 1995. Vascularization of the mouse embryo: a study of flk-2, tek, tie, and vascular endothelial growth factor expression during development. Dev. Dyn. 203:80–92.

Dumont, D. J., G. Gradwohl, G. H. Fong, M. C. Puri, M. Gertsenstein, A. Auerbach, and M. L. Breitman. 1994. Dominant-negative and targeted null mutations in the endothelial receptor tyrosine kinase, tek, reveal a critical role in vasculogenesis of the embryo. Genes Dev. 8:1897–1909.

Dumont, J. D., T. P. Yamaguchi, R. A. Conlon, J. Rossant, and M. L. Breitman. 1992. *tek*, a novel tyrosine kinase gene located on mouse chromosome 4 is expressed in endothelial cells and their presumptive precursors. Oncogene 7:1471–1480.

Ferrara, N., K. Carver-Moore, H. Chan, M. Dowd, L. Lu, K. S. O'Shea, L. Powell-Braxton, K. J. Hillan, and M. W. Moore. 1996. Heterozygous embryonic lethality induced by targeted inactivation of the VEGF gene. Nature 380:439–442.

Fiorella, M. L., D. A. Ross, R. I. White, C. Sabba, and R. Fiorella. 2004. Hereditary haemorrhagic telangiectasia: state of the art. Acta Otorhinolaryngol. Ital. 24:330–336.

Flenniken, A. M., N. W. Gale, G. D. Yancopoulos, and D. G. Wilkinson. 1996. Distinct and overlapping expression patterns of ligands for Eph-related receptor tyrosine kinases during mouse embryogenesis. Dev. Biol. 179:382–401.

Fong, G.-H., J. Rossant, M. Gertsenstein, and M. L. Breitman. 1995. Role of the Flt-1 receptor tyrosine kinase in regulating the assembly of vascular endothelium. Nature 376:66–70.

Fong, G. H., L. Y. Zhang, D. M. Bryce, and J. Peng. 1999. Increased hemangioblast commitment, not vascular disorganization, is the primary defect in flt-1 knock-out mice. Development 126:3015–3025.

Fortini, M. E., and S. Artavanis-Tsakonas. 1994. The suppressor of hairless protein participates in Notch receptor signaling. Cell 79:273–282.

Francis, S. E., K. L. Goh, K. Hodivala-Dilke, B. L. Bader, M. Stark, D. Davidson, and R. O. Hynes. 2002. Central roles of alpha5beta1 integrin and fibronectin in vascular development in mouse embryos and embryoid bodies. Arterioscler. Thromb. Vasc. Biol. 22:927–933.

Garcia-Martinez, V., and G. C. Schoenwolf. 1993. Primitive-streak origin of the cardiovascular system in avian embryos. Dev. Biol. 159:706–719.

Gerety, S. S., H. U. Wang, Z. F. Chen, and D. J. Anderson. 1999. Symmetrical mutant phenotypes of the receptor EphB4 and its specific transmembrane ligand ephrin-B2 in cardiovascular development. Mol. Cell 4:403–414.

Hauschka, S. D. 2001. Myocardin: a novel potentiator of SRF-mediated transcription in cardiac muscle. Mol. Cell 8:1–2.

Helbling, P. M., D. M. E. Saulnier, V. Robinson, J. H. Christiansen, D. G. Wilkinson, and A. W. Brandli. 1999. Comparative analysis of embryonic gene expression defines potential interaction sites for *Xenopus* EphB4 receptors with ephrin-B ligands. Dev. Dyn. 216:361–373.

Hellstrom, M., M. Kalen, P. Lindahl, A. Abramsson, and C. Betsholtz. 1999. Role of PDGF-B and PDGFR-beta in recruitment of vascular smooth muscle cells and pericytes during embryonic blood vessel formation in the mouse. Development 126:3047–3055.

Herzog, Y., C. Kalcheim, N. Kahane, R. Reshef, and G. Neufeld. 2001. Differential expression of neuropilin-1 and neuropilin-2 in arteries and veins. Mech. Dev. 109:115–119.

Hogan, K. A., and V. L. Bautch. 2004. Blood vessel patterning at the embryonic midline. Curr. Top. Dev. Biol. 62:55–85.

Hoodless, P. A., and J. L. Wrana. 1998. Mechanism and function of signaling by the TGF beta superfamily. Curr. Top. Microbiol. Immunol. 228:235–272.

Hungerford, J. E., J. P. Hoeffler, C. W. Bowers, L. M. Dahm, R. Falchetto, J. Shabanowitz, D. F. Hunt, and C. D. Little. 1997. Identification of a novel marker for primordial smooth muscle and its differential expression pattern in contractile vs noncontractile cells. J. Cell Biol. 137:925–937.

Iida, K., H. Koseki, H. Kakinuma, N. Kato, Y. Mizutani-Koseki, H. Ohuchi, H. Yoshioka, S. Noji, K. Kawamura, Y. Kataoka, F. Ueno, M. Taniguchi, N. Yoshida, T. Sugiyama, and N. Miura. 1997. Essential roles of the winged helix transcription factor MFH-1 in aortic arch patterning and skeletogenesis. Development 124:4627–4638.

Jones, N., Z. Master, J. Jones, D. Bouchard, Y. Gunji, H. Sasaki, R. Daly, K. Alitalo, and D. J. Dumont. 1999. Identification of Tek/Tie2 binding partners. Binding to a multifunctional docking site mediates cell survival and migration. J. Biol. Chem. 274:30896–30905.

Kearney, J. B., C. A. Ambler, K. A. Monaco, N. Johnson, R. G. Rapoport, and V. L. Bautch. 2002. Vascular endothelial growth factor receptor Flt-1 negatively regulates developmental blood vessel formation by modulating endothelial cell division. Blood 99:2397–2407.

Kirby, M. L., P. Hunt, K. T. Wallis, and P. Thorogood. 1997. Normal development of the cardiac outflow tract is not dependent on normal patterning of the aortic arch arteries. Dev. Dyn. 208:34–47.

Korhonen, J., A. Polvi, J. Partanen, and K. Alitalo. 1994. The mouse tie receptor tyrosine kinase gene: expression during embryonic angiogenesis. Oncogene 9:395–403.

Krantz, I. D., R. P. Colliton, A. Genin, E. B. Rand, L. H. Li, D. A. Piccoli, and N. B. Spinner. 1998. Spectrum and frequency of Jagged1 (*JAG1*) mutations in Alagille syndrome patients and their families. Am. J. Hum. Genet. 62:1361–1369.

Krebs, L. T., Y. Z. Xue, C. R. Norton, J. R. Shutter, M. Maguire, J. P. Sundberg, D. Gallahan, V. Closson, J. Kitajewski, R. Callahan, G. H. Smith, K. L. Stark, and T. Gridley. 2000. Notch signaling is essential for vascular morphogenesis in mice. Genes Dev. 14:1343–1352.

Larsson, J., M. J. Goumans, L. J. Sjostrand, M. A. van Rooijen, D. Ward, P. Leveen, X. Xu, P. ten Dijke, C. L. Mummery, and S. Karlsson. 2001. Abnormal angiogenesis but intact hematopoietic potential in TGF-beta type I receptor-deficient mice. EMBO J. 20:1663–1673.

LaRue, A. C., V. A. Mironov, W. S. Argraves, A. Czir¢k, P. A. Fleming, and C. J. Drake. 2003. Patterning of embryonic blood vessels. Dev. Dyn. 228:21–29.

Lawson, N. D., N. Scheer, V. N. Pham, C. H. Kim, A. B. Chitnis, J. A. Campos-Ortega, and B. M. Weinstein. 2001. Notch signaling is required for arterial-venous differentiation during embryonic vascular development. Development 128:3675–3683.

Lawson, N. D., and B. M. Weinstein. 2002. In vivo imaging of embryonic vascular development using transgenic zebrafish. Dev. Biol. 248:307–318.

Letamendia, A., P. Lastres, L. M. Botella, U. Raab, C. Langa, B. Velasco, L. Attisano, and C. Bernabeu. 1998. Role of endoglin in cellular responses to transforming growth factor-beta. A comparative study with betaglycan. J. Biol. Chem. 273:33011–33019.

Li, S., D.-Z. Wang, Z. Wang, J. A. Richardson, and E. N. Olson. 2003. The serum response factor coactivator myocardin is required for vascular smooth muscle development. Proc. Natl. Acad. Sci. USA 100:9366–9370.

Lindahl, P., M. Hellstrom, M. Kalen, and C. Betsholtz. 1998. Endothelial–perivascular cell signaling in vascular development: lessons from knockout mice. Curr. Opin. Lipidol. 9:407–411.

Loughna, S., and T. Sato. 2001. Angiopoietin and Tie signaling pathways in vascular development. Matrix Biol. 20:319–325.

Lu, X., F. Le Noble, L. Yuan, Q. Jiang, B. De Lafarge, D. Sugiyama, C. Breant, F. Claes, F. De Smet, J. L. Thomas, M. Autiero, P. Carmeliet, M. Tessier-Lavigne, and A. Eichmann. 2004. The netrin receptor UNC5B mediates guidance events controlling morphogenesis of the vascular system. Nature. 432:179–186.

Macatee, T. L., B. P. Hammond, R. Benjamin, B. R. Arenkiel, L. Francis, D. U. Frank, and A. M. Moon. 2003. Ablation of specific expression domains reveals discrete functions of ectoderm- and endoderm-derived FGF8 during cardiovascular and pharyngeal development. Development 130:6361–6374.

Maisonpierre, P. C., C. Suri, P. F. Jones, S. Bartunkova, S. Wiegand, C. Radziejewski, D. Compton, J. McClain, T. H. Aldrich, N. Papadopoulos, T. J. Daly, S. Davis, T. N. Sato, and G. D. Yancopoulos. 1997. Angiopoietin-2, a natural antagonist for Tie2 that disrupts in vivo angiogenesis. Science 277:55–60.

McAllister, K. A., K. M. Grogg, D. W. Johnson, C. J. Gallione, M. A. Baldwin, C. E. Jackson, E. A. Helmbold, D. S. Markel, W. C. McKinnon, J. Murrell, et al. 1994. Endoglin, a TGF-beta binding protein of endothelial cells, is the gene for hereditary haemorrhagic telangiectasia type 1. Nat. Genet. 8:345–51.

McBride, J. L., and J. C. Ruiz. 1998. Ephrin-A1 is expressed at sites of vascular development in the mouse. Mech. Dev. 77:201–204.

McCright, B., X. Gao, L. Shen, J. Lozier, Y. Lan, M. Maguire, D. Herzlinger, G. Weinmaster, R. Jiang, and T. Gridley. 2001. Defects in development of the kidney, heart and eye vasculature in mice homozygous for a hypomorphic *Notch2* mutation. Development 128:491–502.

Millauer, B., S. Wizigmann-Voos, H. SchnÅrch, R. Martinez, N. P. H. Moller, W. Risau, and A. Ullrich. 1993. High affinity VEGF binding and developmental expression suggest Flk-1 as a major regulator of vasculogenesis and angiogenesis. Cell 72:835–846.

Milunsky, A., C. Konialis, S. H. Shim, T. A. Maher, K. Spengos, M. Ito, and C. Pangalos. 2005. The prenatal diagnosis of cerebral autosomal dominant arteriopathy with subcortical infarcts and leukoencephalopathy (CADASIL) by mutation analysis. Prenat. Diagn. 25:1057–1058.

Moser, M., O. Binder, Y. Wu, J. Aitsebaomo, R. Ren, C. Bode, V. L. Bautch, F. L. Conlon, and C. Patterson. 2003. BMPER, a novel endothelial cell precursor-derived protein, antagonizes bone morphogenetic protein signaling and endothelial cell differentiation. Mol. Cell Biol. 23:5664–5679.

Neufeld, G., O. Kessler, and Y. Herzog. 2002. The interaction of Neuropilin-1 and Neuropilin-2 with tyrosine-kinase receptors for VEGF. Adv. Exp. Med. Biol. 515:81–90.

Oda, T., A. G. Elkahloun, B. L. Pike, K. Okajima, I. D. Krantz, A. Genin, D. A. Piccoli, P. S. Meltzer, N. B. Spinner, F. S. Collins, and S. C. Chandrasekharappa. 1997. Mutations in the human *Jagged1* gene are responsible for Alagille syndrome. Nat. Genet. 16:235–242.

Oh, S. P., T. Seki, K. A. Goss, T. Imamura, Y. Yi, P. K. Donahoe, L. Li, K. Miyazono, P. ten Dijke, S. Kim, and E. Li. 2000. Activin receptor-like kinase 1 modulates transforming growth factor-beta 1 signaling in the regulation of angiogenesis. Proc. Natl. Acad. Sci. USA 97:2626–2631.

Oike, Y., Y. Ito, K. Hamada, X. Q. Zhang, K. Miyata, F. Arai, T. Inada, K. Araki, N. Nakagata, M. Takeya, Y. Y. Kisanuki, M. Yanagisawa, N. W. Gale, and T. Suda. 2002. Regulation of vasculogenesis and angiogenesis by EphB/ephrin-B2 signaling between endothelial cells and surrounding mesenchymal cells. Blood 100:1326–1333.

Park, C., I. Afrikanova, Y. S. Chung, W. J. Zhang, E. Arentson, G. G. Fong, A. Rosendahl, and K. Choi. 2004. A hierarchical order of factors in the generation of FLK1- and SCL-expressing hematopoietic and endothelial progenitors from embryonic stem cells. Development 131:2749–2762.

Park, K. W., C. M. Morrison, L. K. Sorensen, C. A. Jones, Y. Rao, C. B. Chien, J. Y. Wu, L. D. Urness, and D. Y. Li. 2003. Robo4 is a vascular-specific receptor that inhibits endothelial migration. Dev. Biol. 261:251–267.

Pepper, M. S. 1997. Transforming growth factor-beta: vasculogenesis, angiogenesis, and vessel wall integrity. Cytokine Growth Factor Rev. 8:21–43.

Peters, N., C. Opherk, A. Danek, C. Ballard, J. Herzog, and M. Dichgans. 2005. The pattern of cognitive performance in CADASIL: a monogenic condition leading to subcortical ischemic vascular dementia. Am. J. Psychiatry 162:2078–2085.

Risau, W. 1986. Developing brain produces an angiogenesis factor. Proc. Natl. Acad. Sci. USA 83:3855–3859.

Robert, B., P. L. St John, and D. R. Abrahamson. 1998. Direct visualization of renal vascular morphogenesis in Flk1 heterozygous mutant mice. Am. J. Physiol. 275:F164–172.

Roberts, D. M., J. B. Kearney, J. H. Johnson, M. P. Rosenberg, R. Kumar, and V. L. Bautch. 2004. The vascular endothelial growth factor (VEGF) receptor Flt-1 (VEGFR-1) modulates Flk-1 (VEGFR-2) signaling during blood vessel formation. Am. J. Pathol. 164:1531–1535.

Sariola, H., P. Ekblom, E. Lehtonen, and L. Saxen. 1983. Differentiation and vascularization of the metanephric kidney grafted on the chorioallantoic membrane. Dev. Biol. 96:427–435.

Sato, T. N., Y. Qin, C. A. Kozak, and K. L. Audus. 1993. tie-1 and tie-2 define another class of putative receptor tyrosine kinase genes expressed in early embryonic vascular system. Proc. Natl. Acad. Sci. USA 90:9355–9358.

Sato, T. N., Y. Tozawa, U. Deutsch, K. Wolburg-Buchholz, Y. Fujiwara, M. Gendron-Maguire, T. Gridley, H. Wolburg, W. Risau, and Y. Qin. 1995. Distinct roles of the receptor tyrosine kinases Tie-1 and Tie-2 in blood vessel formation. Nature 376:70–74.

Schnurch, H., and W. Risau. 1993. Expression of tie-2, a member of a novel family of receptor tyrosine kinases, in the endothelial cell lineage. Development 119:957–968.

Schroeter, E. H., J. A. Kisslinger, and R. Kopan. 1998. Notch-1 signalling requires ligand-induced proteolytic release of intracellular domain. Nature 393:382–386.

Shalaby, F., J. Rossant, T. P. Yamaguchi, M. Gertsenstein, X.-F. Wu, M. L. Breitman, and A. C. Schuh. 1995. Failure of blood-island formation and vasculogenesis in Flk-1-deficient mice. Nature 376:62–66.

Shirayoshi, Y., Y. Yuasa, T. Suzuki, K. Sugaya, E. Kawase, T. Ikemura, and N. Nakatsuji. 1997. Proto-oncogene of int-3, a mouse Notch homologue, is expressed in endothelial cells during early embryogenesis. Genes Cells 2:213–224.

Shutter, J. R., S. Scully, W. Fan, W. G. Richards, J. Kitajewski, G. A. Deblandre, C. R. Kintner, and K. L. Stark. 2000. Dll4, a novel Notch ligand expressed in arterial endothelium. Genes Dev. 14:1313–1318.

Sorensen, L. K., B. S. Brooke, D. Y. Li, and L. D. Urness. 2003. Loss of distinct arterial and venous boundaries in mice lacking endoglin, a vascular-specific TGFa coreceptor. Dev. Biol. 261:235–250.

Stalmans, I. 2005. Role of the vascular endothelial growth factor isoforms in retinal angiogenesis and DiGeorge syndrome. Verh. K. Acad. Geneeskd. Belg. 67:229–276.

Stewart, P. A., and M. J. Wiley. 1981. Developing nervous tissue induces formation of blood–brain barrier characteristics in invading endothelial cells: a study using quail–chick transplantation chimeras. Dev. Biol. 84:183–192.

Struhl, G., and A. Adachi. 1998. Nuclear access and action of notch in vivo. Cell 93:649–660.

Takashima, S., M. Kitakaze, M. Asakura, H. Asanuma, S. Sanada, F. Tashiro, H. Niwa, J. J. Miyazaki, S. Hirota, Y. Kitamura, T. Kitsukawa, H. Fujisawa, M. Klagsbrun, and M. Hori. 2002. Targeting of both mouse neuropilin-1 and neuropilin-2 genes severely impairs developmental yolk sac and embryonic angiogenesis. Proc. Natl. Acad. Sci. USA 99:3657–3662.

Urness, L. D., L. K. Sorensen, and D. Y. Li. 2000. Arteriovenous malformations in mice lacking activin receptor-like kinase-1. Nat. Genet. 26:328–331.

Uyttendaele, H., V. Closson, G. Y. Wu, F. Roux, G. Weinmaster, and J. Kitajewski. 2000. *Notch4* and *Jagged-1* induce microvessel differentiation of rat brain endothelial cells. Microvasc. Res. 60:91–103.

Uyttendaele, H., G. Marazzi, G. Wu, Q. Yan, D. Sassoon, and J. Kitajewdki. 1996. *Notch4/int-3*, a mammary proto-oncogene, is an endothelial cell-specific mammalian Notch gene. Development 122:2251–2259.

Vincent, P., H. Plauchu, J. Hazan, S. Faure, J. Weissenbach, and J. Godet. 1995. A third locus for hereditary haemorrhagic telangiectasia maps to chromosome 12q. Hum. Mol. Genet. 4:945–949.

Visvader, J. E., Y. Fujiwara, and S. H. Orkin. 1998. Unsuspected role for the T-cell leukemia protein SCL/tal-1 in vascular development. Genes Dev. 12:473–479.

Waldo, K. L., D. Kumiski, and M. L. Kirby. 1996. Cardiac neural crest is essential for the persistence rather than the formation of an arch artery. Dev. Dyn. 205:281–292.

Wang, D., P. S. Chang, Z. Wang, L. Sutherland, J. A. Richardson, E. Small, P. A. Krieg, and E. N. Olson. 2001. Activation of cardiac gene expression by myocardin, a transcriptional cofactor for serum response factor. Cell 105:851–862.

Wang, H. U., Z. F. Chen, and D. J. Anderson. 1998. Molecular distinction and angiogenic interaction between embryonic arteries and veins revealed by ephrin-B2 and its receptor Eph-B4. Cell 93:741–753.

Xue, Y. Z., X. Gao, C. E. Lindsell, C. R. Norton, B. Chang, C. Hicks, M. Gendron-Maguire, E. B. Rand, G. Weinmaster, and T. Gridley. 1999. Embryonic lethality and vascular defects in mice lacking the Notch ligand JAGGED1. Hum. Mol. Genet. 8:723–730.

Yamaguchi, T. P., D. J. Dumont, R. A. Conlon, M. L. Breitman, and J. Rossant. 1993. flk-1, an flt-related receptor tyrosine kinase is an early marker for endothelial cell precursors. Development 118:489–498.

Yamashita, J., H. Itoh, M. Hirashima, M. Ogawa, S. Nishikawa, T. Yurugi, M. Naito, K. Nakao, and S. Nishikawa. 2000. Flk1-positive cells derived from embryonic stem cells serve as vascular progenitors. Nature 408:92–96.

Yuan, Z. R., T. Kohsaka, T. Ikegaya, T. Suzuki, S. Okano, J. Abe, N. Kobayashi, and M. Yamada. 1998. Mutational analysis of the *Jagged 1* gene in Alagille syndrome families. Hum. Mol. Genet. 7:1363–1369.

Zhong, T. P., S. Childs, J. P. Leu, and M. C. Fishman. 2001. Gridlock signalling pathway fashions the first embryonic artery. Nature 414:216–220.

Zhong, T. P., M. Rosenberg, M. A. P. K. Mohideen, B. Weinstein, and M. C. Fishman. 2000. *gridlock*, an HLH gene required for assembly of the aorta in zebrafish. Science 287:1820–1824.

3

Cardiogenic Fields and Heart Tube Formation

All vertebrates go through a type of development in which a primary PLEURIPOTENTIAL FIELD of cells is established that is subdivided into organ fields as development proceeds. Heart development is initiated when bilateral CARDIOGENIC FIELDS are established in the mesodermal GERM LAYER. These cardiogenic fields become spatially and molecularly subdivided into chamber-forming regions or fields. The mode in which the bilateral fields are brought together and fuse, as well as how the chamber forming regions are established, contribute to the complexity in understanding heart tube formation. The cardiogenic fields provide the myocardium and some of the endocardium used to build the heart tube. This chapter focuses on the myocardium, although formation of the heart tube necessitates formation of an endocardial tube, and these steps are covered briefly at the end of the chapter. The endocardium as a separate entity is covered in Chapter 9. An initial heart tube forms and begins to beat to initiate circulation even though more myocardium and endocardium are added to the INFLOW AND OUTFLOW (VENOUS AND ARTERIAL, RESPECTIVELY) POLES to lengthen the tube. The final myocardium is added to the arterial and venous poles from part(s) of the cardiogenic field that does not differentiate as myocardium with the rest of the cardiogenic mesoderm to form the initial heart tube. The cells in this subdivision of the cardiogenic fields are set aside during formation of the initial myocardial heart tube and are added later to lengthen the tube.

Myocardial Progenitors

Confusion regarding the location of the myocardial progenitors has existed because (1) they represent a moving target, (2) the distinction between cell potential and CELL LINEAGE has not been clear, and (3) the best tracing studies have been done in explanted chick embryos that do not survive to the time at which all the myocardium has been incorporated into the heart tube. The myocardial cells are generated from epiblast cells that ingress through the primitive streak during gastrulation to become part of the mesodermal germ layer (Fig. 3.1). Thus, the cells are in different locations at different times in development. This is further confused by the fact that epiblast cells with myocardial potential do not have to undergo gastrulation to become myocardial if they are placed in appropriate conditions.

The earliest studies of cells with myocardial POTENTIAL were done by EXPLANTING various tissues that sometimes included all three germ layers. These explantation assays yield information about whether a cell can become myocardial, that is, its potency or potential, but not about what it will become in its correct spatiotemporal location in the embryo, that is, its CELL FATE. Generally, many more cells have the potential to be myocardial than will actually differentiate as myocardium in the embryo. Thus, studies of cell potential have to be interpreted in light of cell marking experiments.

Most in vivo tracing studies have been done in cultured chick embryos that live only about 24–48 h after being explanted. Because a cardiac tube has formed by this time, it was incorrectly assumed that all of the myocardial cells had been incorporated. Recent studies show that myocardium is added to both ends of the heart tube for some time after the tube forms.

Historical Perspective

As introduced in the preceding text, two types of experiments have been done to establish the location of the cardiogenic fields. The earliest studies were done via explantation, which provided information about potency of a tissue rather than cell lineage or fate. Potency gives information about what a

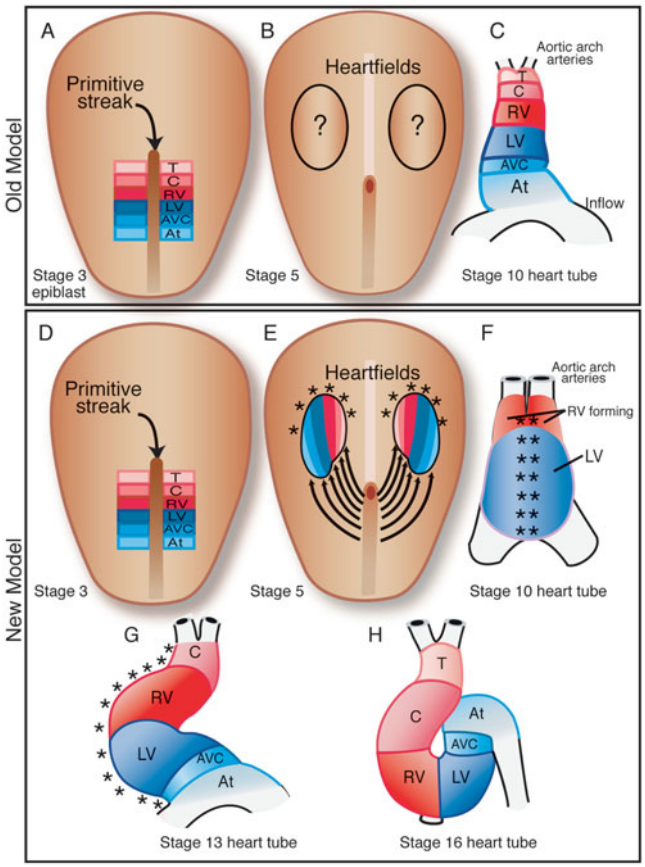

Figure 3.1. Location of the myocardial progenitors in the chick primitive streak, cardiogenic fields and heart tube. (*A–C*) Position in the primitive streak and heart tube but it was not understood until recently how the organization in the cardiogenic fields related to that in the primitive streak and heart tube. As shown in *D–H*, the cells are organized rostrocaudally in the primitive streak and heart tube but in the cardiogenic fields, the cells are organized mediolaterally. The arrows in *E* indicate how migration from the primitive streak causes the rearrangement. Asterisks at the cranial end of the cardiogenic field illustrate that the cranialmost part of the field becomes the ventral midline which, after looping, becomes the right border.

cell has the potential to become, but this does not necessarily correspond to cell fate, which can be obtained only from FATE MAPPING by labeling and following individual cells in situ. In some of the earliest experiments, mesodermal cells were explanted into culture or into chick eggs as CHORIOALLANTOIC GRAFTS (Rawles, 1943). Cultures or grafts that beat were considered to constitute the heart field. Explanted fragments of the BLASTODERM (presumably epiblast and hypoblast) helped localize cells with cardiogenic potential more precisely. The cells with myocardial potential were found to be restricted to the caudal half of the blastoderm near the cephalic end of the primitive streak (Hunt, 1932; Rawles, 1936; Rudnick, 1938; Spratt, 1942). The most precise myocardial potential map located two large bilateral areas of mesoderm extending from 0.2 mm on either side of the NODE to the edge of the embryo. Rostrally the areas extend to the tip of the HEAD PROCESS and posteriorly 0.4 mm caudal to the node (Rawles, 1943). Myocardial potency diminishes toward the periphery of these regions, and there are no asymmetric differences in the shape and extent of the two areas. One of the problems with the early potency mapping has to do with the method of tissue explantation. Many of these studies used all the layers of the blastodisc and thus myocardial potential of cells in the epiblast was not distinguished from myocardial potential of cells located in the mesoderm.

The early fate mapping studies, by contrast, were able to mark EPIBLAST or MESODERM. However, many of these early maps were generated before precise embryo staging was established and before a procedure for whole embryo culture was available (Hamburger and Hamilton, 1951; New, 1955). Thus, the earlier studies are less precise and repeatable than studies done since the late 1950s. Also, because whole embryos in culture do not develop well after 36–48 h and myocardial cells contributed to the heart during the looping period are added very late, their existence was unappreciated until very recently. Fate mapping has been done using several methods: labeling with vital dyes, iron particles, autoradiography, quail-chick chimeras, and most recently fluorescent dye labeling. Vital dye labeling first showed that tissues with cardiogenic potential were present in the early blastoderm, an imprecisely defined cell origin (Graper, 1907; Pasteels, 1936).

Epiblast Origin of Cardiogenic Cells

The fate maps of all the vertebrates appear to follow a generally similar plan. The most precise fate map of the avian epiblast was established using fluorescent dye injection in very small, well-defined regions of intermediate primitive streak-stage embryos (Fig. 3.2) (Hatada and Stern, 1994; Lopez-Sanchez et al., 2001). The presumptive cardiac cells are located in the epiblast just lateral to the primitive streak and caudal to the node (red in Fig. 3.2). The cells in this region contribute to the initial heart tube in rostrocaudal order, that is, the cells located more rostrally in the epiblast contribute to the more rostral portions of the tubular heart, and the more caudally located cells in the epiblast contribute to the more caudal portions of the heart tube at stages 10–11. As the primitive streak forms, cells with heart-forming potential are localized mainly in the caudal half of the epiblast near the primitive streak (Hunt, 1932; Rawles, 1936; Spratt, 1942).

The epiblast origin and position of the heart-forming cells in the mouse are similar to the chick. In the mouse, the earliest heart precursors can be traced to approximately 50 founder cells located on both sides of the midline in the epiblast of early gastrula stage embryos (E6.5)(Tam et al., 1997). The fate map of the mouse epiblast at the early primitive streak stage is topologically similar to that of other vertebrates (Lawson and Pedersen, 1992). The cardiogenic potency of cells in the epiblast of the early primitive streak-stage mouse embryo was

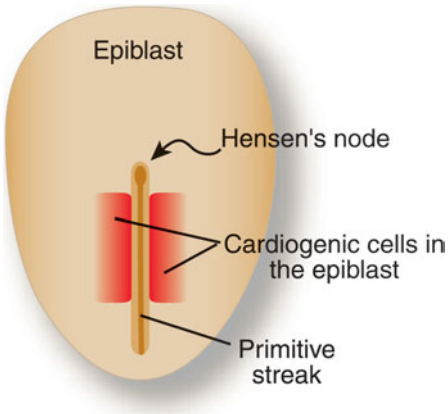

Figure 3.2. Location of cardiogenic cells in the epiblast prior to gastrulation. (Adapted from Lopez-Sanchez et al., 2001.)

tested by transplanting them to a region of the epiblast known to be non-cardiogenic. It was found that cells in the rostral and caudal epiblast of early primitive streak-stage mouse embryos have similar cardiogenic potency. The epiblast-derived cells differentiate to myocardial cells after being transplanted directly to the cardiogenic field of the late primitive streak embryo without ingressing through the primitive streak or moving within the mesoderm, suggesting that ingression is not critical for specification of myocardial fate (Tam and Behringer, 1997; Tam et al., 1997).

Heart Progenitors in the Primitive Streak

The earliest lineage tracing studies were done using a radioactive analogue of thymidine, tritiated thymidine. In this tracing technique, embryos are incubated with tritiated thymidine, which incorporates into all of the nuclei during the synthesis phase of cell division. Labeled cells are then removed and transplanted to the same location they were removed from in an unlabeled host embryo, which is then allowed to develop to the desired stage. On the basis of this marking technique, the prospective heart mesoderm was thought to originate generally from the middle of the primitive streak in a rostrocaudal order that mirrors the rostrocaudal order in the primary heart tube (Fig. 3.1)(Rosenquist, 1970). Using quail-chick chimeras and fluorescent dye marking of the primitive streak, it was later found that the cardiogenic precursors are located more rostrally in the primitive streak (Antin et al., 1994; Garcia-Martinez and Schoenwolf, 1993; Rosenquist, 1970; Rosenquist and DeHaan, 1966; Tam et al., 1997). The exception is the extreme rostral end of the streak, which contributes cells mainly to prospective head mesenchyme and foregut endoderm at early streak stages (Schoenwolf et al., 1992). The cardiogenic cells form both endocardium and myocardium, and in addition, two non-cardiac populations: the dorsal mesocardium and PARIETAL PERICARDIUM. The dorsal mesocardium attaches the heart tube to the ventral pharynx but disappears when the tube begins to loop. The parietal pericardium forms the sac that encloses the heart. The node contributes endocardial but no myocardial cells to the conus, and no other prospective myocardial cells can be found in the streak at these late gastrulation stages. The cells in the primitive streak are located in the same rostrocaudal sequence as that found in the heart, which is referred to as COALIGNMENT (Garcia-Martinez and Schoenwolf, 1993). This means that the most rostral cells in the streak form the most rostral region of the heart tube, and the cells most caudal in the streak form the most caudal region of the heart tube (Fig. 3.1).

Marking of primitive streak cells by REPLICATION-INCOMPETENT RETROVIRUS shows that both endocardial and myocardial cells are in the rostral primitive streak at stage 3 and already represent two separate cell lineages (see Chapter 9 for further details) (Wei and Mikawa, 2000).

Ingression of cardiogenic mesoderm in the mouse is very similar to that in the chick. During a narrow window of development, the presumptive cardiogenic cells ingress through the primitive streak with other cells destined for rostral structures such as head mesoderm (Kinder et al., 1999). As in the chick, the first cells that leave the primitive streak are destined to become extraembryonic tissues of the yolk sac and AMNION. A mesodermal marker, MESP1, has been used to trace the first mesodermal cells that ingress through the primitive streak. The first Mesp1-expressing cells that ingress through the primitive streak are incorporated as the mesodermal component of the amnion, and the next mesodermal population contributes mainly to the myocardium of the heart tube but not to the endocardium (Saga et al., 1999). Cardiogenic mesoderm ingresses at the rostral and middle segments of the primitive streak (Kinder et al., 1999). Almost no information is available about the control of these early steps, and our knowledge about induction of cardiogenesis really begins with the formation of the heart fields. Migration of the cells from the primitive streak to form the cardiogenic fields depends on expression of Mesp1 (Saga et al., 1999). The function of Mesp1 is still not known but in *Mesp1*-null mice the cardiogenic progenitors fail to migrate to form the cardiogenic fields (Kitajima et al., 2000).

It is not known if coalignment of cells in the primitive streak and heart tube is present in the mouse and if the endocardial and myocardial progenitors in the primitive streak represent completely separate lineages as they do in the chick.

Cardiogenic Mesoderm

After their ingression through the primitive streak, the cardiogenic mesodermal cells rapidly move laterally and cranially until they assume residence in the lateral plate mesoderm (Yang et al., 2002). The heart founders located here, bilaterally in the anterior lateral plate mesoderm, have been designated

the cardiogenic fields. However, the exact boundaries of the cardiogenic fields in the mesoderm have been elusive (Fig. 3.3). The position of this mesoderm has been the subject of many investigations using physical marking techniques and molecular markers of myocardial transcriptional regulators, especially NKX2.5. There are many discrepancies in the exact location of the cardiogenic mesoderm, perhaps because of differences in different species used and in part because the cardiogenic mesoderm moves continuously after the cells leave the primitive streak, presenting a moving target. Recent tracing studies suggest that the heart fields at early somite stages extend craniocaudally from the level of the BUCCOPHARYNGEAL MEMBRANE to about somites 2–3, and mediolaterally from the PARAXIAL MESODERM almost to the edge of the embryonic disc (Abu-Issa and Kirby, unpublished). In addition, because different parts of the heart have recently been found to arise from distinct regions of the cardiogenic mesoderm, several subdivisions can be recognized molecularly. In the mouse two subdivisions of the field are recognized at E7 by differential ISLET (ISL)1 and MYOSIN LIGHT CHAIN (MLC)2a expression (Fig. 3.4)(Cai et al., 2003). The medial part of the field expresses Isl1 and gives rise to the right ventricle and conotruncal myocardium and the Mlc2a-expressing region gives rise to the atria, atrioventricular canal, and left ventricle.

While most of the early studies in chick showed bilateral cardiogenic fields, some studies described a single cardiogenic field as a "horseshoe-shaped zone" or "cardiac crescent" continuous across the midline, cranial to the prechordal plate (DeHaan, 1963, 1963; Rosenquist, 1970). However, when tritiated thymidine-labeled mesoderm/endoderm from the crescent

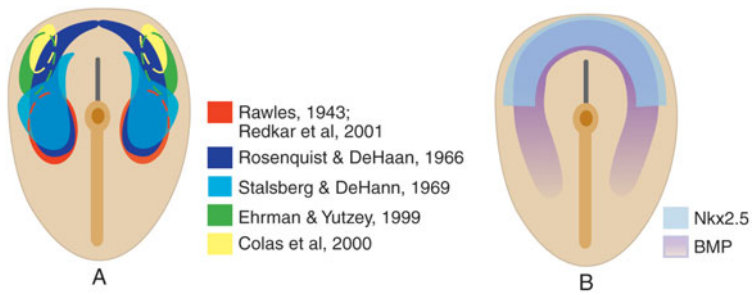

Figure 3.3. Location of *Nkx2.5* and *Bmp4* expression in relation to the various maps of the cardiogenic fields in the mesoderm in chick at approximately stage 5.

Figure 3.4. Expression of Isl1 (*green*) and MLC2a (*red*) messages showing subdivision of the cardiogenic field in the mouse. (*A*) ED7; (*B*) ED7.5; (*C*) ED8.0 (2 somite pairs); (*D*) ED8.25 (5 somite pairs); (*E*) ED8.5 (8 somite pairs). (From Cai et al., 2003, with permission.)

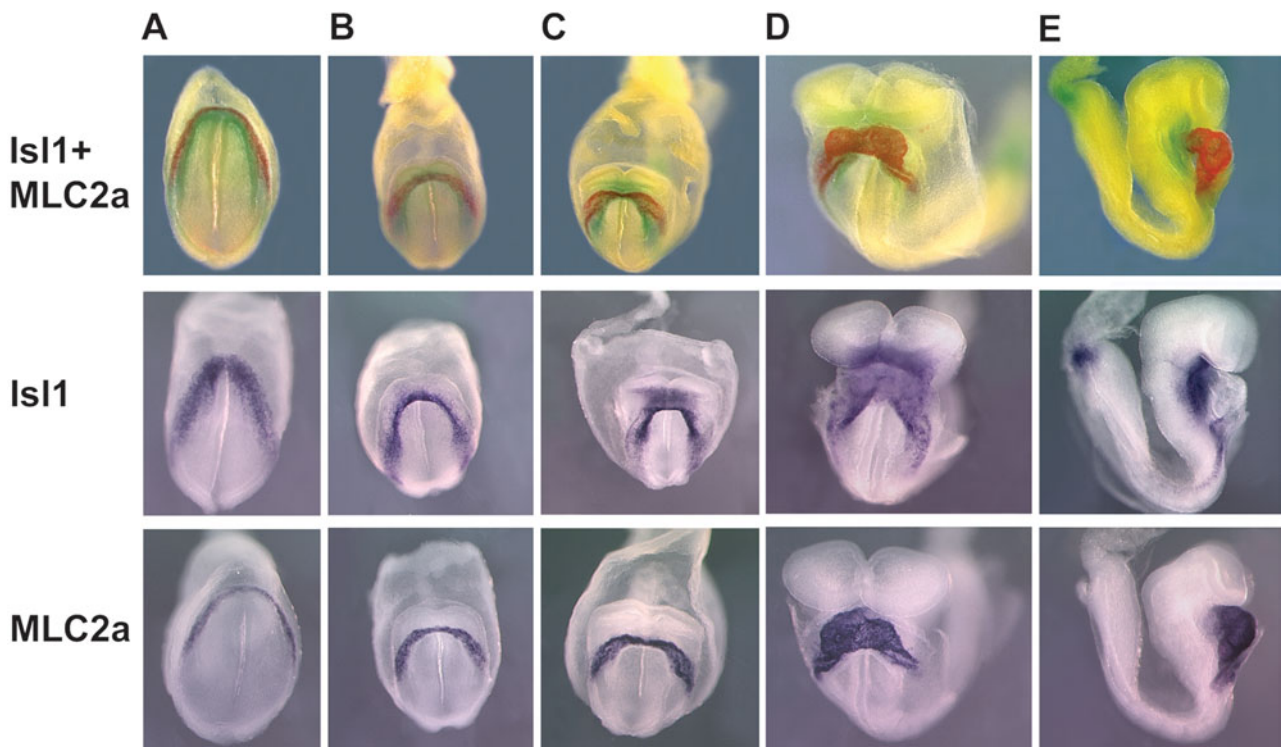

was transplanted, no cells from the paramedian positions cranial to the prechordal plate contributed to the heart tube, essentially refuting the idea of a continuous crescent prior to formation of the foregut pocket (Stalsberg and DeHaan, 1969). Thus, in the chick at stage 5, the heart-forming regions are clearly organized in two separate regions with a gap of about 0.8 mm between them. At the same time, it was found that the heart fields are substantially narrower than the fields of heart-forming potency described earlier (Fig. 3). (Rawles, 1943; Rosenquist and DeHaan, 1966). Recently, using molecular markers, it has been shown in avians and amphibians that two separate bilateral cardiogenic fields form that are not joined across the midline, confirming previous marking studies of Stalsberg and DeHaan (Colas et al., 2000; Stalsberg and DeHaan, 1969). Even though two independent cardiogenic fields exist in the chick, in the mouse it is difficult to see independent bilateral cardiogenic fields, suggesting that there is a continuous migration of cells from the primitive streak to the lateral plate and to the midline. Thus, the mouse most likely has bilateral cardiogenic fields, but these fields merge cranially so rapidly that it is difficult to see the independent cardiogenic fields. This has resulted in the mouse cardiogenic field being described universally as a single, crescent-shaped region.

Many other studies have attempted to locate the cardiogenic fields using molecular markers such as *Nkx2.5* and *GATA4*, transcription factors involved in myocardiogenesis. Because these factors are expressed in the endoderm in addition to mesoderm, the interpretation of their expression led to incorrect conclusions about the existence of a cardiac crescent in the chick (Fig. 3.3) (Schultheiss et al., 1995). A recent study combined physical cell marking with molecular expression studies (Redkar et al., 2001). This study brought to light a new puzzle in that cells identified as myocardial lineage by mapping using physical markers do not fit into the pattern of myocardial gene expression, in this case *Nkx2.5*, a transcription factor required for myocardial gene expression. These investigators used injections of two different fluorescent dyes on a coordinate grid system in which the dimensions of the grid were adjusted proportionately to fit the size of each embryo. At stage 4, the rostral boundary of the cardiogenic mesenchyme is just cranial to Henson's node, with the caudal boundary caudal to Henson's node (Fig. 3.2). At stage 5, the cardiogenic field is located at about the same rostrocaudal position and more medially with respect to the embryonic axis. The medial border of the cardiogenic field at stage 5 is about 0.3 mm lateral to the primitive streak, with the anterior border located cranial to the node and the caudal border extending one-fourth of the distance down the primitive streak (Redkar et al., 2001). A notable feature between stages 5 and 6 is the elongation of the cardiogenic field in the craniocaudal axis. It is at stage 6 that the cardiogenic field aligns almost perfectly with Bmp2 expression. However, the caudal portion of the cardiogenic fields is still not Nkx2.5 positive. The Nkx2.5-positive area is continuous across the midline in a horseshoe shape following the developing anterior intestinal portal. In the chick there is no mesoderm located across the midline and this *Nkx2.5* expression is in the endoderm. Therefore *Nkx2.5* marks some but not all of the cardiogenic mesoderm as well as noncardiogenic endoderm at these stages of development (Eisenberg, 2002; Patten, 1951). This is important because Nkx2.5 is a major transcription factor thought to be needed for expression of many myocardial genes even though it is not a master gene in the sense that *MyoD* is a master regulator for skeletal muscle (Evans et al., 1995; Harvey, 1999).

Once the cardiogenic field is formed, it seems to become quickly subdivided, as can be seen by differential expression of genes in the field. The subdivisions represent regions of what will become the inflow and outflow portions of the tube. The organization of the cardiogenic fields is also coaligned with organization of the heart tube but the orientation is now such that the rostrocaudal orientation of the heart tube is represented mediolaterally in the cardiogenic fields. The first parts of the heart tube to fuse ventrally originate from the most cranial parts of the cardiogenic fields (Fig. 3.1).

Chamber specification may actually begin in the subdivisions of the cardiogenic fields. In mouse, *Isl1* and *Fgf8* expression identify the medial cells in the cardiogenic field which will become the right ventricle and conotruncus while *Nkx2.5* and *MLC2a* identify the lateral cells in the field which will give rise to the atrium, atrioventricular canal, and left ventricle (Fig. 3.3).

In fish and amphibian embryos, the cardiogenic mesoderm regenerates after ablation; however, in avians, removal of all or any subset of the cells identified as cardiogenic results in the loss of corresponding cardiac structures. In contrast to the expression-marking studies, ablation studies indicate that removal of any of the *Nkx2.5*-expressing cells in the anterior lateral mesoderm results in the loss of corresponding heart structures (Ehrman and Yutzey, 1999).

Initial Tube Formation: Atrium, Atrioventricular Canal, Left Ventricle, Proximal Right Ventricle

The cardiogenic fields initially give rise to the straight heart tube which is seen first at stage 10 in the chick embryo. The idea that it is a tube is a misconception, however, because the dorsal myocardial seam adjacent to the foregut has not closed at this time (Fig. 3.5). The myocardium in the process of forming the tubular heart represents the primordium of the trabeculated portions of the right and left ventricles (de la Cruz et al., 1991). The conus is added cranially and the atrioventricular canal and atria caudally from the cardiogenic mesoderm (Buckingham, 2005; de la Cruz et al., 1991; Meilhac et al., 2003). The atrioventricular canal and atria are added from a region that has been called second heart field but that is in reality just a subdivision of the cardiogenic mesoderm (Fig. 3.1).

Anterior Heart Field: Right Ventricle and Conus

The term ANTERIOR HEART FIELD was defined differently by two different labs (Fig. 3.6) (Kelly et al., 2001; Mjaatvedt et al., 2001). In the mouse the anterior heart field, which is located

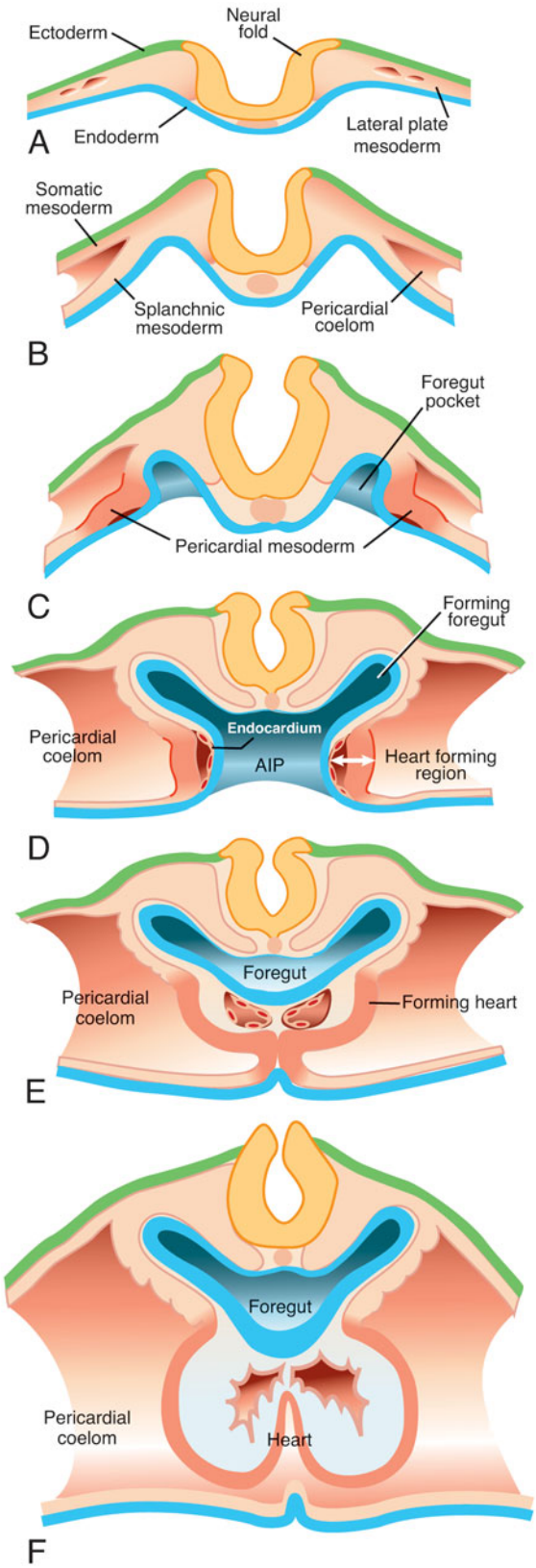

Figure 3.5. Diagrammatic representation of the formation of the heart, foregut pocket, and coelom in the chick.

in the medial part of the cardiogenic field, gives rise to the distal portion of the right ventricle and conus (Figs. 3.4 and 3.6) (Cai et al., 2003; Kelly et al., 2001). In the chick, the anterior heart field was defined as the mesoderm surrounding the outflow tract and adding the conotruncal myocardium to the outflow myocardium (Mjaatvedt et al., 2001). The term "anterior heart field" was suggested by de la Cruz, whose group carried out marking experiments in ovo showing that the heart tube lengthens during looping by accretion of cells from the inflow and outflow ends (Arguello et al., 1975; de la Cruz et al., 1977, 1987, 1989, 1991). A study of the outflow limb of the looped heart tube showed that the majority of the conus and truncus (cranial part of the outflow limb) are added during looping, which occurs between stages 13 and 22 in chick embryos (de la Cruz et al., 1977).

The fact that myocardial cells are added to the outflow of the heart tube was confirmed in mouse by a genetic marking study using a lacZ insertion upstream of the Fgf10 locus (Kelly et al., 2001). LacZ activity was found in the entire ascending limb of the looped heart, that is, right ventricle, conus, and truncus (Fig. 3.6). The lacZ-positive outflow myocardium was continuous with the splanchnic mesoderm and the mesodermal core of the pharyngeal arches. It should be noted that pharyngeal arches 1 and 2 have substantial mesodermal cores while the mesodermal contribution to arches 3, 4 and 6 is much less. Using DiI labeling, these investigators showed that the pharyngeal mesoderm progressively moved into the lengthening heart tube. This movement of the pharyngeal mesoderm and the difference seen in the location of Fgf10 mRNA versus β-galactosidase activity suggest that the areas of lacZ expression translocate into and become components of the heart. Although the data are based only on the lacZ expression pattern and without external marking, it has been proposed that this field represents a separate population of cells located medial to, but separate from, the classically defined cardiogenic heart fields and called the anterior heart field (Kelly et al., 2001). The fact that these cells are different from the more lateral cells in the cardiogenic fields was further suggested by Isl1 expression. Isl1 is expressed by the Fgf10-positive cardiogenic mesenchyme that represents the medial cells in the cardiogenic fields designated anterior heart field. Expression and lineage tracing data show that Isl1 is expressed in a more medial/posterior field relative to cells expressing MLC2a at E7.0. The MLC2a-positive cells contribute mainly to the atrium, atrioventricular canal and left ventricle while the Isl1-positive cells move cranially and are added mainly to the outflow limb (right ventricle and conotruncus) of the looped heart, although a few also end up in the atria (Cai et al., 2003). This pattern mimics that seen in the Fgf10–lacZ insertion and supports the idea that a unique group of cells that will form the outflow limb has already been specified in the cardiogenic field. Mutation of Isl1 results, as predicted, in embryonic hearts lacking the right ventricle and conus (Cai et al., 2003).

In the chick, the cranial part of the right ventricle and proximal outflow (conus) are part of the initial tubular heart, although they appear to be divided from the ventral pharynx

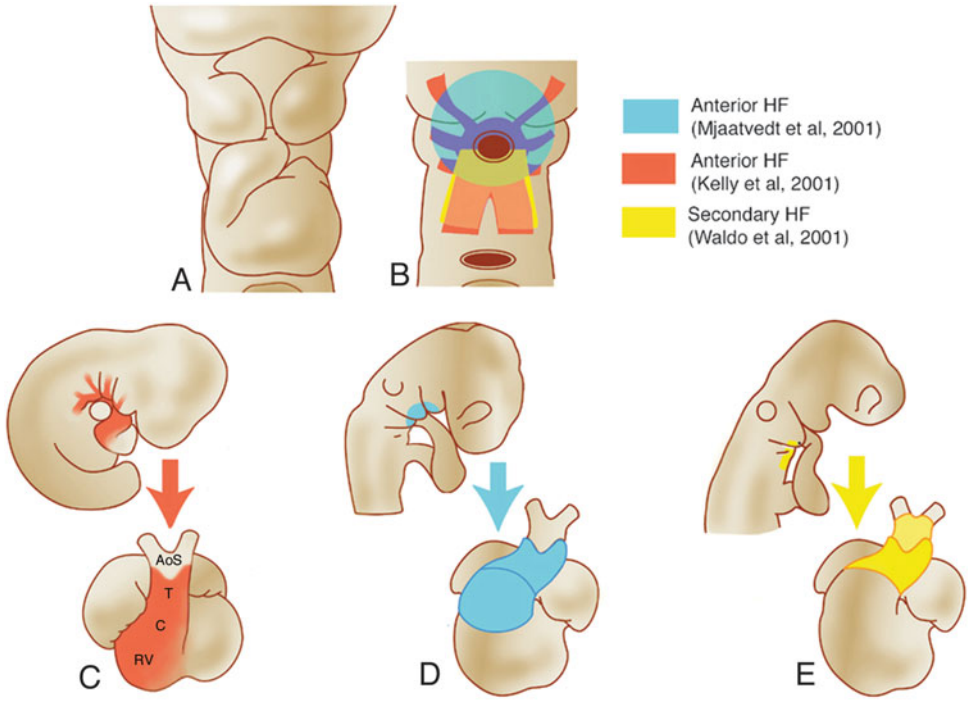

Figure 3.6. Anterior versus secondary heart fields. (From Abu-Issa et al., 2004, with permission.)

somewhat later than the left ventricle and caudal right ventricle (Manner, 2000). The differences in chick and mouse with regard to addition of pharyngeal mesoderm through the outflow may have to do with the more rapid closure of the foregut and shortened craniocaudal space in the ventral pharynx where the heart forms in mouse (Fig. 3.7). However, new studies suggest that the right ventricle and conus in chick and mouse are both derived from the medial portion of the cardiogenic field and that the cells are added to the heart tube in a similar manner (Abu-Issa and Kirby, unpublished).

In the chick the "anterior heart field" was defined by explantation of the mesenchyme around the attachment of the heart tube to the pharynx (Mjaatvedt et al., 2001). The explanted pieces of mesenchyme developed as beating cardiomyocytes. An additional feature of this study was that the cardiogenic mesoderm was removed before heart tube formation, which prevented the heart tube from forming except for a small CONOTRUNCAL segment. Although this was interpreted as evidence that the anterior heart field is not part of the cardiogenic mesoderm, it does not rule out the alternative interpretation that the very medial part of the cardiogenic field was not ablated. Recent tracing studies in the chick show that the cardiogenic mesoderm that contributes to the conus and truncus is located very medially and it is possible that the ablations missed this part of the cardiogenic field (Abu-Issa and Kirby, unpublished).

Secondary Heart Field: Arterial Pole

Physical marking techniques and expression in chick showed that the definitive outflow tract (truncus) is derived from a rapidly elongating band of cephalic undifferentiated mesoderm, located in pharyngeal mesenchyme immediately adjacent and primarily caudal to the distal end of the heart tube (Fig. 3.6) (Mjaatvedt et al., 2001; Waldo et al., 2001). Gene expression revealed that these PROGENITOR cells of the outflow myocardium recapitulate the EXPRESSION PROFILE of *Nkx2.5* and *Gata4* seen in the cardiogenic field (Waldo et al., 2001; Ward et al., 2005).

More recent studies suggest that the secondary heart field contributes myocardium and smooth muscle only to the arterial pole which is defined as the region of transition from myocardium at the semilunar valves to the base of great arterial vessels, that is, the distal myocardium of the outflow tract (truncus) and smooth muscle in the TUNICA MEDIA at the base of the arterial trunks (Waldo et al., 2005). The arterial pole will be discussed in more detail in Chapter 6.

How Many Heart Fields Exist?

The current evidence points to complex patterning in the bilateral cardiogenic mesoderm rather than the existence of multiple fields. If this is true and there is only a single cardiogenic field, albeit bilateral, with various subdivisions. The task at hand is to find a common language to characterize these regions (Abu-Issa et al., 2004).

The differences between secondary and anterior heart fields may reflect simply differences of the stages analyzed and the tissues and techniques for cell marking. If all the cells in the various heart fields described originate in the bilateral cardiogenic fields, these differences reflect an unsuspected and complex patterning of the cardiogenic mesoderm such that

cells in different locations go through all of the early steps in commitment but are then inhibited from differentiating as myocardium when the tubular heart is first formed. The inhibited cardiogenic cells are then added to the poles of the heart tube during later development. A great deal of molecular data has accrued in the last few years suggesting that regional differences in myocardial cells are established early (Christoffels et al., 2000; Franco et al., 2000). The current data argue that the regional differences are established even earlier than originally suspected. However, the data from the *Isl1*-null mouse also argue that the story may be more complex than a simple model of the cardiogenic field being divided into prospective regions; instead, the heart is constructed from several populations in the bilateral cardiogenic fields that converge in a coordinated fashion from different locations and at different times with different programs. This idea is supported by a novel lineage tracing study based on the use of a novel *laacZ* reporter gene, targeted to the α-cardiac actin locus. This clonal analysis demonstrates the existence of two cell populations with differing birth dates that segregate early from a common precursor. The left ventricle is derived exclusively from cells with the earliest birth dates, and the outflow tract is derived exclusively from cells with later birth dates, while all other regions of the heart are colonized by a mixture of cells from both populations (Meilhac et al., 2003).

Figure 3.7. Earliest formation of the heart tube in the chick (*A* and *B*) and mouse (*C* and *D*) illustrates basic differences in the way the heart tube forms. In the chick a long distance between the forebrain and the anterior intestinal portal (*asterisk*) allows the tube to form along the ventral pharynx. In the mouse the shortened distance between the forebrain and anterior intestinal portal forces the tube to loop and acquire cells from the poles rather than along the sides as happens in the chick. (*A* and *B* from Manner, 2000, with permission; *C* and *D* courtesy of K. K. Sulik, Embryo Images at www.med.unc.edu/embryo_images/.)

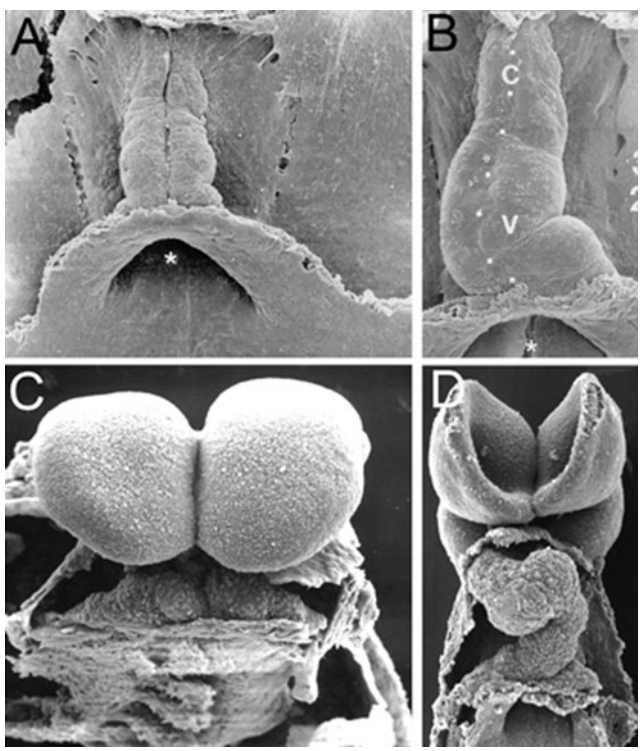

Formation of the Heart Tube

Between stages 7 and 8, the lateral plate mesoderm divides into dorsal (SOMATIC) and ventral (splanchnic) layers. The pericardial coelom is created by the splitting of the two layers (Fig. 3.8). The cardiac cells become a separate compartment from a seemingly HOMOGENEOUS population of lateral plate mesoderm cells in the bilateral cardiogenic fields (Fig. 3.9). Mesoderm splitting was first noted in the rabbit by Van der Stricht in 1895 (Sabin, 1920). The separation of the splanchnic and somatic mesoderm and formation of the epithelial cardiogenic cell population in the chick initiates cranially and proceeds caudally (Fig. 3.9). As the precardiomyocytes differentiate to form the myocardial sleeve of the heart tube, they are ready to begin beating. N-CADHERIN is evenly distributed within the heart forming region in the mesoderm and endoderm at stages 5 to early 6 (Fig. 3.8). It is gradually restricted to the central regions of the mesoderm at FOCI of small cavities that appear at stage 7. The cavities coalesce to form the pericardial coelom (Linask, 1992). The precardiomyocytes in the splanchnic mesoderm undergo mesenchymal-to-epithelial transformation, during which N-cadherin is localized to the apical surface of the presumptive myocardial epithelium.

Figure 3.8. Scanning electron micrographs of chick embryos cut transversely. (*A*) Initial split of the lateral plate mesoderm to form the pericardial coelom (PC) between somatic (outer) and splanchnic (inner) layers. The red hatching indicates the cardiogenic field. (*B*) A more caudal section where the lateral plate mesoderm has not yet split. (From Schoenwolf, 2001, with permission.)

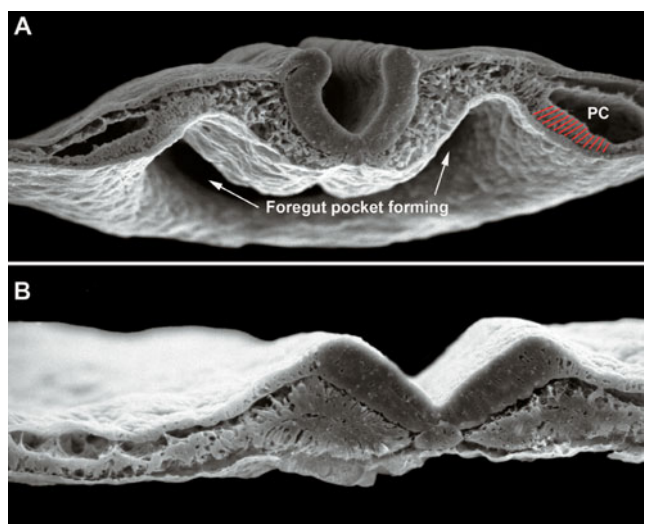

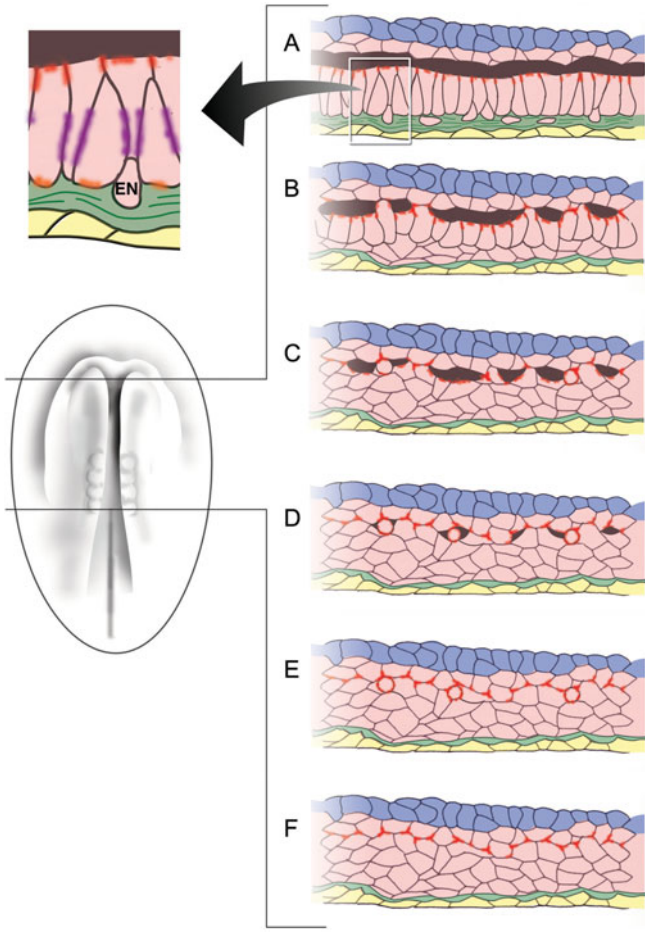

Figure 3.9. (*A–F*) Cranial to caudal progression of cardiac compartment formation. *Blue* represents ectoderm cells; *pink*, mesoderm; *yellow*, endoderm; *black*, coelom cavities; *green*, fibronectin matrix localization; *bright red*, apical localization of N-cadherin/β-catenin; *magenta* and EN, endocardial cells. (A) Endocardial cells (EN) are sort ventrally localizing in fibronectin-rich area. Magnification illustrates the polarized pattern of Na^+, K^+-ATPase (*purple*), N-cadherin (*red*), and integrin (*orange*). (*B*) Coalescence of the spaces that will become the coelomic cavity and concurrent mesenchymal-to-epithelial transformation of the precardiac mesoderm. (*C–E*) Restriction of N-cadherin/β-catenin expression to patches and formation of the coelomic cavity. N-cadherin is restricted to the dorsal boundary of the mesoderm. (From Linask, 2003, with permission.)

The N-cadherin is eventually incorporated into the cell junctions of the beating myocardium (Linask, 1992). Because the cadherins are calcium-dependent cell adhesion molecules that are associated with cell sorting, N-cadherin may function in separation of the splanchnic from the somatic mesoderm to form the pericardial coelom. If cadherin function is perturbed, heart development is arrested, and MYOFIBRILLOGENESIS is inhibited (Linask et al., 1997).

The thickened precardiac mesodermal plate separates from the splanchnic layer in close association with the endoderm. Endocardium appears between these two layers. While the myocardium derives from a cohesive mesothelial layer, the endocardium is formed from small groups of cells that separate from the splanchnic mesoderm between stages 5 and 8 and follow routes independent of the myocardial cells (Sabin, 1920). The endocardial cells migrate and become localized between the developing myocardium above and the endoderm below (Fig. 3.5). Sparsely localized endothelial cells become arranged in a columnar fashion. The endocardial cells are first noted by their exclusion from the myocardial compartment (Fig. 3.9). N-cadherin may also be important in specific cell sorting of the myocardial and endocardial cell lineages (Linask and Lash, 1993). CATENINS associate with the cytoplasmic domain of calcium-dependent cadherins, including N-cadherin. The catenins link the cadherins to the actin cytoskeleton and are necessary for cadherin-mediated cell adhesion. β-catenin is in the Wnt signaling pathway and is associated with N-cadherin during heart tube formation (Linask et al., 1997). N-cadherin is downregulated and vascular (VE) cadherin is upregulated in the excluded endocardial cells (Linask et al., 1997). The induction of endocardial cells may be the result of vascular endothelial growth factor (Vegf) signaling and presence of matrix molecules such as fibronectin (Linask, 2003). The endocardial cells continue to be sorted and coalesce ventrally adjacent to the endoderm to form the endothelial–endocardial population. This sorting suggests that the endocardial population has a common origin with cardiomyocytes, although lineage tracing suggests that the specification occurs during gastrulation (Eisenberg and Markwald, 1997; Mikawa et al., 1992).

Contributions of the left and right heart-forming regions are strictly to the left and right sides of the cardiac tube but both sides contribute to both ventricles. Heart differentiation does not depend on convergence of the heart primordia as two beating heart tubes form, one on the left and one on the right of the embryo. These "hearts" form left and right ventricles, an atrioventricular canal and an atrium and undergo looping (Li et al., 2004).

Fibronectin deposition at the midline is required for the movement of myocardial precursors. In the complete absence of fibronectin, ADHERENS JUNCTIONS between the myocardial precursors do not form properly, suggesting that cell-matrix interactions are required for epithelial organization and that epithelial integrity is important for migration of the myocardial progenitors (Trinh and Stainier, 2004). TENASCIN-C, an extracellular matrix protein, is also associated with cell motility (Erickson, 1993; Jones and Jones, 2000). It is expressed in the cardiogenic fields and disappears once the heart fields fuse (Akhurst et al., 1990; Crossin and Hoffman, 1991; Hurle et al., 1990; Imanaka-Yoshida et al., 2003; Sugi and Markwald, 1996, Zhang et al., 1993). However, tenascin-C-null mice do not show a distinct phenotype and the function of tenascin-C in heart tube formation remains elusive (Saga et al., 1992).

RHO GTPASES act as molecular switches controlling numerous signaling pathways by cycling between active and inactive conformational states (Etienne-Manneville and Hall, 2002). The Rho GTPases play a role in regulating the actin cytoskeleton,

influencing cell polarity, microtubule dynamics, membrane transport pathways, and transcriptional activity. A single GTPase can coordinately activate specific signaling pathways. RhoA was identified from a screen of stage 6–9 chick heart primordia. Its message and protein are highly expressed in the anterior lateral plate, heart primordium, and anterior intestinal portal (Kaarbo et al., 2003). Inhibition of RhoA using siRNA results in cardia bifida. Thus, while RhoA is implicated in heart tube fusion, the cellular details of its involvement are not yet understood.

A distinct orientation of cells in the cardiogenic field becomes evident in the stage 6 chick embryo. Directional movement of the precardiac cells begins at this stage and continues through stages 7 and 8. By stage 8 the cells arrive at the lateral sides of the anterior intestinal portal. The cells move by virtue of their association with the underlying endoderm. There is an increase in fibronectin in the heart-forming region and at the lateral sides of the anterior intestinal portal. The cells are oriented perpendicular to the ANTERIOR INTESTINAL PORTAL (Linask and Lash, 1986). The transition of nondifferentiated mesoderm to myocardium occurs over a short time, in the chick between Hamburger-Hamilton stages 4–8.

Heart tube and foregut formation are interrelated (Fig. 3.9). Endodermal folding creates the foregut pocket bounded caudally by the anterior intestinal portal. The FOREGUT POCKET is initially a broad but shallow arc across the midline that narrows as it lengthens craniocaudally. The cardiogenic fields move from their bilateral positions to the embryonic ventral midline as the anterior intestinal portal elongates the foregut. Stalsberg and DeHaan suggest that the foregut elongates as a result of tension applied at the anterior intestinal portal (Stalsberg and DeHaan, 1968). They suggest that the tension arises from the regression of the primitive streak and elongation of the notochord. The same force may be transmitted to the subjacent splanchnic mesoderm, acting to drag that layer medially and caudally. In the classic model of heart formation (see later) prospective heart tissue moves medially, adding to the caudal or inflow end of the heart as the anterior intestinal portal moves caudally to elongate the foregut. The lateral wings of the cardiogenic crescent swing ventromedially to fuse in the midline. DeHaan showed, using movies, that the myocardial mesoderm is not carried passively into the midline by the folding endoderm but moves cephalically over that layer between stages 5 and 7 (DeHaan, 1963). CARDIA BIFIDA occurs in the *Gata4*-null mouse and this phenotype can be rescued by wild-type extraembryonic tissues. Thus, foregut and heart tube formation may both be dependent on visceral (extraembryonic) endoderm (Narita et al., 1997). Several mutations in mice are associated with cardia bifida. *Gata4*-null mice have already been mentioned. *HYPOXIA INDUCIBLE FACTOR (HIF)1α*-null mutation in mice causes cardia bifida in some embryos, suggesting that the process is sensitive to oxygen (Compernolle et al., 2003). In zebrafish, a gene mutation called *miles apart*, is associated with cardia bifida. The *miles apart* gene encodes sphingosine-1-phosphate receptor, which binds lysosphingolipids. These receptors transmit signals into the cells on which they are found via guanine nucleotide–binding proteins. In the case of the *miles apart* mutant allele, downstream signaling is disrupted (Kupperman et al., 2000). Sphingosine-1-phosphate is the ligand that binds to the receptor to guide migration of the heart primordia (Kupperman et al., 2000). However, the *miles apart* gene product does not need to be expressed by the migrating heart precursor cells themselves, as cells with mutations in *miles apart* migrate normally when transplanted into normal embryos. *Miles apart* messenger RNA is found in paraxial cells, located on either side of the midline, and these cells may direct cardiac precursor cells to the midline. Analogous cells have not been described in other animals. Inhibition of Ras-GTPase in chick also causes cardia bifida (Wei et al., 2001).

There has been disagreement over when, and if, the cardiogenic field becomes organized craniocaudally in a colinear arrangement with the heart tube. Recently, a new model of heart tube development that differs fundamentally from the classic model was introduced (Abu-Issa et al., 2004; Cai et al., 2003; DeHaan, 1965; Harvey, 2002; Kelly et al., 2001). The old model proposed that the early cardiogenic field is arranged with colinear polarity with the heart tube and that the bilateral cardiogenic fields simply fuse in a zipper-like fashion to give rise to the heart tube (DeHaan, 1965). In contrast, the new model shows that the heart ascending limb/outflow precursors cells form from the anterior heart field originally located medial–posterior to the lateral–anterior descending limb/inflow precursor cells (Fig. 3.1). The outflow and inflow precursors invert their position to give rise to their prospective segments (Harvey, 2002). The inversion is accomplished by a 120° rotation of the heart field along with the coelomic cavity in the same direction and concomitant with the formation of the foregut pocket (Abu-Issa et al., 2004). The heart fields then fuse anteriorly at the midline. Cells are added to the forming heart tube after this fusion as a continuous stream. This model accounts for maintenance of the caudal–cranial polarity found in the primitive streak and heart tube, and the deduced 120° rotation of the cardiogenic plate found in early human heart development (Fig. 3.10) (Davis, 1927; Garcia-Martinez and Schoenwolf, 1993; Lopez-Sanchez et al., 2001).

After epithelialization of the cardiomyocytes, myofibrillogenesis and initiation of electrical activity begin (Kamino, 1991; Tokuyasu and Maher, 1987, 1987). SODIUM–CALCIUM EXCHANGER (NCX-1) is expressed in the heart fields in the chick at stage 7 and in mouse at E7.5. By E8, the protein shows rostrocaudal difference in expression with higher expression cranially. There is also higher expression in the myocardium of the outer curvature than in the inner curvature. Very low expression is seen in the inflow and outflow myocardium (Linask et al., 2001). The early expression of this exchanger is consistent with a role in early rhythmicity. Because calcium is involved in many processes in the cell, including cell adhesion and transcriptional control, regulation of intracellular calcium is of critical importance to cellular differentiation.

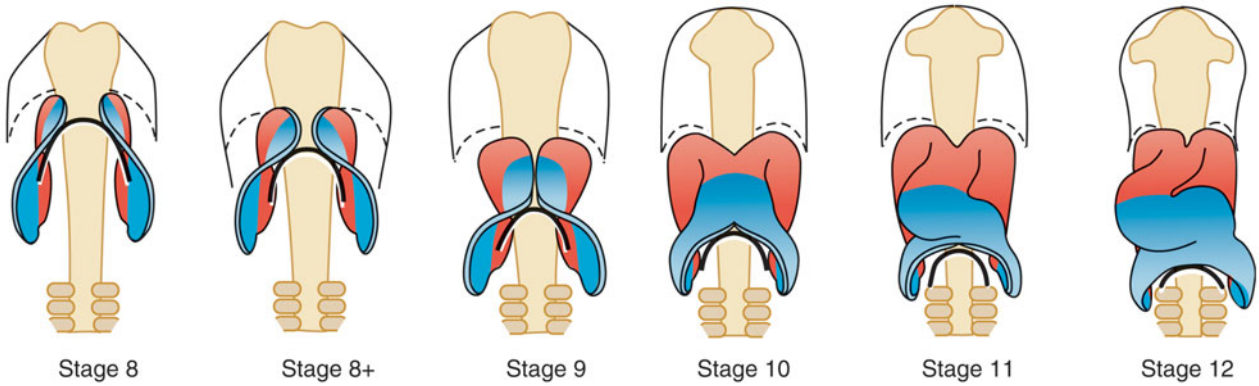

Figure 3.10. Formation of the ventral midline heart tube from the cardiogenic mesenchyme in chick at the stages indicated. *Red* indicates the outflow limb (right ventricle and conus) and *blue* indicates the inflow limb (atrium, atrioventricular canal, left ventricle) of the cardiac tube.

Cardia Bifida in a Neonate

One case of cardia bifida has been reported in a human baby who survived for 5 days after birth. The bilateral hearts had trabeculation patterns characteristic of right and left ventricles with the "chambers" separated by a partial ventricular septum (Aiello and Xavier-Neto, 2006).

REFERENCES

Abu-Issa, R., K. Waldo, and M. L. Kirby. 2004. Heart fields: one, two or more? Dev. Biol. 272:281–285.

Aiello, V. D., and J. Xavier-Neto. 2006. Full intrauterine development is compatible with cardia bifida in humans. Ped. Cardiol. 27:393–394.

Akhurst, R. J., S. A. Lehnert, A. Faissner, and E. Duffie. 1990. TGF beta in murine morphogenetic processes: the early embryo and cardiogenesis. Development 108:645–656.

Antin, P. B., R. G. Taylor, and T. Yatskievych. 1994. Precardiac mesoderm is specified during gastrulation in quail. Dev. Dyn. 200:144–154.

Arguello, C., M. V. De la Cruz, and C. S. Gomez. 1975. Experimental study of the formation of the heart tube in the chick embryo. J. Embryol. Exp. Morph. 33:1–11.

Cai, C. L., X. Liang, Y. Shi, P. H. Chu, S. L. Pfaff, J. Chen, and S. Evans. 2003. Isl1 identifies a cardiac progenitor population that proliferates prior to differentiation and contributes a majority of cells to the heart. Dev. Cell. 5:877–889.

Christoffels, V. M., P. E. Gabets, D. Franco, M. Campione, F. de Jong, W. H. Lamers, Z. Z. Bao, S. Palmer, C. Biben, R. P. Harvey, and A. F. Moorman. 2000. Chamber formation and morphogenesis in the developing mammalian heart. Dev. Biol. 223:266–278.

Colas, J. F., A. Lawson, and G. C. Schoenwolf. 2000. Evidence that translation of smooth muscle alpha-actin mRNA is delayed in the chick promyocardium until fusion of the bilateral heart-forming regions. Dev. Dyn. 218:316–330.

Compernolle, V., K. Brusselmans, D. Franco, A. Moorman, M. Dewerchin, D. Collen, and P. Carmeliet. 2003. Cardia bifida, defective heart development and abnormal neural crest migration in embryos lacking hypoxia-inducible factor-1alpha. Cardiovasc. Res. 60:569–579.

Crossin, K. L., and S. Hoffman. 1991. Expression of adhesion molecules during the formation and differentiation of the avian endocardial cushion tissue. Dev. Biol. 145:227–286.

Davis, C. L. 1927. Development of the human heart from its first appearance to the stage found in embryos of twenty paired somites. Contrib. Embryol. 19:245–284.

de la Cruz, M. V., C. S. Gomez, M. M. Arteaga, and C. Arguello. 1977. Experimental study of the development of the truncus and the conus in the chick embryo. J. Anat. 123:661–686.

de la Cruz, M. V., C. S. Gomez, and R. Cayre. 1991. The developmental components of the ventricles: their significance in congenital cardiac malformations. Cardiol. Young 1:123–128.

de la Cruz, M. V., C. S. Gomez, and M. A. Palomino. 1989. The primitive cardiac regions in the straight tube heart (stage 9-) and their anatomical expression in the mature heart: an experimental study in the chick embryo. J. Anat. 165:121–131.

de la Cruz, M. V., C. Sanchez-Gomez, and J. L. Robledo-Tovi. 1987. Experimental study of the development of the ventricular inlets in the chick embryo. Embryol. Hefte 1:25–37.

DeHaan, R. L. 1963. Migration patterns of the precardiac mesoderm in the early chick embryo. Exp. Cell Res. 29:544–560.

DeHaan, R. L. 1963. Organization of the cardiogenic plate in the early chick embryo. Acta Embryol. Morphol. Exp. 6:26–38.

DeHaan, R. L. 1965. Morphogenesis of the vertebrate heart. In: Organogenesis., ed. DeHaan, R. L. and H. Ursprung, 377–419. New York: Holt, Rinehart & Winston.

Ehrman, L. A., and K. E. Yutzey. 1999. Lack of regulation in the heart forming region of avian embryos. Dev. Biol. 207:163–175.

Eisenberg, L. 2002. Belief versus scientific observation: the curious story of the precardiac mesoderm. Anat. Rec. 266:194–197.

Erickson, H. P. 1993. Tenascin-C, tenascin-R and tenascin-X: a family of talented proteins in search of functions. Curr. Opin. Cell Biol. 5:869–876.

Etienne-Manneville, S., and A. Hall. 2002. Rho GTPases in cell biology. Nature 420:629–635.

Evans, S. M., W. Yan, M. P. Murillo, J. Ponce, and N. Papalopulu. 1995. *tinman*, a *Drosophila* homeobox gene required for heart and visceral mesoderm specification, may be represented by a family

of genes in vertebrates: *XNkx-2.3*, a second vertebrate homologue of *tinman*. Development 121:3889–3899.

Franco, D., M. Campione, R. Kelly, P. S. Zammit, M. Buckingham, W. H. Lamers, and A. F. M. Moorman. 2000. Multiple transcriptional domains, with distinct left and right components, in the atrial chambers of the developing heart. Circ. Res. 87:984–991.

Garcia-Martinez, V., and G. C. Schoenwolf. 1993. Primitive-streak origin of the cardiovascular system in avian embryos. Dev. Biol. 159:706–719.

Graper, L. 1907. Untersuchungen uber die Hertzbildung der Vogel. Arch. Entw-mech. Org. 24:375–410.

Hamburger, V., and H. L. Hamilton. 1951. A series of normal stages in the development of the chick embryo. J. Morphol. 88:49–92.

Harvey, R. 2002. Patterning the vertebrate heart. Nat. Rev. Genet. 3:544–556.

Harvey, R. P. 1999. Seeking a regulatory roadmap for heart morphogenesis. Semin. Cell Dev. Biol. 1:99–107.

Hatada, Y., and C. D. Stern. 1994. A fate map of the epiblast of the early chick embryo. Development 120:2879–2889.

Hunt, T. E. 1932. Potencies of transverse levels of the chick blastoderm in the definitive streak stage. Anat. Rec. 55:41–70.

Hurle, J. M., V. Garcia-Martinez, and M. A. Ros. 1990. Immunofluorescent localization of tenascin during the morphogenesis of the outflow tract of the chick embryo heart. Anat. Embryol. (Berl.) 181:149–155.

Imanaka-Yoshida, K., K. Matsumoto, M. Hara, T. Sakakura, and T. Yoshida. 2003. The dynamic expression of tenascin-C and tenascin-X during early heart development in the mouse. 71:291–298.

Jones, P. L., and F. S. Jones. 2000. Tenascin-C in development and disease: gene regulation and cell function. Matrix Biol. 19:581–596.

Kaarbo, M., D. I. Crane, and W. G. Murrell. 2003. RhoA is highly upregulated in the process of early heart development of the chick and important for normal embryogenesis. Dev. Dyn. 227:35–47.

Kamino, K. 1991. Optical approaches to ontogeny of electrical activity and related functional organization during early heart development. Physiol. Rev. 71:53–91.

Kelly, R. G., N. A. Brown, and M. E. Buckingham. 2001. The arterial pole of the mouse heart forms from Fgf10-expressing cells in pharyngeal mesoderm. Dev. Cell 1:435–440.

Kinder, S. J., T. E. Tsang, G. A. Quinlan, A. K. Hadjantonakis, A. Nagy, and P. P. Tam. 1999. The orderly allocation of mesodermal cells to the extraembryonic structures and the anteroposterior axis during gastrulation of the mouse embryo. Development 126:4691–4701.

Kitajima, S., A. Takagi, T. Inoue, and Y. Saga. 2000. MesP1 and MesP2 are essential for the development of cardiac mesoderm. Development 127:3215–3226.

Kupperman, E., S. An, N. Osborne, S. Waldron, and D. Y. Stainier. 2000. A sphingosine-1-phosphate receptor regulates cell migration during vertebrate heart development. Nature 406:192–195.

Lawson, K. A., and R. A. Pedersen. 1992. Clonal analysis of cell fate during gastrulation and early neurulation in the mouse. Ciba Found. Symp. 165:3–21.

Li, S., D. Zhou, M. M. Lu, and E. E. Morrisey. 2004. Advanced cardiac morphogenesis does not require heart tube fusion. Science 305:1619–1622.

Linask, K. K. 1992. N-Cadherin localization in early heart development and polar expression of Na^+, K^+-ATPase, and integrin during pericardial coelom formation and epithelialization of the differentiating myocardium. Dev. Biol. 151:213–224.

Linask, K. K. 2003. Regulation of heart morphology: current molecular and cellular perspectives on the coordinated emergence of cardiac form and function. Birth Defects Res. C Embryo Today 69:14–24.

Linask, K. K., M. D. Han, M. Artman, and C. A. Ludwig. 2001. Sodium-calcium exchanger (NCX-1) and calcium modulation: NCX protein expression patterns and regulation of early heart development. Dev. Dyn. 221:249–264.

Linask, K. K., K. A. Knudsen, and Y. H. Gui. 1997. N-cadherin-catenin interaction: necessary component of cardiac cell compartmentalization during early vertebrate heart development. Dev. Biol. 185:148–164.

Linask, K. K., and J. W. Lash. 1986. Precardiac cell migration: fibronectin localization at mesoderm-endoderm interface during directional movement. Dev. Biol. 114:87–101.

Linask, K. K., and J. W. Lash. 1993. Early heart development: dynamics of endocardial cell sorting suggests a common origin with cardiomyocytes. Dev. Dyn. 195:62–69.

Lopez-Sanchez, C., V. Garcia-Martinez, and G. C. Schoenwolf. 2001. Localization of cells of the prospective neural plate, heart and somites within the primitive streak and epiblast of avian embryos at intermediate primitive-streak stages. Cell Tissue Organs 169: 334–346.

Manner, J. 2000. Cardiac looping in the chick embryo: a morphological review with special reference to terminological and biomechanical aspects of the looping process. Anat. Rec. 259:248–262.

Meilhac, S. M., R. G. Kelly, D. Rocancourt, S. Eloy-Trinquet, J.-F. Nicolas, and M. E. Buckingham. 2003. A retrospective clonal analysis of the myocardium reveals two phases of clonal growth in the developing mouse heart. Development 130:3877–3889.

Mikawa, T., A. Borisov, A. M. C. Brown, and D. A. Fischman. 1992. Clonal analysis of cardiac morphogenesis in the chick embryo using a replication-defective retrovirus. I. Formation of the ventricular myocardium. Dev. Dyn. 193:11–23.

Mjaatvedt, C. H., T. Nakaoka, R. Moreno-Rodriguez, R. A. Norris, M. J. Kern, C. A. Eisenberg, D. Turner, and R. R. Markwald. 2001. The outflow tract of the heart is recruited from a novel heart-forming field. Dev. Biol. 238:97–109.

Narita, N., M. Bielinska, and D. B. Wilson. 1997. Wild-type endoderm abrogates the ventral developmental defects associated with GATA-4 deficiency in the mouse. Dev. Biol. 189:270–274.

New, D. A. T. 1955. A new technique for the cultivation of the chick embryo in vitro. J. Embryol. Exp. Morph. 3:320–331.

Pasteels, J. 1936. Critique et controle experimental des conceptions de P. Wintrebert sur la gastrulation du Discoglosse. Arch. Biol. 47: 631–677.

Patten, B. M. 1951. Early Embryology of the Chick. Philadelphia: Blakiston.

Rawles, M. 1943. The heart-forming areas of the early chick blastoderm. Physiol. Zool. 16:22.

Rawles, M. E. 1936. A study in the localization of organ-forming areas in the chick blastoderm of the head-process stage. J. Exp. Zool. 72:271–315.

Redkar, A., M. Montgomery, and J. Litvin. 2001. Fate map of early avian cardiac progenitor cells. Development 128:2269–2279.

Rosenquist, G. C. 1970. Location and movements of cardiogenic cells in the chick embryo: the heart-forming portion of the primitive streak. Dev. Biol. 22:461–475.

Rosenquist, G. C., and R. L. DeHaan. 1966. Migration of precardiac cells in the chick embryo: a radioautographic study. Carnegie Inst. Wash. Publ. 625, Contrib. Embryol. 38:111–121.

Rudnick, D. 1938. Differentiation in culture of pieces of early chick blastoderm. Ann. NY Acad. Sci. 49:761–772.

Sabin, F. R. 1920. Studies on the origin of the blood vessels and of red blood corpuscles as seen in the living blastoderm of chick during the second day of incubation. Contrib. Embryol. Carnegie Inst. Wash. 9:215–262.

Saga, Y., S. Miyagawa-Tomita, A. Takagi, S. Kitajima, J. Miyazaki, and T. Inoue. 1999. MesP1 is expressed in the heart precursor cells and required for the formation of a single heart tube. Development 126:3437–3447.

Saga, Y., T. Yagi, Y. Ikawa, T. Sakakura, and S. Aizawa. 1992. Mice develop normally without tenascin. Genes Dev. 6:1821–1831.

Schoenwolf, G. C. 2001. Laboratory Studies of Vertebrate and Invertebrate Embryos. Guide and Atlas of Descriptive and Experimental Development. Upper Saddle River, NJ: Prentice-Hall.

Schoenwolf, G. C., V. Garcia-Martinez, and M. S. Dias. 1992. Mesoderm movement and fate during avian gastrulation and neurulation. Dev. Dyn. 193:235–248.

Schultheiss, T. M., S. Xydas, and A. B. Lassar. 1995. Induction of avian cardiac myogenesis by anterior endoderm. Development 121: 4203–4214.

Spratt, N. T. 1942. Location of organ-specific regions and their relationship to the development of the primitive streak in the early chick blastoderm. J. Exp. Zool. 89:69–101.

Stalsberg, H., and R. L. DeHaan. 1968. Endodermal movements during foregut formation in the chick embryo. Dev. Biol. 18:198–215.

Stalsberg, H., and R. L. DeHaan. 1969. The precardiac areas and formation of the tubular heart in the chick embryo. Dev. Biol. 19:128.

Sugi, Y., and R. R. Markwald. 1996. Formation and early morphogenesis of endocardial endothelial precursor cells and the role of endoderm. Dev. Biol. 175:66–83.

Tam, P. P., and R. R. Behringer. 1997. Mouse gastrulation: the formation of a mammalian body plan. Mech. Dev. 68:3–25.

Tam, P. P. L., M. Parameswaran, S. J. Kinder, and R. P. Weinberger. 1997. The allocation of epiblast cells to the embryonic heart and other mesodermal lineages: the role of ingression and tissue movement during gastrulation. Development 124:1631–1642.

Tokuyasu, K. T., and P. A. Maher. 1987. Immunocytochemical studies of cardiac myofibrillogenesis in early chick embryos. I. Presence of immunofluorescent titin spots in premyofibril stages. J. Cell Biol. 105:2781–2793.

Tokuyasu, K. T., and P. A. Maher. 1987. Immunocytochemical studies of cardiac myofibrillogenesis in early chick embryos. II. Generation of á-actinin dots within titin spots at the time of the first myofibril formation. J. Cell Biol. 105:2795–2801.

Trinh, L. A., and D. Y. Stainier. 2004. Fibronectin regulates epithelial organization during myocardial migration in zebrafish. Dev. Cell. 6:371–382.

Waldo, K. L., M. R. Hutson, C. C. Ward, M. Zdanowicz, H. A. Stadt, D. Kumiski, R. Abu-Issa, and M. L. Kirby. 2005. Secondary heart field contributes myocardium and smooth muscle to the arterial pole of the developing heart. Dev. Biol. 281:78–90.

Waldo, K. L., D. H. Kumiski, K. T. Wallis, H. A. Stadt, M. R. Hutson, D. H. Platt, and M. L. Kirby. 2001. Conotruncal myocardium arises from a secondary heart field. Development 128: 3179–3188.

Ward, C., H. A. Stadt, M. R. Hutson, and M. L. Kirby. 2005. Ablation of the secondary heart field leads to tetralogy of Fallot and pulmonary atresia. Dev. Biol. 284:72–83.

Wei, L., W. Roberts, L. Wang, M. Yamada, S. X. Zhang, Z. Y. Zhao, S. A. Rivkees, R. J. Schwartz, and K. Imanaka-Yoshida. 2001. Rho kinases play an obligatory role in vertebrate embryonic organogenesis. Development 128:2953–2962.

Wei, Y., and T. Mikawa. 2000. Fate diversity of primitive streak cells during heart field formation in ovo. Dev. Dyn. 219:505–513.

Yang, X., D. Dormann, A. Munsterberg, and C. J. Weijer. 2002. Cell movement patterns during gastrulation in the chick are controlled by positive and negative chemotaxis mediated by FGF4 and FGF8. Dev. Cell 3:425–437.

Zhang, H. Y., M. Kluge, R. Timpl, M. L. Chu, and P. Ekblom. 1993. The extracellular matrix glycoproteins BM-90 and tenascin are expressed in the mesenchyme at sites of endothelialmesenchymal conversion in the embryonic mouse heart. Differentiation 52:211–220.

This page intentionally left blank

4

Induction and Differentiation of the Myocardium

As discussed in Chapter 3, the cardiogenic fields contain both endocardial and myocardial precursors. This chapter is also concerned with the myocardium, but in this case, we focus on the INDUCTION and DIFFERENTIATION

As discussed in Chapter 3, the cardiogenic fields contain both endocardial and myocardial precursors. This chapter is also concerned with the myocardium, but in this case, we focus on the INDUCTION and DIFFERENTIATION of the myocardial cell lineage in the cardiogenic fields. The endocardium is considered in Chapter 9. The development of specialized cell types is referred to as differentiation. Differentiation of a cell is preceded by COMMITMENT of the cell to a particular fate or cell type. The process of commitment occurs in two stages. The first stage is called SPECIFICATION. A myocardial cell is specified if it develops into a myocardial cell when it is placed in a neutral environment; in other words, the environment is not particularly conducive to myocardial differentiation, but the cell develops as a myocardial cell nonetheless. The second stage of commitment is called DETERMINATION. A myocardial cell that has been determined develops AUTONOMOUSly into a myocardial cell when it is placed in an environment that is actually antagonistic to development of the myocardial cell lineage. In the embryo, the map of cells that have been either specified to a myocardial cell lineage or have the potential to become myocardium is larger than the fate map (see Chapter 3 for an explanation of fate map) of cells that are determined to be myocardial. The stages of myocardial commitment are brought about by a series of inductions that depend on signals from neighboring cells. In an induction, a particular tissue or tissues emit signals in the form of growth factors or MORPHOGENs that induce a particular response in a target cell that is competent to decode the signal, that is, the target cell has receptors and intracellular signaling pathways necessary to transduce or read the signal. In the case of the myocardium, inductive signals are produced by both the HYPOBLAST (chick) or VISCERAL ENDODERM (mouse) and definitive endoderm. A specified cell is one that is competent to respond appropriately to subsequent inductive signals. One of the factors that makes a cell competent is its expression of receptors for various inductive signals. The initial response of the determined cell is to express sets of transcriptional regulators characteristic of a particular cell type. In the case of myocardium, Nkx2.5 and Gata4 are two of the first to be expressed. These transcriptional regulators then orchestrate differentiation, which is the morphological appearance of cell specializations characteristic of a particular cell lineage, in this case the proteins that comprise the contractile apparatus and particular membrane properties that make an initially spontaneously contractile cell type (Fig. 4.1).

Myocardial Induction

Explants of prospective heart mesoderm isolated from mid- or late NEURULA stages are capable of heart formation in nearly 100% of cases, indicating that the specification of cardiogenic mesoderm is complete by mid-neurula stages (Sater and Jacobson, 1989). Figuring out which tissues are responsible for myocardial induction is difficult because it necessitates isolating small regions of tissues for testing. Fortunately, separation and recombination of tissues in chick is possible as early as pregastrulation stages. Co-culturing isolated chick epiblast with hypoblast from pregastrulation stage embryos results in myocardiogenesis directly from the epiblast. This suggests, first, that ingression of epiblast cells through the primitive streak is not required for myocardial induction, and second, that hypoblast is involved in myocardial specification because epiblast without the accompanying hypoblast does not differentiate as myocardium (Fig. 4.2). If a signal from the hypoblast is needed for myocardial specification, factors in the culture medium must induce the subsequent determination and differentiation steps. The hypoblast gradually loses it ability to induce myocardium by gastrulation stages 4–5 in the chick (Yatskievych et al., 1997). The mouse equivalent of the chick hypoblast is the anterior visceral endoderm (Chapman et al.,

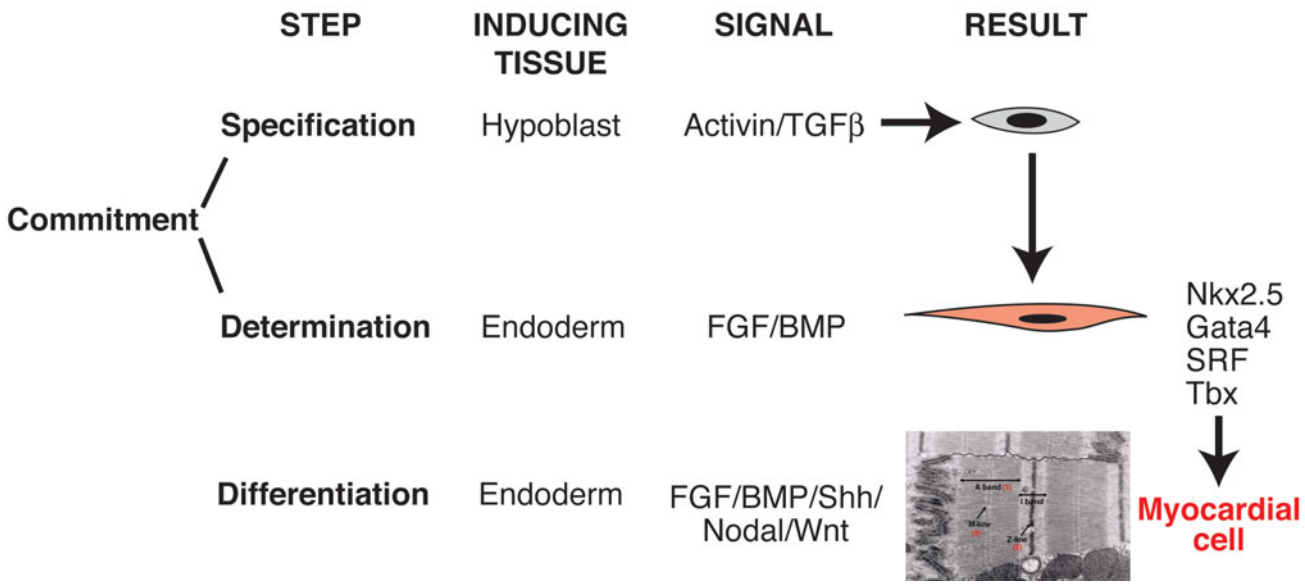

Figure 4.1. Simplified version of myocardial differentiation. Activin/TGF-β signaling from the hypoblast initiates myocardial specification. FGF and BMP signaling initiates myocardial determination by turning on myocardial transcription factors *Nkx2.5*, *Gata4,* and *MEF2*. Determination is quickly followed by myocardial cell differentiation which is promoted by other signaling factors such as Shh, Nodal and non-canonical Wnt11. (Electron micrograph from Severs, 2000, with permission.)

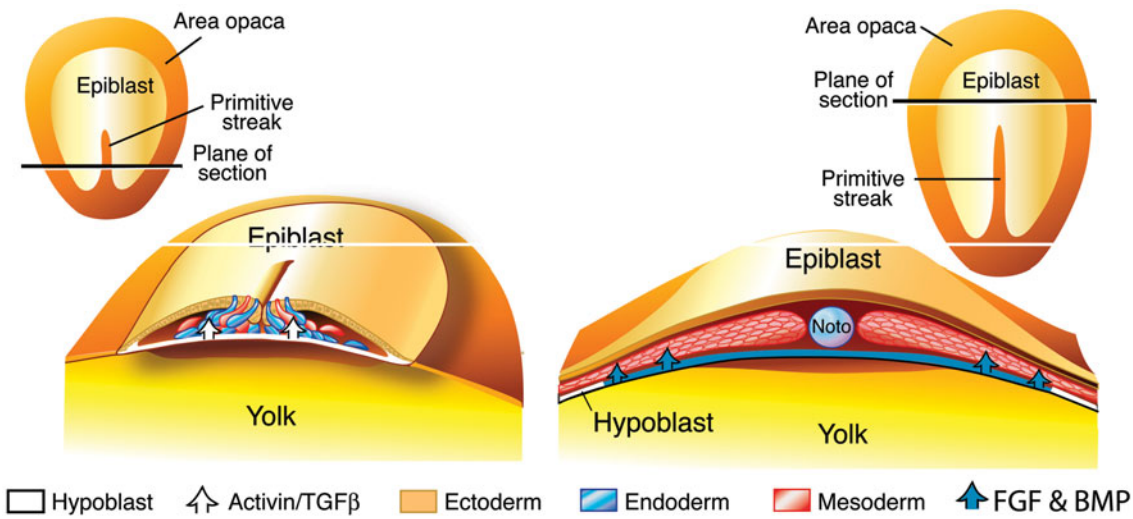

Figure 4.2. Two stages of cardiac specification and determination in the chick. On the *left*, the signals from the hypoblast cause specification of the newly forming mesodermal cells during early gastrulation. Determination and differentiation are induced by the anterolateral endoderm shown on the *right*.

2003). Anterior visceral endoderm has not been examined for its ability to induce myocardium.

While the hypoblast induces the initial step in myocardial commitment, the anterolateral endoderm appears to regulate the determination and differentiation steps of myocardial cells (Fig. 4.2) (Lough and Sugi, 2000). The anterolateral endoderm has no ability to induce myocardium in epiblast but it is a potent inducer of the emerging mesoderm from the primitive streak and of cardiogenic mesoderm, that is, mesoderm that has undergone specification by the hypoblast (Antin et al., 1994; Yatskievych et al., 1997). The endoderm initiates expression of Gata and Nkx family members. Expression of these genes is required for terminal cardiac myocyte differentiation and indicates that the mesoderm is determined. In urodeles, co-culture of anterior endoderm and presumptive heart mesoderm from early neurula embryos leads to differentiation of a beating heart, indicating that, after myocardial determination, the final step of differentiation occurs rapidly (Jacobson, 1960, 1961; Jacobson and Duncan, 1968). However, *Nkx* and *Gata* genes are expressed more widely in the mesoderm than in myocardial precursors and some of the cells that express *Gata* and *Nkx* genes do not ultimately differentiate as myocardium.

Anterolateral endoderm specifically has the capability to induce myocardiogenesis even in cells that are not in the cardiogenic mesoderm. When cells from the caudal primitive streak (outside of the cardiogenic fields) are cultured with anterolateral endoderm, the cells express myocardial markers. The inductive interaction occurs even when a porous barrier is placed between the endoderm and mesoderm, indicating that direct contact is not needed for the induction (Schultheiss et al., 1995). The endoderm loses its ability to induce myocardial differentiation although the timing of this loss is somewhat controversial. After about stages 4+ to 5−, the endoderm no longer supports terminal differentiation of precardiac mesoderm in culture (Gannon and Bader, 1995; Sugi and Lough, 1994). However, removal of the endoderm underlying the precardiac mesoderm from stage 5 and older chick embryos still leads to defective cardiogenesis (Orts-Llorca, 1963).

Factors that Induce Myocardiogenesis

In chick, the signal from the hypoblast that induces myocardial specification may be activin or some other members of the transforming growth factor (TGF)β family (Ladd et al., 1998). Multiple signals from the anterolateral endoderm are most likely required to induce myocardial differentiation, and these are balanced by factors that inhibit myocardial differentiation (Fig. 4.3). Many of the positive factors are generated by anterolateral endoderm while some inhibitory factors are known to arise from midline structures (Fig. 4.4). The candidates that promote myocardial differentiation include bone morphogenetic protein (BMP) and fibroblast growth factor (FGF) family members (Sugi and Lough, 1995). BMP2 and FGF4 cause a combination of differentiation and proliferation, respectively, and their combined action appears to promote myocardial differentiation (Hyer and Mikawa, 1997; Lough et al., 1996). While brief application of both BMP2 and FGF4 can induce myocardiogenesis in a modest number of cells from non-cardiogenic mesoderm, 100% of explants can be forced to differentiate by brief FGF4 treatment followed by continuous BMP2 treatment (Barron et al., 2000). There is some evidence that other factors facilitate myocardial differentiation including non-canonical Wnt signaling and Sonic hedgehog (Shh).

TGFβ Family: TGFβ, BMP, Activin

Activin/TGF-β and BMP2/BMP4 have distinct and reciprocal cardiomyogenic mesoderm-inducing capacities that mimic the tissues in which they are expressed, that is, the hypoblast and anterior lateral endoderm, respectively (Ladd et al., 1998). Activin, TGFβ and certain BMPs, which are members of the TGFβ superfamily, can reproduce aspects of cardiogenesis but none of these signaling peptides by themselves can induce the full range of activities elicited by the inducing tissues, nor do they show the capacity to convert non-cardiogenic mesoderm toward a myocardial phenotype. In the most simplified scheme, activin promotes anterior character in MESENDODERM, creating a permissive environment for BMP/FGF induction of myocardiogenesis (Ladd et al., 1998). Application of BMP2-soaked beads to regions of non-cardiogenic mesoderm in vivo elicits ectopic expression of the cardiac transcription factors Nkx2.5 and Gata4, and exposure to the secreted protein NOGGIN, which antagonizes BMP activity, completely inhibits differentiation of the precardiac mesoderm (Fig. 4.3) (Schneider and Mercola, 2001; Schultheiss et al., 1997). Components of the BMP signaling cascade including the BMP receptors and intracellular signaling components are co-expressed in the cardiogenic mesoderm (Monzen et al., 1999; Shi et al., 2000). Forced expression of dominant negative BMP receptors in the cardiogenic mesoderm results in the reduction or absence of heart formation (Shi et al., 2000).

Figure 4.3. A summary of the transcriptional regulators (*tan*) induced in cardiogenic mesoderm (*red*) and the signaling factors that promote (*green*) or inhibit (*pink*) myocardial differentiation.

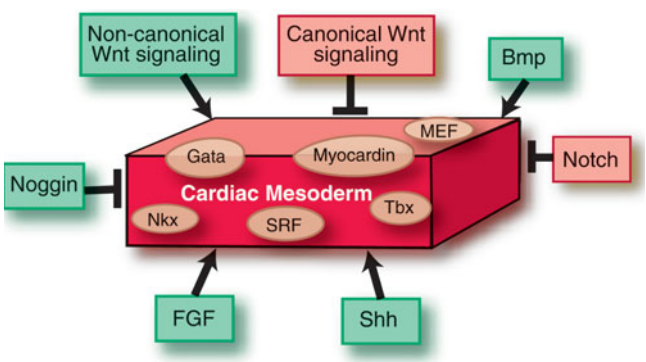

Figure 4.4. Spatial relationship between cardiac inducing factors, which are mainly secreted by pharyngeal endoderm (*green*) and inhibitory factors such as canonical Wnt signals that are secreted by ectodermal tissue (*blue*) and Noggin that is expressed in the notochord (*lavender*). Cardiogenic mesoderm (*deep red*) is formed only in splanchnic mesoderm, which remains in close contact to pharyngeal endoderm. (Adapted from Brand, 2003.)

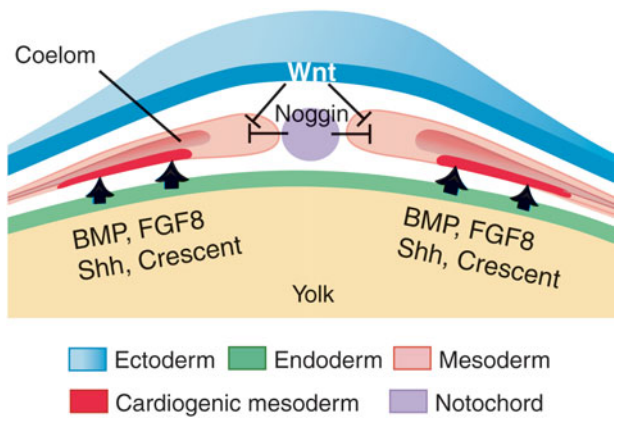

In addition to its role in myocyte differentiation, BMP2 also modulates functional properties of differentiated myocardium. In vitro, it increases the percentage of fractional shortening of terminally differentiated cardiomyocytes (Ghosh-Choudhury et al., 2003).

Fibroblast Growth Factors

It is clear from a number of studies that the Fgf family is important in several different aspects of myocardial development. The first of these is differentiation. Fgf has a cardiomyogenic effect in regions where Bmp signaling is also present (Alsan and Schultheiss, 2002). Fgf2 and -4 have been the most studied members of the Fgf family in mice and chick heart development. However, it is Fgf8 that is expressed in, and required for, development of the zebrafish heart precursors, particularly during initiation of cardiac gene expression. Recent evidence indicates that Fgf8 is also the inductive family member in mouse and chick (Alsan and Schultheiss, 2002; Abu-Issa et al., 2002; Frank et al., 2002). Fgf8 is initially expressed by cardiomyogenic precursors and later in ventricular myocardium, and its expression is required for the expression of Nkx2.5 and Gata4. In zebrafish embryos with the ACEREBELLAR phenotype, the *Fgf8* gene is mutated (Reifers et al., 2000). Homozygous acerebellar embryos do not establish normal circulation because development of the ventricle is severely abnormal. Morpholino knockdown or pharmacological inhibition of Fgf8 signaling during heart development phenocopies the acerebellar heart phenotype (Araki and Brand, 2001). In the *Fgf8* hypomorphic mouse, development of the right ventricle and outflow tract are attenuated, although the atria, atrioventricular canal and left ventricle appear to form, suggesting that only the most medial subset of the myocardial precursors in the cardiogenic field require Fgf8 signaling. From the mutant phenotypes, it appears that Fgf8 signaling may be more important for development of the myocardial precursors located in the medial parts of the cardiogenic fields (right ventricle, conus and truncus) than those located laterally.

Further evidence that Fgf signaling is necessary for cardiomyocyte lineage differentiation has been confirmed in *Fgf receptor* (*Fgfr*)*1*-null EMBRYOID BODIES (Dell'Era et al., 2003). Embryonic stem (ES) cells differentiate as embryoid bodies when removed from the factors that maintain their stem cell potential and grown in hanging drop cultures. The embryoid bodies differentiate both myocardial and endothelial cells. When Fgfr1-null ES cells are grown as embryoid bodies, they do not differentiate myocardial islands even though endothelial cell differentiation is normal. The myocardial cell lineage can be partially rescued by treatment with phorbol ester, which activates the protein kinase C (PKC) pathway. PKC is activated by the receptors for many signaling factors. The fact that activation of PKC can rescue myocardial differentiation suggests that PKC signaling is activated downstream of the Fgfr1. It must also interact with the Fgf intracellular signaling components Mek/Erk, which are the part of the mitogen-activated protein kinase (Mapk) pathway that alters gene transcription in a cell responding to FGF signaling (Dell'Era et al., 2003). Transcriptional activity of MYOCYTE ENHANCER FACTOR (MEF)2, one of the obligatory myocardial transcriptional activators, is regulated by Mapk activation and phosphoinositol 3 (PI3) kinase, another intracellular enzyme that is activated by Fgf8 signaling.

Fgfs continue to affect myocardial growth and function after a fully functional myocardium develops. Fgfr1, which is present in low abundance in the cardiogenic fields, reaches a peak of expression just after looping is finished when punctate deposits of the receptor can be seen in the myocardium (Sugi et al., 1995). Incubation of hearts with a neutralizing antibody to Fgfr1 retards proliferation and formation of multiple layers of cardiac myocytes. In addition, Fgf signaling affects transcription of cardiomyocyte-specific proteins during a limited window of development. Treatment of cardiac myocytes during the looping stages with Fgf2 increases TROPONIN T and DESMIN expression, which is a sign of further differentiation (Velez et al., 1994, 2000). After septation, myocyte growth and transcription are thought to become Fgf independent (Velez et al., 1994).

Fgfs can alter functional properties of immature myocardial cells. Fgf2 has a negative INOTROPIC effect on adult cardiac myocytes that could result from alterations in intracellular calcium HOMEOSTASIS, and there is some evidence that development of the myocardial calcium transient in immature myocardium is affected by Fgfs (Ishibashi et al., 1997). Fgf signaling appears to be necessary for transcription of genes subserving the CALCIUM TRANSIENT, for example, myocardial L-type calcium channel expression is reduced by excess Fgf8 signaling (Farrell et al., 2001). The ligand for Fgf signaling may be Fgf2, which is found in substantial deposits in the myocardium during looping, or Fgf8, which is expressed by the pharyngeal endoderm and ectoderm (Zhu et al., 1996).

Sonic Hedgehog

SONIC HEDGEHOG (SHH) is an important signaling factor for a variety of developmental pathways during embryogenesis and may play a role in cardiomyogenesis. It is expressed by the pharyngeal endoderm. Mice that lack the SMOOTHENED receptor, which is required for Shh signaling, show delayed induction of *Nkx2.5* in cardiomyocytes (Zhang et al., 2001). Further, Shh induces cardiomyogenesis in a multipotent cell line in culture after cellular aggregation when the cells begin to express Gata4, Mef2C, and Nkx2.5 (Gianakopoulos and Skerjanc, 2005). However, the significance of this in vivo is still not known.

Wnts

WNTS are secreted cysteine-rich glycoproteins that act as short-range ligands to activate and repress downstream targets. In myocardial cells the ligands that activate β-catenin as

a transcriptional regulator actually repress myocardial differentiation and therefore must be blocked for heart induction. This is called canonical Wnt signaling and is covered in the next section. Some Wnt ligands activate cJun-N-terminal kinase (Jnk) rather than β-catenin and this is called non-canonical Wnt signaling. The non-canonical Wnt signaling pathway is thought to enhance myocardial differentiation (Fig. 4.5) (Solloway and Harvey, 2003). Wnt11, expressed in endoderm and mesoderm, activates Jnk (Marlow et al., 2002). Because this pathway does not act through β-catenin, it is considered to activate non-canonical Wnt signaling. Wnt11 not only acts through a different intracellular pathway, but it also inhibits canonical Wnt signaling through β-catenin. The Wnt antagonists Dickkopf (Dkk)-1 and Crescent competitively bind Wnts that act through the Frizzled receptor to inhibit Wnt signaling via the canonical pathway. These Wnt inhibitors actually stimulate Wnt/JNK signaling and promote myocardial differentiation.

Factors that Inhibit Myocardiogenesis

Wnt/β-Catenin: Canonical Wnt Signaling and Repression of Cardiogenesis

Wnt3A and Wnt8 signal through β-catenin and thus initiate canonical Wnt signaling (Fig. 4.5). Both Wnt3A and Wnt8 inhibit myocardial differentiation. Conversely, inhibition of Wnt3A or Wnt8 signaling by Wnt antagonists promotes cardiomyogenesis. Wnt antagonists DICKKOPF (DKK)1 and CRESCENT can induce heart formation in explants of cardiogenic mesoderm while other Wnt antagonists including FRIZBEE (FRZB) lack this ability (Schneider and Mercola, 2001). β-Catenin is one of the best characterized intracellular effectors of the canonical Wnt signaling pathway (Moon et al., 2002). Canonical Wnt signaling stabilizes cytoplasmic β-catenin, allowing it to enter the nucleus, associate with transcription factors of the Tcf/Lef FAMILY, and activate transcription of target genes. Ectopic expression of GLYCOGEN SYNTHASE KINASE (Gsk)3β, which inhibits classical β-catenin-mediated Wnt signaling by destabilizing β-catenin and allowing it to be degraded, also induces cardiogenesis in cardiogenic mesoderm. Both Dkk-1 and Crescent are produced by the node during gastrulation and may initiate cardiogenesis by establishing a zone of low Wnt signaling (Schneider and Mercola, 2001). Thus, it has been proposed that a Wnt activity gradient along the anteroposterior axis intersects Bmp along the dorsoventral axis to induce cardiogenesis in a region of high Bmp and low Wnt activity (Marvin et al., 2001). Interestingly, null mutation of β-catenin in mice leads to formation of multiple sites of myocardial differentiation in the endoderm (Lickert et al., 2002). Cardiogenesis-inhibiting Wnts are also expressed by the NEURAL ECTODERM and may help to limit the medial extent of the cardiogenic mesenchyme (Fig. 4.5).

Figure 4.5. Non-canonical Wnt signaling initiates myocardial differentiation. Inhibitors of canonical Wnt/β-catenin plus signaling by non-canonical Wnt ligands control initial induction of myocardial transcription factors.

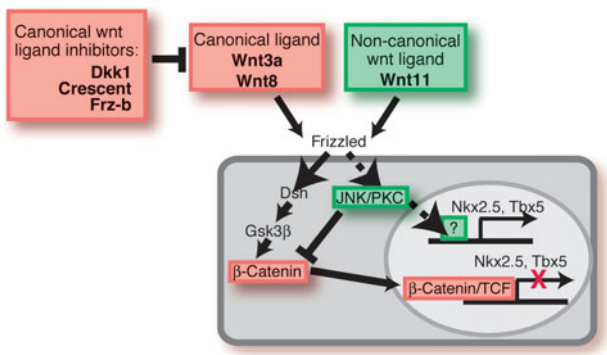

Restriction of the Primary Heart Fields by Notch Signaling

All cells that become cardiomyocytes have to express Nkx2.5 before they differentiate but not all cells that express Nkx2.5 will become cardiomyocytes. In the frog, Notch1 receptor is co-expressed with Nkx2.5 in the cardiogenic mesoderm. The Notch ligand Serrate1 is restricted to the cells that do not differentiate as cardiomyocytes but will become the dorsal mesocardium and pericardial cavity (Rones et al., 2000). Notch signaling inhibits these cells from expressing a myocardial phenotype. The Notch family has recently been shown to block cardiomyogenesis, perhaps by blocking DNA binding by heterodimerized Mef2C. Responsiveness to Notch requires a 12-amino acid region of Mef2C immediately adjacent to the DNA-binding domain that is unique to this Mef2 isoform. This region of Mef2C interacts directly with the ankyrin repeat region of the Notch receptor (Wilson-Rawls et al., 1999).

Notch signaling regulates transcription via members of the HAIRY-RELATED TRANSCRIPTION FACTOR (Hrt) family. Hrt proteins physically interacted with Gata proteins, which results in inhibition of Gata-dependent transcriptional activation of

Figure 4.6. Notch signaling in the *Nkx2.5/Gata4*-positive cardiogenic mesoderm limits the formation of myocardium from the medial part of the field to form dorsal mesocardium. The dorsal mesocardium retains its myocardial potential and will add myocardium to both the inflow and outflow poles during looping (see Chapter 6).

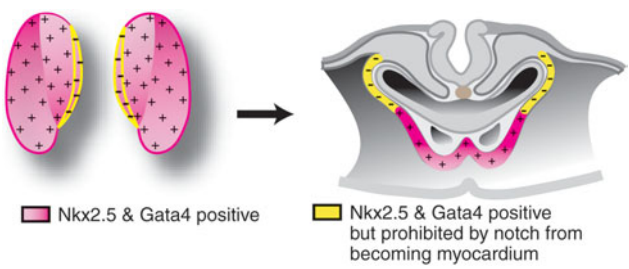

cardiac-specific genes. This inhibition is sensitive to growth factor signaling because AKT1/PKB, a focal point for growth factor signaling transduced via PHOSPHOINOSITIDE-3 (PI3) KINASE, removes the Hrt-mediated inhibition of GATA-dependent transcription.

Noggin

Bmp signaling is an important factor in induction of myocardiogenesis. The Bmp inhibitor noggin has been shown to inhibit Bmp signaling, which leads to a failure in Nkx2.5 expression and inhibition of myogenesis in cultured cells (Jamali et al., 2001). It is not known what the significance of this is in vivo, although Noggin is expressed in the notochord, which is close to the medial part of the cardiogenic fields where myocardium differentiates last (Fig. 4.6).

Transcriptional Regulation of Myocardiogenesis

A master regulator that is capable of triggering cardiac myogenesis in a manner analogous to the role played by MyoD in skeletal myogenesis has not been identified. A master myocardial gene probably does not exist. Rather, transcriptional regulation of myocardial development is by multimeric complexes of transcription factors. These complexes can be comprised of as many as 20 different proteins. The loss of any one factor appears to make transcriptional regulation of myocardial gene transcription less efficient but does not eliminate the myocardial cell lineage. Many cardiac transcription factors interact directly with DNA, allowing increased stability of the transcriptional complexes, synergistic activation of target genes, and recruitment of individual factors to enhancers that lack specific binding sites (Chen and Schwartz, 1996; Morin et al., 2000; Wang et al., 2001). The transcriptional regulators that have been most studied include members of the Nkx2, Gata, Mef2, TBX (T-BOX), IRIQUOIS (IRX), and HAND families of transcription factors (Fishman and Chien, 1997).

The transcription factors associated with myocardial differentiation fall into two major classes: those associated with positive transcription factor regulatory circuits and those associated with negative regulatory circuits. Myocardial induction is accompanied by positive feed-forward with mutual cross-regulatory circuitry (Bruneau, 2002). For example, Nkx2.5 and Hand2 expression is regulated by Gata, while Gata gene expression is regulated by Nkx2.5. Nkx2.5 and Hand2 are required for full expression of Hand1 and Irx4, while Irx4 is required for expression of Hand1. Hand2 and Tbx4 are required for Irx4 expression (Bruneau, 2002; Bruneau et al., 2000; Lien et al., 1999; McFadden et al., 2000; Molkentin et al., 2000).

NK Homeodomain Transcription Factors

At least five members of the *Nkx2* gene family are expressed during vertebrate heart development. The *Nkx2.5* gene was identified by virtue of its homology to *TINMAN*, found in a *Drosophila* mutant screen, and its protein product plays a similar role in development (Lyons et al., 1995). However, unlike its vertebrate counterpart, null mutation of *tinman* in *Drosophila* results in a complete failure of cardioblast development. Thus, *tinman* does play the role of a myocardial master gene in *Drosophila*. However, we argue in Chapter 14 that *Drosophila* cardioblasts are not the equivalent of vertebrate myocardial cells and so the fact that *tinman* serves as a cardioblast master gene should not raise the expectation that its equivalent in vertebrate myocardial cells should be a master gene.

Nkx2.5 is one of the earliest markers of avian mesoderm fated to give rise to cardiac muscle (Fig. 4.7) (Schultheiss et al., 1995). The region that is identified as the cardiogenic field is defined medially, laterally, and posteriorly by Nkx2.5 gene expression. Removal of all or part of the Nkx2.5-expressing region results in the loss of corresponding heart structures—atrium, atrioventricular canal and ventricle—suggesting that the embryo is unable to regenerate cardiac tissue after Nkx2.5 expression is initiated (Chen and Fishman, 1996; Ehrman and Yutzey, 1999; Mjaatvedt et al., 2001; Tonissen et al., 1994).

Nkx2.5 interacts with serum response factor (Srf), Gata4, and Tbx5 to promote the expression of a number of myocardial genes including *natriuretic peptide precursor* (*Nppa*), *myosin light chain* (*Mlc*)*2v*, *Mef2C*, *Hand1*, and *α-smooth muscle actin* (Chen and Schwartz, 1996; Chen et al., 1996; Tanaka et al., 1999). Mice with null mutations of *Nkx2.5* develop beating, although small, hearts but ultimately die of heart failure. The fact that the heart can develop to a beating stage suggests that there are redundant factors that can substitute for *Nkx2.5*, or as mentioned earlier, that the transcriptional complexes are less efficient but still functional without *Nkx2.5* (Lyons et al., 1995). Chimeric mice, generated by injection of *Nkx2.5*-null EMBRYONIC STEM (ES) CELLS into wild-type BLASTOCYSTS, develop

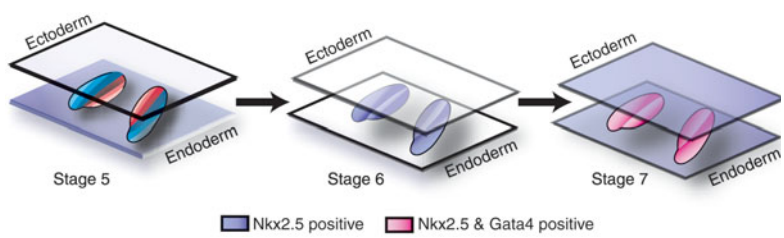

Figure 4.7. Position and subdivisions in the cardiogenic mesoderm located between ectoderm and endoderm. Onset of *Nkx2.5* expression is at stage 6 followed by *Gata4* expression at stage 7 in the cardiogenic mesoderm.

no myocardial descendants of the mutant ES cells although the *Nkx2.5*-null ES cells are found in all other organs (Tanaka et al., 1999). This further suggests that *Nkx2.5* plays a fundamental role in promoting the myocardial phenotype. In humans, an *NKX2.5* mutation is associated with TETRALOGY OF FALLOT, ATRIAL SEPTAL DEFECT, and ATRIOVENTRICULAR CONDUCTION BLOCK (Goldmuntz et al., 2002; Schott et al., 1998). Embryos with double null mutation of *Nkx2.5* and *Hand 2* have only a single chamber which is molecularly defined as the atrium (Yamagishi et al., 2001).

In transgenic mice, deletion or targeted mutation of the Smad consensus regions from the *Nkx2.5* promoter delays or inhibits induction of *Nkx2.5* gene expression during early heart formation. The Smad consensus region confers the ability of the gene to be responsive to Bmp signaling which is one of the signals important for myocardial induction (Liberatore et al., 2002). Cardiac expression of Nkx2.5 is maintained throughout development. However, Nkx2.5 expression is not limited to cardiogenic mesenchyme or myocardium. The gene is also expressed in the pharyngeal endoderm, developing pharyngeal arches, spleen, thyroid, and tongue. Approximately 3 kb of 5′ flanking sequence is sufficient to activate gene expression in the cardiogenic fields as early as E7.25 in the mouse. A 505-base pair (bp) regulatory element has been identified that contains multiple identified binding sites for other transcriptional regulators. These include Gata, NK ELEMENT (NKE), and basic helix–loop-helix (bHLH). The presence of consensus binding sites for other developmentally important regulatory factors within the 505-bp element suggests that combinatorial interactions between multiple regulatory factors are responsible for the initial activation of Nkx2.5 in the cardiac primordia (Searcy et al., 1998). This regulatory element is sufficient for gene activation in cardiogenic mesenchyme, pharynx, and spleen. Mutation of the Gata binding sites eliminates *Nkx2.5* gene activation in these primordia.

Gata Factors

Three members of the Gata family of transcription factors, Gata4, -5, and -6 genes, are expressed by precardiac cells (Fig. 4.7). These *Gata* genes comprise what is known as the cardiac subfamily (Alsan and Schultheiss, 2002; Molkentin, 2000). Each is expressed in a similar pattern within gastrulating cells of the primitive streak, before determination of the cardiomyocyte progenitors, and later within the cardiogenic mesoderm and the endoderm that underlies it. Gata5 becomes restricted to the endocardium, while Gata4 and -6 are expressed in the myocardium. The expression pattern of Gata4 in the putative heart field encompasses that of Nkx2.5, but extends to a larger portion of the lateral plate mesoderm (Molkentin, 2000; Serbedzija et al., 1998). The *Gata* gene family encodes transcription factors characterized by zinc-finger motifs required for DNA recognition, binding and transcriptional activation (Weiss and Orkin, 1995). Members of the cardiac Gata subfamily of transcription factors bind to a specific motif in the promoter regions of many cardiac-specific genes (Zaffran and Frasch, 2002). It has been proposed that combinatorial interaction among Gata factors or between Gata factors and other cofactors may differentially control various stages of cardiogenesis (Charron and Nemer, 1999). Gata4 protein interacts with Srf, Nkx2.5, Mef2C, FRIEND OF GATA (FOG)2, and NUCLEAR FACTOR OF ACTIVATED T CELLS (NFAT)C (Molkentin et al., 1998; Morin et al., 2000; Svensson et al., 1999).

The activity of Gata4 protein is thought to be regulated by growth factor signaling because it is phosphorylated by p38 MAP kinase acting downstream of Rho family GTPases which promote transcriptional activation of the *RhoA* gene itself and SARCOMERE assembly (Charron and Nemer, 1999).

Gata transcription factors play a key role in regulating the expression of many of the genes encoding myocardial contractile proteins including cardiac *troponin I* (*TnI*), a gene that is expressed exclusively in cardiac myocytes. Other genes known to be regulated by Gatas are cardiac *troponin C* (*TnC*), *slow myosin heavy chain* (*Mhc*)*3*, and *α-cardiac actin* (Durocher et al., 1997; Sepulveda et al., 1998). In addition, a number of other genes are responsive to Gata factors. These include early expression of *Nkx2.5*, *Nppa*, a cardiac subtype of the *muscarinic acetylcholine receptor*, and the *sodium-calcium exchanger* (Cheng et al., 1999; Nicholas and Philipson, 1999).

Even though Gata factors are thought to be important in myocardial gene regulation, the phenotype of the *Gata4*-deficient mouse indicates a developmental problem that is unrelated to myocardial transcriptional regulation. In *Gata4* null mice, the heart fields fail to fuse at the midline resulting in cardia bifida (Kuo et al., 1997; Molkentin et al., 1997). The cardia bifida is caused by a paucity of, or poorly functional, extraembryonic tissues, most likely visceral endoderm (Watt et al., 2004). ANTISENSE OLIGOMERS designed to deplete transcripts encoding Gata4, -5, and -6 in chick embryos also result in a high percentage of cardiac bifida without affecting myocardial differentiation (Jiang et al., 1998). Similarly, chimeric mice that harbor *Gata*4-null ES cells do incorporate descendants of these cells into the fully formed beating heart indicating that the defect is not intrinsic to the myocardial cell lineage (Kuo et al., 1997; Narita et al., 1997).

T-Box Transcription Factors

T-box (Tbx) transcription factors (Tbx) act as repressors or activators of downstream gene targets. Most of the target genes are still not identified. Some of the Tbx transcriptional regulators are exclusively repressors or activators; others appear to function in particular instances as either repressors or activators. Tbx proteins bind to T-BOX BINDING ELEMENTS (Tbe)s in the promoter regions of their target genes. Transcripts of Tbx1, -2, -3, -5, -12, and -20 are expressed in overlapping patterns during early myocardial differentiation (Ahn et al., 2000; Carson et al., 2000; Hayata et al., 1999; Yamada et al., 2000). Little is known about the functions of Tbx3, -12, and -20.

The expression domains of Tbx2 and -3 overlap with regions that express Bmp2, and treatment of embryos with exogenous Bmp2 leads to the expression of Tbx2 and -3 (Yamada et al., 2000). Tbx2 is expressed in the myocardial cells that do not express atrial natriuretic factor (Anf protein transcribed form the *Nppa* gene) and is thus thought to repress Anf expression. It is expressed in the atrium and atrioventricular canal of developing chick and mouse heart at the same time as Nppa message is restricted to the developing ventricular myocardium. Later Tbx2 expression is limited to the atrioventricular myocardium, where it again appears to repress Nppa expression. Tbx2 complexes with Nkx2.5 on the TbeNke motifs in the *Nppa* promoter (Habets et al., 2002).

Tbx5 is expressed in the bilateral cardiac primordia of mouse, *Xenopus*, chick, and fish embryos, although its expression is rapidly restricted to caudal areas that represent the prospective atria, atrioventricular canal, and left ventricle (Begemann and Ingham, 2000; Bruneau et al., 1999; Chapman et al., 1996; Horb and Thomsen, 1999). Haploinsufficiency or null mutation of *Tbx5* results in hypoplasia of the inflow regions of the heart with reductions in Nkx2.5 and Gata4 expression (Bruneau et al., 2001; Horb and Thomsen, 1999). Tbx5 directly interacts with Nkx2.5, and haploinsufficiency markedly decreases expression of Nppa and connexin 40 (Cx40). Forced ectopic expression of Tbx5 in the cranial region of the cardiogenic fields causes abnormal ventricular morphogenesis and reduced expression of a ventricle-specific contractile protein, Mlc2V. All of these features suggest that Tbx5 is associated with atrial chamber-specific transcription (Liberatore et al., 2000). Tbx5 is also thought to play a role in controlling cell growth because forced overexpression in embryonic chick ventricular myocardium inhibits myocardial growth and trabeculation by suppressing cardiomyocyte proliferation. In human embryonic hearts, Tbx5 expression is inversely related to proliferation (Hatcher et al., 2001). Further, cell lines overexpressing wild-type Tbx5 start to beat earlier and express cardiac-specific genes more abundantly than control cells of the same cell line (Hiroi et al., 2001). These studies suggest that there may be a delicate balance between proliferation and differentiation of the myocardium and formation of secondary myocardial structures including chamber specification and trabeculation. Tbx5 expression may be controlled by another Tbx family member. The ZEBRAFISH T-BOX GENE, *HRT*, is a homologue of *Tbx20* which is expressed in the developing heart. Overexpression of hrT in zebrafish causes a significant downregulation of Tbx5 (Szeto et al., 2002).

Point mutations or null expression of Tbx1 and -5 are associated with human congenital heart defects that are covered in Chapter 15.

Mef2

The *Mef2* family of genes is part of the superfamily of Mads (Mcm1, agamous, deficiens, serum response factor-box) transcription factors that are essential for differentiation of all muscle lineages (Black and Olson, 1998). The gene family includes *Mef2A, Mef2B, Mef2C*, and *Mef2D*. Mef2A expression starts in precardiac mesoderm and continues in the heart tube, atrium, and ventricle (Buchberger and Arnold, 1999). Mef2C expression in an embryonic carcinoma cell line upregulates a wide spectrum of cardiac specific genes, which include *Gata4, Nkx2.5*, *α-cardiac actin*, and *cardiac Mhc* (Skerjanc et al., 1998). Mef2 proteins are positively regulated by phosphorylation, suggesting that their activity is regulated by cell signaling (Kasahara and Izumo, 1999; Lu et al., 2000).

Inactivation of the *Mef2C* gene causes arrest of cardiac development with lack of specification of the right ventricle and downregulation of a number of cardiac-specific genes including *Hand2*, which is required for specification of right ventricular myocardium (Lin et al., 1997). Most prominent is the absence of myosin heavy chain (Mhc)-expressing myoblasts and differentiated muscle fibers (Bour et al., 1995). Because most of the promoters for the downregulated genes contain no or low-affinity Mef2 binding sites and they are not significantly activated by any Mef2 proteins, Mef2 may act as a cofactor. In fact, there is evidence that Mef2 potentiates the transcriptional activity of Gata factors (Morin et al., 2000). Although each of these transcription factors is expressed homogeneously throughout the heart field and myocardium, the phenotype may be due to the fact that a heterodimerized Mef2C–Gata DNA binding complex confers significantly higher levels of promoter activity in the right ventricle than in the left (Ross et al., 1996).

Serum Response Factor

Serum response factor (Srf) is coexpressed with Nkx2.5 and Gata4 in the cardiogenic fields. It is also a member of the Mads-box family of transcriptional regulators, and it mediates rapid transcriptional response to various extracellular signaling factors. Srf interacts with myocardin and Gata4 and many noncardiac genes because *Srf*-null mutants die at gastrulation without forming mesoderm (Arsenian et al., 1998; Belaguli et al., 2000; Wang et al., 2001; Weinhold et al., 2000). Binding sites for Srf are known as CARG BOXES, which are present in many cardiac promoters. Srf is thought to activate muscle genes by recruiting myogenic accessory factors such as myocardin that are expressed in cardiac and smooth muscle (Wang et al., 2001). The function of Srf is negatively regulated by HOP, a protein containing a small homeobox motif that is unable to bind DNA by itself (Chen et al., 2002; Shin et al., 2002).

Hands

The bHLH transcription factors, Hand1 and Hand2, are expressed in the pharyngeal arches and heart. In the mouse, Hand1 expression begins during preimplantation development.

After implantation, its expression is restricted to placental trophoblast cells and later to embryonic cardiac and neural crest cells. Asymmetric expression of this gene in the murine heart is first observed in the caudal part of the heart tube that becomes the presumptive left ventricle when the heart loops (Biben and Harvey, 1997). In *Nkx2.5*-null mice, Hand1 fails to be expressed in the left ventricle. However, development of *Hand1*-null mice embryos is arrested at E7.5, not because of a problem with heart development but because of defects in TROPHOBLAST giant cell differentiation (Firulli et al., 1998; Riley et al., 1998). Although the early mortality can be rescued by the aggregation of mutant embryos with wild-type TETRAPLOID EMBRyos, the *Hand1* chimeras die prior to cardiac looping.

Hand2 is expressed in the presumptive right ventricle and in the pharyngeal arches. Mice that are homozygous null for *Hand2* lack the third and fourth pharyngeal arches and have hypoplastic first and second arches (Srivastava et al., 1997). These mice also fail to develop a right ventricle, although Hand2 is not required for specification of the right ventricle as indicated by the expression of Mlc2V, which is a marker of right ventricle specification and is normal in this mutant.

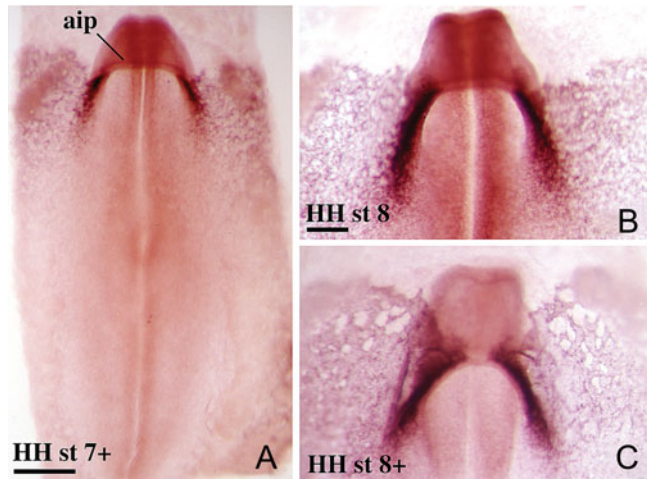

Figure 4.8. Expression of α-smooth muscle actin message is the first sign of myocardial differentiation in the chick embryo. It occurs well before fusion of the cardiogenic fields. (*A–C*) Progressive steps in bringing the bilateral cardiogenic fields to the ventral midline for fusion. (From Colas et al., 2000, with permission.)

Myocardial Contractile Protein Gene Expression

The first contractile gene to be expressed by myocardial cells is smooth muscle α-actin message, which first appears at stage 5 in the chick (Colas et al., 2000; Kruithof et al., 2003). For some unknown reason, transcription continues but translation of the smooth muscle alpha actin protein is delayed for several stages after the message appears (Fig. 4.8) (Colas et al., 2000). In chick, expression of sarcomeric myosin heavy chain protein (MyHC) is first detected at stage 7 (0–3 pairs of somites) which is about 10 hours before the first contractions can be seen (Han et al., 1992).

In mouse, myosin and cardiac actin proteins are first seen at E7.5–8 and the heart begins contracting at E8.5 (Lyons et al., 1990; Sassoon et al., 1988). Between E7.5 and 8, the newly formed cardiac tube begins to express Mhcα, Mhcβ, Mlc1A (atrial), and Mlc1V (ventricular) proteins at high levels throughout the myocardium (Lyons et al., 1990).

Myofibrillogenesis

Myocardial cells are striated muscle cells and the hallmark of striated muscle cells is myofibrils, which are visible threads that run parallel with the long axis of the cell. The myofibrils are composed of numerous myofilaments and these provide the basis of the cells' ability to contract. Myofibrillar assembly is an important step in myogenesis. Assembly of myofibrils begins with premyofibrils and progresses to mature myofibrils. Precardiac mesoderm displays arrays of stress fibers with alternating bands of non-muscle isoforms of α-actinin and myosin IIB. To these are added fibrils composed of actin, additional non-muscle myosin IIB, and sarcomeric α-actinin. Just before beating begins, both non-muscle and muscle myosin IIB localize in some of the fibrils. These begin as thin bundles, dispersed in the cytoplasm, and progress to small aligned A-band-sized aggregates. As the Z-bands form, the amount of non-muscle myosin decreases, and the cells begin beating (Du et al., 2003). In the chick, no striations or periodic repeats can be seen in the presumptive myocytes until stage 10. Myosin is first distributed in the apical regions of the myocytes adjacent to the PERICARDIAL COELOM (Cebra-Thomas et al., 2003; Gibson-Brown et al., 1998; Han et al., 1992).

In mouse, sarcomeric proteins are expressed and myofibril assembly occurs before the first contractions at E8.5. Actinin, titin, and actin make up dense body-like structures that organize sarcomere assembly. The maturation of the sarcomeres is characterized by two events. First, is the formation of M-LINE EPITOPES OF TITIN with respect to Z-DISK epitopes, and second, MYOMESIN and myosin binding protein-C are sequentially incorporated into the M-line (Fig. 4.9). The dense body-like structures serve as a ruler for sarcomere assembly as soon as the C-TERMINI of titin have become localized. Assembly of thin and thick filaments occurs independently during myofibrillogenesis, and myomesin appears to be important for integrating thick filaments with the M-line end of titin (Ehler et al., 1999).

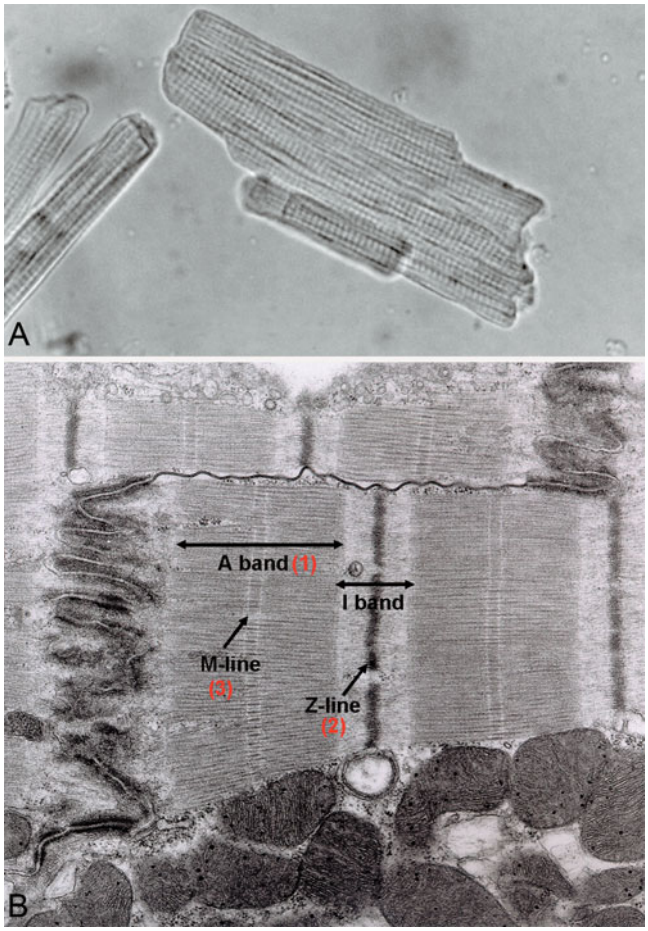

Figure 4.9. (*A*) Phase-contrast micrograph of a cultured neonatal cardiomyocyte showing clear striations of the sarcomeres in the myofibrils. (Photo courtesy of C. E. Sears and B. Casadei.) (*B*) Electron micrograph showing organization of a sarcomere in a differentiated myocardial cell with the order indicated in red numbers that the different components form to build a myofibril. (Adapted from Severs, 2000, with permission.)

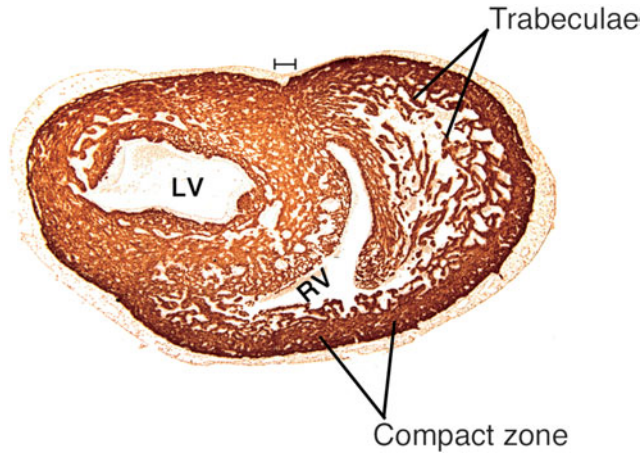

Figure 4.10. Compact and trabecular myocardium in a day 9 chick heart.

Myocardial Growth

Early myocardial development is characterized by subdivision of the myocardial wall into an outer, highly mitotic COMPACT ZONE and an inner trabecular zone with much less proliferative activity (Fig. 4.10) (Jeter and Cameron, 1971; Manasek, 1968; Thompson, 1995; Tokuyasu, 1990). The early myocardium is avascular because it is adequately nourished by diffusion through the endocardium through trabecular channels that increase the endocardial surface area (Rychter and Ostadal, 1971; Rychterova, 1971). The compact zone is essential for myocardial growth while the trabeculated myocardium functions in myocardial perfusion. Signaling from the endocardium is necessary for formation of the trabeculae by the compact myocardium. NEUREGULIN and its receptor tyrosine kinases, ERBB2 and erbB4, are involved in the appearance of the trabeculae, as disruption of neuregulin signaling blocks formation of the trabeculae from an apparently normal compact myocardium (Gassmann et al., 1995; Lee et al., 1995; Meyer and Birchmeier, 1995).

Clonal analysis of mouse myocardial proliferation suggests that myocardial cells and their precursors follow a proliferative mode of growth rather than growth from a stem cell population. The proliferative mode has two phases: an initial dispersive phase followed by coherent cell growth (Meilhac et al., 2003). Clusters of cells are dispersed along the long axis of the heart tube. Coherent growth then occurs locally as the tube elongates. At later stages, wedge-shaped clusters span the wall.

Myocardial cells proliferate until birth in the mouse and rat, and hatching in the chick (Li et al., 1996, 1997; Soonpaa et al., 1996). The major increase in thickness of the ventricular wall between E11.5 and 14.5 in the mouse and E8–14 in the chick is due to proliferation (Erokhina, 1968; Rychterova, 1978, 1971). The highest rate of proliferation is in the compact layer just below the epicardium and is dependent on signaling from the epicardium to maintain proliferation (Chen TH et al., 2002; Tokuyasu, 1990).

Regulation of myocardial cell proliferation is an important factor in cardiac morphogenesis. The *JUMONJI* gene encodes an AT rich interaction domain that binds DNA (Kortschak et al., 2000). Jumonji downregulates cell proliferation of cardiac myocytes by repressing cyclin D1 expression (Toyoda et al., 2003). Non-muscle myosin heavy chain II-B is essential for normal CYTOKINESIS of cardiomyocytes, and animals that lack non-muscle myosin heavy chain II-B have enlarged hearts with increased binucleation and cell size during the embryonic period (Takeda et al., 2003).

Animals that lack an epicardium by either mutations in VASCULAR CELL ADHESION MOLECULE (VCAM)1, α4 integrin, WILMS' TUMOR (WT)1, or because of physical disruption of the proepicardium show hypoplastic myocardial wall, ventricular septal defects, and cardiac failure (Gittenberger-de Groot

et al., 2000; Kreidberg et al., 1993; Kwee et al., 1995; Manner et al., 2001; Moore et al., 1999; Yang et al., 1995).

Null mutation of RETINOIC ACID RECEPTOR (Rar)α and retinoid-X receptor (RXR)α, erythropoietin, or erythropoietin receptor also cause hypoplastic myocardial growth. RETINOIC ACID (RA) secreted by the epicardium induces another soluble factor in the epicardium that regulates proliferation in myocardial cells (Chen TH et al., 2002; Stuckmann et al., 2003). The epicardium is the principal source of RA in the developing heart, and RETINALDEHYDE DEHYDROGENASE (RALDH)2, the rate-limiting enzyme in RA synthesis, is highly expressed in the epicardium but not in the myocardium (Moss et al., 1998).

The early dependence of myocardial proliferation on Fgf was shown by expression of a DOMINANT NEGATIVE Fgfr1 construct in developing myocardium (Mima et al., 1995). Fgf2 and Fgfr1 expression is higher in the compact myocardium where proliferation is higher than in the trabeculae. The level of myocyte proliferation is reduced in epicardium-deficient hearts, and Fgf2 and Fgfr1 mRNA levels are reduced proportional to the amount of epicardium that is missing (Pennisi et al., 2003).

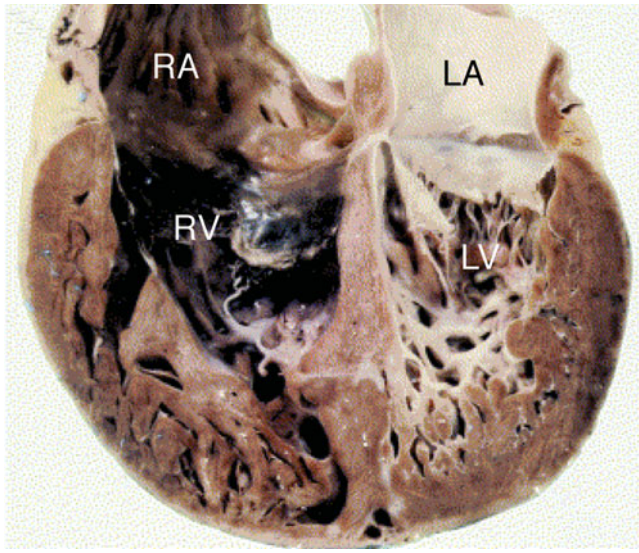

Figure 4.11. Trans-sectional anterior view of the dorsal half of the heart of a 21-year-old man. Note the numerous trabeculae and deep recesses with marked fibroelastosis (*white*) of the left ventricle. (From Oechslin et al., 2000, with permission.)

Myocardial Bioenergetics During Development

Nfat is associated with changes in gene expression and myocyte function. Null mutation of *Nfatc3* and *Nfatc4* shows that they are required during cardiac morphogenesis for mitochondrial energy metabolism to maintain myocardial function and proliferation. In the mutants, cardiac mitochondria are swollen with abnormal CRISTAE along with reduction of enzymatic activity of COMPLEX II AND IV of the respiratory chain and mitochondrial oxidative activity (Bushdid et al., 2003). Nfat regulates the expression of metabolic proteins such as adenyl succinate synthase I and carnitine palmitoyltransferase I (Moore et al., 2001; Xia et al., 2000). Combined disruption of the *Nfatc3* and *Nfatc4* genes results in death at E11. The ventricular gene profile established at E10.5–11.5 in mouse development includes chamber restriction of contractile protein, Ca^{2+} handling and metabolic gene expression (Shepard et al., 1998). In rat embryos at comparable ages, cardiac mitochondrial maturation occurs, and there is increased dependence on oxidative phosphorylation for energy production (Fantel and Person, 2002; Lopaschuk et al., 1992; Shepard et al., 1998).

Myocardial Developmental Disorders

Noncompaction of the Myocardium and Hypertrabeculation

Noncompaction of the ventricular wall is a rare developmental anomaly characterized by numerous, loosely compacted, and prominent ventricular trabeculations with deep intertrabecular recesses (Fig. 4.11). It was first described in the pediatric population in 1990 and later in adults (Chin et al., 1990; Oda et al., 2005). The disorder may be associated with several cardiac malformations, facial DYSMORPHISM, and FAMILIAL RECURRENCE. It is caused by failure of the myocardium to differentiate normally during embryonic development. The noncompaction can affect only one or both ventricles (Fig. 4.11). Mutations in the X-linked *G4.5* gene (Xq28 region) are responsible for cases of isolated left ventricular noncompaction in male infants. A recent study showed linkage of autosomal dominant left ventricular noncompaction with adult onset to chromosome 11p15 (Sasse-Klaassen et al., 2004). The disease carries a risk of association with other cardiac anomalies, progressive left ventricular dysfunction, systemic EMBOLISM, and lethal ARRHYTHMIAS.

Cardiomyopathy

Idiopathic dilated CARDIOMYOPATHY (Table 4.1) is the diagnosis when all other causes of left ventricular dilation and SYSTOLIC dysfunction have been excluded. When it occurs in families it is known as familial dilated cardiomyopathy, which may be as much as 20%–50% of IDIOPATHIC dilated cardiomyopathy cases. Sixteen genes are associated with AUTOSOMAL dominant familial dilated cardiomyopathy. Familial dilated cardiomyopathy demonstrates incomplete penetrance, variable expression, and significant locus and ALLELIC heterogeneity, making clinical and genetic diagnosis complex (Burkett and Hershberger, 2005). Most genes associated with cardiomyopathies code for proteins associated with the contractile apparatus or with mitochondrial energy handling mechanisms.

Table 4.1.
Genes Associated with Cardiomyopathies

Gene	Protein	Function	References
		Autosomal Dominant FDC	
ACTC	Cardiac actin	Sarcomeric protein; muscle contraction	Olson et al., 1998
DES	Desmin	Dystrophin-associated glycoprotein complex; transduces contractile forces	Li et al., 1999
SGCD	δ-Sarcoglycan	Dystrophin-associated glycoprotein complex; transduces contractile forces	Tsubata et al., 2000
TMYH7	β-Myosin heavy chain	Sarcomeric protein; muscle contraction	Daehmlow et al., 2002; Kamisago et al., 2000
TNNT2	Cardiac troponin T	Sarcomeric protein; muscle contraction	Hanson et al., 2002, Kamisago et al., 2000; Li et al., 2001
TPM1	α-Tropomyosin	Sarcomeric protein; muscle contraction	Olson et al., 2001
TTN	Titin	Sarcomere structure/extensible scaffold for other proteins	Gerull et al., 2002
VCL	Metavinculin	Sarcomere structure; intercalated discs	Olson et al., 2002
MYBPC	Myosin-binding protein C	Sarcomeric protein; muscle contraction	Daehmlow et al., 2002
MLP/CSRP3	Muscle LIM protein	Sarcomere stretch sensor/Z discs	Knoll et al., 2002
ACTN2	α-Actinin-2	Sarcomere structure; anchor for myofibrillar actin	Mohapatra et al., 2003
PLN	Phospholamban	Sarcoplasmic reticulum Ca^{++} regulator; inhibits SERCA2 pump	Haghighi et al., 2003; Schmitt et al., 2003
ZASP/LBD3	Cypher/LIM binding domain 3	Cytoskeletal assembly; involved in targeting and clustering of membrane proteins	Vatta et al., 2003
MYH6	α-Myosin heavy chain	Sarcomeric protein; muscle contraction	Taylor et al., 2003
ABCC	SUR2A	Regulatory subunit of Kir6.2, an inwardly rectifying cardiac K_{ATP} channel	Bienengraeber et al., 2004
LMNA	Lamin A/C	Inner leaflet, nuclear membrane protein; confers stability to nuclear membrane; gene expression	Arbustini et al., 2002; Becane et al., 2000; Brodsky et al., 2000; Fatkin et al., 1999; Hershberger et al., 2002; Jakobs et al., 2001; Sebillon et al., 2003; Taylor et al., 2003
		X-linked FDC	
DMD	Dystrophin	Primary component of dystrophin-associated glycoprotein complex; transduces contractile force	Mima et al., 1995; Muntoni et al., 1993; Towbin et al., 1993
TAZ/G4.5	Tafazzin	Unknown	Bione et al., 1996; D'Adamo et al., 1997; Farrell et al., 2001
		Recessive FDC	
TNN13	Cardiac troponin I	Sarcomeric protein, muscle contraction	Murphy et al., 2004

bp, base pair; CSD, conduction system disease; DCM, dilated cardiomyopathy; DNA, deoxyribonucleic acid; FDC, familial dilated cardiomyopathy; HF, heart failure; IDC, idiopathic dilated cardiomyopathy; LV, left ventricle; LVE, left ventricular enlargement; MD, muscular dystrophy; MM, missense mutation; NM, nonsense mutation; NSVT, non-sustained ventricular tachycardia; pts, patients; SCD, sudden cardiac death.
Adapted from (Burkett and Hershberger, 2005).

REFERENCES

Abu-Issa, R., G. Smyth, I. Smoak, K.-I. Yamamura, and E. Meyers. 2002. *Fgf8* is required for pharyngeal arch and cardiovascular development in the mouse. Development 129:4613–4625.

Ahn, D., I. Ruvinsky, A. C. Oates, L. M. Silver, and R. K. Ho. 2000. *tbx20* a new vertebrate T-box gene expressed in the cranial motor neurons and developing cardiovascular structures in zebrafish. Mech. Dev. 95:253–258.

Alsan, B. H., and T. M. Schultheiss. 2002. Regulation of avian cardiogenesis by Fgf8 signaling. Development 129:1935–1943.

Antin, P. B., R. G. Taylor, and T. Yatskievych. 1994. Precardiac mesoderm is specified during gastrulation in quail. Dev. Dyn. 200:144–154.

Araki, I., and M. Brand. 2001. Morpholino-induced knockdown of *fgf8* efficiently phenocopies the acerebellar (ace) phenotype. Genesis 30:157–159.

Arbustini, E., A. Pilotto, A. Repetto, M. Grasso, A. Negri, M. Diegoli, C. Campana, L. Scelsi, E. Baldini, A. Gavazzi, and L. Tavazzi. 2002. Autosomal dominant dilated cardiomyopathy with atrioventricular block: a lamin A/C defect-related disease. J. Am. Coll. Cardiol. 39:981–990.

Arsenian, S., B. Weinhold, M. Oelgeschlager, U. Rüther, and A. Nordheim. 1998. Serum response factor is essential for mesoderm formation during mouse embryogenesis. EMBO J. 17:6289–6299.

Barron, M., M. Gao, and J. Lough. 2000. Requirement for BMP and FGF signaling during cardiogenic induction in non-precardiac mesoderm is specific, transient, and cooperative. Dev. Dyn. 218:383–393.

Becane, H. M., G. Bonne, S. Varnous, A. Muchir, V. Ortega, E. H. Hammouda, J. A. Urtizberea, T. Lavergne, M. Fardeau, B. Eymard, S. Weber, K. Schwartz, and D. Duboc. 2000. High incidence of sudden death with conduction system and myocardial disease due to lamins A and C gene mutation. Pacing Clin. Electrophysiol. 23:1661–1666.

Begemann, G., and P. W. Ingham. 2000. Developmental regulation of *Tbx5* in zebrafish embryogenesis. Mech. Dev. 90:299–304.

Belaguli, N. S., J. L. Sepulveda, V. Nigam, F. Charron, M. Nemer, and R. J. Schwartz. 2000. Cardiac tissue enriched factors serum response factor and GATA-4 are mutual coregulators. Mol. Cell. Biol. 20:7550–7558.

Biben, C., and R. P. Harvey. 1997. Homeodomain factor *Nkx2–5* controls left/right asymmetric expression of bHLH gene eHand during murine heart development. Genes Dev. 11:1357–1369.

Bienengraeber, M., T. M. Olson, V. A. Selivanov, E. C. Kathmann, F. O'Cochlain, F. Gao, A. B. Karger, J. D. Ballew, D. M. Hodgson, L. V. Zingman, Y. P. Pang, A. E. Alekseev, and A. Terzic. 2004. *ABCC9* mutations identified in human dilated cardiomyopathy disrupt catalytic KATP channel gating. Nat. Genet. 36:382–387.

Bione, S., P. D'Adamo, E. Maestrini, A. K. Gedeon, P. A. Bolhuis, and D. Toniolo. 1996. A novel X-linked gene, *G4.5*, is responsible for Barth syndrome. Nat. Genet. 12:385–389.

Black, B. L., and E. N. Olson. 1998. Transcriptional control of muscle development by myocyte enhancer factor-2 (MEF2) proteins. Annu. Rev. Cell Dev. Biol. 14:167–196.

Bour, B. A., M. A. O'Brien, W. L. Lockwood, E. S. Goldstein, R. Bodmer, P. H. Taghert, S. M. Abmayr, and H. T. Nguyen. 1995. *Drosophila MEF2*, a transcription factor that is essential for myogenesis. Genes Dev. 9:730–741.

Brand, T. 2003. Heart development: molecular insights into cardiac specification and early morphogenesis. Dev. Biol. 258:1–19.

Brodsky, G. L., F. Muntoni, S. Miocic, G. Sinagra, C. Sewry, and L. Mestroni. 2000. Lamin A/C gene mutation associated with dilated cardiomyopathy with variable skeletal muscle involvement. Circulation 101:473–476.

Bruneau, B. G. 2002. Transcriptional regulation of vertebrate cardiac morphogenesis. Circ. Res. 90:509–519.

Bruneau, B. G., Z.-Z. Bao, M. Tanaka, J. J. Schott, S. Izumo, C. L. Cepko, J. G. Seidman, and C. E. Seidman. 2000. Cardiac expression of the ventricle-specific homeobox gene *Irx4* is modulated by *Nkx2–5* and *dHand*. Dev. Biol. 217:266–277.

Bruneau, B. G., M. Logan, N. Davis, T. Levi, C. J. Tabin, J. G. Seidman, and C. E. Seidman. 1999. Chamber-specific cardiac expression of *Tbx5* and heart defects in Holt-Oram syndrome. Dev. Biol. 211:100–108.

Bruneau, B. G., G. Nemer, J. P. Schmitt, F. Charron, L. Robitaille, S. Caron, D. A. Conner, M. Gessler, M. Nemer, C. E. Seidman, and J. G. Seidman. 2001. A murine model of Holt-Oram syndrome defines roles of the T-box transcription factor *Tbx5* in cardiogenesis and disease. Cell 106:709–721.

Buchberger, A., and H. H. Arnold. 1999. The MADS domain containing transcription factor *cMef2a* is expressed in heart and skeletal muscle during embryonic chick development. Dev. Genes Evol. 209:376–381.

Burkett, E. L., and R. E. Hershberger. 2005. Clinical and genetic issues in familial dilated cardiomyopathy. J. Am. Coll. Cardiol. 45:969–981.

Bushdid, P. B., H. Osinska, R. R. Waclaw, J. D. Molkentin, and K. E. Yutzey. 2003. *NFATc3* and *NFATc4* are required for cardiac development and mitochondrial function. Circ. Res. 92: 1305–1313.

Carson, C. T., E. R. Kinzler, and B. A. Parr. 2000. *Tbx12*, a novel T-box gene, is expressed during early stages of heart and retinal development. Mech. Dev. 96:137–140.

Cebra-Thomas, J. A., J. Bromer, R. Gardner, G. K. Lam, H. Sheipe, and S. F. Gilbert. 2003. T-box gene products are required for mesenchymal induction of epithelial branching in the embryonic mouse lung. Dev. Dyn. 226:82–90.

Chapman, D. L., N. Garvey, S. Hancock, M. Alexiou, S. I. Agulnik, J. J. Gibson-Brown, J. Cebra-Thomas, R. J. Bollag, L. M. Silver, and V. E. Papaioannou. 1996. Expression of the T-box family genes, *Tbx1–Tbx5*, during early mouse development. Dev. Dyn. 206:379–390.

Chapman, S. C., F. R. Schubert, G. C. Schoenwolf, and A. Lumsden. 2003. Anterior identity is established in chick epiblast by hypoblast and anterior definitive endoderm. Development 130:5091–5101.

Charron, F., and M. Nemer. 1999. GATA transcription factors and cardiac development. Semin. Cell Dev. Biol. 10:85–91.

Chen, C. Y., J. Croissant, M. Majesky, S. Topouzis, T. McQuinn, M. J. Frankovsky, and R. J. Schwartz. 1996. Activation of the cardiac alpha-actin promoter depends upon serum response factor, *Tinman* homologue, *Nkx-2.5*, and intact serum response elements. Dev. Genet. 19:119–130.

Chen, C.-Y., and R. Schwartz. 1996. Recruitment of the *tinman* homolog *Nkx2.5* by serum response factor activates cardiac α-actin gene transcription. Mol. Cell. Biol. 16:6372–6384.

Chen, F., H. Kook, R. Milewski, A. D. Gitler, M. M. Lu, J. Li, R. Nazarian, R. Schnepp, K. Jen, C. Biben, G. Runke, J. P. Mackay,

J. Novotny, R. J. Schwartz, R. P. Harvey, M. C. Mullins, and J. A. Epstein. 2002. *Hop* is an unusual homeobox gene that modulates cardiac development. Cell 110:713–723.

Chen, J.-N., and M. C. Fishman. 1996. Zebrafish *tinman* homolog demarcates the heart field and initiates myocardial differentiation. Development 122:3809–3816.

Chen, T. H., T. C. Chang, J. O. Kang, B. Choudhary, T. Makita, C. M. Tran, J. B. Burch, H. Eid, and H. M. Sucov. 2002. Epicardial induction of fetal cardiomyocyte proliferation via a retinoic acid-inducible trophic factor. Dev. Biol. 250:198–207.

Cheng, G. M., T. P. Hagen, M. L. Dawson, K. V. Barnes, and D. R. Menick. 1999. The role of GATA, CArG, E-box, and a novel element in the regulation of cardiac expression of the Na^{+}-Ca^{2+} exchanger gene. J. Biol. Chem. 274:12819–12826.

Chin, T. K., J. K. Perloff, R. G. Williams, K. Jue, and R. Mohrmann. 1990. Isolated noncompaction of left ventricular myocardium. A study of eight cases. Circulation 82:507–513.

Colas, J. F., A. Lawson, and G. C. Schoenwolf. 2000. Evidence that translation of smooth muscle alpha-actin mRNA is delayed in the chick promyocardium until fusion of the bilateral heart-forming regions. Dev. Dyn. 218:316–330.

D'Adamo, P., L. Fassone, A. Gedeon, E. A. Janssen, S. Bione, P. A. Bolhuis, P. G. Barth, M. Wilson, E. Haan, K. H. Orstavik, M. A. Patton, A. J. Green, E. Zammarchi, M. A. Donati, and D. Toniolo. 1997. The X-linked gene *G4.5* is responsible for different infantile dilated cardiomyopathies. Am. J. Hum. Genet. 61:862–867.

Daehmlow, S., J. Erdmann, T. Knueppel, C. Gille, C. Froemmel, M. Hummel, R. Hetzer, and V. Regitz-Zagrosek. 2002. Novel mutations in sarcomeric protein genes in dilated cardiomyopathy. Biochem. Biophys. Res. Commun. 298:116–120.

Dell'Era, P., R. Ronca, L. Coco, S. Nicoli, M. Metra, and M. Presta. 2003. Fibroblast growth factor receptor-l is essential for in vitro cardiomyocyte development. Circ. Res. 93:414–420.

Du, A., J. M. Sanger, K. K. Linask, and J. W. Sanger. 2003. Myofibrillogenesis in the first cardiomyocytes formed from isolated quail precardiac mesoderm. Dev. Biol. 257:382–394.

Durocher, D., F. Charron, R. Waren, R. Schwartz, and M. Nemer. 1997. The cardiac transcription factors *Nkx2–5* and GATA-4 are mutual cofactors. EMBO J. 16:5687–5696.

Ehler, E., B. M. Rothen, S. P. Hmmerle, M. Komiyama, and J. C. Perriard. 1999. Myofibrillogenesis in the developing chicken heart: assembly of Z-disk, M-line and the thick filaments. J. Cell Sci. 112:1529–1539.

Ehrman, L. A., and K. E. Yutzey. 1999. Lack of regulation in the heart forming region of avian embryos. Dev. Biol. 207:163–175.

Erokhina, E. L. 1968. [Proliferation dynamics of cellular elements in the differentiating mouse myocardium]. Tsitologiia 10:1391–1409.

Fantel, A. G., and R. E. Person. 2002. Involvement of mitochondria and other free radical sources in normal and abnormal fetal development. Ann. NY Acad. Sci. 959:424–433.

Fatkin, D., C. MacRae, T. Sasaki, M. R. Wolff, M. Porcu, M. Frenneaux, J. Atherton, H. J. Vidaillet, Jr., S. Spudich, U. De Girolami, J. G. Seidman, C. Seidman, F. Muntoni, G. Muehle, W. Johnson, and B. McDonough. 1999. Missense mutations in the rod domain of the *lamin A/C* gene as causes of dilated cardiomyopathy and conduction-system disease. N. Engl. J. Med. 341:1715–1724.

Firulli, A. B., D. G. McFadden, Q. Lin, D. Srivastava, and E. N. Olson. 1998. Heart and extra-embryonic mesodermal defects in mouse embryos lacking the bHLH transcription factor Hand1. Nat. Genet. 18:266–270.

Fishman, M. C., and K. R. Chien. 1997. Fashioning the vertebrate heart: earliest embryonic decisions. Development 124: 2099–2117.

Frank, D., L. Fotheringham, J. Brewer, L. Muglia, Tristani-Firouzi, M. Capecchi, and A. Moon. 2002. An *Fgf8* mouse mutant phenocopies human 22q11 deletion syndrome. Development 129: 4591–4603.

Gannon, M., and D. Bader. 1995. Initiation of cardiac differentiation occurs in the absence of anterior endoderm. Development 121:2439–2450.

Gassmann, M., F. Casagranda, D. Orioli, H. Simon, C. Lai, R. Klein, and G. Lemke. 1995. Aberrant neural and cardiac development in mice lacking the ErbB4 neuregulin receptor. Nature 378: 390–394.

Gerull, B., M. Gramlich, J. Atherton, M. McNabb, K. Trombitas, S. Sasse-Klaassen, J. G. Seidman, C. Seidman, H. Granzier, S. Labeit, M. Frenneaux, and L. Thierfelder. 2002. Mutations of *TTN*, encoding the giant muscle filament titin, cause familial dilated cardiomyopathy. Nat. Genet. 30:201–204

Ghosh-Choudhury, N. G., S. L. Abboud, L. Mahimainathan, B. Chandrasekar, and G. G. Choudhury. 2003. Phosphatidylinositol 3-kinase regulates bone morphogenetic protein-2 (BMP-2)-induced myocyte enhancer factor 2A-dependent transcription of BMP-2 gene in cardiomyocyte precursor cells. J. Biol. Chem. 278:21998–22005.

Gianakopoulos, P. J. and I. S. Skerjanc. 2005. Hedgehog signaling induces cardiomyogenesis in P19 cells. J. Biol. Chem. 280:21022–21028.

Gibson-Brown, J. J., S. I. Agulnik, L. M. Silver, and V. E. Papaioannou. 1998. Expression of T-box genes *Tbx2–Tbx5* during chick organogenesis. Mech. Dev. 74:165–169.

Gittenberger-de Groot, A. C., M. P. F. M. Peeters, M. Bergwerff, M. M. T. Mentink, and R. E. Poelmann. 2000. Epicardial outgrowth inhibition leads to compensatory mesothelial outflow tract collar and abnormal cardiac septation and coronary formation. Circ. Res. 87:969–971.

Goldmuntz, E., E. Geiger, and D. W. Benson. 2002. *Nkx2.5* mutations in patients with tetralogy of fallot. Circulation 104:2565–2568.

Habets, P. E. M. H., A. F. M. Moorman, D. E. W. Clout, M. A. van Roon, M. Lingbeek, M. van Lohuizen, M. Campione, and V. M. Christoffels. 2002. Cooperative action of *Tbx2* and *Nkx2.5* inhibits ANF expression in the atrioventricular canal: implications for cardiac chamber formation. Genes Dev. 16:1234–1246.

Haghighi, K., F. Kolokathis, L. Pater, R. A. Lynch, M. Asahi, A. O. Gramolini, G. C. Fan, D. Tsiapras, H. S. Hahn, S. Adamopoulos, S. B. Liggett, G. W. Dorn, 2nd, D. H. MacLennan, D. T. Kremastinos, and E. G. Kranias. 2003. Human phospholamban null results in lethal dilated cardiomyopathy revealing a critical difference between mouse and human. J. Clin. Invest. 111:869–876.

Han, Y., J. E. Dennis, L. Cohen-Gould, D. M. Bader, and D. A. Fischman. 1992. Expression of sarcomeric myosin in the presumptive myocardium of chicken embryos occurs within six hours of myocyte commitment. Dev. Dyn. 193:257–265.

Hanson, E. L., P. M. Jakobs, H. Keegan, K. Coates, S. Bousman, N. H. Dienel, M. Litt, and R. E. Hershberger. 2002. Cardiac troponin T lysine 210 deletion in a family with dilated cardiomyopathy. J. Card. Fail. 8:28–32.

Hatcher, C. J., M.-S. Kim, C. S. Mah, M. M. Goldstein, B. Wong, T. Mikawa, and C. T. Basson. 2001. TBX5 transcription factor regulates cell proliferation during cardiogenesis. Dev. Biol. 230:177–188.

Hayata, T., H. Kuroda, A. Eisaki, and M. Asashima. 1999. Expression of *Xenopus* T-box transcription factor, *tbx2* in *Xenopus* embryo. Dev. Genes Evol. 209:625–628.

Hershberger, R. E., E. L. Hanson, P. M. Jakobs, H. Keegan, K. Coates, S. Bousman and M. Litt. 2002. A novel lamin A/C mutation in a family with dilated cardiomyopathy, prominent conduction system disease, and need for permanent pacemaker implantation. Am. Heart J. 144:1081–1086.

Hiroi, Y., S. Kudoh, K. Monzen, Y. Ikeda, Y. Yazaki, R. Nagai, and I. Komuro. 2001. *Tbx5* associates with *Nkx2–5* and synergistically promotes cardiomyocyte differentiation. Nat. Genet. 28:276–280.

Horb, M. E., and G. H. Thomsen. 1999. Tbx5 is essential for heart development. Development 126:1739–1751.

Hyer, J., and T. Mikawa. 1997. Retroviral techniques for studying organogenesis with a focus on heart development. Mol. Cell. Biochem. 172:23–35.

Ishibashi, Y., Y. Urabe, H. Tsutsui, S. Kinugawa, M. Sugimachi, M. Takahashi, S. Yamamoto, H. Tagawa, K. Sunagawa, and A. Takeshita. 1997. Negative inotropic effect of basic fibroblast growth factor on adult rat cardiac myocyte. Circulation 96: 2501–2504.

Jacobson, A. G. 1960. Influences of ectoderm and endoderm on heart differentiation in the newt. Dev. Biol. 2:138–154.

Jacobson, A. G. 1961. Heart determination in the newt. J. Exp. Zool. 146:139–151.

Jacobson, A. G., and J. T. Duncan. 1968. Heart induction in salamanders. Exp. Zool. 167:79–103.

Jakobs, P. M., E. L. Hanson, K. A. Crispell, W. Toy, H. Keegan, K. Schilling, T. B. Icenogle, M. Litt, and R. E. Hershberger. 2001. Novel *lamin A/C* mutations in two families with dilated cardiomyopathy and conduction system disease. J. Card. Fail. 7:249–256.

Jamali, M., C. Karamboulas, P. J. Rogerson, and I. S. Skerjanc. 2001. BMP signaling regulates *Nkx2–5* activity during cardiomyogenesis. FEBS Lett. 509:126–130.

Jeter, J. R., and I. L. Cameron. 1971. Cell proliferation patterns during cytodifferentiation in embryonic chick tissues: liver, heart and erythrocytes. J. Embryol. Exp. Morph. 23:403–422.

Jiang, Y., S. Tarzami, J. B. E. Burch, and T. Evans. 1998. Common role for each of the *cgata-4/5/6* genes in the regulation of cardiac morphogenesis. Dev. Genet. 22:263–277.

Kamisago, M., S. D. Sharma, S. R. DePalma, S. Solomon, P. Sharma, B. McDonough, L. Smoot, M. P. Mullen, P. K. Woolf, E. D. Wigle, J. G. Seidman, and C. E. Seidman. 2000. Mutations in sarcomere protein genes as a cause of dilated cardiomyopathy. N. Engl. J. Med. 343:1688–1696.

Kasahara, H., and S. Izumo. 1999. Identification of the in vitro casein kinase II phosphorylation site within the homeodomain of the cardiac tissue-specifying homeobox gene product *Csx/Nkx2.5*. Mol. Cell Biol. 19:526–536.

Knoll, R., M. Hoshijima, H. M. Hoffman, V. Person, I. Lorenzen-Schmidt, M. L. Bang, T. Hayashi, N. Shiga, H. Yasukawa, W. Schaper, W. McKenna, M. Yokoyama, N. J. Schork, J. H. Omens, A. D. McCulloch, A. Kimura, C. C. Gregorio, W. Poller, J. Schaper, H. P. Schultheiss, and K. R. Chien. 2002. The cardiac mechanical stretch sensor machinery involves a Z disc complex that is defective in a subset of human dilated cardiomyopathy. Cell 111:943–955

Kortschak, R. D., P. W. Tucker, and R. Saint. 2000. ARID proteins come in from the desert. Trends Biochem. Sci. 25:294–299.

Kreidberg, J. A., H. Sariola, J. M. Loring, M. Maeda, J. Pelletier, D. Housman, and R. Jaenisch. 1993. WT-1 is required for early kidney development. Cell 74:679–691.

Kruithof, B. P. T., M. van den Hoff, S. Tesink-Taekema, and A. F. Moorman. 2003. Recruitment of intra- and extracardiac cells into the myocardial lineage during mouse development. Anat. Rec. 271:303–314.

Kuo, C. T., E. E. Morrisey, R. Anandappa, K. Sigrist, M. M. Lu, M. S. Parmacek, C. Soudais, and J. M. Leiden. 1997. GATA4 transcription factor is required for ventral morphogenesis and heart tube formation. Genes Dev. 11:1048–1060.

Kwee, L., H. S. Baldwin, H. M. Shen, C. L. Stewart, C. Buck, C. A. Buck, and M. A. Labow. 1995. Defective development of the embryonic and extraembryonic circulatory systems in vascular cell adhesion molecule (VCAM-1) deficient mice. Development 121:489–503.

Ladd, A. N., T. A. Yatskievych, and P. B. Antin. 1998. Regulation of avian cardiac myogenesis by activin/TGFbeta and bone morphogenetic proteins. Dev. Biol. 204:407–419.

Lee, K.-F., H. Simon, H. Chen, B. Bates, M.-C. Hung, and C. Hauser. 1995. Requirement for neuregulin receptor erbB2 in neural and cardiac development. Nature 378:394–398.

Li, D., G. Z. Czernuszewicz, O. Gonzalez, T. Tapscott, A. Karibe, J. B. Durand, R. Brugada, R. Hill, J. M. Gregoritch, J. L. Anderson, M. Quinones, L. L. Bachinski, and R. Roberts. 2001. Novel cardiac troponin T mutation as a cause of familial dilated cardiomyopathy. Circulation 104:2188–2193.

Li, D., T. Tapscoft, O. Gonzalez, P. E. Burch, M. A. Quinones, W. A. Zoghbi, R. Hill, L. L. Bachinski, D. L. Mann, and R. Roberts. 1999. Desmin mutation responsible for idiopathic dilated cardiomyopathy. Circulation 100:461–464.

Li, F., X. Wang, J. M. Capasso, and A. M. Gerdes. 1996. Rapid transition of cardiac myocytes from hyperplasia to hypertrophy during postnatal development. J. Mol. Cell. Cardiol. 28:1737–1746.

Li, F., X. Wang, and A. M. Gerdes. 1997. Formation of binucleated cardiac myocytes in rat heart: II. Cytoskeletal organisation. J. Mol. Cell. Cardiol. 29:1553–1565.

Liberatore, C. M., R. D. Searcy-Schrick, E. B. Vincent, and K. E. Yutzey. 2002. *Nkx-2.5* gene induction in mice is mediated by a smad consensus regulatory region. Dev. Biol. 244:243–256.

Liberatore, C. M., R. D. Searcy-Schrick, and K. E. Yutzey. 2000. Ventricular expression of *tbx5* inhibits normal heart chamber development. Dev. Biol. 223:169–180.

Lickert, H., S. Kutsch, B. Kanzler, Y. Tamai, M. M. Taketo, and R. Kemler. 2002. Formation of multiple hearts in mice following deletion of beta-catenin in the embryonic endoderm. Dev. Cell 3:171–181.

Lien, C. L., C. Z. Wu, B. Mercer, R. Webb, J. A. Richardson, and E. N. Olson. 1999. Control of early cardiac-specific transcription of *Nkx2–5* by a GATA-dependent enhancer. Development 126:75–84.

Lin, Q., J. Schwarz, C. Bucana, and E. N. Olson. 1997. Control of mouse cardiac morphogenesis and myogenesis by transcription factor *MEF2C*. Science 276:1405–1407.

Lopaschuk, G. D., R. L. Collins-Nakai, and T. Itoi. 1992. Developmental changes in energy substrate use by the heart. Cardiovasc. Res. 26:1172–1180.

Lough, J., M. Barron, M. Brogley, Y. Sugi, D. L. Bolender, and X. Zhu. 1996. Combined BMP-2 and FGF-4, but neither factor alone,

induces cardiogenesis in non-precardiac embryonic mesoderm. Dev. Biol. 178:198–202.

Lough, J., and Y. Sugi. 2000. Endoderm and heart development. Dev. Dyn. 217:327–342.

Lu, J., T. A. McKinsey, R. L. Nicol, and E. N. Olson. 2000. Signal-dependent activation of the MEF2 transcription factor by dissociation from histone deacetylases. Proc. Natl. Acad. Sci. USA 97:4070–4075.

Lyons, G. E., S. Schiaffino, D. Sassoon, P. Barton, and M. Buckingham. 1990. Developmental regulation of myosin gene expression in mouse cardiac muscle. J. Cell Biol. 111:2427–2436.

Lyons, I., L. Parsons, L. Hartley, R. Li, J. E. Andrews, L. Robb, and R. P. Harvey. 1995. Myogenic and morphogenetic defects in the heart tubes of murine embryos lacking the homeo box gene *Nkx2–5*. Genes Dev. 9:1654–1666.

Manasek, F. J. 1968. Embryonic development of the heart I: A light and electron microscope study of myocardial development in the early chick embryo. J. Morphol. 125:329–366.

Manner, J., J. M. Perez-Pomares, D. Macias and R. Munoz-Chapuli. 2001. The origin, formation and developmental significance of the epicardium: a review. Cells Tissues Organs 169:89–103.

Marlow, F., J. Topczewski, D. Sepich, and L. Solnica-Krezel. 2002. Zebrafish Rho kinase 2 acts downstream of Wnt11 to mediate cell polarity and effective convergence and extension movements. Curr. Biol. 12:876–884.

Marvin, M. J., G. Di Rocco, A. Gardiner, S. M. Bush, and A. B. Lassar. 2001. Inhibition of Wnt activity induces heart formation from posterior mesoderm. Genes Dev. 15:316–327.

McFadden, D. G., C. J., J. A. Richardson, D. Srivastava, A. B. Firulli, and E. N. Olson. 2000. A GATA-dependent right ventricular enhancer controls *dHAND* transcription in the developing heart. Development 127:5331–5341.

Meilhac, S. M., R. G. Kelly, D. Rocancourt, S. Eloy-Trinquet, J.-F. Nicolas, and M. E. Buckingham. 2003. A retrospective clonal analysis of the myocardium reveals two phases of clonal growth in the developing mouse heart. Development 130:3877–3889.

Meyer, D., and C. Birchmeier. 1995. Multiple essential functions of neuregulin in development. Nature 378:386–390.

Mima, T., H. Ueno, D. A. Fischman, L. T. Williams, and T. Mikawa. 1995. Fibroblast growth factor receptor is required for in vivo cardiac myocyte proliferation at early embryonic stages of heart development. Proc. Natl. Acad. Sci. USA 92:467–471.

Mjaatvedt, C. H., T. Nakaoka, R. Moreno-Rodriguez, R. A. Norris, M. J. Kern, C. A. Eisenberg, D. Turner, and R. R. Markwald. 2001. The outflow tract of the heart is recruited from a novel heart-forming field. Dev. Biol. 238:97–109.

Mohapatra, B., S. Jimenez, J. H. Lin, K. R. Bowles, K. J. Coveler, J. G. Marx, M. A. Chrisco, R. T. Murphy, P. R. Lurie, R. J. Schwartz, P. M. Elliott, M. Vatta, W. McKenna, J. A. Towbin, and N. E. Bowles. 2003. Mutations in the muscle LIM protein and alpha-actinin-2 genes in dilated cardiomyopathy and endocardial fibroelastosis. Mol. Genet. Metab. 80:207–215.

Molkentin, J., Q. Lin, S. Duncan, and E. Olson. 1997. Requirement of the transcription factor GATA4 for heart tube formation and ventral morphogenesis. Genes Dev. 11:1061–1072.

Molkentin, J. D. 2000. The zinc finger-containing transcription factors GATA-4, -5, and -6—Ubiquitously expressed regulators of tissue-specific gene expression. J. Biol. Chem. 275:38949–38952.

Molkentin, J. D., C. Antos, B. Mercer, T. Taigen, J. M. Miano, and E. N. Olson. 2000. Direct activation of a GATA6 cardiac enhancer by *Nkx2.5*: Evidence for a reinforcing regulatory network of *Nks2.5* and GATA transcription factors in the developing heart. Dev. Biol. 217:301–309.

Molkentin, J. D., J. R. Lu, C. L. Antos, B. Markham, J. Richardson, J. Robbins, S. R. Grant, and E. N. Olson. 1998. A calcineurin-dependent transcriptional pathway for cardiac hypertrophy. Cell 93:215–228.

Monzen, K., I. Shiojima, Y. Hiroi, S. Kudoh, T. Oka, E. Takimoto, D. Hayashi, T. Hosoda, A. Habara-Ohkubo, T. Nakaoka, T. Fujita, Y. Yazaki, and I. Komuro. 1999. Bone morphogenetic proteins induce cardiomyocyte differentiation through the mitogen-activated protein kinase kinase kinase TAK1 and cardiac transcription factors *Csx/Nkx-2.5* and GATA-4. Mol. Cell Biol. 19:7096–7105.

Moon, R. T., B. Bowerman, M. Boutros, and N. Perrimon. 2002. The promise and perils of Wnt signaling through β-catenin. Science 296:1644–1646.

Moore, A. W., L. McInnes, J. Kreidberg, N. D. Hastie, and A. Schedl. 1999. YAC complementation shows a requirement for Wt1 in the development of epicardium, adrenal gland and throughout nephrogenesis. Development 126:1845–1857.

Moore, M. L., G. L. Wang, N. S. Belaguli, R. J. Schwartz, and J. B. McMillin. 2001. GATA-4 and serum response factor regulate transcription of the muscle-specific carnitine palmitoyltransferase I beta in rat heart. J. Biol. Chem. 276:1026–1033.

Morin, S., F. Charron, L. Robitaille, and M. Nemer. 2000. GATA-dependent recruitment of MEF2 proteins to target promoters. EMBO J. 19:2046–2055.

Moss, J. B., J. Xavier-Neto, M. D. Shapiro, S. M. Nayeem, P. McCaffery, U. C. Drager, and N. Rosenthal. 1998. Dynamic patterns of retinoic acid synthesis and response in the developing mammalian heart. Dev. Biol. 199:55–71.

Muntoni, F., M. Cau, A. Ganau, R. Congiu, G. Arvedi, A. Mateddu, M. G. Marrosu, C. Cianchetti, G. Realdi, A. Cao, et al. 1993. Brief report: deletion of the dystrophin muscle-promoter region associated with X-linked dilated cardiomyopathy. N. Engl. J. Med. 329:921–925.

Murphy, R. T., J. Mogensen, A. Shaw, T. Kubo, S. Hughes, and W. J. McKenna. 2004. Novel mutation in cardiac troponin I in recessive idiopathic dilated cardiomyopathy. Lancet 363:371–372.

Narita, N., M. Bielinska, and D. B. Wilson. 1997. Cardiomyocyte differentiation by GATA-4-deficient embryonic stem cells. Development 124:3755–3764.

Nicholas, S. B., and K. D. Philipson. 1999. Cardiac expression of the Na(+)/Ca(2+) exchanger NCX1 is GATA factor dependent. Am. J. Physiol. 277:H324–330.

Oda, Y., S. Tsunoda, T. Doue, Y. Iida, and H. Matsubara. 2005. Clinical characteristics and morphologic features of isolated noncompaction of the ventricular myocardium: electrocardiogram-gated magnetic resonance imaging can elucidate more accurate biventricular structures. Heart Vessels 20:126–127.

Oechslin, E. N., C. H. Attenhofer Jost, J. R. Rojas, P. A. Kaufmann, and R. Jenni. 2000. Long-term follow-up of 34 adults with isolated left ventricular noncompaction: a distinct cardiomyopathy with poor prognosis. J. Am. Coll. Cardiol. 36:493–500.

Olson, T. M., S. Illenberger, N. Y. Kishimoto, S. Huttelmaier, M. T. Keating, and B. M. Jockusch. 2002. Metavinculin mutations alter actin interaction in dilated cardiomyopathy. Circulation 105: 431–437.

Olson, T. M., N. Y. Kishimoto, F. G. Whitby, and V. V. Michels. 2001. Mutations that alter the surface charge of alpha-tropomyosin

are associated with dilated cardiomyopathy. J. Mol. Cell. Cardiol. 33:723–732.

Olson, T. M., V. V. Michels, S. N. Thibodeau, Y. S. Tai, and M. T. Keating. 1998. Actin mutations in dilated cardiomyopathy, a heritable form of heart failure. Science 280:750–752.

Orts-Llorca, F. 1963. [Influence of the endoblast in the morphogenesis and late differentiation of the chick heart]. Acta Anat. (Basel) 52:202–214.

Pennisi, D. J., V. L. T. Ballard, and T. Mikawa. 2003. Epicardium is required for the full rate of myocyte proliferation and levels of expression of myocyte mitogenic factors FGF2 and its receptor FGFR-1, but not for transmural myocardial patterning in the embryonic chick heart. Dev. Dyn. 228:161–172.

Reifers, F., E. C. Walsh, S. Leger, D. Y. R. Stainier, and M. Brand. 2000. Induction and differentiation of the zebrafish heart requires fibroblast growth factor 8 (fgf8/acerebellar). Development 127:225–235.

Riley, P., L. Anson-Cartwright, and J. C. Cross. 1998. The *Hand1* bHLH transcription factor is essential for placentation and cardiac morphogenesis. Nat. Genet. 18:271–275.

Rones, M. S., K. A. McLaughlin, M. Raffin, and M. Mercola. 2000. Serrate and Notch specify cell fates in the heart field by suppressing cardiomyogenesis. Development 127:3865–3876.

Ross, R. S., S. Navankasattusas, R. P. Harvey, and K. R. Chien. 1996. An HF-1a/HF-1b/MEF-2 combinatorial element confers cardiac ventricular specificity and establishes an anterior-posterior gradient of expression. Development 122:1799–1809.

Rychter, Z., and B. Ostadal. 1971. Mechanism of the development of coronary arteries in chick embryos. Folia Morphol. 19:113–124.

Rychterova, V. 1971. Principle of growth in thickness of the heart ventricular wall in the chick embryo. Folia Morphol. 19:262–272.

Rychterova, V. 1978. Development of proliferation structure of the ventricular heart wall in the chick embryo between the 6th and 14th day of embryogenesis. Folia Morphol. 26:131–143.

Sasse-Klaassen, S., S. Probst, B. Gerull, E. Oechslin, P. Nurnberg, A. Heuser, R. Jenni, H. C. Hennies, and L. Thierfelder. 2004. Novel gene locus for autosomal dominant left ventricular noncompaction maps to chromosome 11p15. Circulation 109:2720–2723.

Sassoon, D. A., I. Garner, and M. Buckingham. 1988. Transcripts of alpha-cardiac and alpha-skeletal actins are early markers for myogenesis in the mouse embryo. Development 104:155–164.

Sater, A. K., and A. G. Jacobson. 1989. The specification of heart mesoderm occurs during gastrulation in *Xenopus laevis*. Development 105:821–830.

Schmitt, J. P., M. Kamisago, M. Asahi, G. H. Li, F. Ahmad, U. Mende, E. G. Kranias, D. H. MacLennan, J. G. Seidman, and C. E. Seidman. 2003. Dilated cardiomyopathy and heart failure caused by a mutation in phospholamban. Science 299:1410–1413.

Schneider, V. A., and M. Mercola. 2001. Wnt antagonism initiates cardiogenesis in *Xenopus laevis*. Genes Dev. 15:304–315.

Schott, J. J., D. W. Benson, C. T. Basson, W. Pease, G. M. Silberbach, J. P. Moak, B. J. Maron, C. E. Seidman, and J. G. Seidman. 1998. Congenital heart disease caused by mutations in the transcription factor *NKX2–5*. Science 281:108–111.

Schultheiss, T. M., J. B. E. Burch, and A. B. Lassar. 1997. A role for bone morphogenetic proteins in the induction of cardiac myogenesis. Genes Dev. 11:451–462.

Schultheiss, T. M., S. Xydas, and A. B. Lassar. 1995. Induction of avian cardiac myogenesis by anterior endoderm. Development 121:4203–4214.

Searcy, R. D., E. B. Vincent, C. M. Liberatore, and K. E. Yutzey. 1998. A GATA-dependent nkx-2.5 regulatory element activates early cardiac gene expression in transgenic mice. Development 125: 4461–4470.

Sebillon, P., C. Bouchier, L. D. Bidot, G. Bonne, K. Ahamed, P. Charron, V. Drouin-Garraud, A. Millaire, G. Desrumeaux, A. Benaiche, J. C. Charniot, K. Schwartz, E. Villard, and M. Komajda. 2003. Expanding the phenotype of LMNA mutations in dilated cardiomyopathy and functional consequences of these mutations. J. Med. Genet. 40:560–567.

Sepulveda, J., N. Belagull, V. Nigam, C.-Y. Chen, M. Nemer, and R. J. Schwartz. 1998. GATA-4 and Nkx-2.5 coactivate *Nkx-2* DNA binding targets: role for regulating early cardiac gene expression. Mol. Cell Biol. 3405–3415.

Serbedzija, G. N., J. N. Chen, and M. C. Fishman. 1998. Regulation in the heart field of zebrafish. Development 125:1095–1101.

Severs, N. J. 2000. The cardiac muscle cell. Bioessays 22:188–199.

Shepard, T. H., L. A. Muffley, and L. T. Smith. 1998. Ultrastructural study of mitochondria and their cristae in embryonic rats and primate (*N. nemistrina*). Anat. Rec. 252:383–392.

Shi, Y., S. Katsev, C. Cai, and S. Evans. 2000. BMP signaling is required for heart formation in vertebrates. Dev. Biol. 224:226–237.

Shin, C. H., Z.-P. Liu, R. Passier, C.-L. Zhang, D.-Z. Wang, T. Harris, H. Yamagishi, J. A. Richardson, G. Childs, and E. N. Olson. 2002. Modulation of cardiac growth and development by HOP, an unusual homeodomain protein. Cell 110:725–735.

Skerjanc, I. S., H. Petropoulos, A. G. Ridgeway, and S. Wilton. 1998. Myocyte enhancer factor 2C and *Nkx2–5* up-regulate each other's expression and initiate cardiomyogenesis in P19 cells. J. Biol. Chem. 273:34904–34910.

Solloway, M. J., and R. P. Harvey. 2003. Molecular pathways in myocardial development: a stem cell perspective. Cardiovasc. Res. 58:264–277.

Soonpaa, M. H., K. K. Kim, L. Pajak, M. Franklin, and L. J. Field. 1996. Cardiomyocyte DNA synthesis and binucleation during murine development. Am. J. Physiol. 271:H2183–2189.

Srivastava, D., T. Thomas, Q. Lin, M. L. Kirby, D. Brown, and E. N. Olson. 1997. Regulation of cardiac mesodermal and neural crest development by the bHLH transcription factor, *dHAND*. Nat. Genet. 16:154–160.

Stuckmann, I., S. Evans, and A. B. Lassar. 2003. Erythropoietin and retinoic acid, secreted from the epicardium, are required for cardiac myocyte proliferation. Dev. Biol. 255:334–349.

Sugi, Y., and J. Lough. 1994. Anterior endoderm is a specific effector of terminal cardiac myocyte differentiation of cells from the embryonic heart forming region. Dev. Dyn. 100: 155–162.

Sugi, Y., and J. Lough. 1995. Activin-A and FGF-2 mimic the inductive effects of anterior endoderm on terminal cardiac myogenesis in vitro. Dev. Biol. 168:567–574.

Sugi, Y., J. Sasse, M. Barron, and J. Lough. 1995. Developmental expression of fibroblast growth factor receptor-1 (cek-1;flg) during heart development. Dev. Dyn. 202:115–125.

Svensson, P. J., D. Von Tell, M. L. Molander, M. Anvret, and A. Nordenskjold 1999. A heterozygous frameshift mutation in the endothelin-3 (*EDN-3*) gene in isolated Hirschsprung's disease. Pediatr. Res. 45:714–717.

Szeto, D. P., K. J. P. Griffin, and D. Kimelman. 2002. hrT is required for cardiovascular development in zebrafish. Development 129: 5093–5101.

Takeda, K., H. Kishi, X. F. Ma, Z. X. Yu, and R. S. Adelstein. 2003. Ablation and mutation of nonmuscle myosin heavy chain II-B results in a defect in cardiac myocyte cytokinesis. Circ. Res. 93:330–337.

Tanaka, M., Z. Chen, S. Bartunkova, N. Yamasaki, and S. Izumo. 1999. The cardiac homeobox gene *Csx/Nkx2.5* lies genetically upstream of multiple genes essential for heart development. Development 126:1269–1280.

Taylor, M. R., P. R. Fain, G. Sinagra, M. L. Robinson, A. D. Robertson, E. Carniel, A. Di Lenarda, T. J. Bohlmeyer, D. A. Ferguson, G. L. Brodsky, M. M. Boucek, J. Lascor, A. C. Moss, W. L. Li, G. L. Stetler, F. Muntoni, M. R. Bristow, and L. Mestroni. 2003. Natural history of dilated cardiomyopathy due to *lamin A/C* gene mutations. J. Am. Coll. Cardiol. 41:771–780.

Thompson, C. B. 1995. Apoptosis in the pathogenesis and treatment of disease. Science 267:1456–1462.

Tokuyasu, K. T. 1990. Co-development of embryonic myocardium and myocardial circulation. In: Developmental Cardiology: Morphogenesis and Function, ed. Clarke, E. B. and A. Takao, 205–208. Mount Kisco, NY: Futura.

Tonissen, K. F., T. A. Drysdale, T. J. Lints, R. P. Harvey, and P. A. Krieg. 1994. *XNkx-2.5*, a *Xenopus* gene related to *Nkx-2.5* and *tinman*: evidence for a conserved role in cardiac development. Dev. Biol. 162:325–328.

Towbin, J. A., J. F. Hejtmancik, P. Brink, B. Gelb, X. M. Zhu, J. S. Chamberlain, E. R. McCabe, and M. Swift. 1993. X-linked dilated cardiomyopathy. Molecular genetic evidence of linkage to the Duchenne muscular dystrophy (dystrophin) gene at the Xp21 locus. Circulation 87:1854–1865.

Toyoda, M., H. Shiratori, K. Nakajima, M. Kojima, M. Takahashi, M. Kubota, R. Suzuki-Migishima, Y. Motegi, M. Yokoyama, and T. Takeuchi. 2003. jumonji downregulates cardiac cell proliferation by repressing cyclin D1 expression. Dev. Biol. 5: 85–97.

Tsubata, S., K. R. Bowles, M. Vatta, C. Zintz, J. Titus, L. Muhonen, N. E. Bowles, and J. A. Towbin. 2000. Mutations in the human delta-sarcoglycan gene in familial and sporadic dilated cardiomyopathy. J. Clin. Invest. 106:655–662.

Vatta, M., B. Mohapatra, S. Jimenez, X. Sanchez, G. Faulkner, Z. Perles, G. Sinagra, J. H. Lin, T. M. Vu, Q. Zhou, K. R. Bowles, A. Di Lenarda, L. Schimmenti, M. Fox, M. A. Chrisco, R. T. Murphy, W. McKenna, P. Elliott, N. E. Bowles, J. Chen, G. Valle, and J. A. Towbin. 2003. Mutations in Cypher/ZASP in patients with dilated cardiomyopathy and left ventricular non-compaction. J. Am. Coll. Cardiol. 42:2014–2027.

Velez, C., A. E. Aránega, J. A. Marchal, C. Melguizo, J. C. Prados, E. Carrillo, and A. Aránega. 2000. Development of chick cardiomyocytes: modulation of intermediate filaments by basic fibroblast and platelet-derived growth factors. Cells Tissues Organs 167:163–170.

Velez, C., A. E. Aranega, C. Melguizo, J. E. Fernandez, J. Prados, and A. Aranega. 1994. Modulation of contractile protein troponin-T in chick myocardial cells by basic fibroblast growth factor and platelet-derived growth factor during development. J. Cardiovasc. Pharmacol. 24:906–913.

Wang, D., P. S. Chang, Z. Wang, L. Sutherland, J. A. Richardson, E. Small, P. A. Krieg, and E. N. Olson. 2001. Activation of cardiac gene expression by myocardin, a transcriptional cofactor for serum response factor. Cell 105:851–862.

Watt, A. J., M. A. Battle, J. Li, and S. A. Duncan. 2004. GATA4 is essential for formation of the proepicardium and regulates cardiogenesis. Proc. Natl. Acad. Sci. USA 101:12573–12578.

Weinhold, B., G. Schratt, S. Arsenian, J. Berger, K. Kamino, H. Schwarz, U. Ruther, and A. Nordheim. 2000. *Srf*(-/-) ES cells display non cell-autonomous impairment in mesodermal differentiation. EMBO J. 19:5835–5844.

Weiss, M. J. and S. H. Orkin. 1995. GATA transcription factors: key regulators of hematopoiesis. Exp. Hematol. 23:99–107.

Wilson-Rawls, J., J. D. Molkentin, B. L. Black, and E. N. Olson. 1999. Activated notch inhibits myogenic activity of the MADS-box transcription factor myocyte enhancer factor 2C. Mol. Cell Biol. 19:2853–2862.

Xia, Y., J. B. McMillin, A. Lewis, M. Moore, W. G. Zhu, R. S. Williams, and R. E. Kellems. 2000. Electrical stimulation of neonatal cardiac myocytes activates the NFAT3 and GATA4 pathways and up-regulates the adenylosuccinate synthetase 1 gene. J. Biol. Chem. 275:1855–1863.

Yamada, M., J. P. Revelli, G. Eichele, M. Barron, and R. J. Schwartz. 2000. Expression of chick *Tbx-2, Tbx-3*, and *Tbx-5* genes during early heart development: evidence for BMP2 induction of Tbx2. Dev. Biol. 228:95–105.

Yamagishi, H., C. Yamagishi, O. Nakagawa, R. P. Harvey, E. N. Olson, and D. Srivastava. 2001. The combinatorial activities of *Nkx2.5* and *dHAND* are essential for cardiac ventricle formation. Dev. Biol. 289:190–203.

Yang, J. T., H. Rayburn, and R. O. Hynes. 1995. Cell adhesion events mediated by à4 integrins are essential in placental and cardiac development. Development 121:549–560.

Yatskievych, T. A., A. N. Ladd, and P. B. Antin. 1997. Induction of cardiac myogenesis in avian pregastrula epiblast: the role of the hypoblast and activin. Development 124:2561–2570.

Zaffran, S., and M. Frasch. 2002. Early signals in cardiac development. Circ. Res. 91:457–469.

Zhang, X. M., M. Ramalho-Santos, and A. P. McMahon. 2001. Smoothened mutants reveal redundant roles for Shh and Ihh signaling including regulation of L/R asymmetry by the mouse mode. Cell 105:781–792.

Zhu, X., J. Sasse, D. McAllister, and J. Lough. 1996. Evidence that fibroblast growth factors 1 and 4 participate in regulation of cardiogenesis. Dev. Dyn. 207:429–438.

5 Tony L. Creazzo

Functional Developmental Biology of the Myocardium

Much of the biochemistry and physiology as well as morphology of heart development has been studied most rigorously in avian species, particularly the chick embryo because, like mammals, they have four-chambered hearts. With the advent of new technologies, mouse and zebrafish embryos have become important models particularly for genetic studies of early morphogenesis. However, detailed physiological studies remain difficult in these species and much of what is known in development still relies on results from the chick embryo. In the chick, development of various systems in the heart and muscle appears to be somewhat accelerated compared with that in mammals. This is not surprising considering that the chick must emerge on its own from its shell and must be able to function autonomously very quickly to survive. Small mammalian species have been used particularly in studies of later development including rat, rabbit, and now the mouse. In these species, the neonates are quite helpless at birth and development of mechanisms involved in cardiac contractile function is much delayed compared with that in humans. The rate of development in humans appears to fall somewhere between the chick and these mammalian species. It is important to note that regardless of variations in the rate of development, the cellular mechanisms necessary for generating rhythmic contractile force in mature hearts are qualitatively the same for birds and mammals. The specific proteins involved are highly conserved among these species with a very high degree of amino acid sequence identity.

Ion Channels and the Myocardial Action Potential

The heart is an electrically excitable tissue in that the plasma membranes of individual myocytes comprising the myocardium are rhythmically depolarized. The heart is dependent on action potentials (AP), time-dependent changes in the electrical potential of the surface plasma membrane (Fig. 5.1), to propagate the signal for the heart beat and to initiate the contraction of the myocardium in a process termed excitation–contraction coupling (discussed below). APs are generated through the activity of ION CHANNELS (Fig. 5.2). These are transmembrane proteins with an aqueous pore that conduct small mono- and

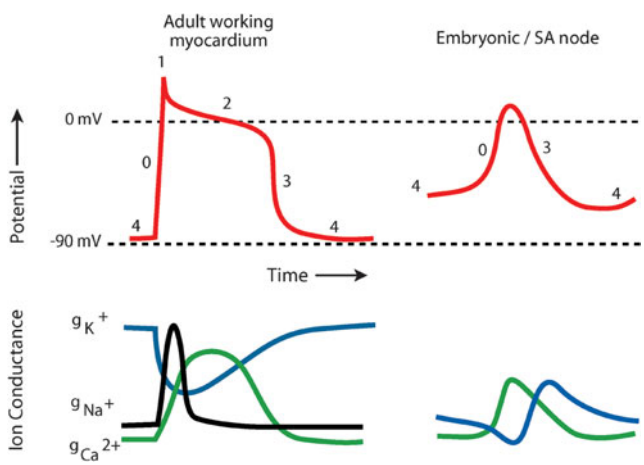

Figure 5.1. Cardiac action potentials. Shown are idealized action potentials (AP) from a mature ventricular and an early embryonic myocyte. Embryonic myocytes from the early stages of heart development (e.g., heart tube stage and for a short time after) are capable of spontaneous activity, and thus APs that resemble those measured in the pacemaking SA node myocytes of the adult heart. These include a slow diastolic depolarization and a slow upstroke velocity in the first phase of the AP. Note the absence of the overshoot and plateau phases (1 and 2, respectively). Also, the peak of the action potential is at a lower potential compared with the mature ventricular AP. The relative time course and magnitude of sodium, calcium, and potassium conductances (g) generating the AP are illustrated below. See the text for a brief discussion of the ionic basis for these differences. The membrane potential is given in millivolts (mV).

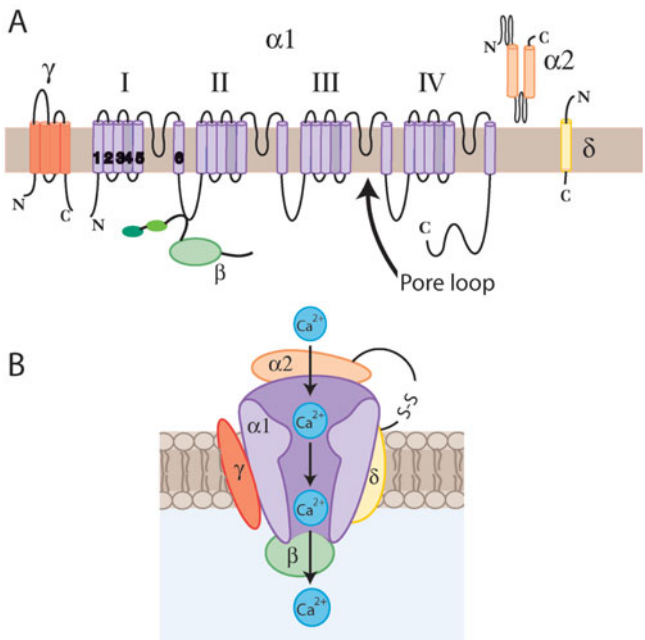

Figure 5.2. Diagram of the L-type calcium channel and accessory protein subunits. (*A*) Shown is a two-dimensional diagram illustrating the linear structure of the pore-forming α1 subunit and the accessory proteins α2-, δ-, and β-subunits. The cylinders represent coiled α-helical segments generally 21 amino acids in length. The α1-subunit consists of four groups of six α-helices (internally homologous repeats) with a pore-forming loop between helix segments 5 and 6 (numbered from left to right as shown in α-helix I) in each group. Segment four of each group (shaded) comprises the voltage sensor with a positively charge amino acid for each three amino acid turn of the helix (seven total). There are cytoplasmic loops that contain sites for regulation of channel activity by protein kinases and calmodulin in addition to a site for binding of the β regulatory subunit. (*B*) Shown is a cut-away three-dimensional diagram of the calcium channel subunits. Each of the internally homologous repeats with their pore-forming loops of α1 is arranged like staves in a barrel.

divalent ions. Ion channels open and close stochastically with a PROBABILITY (P_O) of being in an open conducting state that is quantitatively characteristic and descriptive for each of the many different ion channels. VOLTAGE-GATED ION CHANNELS respond to changes in membrane potential by increasing their probability of being in the open state (increased P_o). In ligand-gated channels, the P_o is increased in response to specific stimulation by neurotransmitters and hormones. Some ion channels are gated by calcium ions (Ca^{2+}). Background ion channels are constitutively active (i.e., in a conducting state with a P_o that is not voltage-dependent) but their P_o can be often be modified by changes in environmental conditions (e.g., acidosis) and in response to hormones. There are also mechanically gated channels (that open in response to stretch). Examples of all of these different ion channel gating mechanisms are found in the heart.

With the advent of patch clamp technology in the late 1970s, combined with advances in molecular biological approaches beginning in the late 1980s, a wealth of knowledge has been gained on the function of ion channels in normal physiological and in pathological processes, including the discovery of a number of inherited ion channel-related diseases (CHANNELOPATHIES) (Jurkat-Rott and Lehmann–Horn, 2005). In cardiac tissue, the focus of research has been largely on the adult, with much less attention given to embryonic development of ion channels and APs. Nonetheless, noteworthy differences in the pattern of ion channel expression and consequent effects on AP shape in the early embryonic heart compared to the adult have been identified. These differences have added significance because there is at least a partial resurgence of the embryonic expression pattern in adult cardiomyopathies and heart failure. Cardiac APs in adult heart have been extensively studied and are discussed only minimally here (Fig. 5.1) (Fozzard and Arnsdorf, 1997; Katz, 1992).

An important note is that the ion channel nomenclature as applied by physiologists and later by molecular biologists has not been fully reconciled and remains somewhat confusing. The problem has been that a particular ionic current such as the Ca^{2+} current has generally been found to be composed of a combination of more than one molecular isoform of the channel. Table 5.1 illustrates the various nomenclatures for the major membrane currents and underlying ion channel isoforms found in heart.

The APs of the adult atrial and ventricular myocardium, with the exception of nodal myocytes, resemble the diagramed APs shown in Fig. 5.1. There are regional differences primarily in the duration of the AP (phase 2), which is longest in the mid-ventricular myocardium, shortest in atrial myocytes, and nonexistent in nodal PACEMAKER CELLS. These differences reflect a variable expression pattern in the complement of ion channels and ion transporters that are contributing to the AP. A large variety of ion channels contribute to the shape and duration of the AP (Roden et al., 2002). These include channels that are gated by MEMBRANE POTENTIAL generally by AP DEPOLARIZATION but also during the REPOLARIZATION phase of the AP; ligand gated channels that modify the rate of AP generation as well as membrane electrical stability and the AP shape; and background channels that determine the resting or DIASTOLIC POTENTIAL and contribute to electrical stability. Expression of more than 70 ion channel pore-forming α-SUBUNITS and auxiliary protein genes have been detected and differentially expressed in the heart (Marionneau et al., 2005). A few ion transport mechanisms, particularly the Na^+/Ca^{2+} exchanger (discussed later) and the Na^+, K^+-ATPase, also contribute to membrane potential and AP shape.

Despite this bewildering array of ion channel and transport proteins, it bears keeping in mind that the proteins contributing to membrane potential and AP shape selectively conduct only four ions (Na^+, Ca^{2+}, K^+, AND Cl^-). Thus, it is possible to describe the AP in terms of these four ionic conductances. The rapid and sharp upstroke and peak (phase 0) of the myocardial AP is produced by a rapid influx of Na^+ from fast activated and inactivated voltage-gated Na^+

Table 5.1
Major Cardiac Ion Channels

IUPHAR*	Membrane Current	Gene & Other Names	Physiological Activity
CaV1.2, CaV1.3	L-type Ca^{2+}, ICaL	α1C, α1D, dihydropyridine-sensitive	Ca^{2+} entry, depolarization, pacemaking (?)
CaV3.1, CaV3.2	T-type Ca^{2+}, ICaT	α1G, α1H	Ca^{2+} entry, depolarization, pacemaking (?)
NaV1.5	Na current, INa	SCN5A, tetrodotoxin-sensitive	Rapid depolarization, AP upstroke
KV4.3	Transient outward K^+, Ito	Voltage gated K^+ channel, A-type	Early repolarization
KV7.1	Delayed rectifier-slow, IKs	KCNQ1, LQT1	Repolarizing K^+ current, slow component
KV11.1	Delayed rectifier-rapid K^+, IKr	KCNH2, HERG, LQT2	Repolarizing K^+current, rapid component
K2p3.1	Not characterized	TASK-1, KCNK3	Background K^+ current (?)
HCN1, HCN2, HCN4	Hyperpolarization-activated, If, Ih	Cyclic nucleotide gated cation channel, pacemaker current, funny current	Pacemaking
Kir2.1	Inward rectifier, IK1	KCNJ2	Background K^+ current, resting potential
Kir3.1	G-protein gated K^+, IK(Ach)	GIRK1, Gβγ-activated	Receptor activated hyperpolarizing current
Kir6.1	ATP depletion K^+, IK(ATP)	ATP-dependent channel	Hyperpolarization during hypoxia (i.e. metabolic stress)
Ncx1**	Na^+/Ca^{2+} exchange, Incx	Na^+/Ca^{2+} exchanger	Ca^{2+} extrusion, Ca entry, pacemaking (?)

* International union of pharmacology ion channel compendium
** Technically not an ion channel but transports a single net positive charge for each Ca^{2+} transported in the opposite direction

channels (Fig. 5.1). The early repolarization (phase 1) is due to voltage-dependent activation of a transient outward K^+ channel. The AP plateau (phase 2) is maintained primarily by the opening of voltage-gated Ca^{2+} channels. The final repolarization (phase 3) is due primarily to delayed activation of voltage-gated K^+ channels as well as the inactivation of Ca^{2+} channels. In the final phase 4, all voltage-gated ion channel activity has ceased and the membrane potential is maintained near the K^+ equilibrium potential (~90 mV) by constitutively active background K^+ channels. Cl^- channels are thought to provide only minimal contribution to the cardiac AP. The shape of the AP as well as heart rate is modified by autonomic neurotransmitters released by the sympathetic and parasympathetic nervous systems (Chapter 13) that modulate the activity of many of these channels. Note that the AP shape of SA and AV nodal cells, which resemble embryonic APs, is considerably different from the APs of the working myocardium (Fig. 5.1). The shape of these APs is dependent on a somewhat different complement of ion channels and these are discussed in greater detail below.

Embryonic Action Potentials: Ca^{2+}

For the most part, action potentials in the developing heart after around mid-gestation are similar to those in adults. However, the earlier in development one looks the more the electrical activity of myocytes, including those in the ventricles and certainly earlier in the primitive heart tube, resembles that in myocytes of the adult sinoatrial (SA) node (Fig. 5.1) (Sperelakis, 1982; Sperelakis and Pappano, 1983). Indeed, it appears that SA nodal myocytes retain many of the characteristics of embryonic cardiac myocytes. Like embryonic myocytes, nodal cells are small, they lack TRANSVERSE TUBULES (t-tubules), the myofibrils are not well organized, and nodal cells are spontaneously active. The action potentials of early embryonic myocytes and SA nodal cells have a much slower rate of rise (small dV/dT) and the diastolic potential is more depolarized compared with a mature atrial or ventricular myocyte. The small dV/dT is due to the fact that voltage-activated Na^+ channels are either absent or are in an inactive state (Satin et al., 1988). Thus in the earliest embryonic myocytes, the rising phase of the action potential is dependent on the voltage-dependent activity of L- AND T-TYPE Ca^{2+} CHANNELS. These action potentials are not affected by Na^+ channel blockers but can be completely inhibited by blocking Ca^{2+} channel activity. The more depolarized diastolic membrane potential is due to poor K^+ permeability resulting from the presence of few background INWARD RECTIFIER K^+ channels (Kir) and a background inward Na^+ conductance. Thus, the diastolic potential is shifted away from the K^+ equilibrium potential to about −50 mV (Josephson and Sperelakis, 1990; Linden et al., 1982; Masuda and Sperelakis, 1993). This brings the membrane potential closer to the activation range for Ca^{2+} channels, which activate at a more depolarized potential than the Na^+

channel. In the chick and probably in mammalian embryos, essentially all of the myocytes in the early heart tube and immature ventricles beat spontaneously when isolated by enzymatic dissociation. The percentage of beating myocytes isolated from the ventricles decreases with development such that by midgestation, spontaneously beating ventricular myocytes are not observed.

Cardiac Autorhythmicity

Much has been learned recently about the ionic basis for the pacemaking diastolic depolarization in spontaneously active adult SA nodal myocytes. However, controversy remains and the precise mechanisms have not been definitively established. Essentially, there is a net inward pacemaking current probably carried by I_F along with a sustained Na^+ influx that is coupled with a slow turning off of the delayed repolarizing K^+ currents (I_{KR} and I_{Ks}). At least three Ca^{2+} channels are expressed in SA nodal myocytes and thought to play a role in pacing activity. These are two isoforms of L-type (α_{1C} and α_{1D}) and at least one of T-type (α_{1G}) of Ca^{2+} channels (Bohn et al., 2000). In the early 1980s, DiFrancesco first reported and characterized I_f for "funny current" because of its slow activation upon repolarization of the AP (DiFrancesco, 1993; Moroni et al., 2001). This current, often termed the "pacemaker" current, is thought to be a major contributor to the diastolic depolarization. Four I_f channel genes have been cloned and all are expressed in SA and AV nodes, and in Purkinje fibers (Stieber et al., 2004). These channels are gated directly by cAMP and the four isoforms are referred to as HCN1–4 FOR HYPERPOLARIZATION-ACTIVATED CYCLIC NUCLEOTIDE-GATED. More recent evidence has identified another inward current that may contribute significantly to the pacemaker diastolic depolarization. The current is due to a net inward flux of positive charge carried by a transport protein that also functions to extrude Ca^{2+} as part of the EC coupling process. This is the cardiac NA^+/CA^{2+} EXCHANGER (NCX1) which exchanges one Ca^{2+} for three Na^+ (Bers, 2001; Kimura et al., 1986; Reeves et al., 1984).

The Pacemaker Current, I_f

I_f (HCN) channels conduct Na^+ and K^+ roughly equally but conduct mainly Na^+ at hyperpolarized potentials, which produces an inward current. Because activation can occur in the diastolic range of potentials and the channels are conducting primarily Na^+ in this range, I_f was at first considered the major current responsible for generating the pacemaker depolarization. There quickly arose some difficulties with a purely I_f model of pacemaking (Lipsius and Bers, 2003). First, the activation threshold of I_f is too negative (more negative than -60 mV) to solely account for the diastolic depolarization, especially in nodal cells, which have a MAXIMUM DIASTOLIC POTENTIAL (MDP) more positive than -60 mV. Second, cesium blockade of I_f appears to only slow the rate of spontaneous beating. In spontaneously active chick embryonic myocytes, activation of I_f is detectable only after depolarization to -100 mV, which is considerably more negative than the MDP. The loss of spontaneous beating of ventricular myocytes with development does correlate with decreased I_f, although the actual cause of the loss of spontaneous activity is probably much more related to the increasing K^+ permeability and membrane hyperpolarization that results from developmentally increasing expression of background K^+ (Kir) channels (Brochu et al., 1992; Linden et al., 1982; Nagashima et al., 2001; Yasui et al., 2001).

Regardless, knockout of HCN4, which constitutes 80% of the I_f channels in mouse heart, is embryonic lethal, with death occurring between E9.5 and 11.5 (Stieber et al., 2004). HCN4 knockout slows the beat rate by about 40% but does not stop it altogether. I_f is likely important for autonomic regulation of heart rate as adrenergic stimulated increase in cAMP shifts the activation to more positive potentials, leading to greater activation of the current on AP repolarization in pacing myocytes and an increase in heart rate (Abi-Gerges et al., 2000; DiFrancesco and Robinson, 2002). It should be noted that adrenergic innervation does not become functional until very late in development, long after loss of autorhythmicity in ventricular myocytes (Higgins and Pappano, 1981; Kirby et al., 1989). However, circulating levels of catecholamines, secreted hormonally by the forming sympathetic chain ganglia and adrenal medulla, can be quite high, particularly in response to periodic hypoxic stress which is normal for mammalian and avian embryos (Mulder et al., 2000; Portbury et al., 2003; Stewart and Kirby, 1985). An interesting possibility is that the HCN4-null is embryonic lethal because of an inability of the heart to respond to hypoxic stress which leads to a decrease in heart rate in the embryo (bradycardia). Regardless, I_f channels appear to have an important role in regulating heart rate during development.

Noteworthy is that a zebrafish mutation in an HCN homolog ("slo mo") has reduced I_f and BRADYCARDIA although the homozygous mutation does not appear to be lethal (Baker et al., 1997; Warren et al., 2001).

Cardiac Na-Ca Exchanger (NCX1)

Much of what is currently known about the physiology of rhythmicity in early heart development has been garnered from studies of chick heart development in the 1970s and early 1980s (reviewed by Sperelakis, 1982; Sperelakis and Pappano, 1983). That the removal of extracellular Na^+ abolished spontaneous activity in embryonic myocytes was first demonstrated more than 30 years ago by Sperelakis and colleagues in the chick embryo (Shigenobu and Sperelakis, 1972). Because of the slow upstroke of the rising phase of the AP, TETRODOTOXIN (TTX)-insensitive Na^+ dependence, and VERAPAMIL inhibition of spontaneous activity, these investigators proposed that early cardiac APs were dependent on a slow verapamil sensitive/TTX-insensitive Na^+ channel. However, no such voltage-sensitive Na^+ channel has been identified. It is

now clear that the rising phase of the AP is due to L- AND T-TYPE Ca^{2+} CURRENTS, I_{Ca}, and $I_{Ca,T}$, both of which are present in embryonic cardiac myocytes and could account for the verapamil sensitivity. More recent evidence suggests that the Na^+-dependence of embryonic pacemaking may at least in part be due to the inward current generated by the cardiac Na^+-Ca^{2+} exchanger (NCX1) at diastolic potentials (Koushik et al., 2001; Wakimoto et al., 2000). In the absence of NCX1 and unlike the HCN knockouts, the embryo never develops a heart beat although normal Ca^{2+} transients can be elicited by electrical field stimulation (Koushik et al., 2001; Reuter et al., 2003). Interestingly, the heart is able to undergo looping, chamber specification, and trabeculation, and the embryo can survive to about E11 apparently from simple diffusion of O_2 from the maternal circulation. Myofibrillar organization is also much disrupted, suggesting that contractile activity is necessary for the development of well-formed myofibrils with Z-line structure.

NCX1 is the principal Ca^{2+} efflux mechanism across the plasma membrane in myocardial cells. NCX1 moves 3 Na^+ across the plasma membrane in exchange for a single Ca^{2+} moving in the opposite direction (Fig. 5.3) (Kimura et al., 1986; Reeves et al., 1984). In normally polarized cells it moves Ca^{2+} out of the cell (forward mode) but can contribute to Ca^{2+} influx (reverse mode) when the cell is depolarized during the peak and early plateau phase of the AP (Haddock et al., 1997; Reeves et al., 1994). Because NCX1 working in its normal forward mode leads to a net movement of positive charge into the cell, a depolarizing current, I_{NCX}, is generated. I_{NCX} is relatively small; however, both SA nodal cells and spontaneously active embryonic myocytes are also small and have very high membrane resistances in the potential range of the diastolic depolarization. It has been estimated that as little as 3–4 pA of inward current are needed to reach the AP threshold in SA nodal cells (DiFrancesco, 1993). Thus, it is conceivable that I_{NCX} can contribute significantly to the diastolic depolarization in SA nodal cells and embryonic myocytes. This hypothesis is now well supported by recent evidence in adult cardiac pacemakers. It has been shown that I_{NCX} likely contributes significantly to the latter third of the diastolic depolarization in auxiliary atrial pacemaker cells; and very recently it has been shown that I_{NCX} is essential for autorhythmicity in SA nodal cells (Bogdanov et al., 2001; Huser et al., 2000). In both pacemaker cell types, Ca^{2+}-INDUCED Ca^{2+} RELEASE (CICR) from the SARCOPLASMIC RETICULUM (SR) is the main contributor to elevated Ca^{2+} during the diastolic depolarization for the generation of I_{NCX}. CICR is initiated by activation of T- and L-type Ca^{2+} channels that are probably activated earlier during the diastolic depolarization by another inward current, which could be I_f, the inward current activated on repolarization. However, myocytes in the tubular embryonic heart are thought to lack readily releasable Ca^{2+} from the SR (see later); therefore, these cells may rely mostly on Ca^{2+} entry from the extracellular space to stimulate I_{NCX} and generate the diastolic depolarization.

Action potentials and autorhythmicity in early mammalian heart development have not been well explored, largely because of the difficulty in working with very small mammalian embryos. With the advent of mouse genetics, there are now a growing number of reports generated from cardiac myocytes differentiated from mouse embryonic stem cells (Banach et al., 2003; Viatchenko-Karpinski et al., 1999). While the use of stem cells is promising, the resulting data must be approached with caution. For example, Dudley and colleagues have shown that myocytes differentiated from stem cells have unusual physiology including prolonged APs and easily triggered ARRHYTHMIAS (Zhang et al., 2002).

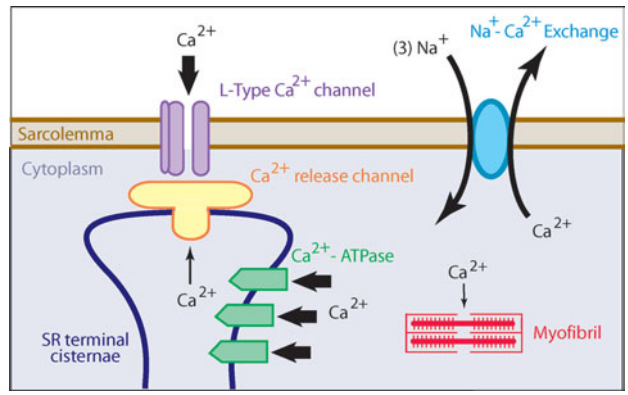

Figure 5.3. Cardiac EC coupling. The diagram illustrates the primary mechanisms for raising and lowering cytosolic Ca^{2+} during the heart beat. Note that the L-type Ca^{2+} channels in the sarcolemma and the Ca^{2+} release channels of the terminal cisterna of sarcoplasmic reticulum (SR) are closely opposed. Ca^{2+} entry from T-type Ca^{2+} channels and reverse Na^+-Ca^{2+} exchange during peak membrane depolarization in systole and from other Ca^{2+} sources are presumed not to be as effective as the L-type channel in initiating Ca^{2+}-induced-Ca^{2+}-release from the SR (CICR; see text). Ca^{2+} is removed from the cytosol primarily by the SR Ca^{2+} ATPase and the Na^+-Ca^{2+} exchanger which normally operates in the forward mode, extruding one Ca^{2+} for every three Na^+ coming into cell. In fetal and newborn hearts, t-tubules are lacking and couplings of the SR with the sarcolemma are at the surface membrane; however, functioning SR is typically sparse in fetal hearts. The obvious implication is that most of the Ca^{2+} entering during systole must come from the extracellular space instead of the SR as occurs in mature hearts. Further, other sources of extracellular Ca^{2+}, such as from T-type channels and reverse Na^+-Ca^{2+} exchange, probably assume greater importance in initiating contraction. Finally, a greater percentage of the systolic Ca^{2+} must be extruded through the Na^+-Ca^{2+} exchanger. Note that the diagram is not to scale and does not indicate the correct stoichiometry. The Ca^{2+} release channel, for example, is far larger than the L-type Ca^{2+} channel and there are at least four times as many.

Cardiac Excitation–Contraction Coupling

Adult Cardiac EC Coupling

Contraction and subsequent relaxation are elicited by a transient rise followed by a decline in cytosolic Ca^{2+} with each heart beat. This process involves a number of steps that are

collectively known as EXCITATION–CONTRACTION (EC) COUPLING. In general, EC coupling is defined as all the steps between depolarization of the surface membrane (sarcolemma) and the subsequent delivery of Ca^{2+} to the contractile proteins. The steps in the EC coupling process of adult cardiac muscle are well described (Fig. 5.3) (Bers, 2001). Briefly stated, sudden depolarization of the sarcolemma leads to activation of voltage-gated Ca^{2+} channels to produce a Ca^{2+} current (I_{Ca}) that peaks within ~10 msec after depolarization. This current provides net Ca^{2+} entry into the myocyte for approximately 30 msec, after which net Ca^{2+} extrusion occurs due to Na^{+}-Ca^{2+} exchange. Contraction does not occur in the absence of I_{Ca}, indicating that this current is essential for the EC coupling process. I_{Ca} increases the concentration of Ca^{2+} in the vicinity of the TERMINAL CISTERNAE of the sarcoplasmic reticulum (SR), which causes release of Ca^{2+} from large stores in the SR. This process is referred to as Ca^{2+}-induced Ca^{2+}-release (CICR) (Fabiato, 1983, 1985). Ca^{2+} release from the SR occurs through ryanodine receptor/Ca^{2+} release channels which appear to be identical to the feet structures that span the space between the sarcolemma and the junctional SR (Nakai et al., 1997). These channels are in close juxtaposition with the dihydropyridine (DHP)-sensitive L-type Ca^{2+} channels of the sarcolemma. The DHP receptor in adult cardiac muscle appears to function as a Ca^{2+} channel and not a voltage sensor that directly controls release of Ca^{2+} from the SR as it does in skeletal muscle (Bers, 2004). Ca^{2+} uptake by the longitudinal SR via a high level of Ca^{2+}-ATPase activity, along with extrusion by the NCX1, leads to a return of intracellular Ca^{2+} to control levels and relaxation of the heart muscle. Most of the Ca^{2+} needed for contraction comes from the SR while the rest comes from the extracellular space primarily via Ca^{2+} channels. Essentially, the amount of Ca^{2+} entering the cytoplasm via the SR during systole (about 80% in larger mammals including humans) is taken back up by the SR and that entering across the plasma membrane mostly via Ca^{2+} channels is extruded by the NCX1 (Bers, 2001). Mitochondria can store and release Ca^{2+} but this mechanism is too slow to contribute noticeably to the Ca^{2+} transient during a single beat. While the sarcolemmal Ca^{2+}-ATPase is sufficient to keep the cytosolic Ca^{2+} low in most cell types, its contribution to Ca^{2+} removal in contracting myocytes is normally quite small.

EC Coupling in Developing Heart

Present information indicates that the general mechanisms involved in EC coupling for adult myocardium described in the preceding text are qualitatively similar in developing cardiac muscle. However, there are important structural and functional differences. Embryonic myocytes regardless of species are small, mononucleated, lack t-tubules, and have poor myofibrillar organization compared with adult cardiomyocytes. This relatively poor cytoplasmic organization is to be expected considering that cardiomyocytes have to contract to keep the embryo alive as well as proliferate as the embryo grows. T-tubule formation, binucleation, and hypertrophy due to increased myofibrillar organization and growth are generally postnatal events. In adult cardiac cardiomyocytes, the structural arrangement of the SR and the specialized junctions that form with t-tubules and the sarcolemma, while complex, have been well described and much is known regarding their function. However, in the embryo, SR development occurs gradually over an extended period of time and the mechanisms that regulate this development are not known. Because T-tubules are not present, SR junctions are formed during development on the peripheral sarcolemma (Flucher and Franzini-Armstrong, 1996).

Ca^{2+} channels, in contrast, are present when cardiomyocytes first begin to beat in the cardiogenic plate and before heart tube formation (Shigenobu et al., 1974; Van Mierop, 1967). The major difference in cardiac EC coupling between embryo and adult hearts is the primary dependence on extracellular Ca^{2+} for contraction during development. Adult myocytes require Ca^{2+} to trigger release from an abundant SR. However, only a small amount of extracellular Ca^{2+} is needed to trigger a much larger cascade from the SR (Bers, 2001). In embryonic and fetal hearts, most of the Ca^{2+} needed for contraction comes from the extracellular space via sarcolemmal Ca^{2+} channels and at least some and perhaps significant Ca^{2+} entry from the NCX1 operating in reverse mode (Balaguru et al., 1997; Bers, 2001; Escobar et al., 2004; Flucher and Franzini-Armstrong, 1996; Haddock et al., 1997, 1999; Sperelakis and Pappano, 1983). While likely present and capable of storing Ca^{2+} to some degree, the SR probably contributes little to CICR because of a paucity of RyR/DHPR Ca^{2+} release units (COUPLONS) (Protasi et al., 1996). Therefore, a second major difference between embryonic and adult EC coupling is that Ca^{2+} removal during relaxation is dependent largely on the NCX1 operating in what is considered its normal forward mode. With maturation of the SR, there is a decline in the percentage of the systolic Ca^{2+} that is extruded by Na^{+}-Ca^{2+} exchange in parallel with an increasing proportion of Ca^{2+} sequestered and released by the SR during EC coupling.

Inositol Tris-Phosphate-Sensitive Ca^{2+} Store

A potentially significant source of intracellular Ca^{2+} in the embryonic heart for EC coupling is the inositol tris-phosphate (IP3)-sensitive store in the endoplasmic reticulum (ER). The IP3-sensitive Ca^{2+} store appears to be prominent in early heart development but is much reduced in adult myocardium (Guo et al., 2001; Kolossov et al., 1998; Li et al., 2002). It is present in progenitor cells before cardiomyogenesis and before functional L-type Ca^{2+} channels are detected (Kolossov et al., 1998). The relatively high level of IP3 Ca^{2+} stores in early myocardial cells suggests a role in Ca^{2+} homeostasis in early heart development. The IP3 store most likely has a role in Ca^{2+}-dependent processes related to differentiation and growth under control of growth factors acting through the PHOSPHOLIPASE C-dependent intracellular signaling pathways (Frey et al., 1999; Rosemblit

et al., 1999). Whether this Ca^{2+} store contributes significantly to EC coupling or cardiac rhythmicity has not been investigated and remains to be determined.

Species Differences in Cardiac EC Coupling

The avian model, particularly the chick embryo, has been of seminal importance in the study of heart development and it continues to be one of the models of choice for many experimental approaches. Embryonic myocytes from avian embryos are very similar to mammalian myocytes. They are small mononucleated cells with less organized myofibrillar structure and lack SR (Manasek, 1968). Major physiological similarities include a reliance on extracellular Ca^{2+} entry for contractility, the presence of T-type Ca^{2+} current in ventricular myocytes, low potassium permeability, and similar action potential characteristics (Aiba and Creazzo, 1992; Kawano and DeHaan, 1989; Linden et al., 1982; Satin and Cribbs, 2000). While the fundamental mechanisms of EC coupling are the same for both adult avian and mammalian species, there are some important structural differences. After birth or hatching there is binucleation and hypertrophy of both mammalian and avian ventricular myocytes but the hypertrophy is much greater in mammals. As a result, mammalian ventricular myocytes develop an extensive t-tubule system to facilitate uniform release of SR Ca^{2+} throughout the cell. The smaller avian ventricular myocytes do not have a t-tubule system and in this respect resemble in size and structure the mammalian atrial myocytes that also lack t-tubules. Avian ventricular myocytes instead develop an extensive "non- or extrajunctional" SR (Ca^{2+} release sites) throughout the cytoplasm that is, in addition to the junctional SR, located at the surface plasma membrane. The mammalian equivalent of extrajunctional SR is referred to as "corbular" SR which is insignificant in ventricle but may be of consequence in the atrium. Extrajunctional SR and the t-tubule system begin to appear shortly after hatching or birth in avian and mammalian ventricular myocytes, respectively (Junker et al., 1994; Sommer, 1995).

Major Proteins in EC Coupling

L-Type Ca^{2+} Channels

The voltage-activated cardiac L-type Ca^{2+} channel is all important in adult heart for providing trigger Ca^{2+} for CICR from the SR (Fig. 5.2). These Ca^{2+} channels form dense random arrays at junctional sites of the sarcolemma with the SR. The cardiac L-type channel is a relatively large multimeric protein (~250,000 Da). It consists of a cardiac specific α1C subunit (CaV1.2) with four transmembrane domains each with a pore-forming segment and β and α2-δ accessory subunits. The α1C subunit spans the sarcolemma and the pore segments together form the Ca^{2+}-conducting pore. Each of the transmembrane domains also contains a voltage sensor that undergoes a conformational change during membrane depolarization. In addition, the α1C subunit includes ALLOSTERICALLY COUPLED binding sites for drugs that are mostly inhibitors of channel function. These are the DIHYDROPYRIDINES such as nifedipine and bay K 8644 (an activator), PHENYLALKAMINES such as verapamil, and the BENZOTHIAZEPINES. The other subunits are essential for normal channel activity as the α1C subunit functions poorly in their absence (McDonald et al., 1994; Sather and McCleskey, 2003).

Although there is only a single adult form of α1C, there appear to be one or more fetal forms generated by exon splicing expressed during development (Diebold et al., 1992; Liu et al., 2000). In the mouse, it has been shown that α1C and to a lesser extent α1D (CaV1.3) isoforms contribute to $I_{Ca,L}$ in the embryonic heart (Klugbauer et al., 2002). Interestingly, null mutation of α1C is lethal in mouse only after E14. In this knockout, the heart is able to compensate for the loss of α1C by upregulation of a splice variant of α1D which, however, is insufficient for survival later in fetal development (Seisenberger et al., 2000; Xu et al., 2003). In adult heart, α1D is found mostly in nodal cells and is expressed at a low level in comparison with α1C. α1D has a slightly more negative voltage threshold for activation than α1C and, therefore, is active earlier during the AP.

Increasingly, it is becoming apparent that L-type Ca^{2+} channel activity is involved in gene transcription in processes that are now collectively referred to as excitation–transcription coupling (Maier and Bers, 2002). It is known, for example, that CALMODULIN is tethered to the L-type DHPR Ca^{2+} channel where it can be activated by incoming Ca^{2+} and increase the activity of the RAS/MITOGEN ACTIVATED PROTEIN KINASE (MAPK) which regulates gene transcription (Bers, 2004; Dolmetsch et al., 2001; Soldatov, 2003). Calmodulin activation is integral to the mechanism of Ca^{2+}-dependent Ca^{2+} channel inactivation and it now seems likely that calmodulin and the L-type channels exist as a multimeric protein complex that is capable of transmitting signals to the nucleus. The best studied example of such signaling is in the central nervous system where Ca^{2+} entry via L-type channels activates the tethered calmodulin that in turn activates calmodulin-sensitive kinases in hippocampal pyramidal neurons. These translocate to the nucleus and phosphorylate CAMP RESPONSIVE ELEMENT (CREB) binding protein, leading to gene transcription which is thought to be important for learning and memory (Mermelstein et al., 2001).

T-Type Ca^{2+} Channels

A second major class of voltage-gated Ca^{2+} channels is found in heart (McDonald et al., 1994; Perez-Reyes, 2003). These are the T-type Ca^{2+} channels that in adult are found in nodal cells, atrial myocytes, and in the conducting system but not in ventricular myocytes. These channels are characteristically expressed in myocytes that are capable of generating spontaneous action potentials (i.e., pacemaking myocytes). T-type channels have a lower or more negative voltage threshold for activation than L-type channels. Therefore, a proportion of

T-type channels is activated, particularly during the latter half of the diastolic depolarization, further contributing to the inward current generating the pacemaker potential (Bogdanov et al., 2001; Lipsius and Bers, 2003; Zhou and Lipsius, 1994). The T-type Ca^{2+} channel is blocked by low concentrations of nickel ions, but unlike in L-type channels, there are no specific inhibitors for this channel comparable to nifedipine, for example, which is highly selective for L-type Ca^{2+} channels. In comparison with L-type, T-type Ca^{2+} current is activated at more hyperpolarized potentials, has faster onset and decay kinetics, and does not show Ca^{2+}-dependent inactivation. The T-type channel contribution to the total Ca^{2+} current tends to be minor and probably does not contribute significantly to CICR because, unlike the L-type channel, it apparently lacks the close association with Ca^{2+} release channels in SR. In contrast with the mature adult heart, T-type channels are present in ventricular myocytes throughout most heart development although expression declines and they are probably absent at near term (Aiba and Creazzo, 1992; Bean, 1985; Creazzo et al., 2004; Kawano and DeHaan, 1990; Kitchens et al., 2003). This is consistent with the observation that early in development embryonic ventricular myocytes are capable of spontaneous beating although the exact role of this channel in autorhythmicity is not well understood. T-type Ca^{2+} channels may contribute to EC coupling during early development when functional SR is sparse, but this has not been studied in great detail (Kitchens et al., 2003).

Of the three known T-type Ca^{2+} channel isoforms, two (α1G and α1H; CaV3.1 and CaV3.2, respectively) are expressed in adult heart whereas the third isoform, α1I, (CaV3.3) appears to be expressed in the nervous system (as are α1G and α1H) (Cribbs et al., 2001; Perez-Reyes, 2003; Perez-Reyes et al., 1998, 1999). The expression of T-type Ca^{2+} channels is developmentally regulated. Both α1H and α1G subunits were reported to be present in embryonic heart (Cribbs et al., 2001; Ferron et al., 2002; Perez-Reyes, 2003). However, embryonic heart is more likely to express α1H (Larsen et al., 2002; Niwa et al., 2004; Perez-Reyes, 2003). It is interesting that there is a developmental switch between α1H and α1G expression in myocardium during the embryonic and postnatal periods. In rodent heart, α1H expression is predominant over α1G in the embryonic period but is essentially absent by postnatal week 4 (Larsen et al., 2002; Niwa et al., 2004). Functional studies further indicate that only α1G contributes to T-type calcium currents in postnatal rat cardiomyocytes although α1H transcript can be detected (Ferron et al., 2002). The reason why there is differential expression of T-type calcium channels in mature and embryonic heart is unknown.

The SR Ca^{2+} Release Channel

The cardiac Ca^{2+} release channel or the RYANODINE RECEPTOR (RyR), as it is commonly called because of a binding site for this plant alkaloid, is present in the membrane terminal dilations of the SR which form junctions with regions of the sarcolemma. In the mature heart, these junctions contain densely packed arrays of L-type Ca^{2+} channels with 4–8 RyRs for each Ca^{2+} channel depending on the species (Bers, 2001, 2004; Katz, 1992; Meissner, 1994). There are three isoforms (RyR1–3). The cardiac isoform is predominately RyR2. RyR1 and RyR3 are more prevalent in skeletal muscle and nervous system, respectively. The cardiac RyR2 Ca^{2+} release channel has multiple Ca^{2+} binding sites and is activated by Ca^{2+} entering via the L-type channel (i.e., CICR). There are only a few nanometers of space separating the release channel from the voltage-activated Ca^{2+} channel; therefore the release channel briefly "sees" a very high concentration of Ca^{2+} in this restricted space following membrane depolarization. The RyR protein is a tetramer with four identical subunits, each with a molecular mass of 550,000 Da. This is the largest known ion channel and it is readily visible by transmission electron microscopy. An array of RyR tetramers resemble feet walking along the t-tubule, and thus electron microscopists have whimsically labeled it the "foot" protein. There is now considerable evidence indicating that cardiac RyR2 exist as a central component to an even larger macromolecular complex that includes regulatory proteins such as protein phosphatases 1 and 2A, protein kinase A, calmodulin, and FKB BINDING PROTEIN, and it is bound to SR luminal proteins including CALSEQUESTRIN (discussed later), JUNCTION and TRIADIN as well (Bers, 2004; Marx et al., 2000). These proteins have varying effects on the channel gating properties.

In development, RyR2 foot proteins begin to appear in the SR membrane as soon as the SR junction with the sarcolemma forms (Flucher and Franzini-Armstrong, 1996; Protasi et al., 1996). These slowly accumulate, apparently simultaneously with accumulation of L-type channels in overlying patches in the sarcolemma, until the SR junctional membrane is densely packed with foot proteins and is considered mature. These data in chick embryo are consistent with a report in which Ca^{2+} sparks, the basic unit of Ca^{2+} release as measured with fluorescent Ca^{2+} indicators and confocal microscopy, are detected only postnatally in rat coincident with the appearance of SR junctions along the forming t-tubules (Seki et al., 2003). Generally, it can be said that SR is present very early in heart development and may serve as a significant store of intracellular Ca^{2+}. However, junctional Ca^{2+} release sites are rare and there probably is little CICR in early EC coupling although, this has not yet been determined.

SR Ca^{2+}-ATPase

SR Ca-ATPase activity becomes detectable in the developing heart coincident with the time of appearance of the SR junctional complexes (Flucher and Franzini-Armstrong, 1996). Membrane Ca^{2+}-ATPases are found in all cells and there are a number of genes that code for them and splice variants. The cardiac specific SR Ca-ATPase has been labeled SERCA2. Study of SERCA2 has been facilitated by the availability of specific antagonists and much is known of its role in EC coupling (Bers, 2001; Flucher and Franzini-Armstrong, 1996; Katz, 1992). The importance of this protein in removing Ca^{2+} from the cytoplasm during relaxation would be expected to increase

as the proportion of the SR contribution to the rise in cytosolic Ca^{2+} during systole increases with development (Creazzo et al., 2004; Reed et al., 2000). In human, the amount of SERCA2 protein increases approximately threefold from 8 weeks of gestation to adult (Qu and Boutjdir, 2001). A second inhibitory protein, PHOSPHOLAMBAN, exists in close association the SERCA2. Inhibition of the ATPase activity by phospholamban is removed by cAMP-dependent phosphorylation such as that following β-adrenergic receptor stimulation. Phospholamban activity is detectable along with the earliest appearance of SERCA2 (Vetter et al., 1986, 1995; Will et al., 1983). Note that the SR serves as an important Ca^{2+} buffer second only to troponin C (discussed later) in its ability to rapidly buffer intracellular Ca^{2+} entering during systole. In fact, only 1%–3% of the Ca^{2+} entering the cytoplasm from the SR release and voltage-gated Ca^{2+} channels is detectable as a Ca^{2+} transient when it is measured using fluorescent Ca^{2+} indicators (Berlin et al., 1994; Bers, 2001; Creazzo et al., 2004). The rest is rapidly bound by Ca^{2+} buffers that include the SR, troponin C, calmodulin, and other cytoplasmic components.

Na^+-Ca^{2+} Exchange

Na^+-Ca^{2+} exchange activity is a potent mechanism for extruding Ca^{2+} in both adult and developing hearts (Flucher and Franzini-Armstrong, 1996; Hilgemann, 1996). Obviously, its importance in EC coupling in the developing heart, where functional SR may be sparse, is much more significant. While gene and protein expression in normal and pathological conditions are well characterized, study of its physiological role and mechanisms of regulation have been difficult and questions remain. Specific antagonists for its activity have only recently become available; however, their use is problematic. Study is further complicated by the fact that this protein is always "on." Its activity is highly dependent on the electrochemical gradients for both Na^+ and Ca^{2+}. Thus, when there is high cytosolic Ca^{2+} and the membrane is depolarized, such as during peak systole, the Na^+-Ca^{2+} exchange is reversed and it becomes a mechanism for further raising cytosolic Ca^{2+}. This observation, along with difficulties in precise measurement, has led to considerable controversy concerning its role in EC coupling. In adult hearts, it seems unlikely Na^+-Ca^{2+} exchange contributes significantly to CICR since the L-type Ca^{2+} channel appears to have preferential access to the Ca^{2+} release channel. However, in the embryonic heart, in which SR is sparse and the myocytes are relatively small, reverse Na^+-Ca^{2+} exchange could contribute significantly to the Ca^{2+} transient (Haddock et al., 1997; Vetter et al., 1986, 1995). There is evidence in fetal and neonatal rabbit to suggest that there is significant Ca^{2+} entry via reverse exchange during the peak and plateau of the AP contributing to EC coupling (Haddock et al., 1997, 1999).

It should be noted that mouse targeted knockout of NCX1 restricted to the embryonic ventricle in 80%–90% of myocytes was surprisingly not embryo lethal (Henderson et al., 2004). The homozygote embryos survive to maturity with a relatively normal heart beat and Ca^{2+} extrusion. While not explicitly discussed in the original report, it should not be surprising that NCX1 is not needed for Ca^{2+} extrusion in the adult mouse. Small rodents rely on SR Ca^{2+} release for greater than 95% of the Ca^{2+} required for EC coupling. Therefore in this mutant, the sarcolemmal Ca^{2+}-ATPase appears to be sufficient for extruding Ca^{2+} entry via Ca^{2+} channels.

Calsequestrin

Calsequestrin is a low-affinity, high-capacity Ca^{2+} binding protein localized to the terminal dilations of junctional SR (Bers, 2001; Flucher and Franzini-Armstrong, 1996). It is readily detectable by electron microscopy as a follicular density within the SR. Its role is to increase the Ca^{2+} storage capacity of the SR. In heart development, its appearance in the SR is slightly delayed but can be detected shortly after the appearance of foot proteins. The implication is that the early SR cannot store as much Ca^{2+} as more mature SR. This may result in a smaller SR contribution to the Ca^{2+} transient and the SR can be more easily depleted of its Ca^{2+} store. However, calsequestrin function in developing cardiomyocytes has not been well studied.

The Contractile Apparatus

In development, there are significant isoform changes in the major contractile proteins of the heart which influence the contractile process (Swynghedauw, 1986). These isoform changes account for an increase in the rate of contraction and a decrease in the Ca^{2+} sensitivity of the contractile apparatus. The study of these isoform changes and their effect on contractility have been complicated by the fact that differentiation is not synchronous and mitosis can continue while the contractile proteins appear. Myocytes expressing different protein isoforms can be found side by side in the developing myocardium.

The contractile apparatus in adult cardiac tissue has been extensively studied and much is known regarding its structure, biophysics, and molecular biology. The basic contractile mechanisms have been known for many years and are very well described in review articles and textbooks (Fozzard, 1991; Katz, 1992; Robbins, 2000; Swynghedauw, 1986). While studies of cardiac function in relationship to the contractile apparatus are lacking, there is good information available on the development of the major contractile proteins. It should be noted that with the advent of transgenic mouse technology, much has been learned recently about the regulation of cardiac gene expression especially in early development and with respect to the myosin genes (see Chapter 4) (Robbins, 1996, 2000). The present discussion is confined to changes in expression of the major contractile proteins that occur during development and the possible effects of these developmental changes on cardiac contractility. It should be noted that re-expression of embryonic myosin and other contractile protein isoforms

in adult heart occurs in cardiomyopathic disease states, suggesting a reactivation of the fetal developmental program for isoform expression.

During early development of the myocardium, there is a paucity of myofibrils and those that are present are not aligned or well organized. Later in development, myofibrils are abundant and aligned (Manasek, 1970; Sperelakis and Pappano, 1983). Contractility, measured as force per unit of cross-sectional area of myocardial strips, increases significantly throughout development and may continue for some time postnatally (Godt et al., 1991; Reiser et al., 1994; Siedner et al., 2003). It was assumed that the increase in force with development was due to accumulation of contractile proteins. More recently, it has been demonstrated that the underlying cause for the increase in force is more complicated (Siedner et al., 2003). In early development, the increase in force is due to better organization of myofibrils rather than an increase in contractile proteins such as myosin heavy chain (MHC, see discussion later). Perinatally, there is an increase in contractile proteins in addition to further increase in organization. The second major change that occurs is a developmental decrease in the Ca^{2+} sensitivity for contraction (Fogaca et al., 1993; Godt et al., 1991; Metzger et al., 1994; Reiser et al., 1994; Siedner et al., 2003; Solaro et al., 1988). Ca^{2+} is obligatory for contraction. In mouse, the amount of Ca^{2+} for generation of half-maximal isometric tension increases about threefold from early heart development to adult (~0.63–2.0 μM) (Siedner et al., 2003). The majority of the shift in Ca^{2+} sensitivity is due to a switch in troponin-I (TnI) isoforms (discussed later).

There are essentially six proteins that are involved in contraction of striated muscle and are the primary constituents of the SARCOMERES, the fundamental units of the contractile apparatus. The interactions of these proteins require Ca^{2+} and hydrolysis of ATP to generate force. Although there are some exceptions, contractile proteins exhibit more tissue specificity than species specificity (Swynghedauw, 1986). The contractile proteins and their interactions and tissue specificity, along with developmental considerations, are discussed in the following section.

Myosin: Adult Structure and Function

The myosin molecule consists of two heavy chains and two pairs of light chains with a total molecular mass of about 450,000 Da. These subunits are members of multigene families (Katz, 1992; Swynghedauw, 1986). The bulk of the protein is made up of the two heavy chain subunits (MHCs) which are the major determinants of contractile ATPase activity and the velocity of shortening in living muscle. Each heavy chain consists of a filamentous tail, which lends rigidity to the structure, and a globular head that pivots or hinges on the tail and contains the site for ATPase activity. There are two heavy chain genes, α and β, and the atria and ventricles each have their own specific set. The α and β heavy chains have fast and slow ATPase activity, respectively. Accordingly, there are three ventricular myosin isoforms. V1 and V3 consist of αα and ββ heavy chains, respectively, and a V2 myosin consisting of αβ heavy chains which typically exist in smaller amounts than V1 and V3. V1, V2, and V3 have fast, intermediate, and slow ATPase activities, respectively. The ratios of these three isoforms present in ventricles correlates with heart rate (speed of myocyte shortening) in species. Rats and mice with very fast heart rates have a high proportion of V1. Intermediate ventricles, such as rabbits, have a high proportion of V3. Humans and larger animals have little or no V1. An intermediate αβ isoform corresponding to V2 does not exist in atria. A1 and A2 forms in the atria consist of αα and ββ combinations with very fast and slow ATPase activities respectively. A1 predominates in most mammalian ventricles.

There are three MYOSIN LIGHT CHAINS (MLC) found in human ventricles, MLC1–3. MLC2 can be phosphorylated by calcium, calmodulin-dependent protein kinases and amplify force development during systole. Phosphorylation of MLC2 probably serves to amplify force development during systole when the cytosolic calcium level is high. MLC1 and MLC3 are alternative splice products from the same gene and may contribute to some of the biological variability among species. Different light chain genes are found in the atria and ventricles. The adult atrium contains mostly MLC2.

Developmental Changes in Myosin

Myosin is probably the earliest of the key contractile proteins to be expressed in the developing heart and can be found in the cardiogenic mesoderm before formation of the primitive heart tube (Han et al., 1992; van der Loop et al., 1992). In the chick embryo, myosin is detected within 6 h of commitment of mesodermal cells to the cardiomyocyte lineage (Han et al., 1992). Interestingly, cardiomyocytes begin beating even before sarcomeres and the striated organization of myosin is observed (van der Loop et al., 1992). In rodent ventricle, there is a shift from V3 to the V1 (slow to fast) form of MHC which is complete by late fetal life (Swynghedauw, 1986). In larger animals, including human, V3 is also the predominate isoform expressed in late fetal life; however, V1 is transiently expressed after birth, with V3 becoming the most abundant isoform in adults. The shift to the A1 (fast) isoform in atria probably occurs very early during development in most species but this has not been well investigated. Rat and fetal human ventricles and atria contain an embryonic MLC isoform that is non-phosphorylatable and appears identical to that observed in fetal skeletal muscle. Phosphorylatable isoforms appear after birth in the ventricles while expression of the fetal isoform is maintained in atria and the conductive Purkinje tissue.

Actin

Actin has a highly conserved structure and is found in all eukaryotic cells. It can exist independently as "globular" G-actin (41,700 Da) but readily polymerizes in the presence of cations (salts) and ATP to form "fibrous" F-actin. The two most

important biological properties of actin are that it activates myosin ATPase and that it interacts physiochemically with myosin. The F-actin polymer, along with tropomyosin and the troponin complex, constitutes the thin filament component of the sarcomere. In the hearts of small mammals there are two isoforms. The α-skeletal actin is present during fetal life and this is replaced by α-cardiac actin in adult. Human hearts contain mainly α-cardiac actin along with a small amount of skeletal α-actin (Katz, 1992).

Tropomyosin

The most important function of tropomyosin is its ability, along with troponin, to respond to the calcium signal during systole and activate the actin–myosin interactions responsible for muscle contraction. It binds stoichiometrically with F-actin, and in this capacity adds rigidity to the thin filament. The tropomyosin molecule exists as either a homodimer or a heterodimer containing either of both of two isoforms, α and β, and each with a molecular mass of 34,000 Da. Tropomyosin in the hearts of smaller animals is made up mostly of α2-dimers while the hearts of larger mammals contain significant amounts of the β-subunit. Roughly equal proportions of α- and β-isoforms exist in adult human atria and ventricles. The proportion of the β-isoform is less in the fetus but increases with development. Interestingly, the content of the β-isoform in a number of species and developmental stages appears inversely correlated with heart rate (Katz, 1992).

The Troponin Complex

The troponin complex consists of three proteins: troponin C, I, and T (TnC, I and T). It is the binding of Ca^{2+} to TnC during the transient rise in cytoplasmic Ca^{2+} in the EC coupling process that initiates a conformational change in tropomyosin and exposes the myosin binding sites on actin. Cardiac TnC differs from the fast skeletal isoform in that it has lost one of the two low affinity binding sites for Ca^{2+}. It is TnI that actually regulates the interaction of tropomyosin with actin. TnT serves to bind the troponin complex to tropomyosin (Katz, 1992). TnC is the same in both atrial and ventricular myocardium and does not seem to vary with development. The embryonic and neonatal isoform of TnI is identical to the slow skeletal muscle TnI isoform and there is a developmental switch to the cardiac isoform late in fetal development (Sabry and Dhoot, 1989; Saggin et al., 1988; Westfall et al., 1996). Two isoforms of TnT are expressed in the developing chick heart (Sabry and Dhoot, 1989). One isoform predominates during early development and this isoform is gradually replaced by an adult form (Cooper and Ordahl, 1985; Sabry and Dhoot, 1989). It was speculated that isoform switching to an adult form of TnT in mammalian and avian hearts accounts for the developmental decrease in sensitivity of the cardiac contractile apparatus to Ca^{2+} (Godt et al., 1991; McAuliffe et al., 1990; Reiser and Lindley, 1990). However, a more recent report has now provided excellent evidence that it is the switch from the slow skeletal to the cardiac TnI isoform that likely accounts for most of the development decrease in Ca^{2+} sensitivity (Siedner et al., 2003). Studies in the mammalian heart also suggest that the neonatal or slow skeletal form of TnI may play a role in the relative insensitivity of the neonatal contractile apparatus to acidosis (Godt et al., 1991; Solaro et al., 1988, 1989).

Contractility, Hemodynamics, and the Frank–Starling Relationship

It has been demonstrated in a number of species that muscular strips from fetal myocardium cannot generate the amount of force produced by strips from adult myocardium (Teitel et al., 1992). This is true at all muscle lengths along the force–tension curve (or pressure–volume relationships; see Fig. 5.3). Much of this diminished contractility is probability attributable to a lower density of functioning contractile units. Other factors, such as those discussed above, undoubtedly play a role as well. These could include differences in function of fetal isoforms of contractile and EC coupling proteins, less organized myofibrillar structure, less functional SR, and lack of t-tubules. In contrast, several animal studies have shown an acute increase in myocardial contractility within the first few days after birth to levels above the adult (Colan et al., 1992). This has been demonstrated in newborn lamb, a common model for fetal and newborn heart studies because of size similarity with human (Anderson and Wilcox, 1992). A Doppler and two-dimensional echocardiographic study in normal human neonates and infants indicates a reduction in contractility and systolic function with growth (Colan et al., 1992). This reduced contractility appears greater than could be accounted for solely by the increased afterload and wall stress that occurs after birth.

Starling's Law

The Frank–Starling relationship or Starling's Law of the heart is characterized by an increase in systolic pressure with increasing ventricular volume (Fig. 5.4) (Katz, 1992; Shroff et al., 1990). This is analogous to the increase force (i.e., peak systolic pressure) generated in cardiac muscle strips with increased lengthening of sarcomeres (i.e., end-diastolic distention) until the maximum overlap of actin and myosin for cross-bridge interaction is achieved and the A band is at its longest (sarcomere length = 2.2 μm). Obviously, increasing length further decreases the efficiency of cross-bridge formation and force generation then decreases. This relationship is illustrated by the curve in Fig. 5.4, which shows both an ascending and descending limb with increased volume. The decreased cross-bridge efficiency when stretching beyond 2.2 μm may be counteracted to some extent by an increase in the Ca^{2+} sensitivity of the contractile apparatus (Gordon et al., 2000). The Starling relationship

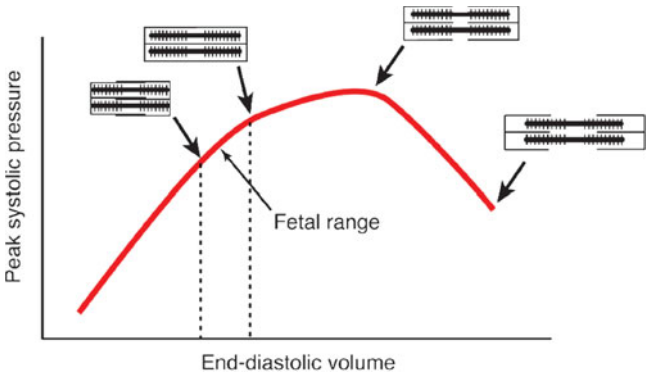

Figure 5.4. The Frank–Starling relationship. Shown is an idealized Starling relationship between peak systolic pressure and end-diastolic volume. The relative overlap of myosin and actin filaments is shown for each limb of the curve. The heart is able to compensate for increased diastolic filling with an increase in the force of contraction measured as an increase in peak systolic pressure (ascending limb of the curve). If the diastolic volume is too great then the ability to generate pressure begins to decline (descending limb) as the sarcomeres are overstretched and not as efficient. However, the heart has a high compliance and this does not normally occur. The fetal heart appears to operate along a narrow range near the top of the ascending limb of the Starling curve indicating less of an ability to respond to cardiovascular stress than the adult heart.

differs from the length–tension curve in that the relationships are between pressure and volume. Second, the high compliance of the myocardium tends to impede high filling levels, which helps protect against overstretching. It is unlikely that the normal ventricle ever dilates to the point that the descending limb of the Starling curve is achieved. Starling's Law maintains the balance between the venous return and the cardiac output by increasing stroke volume along the ascending limb when more blood returns to the heart. Thus, the relationship is important in making adjustments to circulatory dynamics on a beat-to-beat basis such as occur with changes in body position. More drastic changes in circulatory dynamics, such as with exercise, are mediated by changes in contractility. The result of increased or decreased contractility is the generation of a new Starling curve with a new maximum higher or lower achievable pressure. As an example, it should be clear from the discussion earlier in this chapter that interventions that raise or lower cytosolic Ca^{2+} levels produce corresponding changes in contractility and a new Starling relationship.

Starling's Law in the Developing Heart

The presence of a fetal Frank–Starling relationship has been demonstrated, generally in studies employing the fetal lamb as a model (Anderson and Wilcox, 1992; Teitel et al., 1992). A key observation that has emerged from these studies is that the fetal heart appears to be operating close to the top of the ascending limb of the Starling curve (Fig. 5.4). Thus, there is less reserve in response to circulatory stress. Given the fetal environment (analogous to a "tropical island"), a limited Starling response would normally not pose any problems (Teitel et al., 1992). In agreement with the hemodynamic studies, the isolated fetal myocardium does demonstrate an impaired response to stretch. This diminished response to stretch indicates that some of the impairment of the Starling mechanism is likely to be due to fewer and less mature contractile units. However, there appear to be other contributing and as yet not well understood factors. These include greater myocardial stiffness and differences in the fetal circulation such as a very compliant umbilical–placental unit and an already dilated vascular bed that limits changes in preload (Teitel et al., 1992). The marked and immediate increase in left ventricular volume with birth may transiently expend most of the immature heart's Frank–Starling reserve, so that there is even less ability to respond to circulatory stress (Anderson and Wilcox, 1992). The sudden increase in ventricular volume may in some way be related to the rapid increase in contractility seen after birth (see earlier) but this has not been studied.

Cardiac Physiology and Congenital Heart Disease

A number of single-gene mutations of ion channels and contractile proteins have been identified in human congenital heart disease. The best characterized of these mutations are associated with LONG QT disease (Chapter 12) and familial cardiomyopathy (Chapter 4) and can have effects on cardiac function ranging from subtle to profound. It has also been suggested that some forms of SA node dysfunction, conditions collectively known as sick sinus syndrome, may be related to altered I_f current from a mutation in one of the HCN genes (Stieber et al., 2004). Inherited Long QT disease (LQT) manifests itself in the electrocardiogram as a prolongation of the QT interval, which is a temporal measure of ventricular repolarization (about 0.4 sec in humans). The QT interval reflects the length of the plateau phase of the cardiac action potential and is a useful clinical index of action potential duration. Ion channel defects that effectively prolong the duration of inward depolarizing membrane current by loss of function of voltage-gated K^+ channels or similarly decrease outward repolarizing current by gain of function of voltage-gated Na^+ channels will increase the action potential duration and be reflected by a prolonged QT interval (Keating and Sanguinetti, 1996). While most cardiomyopathies are secondary, resulting from hypertension and valvular heart disease, genetic factors are clearly important. Familial hypertrophic cardiomyopathy (FHC) is a heterogeneous autosomal dominant disorder involving mutations in contractile protein genes. It is characterized by thickening of the ventricular walls (hypertrophy), impaired relaxation, and reduced ability for the heart to fill (Edwards et al., 1996; Sanguinetti et al., 1996).

An important rationale for the study of myocardial function in development is that adult cardiomyopathic disease, whether acquired or inherited, generally leads to at least partial reactivation of fetal gene expression. These include genes for ion channels and SR proteins involved in EC coupling and contractile proteins.

Inherited Long QT and cardiomyopathies result from single point mutations. Ultimately of greater importance for human heart disease may be less direct affects on ion channel and contractile protein expression from alterations in the growth factor milieu and cell signaling mechanisms regulating gene transcription. Altered cell signaling may not only affect development of cardiac function but may also account for impaired function and abnormal growth in adult heart disease. A potential significant example of altered cell signaling is neural crest associated heart disease (Chapter 11). In animal models, ablation of the cardiac neural crest or reduced neural crest cell migration leads to impaired cardiac EC coupling which appears to involve altered FGF8 signaling in the myocardium (Creazzo et al., 1998; Farrell et al., 2001; Waldo et al., 1999).

REFERENCES

Abi-Gerges, N., G. J. Ji, Z. J. Lu, R. Fischmeister, J. Hescheler, and B. K. Fleischmann. 2000. Functional expression and regulation of the hyperpolarization activated non-selective cation current in embryonic stem cell-derived cardiomyocytes. J. Physiol. 523 Pt 2:377–389.

Aiba, S., and T. L. Creazzo. 1992. Calcium currents in hearts with persistent truncus arteriosus. Am. J. Physiol. 262:H1182–H1190.

Anderson, R. H., and B. R. Wilcox. 1992. The surgical anatomy of ventricular septal defect. J. Card. Surg. 7:17–35.

Baker, K., K. S. Warren, G. Yellen, and M. C. Fishman. 1997. Defective "pacemaker" current (Ih) in a zebrafish mutant with a slow heart rate. Proc. Natl. Acad. Sci. USA 94:4554–4559.

Balaguru, D., P. S. Haddock, J. L. Puglisi, D. M. Bers, W. A. Coetzee, and M. Artman. 1997. Role of the sarcoplasmic reticulum in contraction and relaxation of immature rabbit ventricular myocytes. J. Mol. Cell. Cardiol. 29:2747–2757.

Banach, K., M. D. Halbach, P. Hu, J. Hescheler, and U. Egert. 2003. Development of electrical activity in cardiac myocyte aggregates derived from mouse embryonic stem cells. Am. J. Physiol. 284: H2114–H2123.

Bean, B. P. 1985. Two kinds of calcium channels in canine atrial cells. Differences in kinetics, selectivity, and pharmacology. J. Gen. Physiol. 86:1–30.

Berlin, J. R., J. W. Bassani, and D. M. Bers. 1994. Intrinsic cytosolic calcium buffering properties of single rat cardiac myocytes. Biophys. J. 67:1775–1787.

Bers, D. M. 2001. Excitation–Contraction Coupling and Cardiac Contractile Force. Norwell, MA: Kluwer.

Bers, D. M. 2004. Macromolecular complexes regulating cardiac ryanodine receptor function. J. Mol. Cell. Cardiol. 37:417–429.

Bogdanov, K. Y., T. M. Vinogradova, and E. G. Lakatta. 2001. Sinoatrial nodal cell ryanodine receptor and Na^+-Ca^{2+} exchanger: molecular partners in pacemaker regulation. Circ. Res. 88:1254–1258.

Bohn, G., S. Moosmang, H. Conrad, A. Ludwig, F. Hofmann, and N. Klugbauer. 2000. Expression of T- and L-type calcium channel mRNA in murine sinoatrial node. FEBS Lett. 481:73–76.

Brochu, R. M., J. R. Clay, and A. Shrier. 1992. Pacemaker current in single cells and in aggregates of cells dissociated from the embryonic chick heart. J. Physiol. 454:503–515.

Colan, S. D., I. A. Parness, P. J. Spevak, and S. P. Sanders. 1992. Developmental modulation of myocardial mechanics: age- and growth-related alterations in afterload and contractility. J. Am. Coll. Cardiol. 19:619–629.

Cooper, T. A., and C. P. Ordahl. 1985. A single cardiac troponin T gene generates embryonic and adult isoforms via developmentally regulated alternate splicing. J. Biol. Chem. 260: 11140–11148.

Creazzo, T. L., J. Burch, and R. E. Godt. 2004. Calcium buffering and excitation–contraction coupling in developing avian myocardium. Biophys. J. 86:966–977.

Creazzo, T. L., R. E. Godt, L. Leatherbury, S. J. Conway, and M. L. Kirby. 1998. Role of cardiac neural crest cells in cardiovascular development. Annu. Rev. Physiol. 60:267–286.

Cribbs, L. L., B. L. Martin, E. A. Schroder, B. B. Keller, B. P. Delisle, and J. Satin. 2001. Identification of the T-type calcium channel (CaV3.1d) in developing mouse heart. Circ. Res. 88:403–407.

Diebold, R. J., W. J. Koch, P. T. Ellinor, J. J. Wang, M. Muthuchamy, D. F. Wieczorek, and A. Schwartz. 1992. Mutually exclusive exon splicing of the cardiac calcium channel alpha 1 subunit gene generates developmentally regulated isoforms in the rat heart. Proc. Natl. Acad. Sci. USA 89:1497–1501.

DiFrancesco, D. 1993. Pacemaker mechanisms in cardiac tissue. Annu. Rev. Physiol. 55:455–472.

DiFrancesco, D., and R. B. Robinson. 2002. b-modulation of pacemaker rate: novel mechanism or novel mechanics of an old one? Circ. Res. 90:E69.

Dolmetsch, R. E., U. Pajvani, K. Fife, J. M. Spotts, and M. E. Greenberg. 2001. Signaling to the nucleus by an L-type calcium channel-calmodulin complex through the MAP kinase pathway. Science 294:333–339.

Edwards, J. G., G. E. Lyons, B. K. Micales, A. Malhotra, S. Factor, and L. A. Leinwand. 1996. Cardiomyopathy in transgenic *myf5* mice. Circ. Res. 78:379–387.

Escobar, A. L., R. Ribeiro-Costa, C. Villalba-Galea, M. E. Zoghbi, C. G. Perez, and R. Mejia-Alvarez. 2004. Developmental changes of intracellular Ca^{2+} transients in beating rat hearts. Am. J. Physiol. 286:H971–H978.

Fabiato, A. 1983. Calcium-induced release of calcium from the cardiac sarcoplasmic reticulum. Am. J. Physiol. 245:C1–14.

Fabiato, A. 1985. Simulated calcium current can both cause calcium loading in and trigger calcium release from the sarcoplasmic reticulum of a skinned canine cardiac Purkinje cell. J. Gen. Physiol. 85:291–320.

Farrell, M. J., J. L. Burch, K. Wallis, L. Rowley, D. Kumiski, H. Stadt, R. E. Godt, T. L. Creazzo, and M. L. Kirby. 2001. FGF-8 in the ventral pharynx alters development of myocardial calcium transients after neural crest ablation. J. Clin. Invest. 107:1509–1517.

Ferron, L., V. Capuano, E. Deroubaix, A. Coulombe, and J. F. Renaud. 2002. Functional and molecular characterization of a T-type Ca^{2+} channel during fetal and postnatal rat heart development. J. Mol. Cell. Cardiol. 34:533–546.

Flucher, B. E., and C. Franzini-Armstrong. 1996. Formation of junctions involved in excitation-contraction coupling in skeletal and cardiac muscle. Proc. Natl. Acad. Sci. USA 93:8101–8106.

Fogaca, R. T. H., K. S. Warren, J. J.-C. Lin, T. M. Nosek, and R. E. Godt. 1993. Contractile alterations during myocardial development in the chick subsequent to ablation of cardiac neural crest. J. Cell. Biochem. Supplement 17D:211.

Fozzard, H. A. 1991. Excitation–contraction coupling in the heart. Adv. Exp. Med. Biol. 308:135–142.

Fozzard, H. A., and M. F. Arnsdorf. 1997. Cardiac Electrophysiology. In: The Heart and Cardiovascular System: Scientific Foundations, ed. Fozzard, H. A., E. Haber, R. B. Jennings, A. M. Katz, and H. E. Morgan, 63–98. New York: Raven Press.

Frey, B. M., B. F. Reber, B. S. Vishwanath, G. Escher, and F. J. Frey. 1999. Annexin I modulates cell functions by controlling intracellular calcium release. FASEB J. 13:2235–2245.

Godt, R. E., R. T. H. Fogaca, and T. M. Nosek. 1991. Changes in force and calcium sensitivity in the developing avian heart. Can. J. Physiol. Pharmacol. 69:1692–1697.

Gordon, A. M., E. Homsher, and M. Regnier. 2000. Regulation of contraction in striated muscle. Physiol. Rev. 80:853–924.

Guo, L., J. Lynch, K. Nakamura, L. Fliegel, H. Kasahara, S. Izumo, I. Komuro, L. B. Agellon, and M. Michalak. 2001. COUP-TF1 antagonizes *Nkx2.5*-mediated activation of the calreticulin gene during cardiac development. J. Biol. Chem. 276:2797–2801.

Haddock, P. S., W. A. Coetzee, and M. Artman. 1997. Na^+/Ca^{2+} exchange current and contractions measured under Cl^--free conditions in developing rabbit hearts. Am. J. Physiol. 273: H837–H846.

Haddock, P. S., W. A. Coetzee, E. Cho, L. Porter, H. Katoh, D. M. Bers, M. S. Jafri, and M. Artman. 1999. Subcellular $[Ca^{2+}]i$ gradients during excitation–contraction coupling in newborn rabbit ventricular myocytes. Circ. Res. 85:415–427.

Han, Y., J. E. Dennis, L. Cohen-Gould, D. M. Bader, and D. A. Fischman. 1992. Expression of sarcomeric myosin in the presumptive myocardium of chicken embryos occurs within six hours of myocyte commitment. Dev. Dyn. 193:257–265.

Henderson, S. A., J. I. Goldhaber, J. M. So, T. Han, C. Motter, A. Ngo, C. Chantawansri, M. R. Ritter, M. Friedlander, D. A. Nicoll, J. S. Frank, M. C. Jordan, K. P. Roos, R. S. Ross, and K. D. Philipson. 2004. Functional adult myocardium in the absence of Na^+-Ca^{2+} exchange: cardiac-specific knockout of NCX1. Circ. Res. 95:604–611.

Higgins, D., and A. J. Pappano. 1981. Developmental changes in the sensitivity of the chick embryo ventricle to ß-adrenergic agonist during adrenergic innervation. Circ. Res. 48:245–253.

Hilgemann, D. W. 1996. The cardiac Na-Ca exchanger in giant membrane patches. Ann. NY Acad. Sci. 779:136–158.

Huser, J., L. A. Blatter, and S. L. Lipsius. 2000. Intracellular Ca^{2+} release contributes to automaticity in cat atrial pacemaker cells. J. Physiol. 524 Pt 2:415–422.

Josephson, I. R., and N. Sperelakis. 1990. Developmental increases in the inwardly-rectifying K^+ current of embryonic chick ventricular myocytes. Biochim. Biophys. Acta 1052:123–127.

Junker, J., J. R. Sommer, M. Sar, and G. Meissner. 1994. Extended junctional sarcoplasmic reticulum of avian cardiac muscle contains functional ryanodine receptors. J. Biol. Chem. 269:1627–1634.

Jurkat-Rott, K., and F. Lehmann-Horn. 2005. Muscle channelopathies and critical points in functional and genetic studies. J. Clin. Invest. 115:2000–2009.

Katz, A. M. 1992. Heart failure in 2001: a prophecy. Am. J. Cardiol. 70:C126–C131.

Kawano, S., and R. L. DeHaan. 1989. Low-threshold current is major calcium current in chick ventricle cells. Am. J. Physiol. 256: H1505–508.

Kawano, S., and R. L. DeHaan. 1990. Analysis of the T-type calcium channel in embryonic chick ventricular myocytes. J. Membr. Biol. 116:9–17.

Keating, M. T., and M. C. Sanguinetti. 1996. Molecular genetics insights into cardiovascular disease. Science 272:681–685.

Kimura, J., A. Noma, and H. Irisawa. 1986. Na-Ca exchange current in mammalian heart cells. Nature 319:596–597.

Kirby, M. L., T. L. Creazzo, and J. L. Christiansen. 1989. Chronotropic responses of chick hearts to field stimulation following various neural crest ablations. Circ. Res. 65:1547–1554.

Kitchens, S. A., J. Burch, and T. L. Creazzo. 2003. T-type Ca^{2+} current contribution to Ca^{2+}-induced Ca^{2+} release in developing myocardium. J. Mol. Cell. Cardiol. 35:515–523.

Klugbauer, N., A. Welling, V. Specht, C. Seisenberger, and F. Hofmann. 2002. L-type Ca^{2+} channels of the embryonic mouse heart. Eur. J. Pharmacol. 447:279–284.

Kolossov, E., B. K. Fleischmann, Q. Liu, W. Bloch, S. Viatchenko-Karpinski, O. Manzke, G. J. Ji, H. Bohlen, K. Addicks, and J. Hescheler. 1998. Functional characteristics of ES cell-derived cardiac precursor cells identified by tissue-specific expression of the green fluorescent protein. J. Cell Biol. 143:2045–2056.

Koushik, S. V., J. Wang, R. Rogers, D. L. Moskophidis, N. A., T. L. Creazzo, and S. J. Conway. 2001. Targeted inactivation of the sodium-calcium exchanger (Ncx1) results in the lack of a heartbeat and abnormal myofibrillar organization. FASEB J. 15:1209–1211.

Larsen, J. K., J. W. Mitchell, and P. M. Best. 2002. Quantitative analysis of the expression and distribution of calcium channel alpha 1 subunit mRNA in the atria and ventricles of the rat heart. J. Mol. Cell. Cardiol. 34:519–532.

Li, J., M. Puceat, C. Perez-Terzic, A. Mery, K. Nakamura, M. Michalak, K. H. Krause, and M. E. Jaconi. 2002. Calreticulin reveals a critical Ca^{2+} checkpoint in cardiac myofibrillogenesis. J. Cell. Biol. 158:103–113.

Linden, J., S. Vogel, and N. Sperelakis. 1982. Sensitivity of Ca-dependent slow action potentials to methacholine is induced by phosphodiesterase inhibitors in embryonic chick ventricles. J. Pharmacol. Exp. Therap. 222:383–388.

Lipsius, S. L., and D. M. Bers. 2003. Cardiac pacemaking: I_f vs. Ca^{2+}, is it really that simple? J. Mol. Cell. Cardiol. 35:891–893.

Liu, L., D. S. O'Hara, S. E. Cala, I. Poornima, R. N. Hines, and J. D. Marsh. 2000. Developmental regulation of the L-type calcium channel alpha1C subunit expression in heart. Mol. Cell. Biochem. 205:101–109.

Maier, L. S., and D. M. Bers. 2002, Calcium, calmodulin, and calcium-calmodulin kinase II: Heartbeat to heartbeat and beyond. J. Mol. Cell. Cardiol. 34:919–939.

Manasek, F. J. 1968. Embryonic development of the heart I: A light and electron microscope study of myocardial development in the early chick embryo. J. Morphol. 125:329–366.

Manasek, F. J. 1970. Histogenesis of the embryonic myocardium. Am. J. Cardiol. 25:149–168.

Marionneau, C., B. Couette, J. Liu, H. Li, M. E. Mangoni, J. Nargeot, M. Lei, D. Escande, and S. Demolombe. 2005. Specific pattern of ionic channel gene expression associated with pacemaker activity in the mouse heart. J. Physiol. 562:223–234.

Marx, S. O., S. Reiken, Y. Hisamatsu, T. Jayaraman, D. Burkhoff, N. Rosemblit, and A. R. Marks. 2000. PKA phosphorylation dissociates FKBP12.6 from the calcium release channel (ryanodine receptor): defective regulation in failing hearts. Cell 101: 365–376.

Masuda, H., and N. Sperelakis. 1993. Inwardly rectifying potassium current in rat fetal and neonatal ventricular cardiomyocytes. Am. J. Physiol. 265:H1107–H111.

McAuliffe, J. J., L. Z. Gao, and R. J. Solaro. 1990. Changes in myofibrillar activation and troponin C Ca^{2+} binding associated with troponin T isoform switching in developing rabbit heart. Circ. Res. 66:1204–1216.

McDonald, T. F., S. Pelzer, W. Trautwein, and D. J. Pelzer. 1994. Regulation and modulation of calcium channels in cardiac, skeletal, and smooth muscle cells. Physiol. Rev. 74:365–507.

Meissner, G. 1994. Ryanodine receptor/Ca^{2+} release channels and their regulation by endogenous effectors. Annu. Rev. Physiol. 56:485–508.

Mermelstein, P. G., K. Deisseroth, N. Dasgupta, A. L. Isaksen, and R. W. Tsien. 2001. Calmodulin priming: nuclear translocation of a calmodulin complex and the memory of prior neuronal activity. Proc. Natl. Acad. Sci. USA 98:15342–15347.

Metzger, J. M., W. I. Lin, and L. C. Samuelson. 1994. Transition in cardiac contractile sensitivity to calcium during the in vitro differentiation of mouse embryonic stem cells. J. Cell Biol. 126:701–711.

Moroni, A., L. Gorza, M. Beltrame, B. Gravante, T. Vaccari, M. E. Bianchi, C. Altomare, R. Longhi, C. Heurteaux, M. Vitadello, A. Malgaroli, and D. DiFrancesco. 2001. Hyperpolarization-activated cyclic nucleotide-gated channel 1 is a molecular determinant of the cardiac pacemaker current I(f). J. Biol. Chem. 276:29233–29241.

Mulder, A. L. M., J. M. C. G. vanGolde, A. A. C. vanGoo, D. A. Giussani, and C. E. Blanco. 2000. Developmental changes in plasma catecholamine concentrations during normoxia and acute hypoxia in the chick embryo. J. Physiol. (Lond.) 527: 593–599.

Nagashima, M., N. Tohse, K. Kimura, Y. Yamada, N. Fujii, and H. Yabu. 2001. Alternation of inwardly rectifying background K^+ channel during development of rat fetal cardiomyocytes. J. Mol. Cell. Cardiol. 33:533–543.

Nakai, J., T. Ogura, F. Protasi, C. Franzini-Armstrong, P. D. Allen, and K. G. Beam. 1997. Functional nonequality of the cardiac and skeletal ryanodine receptors. Proc. Natl. Acad. Sci. USA 94:1019–1022.

Niwa, N., K. Yasui, T. Opthof, H. Takemura, A. Shimizu, M. Horiba, J. K. Lee, H. Honjo, K. Kamiya, and I. Kodama. 2004. CaV3.2 subunit underlies the functional T-type Ca^{2+} channel in murine hearts during the embryonic period. Am. J. Physiol. 286: H2257–H2263.

Perez-Reyes, E. 2003. Molecular physiology of low-voltage-activated t-type calcium channels. Physiol. Rev. 83:117–161.

Perez-Reyes, E., L. L. Cribbs, A. Daud, A. E. Lacerda, J. Barclay, M. P. Williamson, M. Fox, M. Rees, and J. H. Lee. 1998. Molecular characterization of a neuronal low-voltage-activated T-type calcium channel. Nature 391:896–900.

Perez-Reyes, E., J. H. Lee, and L. L. Cribbs. 1999. Molecular characterization of two members of the T-type calcium channel family. Ann. NY Acad. Sci. 868:131–143.

Portbury, A. L., R. Chandra, M. Groelle, M. K. McMillian, A. Elias, J. R. Herlong, M. Rios, S. Roffler-Tarlov, and D. M. Chikaraishi. 2003. Catecholamines act via a beta-adrenergic receptor to maintain fetal heart rate and survival. Am. J. Physiol. 284: H2069–2077.

Protasi, F., X.-H. Sun, and C. Armstrong. 1996. Formation and maturation of the calcium release apparatus in developing and adult avian myocardium. Dev. Biol. 173:265–278.

Qu, Y. X., and M. Boutjdir. 2001. Gene expression of SERCA2a and L- and T-type Ca channels during human heart development. Pediatr. Res. 50:569–574.

Reed, T. D., G. J. Babu, Y. Ji, A. Zilberman, M. V. Heyen, F. Wuytack, and M. Periasamy. 2000. The expression of SR calcium transport ATPase and the Na^+/Ca^{2+} exchanger are antithetically regulated during mouse cardiac development and in hypo/hyperthyroidism. J. Mol. Cell. Cardiol. 32:453–464.

Reeves, J. P., M. Condrescu, G. Chernaya, and J. P. Gardner. 1994. Na^+/Ca^{2+} antiport in the mammalian heart. J. Exp. Biol. 196: 375–388.

Reeves, J. P., C. C. Hale, P. de la Pena, R. S. Slaughter, T. Boulware, J. Froehlich, G. Kaczorowski, and E. Cragoe. 1984. A model for the cardiac sodium-calcium exchange carrier. Prog. Clin. Biol. Res. 168:77–82.

Reiser, P. J. and B. D. Lindley. 1990. Activation in frog atrial trabeculae: dependence on temperature and length. Am. J. Physiol. 258:H1087–H1096.

Reiser, P. J., M. V. Westfall, S. Schiaffino, and R. J. Solaro. 1994. Tension production and thin-filament protein isoforms in developing rat myocardium. Am. J. Physiol. 267:H1589–H1596.

Reuter, H., S. A. Henderson, T. Han, G. A. Mottino, J. S. Frank, R. S. Ross, J. I. Goldhaber, and K. D. Philipson. 2003. Cardiac excitation-contraction coupling in the absence of Na^+-Ca^{2+} exchange. Cell Calcium 34:19–26.

Robbins, J. 1996. Hypertrophic cardiomyopathy: a case study in converging pathways. J. Clin. Invest. 98:2433–2434.

Robbins, J. 2000. Remodeling the cardiac sarcomere using transgenesis. Annu. Rev. Physiol. 62:261–287.

Roden, D. M., J. R. Balser, A. L. George, Jr., and M. E. Anderson. 2002. Cardiac ion channels. Annu. Rev. Physiol. 64:431–475.

Rosemblit, N., M. C. Moschella, E. Ondriasa, D. E. Gutstein, K. Ondrias, and A. R. Marks. 1999. Intracellular calcium release channel expression during embryogenesis. Dev. Biol. 206:163–177.

Sabry, M. A., and G. K. Dhoot. 1989. Identification and pattern of expression of a developmental isoform of troponin I in chicken and rat cardiac muscle. J. Muscle Res. Cell Motility 10:85–91.

Sabry, M. A., and G. K. Dhoot. 1989. Identification of and changes in the expression of troponin T isoforms in developing avian and mammalian heart. J. Mol. Cell. Cardiol. 21:85–91.

Saggin, L., S. Ausoni, L. Gorza, S. Sartore, and S. Schiaffino. 1988. Troponin T switching in the developing rat heart. J. Biol. Chem. 263:18488–18492.

Sanguinetti, M. C., M. E. Curran, A. Zou, J. Shen, P. S. Spector, D. L. Atkinson, and M. T. Keating. 1996. Coassembly of K(V)LQT1 and minK (IsK) proteins to form cardiac I_{Ks} potassium channel. Nature 384:80–83.

Sather, W. A., and E. W. McCleskey. 2003. Permeation and selectivity in calcium channels. Annu. Rev. Physiol. 65:133–159.

Satin, J., and L. L. Cribbs. 2000. Identification of a T-type Ca^{2+} channel isoform in murine atrial myocytes (AT-1 cells). Circ. Res. 86:636–642.

Satin, J., S. Fujii, and R. L. DeHaan. 1988. Development of cardiac beat rate in early chick embryos is regulated by regional cues. Dev. Biol. 129:103–113.

Seisenberger, C., V. Specht, A. Welling, J. Platzer, A. Pfeifer, S. Khbandner, J. Striessnig, N. Klugbauer, R. Feil, and F. Hofmann. 2000. Functional embryonic cardiomyocytes after disruption of the L-type a1C (*Cav1.2*) calcium channel gene in the mouse. J. Biol. Chem. 275:39193–39199.

Seki, S., M. Nagashima, Y. Yamada, M. Tsutsuura, T. Kobayashi, A. Namiki, and N. Tohse. 2003. Fetal and postnatal development of Ca^{2+} transients and Ca^{2+} sparks in rat cardiomyocytes. Cardiovasc. Res. 58:535–548.

Shigenobu, K., J. A. Schneider, and N. Sperelakis. 1974. Verapamil blockade of slow Na^{+} and Ca^{++} responses in myocardial cells. J. Pharmacol. Exp. Ther. 190:280–288.

Shigenobu, K., and N. Sperelakis. 1972. Calcium current channels induced by catecholamines in chick embryonic hearts whose fast sodium channels are blocked by tetrodotoxin or elevated potassium. Circ. Res. 31:932–952.

Shroff, S. G., D. Naegelen, and W. A. Clark. 1990. Relation between left ventricular systolic resistance and contractile rate processes. Am. J. Physiol. 258:H381–394.

Siedner, S., M. Kruger, M. Schroeter, D. Metzler, W. Roell, B. K. Fleischmann, J. Hescheler, G. Pfitzer, and R. Stehle. 2003. Developmental changes in contractility and sarcomeric proteins from the early embryonic to the adult stage in the mouse heart. J. Physiol. 548:493–505.

Solaro, R. J., S. C. el-Saleh, and J. C. Kentish. 1989. Ca^{2+}, pH and the regulation of cardiac myofilament force and ATPase activity. Mol. Cell. Biochem. 89:163–167.

Solaro, R. J., J. A. Lee, J. C. Kentish, and D. G. Allen. 1988. Effects of acidosis on ventricular muscle from adult and neonatal rats. Circ. Res. 63:779–787.

Soldatov, N. M. 2003. Ca^{2+} channel moving tail: link between Ca^{2+}-induced inactivation and Ca^{2+} signal transduction. Trends Pharmacol. Sci. 24:167–171.

Sommer, J. R. 1995. Comparative anatomy: in praise of a powerful approach to elucidate mechanisms translating cardiac excitation into purposeful contraction. J. Mol. Cell. Cardiol. 27:19–35.

Sperelakis, N. 1982, Pacemaker mechanisms in myocardial cells during development of embryonic chick heart. In: Cardiac Rate and Rhythm, ed. L. N. Bouman and H. J. Jongsna, 129–165. Leiden: Martinus Nijhoff.

Sperelakis, N., and A. J. Pappano. 1983. Physiology and pharmacology of developing heart cells. Pharmacol. Ther. 22:1–39.

Stewart, D. E., and M. L. Kirby. 1985. Endogenous tyrosine hydroxylase activity in the developing chick heart: a possible source of extraneuronal catecholamines. J. Mol. Cell. Cardiol. 17:389–398.

Stieber, J., F. Hofmann, and A. Ludwig. 2004. Pacemaker channels and sinus node arrhythmia. Trends Cardiovasc. Med. 14:23–28.

Swynghedauw, B. 1986. Developmental and functional adaptation of contractile proteins in cardiac and skeletal muscles. Am. J. Physiol. 66:710–771.

Teitel, D. F., R. J. Klautz, S. C. Cassidy, P. Steendijk, E. T. van der Velde, F. van Bel, and J. Baan. 1992. The end-systolic pressure–volume relationship in young animals using the conductance technique. Eur. Heart J. 13 Suppl E:40–46.

van der Loop, F. T., G. Schaart, W. Langmann, F. C. Ramaekers, and C. Viebahn. 1992. Expression and organization of muscle specific proteins during the early developmental stages of the rabbit heart. Anat. Embryol. (Berl.) 185:439–450.

Van Mierop, L. H. S. 1967. Location of pacemaker in chick embryo heart at the time of initiation of heartbeat. Am. J. Physiol. 212:407–415.

Vetter, R., R. Studer, H. Reinecke, F. Kolar, I. Ostadalova, and H. Drexler. 1995. Reciprocal changes in the postnatal expression of the sarcolemmal Na^{+}-Ca^{2+}-exchanger and SERCA2 in rat heart. J. Mol. Cell. Cardiol. 27:1689–1701.

Vetter, R., H. Will, I. Kuttner, C. Kemsies, and L. Will-Shahab. 1986. Developmental changes of Ca^{++} transport systems in chick heart. Biomed. Biochim. Acta 45:S219–222.

Viatchenko-Karpinski, S., B. K. Fleischmann, Q. Liu, H. Sauer, G. J. J. Gryschenko, and J. Hescheler. 1999. Intracellular Ca^{2+} oscillations drive spontaneous contractions in cardiomyocytes during early development. Proc. Natl. Acad. Sci. USA 96:8264.

Wakimoto, K., K. Kobayashi, M. Kuro-o, A. Yao, T. Iwamoto, N. Yanaka, S. Kita, A. Nishida, S. Azuma, Y. Toyoda, K. Omori, H. Imahie, T. Oka, S. Kudoh, O. Kohmoto, Y. Yazaki, M. Shigekawa, Y. Imai, Y. Nabeshima, and I. Komuro. 2000. Targeted disruption of Na^{+}/Ca^{2+} exchanger gene leads to cardiomyocyte apoptosis and defects in heartbeat. J. Biol. Chem. 275:36991–36998.

Waldo, K. L., M. Zdanowicz, J. Burch, D. H. Kumiski, R. E. Godt, T. L. Creazzo, and M. L. Kirby. 1999. A novel role for cardiac neural crest in heart development. J. Clin. Invest. 103:1499–1507.

Warren, K. S., K. Baker, and M. C. Fishman. 2001. The slow mo mutation reduces pacemaker current and heart rate in adult zebrafish. Am. J. Physiol. 281:H1711–H1719.

Westfall, M. V., L. C. Samuelson, and J. M. Metzger. 1996. Troponin I isoform expression is developmentally regulated in differentiating embryonic stem cell-derived cardiac myocytes. Dev. Dyn. 206:24–38.

Will, H., I., Küttner., R. Vetter, L. Will-Shahab, and C. Kemsies. 1983. Early presence of phospholamban in developing chick heart. FEBS Lett. 155:326–330.

Xu, M., A. Welling, S. Paparisto, F. Hofmann, and N. Klugbauer. 2003. Enhanced expression of L-type Cav1.3 calcium channels in murine embryonic hearts from *Cav1.2*-deficient mice. J. Biol. Chem. 278:40837–40841.

Yasui, K., W. Liu, T. Opthof, K. Kada, J. K. Lee, K. Kamiya, and I. Kodama. 2001. I_f current and spontaneous activity in mouse embryonic ventricular myocytes. Circ. Res. 88:536–542.

Zhang, Y. M., C. Hartzell, M. Narlow, and S. C. Dudley, Jr. 2002. Stem cell-derived cardiomyocytes demonstrate arrhythmic potential. Circulation 106:1294–1299.

Zhou, Z., and S. L. Lipsius. 1994. T-type calcium current in latent pacemaker cells isolated from cat right atrium. J. Mol. Cell. Cardiol. 26:1211–1219.

6

Development of the Poles of the Heart

Although it may seem odd to have a chapter devoted to the poles of the heart, the junction of the ends of the heart with the rest of the body during development is a dynamic relationship and one that has been under appreciated. Normal development of these junctions is critical for normally connected venous inflow and arterial outflow, and many heart defects are the result of incorrect connections at the venous or arterial pole. An important function of the poles is that they provide an entryway for new cells to be added to the heart including myocardial, endocardial, mesenchymal, and neural cells. They provide access to the endocardial and cardiac jelly layers located beneath the myocardium. This is especially important in the outflow tract, where little mesenchyme is available from any other source. The original mapping studies to identify the cardiogenic fields were done in embryo culture systems to allow access to gastrulation stage embryos. Embryos cultured in this manner have a limited lifespan that does not extend through the looping period, and it is just before and during the looping period that the final myocardial cells are added to the venous and arterial poles, respectively. New studies of both the inflow and outflow reveal a rich contribution of cells to each of the cardiac poles.

"Extracardiac" Cells Needed in Venous and Arterial Pole Development

Development of the initial heart tube is from the cardiogenic fields and all of the progenitors of the conus, right ventricle, left ventricle, atrioventricular canal, and atrial appendages appear to be represented in the early heart tube before the dorsal mesocardium completely disappears, releasing the heart tube from the ventral pharynx. This leaves only the truncus to be added to the arterial pole and the body of the atria and atrial septa to be added to the venous pole. In the mouse, the dorsal mesocardium disappears before the right ventricle forms, necessitating the addition of cells that will form the right ventricle and conus by accretion of cells via the arterial pole. This may explain why a greater part of the ASCENDING LIMB of the mouse heart tube appears to be formed from the pharyngeal mesenchymal cores, although a similar contribution occurs in the chick. Tracing studies have recently shown that only the distal or truncal myocardium arises from the secondary heart field and the conus most likely is derived from the mesodermal cores of pharyngeal arches 1, 2, and 3.

However, normal heart development also depends on cells that are reserved from the cardiogenic fields and do not differentiate at the same time as the cells that form the heart tube, and on other populations that are not derived from the cardiogenic fields at all (see Fig. 1.9). Several groups of cells are necessary for venous pole development. Myocardium is incorporated from the splanchnic mesenchyme and from the walls of the systemic and pulmonary veins. These myocardial cells may have been a peripheral part of the cardiogenic fields but their origin has not been traced. The VESTIBULAR SPINE, a condensation of mesenchyme, is incorporated into the prospective atria from the body wall. The secondary heart field, which has been shown to be part of the cardiogenic fields, contributes myocardial and smooth muscle cells that form the definitive arterial pole. The secondary heart field is initially part of the cardiogenic field but it does not differentiate as myocardium until the looping stage of heart development. Cells from the pharyngeal mesenchyme, including cells derived from the neural crest, populate the cardiac jelly layer between the myocardium and endocardium at the arterial pole. The epicardium, which is discussed in Chapter 10, forms from mesenchyme in or near the septum transversum. It gives rise to the endothelium and smooth muscle of the coronary vasculature as well as all of the connective tissue of the adult heart. Cells derived from the epicardium are the only extracardiac cells that do not enter the heart tube via the poles.

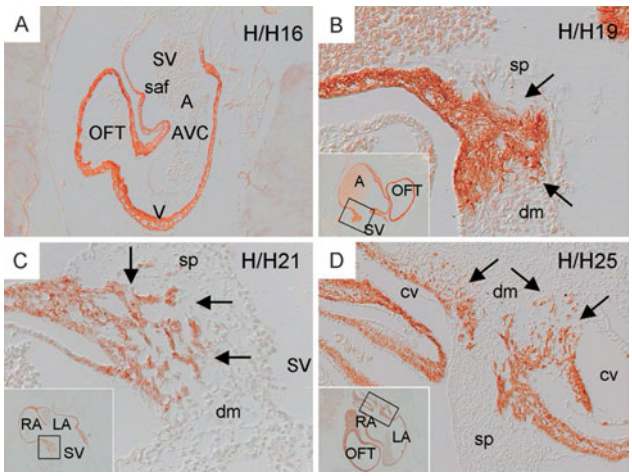

Figure 6.1. MF20 staining for myosin heavy chain shows cells near the venous pole that differentiate as myocardial and are recruited into the developing atria in the chick. SV, sinus venosus; saf, sinoatrial fold; A, atrium; AVC, atrioventricular canal; V, ventricle; OFT, outflow tract; sp, septum primum; dm, dorsal mesocardium; RA, right atrium; LA, left atrium; cv, cardinal vein. (From Van den Hoff et al., 2001, with permission.)

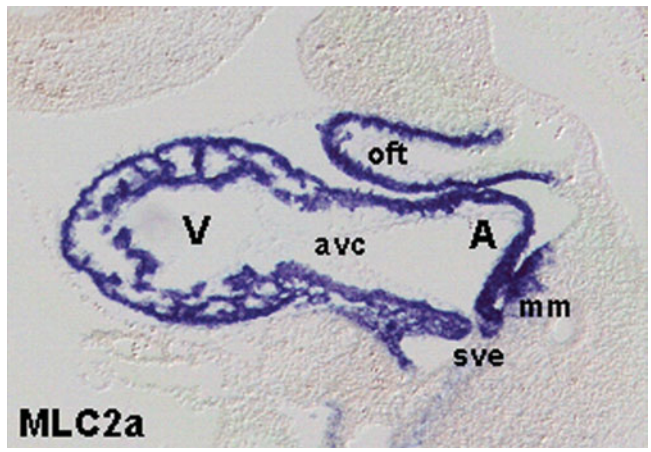

Figure 6.2. Sagittal section through an E9.5 mouse heart stained with MLC2A demonstrates the extent of the inflow myocardium in the splanchnic mesoderm cranial to the inflow pole. mm, mediastinal myocardium; sve, systemic venous entrance; A, atrium; avc, atrioventricular canal; V, ventricle; oft, outflow tract. (From Anderson et al., 2005, with permission.)

Venous Pole

The atrial chambers are formed partly during development of the initial heart tube, but much of the atrial chamber myocardium is recruited from the walls of the great veins and mesenchyme adjacent to the attachment of the venous pole with the body. Explants of mesenchyme near the VENOUS POLE have a stage-dependent potential to spontaneously form myocardial cells in culture. At stage 16 in the chick, cardiac myosin staining is strongest at the sinoatrial fold located at the junction of the sinus venosus and the atrium, and tapers off upstream (Fig. 6.1). At stage 19, fingers of myocardium can be seen differentiating in the mesenchyme distal to the myocardial border of the venous pole. At stage 21, these cardiomyocytes flank the dorsal mesocardium. By stage 25, the myocardial networks have expanded to surround the walls of the superior and inferior vena cava and the nascent pulmonary vein in the dorsal mesocardium (Van den Hoff et al., 2001). While some of this myocardium will continue to provide the tunics of the great veins, much of the walls, that is, endothelium and myocardium, of these proximal great veins will be incorporated into the atria during remodeling.

A similar pattern of myocardial development has been described in the mouse. The splanchnic mesoderm adjacent to the inflow tract is myocardial at E9.5 (Fig. 6.2), and myocardial differentiation continues to occur in the dorsal mesocardium and around the veins. These myocardial cells are recruited to the venous pole from the dorsal mesocardium and surrounding the nascent superior vena cavas and pulmonary vein (Fig. 6.3) (Kruithof et al., 2003).

Remodeling the Venous Pole to Form the Atria and Atrial Septum

As the myocardium remaining at the venous pole is incorporated into the heart tube, the proximal portions of the great veins that have developed myocardial walls begin to be incorporated into the atrial chambers. At around E9.5, the venous pole of the heart tube is relatively symmetrical, with two systemic channels returning blood from the embryo to a collection point called the SINUS VENOSUS. No pulmonary venous drainage has developed in the mouse at this stage (Anderson et al., 2005).

The right atrium is remodeled by incorporation of a large part of the sinus venosus that is covered by myocardium into its dorsal wall. The embryonic sinus venosus defines the region where the right and left horns of the sinus venosus meet. The right and left horns of the sinus venosus collect blood from the CARDINAL, VITELLINE, and UMBILICAL veins, that is, all the venous blood returning to the heart. The slightly constricted junction of the sinus venosus with the atrium is called the SINOATRIAL JUNCTION. This connection is guarded by a SINOATRIAL VALVE that consists of a right and a left leaflet. Each leaflet has traditionally been called a venous valve. The leaflets of the sinoatrial valve are oriented craniocaudally and where they meet cranially, they form a structure called the SEPTUM SPURIUM (Fig. 6.4). The sinoatrial connection gradually shifts to the right side of the single atrial chamber such that all of the systemic venous drainage is confined to what will become the right atrium. In the mature atrium, all of the systemic venous drainage into the right atrium is between the remnants of the sinoatrial valve leaflets that form part of the wall of the right atrium. During this remodeling, the size of the left sinus horn draining the veins from the left side of the body decreases significantly and becomes incorporated into the developing left

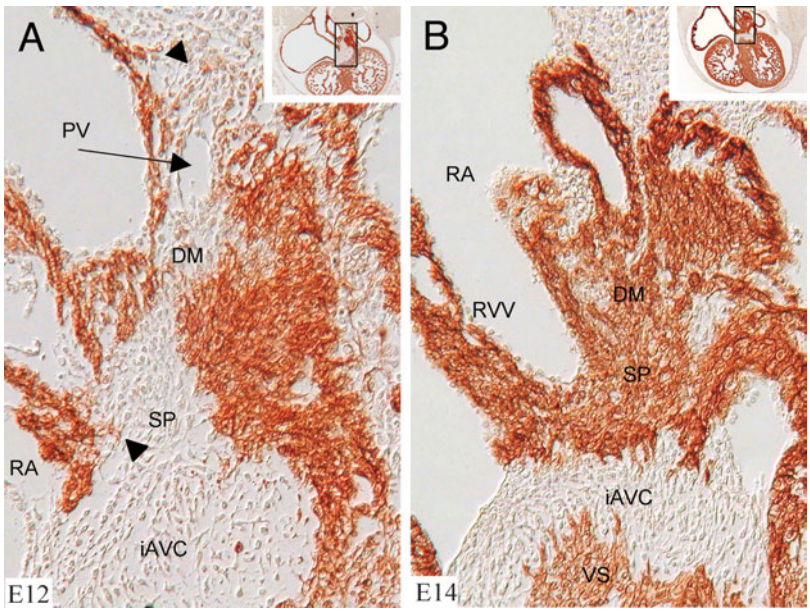

Figure 6.3. Myocardial recruitment to the venous pole from the dorsal mesocardium and concurrent myocardialization of the septum primum and spina vestibuli at E12 (*A*) and 14 (*B*) in the mouse demonstrated with MLC2V staining. *Arrowheads* indicate myocardium being recruited from the dorsal mesocardium (DM). PV (*arrow*), pulmonary vein; RA, right atrium; iAVC, atrioventricular canal; SP, septum primum; RVV, right cusp of the valve of the sinus venosus; VS, ventricular septum. (From Kruithof et al., 2003, with permission.)

atrioventricular groove as the left superior vena cava in the mouse and chick (Fig. 6.4). In humans, the distal left superior vena cava regresses and the proximal part of the remaining vessel (which was originally the left sinus horn), located in the left ATRIOVENTRICULAR GROOVE, becomes the CORONARY SINUS. In both cases the vessel opens into the right atrium (Fig. 6.5) (Knauth et al., 2002). The atrial myocardium originating from the myocardial tube shifts to the right to become the right ATRIAL APPENDAGE (auricle) as myocardium is incorporated into and expands to form the posterior wall and roof of the newly forming right atrial chamber.

The dorsal wall of the left atrium is formed by incorporation of the pulmonary vein. Canalization of the pulmonary vein begins in mouse at E11 from an endothelial strand that opens into an atrial structure called the PULMONARY PIT. This pit is located between two ridges in the back of the nascent left atrium called the left and right pulmonary ridges (Fig. 6.4) (Blom et al., 2001). Once the pulmonary vein forms, the pulmonary pit disappears, placing the opening of the vein adjacent to the atrioventricular junction (Fig. 6.6). The myocardium that has coalesced around the pulmonary vein becomes integrated into the developing left atrium concomitant with the remodeling of the atrioventricular canal and sinus venosus Cai et al., 2003; Soufan et al., 2004). In the mouse at E14, the wall of the pulmonary vein begins to be muscularized by cardiomyocytes (Fig. 6.2). The process of muscularization begins at the junction of the pulmonary vein with the atrial wall and proceeds in the direction of the lungs. By E15, the myocardium of the pulmonary vein has reached the third BIFURCATION. The process continues until E17, when the walls of the pulmonary veins are muscularized to the fifth bifurcation (Kruithof et al., 2003). In the mouse heart, the pulmonary vein remains a single vein with its entrance into the left atrium adjacent to the left atrioventricular junction. By contrast, in the human heart the muscularized pulmonary vein is incorporated into the back of the left atrium to the second bifurcation, resulting in four separate pulmonary vein orifices in the left atrium.

The remodeling of the venous tributaries is important in atrial septation. The primary atrial septum originates from myocardium that differentiates from splanchnic mesoderm near the venous pole. The primary atrial septum formed from this myocardium grows toward the atrioventricular cushions to divide the two atrial chambers. The primary septum and the myocardium forming the posterior wall of the right atrium between the left leaflet of the sinoatrial valve stain positively for PITX2, a marker of left-sided mesenchyme, indicating that part of the posterior wall of the right atrium and the primary septum originate from the left side (Fig. 6.6) (Franco et al., 2000). The primary atrial septum grows on the right side of the pulmonary venous orifice, which confines the newly developed pulmonary venous orifice to the left atrium (Fig. 6.7) (Webb et al., 1998, 2000). A secondary atrial septum forms to the right of the primary atrial septum when the wall between the left leaflet of the sinoatrial valve and primary atrial septum folds into the right atrium. This secondary septum is in reality a superior interatrial fold. Even though it is located in the right atrium it is also Pitx2-positive indicating its origin from mesoderm originating on the left side (Franco et al., 2000). As the right pulmonary veins are incorporated, the wall between them and the left leaflet of the sinoatrial valve fold into the atrium to produce the secondary atrial septum which is in reality a superior interatrial fold (Anderson et al., 2002; Webb et al., 2001). The septum secundum is incorporated to the right of the septum primum.

Normal embryologic development of the pulmonary venous system involves creation of a connection between the left atrium and the pulmonary venous plexus and subsequent regression of pulmonary-to-systemic venous connections.

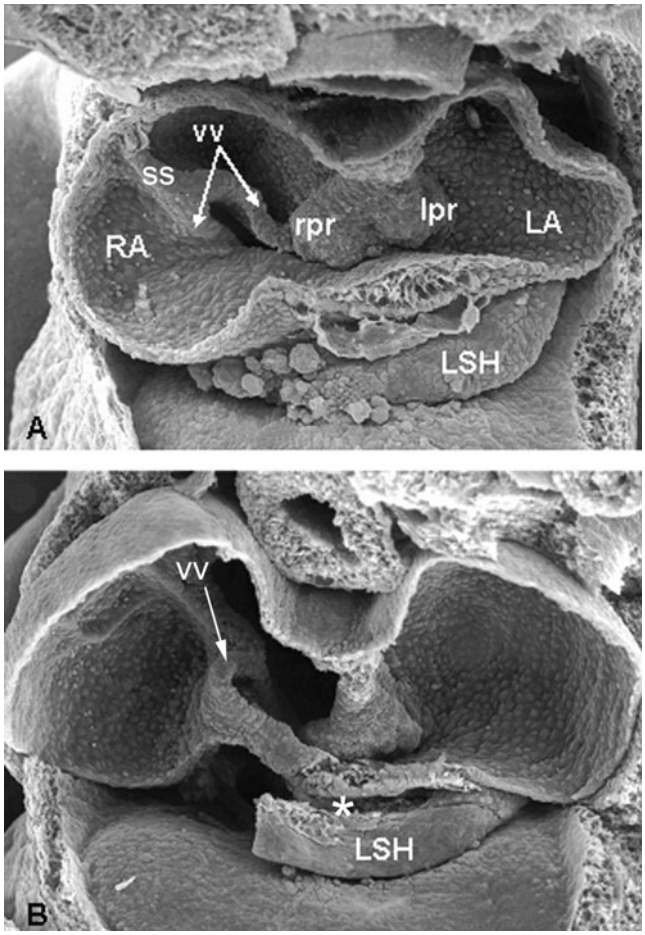

Figure 6.4. Scanning electron micrographs showing cranial views of the heart from an E10.5 mouse embryo. (*A*) The left (lpr) and right (rpr) pulmonary ridges show the position where the pulmonary vein will enter the left atrium when it forms. The left sinus horn (LSH), which will be a persisting left superior vena cava in the mouse, is becoming incorporated into the left atrioventricular junction as the coronary sinus which empties into the right atrium (*asterisk*). The valve leaflets of the sinus valve meet cranially in the septum spurium (SS). (*B*) The sinus valve leaflets can be seen demarcating the entrance of the systemic veins in the back of the right atrium. RA, right atrium; LA, left atrium; rpr, right pulmonary ridge; lpr, left pulmonary ridge. (From Anderson et al., 2005, with permission.)

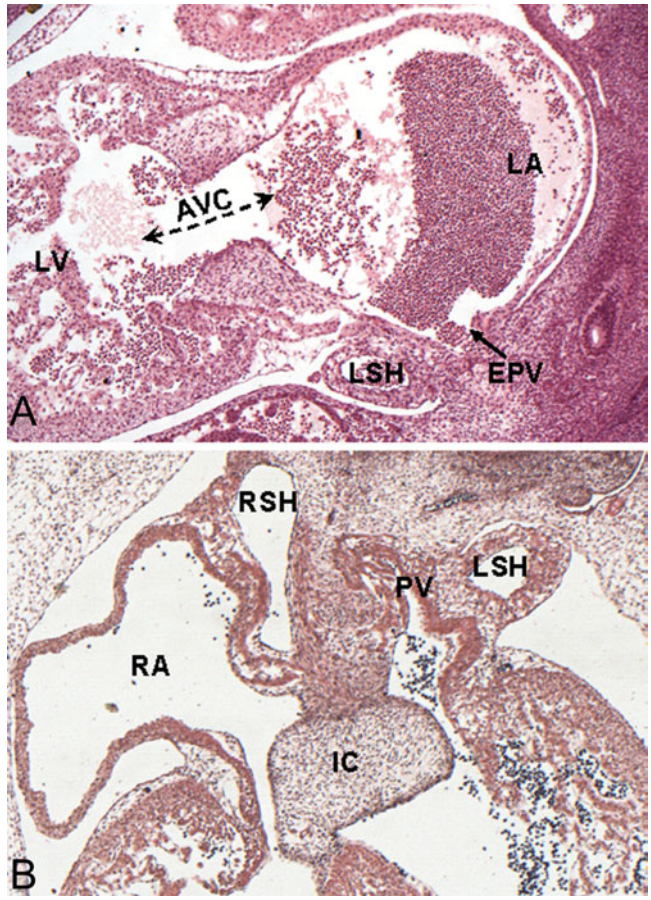

Figure 6.5. Sagittal (*A*) and transverse (*B*) sections through the heart of a Carnegie stage 16 human embryo before formation of the primary atrial septum. At this stage, a single pulmonary vein (PV) opens into the atrium (LA) adjacent to the atrioventricular junction (AVC). The left sinus horn (LSH, future coronary sinus) retains a myocardial wall. LV, left ventricle; RSH, right sinus horn; EPV, entrance to the pulmonary vein; IC, inferior atrioventricular cushion. (From Anderson et al., 2005, with permission.)

Any disruption of this process can result in ANOMALOUS PULMONARY VENOUS DRAINAGE. Because the lungs form as buds from the foregut, the initial venous drainage of the lung buds is through the same cardinal and umbilical-vitelline veins that drain the gut. After the pulmonary vein connects the venous plexus in the lung buds with the left atrium, the systemic venous system regresses, leaving the developing lungs with direct drainage to the left atrium. Anomalous pulmonary venous drainage can result from failure of fusion between the pulmonary vein and the pulmonary venous plexus or from misplacement of the relationship between the proximal pulmonary vein and the forming atrial septum.

The complicated array of myocardial sources that contribute to formation of the atria and atrial septa have been discovered and/or confirmed recently by gene expression profiling. The expression domains of genes that code for atrial natriuretic factor (*Nppa*), myosin light chain (*Mlc*) *3F*, *Mlc2V*, and *Pitx-2* have been used along with transgenic mouse lines expressing *lacZ* under the control of regulatory sequences of the mouse *Mlc1F/3F* gene to map atrial domains. Four transcriptional domains can be seen in the atrial myocardium and these reflect to some extent the patchwork contribution of myocardium to the atria. The domains are the atrioventricular canal that will form the smooth-walled lower atrial rim proximal to the AV valves and ventricles; the atrial appendages formed by myocardium in the initial cardiac tube; the myocardium investing the superior and inferior vena cavas; and the myocardium that originates from splanchnic mesoderm near the attachment of the sinus venosus with the body,

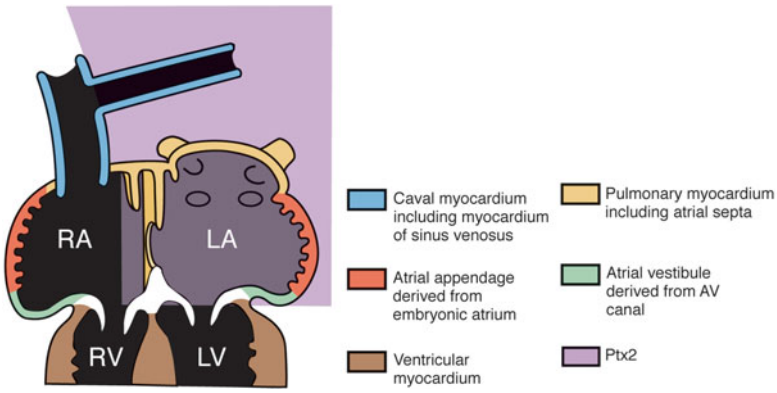

Figure 6.6. Sources of myocardium inferred from the myocardial transcriptional domains described for the mouse atria. The atria are comprised of myocardium from four different sources each with a left and right component identified by the left marker *Pitx2*. RA, right atrium; LA, left atrium; RV, right ventricle; LV, left ventricle. (Adapted from Franco et al., 2000, with permission.)

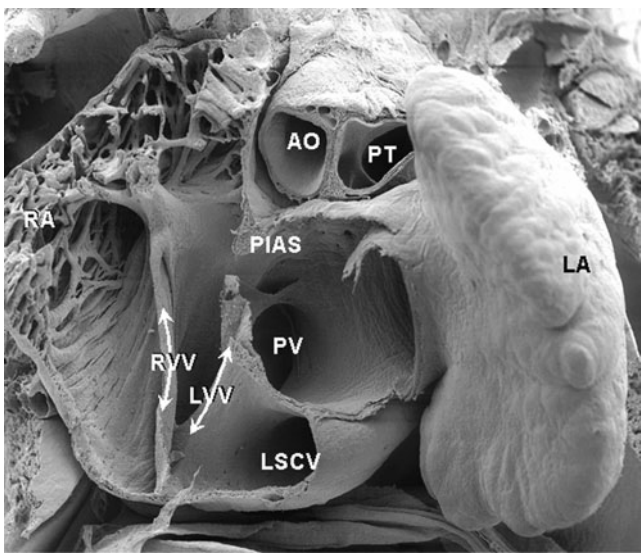

Figure 6.7. Scanning electron micrograph of a newborn mouse heart. The left (LVV) and right (RVV) leaflets of the valve of the sinus venosus located just to the right of the primary atrial septum (PIAS) surround the opening of the systemic veins into the right atrium. The pulmonary vein (PV) enters the left atrium through a solitary venous opening. RA, right atrial appendage; LA, left atrial appendage; LSCV, left superior cardinal vein; AO, aorta; PT, pulmonary trunk. (From Anderson et al., 2005.)

which includes the atrial septum. Each of the transcriptional domains has a distinct left and right component. The systemic and pulmonary inlets show discrete expression patterns that are not seen in the atrial appendages (Fig. 6.6) (Franco et al., 2000).

The right sinus horn grows faster than the left sinus horn and its junction with the atrium takes shape as the right-sided sinoatrial foramen (Davis, 1927). The sinoatrial foramen protrudes into the lumen of the atrium, creating leaflets. As mentioned previously, the commissure connecting the cranial ends of these leaflets continues as the septum spurium in the roof of the right atrium, whereas the caudal or ventricular ends of the leaflets insert near the midline on the spina vestibuli. Shortly after this sinoatrial valve appears, the pulmonary vein can be seen as an endothelial evagination from the atrium into the dorsal mesocardium. The dorsal mesocardium attaching the inflow portion of the heart tube to the back of the pericardial cavity surrounds the orifice of the pulmonary vein, forming a rim. This rim makes the atrial orifice of the pulmonary vein appear to be in a pit on the dorsal atrial lumen (Blom et al., 2001; Webb et al., 1998).

The primary atrial septum is a crescent-shaped muscular septum that originates just cranial and to the right of the pulmonary pit. With the primary atrial septum to its right, the pulmonary vein is committed to what will be the left atrium. The septum grows from the dorsal, cranial wall of the atrium toward the atrioventricular canal. Mesenchyme from the rim of the pulmonary pit and newly generated mesenchyme from the endocardium by epithelial-mesenchymal transformation coats the leading edge of the septum and is called the spina vestibuli (Kim et al., 2001; Tasaka et al., 1996). As the primary atrial septum grows toward the atrioventricular canal, the communication between the nascent left and right atria called the primary atrial foramen gets smaller and then closes when the primary septum fuses with cushion tissue in the atrioventricular canal. Shortly after this fusion the atrioventricular endocardial cushions begin to fuse, creating separate left and right atrioventricular connections (Asami and Koizumi, 1995; Dalgleish, 1976; Igarashi, 1984; Kim et al., 2001). It is actually the mesenchyme on the leading edge of the primary atrial septum that fuses with the superior endocardial cushion. This junction later becomes myocardialized by ingrowth of myocardial cells although the center of the mesenchyme is maintained as a dense connective tissue structure known as Todaro's tendon (Arrechedera et al., 1987; Kim et al., 2001; Webb et al., 1998).

Perforations develop in the cranial portion of the primary atrial septum to maintain communication between the atria as the primary atrial septum closes the primary atrial foramen. These openings coalesce to form the secondary foramen, which continues to enlarge at the expense of the primary atrial septum. The secondary atrial septum develops as an infolding of the dorsal atrial wall to the right of the origin of the primary atrial septum, but it never closes and the opening left below its outer margin is known as the foramen ovale. The secondary atrial septum is difficult to identify in the embryo and

becomes a pronounced fold only during fetal development. The remnant of the primary atrial septum remains as a flap valve leaflet over the foramen ovale. At birth, this leaflet fuses with the edge of the secondary septum to close the foramen ovale forming the fossa ovalis. The lower edge of the fossa ovalis becomes muscularized (Webb et al., 1998).

Vestibular Spine

The vestibular spine or "spina vestibuli" has been a contentious structure. It originates in the splanchnic mesoderm ventral to the foregut, and was thought to remodel into the mesenchymal cap on the primary atrial septum. However, it has recently been shown using lineage tracing that the mesenchymal cap is generated by epithelial-to-mesenchymal transformation from the endocardium coating the septum. This intracardially-generated mesenchyme is continuous with the mesenchyme of the vestibular spine located in the right pulmonary ridge (Mommersteeg et al., 2006). Closure of the atrioventricular canal occurs by introduction of the mesenchyme on the leading edge of the septum primum between the two atrioventricular endocardial cushions (discussed in Chapter 9) (Puerta Fonolla and Orts Llorca, 1978). The process of closing the atrioventricular canal results in closure of the primary foramen by the primary atrial septum. Failure of the mesenchymal cap to fuse with the atrioventricular cushions results in atrial septal defects such as those seen in Holt-Oram syndrome, which is discussed in more detail in Chapter 15 (Li et al., 1997). In a mouse model of Down syndrome, the mesenchymal cap is underdeveloped and does not undergo the growth into the heart seen in normal embryos. This results in atrioventricular canal defects (Webb, 1999).

Even though the vestibular spine does not give rise to the mesenchymal cap on the primary atrial septum, the derivation and position of the spine are important because variability in the connection of the atrial chamber to the body of the embryo, via the dorsal mesocardium and vestibular spine, influence the atrial relationship to the extracardiac midline mesenchyme. The connection with the midline is critical, as this area of attachment encloses the pulmonary pit which is the entry point of the pulmonary vein. Variation in the connection gives the potential for abnormal positioning of the pulmonary vein, which would allow the possibility of abnormal pulmonary venous return (Webb et al., 1999).

Arterial Pole

The junction of the myocardium with the smooth muscle at the base of the aorta and pulmonary trunk constitutes the arterial pole of the mature heart. In the developing heart this junction is represented by the transition from the myocardial covered truncus arteriosus to the mesenchyme-covered aortic sac. The outflow tract of the developing heart has traditionally been called the conotruncus. In the chick these two segments are easily identifiable; however, in human and mouse, the two regions are not so easily distinguished. The conotruncus, which has a smooth-walled lumen, is easily distinguished from the right ventricle, which has a trabeculated lumen. The lumen of the conotruncus is continuous with the aortic sac, which is not invested in myocardium and thus not a cardiac chamber. For much of its development the aortic sac is invested in loose mesenchyme. However, after all of the myocardium has been added to build the cardiac outflow tract, smooth muscle is added from the same splanchnic mesoderm to surround the aortic sac. After septation and extensive remodeling, the conus is incorporated into smooth-walled regions of the ventricles just beneath the pulmonary and aortic semilunar valves known respectively as the infundibulum (conus) and aortic vestibule. The semilunar valves form in the lumen of the remodeled truncus; and the base of the arterial trunks, the aorta, and pulmonary trunk are formed from the smooth muscle-invested aortic sac (Fig. 6.8).

An early study in mice showed that the cells added to the outflow myocardium originate in the splanchnic mesoderm where mesenchymal cells differentiate into cardiomyocytes between E8 and E11 (Viragh and Challice, 1973). A second study also based on the morphological analysis of heart development in humans and rats showed that the outflow pole myocardium is accreted from prepharyngeal mesoderm (de Vries, 1981). Marking experiments and quail-chick chimeras also show that cells in the pharyngeal splanchnic mesoderm caudal to the outflow tract are added to the elongating outflow tract (Fig. 6.9) (Waldo et al., 2001). This is the same region previously termed "prepharyngeal" mesoderm (de Vries, 1981). It is important to understand that this layer is continuous with the myocardial layer and that the other mesenchyme in the pharynx is not on the same tissue plane as the myocardium. Expression studies revealed that these progenitor cells of the outflow myocardium express Nkx2.5 and Gata4, as seen earlier in the cardiogenic fields (Waldo et al., 2001; Ward et al., 2005).

Formation of the Arterial Pole from the Secondary Heart Field

After the initial reports showing that the distal myocardium is added from the secondary heart field, the same region was subsequently found to give rise to the smooth muscle at the myocardial–arterial or ventriculoarterial junction where the semilunar valves form (Waldo et al., 2005). Because the secondary heart field gives rise to both the myocardium and smooth muscle, it is probably best to consider that the secondary heart field gives rise to the arterial pole. The smooth muscle tunic at the base of the aorta and pulmonary trunk is derived from the secondary heart field proximally, and these cells join a more distal smooth muscle tunic derived from NEURAL CREST CELLS (Fig. 6.8). Data from mouse embryos transgenic for lineage tracing of neural crest cells show that the same junctions form in the mouse. This indicates that there are two "seams" at the arterial pole, that is, the myocardial-to-smooth muscle transition derived from the secondary heart

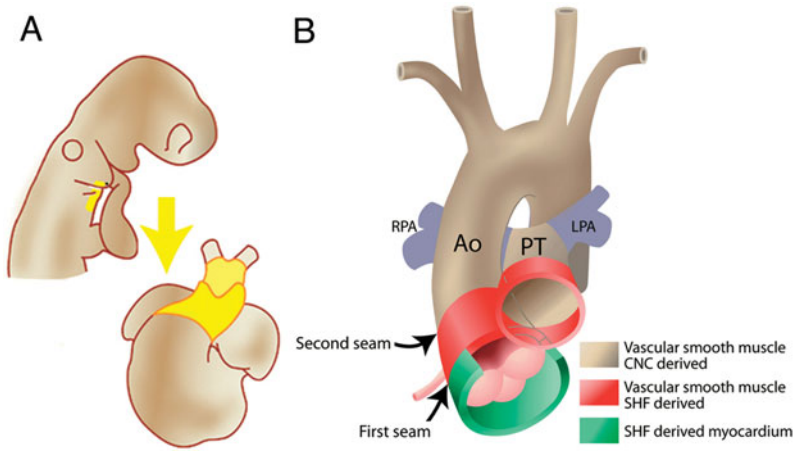

Figure 6.8. Formation of the arterial pole from the secondary heart field. (*A*) Lateral view of the looped heart in a chicken embryo (stage 14) and a frontal view of a stage 22. The *yellow* area represents the secondary heart field which adds the distal myocardium to the heart tube and proximal smooth muscle that surrounds the aortic sac which becomes the proximal portion of the aorta and pulmonary trunks after septation. (*B*) Diagrammatic representation of the seams at the arterial pole of the human heart. The secondary heart field generates myocardium (*green*) and vascular smooth muscle (*red*). A seam is formed where the myocardial cells meet the vascular smooth muscle cells of the tunica media of the aorta and pulmonary trunk. The tunica media of the aorta and pulmonary trunk is derived from secondary heart field proximally (*red*) and the cardiac neural crest distally (*tan*). The interface between these populations creates a second seam. These seams are likely locations of aortic wall dissections. (*A* from Abu-Issa et al., 2004, with permission; *B* from Waldo et al., 2005, with permission.)

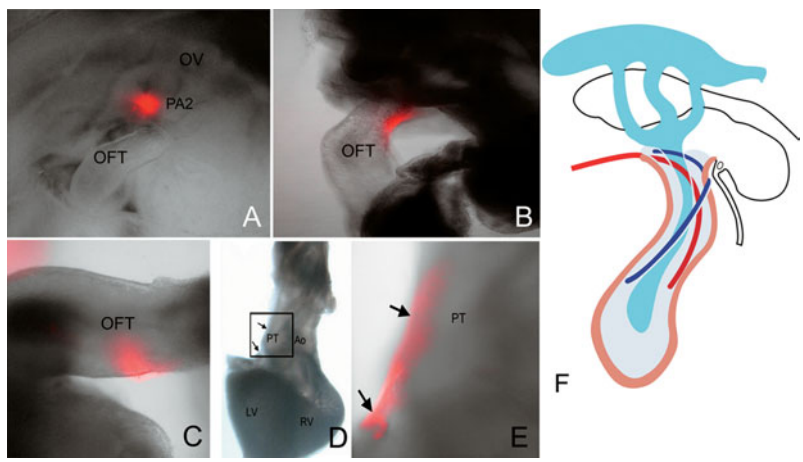

Figure 6.9. Right secondary heart field at stage 14 labeled with fluorescent dye (*A*) just after the injection. (*B*) At 24 hours later the cells have moved into the caudal and left side of the outflow tract. (*C*) After 48 hours the fluorescent cells are in the mid-portion of the caudal wall of the outflow tract and moving toward the left side. (*D*) After 96 hours the cells are at the base of the outflow on the left side. (*E*) Higher magnification of boxed area in (*D*). (*F*) Diagram illustrating that the myocardium from the right secondary heart field (red) spirals behind the outflow and to the left side. Blue represents the putative path of the left secondary heart field cranial and to the right base of the outflow. OV, otic vesicle; OFT, outflow tract; PA2, pharyngeal arch 2; PT, pulmonary trunk; Ao, aorta; LV, left ventricle; RV, right ventricle; L, lumen. (Reprinted from Ward et al., 2005, with permission.)

field at the base of the arterial trunks, and the junction of the secondary heart field-derived smooth muscle with cardiac neural crest-derived smooth muscle (Fig. 6.8).

The initial sign of myocardial cells moving into the outflow tract is HNK1 expression in the Nkx2.5/Gata4-positive mesenchyme underlying the pharyngeal endoderm (Waldo et al., 2001). HNK1 is associated with many types of cells undergoing translocation or differentiation (Canning and Stern, 1988; Tucker et al., 1984; Vincent and Thiery, 1984). The onset of HNK1 expression in the secondary heart field is at stage 14, which coincides with the time at which cells begin to move into the outflow tract and differentiate as myocardium (Arguello et al., 1975; de la Cruz et al., 1977, 1987, 1989). At progressively later stages until about stage 18–20, the length of HNK1-positive outflow myocardium progressively increases (Waldo et al., 2001).

The movement of the presumptive myocardial cells into the outflow tract follows a unique pattern. When the right secondary

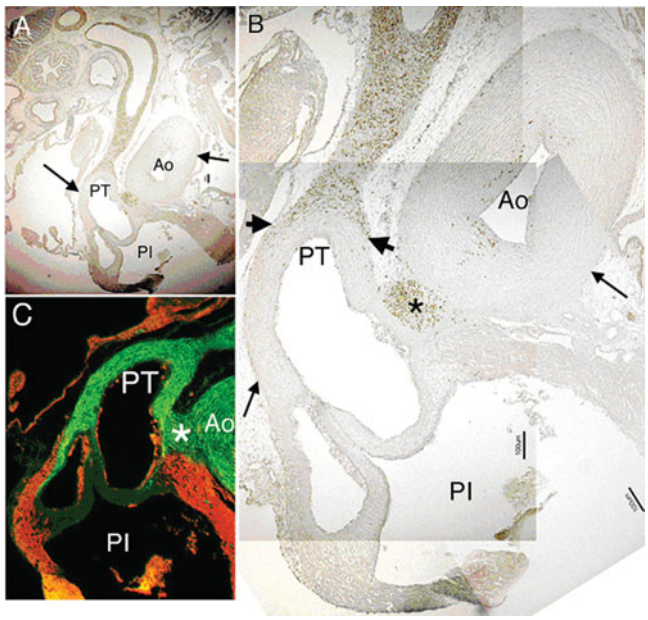

Figure 6.10. Sagittal sections showing that cardiac neural crest cells form the tunica media distal to the cells derived from the secondary heart field in quail-chick chimeras. Quail cells are *brown*, myocardial cells are *red*, and smooth muscle is *green*. The smooth muscle cells from the secondary heart field are negative for the smooth muscle marker until stage 29. All bars in this figure = 100 μm. (From Waldo et al., 2005, with permission.)

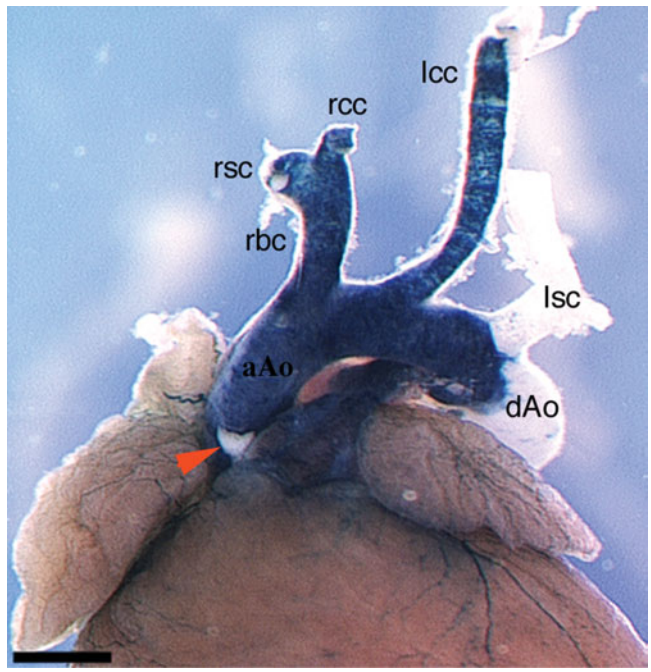

Figure 6.11. Lineage tracing of neural crest cells using plasminogen activator-cre X RARE-lacZ marker. The tunica media at the base of the aorta and pulmonary trunk is not derived from neural crest ectomesenchyme. (From Pietri et al., 2003, with permission.)

heart field is labeled with fluorescent dye prior to the addition of the myocardium in chick embryos the movement of the cells from the secondary heart field can be followed into the outflow tract (Fig. 6.9). The marked myocardial cells can be seen spiraling in the truncal myocardium toward the right ventricle. The cells from the right move into the caudal and then to the left side of the outflow tract while the cells from the left secondary heart field move cranially and rightward in the outflow myocardium. Thus, the right side of the secondary heart field contributes to the left or pulmonary side of the right ventricular outflow and the left secondary heart field contributes to the right or aortic side of the outflow. In contrast, when the secondary heart field is labeled at stage 18, after the addition of the myocardium, smooth muscle precursor cells are added to the caudal wall of the lengthening aortic sac which will become the base of the aorta and pulmonary trunk (Waldo et al., 2005; Ward et al., 2005).

The attachment point of the outflow tract with the pharynx is dynamic, translocating progressively more caudally (Waldo et al., 2001). At stage 12, the outflow joins the pharynx ventral to pharyngeal arch and arch artery 1, and by stage 24 it is located ventral to pharyngeal arches 4–6. This means it has moved along the region of the ventral pharynx that shows Nkx2.5/Gata4 expression (Waldo et al., 2001).

The presumptive smooth muscle from the secondary heart field is added, not by a spiraling migration path like the myocardium, but by dropping into place as the outflow tract moves caudally (Waldo et al., 2005). This means that the right secondary heart field provides smooth muscle to the base of the aorta and the left secondary heart field provides smooth muscle to the base of the pulmonary trunk (Fig. 6.10). These smooth muscle progenitors are unique in that they can be identified for several stages after they are added to the arterial pole only by their failure to express either myocardial or smooth muscle markers except for SM22. They first express smooth muscle contractile proteins at stage 28, which is after outflow septation has been initiated.

Myocardial Induction in the Secondary Heart Field

Several growth factors, including FGF8 and BMP2 and −4, are present in the caudal pharynx and outflow tract during the time that myocardium is added to the heart tube from the secondary heart field (Fig. 6.12). FGF8 is necessary for myocardial induction in both zebrafish and chick (Alsan and Schultheiss, 2002; Reifers et al., 2000). FGF8 is expressed in the endoderm and ectoderm of the lateral pharynx at stage 14 when the myocardium from the secondary heart field begins to differentiate (Waldo et al., 2001; Wendling et al., 2001). This expression is much reduced by stage 18, when outflow lengthening by addition of myocardium is finished (Farrell et al., 2001). Further, the FGF8 HYPOMORPHIC mouse has dramatically reduced development of the entire outflow limb of the looped heart (Abu-Issa et al., 2002; Frank et al., 2002).

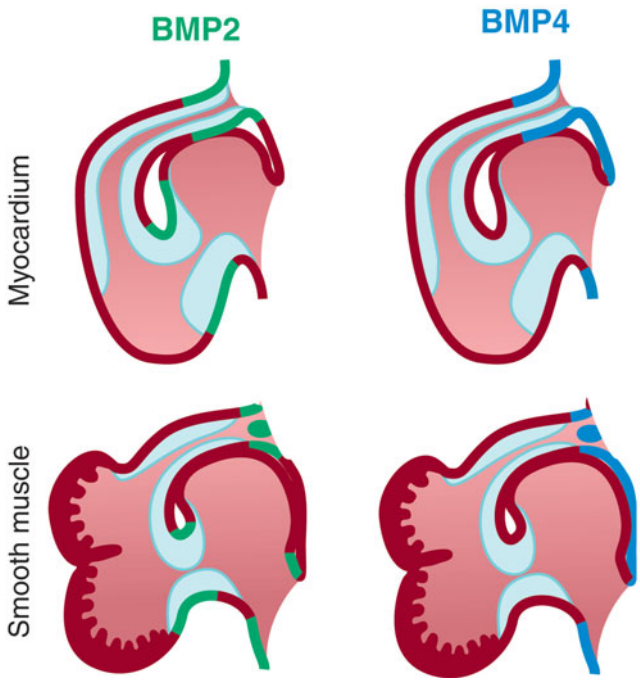

Figure 6.12. Diagrams illustrating the expression of BMP2 and -4 in the distal outflow tract during addition of the myocardium (*top panels*) and smooth muscle (*bottom panels*). (Adapted from Some et al., 2004, with permission.)

Proximity of the outflow myocardium is needed for cells in the secondary heart field to adopt a myocardial phenotype. When secondary heart field grafts are implanted in the lateral wall of the pharynx, not in proximity to the cardiac outflow tract, the grafted cells do not become myocardial. This suggests that the outflow tract moves caudally along the secondary heart field, bringing it in proximity with signaling factors that progressively induce differentiation of the cells into myocardium. The most likely candidates for the induction are BMP2 and -4, which are expressed in the myocardium of the distal outflow tract. Indeed, it has been shown that noggin, a BMP inhibitor, delays differentiation of the myocardial cell phenotype (Somi et al., 2004; Waldo et al., 2001).

In a transgenic mouse expressing a BMP type II receptor that lacks half of the ligand-binding domain and has reduced signaling capability, the mice die at mid-gestation with cardiovascular and skeletal defects. The most striking defect is in the outflow tract, with absence of septation of the conotruncus below the valve level (Delot et al., 2003). These studies suggest that BMP is an important factor in myocardial differentiation from the secondary heart field, but much more work is required to determine whether the inductive sequence is similar to that required in the cardiogenic fields.

Nothing is known about the mechanisms involved in the shift from myocardium to smooth muscle production by the secondary heart field to the arterial pole. The smooth muscle provides the tunica media at the base of the aorta and pulmonary trunk at the level of the aortic and pulmonary sinuses. Because neural crest cells provide the smooth muscle tunics more distally, the smooth muscle cells added by the secondary heart field appear unlabeled in a mouse model with lineage traced neural crest cells (Fig. 6.10).

The coronary artery stems originate in the right and left aortic sinuses. These stems are formed from cells derived from the epicardium and their development is covered more thoroughly in Chapter 10. However, the coronary stems develop by growth of capillary endothelial cells into the wall of the aorta. Multiple capillaries in the right and left aortic sinuses coalesce to form the stems of the right and left coronary arteries. Because abnormal coronary patterning is associated with abnormal development of the secondary heart field, the difference in derivation of the smooth muscle at the base of the arteries versus more distally may provide homing cues to the developing coronary capillaries (Ward et al., 2005).

Malformations Associated with Abnormal Development of the Cardiac Poles

Most congenital cardiac defects affect development of the poles. Historically, knowledge of the embryogenesis of any heart defects has been difficult to attain because of the lack of models in which the pathogenesis of the defect could be studied prospectively. The hero of the era before any models of heart defects became available was Ralph Shaner, who studied naturally occurring defects and examined 20,000 embryonic pigs to find only one in the process of developing complete transposition of the great arteries (Shaner, 1951). Retinoic acid was used as a teratogen to study heart defects, but this teratogen causes a number of other malformations and is better considered under syndromes (Chapter 15). There are now many models available to study some of the cardiac pole malformations and still none for several of the malformations. The following section discusses the human congenital malformations of the cardiac poles in the context of the animal models that now exist to study them.

Venous Pole Malformations

The venous pole is subject to septation defects that may or may not involve abnormal connections of the veins with the atria and with abnormal venous connections that typically occur with or without atrial septation defects. With the exception of atrial septal defects, few animal models are available to study venous pole developmental defects.

Cor Triatriatum

Cor triatriatum is a rare congenital cardiac anomaly. Most commonly, the left atrium is divided into a proximal and distal chamber by a fibromuscular diaphragm with one or more restrictive ostia. The pulmonary veins enter the proximal

chamber and the atrial appendage is distal to the membrane. The proximal chamber is formed by a vestigial common pulmonary vein that has not been appropriately remodeled (absorbed) into the left atrial wall. The pulmonary veins thus drain into this proximal chamber. Most patients present in the first few years of life although some are asymptomatic until the second or third decade. A left superior vena cava is frequently observed with this lesion. This leads to the possibility that impingement of the left superior vena cava on the developing left atrium is a potential pathogenesis (Myers and Jaggers, 2004). No animal models of cor triatriatum have been reported.

Partial and Total Anomalous Pulmonary Venous Connection

PARTIAL ANOMALOUS PULMONARY VENOUS CONNECTION (PAPVC) with intact atrial septum is a rare congenital cardiac defect. In PAPVC a portion of the pulmonary venous blood flow returns to the right atrium. Severity of the symptoms associated with PAPVC depends on how many pulmonary veins return abnormally to the right atrium. A greater number of veins draining anomalously results in more blood returning to the right side of the heart. The defect becomes clinically significant when 50% or more of the pulmonary veins return anomalously. Over a period of many years, excessive pulmonary venous return to the right side of the heart causes right atrial and ventricular dilation. This has a number of consequences, including risk of arrhythmia, right-sided heart failure, and, rarely, development of PULMONARY HYPERTENSION. This means that the clinical evidence of this congenital defect may not be apparent until the patient reaches middle age.

PAPVC occurs in approximately 10% of patients with an atrial septal defect. Typically, the pulmonary vein has an abnormal connection to the superior or inferior vena cava or the right atrium. The most common pattern of PAPVD with atrial septal defect is an anomalous connection with the superior vena cava associated with a superior sinus venosus atrial septal defect. A second pattern of PAPVD is in patients with scimitar syndrome. In these patients, the right pulmonary vein drains to the inferior vena cava. This is often associated with right lung hypoplasia.

TOTAL ANOMALOUS PULMONARY VENOUS RETURN (TAPVR) is a rare congenital malformation in which all four pulmonary veins do not connect to the left atrium, but instead drain into the right atrium by way of an abnormal connection. TAPVR is classified into different types based on the location of the abnormal pulmonary vein connections. In supracardiac total anomalous pulmonary venous return, the pulmonary veins commonly drain through a venous confluence behind the left atrium, via a connecting vein (often termed a vertical vein), to the right BRACHIOCEPHALIC VEIN which drains into an anomalous right-sided superior vena cava, and then into the right atrium. Other patterns of drainage are less common. In some cases, the pulmonary venous drainage occurs through a pulmonary venous confluence to an enlarged coronary sinus rather than persistent left superior vena cava. Less commonly, the confluence drains directly to the right atrium. In infracardiac TAPVR the pulmonary veins drain to the portal vein or the ductus venosus, then to the inferior vena cava and the right atrium. A mixed TAPVR is recognized where the pulmonary venous drainage is through multiple connections to the systemic venous circulation at the supracardiac, cardiac, and/or infracardiac level.

All types of TAPVR are accompanied by an atrial septal defect. Because none of the pulmonary veins connect normally to the left side of the heart, the pulmonary venous return is shunted from the right atrium across the atrial septal defect. Absence of an atrial septal defect with TAPVR is not compatible with survival.

No animal models of anomalous pulmonary venous return have been reported. However, these veins are very fragile even in adults making dissection almost impossible and techniques for visualizing them are not well developed.

Atrial Septal Defects

Because the atrial myocardium is incorporated from several different sources, there are many places where development can occur incorrectly to cause atrial malformations. There are four types of defects that are either actual deficiency in the interatrial septum or act functionally like interatrial septal defects. Primum and secundum atrial septal defects are true defects in the atrial septum and are named for the ostia that are affected rather than the septum. Sinus venosus (high) type and sinus venosus (low, also called coronary sinus) type act functionally like atrial septal defects but are in actuality deficiencies in the walls of the right pulmonary veins or coronary sinus that "unroof" them (Bharati and Lev, 1996). A sinus venosus type defect (high) results from a deficiency in the wall that normally separates the right pulmonary veins from the superior vena cava and right atrium which essentially unroofs the right pulmonary veins (Van Praagh et al., 1994). The right pulmonary veins then drain into the superior vena cava and/or right atrium. The defect is associated with an interatrial communication which is located posterior and superior to the fossa ovalis (Fig. 6.13). The inferior or coronary type of sinus venosus defect is found at the junction of the right atrium and inferior vena cava and may involve unroofing of the coronary sinus. This defect can be associated with abnormal connection of the right lower pulmonary vein to the inferior vena cava. Sinus venosus atrial septal defects represent about 1% of congenital cardiac lesions (Meyers and Jaggers, 2004).

Secundum atrial septal defect is due to an unclosed ostium secundum. This can be caused by several different processes. If the secondary septum (septum secundum) fails to grow properly or if the ostium secundum (in the primary septum) is too large, the secondary septum does not completely cover the opening, resulting in secundum atrial septal defect (Abdulla, 2004).

Primum atrial septal defect occurs when the primary atrial septum (septum primum) does not fuse with the atrioventricular cushions leaving the ostium primum open. As discussed previously, this defect may be associated with a poorly developed

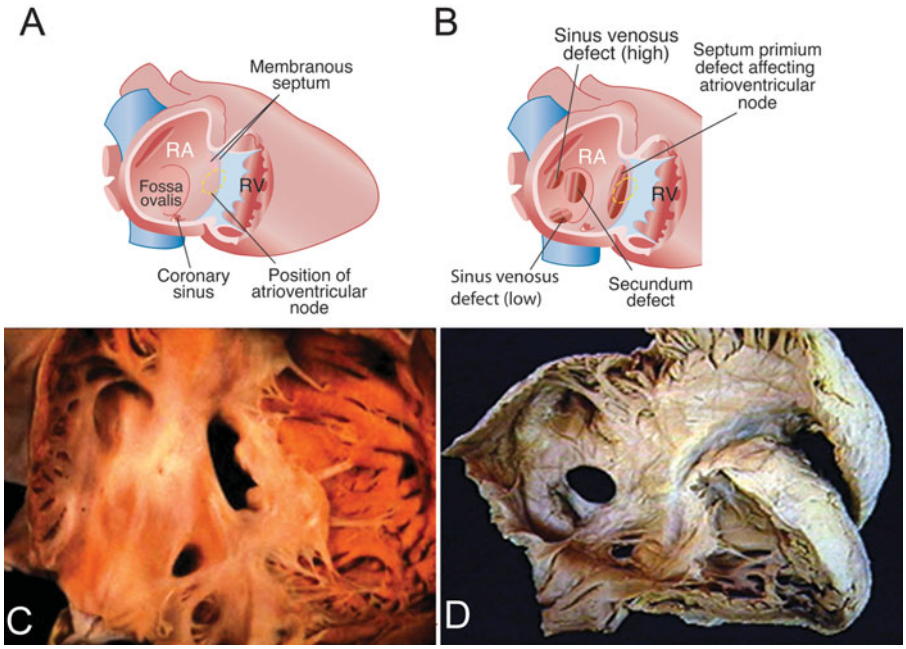

Figure 6.13. Types of atrial septal defect. *A* shows the perspective. *B* is a diagrammatic representation. *C* is a septum secundum defect in a human heart. *D* shows a septum primum defect. (*C* and *D* from Numan, 2002, with permission.)

mesenchymal cap on the primary atrial septum or atrioventricular cushions. If the atrioventricular cushions are defective, the primum type defect is not truly a venous pole malformation but a cushion defect, which is discussed in Chapter 9. Because of the involvement with the atrioventricular cushions that form the atrioventricular valve leaflets, this defect can occur with atrioventricular valve defect or cleft mitral valve (Abdulla, 2004).

In common atrium, the entire atrial septum is missing. Common atrium is associated with mitral valve prolapse (Abdulla, 2004).

Point mutations in *NKX*2.5, *TBX5*, and *GATA4* have been associated with atrial septal defects. Mutations in the *NKX2.5* transcription factor gene cause autosomal dominant familial atrial septal defects in association with progressive atrioventricular block as well as complex congenital heart disease (Schott et al., 1998; Vaughan and Basson, 2000). Point mutations in *TBX5* are associated with the Holt-Oram syndrome which is discussed more thoroughly in Chapter 15. *GATA4* mutations are associated with autosomal dominant familial atrial septal defects of the septum secundum type (Fig. 6.14) (Garg et al., 2003).

A mouse model of atrial septal defect and cardiac conduction abnormalities is associated with *Nkx2.5* haploinsufficiency (Tanaka et al., 2002). The conduction anomalies are discussed in more detail in Chapter 12. Haploinsufficient *Tbx5* mice provide a model of Holt-Oram syndrome which has atrial septal and forelimb defects. The Holt-Oram syndrome is discussed in Chapter 15.

Arterial Pole Malformations

Because of its complicated development the outflow tract is subject to a huge variety of congenital malformations. The malformations that involve primarily the secondary heart field are covered here and those that involve neural crest are covered in Chapter 11.

Ventricular Septal Defect

Ventricular septal defects frequently occur with other malformations of the arterial pole; however, isolated ventricular septal defects can occur anywhere in the ventricular septum. The majority of ventricular septal defects occur in the outflow septum and these are included in our consideration of arterial pole malformations. The most common type of ventricular septal defect is subaortic. The defect extends to the base of the semilunar valve and is considered to be in the conal septum (Bharati and Lev, 1996). It is possible that the volume of conal or truncal myocardium generated from the secondary heart field plays a role in closure of the conal septum because the conal and/or truncal myocardium is used to myocardialized the conal cushions.

Overriding Aorta in Double Outlet Right Ventricle (DORV)

OVERRIDING AORTA is a condition in which the aorta does not wedge properly between the atrioventricular valves (Fig. 6.14). It is always associated with a ventricular septal defect. If the aorta obtains 50% of its blood from the right ventricle, the defect is classified as DOUBLE OUTLET RIGHT VENTRICLE (DORV). DORV represents a continuum of congenital heart defects that ranges from VENTRICULAR SEPTAL DEFECT (VSD), with 50% of the blood entering the aorta coming from the right ventricle, to complete origin of the aorta from the right ventricle. Pathophysiologic description and classification is accomplished by relating the location of the ventricular septal defect to the origin of the great vessels. The ventricular septal defect

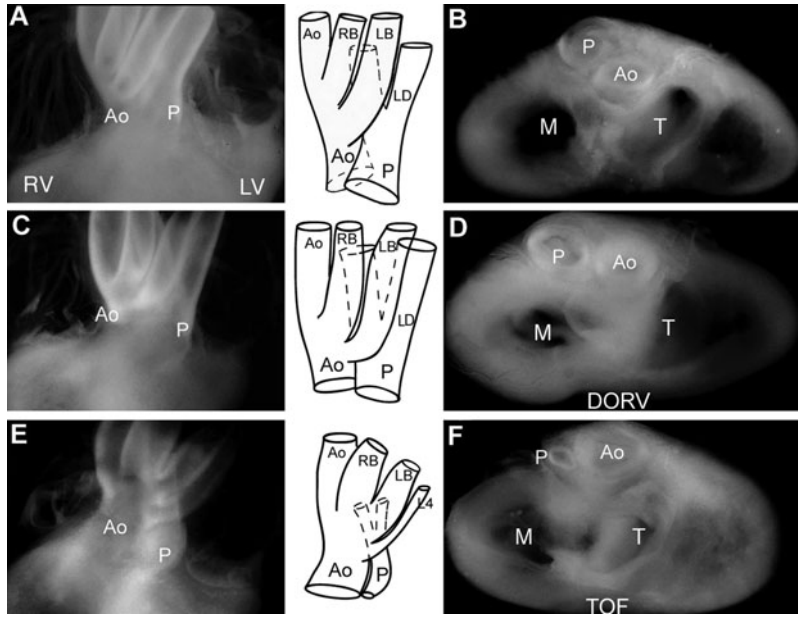

Figure 6.14. (*A*, *C*, and *E*) Ventral view of outflow tract with line drawings to show the position of outflow vessels and arch artery derivatives in day 9 chick hearts. (*B*, *D*, and *F*) Atria have been dissected away to show a four-valve view (ventral is toward the *top*) and the alignment of the outflow vessels. (*A* and *B*) Normal wedging and alignment of the aorta (Ao) behind the pulmonary (P) and between the mitral and tricuspid valves (M and T). The aorta then divides into the left and right brachiocephalic arteries (LB and RB) and a right-sided aortic arch (Ao). The pulmonary trunk divides into the right ductus arteriosus and left ductus arteriosus (LD) (*C* and *D*) Side-by-side orientation of the aorta and pulmonary trunk. In this situation the aorta is overriding and is not wedged between the mitral and tricuspid valves. (*E* and *F*) Aorta displaced to the right and the pulmonary trunk is stenotic showing similar pathology to that seen in tetralogy of Fallot. (From Hutson et al., 2006, with permission.)

can be subaortic, subpulmonary, noncommitted (not committed to either vessel), or doubly committed (underlying both vessels). Most of the ventricular septal defects do not restrict the flow of blood, but many require enlargement during repair to allow unrestricted blood flow.

DORV with noncommitted or remote ventricular septal defect has anatomy and physiology similar to isolated VSD or atrioventricular canal defect. To meet the criteria for DORV with noncommitted ventricular septal defect, the distance between the ventricular septal defect and the aortic and pulmonary outflow tracts should be at least equal to the aortic valve diameter.

Because DORV occurs as an isolated defect in fewer than 50% of patients who have it, classification and description also may take into consideration obstruction of the systemic circulation, ventricular anomalies, coronary artery anomalies, and conduction system abnormalities. Additional ventricular septal defects, anomalies of ventricular rotation, and anomalies of insertion of the subvalvar apparatus of the atrioventricular valves are not uncommon.

Coronary artery abnormalities are related to the relationship of the great arteries with several variations, including anomalous origin of the right coronary artery from the left main coronary artery, duplication of left anterior descending, anomalous origin of left anterior descending from right coronary artery (associated with a subaortic ventricular septal defect and pulmonary stenosis), anterior origin of left anterior descending, right coronary artery immediately beneath pulmonary annulus, and right coronary artery from the posterior aortic sinus/left coronary artery from the left sinus, which is seen with an anterior aorta and subpulmonary ventricular septal defect and is similar to transposition of the great arteries. Coronary artery mispatterning is covered in detail in Chapter 11.

DORV has been reported in association with chromosome 22q11 deletion (L'hermine-Coulomb et al., 2004). The heart defects associated with this deletion have been largely attributed to lack of Tbx1 function. The secondary heart field fails to proliferate normally suggesting that the outflow tract is not lengthened which results in malalignment (Xu et al., 2004).

Dextroposed aorta/double outlet right ventricle can be produced in animal models using a variety of methods including mechanical, teratogen-induced, genetic, and neural crest ablation. DORV with and without coronary artery anomalies can be produced experimentally by ablation of the secondary heart field (Ward et al., 2005). The addition of myocardium from the secondary heart field to the heart during looping appears to be an important mechanism for lengthening the primary heart tube. This lengthening is necessary for proper alignment of the inflow and outflow tracts prior to septation. If the lengthening does not occur normally, VSD and dextroposition of the aorta are the result (Yelbuz et al., 2002). Because the myocardium from the secondary heart field is added by spiraling, this may be important in alignment as the outflow tract settles finally by making a quarter turn to seat or wedge the aorta between the atrioventricular valves (Thompson et al., 1987). Ablation of the secondary heart field also leads to pulmonary stenosis or atresia. Both pulmonary stenosis and overriding aorta are hallmarks of tetralogy of Fallot, which is the prototypical malalignment defect. Classic tetralogy of Fallot is seen in a number of animal models and can be experimentally produced by ablation of the secondary heart field and preventing normal myocardial cell death during septation and remodeling of the outflow tract (Ward et al., 2005; Watanabe et al., 2001).

Reduced dosage of Gata4 results in double outlet right ventricle in the mouse (Pu et al., 2004). Mice homozygous for a *Jumonji* mutation have DORV with abnormal development of the ventricular walls. Jumonji is a nuclear protein that regulates proliferation (Toyoda et al., 2003). It is expressed in the

myocardium of the ventricles and outflow tract. Myocardial cells differentiate but fail to express chamber-specific genes (Lee et al., 2000).

Taussig–Bing Anomaly

TAUSSIG–BING ANOMALY is essentially DORV with pulmonary artery overriding the VSD. In this defect both of the great arteries arise from the right ventricle with the aorta to the right of the pulmonary artery. This is the same relationship of the aorta and pulmonary trunk seen in transposition of the great arteries. The pulmonary semilunar valve is to the right and slightly posterior or side by side with the aortic valve. The left ventricular outflow is directed toward the pulmonary artery. This results in pulmonary artery oxygen saturations greater than aortic saturations. In the absence of pulmonary obstruction or stenosis, DORV with subpulmonary VSD produces physiology similar to transposition of the great arteries. In this case, pulmonary vascular resistance determines pulmonary blood flow. Early-onset pulmonary obstructive vascular disease commonly occurs because of increased pulmonary blood flow and pressures, although cyanosis may be absent with high pulmonary blood flow. High pulmonary blood flow in DORV most frequently occurs with subaortic stenosis and aortic arch obstruction. *Fgf8* hypomorphic mice occasionally have transposed aorta and pulmonary trunk in a phenotype that looks much like the Tausig–Bing anomaly (Abu-Issa et al., 2002). Blocking Fgf8 signaling in chick embryos can also result in TRANSPOSITION OF THE GREAT ARTERIES (Hutson et al., 2006). In this case, the defect is caused by failure of addition of myocardium to the outflow tract from the secondary heart field.

Tetralogy of Fallot

Tetralogy of Fallot comprises a group of heart malformations associated with CYANOSIS after birth. Tetralogy of Fallot has four major components: pulmonary valve stenosis, VSD, dextroposition of the aorta which overrides the VSD, and CONCENTRIC HYPERTROPHY of the right ventricle. Tetralogy of Fallot occurs in 4:10,000 live births and represents 15% of congenital heart disease and 55%–70% of cyanotic congenital malformations (Boudjemline et al., 2000). There is a slight predominance of males over females. The pulmonary stenosis is valvular in 25% of the cases, INFUNDIBULAR in 25%, and both valvular and infundibular in 50% of the cases. The degree of stenosis is variable, from mild to pulmonary valve atresia. When the pulmonary valve is atretic, the defect is referred to as "PSEUDOTRUNCUS," as the physiology is essentially the same as a persistent truncus arteriosus. A fibromuscular or fibrous hypertrophy of the infundibular region can be seen in the infundibular stenosis. When this fibrous hypertrophy is located below the infundibulum, the space between the hypertrophied ring and the valve is called "infundibular camera" or "third ventricle" or "double-chamber right ventricle." In "PENTALOGY" OF FALLOT an atrial septal defect is seen in addition to the four definitive components.

Ablation of the right side of the secondary heart field or blocking Fgf8 signaling during the period when the myocardium is added from the secondary heart field in chick embryos have both been shown to result in pulmonary stenosis and atresia (Fig. 6.13) (Hutson et al., 2006; Ward et al., 2005). The myocardium contributed from the right side of the secondary heart field spirals behind and to the pulmonary side (left) of the outflow tract. When this myocardium is lost by ablation, the pulmonary outflow channel is compromised. Fgf8 is needed for normal proliferation of the myocardial precursors in the secondary heart field. Blocking Fgf8 signaling before the precursors are added to the outflow myocardium results in a situation similar to ablation in that not enough myocardial cells are added to maintain the pulmonary outflow diameter.

Mice hypomorphic for Fgf8 have DORV and tetralogy of Fallot (Abu-Issa et al., 2002; Frank et al., 2002). However, these mice have a number of other defects and it is not possible to say whether low Fgf8 signaling directly affects addition of the secondary heart field to the heart or acts via some other mechanism. NEUROTROPHIN 3 (NT3) is essential for the normal heart development via TRK C receptor tyrosine kinases on cardiac myocytes. It regulates cardiac myocyte proliferation during looping and formation of the ventricular trabeculae. Proliferation later becomes independent of Nt3. Nt3-null mice have atrial and ventricular septal defects, and tetralogy of Fallot (Donovan et al., 1996; Lin et al., 2000). A mutation in a highly conserved glycine residue of Jagged, a Notch ligand expressed in the developing right heart is associated with tetralogy of Fallot (Eldadah et al., 2001). Mutation or microdeletion of *JAGGED1* is also associated with ALLAGILE SYNDROME, discussed in Chapter 15. Disruption of non-muscle myosin heavy chain B is associated with abnormal myocardial development and overriding aorta as is found in both tetralogy of Fallot and double outlet right ventricle (Tullio et al., 1997).

Aortic Stenosis

Aortic stenosis refers to any condition that causes obstruction to blood flow between the left ventricle and the aorta. There are a variety of causes, including muscular obstruction below the aortic valve, obstruction at the valve itself, or aortic narrowing immediately above the valve. The most common form is obstruction at the valve itself, referred to as aortic valvar stenosis. Aortic stenosis has not been reported in an animal model.

Isolated Pulmonary Stenosis or Atresia

Pulmonary stenosis is a condition characterized by obstruction to blood flow from the right ventricle to the pulmonary artery. This obstruction is caused by narrowing or stenosis at one or more of several points from the right ventricle to the

pulmonary artery. It includes obstruction from thickened muscle below the pulmonary valve, narrowing of the valve itself, or narrowing of the pulmonary artery above the valve. The most common form of pulmonary stenosis is obstruction at the valve itself, referred to as pulmonary valvar stenosis.

Null mutation of Cx43 is also associated with pulmonary stenosis but in this case the pulmonary subvalvular myocardium does not function normally because it is replaced with large pockets of smooth muscle (Li et al., 2002).

Transposition of the Great Arteries

Transposition of the great arteries (TGA) is the most common cyanotic heart defect identified in the first week of life, and occurs in approximately 4 in 10,000 infants (Campbell, 2004). In transposition of the great arteries, both the aorta and pulmonary trunk are connected to the wrong ventricle referred to as ventriculoarterial discordance: the aorta arises from the right ventricle while the pulmonary trunk arises from the left ventricle. Thus, oxygenated blood from the lungs returns to the heart only to be sent back to the lungs rather than being delivered to the body. Conversely, oxygen-poor blood returns to the heart from the body and is immediately sent back to the body without being reoxygenated. Survival prior to surgery requires mixing of systemic and pulmonary blood somewhere in the heart or the body. If present, a VSD allows some mixing, but often this is not enough. Other places where mixing may occur are through an atrial septal defect or a patent ductus arteriosus. In nearly a third of cases, the branching pattern of the coronary arteries as they leave the transposed aorta is unusual. Infants may also have narrowing below the pulmonary valve which blocks blood flow from the left ventricle to the lungs.

There are three points of reference for transposition of the great arteries: the position of the arterial trunks, the emergence of the arterial trunks from the ventricular chambers, and the relationship of the ventricles to the atrioventricular valves. In common transposition discordance is between the ventricles and the arteries (ventriculoarterial) with no discordance between the atria and the ventricles, in other words it is "isolated" ventriculoarterial discordance. Transposition can also occur as congenital, physiologically corrected transposition (designated SLL or IDD transposition). This happens when the heart loops to the wrong side or the atria are reversed. These physiological corrections are mostly associated with abnormal SITUS (abnormal placement of the asymmetric organs such as the lungs, liver, spleen, and stomach).

From the embryological aspect, there are two main theories: (1) abnormal rotation of the arterial pole and (2) abnormal development of the outflow septum. To resolve which of these embryogenic mechanisms might occur, a robust animal model is needed. Retinoic acid and some human teratogenic agents produce low percentages of TGA but these are usually accompanying multiple other anomalies. Because TGA is rarely associated with syndromes or extracardiac anomalies, none of these animal models is particularly useful.

The genetic models for TGA harbor null mutations in several different genes: hypomorphic Fgf8, *type IIB activin receptor*, and *CRYPTIC* show the clearest examples of transposition although this phenotype is only one of several outflow defects, that is, double outlet right ventricle and persistent truncus arteriosus, are also seen in these mutants (Abu-Issa et al., 2002; Frank et al., 2002). Retinoic acid shows a dose-dependent differential induction of TGA at high doses and dextroposition of the aorta at low dose (Yasui et al., 1999). Because retinoic acid and the knockouts of the genes associated with retinoid signaling cause such complex phenotypes, it is difficult to assess pathogenesis of transposition in these models. More promising are the gene knockouts of *Activin IIB receptor* and *cryptic*, a member of the EGF-CFC family of membrane-associated proteins (Gaio et al., 1999; Oh and Li, 1997). However, all of these perturbations alter left-right axis determination and ventricular septation, which are defects associated with physiologically corrected transposition. Importantly, in these models transposition occurs only infrequently in the spectrum of other outflow malformations.

In contrast to the other models of transposition, which are physiologically corrected, the *PERLECAN*-null mouse presents common or uncorrected transposition (Costell et al., 2002). The high incidence of common transposition with intact ventricular septum is not found in any other animal models. This makes the *perlecan* model very important because intact septum is found with some frequency in humans with transposition. The *perlecan*-null mouse has what is clinically known as "common" or "isolated" SDD transposition of the great arteries (formerly called D-transposition) (Costell et al., 2002).

Perlecan is a heparan sulfate proteoglycan that is expressed in all basement membranes, in cartilage, and several other mesenchymal tissues during development. Perlecan binds growth factors and interacts with various extracellular matrix proteins and cell adhesion molecules. Since the heparan sulfate side chains bind Fgfs, perlecan may even serve as a low-affinity Fgf receptor (Aviezer et al., 1994; Sharma et al., 1998). Other aspects of the *perlecan*-null phenotype are associated with deterioration of basement membranes suggesting that perlecan is needed for stabilization of basement membranes (Costell et al., 1999).

The mesenchyme of the outflow tract in the *perlecan*-null mouse is disrupted. The outflow ridges serve as a template for septation of the outflow tract. In normal development they spiral in a counterclockwise similar to the spiral seen as myocardium from the secondary heart field is added to the outflow tract. The mesenchyme of the outflow tract has two described origins: endocardial cell-derived mesenchyme that arises by epithelial-to-mesenchymal transformation and cells migrating from the pharyngeal arches (Thompson and Fitzharris, 1979). The cells that migrate from the pharyngeal arches are mostly derived from neural crest but may also be from other sources (Jiang et al., 2000; Waldo et al., 1999). Disruption of the ridge pattern in the lumen of the outflow tract results in formation of a straight outlet septum rather than a spiraling septum. *Perlecan*-null embryos showed no abnormalities in the morphology or

placement of the lungs, liver, stomach, and spleen, which are sentinel organs for assessing normal left–right axis determination. The significance of this should now be obvious as the *perlecan*-null mouse represents the first animal model of common or isolated transposition. It will be interesting to see if the secondary heart field myocardium spirals into the outflow tract of the *perlecan*-null mouse.

Dissecting Aorta

Dissecting aorta is a condition in which bleeding occurs into the wall of the aorta. There are typical sites where the bleeding begins. The secondary heart field adds myocardium and smooth muscle to the cardiac outflow tract and as a result, there are two seams in the arterial pole: first, the myocardial junction with secondary heart field-derived smooth muscle; second, the secondary heart field-derived smooth muscle with the neural crest-derived smooth muscle (Fig. 6.8). Both of these seams are points where aortic dissection frequently occurs in Marfan's and other syndromes.

REFERENCES

Abdulla, R. 2004. Heart Diseases in Children Information Center at http://pediatriccardiology.uchicago.edu. Accessed July 24, 2006.

Abu-Issa, R., G. Smyth, I. Smoak, K. -I. Yamamura, and E. Meyers. 2002. Fgf8 is required for pharyngeal arch and cardiovascular development in the mouse. Development 129:4613–4625.

Abu-Issa, R., K. Waldo, and M. L. Kirby. 2004. Heart fields: one, two or more? Dev. Biol. 272:281–285.

Alsan, B. H., and T. M. Schultheiss. 2002. Regulation of avian cardiogenesis by Fgf8 signaling. Development 129:1935–1943.

Anderson, R. H., N. A. Brown, and A. F. Moorman. 2006. Development and structures of the venous pole of the heart. Dev. Dyn. 235:2–9.

Anderson, R. H., N. A. Brown, and S. Webb. 2002. Development and structure of the atrial septum. Heart 88:104–110.

Arguello, C., M. V. De la Cruz, and C. S. Gomez. 1975. Experimental study of the formation of the heart tube in the chick embryo. J. Embryol. Exp. Morph. 33:1–11.

Arrechedera, H., M. Alvarez, M. Strauss, and C. Ayesta. 1987. Origin of mesenchymal tissue in the septum primum: a structural and ultrastructural study. J. Mol. Cell. Cardiol. 19:641–651.

Asami, I., and K. Koizumi. 1995. Contribution of the spina vestibuli to the atrial septal complex in the human heart. In: Developmental Mechanisms of Heart Disease, ed. Clark, E. B., R. R. Markwald, and A. Takao, 255–260. Armonk, NY: Futura.

Aviezer, D., D. Hecht, M. Safran, M. Eisinger, G. David, and A. Yayon. 1994. Perlecan, basal lamina proteoglycan, promotes basic fibroblast growth factor-receptor binding, mitogenesis, and angiogenesis. Cell 79:1005–1013.

Bharati, S., and M. Lev. 1996. The Pathology of Congenital Heart Disease. A Personal Experience with More than 6,300 Congenitally Malformed Hearts. Futura Publishing Company, Inc., Armonk, NY.

Blom, N. A., A. C. Gittenberger-de Groot, T. H. Jongeneel, M. C. DeRuiter, R. E. Poelmann, and J. Ottenkamp. 2001. Normal development of the pulmonary veins in human embryos and formulation at a morphogenetic concept for sinus venosus defects. Am. J. Cardiol. 87:305–309.

Boudjemline, Y., L. Fermont, J. Le Bidois, A. Fraisse, J. Kachaner, E. Villain, D. Sidi, and D. Bonnet. 2000. Prenatal diagnosis of conotruncal heart diseases. Results in 337 cases. Arch. Mal. Coeur Vaiss. 93:583–586.

Cai, C. L., X. Liang, Y. Shi, P. H. Chu, S. L. Pfaff, J. Chen, and S. Evans. 2003. Isl1 identifies a cardiac progenitor population that proliferates prior to differentiation and contributes a majority of cells to the heart. Dev. Cell. 5:877–889.

Campbell, B. T. 2004. Transposition of the great vessels. Medical Encyclopedia, National Library of Medicine, http://www.nlm.nih.gov/medlineplus/ency/article/001568.htm. Accessed July 24, 2006

Canning, D. R., and C. D. Stern. 1988. Changes in the expression of the carbohydrate epitope HNK-1 associated with mesoderm induction in the chick embryo. Development 104:643–655.

Cardo, M., B. Fernandez, A. C. Duran, J. M. Arque, D. Franco, V. Sans-Coma. 1994. Anomalous origin of the left coronary artery from the pulmonary trunk and its relationship with the morphology of the cardiac semilunar valves in Syrian hamsters. Basic Res. Cardiol. 89:94–99.

Costell, M., R. Carmona, E. Gustafsson, M. Gonzalez-Iriarte, R. Fassler, and R. Munoz-Chapuli. 2002. Hyperplastic conotruncal endocardial cushions and transposition of great arteries in perlecan-null mice. Circ. Res. 91:158–164.

Dalgleish, A. E. 1976. The development of the septum primum relative to atrial septation in the mouse heart. J. Morphol. 149:369–382.

Davis, C. L. 1927. Development of the human heart from its first appearance to the stage found in embryos of twenty paired somites. Contrib. Embryol. 19:245–284.

de la Cruz, M. V., C. S. Gomez, M. M. Arteaga, and C. Arguello. 1977. Experimental study of the development of the truncus and the conus in the chick embryo. J. Anat. 123:661–686.

de la Cruz, M. V., C. S. Gomez, and R. Cayre. 1991. The developmental components of the ventricles: their significance in congenital cardiac malformations. Cardiol. Young 1:123–128.

de la Cruz, M. V., C. S. Gomez, and M. A. Palomino. 1989. The primitive cardiac regions in the straight tube heart (stage 9-) and their anatomical expression in the mature heart: an experimental study in the chick embryo. J. Anat. 165:121–131.

de la Cruz, M. V., C. Sanchez-Gomez, and J. L. Robledo-Tovi. 1987. Experimental study of the development of the ventricular inlets in the chick embryo. Embryol. Hefte 1:25–37.

Delot, E. C., M. E. Bahamonde, M. X. Zhao, and K. M. Lyons. 2003. BMP signaling is required for septation of the outflow tract of the mammalian heart. Development 130:209–220.

deVries, P. 1981. Evolution of precardiac and splanchnic mesoderm in relationship to the infundibulum and truncus. In: Mechanisms of Cardiac Morphogenesis and Teratogenesis, ed. Pexieder, T., 31–48. New York: Raven Press.

Donovan, J., J., A. Kordylewska, Y. N. Jan, and M. F. Utset. 2002. Tetralogy of Fallot and other congenital heart defects in *Hey2* mutant mice. Curr. Biol. 12:1605–1610.

Donovan, M. J., R. Hahn, L. Tessarollo, and B. L. Hempstead. 1996. Identification of an essential nonneuronal function of neurotrophin 3 in mammalian cardiac development. Nat. Genet. 14:210–213.

Eldadah, Z. A., A. Hamosh, N. J. Biery, R. A. Montgomery, M. Duke, R. Elkins, and H. C. Dietz. 2001. Familial tetralogy of Fallot

caused by mutation in the *jagged1* gene. Hum. Mol. Genet. 10:163–169.

Farrell, M. J., J. L. Burch, K. Wallis, L. Rowley, D. Kumiski, H. Stadt, R. E. Godt, T. L. Creazzo, and M. L. Kirby. 2001. FGF-8 in the ventral pharynx alters development of myocardial calcium transients after neural crest ablation. J. Clin. Invest. 107:1509–1517.

Franco, D., M. Campione, R. Kelly, P. S. Zammit, M. Buckingham, W. H. Lamers, and A. F. M. Moorman. 2000. Multiple transcriptional domains, with distinct left and right components, in the atrial chambers of the developing heart. Circ. Res. 87:984–991.

Frank, D., L. Fotheringham, J. Brewer, L. Muglia, Tristani-Firouzi, M. Capecchi, and A. Moon. 2002. An *Fgf8* mouse mutant phenocopies human 22q11 deletion syndrome. Development 129:4591–4603.

Gaio, U., A. Schweickert, A. Fischer, A. N. Garratt, T. Muller T, C. Ozcelik, W. Lankes W, M. Strehle M, S. Britsch S, M. Blum M, and C. Birchmeier C. 1999. A role of the cryptic gene in the correct establishment of the left-right axis. Curr. Biol. 9:1339–1342.

Garg, V., I. S. Kathiriya, R. Barnes, M. K. Schluterman, I. N. King, C. A. Butler, C. R. Rothrock, R. S. Eapen, K. Hirayama-Yamada, K. Joo, R. Matsuoka, J. C. Cohen, and D. Srivastava. 2003. GATA4 mutations cause human congenital heart defects and reveal an interaction with *TBX5*. Nature 424:443–447.

Hutson, M. R., H. A. Stadt, J. Burch, T. L. Creazzo, and M. L. Kirby. 2006. Cardiac outflow alignment is sensitive to levels of FGF8 signaling in the pharynx. Dev. Biol. 295:486–497.

Igarashi, H. 1984. Scanning electron microscopy study on the formation of the atrial septum in rat embryos. Acta Anat. Nippon 59:28–46.

Jiang, X., D. H. Rowitch, P. Soriano, A. P. McMahon, and H. M. Sucov. 2000. Fate of the mammalian cardiac neural crest. Development 127:1607–1616.

Kim, J. S., S. Viragh, A. F. Moorman, R. H. Anderson, and W. H. Lamers. 2001. Development of the myocardium of the atrioventricular canal and the vestibular spine in the human heart. Circ. Res. 88:295–402.

Knauth, A., K. P. McCarthy, S. Webb, S. Y. Ho, S. P. Allwork, A. C. Cook, and R. H. Anderson. 2002. Interatrial communication through the mouth of the coronary sinus. Cardiol. Young 12:364–372.

Kruithof, B. P. T., M. J. B. Van den Hoff, A. Wessels, and A. F. M. Moorman. 2003. Cardiac muscle cell formation after development of the linear heart tube. Dev. Dyn. 227:1–13.

L'hermine-Coulomb, A., L. Houyel, A. Aboura, F. Audibert, D. Dal Soglio, and G. Tachdjian. 2004. Double-outlet right ventricle with absent left ventricle and mitral atresia in a fetus with a deletion 22q12. Prenat. Diagn. 24:708–712.

Lee, Y., A. J. Song, R. Baker, B. Micales, S. J. Conway, and G. E. Lyons. 2000. Jumonji, a nuclear protein that is necessary for normal heart development. Circ. Res. 86:932–938.

Li, Q. Y., R. A. Newbury-Ecob, J. A. Terrett, D. I. Wilson, A. R. J. Curtis, C. H. Yi, T. Gebuhr, P. J. Bullen, S. C. Robson, T. Strachan, D. Bonnet, S. Lyonnet, I. D. Young, J. A. Raeburn, A. J. Buckler, D. J. Law, and J. D. Brook. 1997. Holt-Oram syndrome is caused by mutations in *TBX5*, a member of the Brachyury (T) gene family. Nat. Genet. 15:21–29.

Li, W. E. I., K. Waldo, K. L. Linask, T. Chen, A. Wessels, M. S. Parmacek, M. L. Kirby, and C. W. Lo. 2002. An essential role for connexin43 gap junctions in mouse coronary artery development. Development 129:2031–2042.

Lin, M. I., I. Das, G. M. Schwartz, P. Tsoulfas, T. Mikawa, and B. L. Hempstead. 2000. Trk C receptor signaling regulates cardiac myocyte proliferation during early heart development in vivo. Dev. Biol. 226:180–191.

Mommersteeg, M. T., A. T. Soufan, F. J. de Lange, M. J. B. van den Hoff, R. H. Anderson, V. M. Christoffels, and A. F. M. Moorman. 2006. Two distinct pools of mesenchyme contribute to the development of the atrial septum. Circ. Res. 99:351–353.

Myers, J. L., and J. Jaggers. 2004. Cor triatriatum. eMedicine Specialties http://www.emedicine.com/ped/topic2107.htm. Accessed July 24, 2006:

Numan, M. 2002. Isolated atrial septal defect embryology, clinical presentation, and diagnosis. Heart Views 3:55–60.

Oh, S. P., and E. Li. 1997. The signaling pathway mediated by the type IIB activin receptor controls axial patterning and lateral asymmetry in the mouse. Genes Dev. 11:1812–1826.

Pietri, T., O. Eder, M. Blanche, J. P. Thiery, and S. Dufour. 2003. The human tissue plasminogen activator-Cre mouse: a new tool for targeting specifically neural crest cells and their derivatives in vivo. Dev. Biol. 259:176–187.

Pu, W. T., T. Ishiwata, A. L. Juraszek, Q. Ma, and S. Izumo. 2004. GATA4 is a dosage-sensitive regulator of cardiac morphogenesis. Dev. Biol. 275:235–244.

Puerta Fonolla, A. J., and F. Orts Llorca. 1978. Origin and development of the septum primum. Acta Anat. (Basel). 100:250–257.

Reifers, F., E. C. Walsh, S. Leger, D. Y. R. Stainier, and M. Brand. 2000. Induction and differentiation of the zebrafish heart requires fibroblast growth factor 8 (fgf8/acerebellar). Development 127:225–235.

Schott, J. J., D. W. Benson, C. T. Basson, W. Pease, G. M. Silberbach, J. P. Moak, B. J. Maron, C. E. Seidman, and J. G. Seidman. 1998. Congenital heart disease caused by mutations in the transcription factor *NKX2–5*. Science 281:108–111.

Shaner, R. B. 1951. Complete and corrected transposition of the aorta, pulmonary artery and the ventricle in pig embryos, and a case of corrected transposition in a child. Am. J. Anat. 88:35.

Sharma, B., M. Handler, I. Eichstetter, J. M. Whitelock, M. A. Nugent, and R. V. Iozzo. 1998. Antisense targeting of perlecan blocks tumor growth and angiogenesis in vivo. J. Clin. Invest. 102: 1599–1608.

Somi, S., A. A. M. Buffing, A. F. M. Moorman, and M. J. B. Van Den Hoff. 2004. Dynamic patterns of expression of BMP isoforms 2, 4, 5, 6, and 7 during chicken heart development. Anat. Rec. 279: 636–651.

Soufan, A. T., M. J. van den Hoff, J. M. Ruijter, P. A. de Boer, J. Hagoort, S. Webb, R. H. Anderson, and A. F. Moorman. 2004. Reconstruction of the patterns of gene expression in the developing mouse heart reveals an architectural arrangement that facilitates the understanding of atrial malformations and arrhythmias. Circ. Res. 95:1207–1215.

Tanaka, M., C. I. Berul, M. Ishii, P. Y. Jay, H. Wakimoto, P. Douglas, N. Yamasaki, T. Kawamoto, J. Gehrmann, C. T. Maguire, M. Schinke, C. E. Seidman, J. G. Seidman, Y. Kurachi, and S. Izumo. 2002. A mouse model of congenital heart disease: cardiac arrhythmias and atrial septal defect caused by haploinsufficiency of the cardiac transcription factor *Csx/Nkx2.5*. Cold Spring Harb. Symp. Quant. Biol. 67:317–325.

Tasaka, H., E. L. Krug, and R. R. Markwald. 1996. Origin of the pulmonary venous orifice in the mouse and its relation to the morphogenesis of the sinus venosus, extracardiac mesenchyme (spina vestibuli), and atrium. Anat. Rec. 246:107–113.

Thompson, R. P., V. Abercrombie, and M. Wong. 1987. Morphogenesis of the truncus arteriosus of the chick embryo heart: movements of autoradiographic tattoos during septation. Anat. Rec. 218: 434–440.

Thompson, R. P., and T. P. Fitzharris. 1979. Morphogenesis of the truncus arteriosus of the chick embryo heart: the formation and migration of mesenchymal tissue. Am. J. Anat. 154:545–556.

Toyoda, M., H. Shiratori, K. Nakajima, M. Kojima, M. Takahashi, M. Kubota, R. Suzuki-Migishima, Y. Motegi, M. Yokoyama, and T. Takeuchi. 2003. Jumonji downregulates cardiac cell proliferation by repressing cyclin D1 expression. Dev. Biol. 5:85–97.

Tucker, G. C., H. Aoyama, M. Lipinski, T. Tursz, and J. P. Thiery. 1984. Identical reactivity of monoclonal antibodies HNK-1 and NC-1: conservation in vertebrates on cells derived from the neural primordium and on some leukocytes. Cell Differ. 14:223–230.

Tullio, A. N., D. Accili, V. J. Ferrans, Z. X. Yu, K. Takeda, A. Grinberg, H. Westphal, Y. A. Preston, and R. S. Adelstein. 1997. Nonmuscle myosin II-B is required for normal development of the mouse heart. Proc. Natl. Acad. Sci. USA 94:12407–12412.

Van den Hoff, M. J. B., B. P. T. Kruithof, A. F. M. Moorman, R. R. Markwald, and A. Wessels. 2001. Formation of myocardium after the initial development of the linear heart tube. Dev. Biol. 240:61–76.

Van Praagh, S., M. E. Carrera, S. P. Sanders, J. E. Mayer, R. Van Praagh, R. 1994. Sinus venosus defects: unroofing of the right pulmonary veins—anatomic and echocardiographic findings and surgical treatment. Am. Ht. J. 128:365–379.

Vaughan, C. J., and C. T. Basson. 2000. Molecular determinants of atrial and ventricular septal defects and patent ductus arteriosus. Am. J. Med. Genet. 97:304–309.

Vincent, M., and J. P. Thiery. 1984. A cell surface marker for neural crest and placodal cells: Further evolution in peripheral and central nervous system. Dev. Biol. 103:468–481.

Viragh, S., and C. E. Challice. 1973. Origin and differentiation of cardiac muscle cells in the mouse. J. Ultrastruct. Res. 42:1–24.

Waldo, K. L., M. R. Hutson, C. C. Ward, M. Zdanowicz, H. A. Stadt, D. Kumiski, R. Abu-Issa, and M. L. Kirby. 2005. Secondary heart field contributes myocardium and smooth muscle to the arterial pole of the developing heart. Dev. Biol. 281:78–90.

Waldo, K. L., D. H. Kumiski, K. T. Wallis, H. A. Stadt, M. R. Hutson, D. H. Platt, and M. L. Kirby. 2001. Conotruncal myocardium arises from a secondary heart field. Development 128:3179–3188.

Waldo, K. L., C. W. Lo, and M. L. Kirby. 1999. Connexin 43 expression reflects neural crest patterns during cardiovascular development. Dev. Biol. 208:307–323.

Ward, C., H. A. Stadt, M. R. Hutson, and M. L. Kirby. 2005. Ablation of the secondary heart field leads to tetralogy of Fallot and pulmonary atresia. Dev. Biol. 284:72–83.

Watanabe, M., A. Jafri, and S. A. Fisher. 2001. Apoptosis is required for the proper formation of the ventriculo-arterial connections. Dev. Biol. 240:274–288.

Webb, S., R. H. Anderson, W. H. Lamers, and N. A. Brown. 1999. Mechanisms of deficient cardiac septation in the mouse with trisomy 16. Circ. Res. 84:897–905.

Webb, S., N. A. Brown, and R. H. Anderson. 1998. Formation of the atrioventricular septal structures in the normal mouse. Circ. Res. 82:645–656.

Webb, S., N. A. Brown, R. H. Anderson, and M. K. Richardson. 2000. Relationship in the chick of the developing pulmonary vein to the embryonic systemic venous sinus. Anat. Rec. 259:67–75.

Webb, S., M. Kanani, R. H. Anderson, M. K. Richardson, and N. A. Brown. 2001. Development of the human pulmonary vein and its incorporation in the morphologically left atrium. Cardiol. Young 11:632–642.

Wendling, O., N. B. Ghyselinck, P. Chambon, and M. Mark. 2001. Roles of retinoic acid receptors in early embryonic morphogenesis and hindbrain patterning. Development 128:2031–2038.

Xu, H., M. Morishima, J. N. Wylie, R. J. Schwartz, B. G. Bruneau, E. A. Lindsay, and A. Baldini. 2004. *Tbx1* has a dual role in the morphogenesis of the cardiac outflow tract. Development 131: 3217–3227.

Yasui, H., M. Morishima, M. Nakazawa, M. Ando, and E. Aikawa. 1999. Developmental spectrum of cardiac outflow tract anomalies encompassing transposition of the great arteries and dextroposition of the aorta: pathogenic effect of extrinsic retinoic acid in the mouse embryo. Anat. Rec. 254:253–260.

Yelbuz, T. M., K. L. Waldo, D. H. Kumiski, H. A. Stadt, R. R. Wolfe, L. Leatherbury, and M. L. Kirby. 2002. Shortened outflow tract leads to altered cardiac looping after neural crest ablation. Circulation 106:504–510.

This page intentionally left blank

7

Molecular Control of Looping

Even though the right–left axis of the body is established during early gastrulation, cardiac looping is the first visible sign of right–left ASYMMETRY during embryonic development. In vertebrates the heart always loops to the right. Looping directionality correlates with asymmetric expression of several molecular markers, but how these molecules are translated into biomechanical forces that drive looping remains obscure. The looping process itself is important to bring the initially sequentially ordered regions of the heart tube with serial circulation into the correct conformation for chamber specification and septation to create two parallel circulations.

Morphology of Looping

During the looping process, the initially midline heart tube undergoes a coordinated progression of bending, rotation, and torsion (Fig. 7.1). The initial steps result in a C-shaped loop whose convexity is directed toward the right side of the body (DeHaan, 1965; Garcia-Pelaez and Arteage, 1993; Icardo, 1996; Stalsberg, 1970). The heart tube goes through two major alterations in shape to achieve the C-shaped loop: ventral bending and rightward rotation (Manner, 2000). However, because the dorsal mesocardium is still intact during C-looping (Fig. 7.1A), little movement is possible except by shape changes at the ventral midline or outer curvature which becomes the right border during C-looping. Thus, the ventral bending is actually ballooning of the newly formed ventral wall rather than bending of the whole tube. In the second part of this movement, the heart tube rotates around its craniocaudal axis, bringing the ventral midline (outer curvature) to the right and the initially left surface of the myocardial tube to form the ventral surface of the C-shaped loop (Manner, 2000). An inner curvature is formed from the dorsal midline on the left side (Fig. 7.1). This is referred to as dextral or D-looping.

The C-shaped tube is next converted into an S-shaped loop (Fig. 7.1A) (de la Cruz and Markwald, 1998; Taber, 1995). In this process, the distance between the outflow and inflow attachment points to the foregut is diminished, and the ventricular bend, which was originally cranial to the inflow attachment and atrium is now caudal (Fig. 7.1A).

During the final stage of looping, the atrial and outflow poles converge as the last segment of the outflow tract, the truncus is added, and chamber identity becomes established (Manner et al., 2000; Patten, 1922; Steding and Seidl, 1980). Some investigators consider this the end of the looping process, although others recognize a final "wedging" step that occurs concurrently with and after septation of the aorta and pulmonary trunk, in which the aorta wedges between the atrioventricular valves (Fig. 7.1B and C) (Bouman et al., 1995, 1997; Kirby and Waldo, 1995).

In the broadest sense then, looping involves at least four separate processes: formation of a C-shaped loop, elongation to form an S-shaped loop, convergence of the inflow and outflow poles, and finally, rotation and wedging of the aorta between the atrioventricular valves. In the chick, these steps occur over a prolonged period that extends from fusion of the bilateral heart primordia until the end of outflow septation, or over approximately incubation days 2–8. Another feature of chick heart development that is shared in human heart development is that the initial tube is formed along the ventral pharynx where there is ample craniocaudal space for a relatively long tube to form that represents much of the heart (Fig. 7.2). In mouse, a straight heart tube is never formed because of shortened space between the forebrain and anterior intestinal portal (Fig. 7.3). The heart is never laid out along the ventral pharynx as a straight tube as it is in the chick and human. This necessitates addition of myocardium mostly from the ends of the tube rather than from the sides as in the case of the chick and human. In mouse embryos, heart looping starts at the same time as heart fusion at E8.0, and by E9.0 an S-shaped loop is formed with convergence well underway.

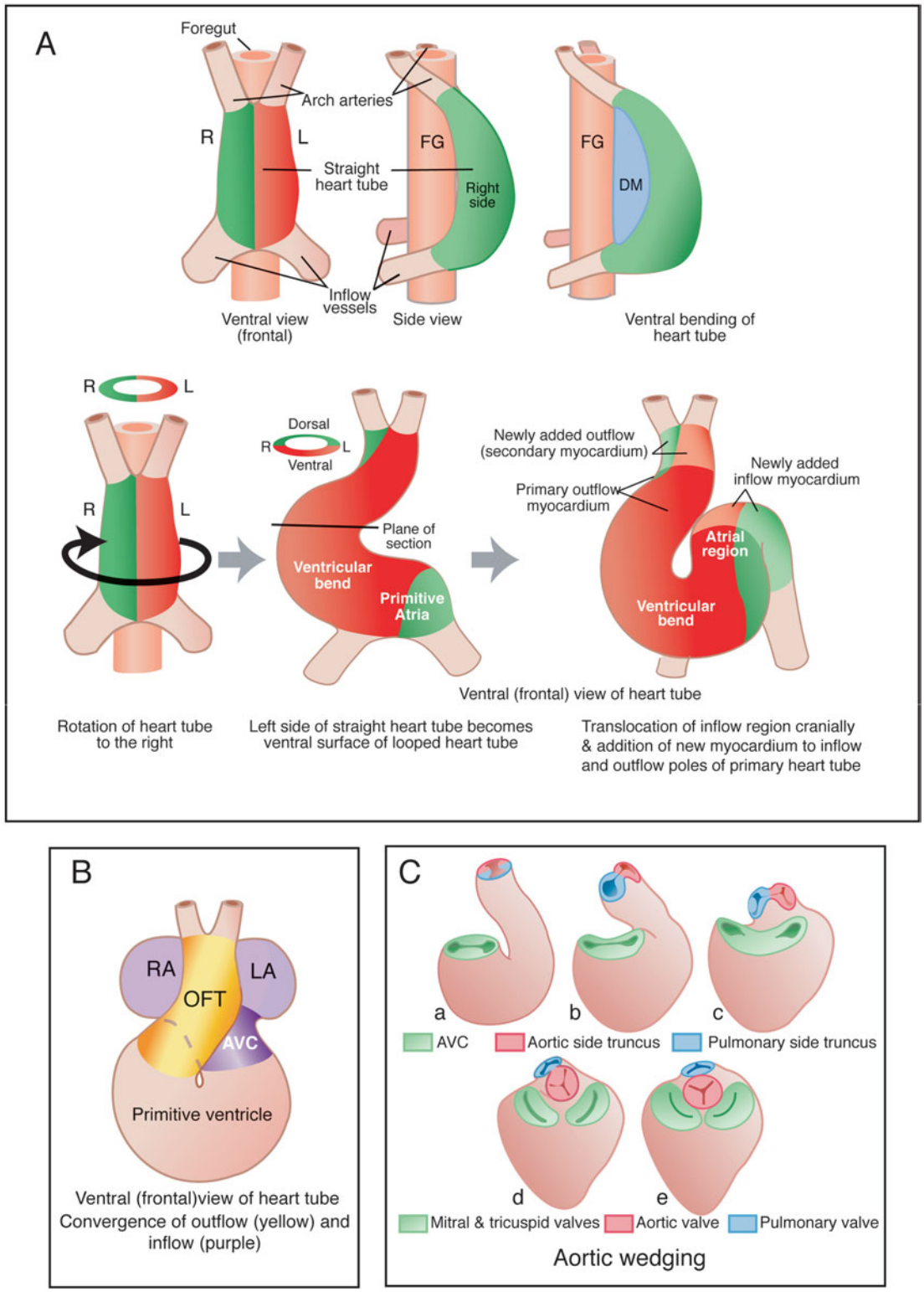

Figure 7.1. Steps in looping and wedging. (*A*) The heart tube forms ventral to the foregut and is open to it at first. Then the heart tube is suspended at its nascent inner curvature from the ventral foregut by the dorsal mesocardium which quickly disappears. Ventral bending occurs first, followed by rotation to the right which brings the left side of the tube to the front and the inner curvature to the left side. Subsequent looping to form the S-shaped loop involves addition of cells at the inflow and outflow poles. (*B*) The outflow tract centers itself between the nascent atrioventricular valves at the atrioventricular canal. (*C*) The aortic side of the outflow tract nestles between the mitral and tricuspid valves as the outflow myocardium is remodeled.

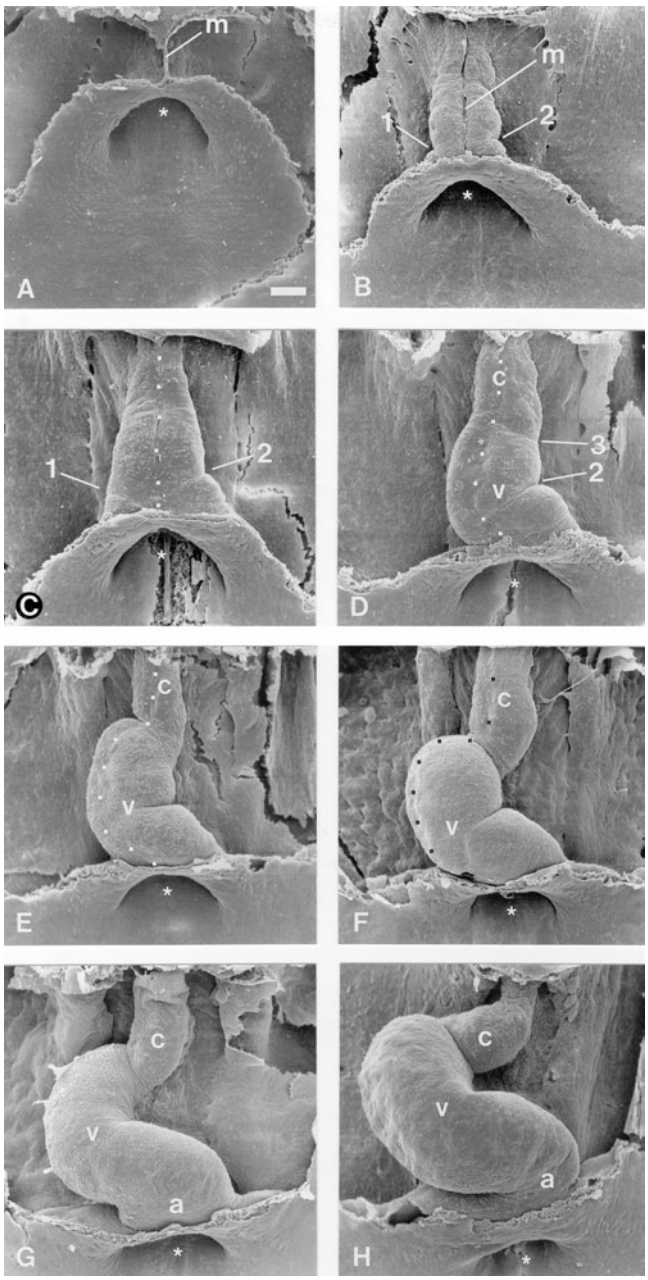

Figure 7.2. Ventral views of chick embryos ranging from stages 9–13 illustrating the steps in formation of the C-shaped loop. (From Manner, 2000, with permission.)

The inflow and outflow are located dorsally, and the presumptive ventricles are ventral. The presumptive right and left ventricles are transversely oriented, i.e., side by side (Ya et al., 1998).

Forces That Drive Heart Looping

Waddington proposed that the direction of head turning is controlled by the asymmetry of heart looping. The first sign of

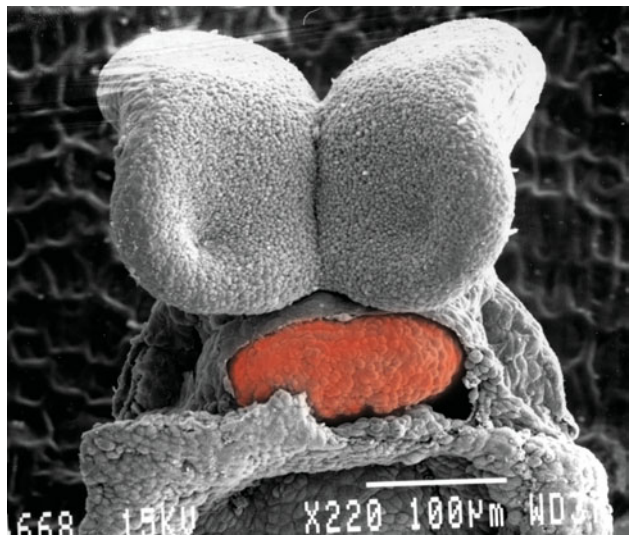

Figure 7.3. The early mouse heart tube (*red*) lies transversely rather than longitudinally at E8. The heart is sandwiched horizontally across the ventral pharynx between the buccopharyngeal membrane/forebrain and the anterior intestinal portal. (Compliments of K. K. Sulik, Embryo Images at http://www.med.unc.edu/embryo_images/.)

body turning occurs when the right eye and ear rotate dorsally (Waddington, 1937). Two supportive studies showed a majority of embryos with body turning correlated with heart looping after mechanical disruptions (Hoyle et al., 1992; Kirby et al., 2003). However, by applying the morphogen Sonic hedgehog (Shh), to the right side of Henson's node and thus altering the embryonic left–right axis during gastrulation (see later), the direction of heart looping and embryonic rotation can be uncoupled (Levin et al., 1997). This suggests that the direction of heart looping is a multistage process involving at least two separate determinative events. The first of these is establishing the right-left axis during gastrulation. A second event may be coordination of a right–left head axis during formation of the foregut pocket when the cardiac tube is formed, but very little is known about stages in left–right determination other than the events at the node and distinctly separated but coordinated subsequent asymmetrical patterns of gene expression in the mesoderm (Kirby et al., 2003).

C-Shaped Loop

Formation of the C-shaped loop consists of two independent steps. The first of these is ventral bending, and the second is rotation to the right side (Latacha et al., 2005). Several studies suggest that the earliest ventral bending component is regulated by forces intrinsic to the heart while the rotation is controlled by factors extrinsic to the heart (Itasaki et al., 1991; Manasek et al., 1984; Manning and McLachlan, 1990; Voronov et al., 2004). In his chick embryology textbook, Patten said that there is already a tendency for the right lateral margin of the heart to show greater convexity than that of the left and that

this asymmetry is due to unequal dilation of the heart wall (Patten, 1922). Other investigators have also maintained that the heart is never a strictly symmetrical, straight tube (Davis, 1927; Orts Llorca and Ruano Gil, 1967). However, while the tube in the chick is not symmetrical as can be appreciated in Fig. 7.2, the right and left lateral margins look quite straight at stages 10 and 11 and a tendency to bend rightward is first seen at stage 11 (Manner, 2000). On the other hand, the cardiac tube in the mouse is constrained by the forebrain/buccopharyngeal membrane cranially and the anterior intestinal portal caudally, making it impossible for a straight tube to form as in the chick (Fig. 7.3). Thus, the mouse heart tube forms in a looped configuration. The human heart tube forms more similarly to the chick than the mouse (K. Sulik, personal communication).

One of the mechanisms considered for the initial rightward asymmetry was that the heart fields contribute unequally to the heart tube that initiates looping. Radioactive thymidine labeling of the primary heart fields showed that contributions of the heart fields to the tube are maintained as right and left in the heart tube and are about equal (Stalsberg, 1969). The right contribution becomes dorsal and the left contribution ventral after looping, but there is no difference in proliferative activity in the linear heart tube that would account for looping (Stalsberg, 1969). However, there is a significantly larger contribution from the right heart field to the cranial portion of the tube and a significantly larger contribution from the left heart field to the caudal portion of the tube at stage 10, that is, right-sided dominance rostrally and left-sided dominance caudally. Producing cardia bifida by preventing the right and left heart primordia from fusing also shows that the cephalic part of the heart loop tends to be larger on the right side and the caudal part of the loop larger in the left half-heart (Van Praagh and DeHaan, 1967). This is also seen in human embryos, in which the right cardiogenic mesoderm contributes more to the presumptive right ventricle and infundibulum than the left cardiogenic mesoderm while the left cardiogenic mesoderm contributes most to the left ventricular primordium (De Vries and Saunders, 1962). In support of this idea, there is a difference in the temporal progression of cardiac differentiation between the left and right sides (Satin et al., 1988). However, a recent study in a mouse mutant that develops cardia bifida showed that looping and subsequent ventricular chamber specification occurs normally in both the left and right hearts, so the significance of cranial right-sided dominance versus caudal left-sided dominance is unclear (Li et al., 2004). Curvatures, alternating dilations, and constrictions occur in each of the cardia bifida half-hearts (Van Praagh and DeHaan, 1967). This suggests that even if there is an unequal contribution of cardiogenic mesoderm to the heart tube from right or left sides, the differences in contributions are not sufficient to account for the degree of bending that occurs during looping. Further, only rightward bending and not ventral bending would be affected by differences in right versus left contributions to the heart tube.

It was suggested that pressure in the cardiac jelly, coupled with a spiraling myocardial fiber layer, causes the heart tube to twist (Manasek, 1983). However, when the cardiac jelly is digested by hyaluronidase, the heart loops normally (Baldwin and Solursh, 1989). This led to the idea that the myocardium itself may be a factor in looping. Indeed, when a crystal of cytochalasin B, an agent that depolymerizes intermediate filaments, is placed on the right side, the heart loops to the left (Itasaki et al., 1991). This suggests that circumferential contractile forces, most likely in the myocardial layer, pull the heart tube to the right forcing it to rotate on the dorsal mesocardium. Thus, cardiac looping could be driven by changes of cell shape that involve differential contraction of the actin cytoskeleton along the heart tube (Taber et al., 1995). However, this is contradicted or perhaps clarified by more recent studies showing that the heart has no intrinsic ability to rotate (Voronov et al., 2004). It does have the ability to bend ventrally, the first step in forming the C-shaped loop. In fact, treatment with low doses of agents that inhibit actin polymerization destabilizes the cytoskeleton and disrupts the ventral bending component of C-shaped looping (Latacha et al., 2005). Indeed, the heart has little to no intrinsic ability to rotate (Manning and McLachlan, 1990; Voronov et al., 2004). This means that the ventral bending but not the rightward rotation is orchestrated by intrinsic force generated by the myocardial cytoskeletal actin but it leaves the factors that control rightward looping unresolved.

Patten suggested that the heart is forced to loop to the right because of physical constraints imposed by the embryo body dorsally and the yolk ventrally (Patten, 1922). A recent study showed that the rotational component depends on external forces provided by the dorsal mesocardium and the omphalomesenteric veins (Voronov et al., 2004). When the heart is dissected from the embryo at stage 10, the left ventricle is formed and is directed toward the right, suggesting that tension at the inflow as the chambers are formed directs the rightward rotation movement (de la Cruz and Markwald, 1998). The stresses generated by the inflow are caused by longitudinal cytoskeletal contractions, which pull precardiac cells through the veins toward the caudal end of the heart (Linask and Lash, 1986, 1988a,b; Toyoizumi et al., 1991). The left vein pushes with greater force, displacing the heart slightly to the right while the dorsal mesocardium locks in the displacement and converts it into a rightward rotation (Fig. 7.4) (Voronov and Taber, 2002).

S-Shaped Loop

After the bending and rightward rotation have been initiated, subsequent morphological changes in the loop are intimately tied to elongation of the heart tube. De la Cruz and colleagues initially showed that only a portion of the mature heart is represented after initial heart tube formation (Arguello et al., 1975; de la Cruz et al., 1987, 1989). Marking studies showed that the initial heart tube in the chick represents primarily what will ultimately become the right ventricle and a small portion of the left ventricle, although more recent data suggest

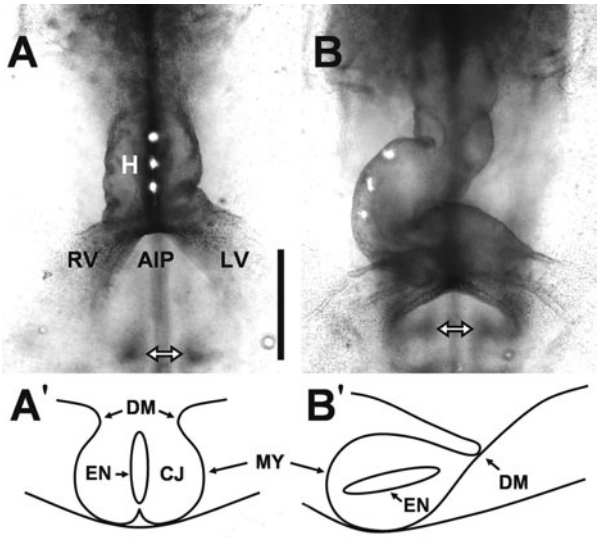

Figure 7.4. Formation of the C-shaped loop. Marks placed in the ventral midline heart tube at stage 10 (*A*) are found on the right border at stage 13 (*B*). Note that the tube is not completely formed at stage 10 (*A′*) and the dorsal mesocardium formed by stage 13 (*B′*) is still intact during formation of the C-shaped loop. EN, endocardium, CJ, cardiac jelly; DM, dorsal mesocardium, RV, right ventricle; AIP, anterior intestinal portal; LV, left ventricle; MY, myocardium . (From Voronov et al. 2004, with permission).

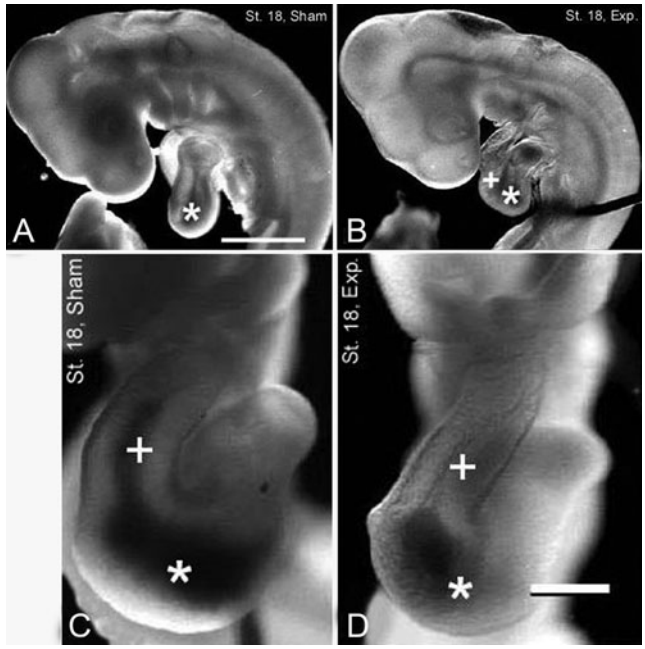

Figure 7.5. Shortened outflow limb caused by failure of myocardium to be added to the truncus is associated with abnormal convergence and wedging in the chick embryo. *A* and *B* show the embryo from a left lateral view and *C* and *D* are frontal views of the heart. (*A*) In a normal embryo the inflow and outflow limbs are not visible. (*B*) In a neural crest-ablated embryo the cardiac loop is abnormal because both the inflow and outflow limbs are visible. (*C*) In the normal embryo, the outflow limb (+) shows a gentle curvature back to its pharyngeal attachment from the convex part of the loop (*). (*D*) In contrast, the outflow limb in a neural crest-ablated embryo looks straight. (Adapted from Yelbuz et al., 2002, with permission).

that the initial mouse cardiac tube is comprised primarily of left ventricle (Kelly et al., 2001). The atria and outflow myocardium are added from the inflow and outflow ends of the tube, respectively, from an Islet1 (Isl1) expressing population of myocardial progenitors (Cai et al., 2003). This population has also been described as corresponding to the second myocardial lineage by retrospective clonal analysis (Meilhac et al., 2003). Addition of cells from the ends of the tube is requisite because the attachment of the tube to the ventral foregut by the dorsal mesocardium disappears as looping begins. This detachment seals the dorsal midline seam of the myocardial tube, making the sides of the tube inaccessible and leaving only the ends of the tube attached and accessible for accretion of cells to the tube. Because of the difference in the way the cardiac tube is formed in the mouse, detachment of the tube from the ventral wall of the foregut starts well before the cells that represent the atria and right ventricle are added and elongation of the loop is largely from the poles. Failure of addition of the cells to the ends of the heart results in abnormal development ranging from absence of the right ventricle and conus, when most of the cells are not added, to conotruncal heart defects when only the distal truncal myocardium is not added (Fig. 7.5) (Cai et al., 2003, Yelbuz et al., 2002).

Convergence

A major factor in convergence of the outflow and inflow poles of the heart appears to be intimately tied to the addition of the cells to the arterial pole from the secondary heart field. If these cells are not added to the lengthening heart tube, the morphology of the S-shaped loop is disturbed not only because it is shorter but also because the outflow tract is not displaced caudally as the caudal arch arteries (aortic arch arteries 3, 4, and 6) open (see Chapter 6 for details). The result is DISCORDANCE in the confluence of the cardiac outflow with the arch vessels that will become the great arteries. A second consequence is that the outflow and inflow poles do not converge (Waldo et al., 2005). Normal development of the secondary heart field depends on appropriate levels of fibroblast growth factor (Fgf) signaling. Ablation of cardiac neural crest, which causes a functional increase in Fgf signaling in the pharynx, interferes with normal addition of the myocardium from the secondary heart field to the developing cardiac outflow tract (Farrell et al., 2001; Hutson et al., 2006). The impact of this failure is that the looped tube is shortened (Fig. 7.5), which prevents convergence of the outflow and inflow limbs, and ultimately results in failure of normal aortic wedging between the mitral and tricuspid valves (Yelbuz et al., 2002).

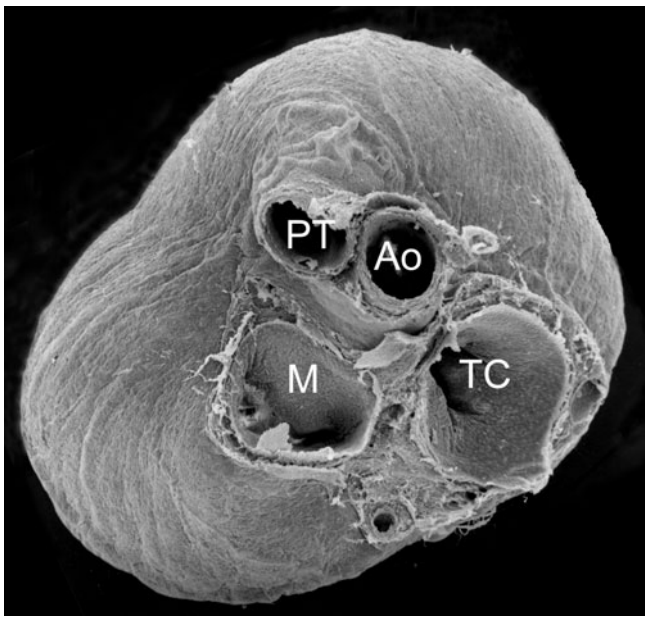

Figure 7.6. Four-valve view of a near-term normal mouse heart. As in all four-chambered hearts, the inflow represented here by the atrioventricular valves and outflow represented by the aorta and pulmonary trunk are converged. In addition, the subaortic outlet is wedged between the aortic leaflet of the mitral valve and the septum. (Image courtesy of K. K. Sulik, Embryo Images at www.med.unc.edu/embryo_images, with permission.)

Wedging

Wedging is the movement of the aorta behind or caudal to the pulmonary trunk (Fig. 7.6). It occurs during septation and is dependent on retraction and rotation of the truncal myocardium by about 45° as shown by tattooing and by changes in cell and fiber orientation during retraction of the conotruncal myocardium (Thompson et al., 1984, 1987). Outflow shortening can also be seen using retrovirally labeled outflow myocardium, which shortens to become a compact ring at the level of the pulmonary infundibulum (see Fig. 8.3) (Watanabe et al., 1998).

When wedging of the aorta fails to happen, the aorta overrides the ventricular septum and settles to the right of its normal position in a configuration called dextroposed aorta (Hutson et al., 2005; Yelbuz et al., 2002). This is one component in CONOTRUNCAL DEFECTS such as tetralogy of Fallot and double outlet right ventricle. Failure of addition of myocardium from the secondary heart field is thus a potential mechanism for genesis of these defects.

Compaction and rotation of the truncal myocardium are accompanied by cell death as shown by TUNEL labeling of DNA fragments and annexin V binding, suggesting that cell death is one mechanism for shortening (Watanabe et al., 1998). Treatment of chick embryos with CASPASE inhibitors to prevent the normal cell death leads to a failure in outflow tract shortening and double outlet right ventricle. Thus, elimination of truncal cardiomyocytes by APOPTOSIS is necessary for normal wedging (Watanabe et al., 2001). The cell death of truncal myocytes is driven by hypoxia. The hypoxia-inducible transcription factor Hif1α is specifically present in the nuclei of truncal myocytes during the wedging period. Vascular endothelial growth factor receptor 2(Vegfr2) expression in the truncal myocardium protects the myocytes that don't die from cell death. Forced overexpression of vascular endothelial growth factor (Vegf) in the conotruncal myocardium leads to double outlet right ventricle, that is, absent wedging (Sugishita et al., 2004a,b).

Establishing the Left–Right Body Axis

The sequence of events leading up to heart looping begins with establishing the left–right axis with respect to the craniocaudal and dorsoventral axes during gastrulation (Levin, 2005). Disruption of either the craniocaudal axis or the midline either mechanically or genetically results in randomization of cardiac looping, suggesting that the craniocaudal axis is intimately linked with establishing the left–right axis (Danos and Yost, 1995; Lowe et al., 2001). The connection with the craniocaudal axis is via the node, which lies at the cranial extremity of the primitive streak and generates axial tissue. Even though we still do not understand the proximate causes of cardiac looping the earlier events in left–right axis formation have become clear because of the discovery of asymmetrical gene expression at the node (Fig. 7.7) (Levin et al., 1995). While these studies have not resolved the forces involved in looping, they have provided important clues to the signaling pathways that control the direction of looping.

The left–right axis is established by a variety of molecules that transduce chiral information into left–right positions and transmit the information to multicellular fields. Some of these molecules have been identified: connexins, H^+/K^+ TRANSPORTERS, SYNDECANS, adhesion molecules, and motor proteins. Subsequent differences in left–right asymmetries rely on "crosstalk" between cells, which involve long-range signaling molecules (or ligands) and cell-surface receptors on receptive cells. Important signaling factors include the TGFβ superfamily members NODAL, VG1, and Activin which are agonists, and LEFTY, an antagonist. Cells receiving the signals express the EGF–CFC FAMILY OF CO-RECEPTORS (Fig. 7.8). The EGF–CFC family of co-receptors are defined by the presence of a signal sequence, an EGF-like domain, a second cysteine-rich domain, and a hydrophobic C terminus. Mutations in the EGF–CFC family of genes in the zebrafish and mouse, or downregulation of expression in the chick, result in abnormal left–right axis specification. While ligand stimulation of the Activin receptor by Nodal and Vg1 requires the EGF–CFC co-receptors, Activin can activate the Activin pathway without a co-receptor. Lefty inhibits Nodal and Vg1 but not Activin signaling by blocking EGF–CFC co-receptors (Fig. 7.8) (Cheng et al., 2003, 2004). Asymmetrically expressed signaling molecules, including secreted proteins in the TGFβ family, FGF8 and Shh, pass left

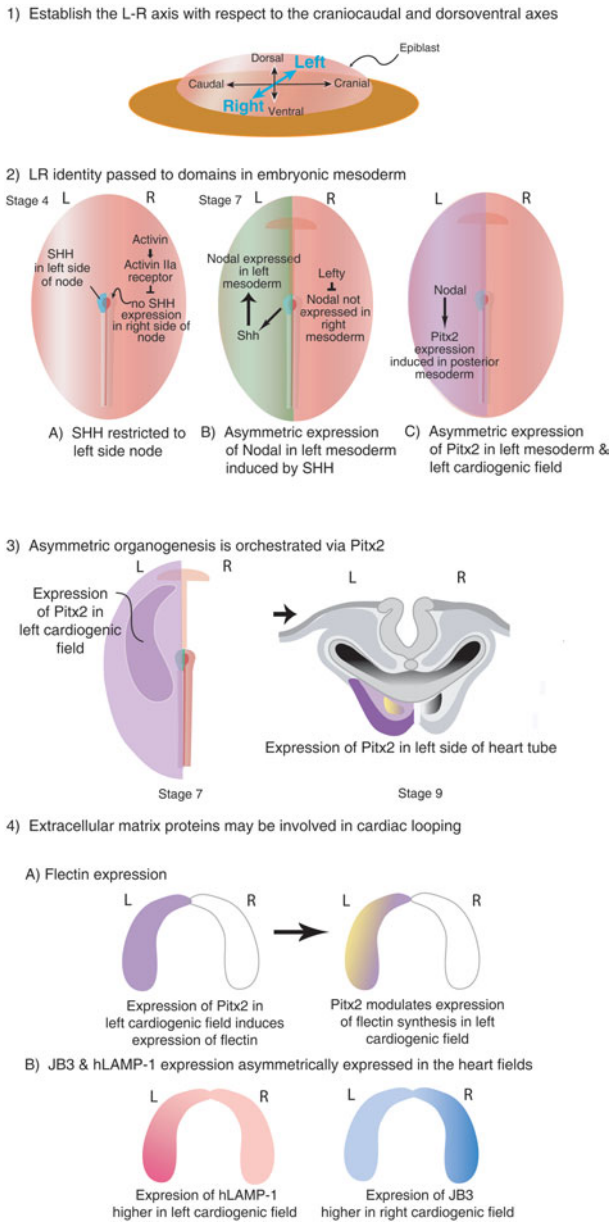

Figure 7.7. Sequence of events that establish the left–right axis in chick that activates left-sided genes in the mesoderm that ultimately lead to cardiac looping.

or right identity to numerous domains in the embryo. Finally, asymmetric organogenesis is orchestrated via Pitx2, Nodal, Lefty2 on the left and Snail on the right (Fig. 7.7) (Bisgrove et al., 1999). While many of these signaling factors are highly conserved, there are some species differences in the details. One difference between chick and mouse is that FGF8 is a right determinant and Shh a left determinant in the chick while in the mouse, FGF8 is a left determinant, and Shh is required to prevent left determinants from being expressed on the right (Meyers and Martin, 1999). Because of these species variations, there is still much uncertainty about the role of many factors that determine the right–left axis.

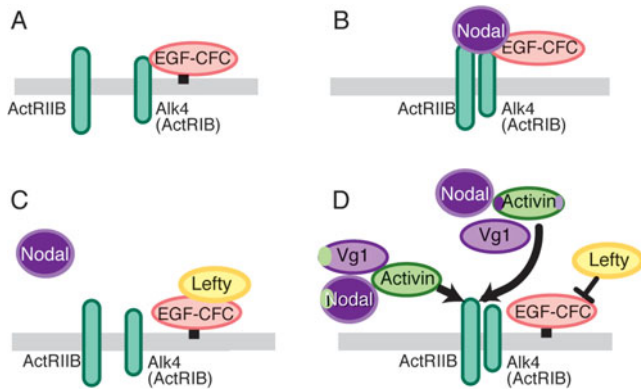

Figure 7.8. Model for TGF-β family interactions. (*A*) Without ligands, the EGF–CGC coreceptor is bound to the type I Alk4 receptor. (*B*) Nodal binds to the receptor complex causing dimerization of ActRIIB with the complex. (*C*) Lefty binds the EGF–CGC coreceptor preventing Nodal from binding to the receptor complex to activate signaling. (*D*) Nodal and Vg1 require the EGF–CFC co-receptor to signal through ActRIIB and Alk4 but Activin does not. (Adapted from Cheng et al., 2004.)

The mouse embryo appears symmetric at E7.75. The node has motile CILIA that move generating leftward nodal flow, which is essential to establish the right–left axis (Fig. 7.9). Ciliogenesis depends on the MICROTUBULE-DEPENDENT MOTOR PROTEIN, KIF3B. This protein functions in intracellular transport of materials required for ciliogenesis. The motile cilia produce a gradient of putative morphogen along the left–right axis in the node (Fig. 7.10) (Nonaka et al., 1998). In mice deficient for KIF3B, the node lacks cilia, a left-sided marker and signaling factor Lefty2, is expressed either bilaterally or not at all, and the left–right asymmetry of heart looping and embryonic turning is randomized.

At E8.25, symmetric perinodal expression of Nodal becomes asymmetric and by E8.5, most of the left lateral plate mesoderm expresses Nodal (Fig. 7.10). Members of the Nodal family are expressed unilaterally in the left lateral plate mesoderm and are thought to confer left-sidedness (Schier and Shen, 2000). Expression of Nodal leads to left-sided expression of Pitx2 in the lateral plate and subsequently in the left side of the heart tube (Mercola and Levin, 2001). Asymmetric expression of Nodal and Pitx2 in the left lateral plate mesoderm coincides with both embryo turning and heart looping. However, as for heart looping, the proximate genes and mechanisms are poorly understood (Constam and Robertson, 2000). While Pitx2 has been considered to be the interface between genes controlling left-sidedness and those controlling the mechanical process of heart looping, looping is not affected in Pitx2-null mice (Kitamura et al., 1999; Lin et al., 1999; Lu et al., 1999).

In the chick, several different genes are asymmetrically expressed at Henson's node, and these are believed to be the source of instructive signals that drive expression of downstream mediators of sidedness (Fig. 7.7A) (King et al., 1998; Levin et al., 1997). An as yet unidentified symmetry-breaking

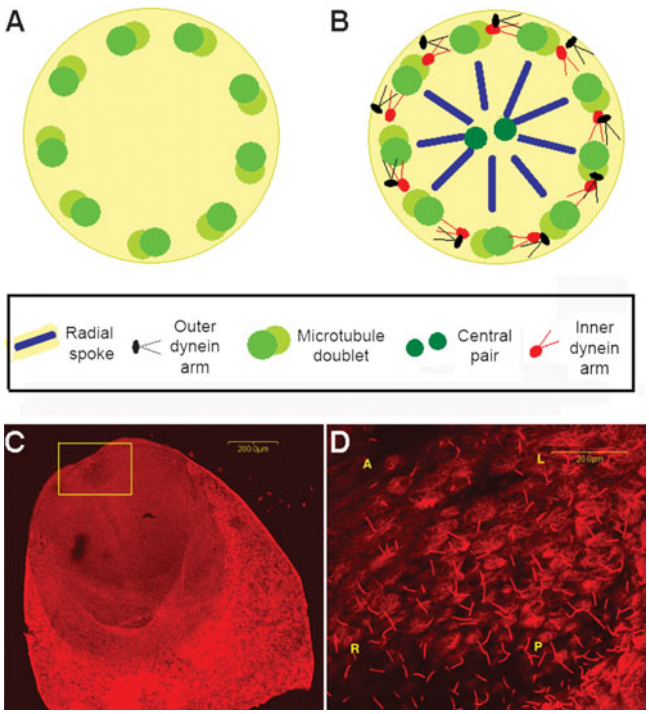

Figure 7.9. Structure and distribution of node monocilia. (*A*) Nine microtubular doublets, each consisting of an A-tubule and a B-tubule found in all cilia. (*B*) Structure of a 9+2 tracheal cilium. A central pair of microtubules is connected to the outer microtubule doublets by radial spokes. Inner and outer arm dynein arms link the outer doublets to each other to generate ATP-driven sliding movement of the axoneme. (*C*) Bowl-shaped mouse node at E7.75 (in the *yellow* rectangle). (*D*) Enlarged view of node monocilia, labeled with anti-acetylated tubulin antibody. There is a single cilium on every node cell. (From McGrath and Brueckner, 2003, with permission.)

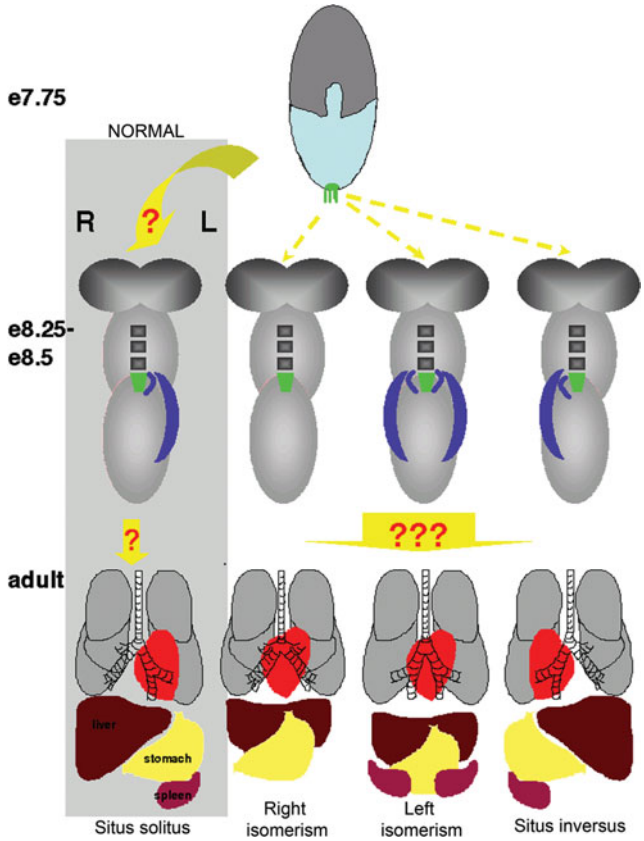

Figure 7.10. Normal and abnormal development of mouse left-right asymmetry. At E7.75 the embryo is symmetric. The node (*green*) contains monocilia that generate leftward nodal flow. At E8.25, nodal expression (*blue*) at the node becomes asymmetric and this is followed by asymmetric expression of nodal and *Pitx2* in the left lateral plate mesoderm. By E8.5 asymmetric gene expression has been translated into asymmetric development of the lungs (*gray*), heart (*red*), liver (*dark brown*), spleen (*light brown*), and gut (*yellow*). Right or left isomerism and situs inversus are all associated with abnormal left–right axis development. Right or left isomerism usually include severe complex cardiac malformations. (From McGrath and Brueckner, 2003, with permission.)

event along the left–right axis in the early chick is translated into differential H^+, K^+-ATPase activity. This in turn results in increased levels of extracellular Ca^{2+} in the left side of Hensens's node and triggers a genetic regulatory cascade that eventually leads to left-sided restriction of Shh. Increased levels of extracellular Ca^{2+} also cause locally confined hyperactivation of the Notch signaling pathway which directly activates expression of Nodal in the left side of Hensen's node (Raya and Izpisua Belmonte, 2004). Perinodal expression of Nodal is subsequently translated to broad domains of Nodal expression in the left lateral plate mesoderm by a mechanism under the control of Shh. As in the mouse, Nodal induces Pitx2 (Campione et al., 1999; Logan et al., 1998; Piedra et al., 1998; Ryan et al., 1998).

Differential expression of Cx43 is required for asymmetric Shh expression at the node in the chick (Levin and Mercola, 1999). It may be that lateral-to-medial signaling instructs the first asymmetric expression at stage 4 when Shh becomes restricted to the left side of the node. Because gap junctional communication allows signals to be transmitted quickly across large distances, it may be important in the spread of asymmetric information in the embryo. Asymmetric Shh expression leads to left-sided expression of Nodal at stage 7 in a small domain of endoderm adjacent to the ectoderm cells expressing Shh and then in a large domain in the lateral plate mesoderm (Levin, 1998; Levin et al., 1995, 1997). Activin induces the expression of Activin receptor IIa on the right side of Henson's node and probably represses Shh expression on the right side at the time that Shh is restricted to the left side of the node (Levin, 1998; Levin et al., 1997). Mutation of a potential regulatory residue in the Cx43 protein is sufficient to cause heterotaxia experimentally, and six children with VISCEROATRIAL HETEROTAXIA syndromes were shown to have point mutations in a phosphorylatable serine or threonine residue in the Cx43 message (Britz-Cunningham et al., 1995; Levin and Mercola, 1998). Transfected cells expressing the mutant Cx43 show

abnormalities in regulation of cell–cell communication as compared with cells expressing normal Cx43 (Britz-Cunningham et al., 1995). Despite uncertainty about the prevalence of this mutation reported in human patients with laterality defects, the mutant protein is both a mild hypomorph and a potent antimorph as determined by the effect of its expression on left–right patterning (Levin and Mercola, 1999, 1998). On the other hand, Cx43-null mice do not show heterotaxia phenotypes (Melloy et al., 1998; Reaume et al., 1995; Sullivan et al., 1998). Because the null phenotype differs dramatically from the mutant phenotype, it is possible that malfunction of the Cx43 gap junctional channel disrupts development more seriously, or at different stages, than its absence.

Nodal affects cardiac looping when it is ectopically expressed on the right side in the chick, and the Nodal hypomorphic mouse has abnormal looping (Levin et al., 1995; (Lowe et al., 2001). Left–right axis abnormalities, including heterotaxia, DEXTROCARDIA, and transposition of the great arteries, are associated with loss-of-function mutations in the EGF–CFC gene *CFC1* (Bamford et al., 2000). EGF–CFC proteins are essential cofactors for Nodal signaling (Schier and Shen, 2000; Shen and Schier, 2000). CFC is expressed asymmetrically in the left side of Hensen's node (Schlange et al., 2001). Antisense oligonucleotide treatment results in a high incidence of abnormal heart looping caused by bilateral expression of Nodal, Pitx2, Nkx3.2, and Caronte, which is due to a transient loss of Lefty1 expression in the midline (Schlange et al., 2001). Furthermore, mice homozygous for a *Lefty1*-null allele manifest left–right malformations and misexpress Lefty2. Mutations have been found in the CYSTEINE-KNOT region of Lefty protein in two human cases of left–right axis perturbations (Kosaki et al., 1999).

Molecular Pathways That Drive Cardiac Looping

Once left–right axis asymmetry is established, the information is transmitted to the cardiogenic fields, and this initiates a program of expression unique to each cardiogenic field. We have only limited information about these molecules (Fig. 7.7). Perturbation of different upstream left–right axis specifying genes leads to abnormal looping and direct disruption of either extracellular matrix molecules and/or cytoskeletal molecules disrupt the normal direction of looping. Thus, it is thought that cytoskeletal and matrix molecules are the effectors of the left–right axis specifying genes but little is known about how the genes are linked to the molecules that effect the biophysical process and even less is known about how the biophysical forces cause looping (Itasaki et al., 1991; Linask et al., 2002; Mercola and Levin, 2001).

Biophysical mechanisms used to shape organogenesis include the extracellular matrix and intracellular cytoskeletal actin bundles (Linask et al., 2002, 2003; Tsuda et al., 1996; Yue et al., 2004). The biophysical mechanism of bending appears to be related to asymmetrical extracellular matrix expression in the left heart field relative to the right (Linask et al., 2002; Smith et al., 1997; Tsuda et al., 1996, 1998).

A plethora of asymmetrically expressed genes has been identified, and these appear to participate in cascades of induction and repression of asymmetric gene pathways on the right and left sides of the midline to ultimately dictate heart situs. Gap junctional communication may propagate signals throughout the epiblast but not across an insulating zone represented by the primitive streak caudally and the notochord cranially. The role of the midline is critical in asymmetric gene expression and heart situs. Because removal of the notochord destabilizes left–right asymmetry, it was initially thought that the midline played a barrier function (Danos and Yost, 1996). In the zebrafish, the *FLOATING HEAD* and *NO TAIL* (*Brachyury*) mutants have notochord defects that are accompanied by the heart looping to the left (Fig. 7.11) (Chin et al., 2000; Halpern et al., 1993). Lefty1, expressed in the midline, inhibits propagation of Nodal signals to the right flank of the embryo, while Lefty2 acts as a feedback inhibitor within the left lateral plate mesoderm (Cheng et al., 2000).

Left–right patterning is mediated proximately by extracellular matrix proteins: FLECTIN, HEART-SPECIFIC LECTIN-ASSOCIATED MATRIX PROTEIN-1 (hLAMP1) and JB3; transcription factors: Pitx2, bHLH family members Hand1 and Hand2, and T-box factors Tbx5 and Tbx20 and signaling factors in the TGFβ family (Angelo et al., 2000; Bruneau et al., 1999; Fernandez-Teran et al., 2000; Hatcher et al., 2000; Sparrow et al., 1998; Srivastava et al., 1995; Takeuchi et al., 2003; Tsuda et al., 1996).

Flectin is an extracellular matrix protein first detected in the cardiogenic mesoderm on the left side at stage 7+ to 8. It subsequently crosses the midline and is expressed in the

Figure 7.11. Zebrafish with normal (left) and reversed looping (right). The mutant is called one-eyed pinhead which has a mutation in the EGF–CGC gene. (From Yan et al., 1999, with permission.)

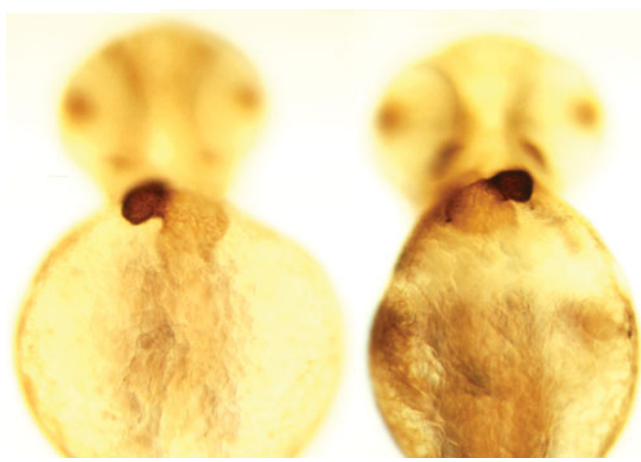

right cardiogenic mesoderm and, possibly more importantly, in the right dorsal mesocardium, the side toward which the tube loops (Linask et al., 2002; Tsuda et al., 1996, 1998). Flectin continues to be asymmetrically expressed in the secondary heart field (Linask et al., 2003). The function of flectin is to make the myocardial wall more pliant or less stiff than the nonexpressing side (Linask, 2003). While flectin has not yet been well characterized, it belongs to the matricellular proteins which interact with multiple cell surface receptors, cytokines, growth factors, proteases, and structural proteins. It has the ability to interact with heparan sulfate and chondroitin sulfate proteoglycans, two of the major components of the cardiac jelly (Mieziewska et al., 1994).

Two other extracellular matrix proteins are differentially expressed in the heart fields: hLAMP1 and the fibrillin-related protein recognized by the antibody JB3. JB3 expression is higher in the right cardiogenic mesoderm, and hLAMP-1 is higher in the left cardiogenic mesoderm. Treatment with retinoic acid equalizes or reverses the expression of these proteins which causes randomized or left heart looping, respectively (Smith et al., 1997).

Pitx2 is a bicoid-related gene that was first cloned in association with RIEGER SYNDROME, an autosomal-dominant human disorder that includes anomalies of the anterior chamber of the eye, dental hypoplasia, and a protuberant umbilicus (Semina et al., 1996). *Pitx2* is associated with heart looping (St. Amand et al., 1998). Asymmetric expression of Pitx2 occurs in the left mesoderm at stage 7. Implantation of an Shh-soaked bead on the right side of embryos induces ectopic Pitx2 expression on that side via Nodal signaling which ultimately results in left-sided heart looping (Campione et al., 1999; Logan et al., 1998; Ryan et al., 1998; Yoshioka et al., 1998). Ectopic expression of Pitx2 is associated with ectopic activation of flectin, and Pitx2 is known to modulate the timing of flectin synthesis normally (Linask et al., 2002; Tsuda et al., 1996). This could be one of the ways Pitx2 directs heart looping. Other than flectin, it is unknown what effectors might be downstream of Pitx2 function. Pitx2 expression domains in the atrial chambers represent those derived from the left side of the early cardiac tube, and consistent with this atrial expression pattern, mice with hypomorphic or null expression of *Pitx2* have right ATRIAL ISOMERISM, abnormal venous return, and atrial septal defects, similar to those observed in heterotaxia (Franco et al., 2000; Gage et al., 1999; Kitamura et al., 1999). Some embryos also have double outlet right ventricle and/or DOUBLE INLET LEFT VENTRICLE (Gage et al., 1999; Kitamura et al., 1999; Lin et al., 1999; Lu et al., 1999). The *Pitx-2* gene expresses multiple message isoforms that are called Pitx2abc. Pitx2c is asymmetrically expressed while Pitx2ab are expressed symmetrically. All of the defects seen with altered Pitx2 expression are associated with the Pitx2c isoform because *Pitx2ab*-null mice have normal heart development.

Hand1 and -2 antisense treatment in chicks results in failure of looping (Srivastava et al., 1995). Hand1 expression is enhanced in the left atrial and ventricular primordia, and *Hand1*-null cells in mouse chimeras are underrepresented in the left caudal region of the linear heart tube (Biben and Harvey, 1997). Data from *Hand1–lacZ* chimeric embryos suggest that Hand1 is specifically required for formation of the outer curvature of the left ventricular myocardium (Riley et al., 2000).

Tbx20 is expressed in the heart fields and Tbx20 morpholino-treated embryos develop a straight heart tube (Griffin et al., 2000; Iio et al., 2001; Kraus et al., 2001; Szeto et al., 2002). *Tbx5* mutant mice also have unlooped hearts (Garrity et al., 2002). However, it is not clear whether the role of *Tbx* genes is in left–right asymmetry development or in promoting heart development to the stages where looping occurs.

BMP4 and its downstream effector phosphorylated Smad1 are normally expressed on the left side of the linear heart tube (Faure et al., 2002). Ectopic expression of BMP4 bilaterally in the heart tube is associated with randomized looping in both zebrafish and *Xenopus* (Breckenridge et al., 2001; Chen et al., 1997).

Animal Models of Abnormal Looping

One of the oldest models of situs inversus is the *IV* MOUSE (Layton, 1976). Approximately 50% of *iv/iv* mice have situs inversus (mirror image reversal of viscera), and 40% have heterotaxia, a condition in which the asymmetric organs, that is, stomach, spleen, liver, and heart have positioned themselves left or right, stochastically (Layton et al., 1993). Mapping of the mutation to LEFT–RIGHT DYNEIN, an intermediate filament required for cilia motility, led to our current knowledge about the function of nodal cilia in establishing asymmetric expression of Shh and Nodal during gastrulation (Supp et al., 1997). Both Lefty1 and Lefty2 are expressed exclusively on the left side of the early mouse embryo, and this asymmetry is lost or reversed in the *iv* mouse (Kosaki and Casey, 1998).

The *INV* (INVERSION OF EMBRYONIC TURNING) mutant mouse was first described as a situs inversus model. Inv codes for a gene named *Inversin* that is disrupted by an insertional mutation. One in 10 of the mice have situs solitus (normal position of all the asymmetric organs), but the majority have situs inversus (mirror image of the asymmetric organs). All of the mice tend to have cardiovascular anomalies, with the most frequent severe malformation consisting of pulmonary infundibular stenosis/atresia with absence of the pulmonary semilunar valve and a ventricular septal defect (McQuinn et al., 2001). Lefty1 and -2 are expressed incorrectly in the *inv* mouse (Kosaki and Casey, 1998). About one-third of the known left–right asymmetry mutations in mice and humans affect genes that have a role in ciliary biogenesis and function. Defects in the genes *Kif3A* and *Kif3B*, encoding components of kinesin, and defects in the gene encoding Tg737 (polaris), all result in embryos with a complete absence of cilia and abnormal development of left–right asymmetry.

These findings led to the discovery that movement of nodal cilia is required to establish molecular asymmetries (McGrath and Brueckner, 2003).

The "no turning" (*nt*) mutant mouse has a spontaneous mutation in an as yet unidentified gene that causes left–right patterning defects. This mutation is recessive lethal and was named *nt* because the mutant embryos fail to undergo embryonic turning. Development of the heart arrests at the looped heart tube stage, with heart failure evidenced by pericardial effusion and pooled blood in various regions of the embryo. The direction of heart looping is randomized, and *Nodal* and *Lefty*, genes that are normally expressed only in the left lateral plate mesoderm, show bilateral expression. Histological analysis indicates that the notochord is present in the early *nt* embryo, but degenerates as development progresses supporting the hypothesis that the notochord plays an active role in left–right patterning (Melloy et al., 1998).

Activin receptor IIB (ActRIIB)-deficient mice show randomized heart looping and malposition of the great arteries. The cardiovascular anomalies are associated with right pulmonary isomerism and splenic abnormalities, recapitulating the clinical symptoms of the human asplenia syndrome (Oh and Li, 1997). Activin signaling induces left-sided Zic3 expression in the mesoderm. Zic3 is a potent activator of nodal-related-1 (*Nr1*) and *Pitx2*, both of which are normally expressed in the left lateral plate mesoderm (Kitaguchi et al., 2000).

Other genes that affect looping have been mentioned previously. These include the transcriptional regulators Pitx2, Hand1, and -2, Tbx20 and -5; and the signaling proteins BMP4 (and its downstream target Smad1), Nodal, and EGF–CFC. Antisense treatment or null mutation of these factors has been discussed previously, and all provide models of abnormal or nonlooping.

Cardiac Malformations Related to Right–Left Axis and Looping Abnormalities

Normal left–right development results in SITUS SOLITUS, with all the asymmetric organs placed on the side of the body where they normally reside. When left–right development does not proceed normally, a range of outcomes is possible. Mirror-image reversal of all the organs is called situs inversus and is usually not associated with significant pathology. However, mixed situs, with part of the organs having normal situs solitus and part with situs inversus results in visceral heterotaxy, which is usually accompanied by complex heart defects. The heart shows a wide spectrum of anomalies in heterotaxia syndromes including atrial and ventricular septal defects, double outlet right ventricle, COMMON ATRIOVENTRICULAR CANAL, double inlet left ventricle, atrial isomerism, sinus venosus type atrial septal defect, and anomalous venous return. The malformations may be isolated or in combination (Goldstein et al., 1998). Complete failure to break bilateral symmetry is thought to result in left isomerism (associated with bilateral multilobed lungs and bilateral spleens) or right isomerism (bilateral one or two-lobed lungs and absent spleen). The isomerisms have associated severe, complex cardiac malformations (McGrath and Brueckner, 2003).

Kartagener's Syndrome

Siewert first described the combination of situs inversus, recurrent respiratory infections with chronic sinusitis, male infertility, and bronchiectasis in 1904. However, Kartagener first recognized the signs as a distinct congenital syndrome in 1933. Most cases are sporadic and may represent recessive inheritance, but occasional dominant transmission has been reported. One-half of patients with Kartagener syndrome have complete situs inversus. Symptoms result from defective cilia motility. Camner and co-workers first suggested ciliary dyskinesia as the cause of Kartagener syndrome in 1975. They described two patients with the syndrome who had immotile cilia and immotile spermatozoa. Mutations in the genes for both dynein intermediate chains and dynein heavy chains have been demonstrated in some families with Kartagener syndrome, providing the molecular link between the structural ciliary defects in Kartagener syndrome and specific ciliary proteins (McGrath and Brueckner, 2003).

Transposition of the Great Arteries

Transposition of the great arteries (TGA) is seen in children with lateralization defects, heterotaxy, and asplenia syndrome. Transposition is rarer in patients with heterotaxy in polysplenia syndrome. In mice with mutation of *Smad2* and *Nodal*, two genes involved in the lateralization process, some transposition occurs with or without right isomerism of the lungs. Moreover, in families with heterotaxy, some cases with congenitally corrected transposition have been reported, and a new gene *CRYPTIC* (EGF–CFC family) which is associated with heterotaxy, has been shown to have point mutations in patients with "isolated" transposition. A recent study on familial recurrence of transposition found TGA and corrected TGA in the same family. This suggests monogenic inheritance (autosomal dominant or recessive) with variable phenotypic expression (Marino et al., 2002).

Visceroatrial Heterotaxia (Ivemark Syndrome)

Ivemark first described the association of asplenia with cardiovascular malformations (Ivemark, 1955). Asplenia and polysplenia were originally treated as separate entities but both were found in single families and have similar patterns of malformations and are now considered part of the same disease process (Pajkrt et al., 2004). Patients with asplenia have right atrial isomerism and otherwise paired right-sided viscera, that is, bilateral trilobed lungs, midline liver, and absence of left-sided organs. There is usually dextrocardia with total

anomalous pulmonary venous connection, complete atrioventricular septal defect, transposition of the great arteries, and pulmonary atresia. In patients with polysplenia, left atrial isomerism is accompanied by bilateral duplication of left-sided structures and malpositioned stomach associated with multiple spleens. Virtually all of the various heart defects have been described in association with heterotaxia (Hackett, 2002). These include atrioventricular septal defect and malaligned outflow and inflow vessels represented by bilateral superior vena cava and interruption of the inferior vena cava (Berg et al., 2003; Pajkrt et al., 2004).

Malfunction of the nodal cilia carry increased risk for heterotaxias with a 50% risk of situs inversus (Afzelius, 2004). Mothers with type 1 diabetes have a 20-fold increased risk of heterotaxia (Martinez-Frias, 2001). Heterotaxy can be caused by single-gene mutations with extensive locus heterogeneity. It is also associated with teratogen exposure. Genes currently implicated in human heterotaxy include *ZIC3*, *LEFTYA*, *CRYPTIC*, *activin receptor type IIB* gene (*ACVR2B*), and *NKX2.5* (Belmont et al., 2004)

REFERENCES

Afzelius, B. A. 2004. Cilia-related diseases. J. Pathol. 204:470–477.

Angelo, S., J. Lohr, K. H. Lee, B. S. Ticho, R. E. Breitbart, S. Hill, H. J. Yost, and D. Srivastava. 2000. Conservation of sequence and expression of Xenopus and zebrafish dHAND during cardiac, branchial arch and lateral mesoderm development. Mech. Dev. 95:231–237.

Arguello, C., M. V. De la Cruz, and C. S. Gomez. 1975. Experimental study of the formation of the heart tube in the chick embryo. J. Embryol. Exp. Morph. 33:1–11.

Baldwin, H. S., and M. Solursh. 1989. Degradation of hyaluronic acid does not prevent looping of the mammalian heart in situ. Dev. Biol. 136:555–559.

Bamford, R. N., E. Roessler, R. D. Burdine, U. Saplakoglu, J. Dela Cruz, M. Splitt, J. Towbin, P. Bowers, B. Marino, A. F. Schier, M. M. Shen, M. Muenke, and B. Casey. 2000. Loss-of-function mutations in the *EGF–CFC* gene *CFC1* are associated with human left-right laterality defects. Nat. Genet. 26:365–369.

Belmont, J. W., B. Mohapatra, J. A. Towbin, and S. M. Ware. 2004. Molecular genetics of heterotaxy syndromes. Curr. Opin. Cardiol. 19:216–220.

Berg, C., A. Geipel, J. Smrcek, M. Krapp, U. Germer, T. Kohl, U. Gembruch, and A. A. Baschat. 2003. Prenatal diagnosis of cardiosplenic syndromes: a 10-year experience. Ultrasound Obstet. Gynecol. 22:451–459.

Biben, C., and R. P. Harvey. 1997. Homeodomain factor *Nkx2-5* controls left/right asymmetric expression of bHLH gene *eHand* during murine heart development. Genes Dev. 11:1357–1369.

Bisgrove, B. W., J. J. Essner, and H. J. Yost. 1999. Regulation of midline development by antagonism of lefty and nodal signaling. Development 126:3253–3262.

Breckenridge, R. A., T. J. Mohun, and E. Amaya. 2001. A role for BMP signalling in heart looping morphogenesis in *Xenopus*. Dev. Biol. 232:191–203.

Bouman, H. G. A., M. L. A. Broekhuizen, A. Mieke, J. Baasten, A. C. Gittenberger-de Groot, and A. C. G. Wenink. 1995. Spectrum of looping disturbances in stage 34 chicken hearts after retinoic acid treatment. Anat. Rec. 243:101–108.

Bouman, H. G. A., M. L. A. Broekhuizen, A. M. J. Baasten, and A. C. G. Gittenberger-de Groot, and A. C. Wenink. 1997. Stereological study of stage 34 chicken hearts with looping disturbances after retinoic acid treatment: Disturbed growth of myocardium and atrioventricular cushion tissue. Anat. Rec. 248:242–250.

Britz-Cunningham, S. H., M. Maithili, B. S. Shah, C. W. Zuppan, and W. H. Fletcher. 1995. Mutations of the connexin43 gap-junction gene in patients with heart malformations and defects of laterality. N. Engl. J. Med. 332:1323–1320.

Bruneau, B.G., M. Logan, N. Davis, T. Levi T, C. J. Tabin, J. G. Seidman, and C. E. Seidman. 1999. Chamber-specific cardiac expression of Tbx5 and heart defects in Holt-Oram syndrome. Dev. Biol. 211:100–108.

Cai, C. L., X. Liang, Y. Shi, P. H. Chu, S. L. Pfaff, J. Chen, and S. Evans. 2003. Isl1 identifies a cardiac progenitor population that proliferates prior to differentiation and contributes a majority of cells to the heart. Dev. Cell. 5:877–889.

Campione, M., H. Steinbeisser, A. Schweickert, K. Deissler, F. Van Bebber, L. A. Lowe, S. Nowotschin, C. Viebahn, P. Haffter, M. R. Kuehn, and M. Blum. 1999. The homeobox gene *Pitx2*: mediator of asymmetric left-right signaling in vertebrate heart and gut looping. Development 126:1225–1234.

Chen, J. N., F. J. Van Eeden, K. S. Warren, A. Chin, C. Nusslein-Volhard, P. Haffter, and M. C. Fishman. 1997. Left-right pattern of cardiac BMP4 may drive asymmetry of the heart in zebrafish. Development 124:4373–4382.

Cheng, A. M., B. Thisse, C. Thisse, and C. V. Wright. 2000. The lefty-related factor Xatv acts as a feedback inhibitor of nodal signaling in mesoderm induction and L-R axis development in *Xenopus*. Development 127:1049–1061.

Cheng, S. K., F. Olale, J. T. Bennett, A. H. Brivanlou, and A. F. Schier. 2003. EGF–CFC proteins are essential coreceptors for the TGF-beta signals Vg1 and GDF1. Genes Dev. 17:31–36.

Cheng, S. K., F. Olale, A. H. Brivanlou, and A. F. Schier. 2004. Lefty blocks a subset of TGFbeta signals by antagonizing EGF–CFC coreceptors. PLoS Biol. 2:E30.

Chin, A. J., M. Tsang, and E. S. Weinberg. 2000. Heart and gut chiralities are controlled independently from initial heart position in the developing zebrafish. Dev. Biol. 227:403–421.

Constam, D. B. and E. J. Robertson. 2000. Tissue-specific requirements for the proprotein convertase Furin/SPC1 during embryonic turning and heart looping. Development 127:245–254.

Danos, M. C., and H. J. Yost. 1995. Linkage of cardiac left-right asymmetry and dorsal-anterior development in *Xenopus*. Development 121:1467–1474.

Danos, M. C., and H. J. Yost. 1996. Role of notochord in specification of cardiac left-right orientation in zebrafish and *Xenopus*. Dev. Biol. 177:96–103.

Davis, C. L. 1927. Development of the human heart from its first appearance to the stage found in embryos of twenty paired somites. Contrib. Embryol. 19:245–284.

DeHaan, R. L. 1965. Morphogenesis of the vertebrate heart. In: Organogenesis ed by R. L. DeHaan and H. Ursprung. New York: Holt, Rinehart & Winston.

de la Cruz, M. V., C. S. Gomez, and M. A. Palomino. 1989. The primitive cardiac regions in the straight tube heart (stage 9-) and

their anatomical expression in the mature heart: an experimental study in the chick embryo. J. Anat. 165:121–131.

de la Cruz, M. V., and R. R. Markwald. 1998. Living Morphogenesis of the Heart. Boston: Birkhauser.

de la Cruz, M. V., C. Sanchez-Gomez, and J. L. Robledo-Tovi. 1987. Experimental study of the development of the ventricular inlets in the chick embryo. Embryol. Hefte 1:25–37.

De Vries, P. A., and J. Z. B. de C. M. Saunders. 1962. Development of the ventricles and spiral outflow tract in the human heart. Carnegie Inst. Wash. Contrib. Embryol. 37:87–114.

Farrell, M. J., J. L. Burch, K. Wallis, L. Rowley, D. Kumiski, H. Stadt, R. E. Godt, T. L. Creazzo, and M. L. Kirby. 2001. FGF-8 in the ventral pharynx alters development of myocardial calcium transients after neural crest ablation. J. Clin. Invest. 107:1509–1517.

Faure, S., P. Santa Barbara, D. J. Roberts, and M. Whitman. 2002. Endogenous patterns of BMP signaling during early chick development. Dev. Biol. 244:44–65.

Fernandez-Teran, M., M. E. Piedra, I. S. Kathiriya, D. Srivastava, J. C. Rodriguez-Rey, and M. A. Ros. 2000. Role of dHAND in the anterior-posterior polarization of the limb bud: implications for the Sonic hedgehog pathway. Development 127:2133–2142.

Franco, D., M. Campione, R. Kelly, P. S. Zammit, M. Buckingham, W. H. Lamers, and A. F. M. Moorman. 2000. Multiple transcriptional domains, with distinct left and right components, in the atrial chambers of the developing heart. Circ. Res. 87:984–991.

Gage, P. J., H. Y. Suh, and S. A. Camper. 1999. Dosage requirement of *Pitx2* for development of multiple organs. Development 126:4643–4651.

Garcia-Pelaez, I. and M. Arteaga. 1993. Experimental study of the development of the truncus arteriosus of the chick embryo heart. I. Time of appearance. Anat. Rec. 237:378–84.

Garrity, D. M., S. Childs, and M. C. Fishman. 2002. The heartstrings mutation in zebrafish causes heart/fin *Tbx5* deficiency syndrome. Development 129:4635–4645.

Goldstein, A. M., B. S. Ticho, and M. C. Fishman. 1998. Patterning the heart's left-right axis: From zebrafish to man. Dev. Genet. 22:278–287.

Griffin, K. J. P., J. Stoller, M. Gibson, S. Chen, D. Yelon, D. Y. R. Stainier, and D. Kimelman. 2000. A conserved role for H15-related T-box transcription factors in zebrafish and *Drosophila* heart formation. Dev. Biol. 218:235–247.

Hackett, B. P. 2002. Formation and malformation of the vertebrate left-right axis. Curr. Mol. Med. 2:39–66.

Halpern, M. E., R. K. Ho, C. Walker, and C. B. Kimmel. 1993. Induction of muscle pioneers and floor plate is distinguished by the zebrafish no tail mutation. Cell 75:99–111.

Hatcher, C.J., M. M. Goldstein, C. S. Mah, C. S. Delia, and C. T. Basson CT. 2000. Identification and localization of tbx5 transcription factor during human cardiac morphogenesis. Dev. Biol. 219:90–95.

Hoyle, C., N. A. Brown, and L. Wolpert. 1992. Development of left/right handedness in the chick heart. Development 115:1071–1078.

Hutson, M. R., P. Zhang, H. A. Stadt, A. Sato, Y.-X. Li, J. Burch, T. L. Creazzo, and M. L. Kirby. 2006. Cardiac arterial pole alignment is sensitive to FGF8 signaling in the pharynx. Dev. Biol. 295:486–497.

Icardo, J. M. 1996. Developmental biology of the vertebrate heart. J. Exp. Zool. 275:144–161.

Iio, A., M. Koide, K. Hidaka, and T. Morisaki. 2001. Expression pattern of novel chick T-box gene, *Tbx20*. Dev. Genes Evol. 211:559–562.

Itasaki, N., H. Nakamura, H. Sumida, and M. Yasuda. 1991. Actin bundles on the right side in the caudal part of the heart tube play a role in dextro-looping in the embryonic chick heart. Anat. Embryol. (Berl.) 183:29–39.

Ivemark, B. I. 1955. Implications of agenesis of the spleen on the pathogenesis of conotruncus anomalies in childhood; an analysis of the heart malformations in the splenic agenesis syndrome, with fourteen new cases. Acta Paediatr. 44:7–110.

Kelly, R. G., N. A. Brown, and M. E. Buckingham. 2001. The arterial pole of the mouse heart forms from Fgf10-expressing cells in pharyngeal mesoderm. Dev. Cell 1:435–440.

King, T., R. S. P. Beddington, and N. A. Brown. 1998. The role of the *brachyury* gene in heart development and left-right specification in the mouse. Mech. Dev. 79:29–37.

Kirby, M. L., A. Lawson, H. Stadt, D. Kumiski, K. Wallis, E. McCraney, K. Waldo, Y. Li, and G. C. Schoenwolf. 2003. Hensen's node gives rise to the ventral midline of the foregut: implications for organizing head and heart development. Dev. Biol. 253:175–188.

Kirby, M.L. and K. L. Waldo. 1995. Neural crest and cardiovascular patterning. Circ. Res. 77:211–215.

Kitaguchi, T., T. Nagai, K. Nakata, J. Aruga, and K. Mikoshiba. 2000. *Zic3* is involved in the left-right specification of the *Xenopus* embryo. Development 127:4787–4795.

Kitamura, K., H. Miura, S. Miyagawa-Tomita, M. Yanazawa, Y. Katoh-Fukui, R. Suzuki, H. Ohuchi, A. Suehiro, Y. Motegi, Y. Nakahara, S. Kondo, and M. Yokoyama. 1999. Mouse *Pitx2* deficiency leads to anomalies of the ventral body wall, heart, extra- and periocular mesoderm and right pulmonary isomerism. Development 126:5749–5758.

Kosaki, K., and B. Casey. 1998. Genetics of human left-right axis malformations. Cell Dev. Biol. 9:89–99.

Kosaki, K., M. T. Bassi, R. Kosaki, M. Lewin, J. Belmont, G. Schauer, and B. Casey. 1999. Characterization and mutation analysis of human LEFTY A and LEFTY B, homologues of murine genes implicated in left-right axis development. Am. J. Hum. Genet. 64:712–721.

Kraus, F., B. Haenig, and A. Kispert. 2001. Cloning and expression analysis of the mouse T-box gene *Tbx20*. Mech. Dev. 100:87–91.

Latacha, K. S., M. C. Remond, A. Ramasubramanian, A. Y. Chen, E. L. Elson, and L. A. Taber. 2005. Role of actin polymerization in bending of the early heart tube. Dev. Dyn. 233:1272–1286.

Layton, W. M., M. W. Layton, M. Binder, D. M. Kurnit, A. J. Hanzlik, M. Van Keuren, and F. G. Biddle. 1993. Expression of the IV (reversed and/or heterotaxic) phenotype in SWV mice. Teratology 47: 595–602.

Layton, W. M. J. 1976. Random determination of a developmental process: reversal of normal visceral asymmetry in the mouse. J. Hered. 67:336–338.

Levin, M. 1998. Left-right asymmetry and the chick embryo. Semin. Cell Dev. Biol. 9:67–76.

Levin, M. 2005. Left-right asymmetry in embryonic development: a comprehensive review. Mech. Dev. 122:3–35.

Levin, M., R. L. Johnson, C. D. Stern, M. Kuehn, and C. Tabin. 1995. A molecular pathway determining left-right asymmetry in chick embryogenesis. Cell 82:803–814.

Levin, M., and M. Mercola. 1998. Gap junctions are involved in the early generation of left-right asymmetry. Dev. Biol. 203:90–105.

Levin, M., and M. Mercola. 1999. Gap junction-mediated transfer of left-right patterning signals in the early chick blastoderm is upstream of Shh asymmetry in the node. Development 126: 4703–4714.

Levin, M., S. Pagan, D. J. Roberts, J. Cooke, M. R. Kuehn, and C. J. Tabin. 1997. Left/right patterning signals and the independent regulation of different aspects of Situs in the chick embryo. Dev. Biol. 189:57–67.

Li, S., D. Zhou, M. M. Lu, and E. E. Morrisey. 2004. Advanced cardiac morphogenesis does not require heart tube fusion. Science 305:1619–1622.

Lin, C. R., C. Kioussi, S. O'Connell, P. Briata, D. Szeto, F. Liu, J. C. Izpis£a-Belmonte, and M. G. Rosenfeld. 1999. *Pitx2* regulates lung asymmetry, cardiac positioning and pituitary and tooth morphogenesis. Nature 401:279–282.

Linask, K. K. 2003. Regulation of heart morphology: current molecular and cellular perspectives on the coordinated emergence of cardiac form and function. Birth Defects Res. C Embryo Today 69:14–24.

Linask, K. K., M. D. Han, K. L. Linask, T. Schlange, and T. Brand. 2003. Effects of antisense misexpression of CFC on downstream flectin protein expression during heart looping. Dev. Dyn. 228:217–230.

Linask, K. K., and J. W. Lash. 1986. Precardiac cell migration: fibronectin localization at mesoderm-endoderm interface during directional movement. Dev. Biol. 114:87–101.

Linask, K. K., and J. W. Lash. 1988a. A role for fibronectin in the migration of avian precardiac cells. I. Dose-dependent effects of fibronectin antibody. Dev. Biol. 129:315–323.

Linask, K. K., and J. W. Lash. 1988b. A role for fibronectin in the migration of avian precardiac cells. II. Rotation of the heart-forming region during different stages and its effects. Dev. Biol. 129:324–329.

Linask, K. K., X. Y. Yu, Y. P. Chen, and M. D. Han. 2002. Directionality of heart looping: Effects of *Pitx2c* misexpression on flectin asymmetry and midline structures. Dev. Biol. 246:407–417.

Logan, M., S. M. Pagan-Westphal, D. M. Smith, L. Paganessi, and C. J. Tabin. 1998. The transcription factor *Pitx2* mediates situs-specific morphogenesis in response to left-right asymmetric signals. Cell 94:307–317.

Lowe, L. A., S. Yamada, and M. R. Kuehn. 2001. Genetic dissection of nodal function in patterning the mouse embryo. Development 128:1831–1843.

Lu, M. F., C. Pressman, R. Dyer, R. L. Johnson, and J. F. Martin. 1999. Function of Rieger syndrome gene in left-right asymmetry and craniofacial development. Nature 401:276–278.

Manasek, F. J. 1983. Control of early embryonic heart morphogenesis: a hypothesis. Ciba Found. Symp. 100:4–19.

Manasek, F. J., Y. Isobe, Y. Shimada, and W. Hopkins. 1984. The embryonic myocardial cytoskeleton, interstital pressure, and the control of morphogenesis. In: Congenital Heart Diseases Causes and Processes, ed. Nora, J., and A. Takao, 359–376. Mount Kisco, NY: Futura.

Manner, J. 2000. Cardiac looping in the chick embryo: a morphological review with special reference to terminological and biomechanical aspects of the looping process. Anat. Rec. 259:248–262.

Manning, A., and J. C. McLachlan. 1990. Looping of chick embryo hearts in vitro. J. Anat. 168:257–263.

Marino, B., M. C. Digilio, P. Versacci, S. Anaclerio, and B. Dallapiccola. 2002. [Transposition of great arteries. Understanding its pathogenesis]. Ital. Heart J. Suppl. 3:154–160.

Martinez-Frias, M. L. 2001. Heterotaxia as an outcome of maternal diabetes: an epidemiological study. Am. J. Med. Genet. 99: 142–146.

McGrath, J., and M. Brueckner. 2003. Cilia are at the heart of vertebrate left-right asymmetry. Curr. Opin. Dev. Genet. 13:385–392.

McQuinn, T. C., D. E. Miga, C. H. Mjaatvedt, A. L. Phelps, and A. Wessels. 2001. Cardiopulmonary malformations in the inv/inv mouse. Anat. Rec. 263:62–71.

Meilhac, S. M., R. G. Kelly, D. Rocancourt, S. Eloy-Trinquet, J.-F. Nicolas, and M. E. Buckingham. 2003. A retrospective clonal analysis of the myocardium reveals two phases of clonal growth in the developing mouse heart. Development 130:3877–3889.

Melloy, P. G., J. L. Ewart, M. F. Cohen, M. E. Desmond, M. R. Kuehn, and C. W. Lo. 1998. No turning, a mouse mutation causing left-right and axial patterning defects. Dev. Biol. 193:77–89.

Mercola, M., and M. Levin. 2001. Left-right asymmetry determination in vertebrates. Ann. Rev. Cell Dev. Biol. 17:779–805.

Meyers, E. N., and G. R. Martin. 1999. Differences in left-right axis pathways in mouse and chick: functions of FGF8 and SHH. Science 285:403–406.

Mieziewska, K., A. Szel, T. Van Veen, G. D. Aguirre, and N. Philp. 1994. Redistribution of insoluble interphotoreceptor matrix components during photoreceptor differentiation in the mouse retina. J. Comp. Neurol. 345:115–124.

Nonaka, S., Y. Tanaka, Y. Okada, S. Takeda, A. Harada, Y. Kanai, M. Kido, and N. Hirokawa. 1998. Randomization of left-right asymmetry due to loss of nodal cilia generating leftward flow of extraembryonic fluid in mice lacking KIF3B motor protein. Cell 95:829–837.

Oh, S. P., and E. Li. 1997. The signaling pathway mediated by the type IIB activin receptor controls axial patterning and lateral asymmetry in the mouse. Genes Dev. 11:1812–1826.

Orts Llorca, F., and D. Ruano Gil. 1967. A causal analysis of the heart curvatures in the chick embryo. Roux Arch. Entwicklungsmech. Organ. 158:52–63.

Pajkrt, E., B. Weisz, H. V. Firth, and L. S. Chitty. 2004. Fetal cardiac anomalies and genetic syndromes. Prenat. Diagn. 24:1104–1115.

Patten, B. M. 1922. The formation of the cardiac loop in the chick. Am. J. Anat. 30:373–397.

Piedra, M. E., J. M. Icardo, M. Albajar, J. C. Rodriguez-Rey, and M. A. Ros. 1998. Pitx2 participates in the late phase of the pathway controlling left-right asymmetry. Cell 94:319–324.

Raya, A., and J. C. Izpisua Belmonte. 2004. Unveiling the establishment of left-right asymmetry in the chick embryo. Mech. Dev. 121:1043–1054.

Reaume, A. G., P. A. de Sousa, S. Kulkarni, B. L. Langille, D. Zhu, T. C. Davies, S. C. Juneja, G. M. Kidder, and J. Rossant. 1995. Cardiac malformation in neonatal mice lacking connexin43. Science 267:1831–1834.

Riley, P. R., M. Gertsenstein, K. Dawson, and J. C. Cross. 2000. Early exclusion of hand1-deficient cells from distinct regions of the left ventricular myocardium in chimeric mouse embryos. Dev. Biol. 277:156–168.

Ryan, A. K., B. Blumberg, C. Rodrigues-Esteban, S. Yonei-Tamura, K. Tamura, T. Tsukui, J. De La Pena, W. Sabbagh, J. Greenwald, S. Choe, D. P. Norris, E. J. Robertson, R. M. Evans, M. G. Rosenfeld, and J. C. Izpisua Belmonte. 1998. *Pitx2* determinnes left-right asymmetry of internal organs in vertebrates. Nature 394:545–551.

Satin, J., S. Fujii, and R. L. DeHaan. 1988. Development of cardiac beat rate in early chick embryos is regulated by regional cues. Dev. Biol. 129:103–113.

Schier, A. F., and M. M. Shen. 2000. Nodal signalling in vertebrate development. Nature 403:385–389.

Schlange, T., I. Schnipkoweit, B. Andree, A. Ebert, M. H. Zile, H. H. Arnold, and T. Brand. 2001. Chick CFC controls Lefty1 expression in the embryonic midline and nodal expression in the lateral plate. Dev. Biol. 234:376–389.

Semina, E. V., R. S. Reiter, N. J. Leysens, M. L. W. Alward, K. W. Small, N. A. Datson, J. Siegel-Bartelt, D. Bierke-Nelson, P. Bitoun, and B. U. Zabel. 1996. Cloning and characterization of a novel bicoid-related homeobox transcription factor gene RIEG, involved in Rieger syndrome. Nat. Genet. 14:391–399.

Shen, M. M., and A. F. Schier. 2000. The EGF–CFC gene family in vertebrate development. TIG 16:303–309.

Smith, S. M., E. D. Dickman, R. P. Thompson, A. R. Sinning, A. M. Wunsch, and R. R. Markwald. 1997. Retinoic acid directs cardiac laterality and the expression of early markers of precardiac asymmetry. Dev. Biol. 182:162–171.

Sparrow, D. B., S. Kotecha, N. Towers, and T. J. Mohun. 1998. Xenopus eHAND: a marker for the developing cardiovascular system of the embryo that is regulated by bone morphogenetic proteins. Mech. Dev. 71:151–163.

Srivastava, D., P. Cserjesi, and E. N. Olson. 1995. A subclass of bHLH proteins required for cardiac morphogenesis. Science 270: 1995–1999.

St Amand, T. R., J. Ra, Y. Zhang, Y. Hu, S. I. Baber, M. Qiu, and Y. Chen. 1998. Cloning and expression pattern of chicken *Pitx2*: a new component in the SHH signaling pathway controlling embryonic heart looping. Biochem. Biophys. Res. Commun. 247:100–105.

Stalsberg, H. 1969. Regional mitotic activity in the precardiac mesoderm and differentiating heart tube in the chick embryo. Dev. Biol. 20:28–45.

Stalsberg, H. 1970. Mechanism of dextral looping of the embryonic heart. Am. J. Cardiol. 25:265–271.

Steding, G. and W. Seidl. 1980. Contribution to the development of the heart. Part I: Normal development. 28:386–409.

Sugishita, Y., D. W. Leifer, F. Agani, M. Watanabe, and S. A. Fisher. 2004. Hypoxia-responsive signaling regulates the apoptosis-dependent remodeling of the embryonic avian cardiac outflow tract. Dev. Biol. 273:285–296.

Sugishita, Y., M. Watanabe, and S. A. Fisher. 2004. Role of myocardial hypoxia in the remodeling of the embryonic avian cardiac outflow tract. Dev. Biol. 267:294–308.

Sullivan, R., G. Y. Huang, R. A. Meyer, A. Wessels, K. K. Linask, and C. W. Lo. 1998. Heart malformations in transgenic mice exhibiting dominant negative inhibition of gap junctional communication in neural crest cells. Dev. Biol. 204:224–234.

Supp, D. M., D. P. Witte, S. S. Potter, and M. Brueckner. 1997. Mutation of an axonemal dynein affects left right asymmetry in inversus viscerum mice. Nature 389:963–966.

Szeto, D. P., K. J. P. Griffin, and D. Kimelman. 2002. *hrT* is required for cardiovascular development in zebrafish. Development 129:5093–5101.

Taber, L. A., I.-E. Lin, and E. B. Clark. 1995. Mechanics of cardiac looping. Dev. Dyn. 203:42–50.

Takeuchi, J.K., M. Ohgi, K. Koshiba-Takeuchi, H. Shiratori H, I. Sakaki I, K. Ogura, Y. Saijoh, and T. Ogura,T. 2003. Tbx5 specifies the left/right ventricles and ventricular septum position during cardiogenesis. Development 130:5953–5964.

Thompson, R. P., V. Abercrombie, and M. Wong. 1987. Morphogenesis of the truncus arteriosus of the chick embryo heart: movements of autoradiographic tattoos during septation. Anat. Rec. 218:434–440.

Thompson, R. P., Y.-M. M. Wong, and T. P. Fitzharris. 1984. Patterns of tensile stress in the developing cardiac truncus. In: Congenital Heart Disease: Causes and Processes, ed. Nora, J. J. and A. Takao, 387–400. Mount Kisco, New York: Futura.

Toyoizumi, R., K. Shiokawa, and S. Takeuchi. 1991. The behavior and cytoskeletal system of chick gastrula mesodermal cells on substrata coated with lines of fibronectin. J. Exp. Zool. 260:345–353.

Tsuda, T., N. Philp, M. H. Zile, and K. K. Linask. 1996. Left-right asymmetric localization of flectin in the extracellular matrix during heart looping. Dev. Biol. 173:39–50.

Tsuda, T., K. Majumder, and K. K. Linask. 1998. Differential expression of flectin in the extracellular matrix and left-right asymmetry in mouse embryonic heart during looping stages. Dev. Genet. 23:203–214.

Van Praagh, R., and R. L. DeHaan. 1967. Morphogenesis of the heart: mechanism of curvature. Carnegie Inst. Embryol. 65:536–537.

Voronov, D. A., P. W. Alford, G. Xu, and L. A. Taber. 2004. The role of mechanical forces in dextral rotation during cardiac looping in the chick embryo. Dev. Biol. 171:339–350.

Voronov, D. A., and L. A. Taber. 2002. Cardiac looping in experimental conditions: effects of extraembryonic forces. Dev. Dyn. 224:413–421.

Waddington, C. H. 1937. The dependence of head curvature on the development of the heart in the chick embryo. J. Exp. Biol. 14:229–231.

Waldo, K. L., M. R. Hutson, M. Zdanowicz, H. A. Stadt, J. Zdanowicz, and M. L. Kirby. 2005. Cardiac neural crest is necessary for normal addition of the myocardium to the arterial pole from the secondary heart field. Dev. Biol. 281:66–77.

Watanabe, M., A. Choudhry, M. Berlan, A. Singal, E. Siwik, S. Mohr, and S. A. Fisher. 1998. Developmental remodeling and shortening of the cardiac outflow tract involves myocyte programmed cell death. Development 125:3809–3820.

Watanabe, M., A. Jafri, and S. A. Fisher. 2001. Apoptosis is required for the proper formation of the ventriculo-arterial connections. Dev. Biol. 240:274–288.

Ya, J., E. B. H. W. Erdtsieck-Ernste, P. A. J. de Boer, M. J. A. van Kempen, H. Jongsma, A. F. M. Moorman, and W. H. Lamers. 1998. Heart defects in connexin 43-deficient mice. Circ. Res. 82:360–366.

Yan, Y. T., K. Gritsman, J. X. Ding, R. D. Burdine, J. D. Corrales, S. M. Price, W. S. Talbot, A. F. Schier, and M. M. Shen. 1999. Conserved requirement for *EGF-CFC* genes in vertebrate left-right axis formation. Genes Dev. 13:2527–2537.

Yelbuz, T. M., K. L. Waldo, D. H. Kumiski, H. A. Stadt, R. R. Wolfe, L. Leatherbury, and M. L. Kirby. 2002. Shortened outflow tract leads to altered cardiac looping after neural crest ablation. Circulation 106:504–510.

Yoshioka, H., C. Meno, K. Koshiba, M. Sugihara, H. Itoh, Y. Ishimaru, T. Inoue, H. Ohuchi, E. V. Semina, J. C. Murray, H. Hamada, and S. Noji. 1998. *Pitx2*, a bicoid-type homeobox gene, is involved in a lefty-signaling pathway in determination of left-right asymmetry. Cell 94:299–305.

Yue, X., T. M. Schultheiss, E. A. McKenzie, and R. D. Rosenberg. 2004. Role of heparan sulfate in dextral heart looping in chick. Glycobiology 14:745–755.

This page intentionally left blank

8

Chamber Specification and Ventricular Septation

As discussed in the previous chapter, the craniocaudal, right–left, and dorsoventral axes are all established for the body during gastrulation. However, except for the craniocaudal axis, the other axes are reinterpreted in the semiautonomous heart tube as it forms and the new axes are the ones that are important in looping, chamber specification, and septation. Based on axial information, many cardiac genes are broadly induced in the cardiogenic fields and early heart tube, and then become restricted to the atria or ventricles as development proceeds based on axis information contained within the heart tube. Chamber specification occurs through distinct transcriptional programs, which govern myocardial identity at various stages of specialization in the forming heart. These transcriptional programs are established based on the craniocaudal and dorsoventral polarity of the heart tube. An understanding of the morphological development of chambers and septation is a first step to appreciate the molecular intricacies of chamber specification and septation.

Morphology of Chamber Development and Septation

As the bilateral heart fields fuse, the earliest tube in the mouse is represented mostly by what will become the inflow limb of the looped heart, that is, the left ventricle, atrioventricular canal, and parts of the atrium. In the chick the prospective right and left ventricles are the earliest identifiable regions (Fig. 8.1). As discussed in Chapter 6, cells are accrued from both the inflow and outflow poles that will supplement this initial population. From the outflow pole the right ventricle, conus and truncus, which comprise the outflow limb of the looped heart, are added. Some remaining atrial myocardium is added from the inflow pole. After C-looping, the deepest convexity of the looped heart separates the inflow from outflow limbs. This bend approximates the position where the ventricular septum will form to separate the right and left

Figure 8.1. Appearance of the bulboventricular fold (2) between the prospective right and left ventricles in the chick at stages 10 (*A*), 11 (*B*), and 14 (*C*) is the first sign of regional specification of the heart tube into an inflow and outflow limb which become obvious by stage 12. m, ventral midline seam, c, conus, v, ventricle, a, atrium, 1, right lateral furrow. (From Manner, 2000, with permission.)

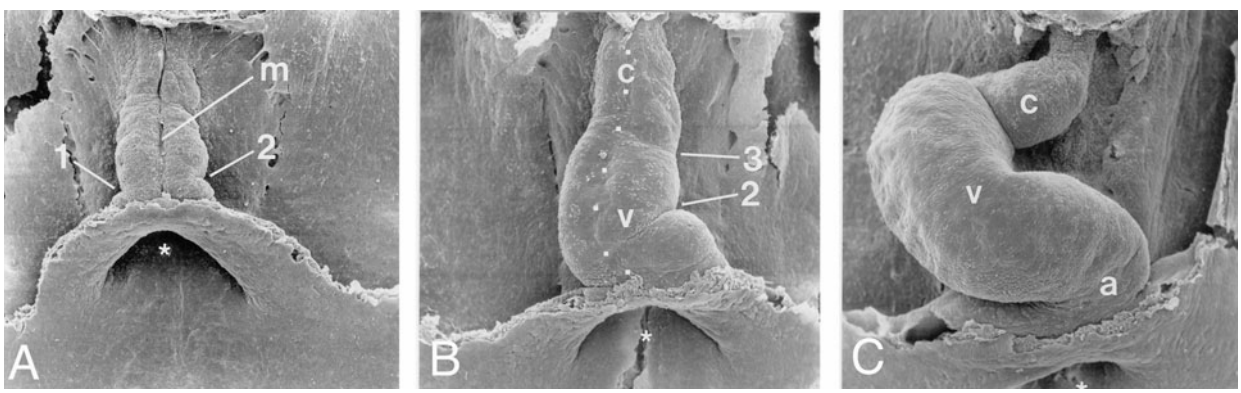

ventricles. The inflow and outflow limbs are gradually sculpted to form the definitive chambers.

Atria and Atrial Septation

As the inflow and outflow poles converge during looping (discussed in Chapter 7), the common atrium enlarges to the right. The enlarged common atrial chamber will be divided later by a primary atrial septum that will create right and left atria. Atrial septation was discussed in detail in Chapter 6 and only the highlights are repeated here. The primary atrial septum is cardiac muscle that is incorporated from splanchnic mesoderm near the venous pole. As the septum extends from the dorsal atrial wall, its leading edge is covered by mesenchyme (Asami and Koizumi, 1995; Mommersteeg et al., 2006; Tasaka et al., 1996; Wessels et al., 1998). The primary atrial septum is augmented by a secondary septum, constructed from a fold of the atrial myocardial wall during fetal life to complete the process of atrial septation.

The left and right atria are derived from the left and right cardiogenic fields respectively and retain the left–right body axis specification. However, the ventricles are composed of myocardium derived from both left and right cardiogenic fields and so left–right have to be reestablished in the ventricular portion of the heart tube. The atria develop symmetrically until the venous inflow is remodeled to the right (Davis, 1927). The venous inflow is remodeled as both sinus horns move rightwards coincident with rapid growth of the atria.

Atrioventricular Canal and Atrioventricular Septation

The lumen of the atrioventricular canal provides the passage between the atrium and the presumptive left ventricle. This canal becomes divided into right and left canals by an atrioventricular septum that is in line with the atrial septum. The right and left canals will be sculpted to form the mitral and tricuspid valves of the mature heart. The details of this septation and subsequent remodeling are in Chapter 9.

Initially, the atrioventricular canal is positioned in line with the left ventricle. However, after separate atrioventricular connections have been established, the right atrium is in direct contact with the right ventricle because of remodeling of the right atrioventricular junction. Growth in the atrioventricular canal is more pronounced on the atrial than on the ventricular side, and on the originally right than on the left side resulting in an asymmetric, funnel-shaped atrioventricular canal (Lamers and Moorman, 2002).

Right and Left Ventricles and the Ventricular Septum

The part of the cardiac loop that joins the inflow and outflow limbs was designated the BULBOVENTRICULAR FOLD in the classical literature. The bulboventricular fold is a narrowed area that represents the division between what will be the right ventricle ("BULBUS") and the left ventricle (Fig. 8.2). Both ventricular chambers are formed by ballooning of the outer curvature myocardium. This occurs concurrently with formation of trabeculae, which are myocardial diverticula extending from the compact, outer wall of the myocardium into the cardiac jelly toward the lumen. Formation of the trabeculae is the first manifestation of the differentiation of the nascent left and right ventricles (Van Mierop and Kutsche, 1985). The ventricular chambers enlarge by growth and expansion of the myocardial wall on the greater or outer curvature (Christoffels et al., 2000). Growth is closely followed by increasing trabeculae, which give the ventricular lumen a spongy appearance (Fig. 8.2). The luminal passage through the bulboventricular fold is called the primary ventricular foramen (or bulboventricular foramen). The ventricular septum grows from the greater curvature at the site of the bulboventricular fold (Fig. 8.2). However, the PRIMARY VENTRICULAR FORAMEN is maintained at the leading edge of this crescent-shaped septum. In fact, the primary ventricular foramen never closes but actually enlarges in the fully developed heart to give left ventricular access to the aortic vestibule (Van Mierop and Kutsche, 1985).

The functional significance of trabeculae in early heart development is unknown. Histological studies in chick and human suggest that coalescence of the trabeculae results in

Figure 8.2. Ventricular morphology in scanning electron micrographs of chick embryos during chamber formation. Ventral halves of frontally dissected stage 17, 21, 25, and 29 hearts viewed from the back. *Arrows* indicate the primary interventricular foramen. LA, left atrium; RA, right atrium; LV, left ventricle; RV, right ventricle; OT outflow tract; asterisk, crest of developing muscular interventricular septum. (From Sedmera et al., 2004, with permission.)

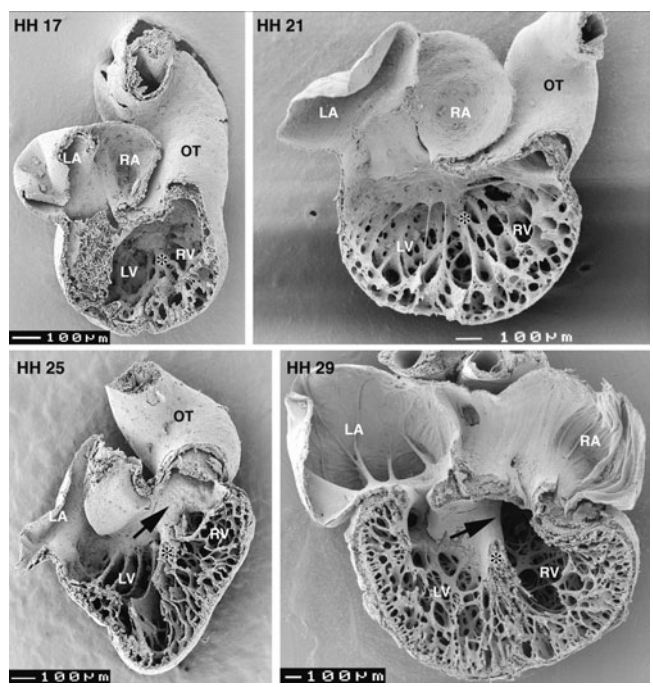

formation of the muscular ventricular septum (Ben-Shachar et al., 1985; Hochstetter, 1906; Morse, 1978; Patten, 1951). Other studies suggest that the muscular septum originates from the part of the ventricular wall that is interposed between the expanding free walls of the future right and left ventricles (Chang, 1932; de la Cruz et al., 1972; Goor and Lillehei, 1975; Streeter, 1948). In fact, both processes may contribute to the growth of the ventricular septum.

In human embryos at 5 weeks, a muscular septum is identifiable between the trabecular portions of both ventricles. The muscular ventricular septum is divided into regions designated the inlet portion of the septum near the atrioventricular septum and valves while the portion nearest the ventricular outflow is designated the outlet septum. The ATRIOVENTRICULAR BUNDLE of His, discussed in Chapter 12, is found on the crest of the caudal portion of the muscular ventricular septum (Kim et al., 2001; Lamers et al., 1995).

The last part of the ventricular septum to form is the MEMBRANOUS SEPTUM which forms from cushion tissue that fills in the opening left between the crest of the ventricular muscular septum and the atrioventricular mesenchymal septum. As the membranous portion of the septum develops, it also forms the primordium for the septal cusp of the tricuspid valve. During sculpting of the septal leaflet it is detached from the interventricular septum at the fifth month of human fetal development (Conte and Grieco, 1984).

Conus, Truncus, and the Outflow Septum

The conus and truncus connect the presumptive right ventricle with the aortic sac. The aortic sac is the collecting point of all the blood at the arterial pole of the heart. It is not covered by myocardium and is thus not part of the heart. However, it is subject to septation along with the myocardial covered outflow tract. The aortic sac in many vertebrates with an undivided pulmonary and systemic circulation is designated ventral aorta.

The myocardium of the conus originates in the anterior heart field along with the right ventricle but the conus differs from the right ventricle in that it never becomes trabeculated (Cai et al., 2003; Kelly et al., 2001; Van Mierop and Kutsche, 1985). Thus, it can be distinguished early as distinct from the right ventricular chamber by its smooth wall. The conus undergoes dramatic remodeling to become incorporated as the smooth-walled pulmonary infundibulum and part of the wall of the aortic vestibule connecting the body of the right ventricle with the pulmonary trunk and the left ventricle with the aorta, respectively.

The most "distal" portion of the outflow of the tubular heart covered by myocardium is called the truncus. The truncus forms the ventricular myocardial portion of the ventriculoarterial junction. The myocardium of the truncus originates from the secondary heart field (Waldo et al., 2001, 2005). This myocardium spirals into the truncus: the myocardium from the right secondary heart field courses caudal and to the left (pulmonary) side of the outflow while that from the left side travels cranial and to the right (aortic) side (Ward et al., 2005). This is the same pattern in which the distal cushions form that ultimately establish the direction of the spiraling outflow septum. Whether the myocardium is added in these spirals or the outflow rotates to create the spiraling myocardium is not known. The truncus is remodeled to become the semilunar valve region of both ventricles during the transition from serial to divided parallel pulmonary and systemic circulations.

From their first appearance conotruncal cardiomyocytes are different from those in the atria and ventricles. They have lower rates of proliferation as well as a more basic panel of contractile proteins, less well-developed sarcoplasmic reticulum, persistent expression of smooth muscle α-actin, and slower impulse conduction than ventricular myocytes of the same developmental stage (Christoffels et al., 2000; Ruzicka and Schwartz, 1988; Thompson et al., 1990). These properties are consistent with the function of the outflow tract as a sphincter rather than a pump. In this case, the outflow tract functions as a sphincter to prevent backflow of blood.

The most proximal parts of the aorta and pulmonary trunk form from the aortic sac, a nonmyocardial covered sinus that receives all of the blood leaving the heart during early development. The aortic sac branches into a series of aortic arch arteries that traverse from ventral to dorsal in the pharyngeal arches to carry blood to the dorsal aorta. The aortic sac is divided into the pulmonary trunk and aorta by the aorticopulmonary septum as an initial step in outflow septation. As outflow septation proceeds, the nascent aorta rotates posterior to the pulmonary trunk and the conotruncal myocardium shortens to about 25% of its original length (de la Cruz et al., 1977; Dor and Corone, 1985; Goor et al., 1972; Thompson et al., 1987). The extent of this remodeling can be especially well appreciated when the myocardium is labeled prior to the remodeling (Fig. 8.3) (Watanabe et al., 1998, 2001). The outflow myocardium reorganizes from tubular to wedge-shaped while septation effects connection of the right ventricle to the pulmonary artery and the left ventricle to the aorta. The semilunar valves of both arterial outlets are formed at the level of the truncus. The remodeling involves incorporation of some of the myocardium into the ventricular outlets and elimination of some myocardium by cell death (Hurle and Ojeda, 1979; Pexieder, 1975; Schaefer et al., 2004; Watanabe et al., 1998). In fact, there is broadly distributed cell death in the proximal outflow myocardium early in remodeling, and concentrated foci of cell death in truncal myocardium underneath the aorta as it moves (wedges) behind the pulmonary artery to connect to the left ventricle.

Septation of the outflow tract is somewhat complicated and is only introduced here; it is covered in detail in Chapter 11. The tissues of the outflow tract are derived from a number of diverse sources. The myocardium is the last to be added to the heart tube as discussed previously while the endocardium is derived from both cardiogenic mesenchyme and noncardiogenic regions of the lateral plate mesoderm and head

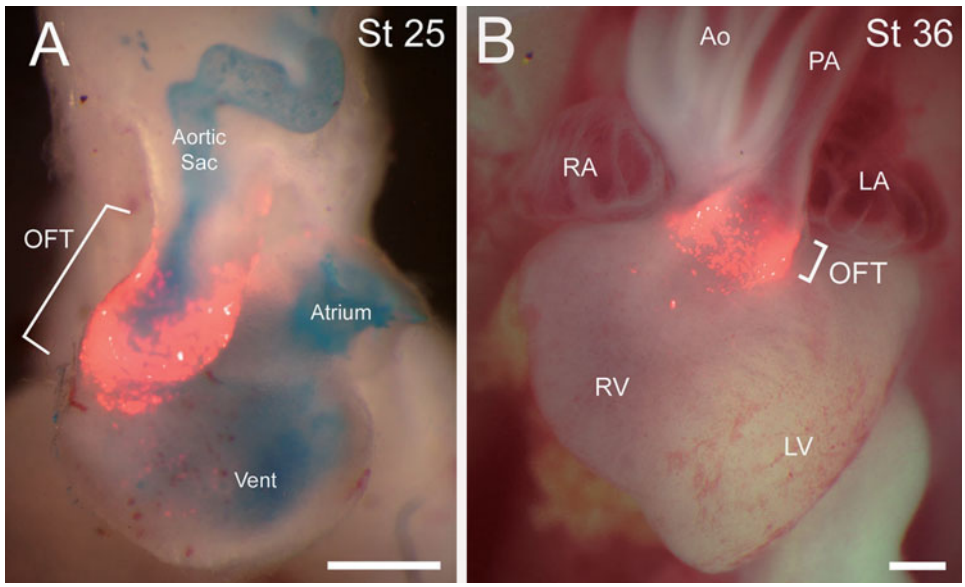

Figure 8.3. Remodeling of the chick outflow myocardium (OFT). (*A*) The OFT myocardium of the stage 25 embryonic day 5 (ED5) chick heart labeled with red fluorescent protein. *(B)* By stage 36 (ED10) the outflow myocardium has been incorporated into the myocardium just below the semilunar valves.RA, right atrium; RV, right ventricle; Ao, aorta; PA, pulmonary artery; LA, left atrium; LV, left ventricle. (From Sugishita et al., 2004, with permission.)

mesenchyme (Coffin and Poole, 1988; Manasek, 1968; Markwald et al., 1996; Mikawa et al., 1996; Noden, 1991; Pardanaud et al., 1987; Sugi and Lough, 1994; Sugi and Markwald, 1996). The mesenchyme in the cardiac jelly of the truncus and conus is contributed by epithelial-mesenchymal transformation from endocardial cells, pharyngeal mesenchyme and ectomesenchymal derivatives of the neural crest (Kirby et al., 1983; Markwald et al., 1977). There is disagreement over the origin of the outflow components owing in part to different hypothetical models of outflow septation that have been proposed (Bartelings and Gittenberger-de Groot, 1989; Laane, 1978a,b, 1979a,b; Thompson and Fitzharris, 1985). A mesenchymal septum grows from the roof of the aortic sac between the origins of arch arteries 4 and 6 dividing the aortic sac into the base of the aorta and pulmonary trunk before entering the outflow tract proper. As the septum grows into the outflow tract, it spirals 180°. During septation, the outflow myocardium is remodeled by a combination of incorporation into the right and left ventricles and cell death. The result is that the aorta is wedged between the mitral and tricuspid valves, behind the pulmonary trunk as discussed previously and in Chapter 7.

Polarity in the Heart Tube

The craniocaudal disposition of cells in the primitive streak during gastrulation is maintained in the heart tube despite the fact that the craniocaudal axis goes through a stage of being oriented mediolaterally in the cardiogenic fields (Abu-Issa and Kirby, 2005). Because of the manner in which the heart fields fuse, craniocaudal is reestablished as it had been in the primitive streak. This axis is particularly important in establishing the relationship of the primitive atrium, atrioventricular canal, and left and right ventricles which will form from caudal to cranial as the heart tube forms. The left cardiogenic field contributes to the left side of the tubular heart, which after rightward looping becomes the ventral or front face of the tube. The right cardiogenic field contributes to the right side of the tubular heart, which becomes the dorsal or back face of the looped tube. Thus, right and left in the body axis become dorsal and ventral in the heart tube. The dorsal midline seam forms from the most caudal region of the cardiogenic field while the ventral midline seam forms from the cranial cardiogenic field. During looping, the ventral midline becomes the right border or greater curvature while the dorsal midline becomes the left border or inner curvature of the looped tube. It is the outer curvature that balloons to form the ventricular chambers.

Craniocaudal Axis

Retinoic acid is an important signal in establishing atrial identity in the caudal region of the heart tube. Endogenous retinoid signaling is highest at the caudal (inflow or atrial) region of the developing heart tube and decreases cranially in the presumptive left ventricular region. The gradient is important for defining the portion of the tube that will be the atria and atrioventricular canal. Retinoic acid is synthesized by retinaldehyde dehydrogenase-2 (Raldh2), which is specifically expressed within the caudal heart region of both mouse and chick. Mouse embryos lacking Raldh2 fail to develop a distinct atrial

chamber (Chazaud et al., 1999; Niederreither et al., 1999, 2001; Xavier-Neto et al., 1999). Evidence suggests that endogenous retinoid signaling in heart development depends on localized presentation of the ligand, with only limited diffusion from the source of its synthesis (Colbert et al., 1996; Moss et al., 1998). Excessive retinoid signaling results in specification of more of the ventricular region as atrial. In the chick, exogenously applied retinoic acid causes a shift in the atrial identity of the primary heart tube into the ventricular portion of the tube (Yutzey et al., 1994). Retinoic acid administered to pregnant mice at E7.5 or chick embryos at gastrulation truncates the ventricular portion of the heart tube and enlarges the atrial portion, resulting in cardiac phenotypes ranging from hearts with reduced ventricles to complete absence of the outflow tract and ventricles (Brunskill et al., 2001; Xavier-Neto et al., 1999; Yutzey et al., 1994).

Retinoid signaling initiates a cascade of gene expression. Gata4, -5, and -6 are expressed in and caudal to the heart forming region of one-somite embryos and in a caudal-to-cranial gradient in the tubular heart with the highest expression caudally (Jiang et al., 1998). *Gata4* is expressed at the anterior intestinal portal and inflow region of the fusing heart tube. It is downregulated in retinoid-deficient embryos (Kostetskii et al., 1999). *Tbx5* is also expressed in a caudal-to-cranial gradient in the tubular heart and this gradient is altered by retinoid signaling(Bruneau et al., 1999). In the *Raldh2*-null heart, the expression of *Tbx5* is restricted to its most caudal expression domain in the atria (Niederreither et al., 2001).

Mediolateral and Dorsoventral Axes

The dorsal and ventral midlines of the heart tube are formed from the cranial and caudal portions of the cardiogenic fields, respectively, and after looping they become the outer and inner curvatures, respectively (Abu-Issa and Kirby, 2005). The ventricular chambers expand from the outer curvature (Moorman and Christoffels, 2003; Moorman AF, 2003). The atria maintain left and right-sided identity with the left and right sides of the body while the ventricles are free to reestablish an endogenous understanding of left and right using mixed parts of the left and right cardiogenic fields. This idea is supported by data showing that left and right ventricles differentiate in both hearts in cardia bifida (Li et al., 2004). By contrast, it appears that the atria must be faithful to the left and right sides of the body so that the asymmetric venous systemic and pulmonary connections are made correctly.

The myocardium of the outer curvature expands to form the ventricles and at the same time differentiates as ventricular chamber or "working" myocardium. The ventricular chamber myocardium has different characteristics from the early myocardium. Before expansion of these chambers, one of the signs of differentiation as chamber myocardium is the combined expression of atrial natriuretic factor (Nppa), Cx40, Cx43, and Chisel. The myocardium of the inner curvature does not express these genes and thus retains the characteristics of the early myocardium. In chick at stage 9, Nppa expression is first observed in a subset of cardiomyocytes localized ventrally (prospective outer curvature) in the fused heart tube and laterally (prospective atria) in the unfused cardiogenic mesoderm suggesting that differentiation of chamber myocardium may have already begun in the cardiogenic mesoderm (Houweling et al., 2002).

Slow conduction is one of the characteristics of the early myocardium and this is lost in the chamber myocardium but retained in the myocardium of the inner curvature, outflow tract, atrioventricular canal, and atria. Because the myocardium of the inner curvature of the heart continues to have slow conduction, Moorman and colleagues believe that it is set aside as conduction myocardium. In fact, the inner curvature myocardium is in an excellent position to contribute to the His bundle and bundle branches (see Chapter 12). While Nppa expression can be used to distinguish chamber myocardium, including the peripheral ventricular conduction system, from embryonic myocardium, during later development Nppa expression is excluded from the myocardium in the interventricular septum and the most proximal part of the bundle branches, whereas the distal bundle branches, trabeculae, and surrounding working myocardium do express Nppa (Houweling et al., 2002).

Chamber-Specific Gene Expression

It is difficult to determine precisely when a chamber is a chamber. The chambers appear to emerge morphologically and molecularly from regions, that is, inflow limb, loop, and outflow limb, via a series of overlapping and nonoverlapping gene expressions some of which are initiated in the bilateral cardiogenic fields. Via expression and repression of specific genes, each chamber finally takes on the morphological and functional characteristics needed for its normal tasks.

A major theme in chamber-specific gene expression is that transcriptional repression and mutually antagonistic pathways are required to establish chamber identity in heart development (Solloway and Harvey, 2003). Many genes are initially expressed throughout the heart tube and later become restricted to a particular chamber. For example, slow myosin heavy chain 3 (sloWMyHC3) is expressed uniformly throughout the heart tube, but is gradually extinguished cranially establishing a craniocaudal gradient that culminates in atrial-specific expression (Wang et al., 1996). The vitamin D receptor specifically represses expression of slowMyHC3 in the ventricles (Wang et al., 1998). However, activation is also an important mechanism in chamber specification. *Irx4*, a homeobox-containing gene, is expressed in a ventricle-specific manner throughout heart development and has been shown to activate ventricular myosin heavy chain-1 (MHC1V) and suppress the expression of atrial myosin heavy chain-1 (MHC1A) in the ventricles (Bao et al., 1999).

Atruim–Atrioventricular Canal–Left Ventricle (Inflow Limb)

The atrial compartment of the myocardium is marked by Gata4, Tbx5, and the orphan receptor COUP-TFII. Gata4 and Nkx2.5 expression domains overlap during early heart tube formation, but *Gata4* is downregulated in the ventricular part of the cardiogenic fields and is maintained only in the presumptive atrial compartment (Jiang et al., 1998). Gata4 expression is severely reduced in retinoic acid-deficient quail embryos and an oversized ventricle is formed with deficient development of the atrium (Dersch and Zile, 1993; Kostetskii et al., 1999). The reduced expression of Gata4 is accompanied by foregut apoptosis, which may be causally related to the malformations of the inflow tract (Ghatpande et al., 2000). Null mutation of Coup-tfII is associated with failure to develop an atrium and sinus venosus (Pereira et al., 1999).

Tbx5-null mice show severe hypoplasia of the atria and left ventricle, while the right ventricle and outflow tract are not affected (Bruneau et al., 2001). In *Raldh2*-null mice, Tbx5 expression is lost and there is severe truncation of the inflow region of the heart (Niederreither et al., 2001). SlowMyHC3 is initially expressed uniformly in the tubular heart. A caudal-to-cranial gradient of expression develops that culminates in atrial chamber-restricted expression of this gene following chamber formation (Fig. 8.4). Two *cis* elements in the promoter of *slowMyHC3* control its regionalized expression/repression. A Gata-binding element promotes expression while a vitamin D receptor binding element represses expression in the ventricle but not in atrium. An inhibitory protein complex composed of vitamin D receptor, RXRα, and Irx4 binds at the vitamin D receptor binding element (Wang et al., 1996, 2001).

Irx4 regulates chamber-specific expression of chick myosin isoforms ventricular myosin heavy chain-1 (VMHC1) and atrial myosin heavy chain-1 (AMHC1) (Bao et al., 1999). Amhc1 is expressed in the caudal heart tube at stage 12 in the chick while Vmhc1 is expressed in all cardiac myocytes at early stages of development (Yutzey and Bader, 1995, Yutzey et al., 1994). In the mouse heart tube α-myosin heavy chain (αMhc) also shows a caudal-to-cranial gradient that becomes confined to the inflow tract, atria, atrioventricular canal (Lyons, 1990, 1994). β-Myosin heavy chain (βMhc) is expressed in a cranial-to-caudal gradient and after looping expression is confined to the outflow tract, ventricles, and atrioventricular canal (Lyons, 1990, 1994).

As a distinct ventricular chamber forms in the mouse between E8 and 10.5, βMhc becomes restricted to the ventricular myocytes. αMhc transcripts continue to decrease in ventricular myocytes until E16, when they are detectable at low levels, but then increase, and finally replace βMhc ventricular muscle by postnatal day 7. Like βMhc, myosin light chain 1V (Mlc1V) transcripts become restricted to ventricular myocytes, but at a slower rate (Lyons et al., 1990).

Between E12.5 and birth, αMhc, Mlc1A, and Mlc2A become transcriptionally restricted to the atria (Fig. 8.5). These genes are downregulated in the compact myocardium of the left ventricle before that of the right ventricle. αMhc protein also accumulates in the right, but not left, compact ventricular myocardium during this period. Downregulation of *αMhc*, *Mlc1A*, and *Mlc2A* in *iv*/*iv* embryos, which have defective left/right patterning, is initiated in the systemic ventricle regardless of its anatomical position on the right or left hand side (Fig. 8.6) (Zammit et al., 2000).

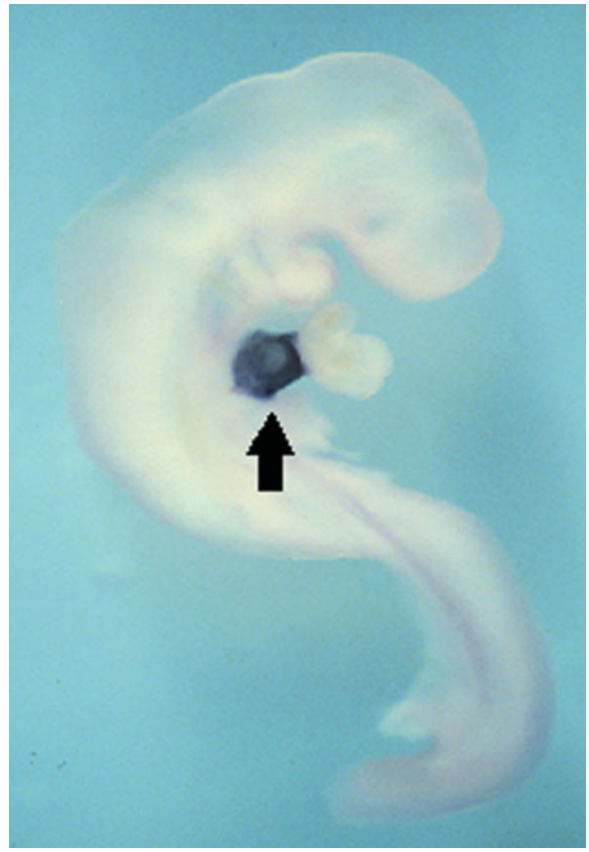

Figure 8.4. Transgenic mouse embryo at 9.0 dpc with 840 bp of the *slowMyHC3* promoter driving human *alkaline phosphatase* reporter in a transgenic mouse. The expression is limited to the developing atrium (arrow). (From Xavier-Neto et al., 1999, with permission.)

Left Ventricle–Right Ventricle (Loop)

One of the first demonstrations of ventricular myogenic gene program was the expression of Mlc2V in the heart tube (O'Brien et al., 1993). At E8.0, Mlc2V expression is high in the ventricular portion of the heart tube, with no detectable expression in the atrium or sinus venosus (Fig. 8.5). Expression is well established in the proximal outflow tract region adjacent to the ventricular segment by E9-10, eventually reaching levels comparable to the trabeculated ventricular myocardium. By E11, prior to the completion of septation, expression becomes restricted to the ventricles (Fig. 8.7) (Kubalak et al., 1994). Ventricle-restricted expression of Mlc2V is by a 250–base-pair ventricular promoter fragment (Ross et al., 1996).

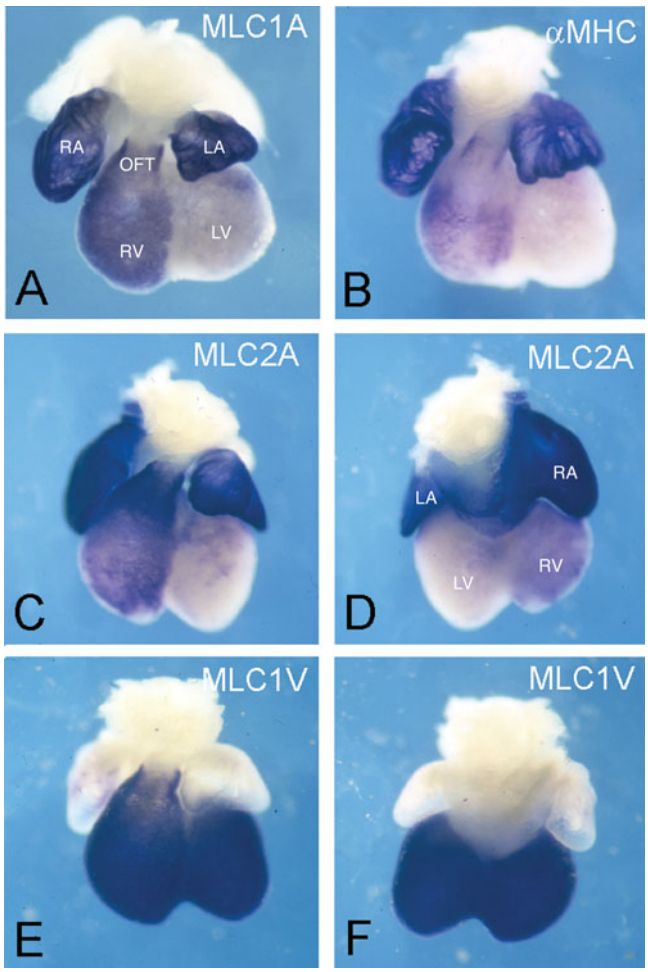

Figure 8.5. Whole-mount in situ hybridization of mouse hearts at E12.5. Left–right differences in expression of MLC1A (*A*), αMHC (*B*), and MLC2A (*C*, ventral view; *D*, dorsal view) in the right ventricle (RV) compared to the left ventricle (LV). MLC1A, αMHC, and MLC2A are all robustly expressed in the atria. MLC1V (*E*, ventral view; *F*, dorsal view) is typical of the expression pattern shared with βMHC and MLC2V, that is, strong expression in the left and right ventricles terminating distal to the atrioventricular canal. αMHC is expressed at a lower level in the outflow tract (OFT) than in the RV, whereas MLC2A transcripts are more abundant in the OFT than in the RV, indicating that the RV and OFT are transcriptionally distinct compartments. RA, right atrium; LA, left atrium. (From Zammit et al., 2000, with permission.)

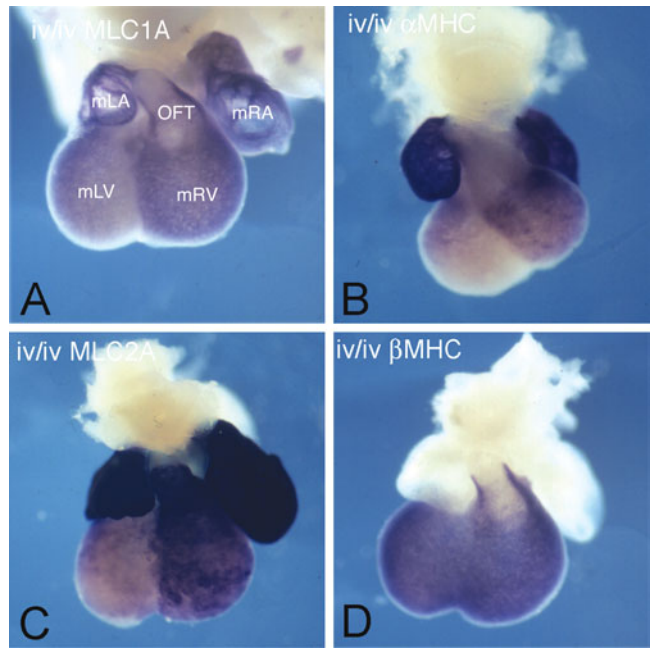

Figure 8.6. Whole-mount in situ hybridization of mouse hearts at E12.5 from embryos with situs inversus (*iv*/*iv*). MLC1A (A), MHC (B), and MLC2A (C) are more strongly expressed in the morphological right (pulmonary) ventricle (mRV) than the morphological left (systemic) ventricle (mLV). βMHC is expressed equally in both ventricles but not in the outflow tract (OFT). mLA, morphological left atrium; mRA, morphological right atrium. (From Zammit et al., 2000, with permission.)

Ventricular chamber specification occurs in discreet zones at the outer curvature of the looping heart tube. These zones are marked by expression of Hand1, Cited1 and Irx1/2/3, gap junction proteins connexin 40 and 43, Nppa, and the cytoskeletal protein Chisel. Irx4 labels ventricular precursor cells in the cardiogenic fields and is exclusively expressed in the left ventricle after chamber formation (Bruneau et al., 2000). Other genes that are not expressed in a chamber-specific manner, including some myofilament genes, are upregulated in chamber myocardium as the chambers are established. Thus, it appears that formation of the definitive chamber myocardium requires a regional myogenic specialization that ultimately leads to unique contractile, excitation and cytoskeletal properties appropriate for each chamber. The related basic helix–loop–helix transcription factor genes *Hand1* and *Hand2* are coexpressed in the primary heart tube but their messages differentially accumulate in the right (Hand2) and left (Hand1) ventricles in the mouse (Fig. 8.8) (Thomas et al., 1998). Similar expression of the *Hand* genes does not occur in the chick. In the mouse, Hand1 is expressed in the left or systemic ventricle in both normal and situs inversus mice indicating chamber specificity of expression rather than right–left axial cues (Thomas et al., 1998). Irx4 labels ventricular precursor cells in the cardiogenic fields and is exclusively expressed in the left ventricle after chamber formation (Bruneau et al., 2000).

Tbx5 is important in left–right ventricle formation and in the placement of the ventricular septum (Fig. 8.9). Tbx5 is expressed in the left ventricle but when its expression is forced ubiquitously, the ventricular septum does not form resulting in a single ventricle. Tbx20 is expressed in the right ventricle but is repressed when Tbx5 is ubiquitously expressed. If misexpression of Tbx5 is only partially in the right ventricle the ventricular septum is shifted to the right creating a small right ventricular chamber and a comparably enlarged left ventricle (Takeuchi et al., 2003).

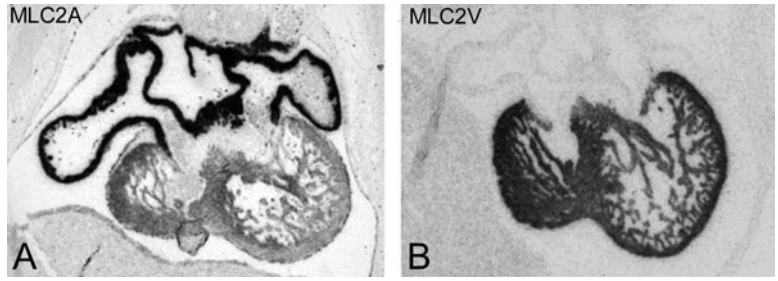

Figure 8.7. MLC2A (*A*) and MLC2V (*B*) immunohistochemistry in the mouse heart at E14.5. (*A*) MLC2A protein is evenly expressed in all the venous myocardial components in addition to the atria. (*B*) MLC2V protein is confined to the ventricular myocardium. (Zammit et al., 2000, with permission.)

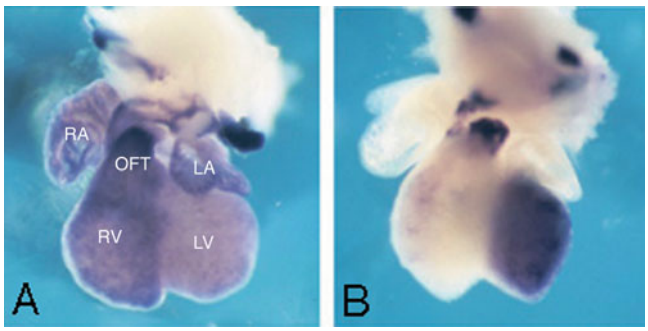

Figure 8.8. Hand1 and Hand2 expression by in situ hybridization in mouse hearts at E12.5. (*A*) Hand2 is expressed strongly in the right ventricle (RV). (*B*) Hand1 expression is restricted to the left ventricle. A cuff of outflow tract (OFT) myocardium shows high expression of both Hands. RA, right atrium; LA, left atrium. (From Zammit et al., 2000, with permission.)

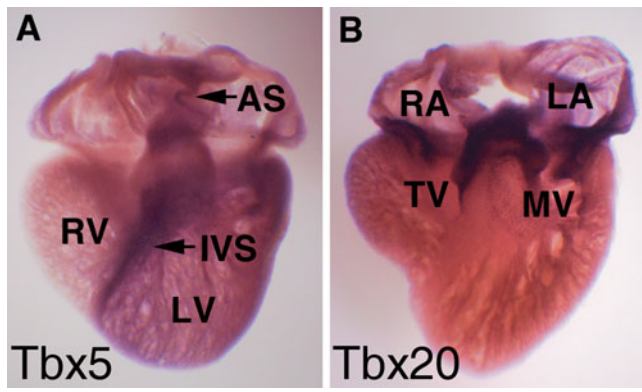

Figure 8.9. Differential expression of T-box genes during heart chamber formation in chick. Expression of chicken Tbx5 and Tbx20 in the heart at 6 days of development. Tbx5 is expressed in the atria and atrial septum (AS) (*arrow*). The position of the interventricular septum (IVS, *arrow*) is coincident with the border of high Tbx5 expression in the left ventricle (LV) and lower expression in the right ventricle (RV). Tbx20 is expressed in the right (RA) and left (LA) atria, and strong expression is apparent in the primordia of the tricuspid and mitral valves. (From Plageman and Yutzey, 2005, with permission.)

Right Ventricle–Outflow Tract (Outflow Limb)

Isl1, Foxh1, and Mef2c are all needed for addition of the right ventricle and outflow tract to the developing heart tube from the cardiogenic mesoderm. Mef2c is a member of the myocyte enhancer factor-2 (Mef2) family of MADS (MCM1, agamous, deficiens, serum response factor)-box transcription factors. These factors bind an AT-rich DNA sequence associated with muscle-specific genes. The *Mef2C* gene is expressed in heart precursor cells before formation of the linear heart tube (Lin et al., 1997). Hand2 is a factor that is specifically expressed by right ventricle in the mouse, and when the cells that form the right ventricle are not added Hand2 is never expressed.

Hand2-null mice fail to form a right-sided (pulmonary) ventricle (Thomas et al., 1998; Srivastava et al., 1997). The search for Mef2C-dependent genes resulted in the identification of a heart-restricted helicase, CHAMP, that probably functions as a negative regulator of cell cycle progression by upregulating the cyclin dependent kinase inhibitor p21 (Liu et al., 2001). In the context of Mef2C function, Champ may be part of a negative regulatory loop that controls right ventricular wall expansion by inhibiting myocardial cell proliferation (Liu and Olson, 2002; Liu et al., 2001). Another potential Mef2C target gene is the Egf–cfc factor, *Crypto*, that is downregulated in *Mef2C*-deficient hearts (Liu et al., 2001). Mef2 proteins are phosphorylation targets of various signal transduction pathways. In particular, p38α and Erk5 can phosphorylate Mef2C and Mef2A (Zhao et al., 1999). Interestingly, *Mekk3*- and *Erk5*-null mice display a phenocopy of the *Mef2C* phenotype and all are deficient in right ventricle formation (Regan et al., 2002; Yang et al., 2000).

The molecular bases of the distinct properties of the conal and truncal myocardium have not been studied systematically. A few transcription factors, such as the homeodomain protein Pitx2c, are selectively expressed in the outflow myocardium but it is not known if the phenotypic differences reflect differences in intrinsic gene regulatory programs or unique external cues (hemodynamics or cell signals) (Liu et al., 2002).

Transcriptional Regulation and Regulatory Modules in Chamber–Specific Gene Expression

Transcriptional regulators that may be important in final chamber specification include Hand1, which is differentially expressed in the dorsoventral axis, Irx4 and Tbx5, which are

differentially expressed in the craniocaudal axis, and Irx5, which is originally expressed in the myocardium of the outer curvature and is later expressed in the atrial myocardium and ventricular trabeculae (Christoffels et al., 2000).

In the absence of Nkx2.5 a number of cardiac genes fail to be expressed or are significantly reduced including *MLC2V*, *Hand1*, and *Nppa* (Lyons et al., 1995; Tanaka et al., 1999a,b). Nkx2.5 functions as an accessory factor to restrict the activity of Tbx factors in the heart.

The T-box transcription factor Tbx5 cooperates with Nkx2.5 to activate expression of a number of genes including *Nppa* and *Cx40*. Another T-box family member, *Tbx2*, encodes a transcriptional repressor that is expressed in a pattern mutually exclusive to Nppa. Tbx2 has the ability to form a repressive complex with Nkx2.5 on the *Nppa* promoter and competes with the transactivating Tbx5–Nkx2.5 complex. Thus, complex formation of positively and negatively regulating factors provides a potential mechanism to generate chamber-specific gene expression (Christoffels et al., 2004).

Transcriptional repression in the myocardium is important in chamber formation. Nppa is initially expressed throughout the chamber myocardium but is downregulated in the prospective ventricular myocardium and restricted to the atrial chamber myocardium. It has been used in many studies as a marker of atrial and atrioventricular specification. Once the atrial markers have been downregulated in the prospective ventricular myocardial cells, they are irreversibly restricted from the atrial cardiomyocyte lineage (Gruber et al., 1998). The limitation of *Nppa* gene expression to atrial myocardium is regulated by combinatorial interactions between Nkx2.5, Gata4, Tbx5, and Srf. A Gata binding site and an NK element (Nke) are not necessary for efficient expression of the *Nppa* gene but they play an essential role in restricting Nppa expression to the atrium (Small and Krieg, 2003). Mutations of the Nke and or proximal Gata element in the *Nppa* promoter results in ectopic Nppa expression in many tissues outside the heart in addition to persistent expression of Nppa in the ventricle and outflow tract myocardium in the frog (Small and Krieg, 2003). The *Nppa* promoter is highly conserved between frog and mammals.

A small fragment of the *Nppa* gene is responsible for the developmental pattern of endogenous *Nppa* gene expression. This same fragment is able to repress cardiac troponin I promoter activity selectively in the embryonic myocardium of the atrioventricular canal. *Tbx2* encodes a transcriptional repressor that is expressed in the embryonic myocardium in a pattern mutually exclusive of Nppa. Tbx2 complexes with Nkx2.5 on the *Nppa* T-box binding element (Tbe) or Nke, and represses *Nppa* promoter activity. Cooperative action of Tbx2 and Nkx2.5 inhibits expression of Nppa in the atrioventricular canal (Fig. 8.9) (Habets et al., 2002). *Tbx2* is expressed in the myocardium of the atrioventricular canal and outflow tract, which retains the characteristics of the inner curvature myocardium. Tbx2 represses the development of chamber myocardium in these regions. Hearts of transgenic embryos that express Tbx2 in the prechamber myocardium fail to form chambers and to express the chamber myocardium-specific genes *Nppa*, *Cx40*, and *Chisel* (Christoffels et al., 2004).

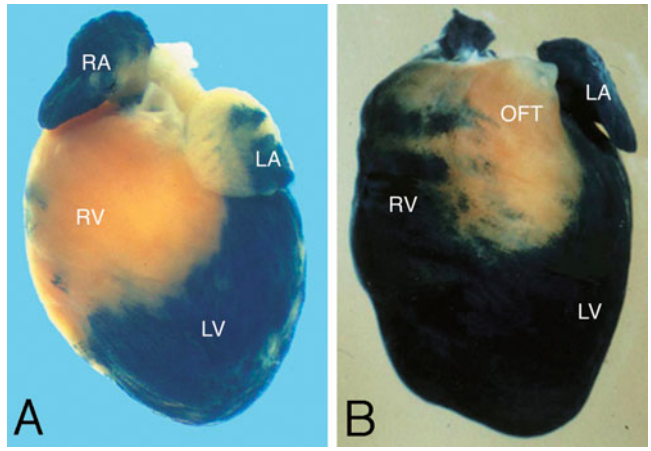

Figure 8.10. "Cardiosensor" mouse heart showing atrial and left ventricular-specific expression of *lacZ* under control of different fragments (contrasted in *A* and *B*) of the *Mlc2V* promoter. RA, right atrium; RV, right ventricle; LA, left atrium; LV, left ventricle; OFT, outflow tract. (From Kelly et al., 1999, with permission.)

Construction of transgenic "cardiosensor" mice with fragments of myocardial promoters driving *lacZ* expression has provided a rich body of information about different promoter elements that respond to chamber-specific cues (Fig. 8.10).

Several T-box transcription factors have been recognized as important in early chamber specification. Tbx5 is expressed in a cranial-to-caudal gradient and activates *Nppa* while Tbx2 represses *Nppa* gene expression in the atrioventricular canal and outflow tract resulting in *Nppa* gene expression that is restricted to the working myocardium of the chambers. Thus Tbx2 is expressed in a pattern mutually exclusive to Nppa. Tbx2 forms a complex with Nkx2.5 on a promoter element in the *Nppa* gene that has both a Tbe and an Nke (Habets et al., 2002).

While Tbx5 is expressed in the inflow limb of the looped cardiac tube, Tbx20 is expressed in the outflow limb. These T-box transcription factors appear to be mutually exclusive. Misexpression of Tbx5 in the ascending limb leads to failure of formation of the ventricular septum and failure of right ventricular markers such as Hand2 to be expressed (Takeuchi et al., 2003).

Tbx5 is expressed throughout the cardiogenic mesoderm and linear heart tube but during chamber specification it acquires a graded distribution with high expression in the atria and low expression in the left ventricle. It is absent in the right ventricle and outflow tract (Bruneau et al., 1999). The early embryonic expression of Tbx5 in the heart primordia and caudal heart tube of mouse and avian embryos is consistent with functions in early atrial lineage development (Bruneau et al., 1999; Liberatore et al., 2000). Misexpression of Tbx5 in the ventricles is correlated with abnormal ventricular

morphology and downregulation of ventricle-specific markers (Liberatore et al., 2000). Targeted mutagenesis of *Tbx5* in mice results in severe hypomorphic development of the atrial region of the primitive heart tube in null embryos that do not survive beyond E10.5 (Bruneau et al., 2001). Conversely, transgenic overexpression of Tbx5 throughout the E8.5–E10.5 heart tube inhibits ventricular chamber maturation and ventricle-specific gene expression (Liberatore et al., 2000). Tbx5 may be a downstream mediator of retinoic acid. In retinoic acid-treated chick embryos, the atrial expression of Tbx5 is expanded cranially (Liberatore et al., 2000). The distribution is also altered in embryos lacking Raldh2 and the embryos have impaired atrial development concomitant with reduced Tbx5 expression (Niederreither et al., 2001). Together, these studies support a critical role for Tbx5 downstream of retinoid signaling in atrial lineage specification and development of the caudal segments of the primitive heart tube (Plageman and Yutzey, 2005).

Tbx2 and Tbx3 are coexpressed in the heart primordia, caudal heart tube, and atrioventricular canal of chicken and mouse embryos (Christoffels et al., 2004; Hoogaars et al., 2004; Yamada et al., 2000). The expression of Tbx2 in these regions is stronger and broader than that of Tbx3, indicating that they may have both overlapping and distinct functions. Unlike Tbx5, Tbx2 and Tbx3 are transcriptional repressors and have been associated with development of the atrioventricular canal and central specialized conduction system (Habets et al., 2002). Targeted mutagenesis of *Tbx2* in mice has not been reported, but transgenic expression of *Tbx2* throughout the primitive heart tube results in loss of heart chamber myocardium (Christoffels et al., 2004).

Tbx20 is expressed in the lateral plate mesoderm and primitive heart tube and becomes localized to the outflow tract and atrioventricular canal during looping. At later stages, Tbx20 is expressed predominantly in the presumptive right ventricle and valves while transcripts are down-regulated in the left ventricle (Iio et al., 2001; Kraus et al., 2001; Stennard et al., 2003; Takeuchi et al., 2003; Yamagishi et al., 2004). Mutations of *Tbx20* have not been reported for mouse or human genes, but its expression pattern is consistent with a role in heart chamber maturation. In zebrafish, loss of *Tbx20* (*HrT*) function causes failure of looping but the atrium and ventricle appear to form (Szeto et al., 2002). Expression of Tbx20 overlaps with Tbx5 in the atria and with Tbx2, -3, and -5 in the atrioventricular canal myocardium, suggesting coordinate regulation of T-box target gene expression in these structures.

Irx4 is a homeodomain-containing transcriptional regulator expressed in the ventricles where it represses atrial chamber-specific gene expression in the ventricles. Deletion of *Irx4* leads to inappropriate expression of the atrial specific slowMyHC in the ventricular myocardium (Bruneau et al., 2001). Repression in the ventricles involves antagonism between Irx4 and the RXRα component of the RXRα/vitamin D receptor (Wang et al., 2001). *Irx5* is another *Irx* family member expressed by the ventricular myocardium (Christoffels et al., 2000).

Roles of Endocardium and Cardiac Jelly in Chamber Formation

The endocardium may be a source of information important to establish the identity of chamber myocardium. Trabeculae form on the inner surface of the ventricular myocardium. The trabeculae are more differentiated and less proliferative than the compact outer layer of myocardium (Moorman et al., 2000; Pasumarthi, 2002). Deletion of the *neuregulin-1* gene, an epidermal growth factor (Egf)-related signaling molecule expressed in the endocardium, or its myocardial receptors ErbB2 or ErbB4 leads to an absence of trabeculae formation and poor compaction of the compact layer (Gassmann et al., 1995; Lee et al., 1995; Meyer and Birchmeier, 1995).

Cardiac jelly is secreted by the myocardium and is important for propagation, integration, regionalization, and/or stabilization of endocardial signals. Mice lacking the *Has2* gene, the major hyaluronic acid synthase gene lack both trabeculae and endocardial cushions which are also dependent on endocardial signals for formation (Camenisch et al., 2000). In zebrafish uridine 5′-diphosphate (Udp)-glucose dehydrogenase which is required for production of hyaluronic acid, heparin sulfate, and chondroitin sulfate is needed for differentiation of the atrioventricular region. The *Jekyll* mutant fish has a mutation in this gene which results in the failure to develop an atrioventricular valve. Because these extracellular matrix glycoproteins are important in cell signaling, it is likely that signaling plays a role in establishing the atrioventricular boundary (Walsh and Stainier, 2001).

Coup-tfII is an orphan nuclear receptor. In the *Coup-tfII* mutant heart, the atria and sinus venosus fail to develop past the primitive tube stage. Reciprocal interactions between the endothelium and the mesenchyme in the vascular system and heart are essential for normal development of these systems. In fact, the expression of Angiopoietin-1, a proangiogenic soluble factor thought to mediate the mesenchymal–endothelial interactions during heart development and vascular remodeling, is downregulated in *Coup-tfII* mutants. This downregulation suggests that Coup-tfII may be required for bidirectional signaling between the endothelial and mesenchymal compartments essential for proper angiogenesis and heart development (Pereira et al., 1999).

Cell–Cell and Cell–Substrate Interactions

Cell–cell and cell–substrate interactions are critically important in myocardial development and differentiation although their importance in chamber specification has not been studied extensively. Cell–cell interactions are required for cardiac morphogenesis, that is, formation of a tubular heart, while cell–substrate interactions are needed for myocardial differentiation and assembly of the contractile apparatus. Atrial and

ventricular Mhc isoform expression seems to depend on cell contact. While cardiac myocytes derived from single isolated progenitors express muscle-specific Mhcs, atrial and ventricular Mhc isoforms are not detected. When the same progenitors are grown at high density or in organ cultures, cell-specific expression of atrial and ventricular isoforms occurs (Gonzalez-Sanchez and Bader, 1990). This indicates a significant role in cell–cell or cell–substrate contacts in chamber-specific contractile isoform expression (see later).

Members of the integrin family of cell surface receptors are important mediators of cell–substrate interactions. The extracellular matrix provides signals to individual cells essential for development and differentiation. β1 integrin is predominantly found in regions of remodeling (trabeculae) in the early mouse heart (10–13 days of gestation). Later in development (15 days of gestation onward), it is abundant in regions containing an elaborate extracellular matrix, such as the valves (Carver et al., 1994).

One of the integrin ligands in the extracellular matrix is fibronectin. Early in heart development, a craniocaudal concentration difference of fibronectin has been implicated in the directional migration of precardiac mesoderm cells which is important in establishing the craniocaudal axis of the heart tube but it is not known if this is important for chamber specification (Linask and Lash, 1988a,b). Versican is an extracellular matrix chondroitin sulfate glycoprotein that exhibits generalized expression in the tubular heart but becomes rapidly downregulated in the atrium and exhibits higher transcript levels on the right side of the ventricular chamber than the left, before the onset of ventricular septation. Versican is expressed strongly in the trabeculated ventricular myocardium, whereas the compact proliferative zone has lower transcript abundance (Henderson and Copp, 1998). Versican is expressed in the outflow tract myocardium and may be necessary for incorporation of the definitive outflow myocardium. Disruption of the versican gene by insertional mutagenesis causes a phenotype similar to that of *Hand2* and *Isl1* null mice in which the right ventricle and conotruncus fail to form (Mjaatvedt et al., 1998). Because these parts of the tube are added from the outflow pole, versican may be needed for normal movement of the cells into the heart.

Cardiac Defects Related to Chamber Specification

Hypoplastic Left Ventricle

In hypoplastic left ventricle, a diminutive left ventricle is not capable of supporting systemic circulation, which depends on the right ventricle and patent ductus arteriosus for perfusion. This is part of a larger spectrum of defects termed hypoplasia of the left heart that can include stenosis or atresia of the mitral and aortic valves, anomalous pulmonary venous connections, atrial septal defect, hypoplasia of the aortic arch, and anomalies of the coronary arteries (Table 8.1). Left ventricular endocardial FIBROELASTOSIS is a crucial feature. Absence of left ventricular inlet results in a thin-walled left ventricle while absence or obstruction of the left ventricular outlet results in a thick walled left ventricle. However, the common denominator of the spectrum is a small, nonfunctional left ventricle, hypoplasia of the ascending aorta, and resulting univentricular circulatory physiology.

Table 8.1.
Left Heart Hypoplasia Can Be Divided into Five Broad Categories

- Mitral and aortic atresia
- Mitral atresia with patent aortic root and ventricular septal defect
- Aortic atresia with patent mitral valve
- Aortic valvar stenosis and dysplasia with patent mitral valve
- Patent, hypoplastic mitral and aortic valves with hypoplasia of the aortic arch and coarctation of the aorta

Ventricular Septal Defect

Tolloid-like 1 (TLL1) is a metalloprotease similar to Bmp1. Null mutation of Tll1 leads to incomplete formation of the muscular interventricular septum and an abnormal and novel position of the aorta. Tll1 expression is specific to precardiac tissue and endocardium in early embryos, and it is found in the developing interventricular septum during later development. Cardiac structures that are not affected in *Tll1*-null embryos, like the atrioventricular cushion mesenchyme, do not express Tll1. Another region that is not affected is the outflow septum where Tll1 expression overlaps with that of Bmp1. This suggests that Bmpl may substitute for Tll1 where they are co-expressed (Clark et al., 1999).

REFERENCES

Bao, Z. Z., B. G. Bruneau, J. G. Seidman, C. E. Seidman, and C. L. Cepko. 1999. Regulation of chamber-specific gene expression in the developing heart by *Irx4*. Science 283:1161–1164.

Bartelings, M. M., and A. C. Gittenberger-de Groot. 1989. The outflow tract of the heart—embryologic and morphologic correlations. Int. J. Cardiol. 22:289–300.

Ben-Shachar, G., R. A. Arcilla, R. V. Lucas, and F. J. Manasek. 1985. Ventricular trabeculations in the chick embryo heart and their contribution to ventricular and muscular septal development. Circ. Res. 57:759–766.

Bruneau, B. G., Z.-Z. Bao, M. Tanaka, J. J. Schott, S. Izumo, C. L. Cepko, J. G. Seidman, and C. E. Seidman. 2000. Cardiac expression of the ventricle-specific homeobox gene *Irx4* is modulated by *Nkx2–5* and *dHand*. Dev. Biol. 217:266–277.

Bruneau, B. G., Z. Z. Bao, D. Fatkin, J. Xavier-Neto, D. Georgakopoulos, C. T. Maguire, C. I. Berul, D. A. Kass, M. L. Kuroski-de Bold, A. J. de Bold, D. A. Conner, N. Rosenthal, C. L. Cepko, C. E. Seidman, and J. G. Seidman. 2001. Cardiomyopathy in *Irx4*-deficient mice is preceded by abnormal ventricular gene expression. Mol. Cell Biol. 21:1730–1736.

Bruneau, B. G., M. Logan, N. Davis, T. Levi, C. J. Tabin, J. G. Seidman, and C. E. Seidman. 1999. Chamber-specific cardiac expression of *Tbx5* and heart defects in Holt-Oram syndrome. Dev. Biol. 211:100–108.

Bruneau, B. G., G. Nemer, J. P. Schmitt, F. Charron, L. Robitaille, S. Caron, D. A. Conner, M. Gessler, M. Nemer, C. E. Seidman, and J. G. Seidman. 2001. A murine model of Holt-Oram syndrome defines roles of the T-box transcription factor *Tbx5* in cardiogenesis and disease. Cell 106:709–721.

Brunskill, E. W., D. P. Witte, K. E. Yutzey, and S. S. Potter. 2001. Novel cell lines promote the discovery of genes involved in early heart development. Dev. Biol. 235:507–520.

Cai, C. L., X. Liang, Y. Shi, P. H. Chu, S. L. Pfaff, J. Chen, and S. Evans. 2003. *Isl1* identifies a cardiac progenitor population that proliferates prior to differentiation and contributes a majority of cells to the heart. Dev. Cell. 5:877–889.

Camenisch, T. D., A. P. Spicer, T. Brehm-Gibson, J. Biesterfeldt, M. L. Augustine, A. J. Calabro, S. Kubalak, S. E. Klewer, and J. A. McDonald. 2000. Disruption of hyaluronan synthase-2 abrogates normal cardiac morphogenesis and hyaluronan-mediated transformation of epithelium to mesenchyme. J. Clin. Invest. 206:349–360.

Carver, W., R. L. Price, D. S. Raso, L. Terracio, and T. K. Borg. 1994. Distribution of beta-1 integrin in the developing rat heart. J. Histochem. Cytochem. 42:167–175.

Chang, C. 1932. On the reaction of the endocardium to the blood stream in the embryonic heart with special reference to the endocardial thinkenings in the atrioventricular canal and bulbous-cordis. Anat. Rec. 51:253–265.

Chazaud, C., P. Chambon, and P. Dolle. 1999. Retinoic acid is required in the mouse embryo for left-right asymmetry determination and heart morphogenesis. Development 126:2589–2596.

Christoffels, V. M., P. E. Gabets, D. Franco, M. Campione, F. de Jong, W. H. Lamers, Z. Z. Bao, S. Palmer, C. Biben, R. P. Harvey, and A. F. Moorman. 2000. Chamber formation and morphogenesis in the developing mammalian heart. Dev. Biol. 223:266–278.

Christoffels, V. M., W. M. H. Hoogaars, A. Tessari, D. E. W. Clout, A. F. M. Moorman, and M. Campione. 2004. T-Box transcription factor *tbx2* represses differentiation and formation of the cardiac chambers. Dev. Biol. 229:763–770.

Christoffels, V. M., A. G. M. Keijser, A. C. Houweling, D. E. W. Clout, and A. F. M. Moorman. 2000. Patterning the embryonic heart: identification of five mouse Iroquois homeobox genes in the developing heart. Dev. Biol. 224:263–274.

Coffin, D. J., and T. J. Poole. 1988. Embryonic vascular development: immunohistochemical identification of the origin and subsequent morphogenesis of the major vessel primordia in quail embryos. Development 102:735–748.

Colbert, M. C., M. L. Kirby, and J. Robbins. 1996. Endogenous retinoic acid signaling colocalizes with advanced expression of the adult smooth muscle myosin heavy chain isoform during development of the ductus arteriosus. Circ. Res. 78:790–798.

Conte, G., and M. Grieco. 1984. Closure of the interventricular foramen and morphogenesis of the membranous septum and ventricular septal defects in the human heart. Anat. Anz. 155:39–55.

Davis, C. L. 1927. Development of the human heart from its first appearance to the stage found in embryos of twenty paired somites. Contrib. Embryol. 19:245–284.

de la Cruz, M. V., C. S. Gomez, M. M. Arteaga, and C. Arguello. 1977. Experimental study of the development of the truncus and the conus in the chick embryo. J. Anat. 123:661–686.

de la Cruz, M. V., S. Munoz-Arma, and L. Munoz-Castellanos. 1972. Development of the Chick Heart. Baltimore, Maryland: The Johns Hopkins University Press.

Dersch, H., and M. H. Zile. 1993. Induction of normal cardiovascular development in the vitamin A-deprived quail embryo by natural retinoids. Dev. Biol. 160:424–433.

Dor, X., and P. Corone. 1985. Migration and torsions in the chick embryo heart: observational evidence and conclusions drawn from experimental intervention. Heart Vessels 1:195–211.

Gassmann, M., F. Casagranda, D. Orioli, H. Simon, C. Lai, R. Klein, and G. Lemke. 1995. Aberrant neural and cardiac development in mice lacking the ErbB4 neuregulin receptor. Nature 378:390–394.

Ghatpande, S., A. Ghatpande, M. Zile, and T. Evans. 2000. Anterior endoderm is sufficient to rescue foregut apoptosis and heart tube morphogenesis in an embryo lacking retinoic acid. Dev. Biol. 219:59–70.

Gonzalez-Sanchez, A., and D. Bader. 1990. In vitro analysis of cardiac progenitor cell differentiation. Dev. Biol. 139:197–209.

Goor, D. A., R. Dische, and C. W. Lillehei. 1972. The conotruncus. I. Its normal inversion and conus absorption. Circulation 46: 375–384.

Goor, D. A., and C. W. Lillehei. 1975. Congenital Malformations of the Heart: Embryology, Anatomy and Operative Considerations, 38–88. New York: Grune & Stratton.

Gruber, P. J., S. W. Kubalak, and K. R. Chien. 1998. Downregulation of atrial markers during cardiac chamber morphogenesis is irreversible in murine embryos. Development 125:4427–4438.

Habets, P. E. M. H., A. F. M. Moorman, D. E. W. Clout, M. A. Van Roon, M. Lingbeek, M. van Lohuizen, M. Campione, and V. M. Christoffels. 2002. Cooperative action of *Tbx2* and *Nkx2.5* inhibits ANF expression in the atrioventricular canal: implications for cardiac chamber formation. Genes Dev. 16:1234–1246.

Habets, P. E. M. H., A. F. M. Moorman, D. E. W. Clout, M. A. van Roon, M. Lingbeek, M. van Lohuizen, M. Campione, and V. M. Christoffels. 2002. Cooperative action of *Tbx2* and *Nkx2.5* inhibits ANF expression in the atrioventricular canal: implications for cardiac chamber formation. Genes Dev. 16:1234–1246.

Henderson, D. J., and A. J. Copp. 1998. Versican expression is associated with chamber specification, septation, and valvulogenesis in the developing mouse heart. Circ. Res. 83:523–532.

Hochstetter, F. 1906. In: Hertwig's Handbuck der Vergleichenden und Experimentellen Entwickelungslehre der Wirbeltiere. 21–166. Jena: G. Fischer.

Hoogaars, W. M., A. Tessari, A. F. Moorman, P. A. de Boer, J. Hagoort, A. T. Soufan, M. Campione, and V. M. Christoffels. 2004. The transcriptional repressor *Tbx3* delineates the developing central conduction system of the heart. Cardiovasc. Res. 62:489–499.

Houweling, A. C., S. Somi, M. J. B. Van den Hoff, A. F. M. Moorman, and V. M. Christoffels. 2002. Developmental pattern of ANF gene expression reveals a strict localization of cardiac chamber formation in chicken. Anat. Rec. 266:93–102.

Hurle, J. M., and J. L. Ojeda. 1979. Cell death during the development of the truncus and conus of the chick embryo heart. J. Anat. 129:427–439.

Iio, A., M. Koide, K. Hidaka, and T. Morisaki. 2001. Expression pattern of novel chick T-box gene, *Tbx20*. Dev. Genes Evol. 211:559–562.

Jiang, Y. M., S. Tarzami, J. B. E. Burch, and T. Evans. 1998. Common role for each of the *cGATA-4/5/6* genes in the regulation of cardiac morphogenesis. Dev. Genet. 22:263–277.

Kelly, R. G., N. A. Brown, and M. E. Buckingham. 2001. The arterial pole of the mouse heart forms from Fgf10-expressing cells in pharyngeal mesoderm. Dev. Cell 1:435–440.

Kelly, R. G., P. S. Zammit, and M. E. Buckingham. 1999. Cardiosensor mice and transcriptional subdomains of the vertebrate heart. Trends Cardiovasc. Med. 9:3–10.

Kim, J. S., S. Viragh, A. F. Moorman, R. H. Anderson, and W. H. Lamers. 2001. Development of the myocardium of the atrioventricular canal and the vestibular spine in the human heart. Circ. Res. 88:295–402.

Kirby, M. L., T. F. Gale, and D. E. Stewart. 1983. Neural crest cells contribute to aorticopulmonary septation. Science 220: 1059–1061.

Kostetskii, I., Y. M. Jiang, E. Kostetskaia, S. Y. Yuan, T. Evans, and M. Zile. 1999. Retinoid signaling required for normal heart development regulates GATA-4 in a pathway distinct from cardiomyocyte differentiation. Dev. Biol. 206:206–218.

Kraus, F., B. Haenig, and A. Kispert. 2001. Cloning and expression analysis of the mouse T-box gene *Tbx20*. Mech. Dev. 100:87–91.

Kubalak, S. W., W. C. Miller-Hance, T. X. O'Brien, E. Dyson, and K. R. Chien. 1994. Chamber specification of atrial myosin light chain-expression precedes septation during murine cardiogenesis. J. Biol. Chem. 269:16961–16970.

Laane, H. M. 1978. The septation of the arterial pole of the heart in the chick embryo. I. Introduction. Acta Morphol. Neerl. Scand. 16:17–27.

Laane, H. M. 1978. The septation of the arterial pole of the heart in the chick embryo. II. Development of the truncus arteriosus of the heart of chick embryos from 4 to 5 days of incubation. Acta Morphol. Neerl. Scand. 16:29–53.

Laane, H. M. 1979. The septation of the arterial pole of the heart in the chick embryo. III. Development of the truncus arteriosus of the heart of chick embryos from 51/2 to 7 days of incubation. Acta Morphol. Neerl. Scand. 17:1–20.

Laane, H. M. 1979. The septation of the arterial pole of the heart in the chick embryo. IV. Discussion. Acta Morphol. Neerl. Scand. 17:21–32.

Lamers, W. H., and A. F. Moorman. 2002. Cardiac septation: a late contribution of the embryonic primary myocardium to heart morphogenesis. Circ. Res. 91:93–103.

Lamers, W. H., S. Viragh, A. Wessels, A. F. M. Moorman, and R. H. Anderson. 1995. Formation of the tricuspid valve in the human heart. Circulation 91:111–121.

Lee, K.-F., H. Simon, H. Chen, B. Bates, M.-C. Hung, and C. Hauser. 1995. Requirement for neuregulin receptor erbB2 in neural and cardiac development. Nature 378:394–398.

Li, S., D. Zhou, M. M. Lu, and E. E. Morrisey. 2004. Advanced cardiac morphogenesis does not require heart tube fusion. Science 305:1619–1622.

Liberatore, C. M., R. D. Searcy-Schrick, and K. E. Yutzey. 2000. Ventricular expression of tbx5 inhibits normal heart chamber development. Dev. Biol. 223:169–180.

Lin, Q., J. Schwarz, C. Bucana, and E. N. Olson. 1997. Control of mouse cardiac morphogenesis and myogenesis by transcription factor MEF2C. Science 276:1405–1407.

Linask, K. K., and J. W. Lash. 1988. A role for fibronectin in the migration of avian precardiac cells. I. Dose-dependent effects of fibronectin antibody. Dev. Biol. 129:315–323.

Linask, K. K., and J. W. Lash. 1988. A role for fibronectin in the migration of avian precardiac cells. II. Rotation of the heart-forming region during different stages and its effects. Dev. Biol. 129: 324–329.

Liu, C. Y., W. Liu, J. Palie, M. F. Lu, N. A. Brown, and J. F. Martin. 2002. *Pitx2c* patterns anterior myocardium and aortic arch vessels and is required for local cell movement into atrioventricular cushions. Development 129:5081–5091.

Liu, Z. P., O. Nakagawa, M. Nakagawa, H. Yanagisawa, R. Passier, J. A. Richardson, D. Srivastava, and E. N. Olson. 2001. CHAMP, a novel cardiac-specific helicase regulated by MEF2C. Dev. Biol. 234:497–509.

Liu, Z. P., and E. N. Olson. 2002. Suppression of proliferation and cardiomyocyte hypertrophy by CHAMP, a cardiac-specific RNA helicase. Proc. Natl. Acad. Sci. USA 99:2043–2048.

Lyons, G. E. 1994. In situ analysis of the cardiac muscle gene program during embryogenesis. Trends Cardiovasc. Med. 4:70–77.

Lyons, G. E., S. Schiaffino, D. Sassoon, P. Barton, and M. Buckingham. 1990. Developmental regulation of myosin gene expression in mouse cardiac muscle. J. Cell Biol. 111:2427–2436.

Lyons, I., L. M. Parsons, L. Hartley, R. Li, J. E. Andrews, L. Robb, and R. P. Harvey. 1995. Myogenic and morphogenetic defects in the heart tubes of murine embryos lacking the homeo box gene *Nkx2–5*. Genes Dev. 9:1654–1666.

Manasek, F. J. 1968. Embryonic development of the heart. I: A light and electron microscope study of myocardial development in the early chick embryo. J. Morphol. 125:329–366.

Manner, J. 2000. Cardiac looping in the chick embryo: a morphological review with special reference to terminological and biomechanical aspects of the looping process. Anat. Rec. 259: 248–262.

Markwald, R., C. Eisenberg, L. Eisenberg, T. Trusk, and Y. Sugi. 1996. Epithelial-mesenchymal transformations in early avian heart development. Acta Anat. (Basel) 156:173–186.

Markwald, R. R., T. P. Fitzharris, and F. J. Manasek. 1977. Structural development of endocardial cushions. Am. J. Anat. 148:85–119.

Meyer, D., and C. Birchmeier. 1995. Multiple essential functions of neuregulin in development. Nature 378:386–390.

Mikawa, T., J. Hyer, N. Itoh, and Y. Wei. 1996. Retroviral vectors to study cardiovascular development. Trends Cardiovasc. Med. 6:79–86.

Mjaatvedt, C. H., H. Yamamura, A. A. Capehart, D. Turner, and R. R. Markwald. 1998. The *Cspg2* gene, disrupted in the hdf mutant, is required for right cardiac chamber and endocardial cushion formation. Dev. Biol. 202:56–66.

Mommersteeg, M. T., A. T. Soufan, F. J. de Lange, M. J. B. van den Hoff, R. H. Anderson, V. M. Christoffels, and A. F. M. Moorman. 2006. Two distinct pools of mesenchyme contribute to the development of the atrial septum. Circ. Res. 99:351–353.

Moorman, A. F., and V. M. Christoffels. 2003. Cardiac chamber formation: development, genes, and evolution. Physiol. Rev. 83:1223–1267.

Moorman, A. F. M., C. A. Schumacher, P. A. J. de Boer, J. Hagoort, K. Bezstarosti, M. J. B. Van den Hoff, G. T. M. Wagenaar, J. M. J. Lamers, F. Wuytack, V. M. Christoffels, and J. W. T. Fiolet. 2000. Presence of functional sarcoplasmic reticulum in the developing heart and its confinement to chamber myocardium. Dev. Biol. 223:279–290.

Morse, D. E. 1978. Scanning electron microscopy of the developing septa in the chick heart. In: Morphogenesis and Malformation of the Cardiovascular System, ed. Rosenquist, G. C. and D. Bergsma, 91–107. New York: Alan R Liss.

Moss, J. B., J. Xavier-Neto, M. D. Shapiro, S. M. Nayeem, P. McCaffery, U. C. Drager and N. Rosenthal. 1998. Dynamic patterns of retinoic acid synthesis and response in the developing mammalian heart. Dev. Biol. 199:55–71.

Niederreither, K., V. Subbarayan, P. Doll, and P. Chambon. 1999. Embryonic retinoic acid synthesis is essential for early mouse post-implantation development. Nat. Genet. 21:444–448.

Niederreither, K., J. Vermot, N. Messaddeq, B. Schuhbaur, P. Chambon, and P. Doll. 2001. Embryonic retinoic acid synthesis is essential for heart morphogenesis in the mouse. Development 128:1019–1031.

Noden, D. M. 1991. Origins and patterning of avian outflow tract endocardium. Development 111:867–876.

O'Brien, T. X., K. J. Lee, and K. R. Chien. 1993. Positional specification of ventricular myosin light chain 2 expression in the primitive murine heart tube. Proc. Natl. Acad. Sci. USA 90: 5157–5161.

Pardanaud, L., C. Altmann, P. Kitos, F. Dieterlen-Lievre, and C. A. Buck. 1987. Vasculogenesis in the early quail blastodisc as studied with a monoclonal antibody recognizing endothelial cells. Development 100:339–349.

Pasumarthi, K. B., and L. J. Field. 2002. Cardiomyocyte cell cycle regulation. Circ.Res. 90:1044–1054.

Patten, B. M. 1951. Early Embryology of the Chick. Philadelphia: Blakiston.

Pereira, F. A., Y. H. Qiu, G. Zhou, M. J. Tsai, and S. Y. Tsai. 1999. The orphan nuclear receptor COUP-TFII is required for angiogenesis and heart development. Genes Dev. 13:1037–1049.

Pexieder, T. 1975. Cell death in the morphogenesis and teratogenesis of the heart. Adv. Anat. Embryol. Cell Biol. 51:3–99.

Plageman, T. F. J., and K. E. Yutzey. 2005. T-box genes and heart development: putting the "T" in heart. Dev. Dyn. 232:11–20.

Regan, C. P., W. Li, D. M. Boucher, S. Spatz, M. S. Su, and K. Kuida. 2002. Erk5 null mice display multiple extraembryonic vascular and embryonic cardiovascular defects. Proc. Natl. Acad. Sci. USA 99:9248–9253.

Ross, R. S., S. Navankasattusas, R. P. Harvey, and K. R. Chien. 1996. An HF-1a/HF-1b/MEF-2 combinatorial element confers cardiac ventricular specificity and establishes an anterior-posterior gradient of expression. Development 122:1799–1809.

Ruzicka, D. L., and R. J. Schwartz. 1988. Sequential activation of alpha-actin genes during avian cardiogenesis: vascular smooth muscle alpha-actin gene transcripts mark the onset of cardiomyocyte differentiation. J. Cell Biol. 107:2575–2586.

Schaefer, K. S., Y. Q. Doughman, S. A. Fisher, and M. Watanabe. 2004. Dynamic patterns of apoptosis in the developing chicken heart. Dev. Dyn. 229:489–499.

Sedmera, D., M. Reckova, M. R. Bigelow, A. Dealmeida, C. P. Stanley, T. Mikawa, R. G. Gourdie, and R. P. Thompson. 2004. Developmental transitions in electrical activation patterns in chick embryonic heart. Anat. Rec. 280:1001–1009.

Small, E. A., and P. A. Krieg. 2003. Transgenic analysis of the atrial natriuretic factor (ANF) promoter: *Nkx2–5* and *GATA-4* binding sites are required for atrial specific expression of ANF. Dev. Biol. 261:116–131.

Solloway, M. J., and R. P. Harvey. 2003. Molecular pathways in myocardial development: a stem cell perspective. Cardiovasc. Res. 58:264–277.

Srivastava, D., T. Thomas, Q. Lin, M. L. Kirby, D. Brown, and E. N. Olson. 1997. Regulation of cardiac mesodermal and neural crest development by the bHLH transcription factor, *dHAND*. Nat. Genet. 16:154–160.

Stennard, F. A., M. W. Costa, D. A. Elliott, S. Rankin, S. J. P. Haast, D. Lai, L. P. A. McDonald, K. Niederreither, P. Dolle, B. G. Bruneau, A. M. Zorn, and R. P. Harvey. 2003. Cardiac T-box factor *Tbx20* directly interacts with *Nkx2–5*, *GATA4*, and *GATA5* in regulation of gene expression in the developing heart. Dev. Biol. 262:206–224.

Streeter, G. L. 1948. Developmental horizons in human embryos. Description of age groups XV, XVI, XVII, and XVIII. Contrib. Embryol. 32:133–203.

Sugi, Y., and J. Lough. 1994. Anterior endoderm is a specific effector of terminal cardiac myocyte differentiation of cells from the embryonic heart forming region. Dev. Dyn. 100:155–162.

Sugi, Y., and R. R. Markwald. 1996. Formation and early morphogenesis of endocardial endothelial precursor cells and the role of endoderm. Dev. Biol. 175:66–83.

Sugishita, Y., M. Watanabe, and S. A. Fisher. 2004. The development of the embryonic outflow tract provides novel insights into cardiac differentiation and remodeling. Trends Cardiovasc. Med. 14:235–241.

Szeto, D. P., K. J. P. Griffin, and D. Kimelman. 2002. *hrT* is required for cardiovascular development in zebrafish. Development 129: 5093–5101.

Takeuchi, J. K., M. Ohgi, K. Koshiba-Takeuchi, H. Shiratori, I. Sakaki, K. Ogura, Y. Saijoh, and T. Ogura. 2003. *Tbx5* specifies the left/right ventricles and ventricular septum position during cardiogenesis. Development 130:5953–5964.

Tanaka, M., Z. Chen, S. Bartunkova, N. Yamasaki, and S. Izumo. 1999. The cardiac homeobox gene *Csx/Nkx2.5* lies genetically upstream of multiple genes essential for heart development. Development 126:1269–1280.

Tanaka, M., S. B. Wechsler, I. W. Lee, N. Yamasaki, J. A. Lawitts, and S. Izumo. 1999. Complex modular cis-acting elements regulate expression of the cardiac specifying homeobox gene *Csx/Nkx2.5*. Development 126:1439–1450.

Thomas, T., H. Kurihara, H. Yamagishi, Y. Kurihara, Y. Yazaki, E. N. Olson, and D. Srivastava. 1998. A signaling cascade involving endothelin-1, *dHAND* and *msx1* regulates development of neural crest-derived branchial arch mesenchyme. Development 125:3005–3014.

Thomas, T., H. Yamagishi, P. A. Overbeek, E. N. Olson, and D. Srivastava. 1998. The bHLH factors, *dHAND* and *eHAND*, specify pulmonary and systemic cardiac ventricles independent of left-right sidedness. Dev. Biol. 196:228–236.

Thompson, R. P., V. Abercrombie, and M. Wong. 1987. Morphogenesis of the truncus arteriosus of the chick embryo heart: movements of autoradiographic tattoos during septation. Anat. Rec. 218:434–440.

Thompson, R. P., and T. P. Fitzharris. 1985. Division of cardiac outflow. In: Cardiac Morphogenesis., ed. Ferrans, V., G. C. Rosenquist and C. Weinstein, Amsterdam: Elsevier.

Thompson, S., J. R. Lindroth, and Y.-U. M. Wong. 1990. Regional differences in DNA-synthetic activity in the preseptation myocardium of the chick. In: Developmental Cardiology: Morphogenesis and

Function, ed. Clarke, E. B. and A. Takao, 219–234. Mount Kisco, NY: Futura.

Van Mierop, L. H. S., and L. M. Kutsche. 1985. Development of the ventricular septum of the heart. Heart Vessels 1:114–119.

Waldo, K. L., M. R. Hutson, C. C. Ward, M. Zdanowicz, H. A. Stadt, D. Kumiski, R. Abu-Issa, and M. L. Kirby. 2005. Secondary heart field contributes myocardium and smooth muscle to the arterial pole of the developing heart. Dev. Biol. 281:78–90.

Waldo, K. L., D. H. Kumiski, K. T. Wallis, H. A. Stadt, M. R. Hutson, D. H. Platt, and M. L. Kirby. 2001. Conotruncal myocardium arises from a secondary heart field. Development 128:3179–3188.

Walsh, E. C., and D. Y. Stainier. 2001. UDP-glucose dehydrogenase required for cardiac valve formation in zebrafish. Science 293:1670–1673.

Wang, F. G., J. W. Nikovits, Z.-Z. Bao, and F. E. Stockdale. 2001. Irx4 forms an inhibitory complex with the vitamin D and retinoic X receptors to regulate cardiac chamber-specific slow MyHC3 expression. J. Biol. Chem. 276:28835–28841.

Wang, G. F., W. Nikovits, Jr., M. Schleinitz, and F. E. Stockdale. 1996. Atrial chamber-specific expression of the slow myosin heavy chain 3 gene in the embryonic heart. J. Biol. Chem. 271: 19836–19845.

Wang, G. F., W. J. Nikovits, M. Schleinitz, and F. E. Stockdale. 1998. A positive GATA element and a negative vitamin D receptor-like element control atrial chamber-specific expression of a slow myosin heavy-chain gene during cardiac morphogenesis. Mol. Cell Biol. 18:6023–6034.

Ward, C., H. A. Stadt, M. R. Hutson, and M. L. Kirby. 2005. Ablation of the secondary heart field leads to tetralogy of Fallot and pulmonary atresia. Dev. Biol. 284:72–83.

Watanabe, M., A. Choudhry, M. Berlan, A. Singal, E. Siwik, S. Mohr, and S. A. Fisher. 1998. Developmental remodeling and shortening of the cardiac outflow tract involves myocyte programmed cell death. Development 125:3809–3820.

Watanabe, M., A. Jafri, and S. A. Fisher. 2001. Apoptosis is required for the proper formation of the ventriculo-arterial connections. Dev. Biol. 240:274–288.

Xavier-Neto, J., C. M. Neville, M. D. Shapiro, L. Houghton, G. F. Wang, W. Nikovits, Jr., F. E. Stockdale, and N. Rosenthal. 1999. A retinoic acid-inducible transgenic marker of sino-atrial development in the mouse heart. Development 126:2677–2687.

Yamada, M., J. P. Revelli, G. Eichele, M. Barron, and R. J. Schwartz. 2000. Expression of chick *Tbx-2*, *Tbx-3*, and *Tbx-5* genes during early heart development: evidence for BMP2 induction of *Tbx2*. Dev. Biol. 228:95–105.

Yamagishi, T., Y. Nakajima, S. Nishimatsu, T. Nohno, K. Ando, and H. Nakamura. 2004. Expression of *tbx20* RNA during chick heart development. Dev. Dyn. 230:576–580.

Yang, J., M. Boerm, M. McCarty, C. Bucana, I. Fidler, Y. Zhuang, and B. Su. 2000. Mekk3 is essential for early embryonic cardiovascular development. Nat. Genet. 24:309–313.

Yutzey, K. E., and D. Bader. 1995. Diversification of cardiomyogenic cell lineages during early heart development. Circ. Res. 77:216–219.

Yutzey, K. E., J. T. Rhee, and D. Bader. 1994. Expression of the atrial-specific myosin heavy chain AMHC1 and the establishment of anteroposterior polarity in the developing chicken heart. Development 120:871–883.

Zammit, P. S., R. G. Kelly, D. Franco, N. Brown, A. F. M. Moorman, and M. E. Buckingham. 2000. Suppression of atrial myosin gene expression occurs independently in the left and right ventricles of the developing mouse heart. Dev. Dyn. 217:75–85.

Zhao, M., L. New, V. V. Kravchenko, Y. Kato, H. Gram, F. di Padova, E. N. Olson, R. J. Ulevitch, and J. Han. 1999. Regulation of the MEF2 family of transcription factors by p38. Mol. Cell Biol. 19:21–30.

This page intentionally left blank

9

Endocardium, Cardiac Cushions, and Valve Development

The endocardium develops from endothelial cells that form bilaterally paired tubes by the process of vasculogenesis. These bilateral tubes fuse in the midline to form a single tubular cardiac intravascular compartment. The midline endothelial tube lies beneath the foregut endoderm and is covered ventrally by the splanchnic mesoderm that is open toward the ventral pharynx in a W or U shape until the two sides fuse dorsally to become a complete myocardial layer of the tubular heart (Fig. 9.1). An important feature of the endocardium is that it gives rise to all of the cushion mesenchyme in the atrioventricular canal and proximal outflow tract by a process of epithelial-to-mesenchymal transformation. This cushion tissue functions as a one-way valve during contraction of the tubular heart and is critical for formation of the atrioventricular valves. The mesenchyme that gives rise to the semilunar valves in the outflow tract is from a mixture of cushion mesenchyme derived from endocardial epithelial-mesenchymal transformation, neural crest, and pharyngeal mesenchyme. Because of the mixing of cell types in the semilunar valves, their development is covered more completely in Chapter 11.

Figure 9.1. Early stage in formation of the ventral midline heart tube. The endocardium forms the initial tube and is only partially invested by myocardium. The endocardial tube has an intimate relationship with the pharyngeal (foregut) endoderm.

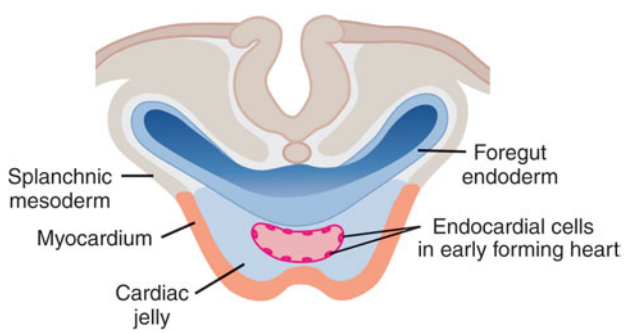

Origin of the Endocardium

All intraembryonic mesoderm contains endothelial precursors that are invasive and have the ability to adapt to any region where they are placed (Noden, 1990). These characteristics distinguish them from all other embryonic mesenchymal cell types. Thus, the control over blood vessel assembly appears to reside in the nonendothelial environment and not in the endothelial precursors themselves. In the heart-forming region, local endothelial cells are likely induced by local signals from either the endoderm or cardiogenic mesenchyme to form bilateral endothelial tubes that will fuse to form the midline endocardial tube.

Mollier proposed in 1906 that the pre-endocardium exists as a cardiogenic crescent (Mollier, 1906). An early tracing study of the cardiac primordia showed that, in general, labeling of the endocardium corresponded with that of the myocardium adjacent to it and that contributions from the right and left heart fields to the endocardium seemed to be about equal (Stalsberg, 1969; Stalsberg and DeHaan, 1969). Because the cardiogenic mesoderm does not form a crescent in chick, the endocardial cells most probably do not form a crescent either. When only one side of the cardiogenic mesoderm is labeled, about 10% of the labeled cells are mixed with unlabeled cells, suggesting either some intermingling of the cells from the two sides or contributions from regions outside the heart fields. However, while no myocardium originated from the midline cranial to the prechordal plate in chick marking experiments, endocardial cells did originate from both median and paramedian implants. Some of the endocardium originates from the ventral midline endoderm that itself originates from the prechordal plate (Kirby et al., 2003).

Retroviral labeling in chick and quail, as well as cell lineage tracing in zebrafish embryos, show definitively that endocardial precursors are present in the heart-forming regions, but

whether they share a common progenitor with the myocardial lineage is not known (Cohen-Gould and Mikawa, 1996; Lee et al., 1994; Lough and Sugi, 2000). A cell line created from gastrulating cells called QCE6 can differentiate into both endocardial and myocardial cells, leaving the possibility open that there is at some point in development a common precursor (Eisenberg and Markwald, 1997). However, retroviral tracing studies in vivo show that the lineages are separated before the time they enter the primitive streak (Wei and Mikawa, 2000). Thus, separation of the progenitors most likely occurs prior to or during gastrulation.

Endocardial Induction

While the endocardial cell lineage is determined at the time of gastrulation, terminal differentiation of endothelial cells in avian embryos, as seen by expression of the quail endothelial cell marker QH1, begins at the two-somite stage (stage 7) in the caudal regions of the bilateral cardiogenic regions (Eisenberg and Markwald, 1997; Wei and Mikawa, 2000). Between the four- and seven-somite stages, endothelial cells within the cardiogenic fields establish connections with endothelial cells outside of the cardiogenic region (Coffin and Poole, 1988). Because the zebrafish mutants *faust* and *cloche* lack endocardial but not other vascular endothelial cells or myocardium, we know that endocardium is molecularly distinct from endothelium (Liao et al., 1997; Reiter et al., 1999). While all endothelial cells in the quail embryo express QH1, the endothelial cells intrinsic to the heart in avians express two additional extracellular antigens, a fibrillin-like protein called JB3 and cytotactin. Appearance of these markers is dependent on endodermal signaling (Sugi and Markwald, 1996).

Expression of the Tie2 receptor is essential for endocardial but not endothelial development (Puri et al., 1999). Tie2 is a receptor tyrosine kinase for the angiopoietin 1 ligand, which is most likely expressed by the myocardial mesenchyme. The fact that the Tie2 receptor is required for endocardial development implies that angiopoietins are involved in formation of the endocardial tube. Angiopoietins are known to stimulate endothelial precursor migration and endothelial cell proliferation (Gill and Brindle, 2005; Kanda et al., 2005).

The initial step of endocardial formation is delamination of the endothelial precursor cells from the precardiac mesoderm (Fig. 9.2). Transforming growth factors beta (TGFβs), but not vascular endothelial growth factor (VEGF), appear to mediate this step when the precardiac mesoderm is tested in culture (Fig. 9.3) (Sugi and Markwald, 2003).

As mentioned previously, zebrafish embryos with the *faust* mutation lack endocardium. This mutation maps to the *Gata5* gene and produces a protein that likely acts as a dominant negative transcriptional regulator (Nemer et al., 1999). Gata5 expression is transient and largely restricted to endocardial cells in the cardiogenic mesenchyme; while Gata4, which is also expressed in the cardiogenic mesenchyme, is only in the premyocardial cells. Later in development, Gata4 is expressed in the endothelial cells lining the great arteries (Kelley et al., 1993). Gata5 is induced concomitant with Flt1 and prior to induction of Tie2, ErbB3, and Connexin (Cx)37 in endothelial differentiation (Fig. 9.4). Nuclear factor of activated T cells (NFATc) is a second transcription factor that is essential for endocardial development. Nfatc is not expressed by extracardiac vascular endothelial cells, suggesting that it may cooperate with Gata5 for terminal endocardial cell differentiation (de la Pompa et al., 1998; Nemer and Nemer, 2002; Ranger et al., 1998).

A mesodermal cell line derived from the hearts of polyomavirus large T-antigen transgenic mice differentiates into endothelial cells when they are treated with retinoic acid (al Moustafa and Chalifour, 1993). Differentiation of these cells leads to downregulation of the early myocardial markers, Gata4, Twist, and Tbx20, and appearance of an endocardial phenotype characterized by the sequential expression of Gata5 and Nfatc (Nemer and Nemer, 2002). Blocking expression of Gata5 and Nfatc inhibits endocardial differentiation.

As the endocardial cells become terminally differentiated, a number of factors are upregulated including epicardin, endothelin-1 (Et1), tenascin X, and endothelial-specific

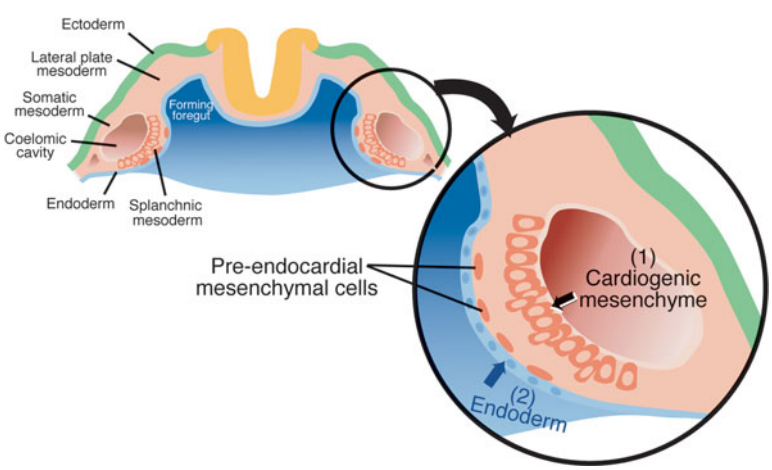

Figure 9.2. Separation of the splanchnic mesoderm in the heart-forming field into pre-endocardial and pre-myocardial cells. The pre-endocardial cells collect subjacent to the endoderm while the pre-myocardial mesenchyme is located adjacent to the coelom.

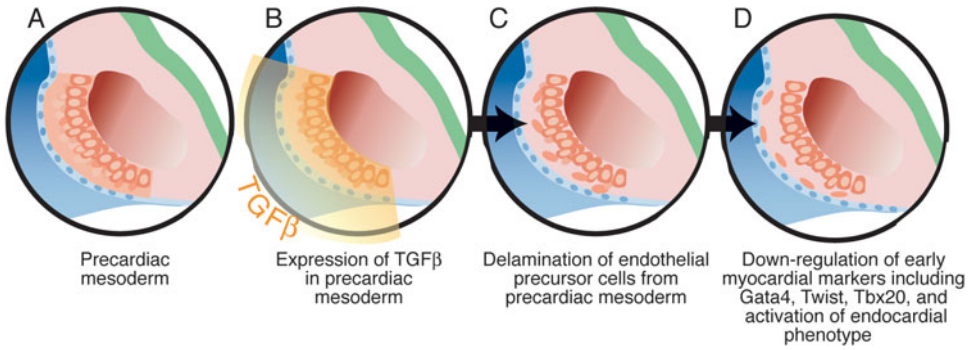

Figure 9.3. Separation of the pre-endocardial cells from the pre-myocardial cells in the splanchnic mesoderm. Tgfβ signaling is important in delamination and downregulation of myocardial markers by the endocardial cells as they leave the cardiogenic mesoderm.

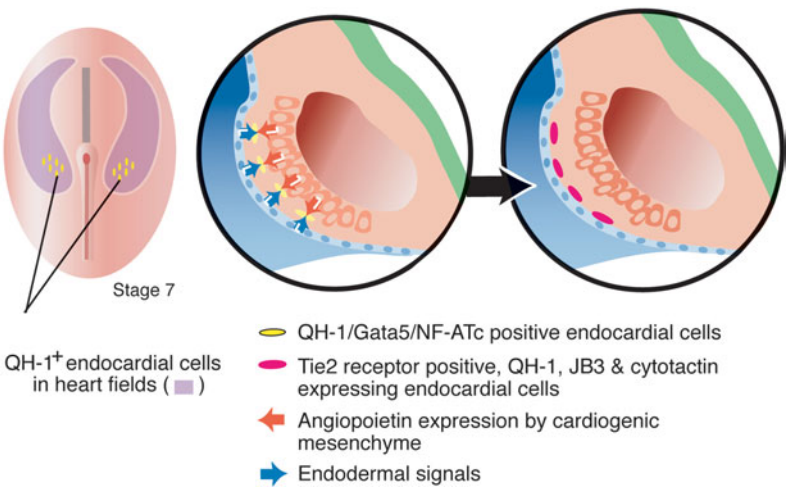

Figure 9.4. Location of the pre-endocardial cells in the heart field identified by QH1 antibody in quail embryos and subsequent steps in differentiation of the endocardial markers.

transcription factor Epas1 (Burch et al., 1995; Kurihara et al., 1995; Tian et al., 1997). Cx37 is found in all endothelial cells, while Cx40 is in all endothelial cells except endocardium (Delorme et al., 1997).

Cardiac Cushions

The cardiac cushions are the primordia of the valves and septa of the adult heart, but they are also critical in maintaining anterograde blood flow in the embryonic heart. Embryos that fail to develop cushions die at about the onset of chamber septation. The atrioventricular endocardial cushions are formed by epithelial-to-mesenchymal transformation (EMT) of the endocardial cells in the atrioventricular canal (Fig. 9.5). While there is some EMT in the proximal outflow tract to form outflow cushions, most of the distal outflow cushion mesenchyme is produced by cells that migrate into the outflow cushions from the pharynx. Cushion formation occurs around E9.5 (between 21 and 28 somites) in the atrioventricular canal of the mouse, and at stages 16–17 (25–28 somites) in the chick (Delot, 2003). The process is slightly later and much less well studied in the outflow tract (beginning at stage 18 in the chick), so most of the information available about the process is based on development of the atrioventricular cushions. Development of the outflow tract cushions is covered with outflow septation in Chapter 11.

Expansion of the cardiac jelly occurs at the junction of the atrium and presumptive left ventricle before cushion mesenchyme forms. The cardiac jelly is secreted by the myocardium (Krug et al., 1985). The cardiac jelly contains highly charged hydrophilic glycosaminoglycans that may promote the expansion, which aids in the invasion of the newly transformed endocardial cells (Manasek, 1970; Manasek et al., 1973). Two atrioventricular cushions are apparent by Carnegie stage 12 in humans, E10.5 in mouse and stage 17 in chick. The ventral (inferior) AV cushion is associated with the inner curvature, and a dorsal (superior) cushion associated with the outer curvature. Central fusion of the atrioventricular endocardial cushions produces the septum intermedium, or atrioventricular septum, that divides the atrioventricular canal into separate right and left orifices (Person et al., 2005). After formation of the atrioventricular septum, the right atrioventricular canal

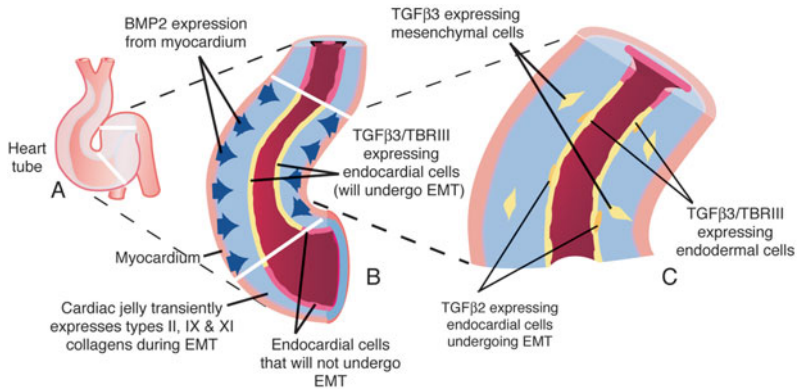

Figure 9.5. Signals involved in formation of the atrioventricular endocardial cushions. (*A*) The region of the heart expanded in *B* and C is between the white lines. (*B*) The signals and their sources that initiate epithelial–mesenchymal transformation and population of the cardiac jelly by mesenchyme. (*C*) Mesenchymal cushion cells in the cardiac jelly.

expands to the right, bringing the atrioventricular septum in line with the ventricular and atrial septa (Wessels and Sedmera, 2003). Formation of the septum ultimately allows formation of the posteroinferior and septal leaflets of the tricuspid valve and the aortic leaflet of the mitral valve. During fusion of the cushions, a second set of smaller cushions forms on the lateral sides of both right and left atrioventricular canals, and these give rise to the remaining valve leaflets.

Although EMT of endocardium to form the cushion mesenchyme was described many years ago, the first direct demonstration that the atrioventricular cushion mesenchyme was derived from endocardium was in a mouse model with permanently marked endothelial cells. The *Tie2-Cre/lacZ* double transgenic mouse demonstrates the lineage of cells derived from the endothelium (Kisanuki et al., 2001). When Cre recombinase is expressed under the *Tie2* reporter, all endothelial cells are permanently marked by a recombination event where *lacZ* is recombined in frame. In these mice, lacZ-expressing cells were found in the cushion tissue of the atrioventricular canal, but only a few were found in the proximal cushions of the cardiac outflow tract. Most of the mesenchymal cells in the proximal cushions were unlabeled, and no labeled mesenchymal cells were found in the distal outflow tract or in the pharyngeal arches. This suggests that most of the cushion tissue of the outflow tract has a different origin from that of the atrioventricular canal. The epicardium may be another source of mesenchymal cells for the atrioventricular cardiac cushions. After septation, epicardially derived cells invade the cushions via the atrioventricular sulcus (Gittenberger-de Groot et al., 1998).

Most of the information about the steps in EMT has been obtained from three-dimensional collagen gels (Fig. 9.2) (Bernanke and Markwald, 1982; Runyan and Markwald, 1983). The steps in EMT defined in this culture system are (1) migration of the endocardium to form a confluent endothelial layer, (2) activation and transformation of the endothelial cells, and (3) invasion. After invasion, the newly formed cushion mesenchymal cells proliferate. The competence to initiate formation of cushion tissue is restricted to the endocardium of the atrioventricular canal. The fact that an antibody called JB3 recognizes its antigen on some endocardial cells but not others (i.e., the ones that give rise to the valves and cushions are JB3-positive) shows that there are at least two subpopulations of endocardial cells in the heart (Wunsch et al., 1994). Endocardium obtained from the ventricular region is not competent to undergo transformation in collagen gel cultures (Runyan and Markwald, 1983). Endocardial cells receive a myocardially produced inductive stimulus. Nuclear factor in activated T cells (Nfatc1) is translocated from the cytoplasm to the nucleus of the endothelial cells. Snail/slug transcription factors are expressed in the endothelial cells. The cells hypertrophy, detach themselves from the endocardial epithelium by down-regulating neural cell adhesion molecule (N-Cam), vascular endothelial (VE)-cadherin, and platelet endothelial cell adhesion molecule 1 (Pecam1) (Baldwin et al., 1994; Crossin and Hoffman, 1991; Timmerman et al., 2004). The endocardial cells extend filopodia into the cardiac jelly and then migrate into the cardiac jelly (Person et al., 2005). By stage 20 in the chick the cardiac jelly of the atrioventricular cushions is densely populated with these cells (Person et al., 2005).

Endocardial Activation and Transformation

Just before endocardial cells detach from their epithelial layer and migrate into the cushion matrix, they begin to swell and at the same time dilate the cisternae of rough endoplasmic reticulum and Golgi complex. The cells then begin to separate (Markwald et al., 1975). Once the cells have separated from the epithelial layer, they extend filopodia into the cardiac jelly and migrate into it. The endocardial cells that do not undergo activation and transformation proliferate to ensure the integrity of the endocardial epithelium.

Factors that Initiate and Limit EMT

The cardiac jelly in the atrioventricular canal contains aggregates identified as "adherons," which are multiprotein complexes that appear to induce EMT (Mjaatvedt et al., 1991). Thus, it is thought that the inductive signals emanate from the myocardium and are transmitted across the cardiac jelly to the receptive endocardium (Fig. 9.5) (Markwald et al., 1984). Because only a fraction of the endocardial cells undergo EMT,

while others maintain intravascular competency, the signals that promote and inhibit EMT must be carefully balanced.

Bmp2 is the first myocardial-derived signal to appear (Fig. 9.6). At the onset of EMT in chick, Bmp2 is expressed by the inducing myocardium, while Tgfβ2 and Tgfβ3 are expressed in the endothelial and invading mesenchymal cells and are needed for endothelial cell activation and mesenchymal cell invasion, respectively (Boyer et al., 1999; Nakajima et al., 2000). Tgfβ2 mediates the initial endothelial cell–cell separation while Tgfβ3 is required for the cell morphological change that enables the migration of cells into the underlying cardiac jelly (Boyer et al., 1999). Atrioventricular canal endocardium expresses Tgfβ3 in response to a myocardial signal other than Tgfβ3. Endocardially generated Tgfβ3 then functions either alone or in combination with Tgfβ2 as an autocrine inducer to transform the cells into invasive mesenchyme (Boyer et al., 1999). One of the functions of Tgfβ2 is to induce expression of Slug, a zinc finger transcription factor that is required for EMT (see later). ActivinβA may also play a role in the formation of cushion mesenchyme (Moore et al., 1998).

Both Tgfβ2 and retinoic acid mediate endothelial expression of the transcription factor Slug, which is required for the initial steps of EMT (Romano and Runyan, 2000). Only a small portion of the endocardial cells located in the areas of EMT are immunolabeled by Slug antibody, but the mechanism for this differential expression is not known (Carmona et al., 2000).

TGFβ signaling is mediated by a complex of type I (TbrI) and type II (TbrII) receptors. Cardiac endothelial cells that undergo EMT express TBRIII (Brown et al., 1999). Endoglin, another receptor mediator of Tgfβ1 and -β3, can be detected on the endocardium as early as 4 weeks in human embryos. It is present at high levels in human endocardial cushion tissue from 5–8 weeks gestation, during heart septation and valve formation. Expression decreases as the valves mature (Qu et al., 1998).

Notch activity is required for expression of snail, a transcriptional repressor that mediates EMT in many tissues. Mice homozygous for *notch1* or *Rbp-Jκ* have hypoplastic cushions with decreased expression of snail and continued expression of VE-cadherin, suggesting that endocardial cells fail to undergo EMT. Indeed, in explant assay, a decreased number of transformed cells can be found in the matrix. Injection of constitutively active Notch intracellular domain in zebrafish causes valve hyperplasia, while antagonism of Notch signaling by the chemical γ-secretase inhibitor N-[*N*-(3,5-difluorophenacetyl)-L-alanyl]-(S)-phenylglycine *t*-butyl ester (DAPT) is associated with valve hypoplasia (Armstrong and Bischoff, 2004; Timmerman et al., 2004).

The endocardium initially universally expresses Nfatc1, but by E11.5 in the mouse it is restricted to regions of the future heart valves (Graef et al., 2001). Translocation of Nfatc to the nucleus is an event that precedes EMT. Both elevated ras signaling, which activates Mapk, and calcineurin are essential for Nfatc1 translocation to the nucleus, where it is a transcriptional regulator. Neurofibromin (Nf1) has ras GTPase-activating activity and can downregulate ras signaling. Nf1 may limit the extent of EMT by downregulation of ras signaling to prevent Nfatc activation or translocation to the nucleus (Gitler et al., 2003). It also plays a role in cushion expansion, discussed later. Mice deficient for Nfatc1 die by E13.5. Two groups reported this null mutation. One group reported failure of EMT in the outflow cushions with subsequent failure of aortic and pulmonary valve development, while the second group reported defective development in both outflow and atrioventricular valves (de la Pompa et al., 1998 Ranger et al., 1998). Nfatc1 is downregulated after EMT and is not seen in the mesenchymal cells populating the cushions.

Mice with mutations in calcineurin B do not localize Nfatc1 to the nucleus, suggesting that this step is regulated by Ca^{2+} (Graef et al., 2001). Calcium signaling may be through gap junctional communication because mutation of Cx45 results in defective endocardial cushion formation similar to that seen in Nfatc1 null mice. In Cx45-deficient mice, Nfatc1 does not translocate to the nucleus (Kumai et al., 2000).

EMT is strongly inhibited in mice deficient for endothelial β-catenin. EMT is accompanied by activation of Wnt signaling through β-catenin/TCF/Lef transcriptional activity (Liebner et al., 2004). Another role of Wnts may be in synthesis of proteoglycans (Walsh and Stainier, 2001). Zebrafish with *adenomatous polyposis coli* (*Apc*) mutation have hyperactive β-catenin and show expanded expression of two matrix proteoglycans, hyaluronic acid synthetase (Has2) and versican. Hyaluronic acid is thought to activate EMT via ras signaling (Fig. 9.8). Wnt6

Figure 9.6. Model of TGFβ/BMP signaling to initiate EMT. Synergistic signaling between BMP and TGFβ facilitates EMT. The type III TGFβ receptor (TGFBRIII) binds the TGFβ ligand and presents it to the TGFβRII. TGFβ promotes expression of Snail/Slug and decreases expression of VE-cadherin. ALK3 and BMPRII have also been shown to be important in cushion development. Smad6 antagonizes the interaction of Smad1 with Smad4, which dampens BMP signaling. (Adapted from Armstrong and Bischoff, 2004.)

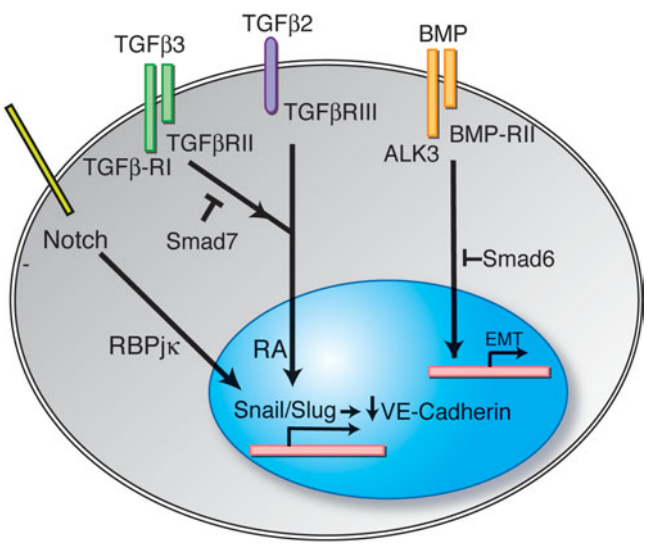

is expressed specifically in the atrioventricular myocardium and is potentially the signaling ligand (Schubert et al., 2002).

Extracellular matrix is important for endocardial cells to be able to populate the cardiac jelly, and it binds growth factors and other molecules that regulate differentiation and migration (Borg et al., 1990; Little and Rongish, 1995). In addition to proteoglycans, collagens form a major component of the cardiac extracellular matrix (Borg et al., 1990). Types II, IX, and XI collagens are transiently expressed, although these collagens have typically been associated with cartilage (Mendler et al., 1989).

Vegf may act to induce proliferation of the endothelial cells and to negatively regulate EMT, and thus cushion formation, depending on its concentration. It is upregulated in a subset of cells in the atrioventricular canal and outflow tract soon after the onset of endocardial cushion formation, perhaps serving to limit the number of endothelial cells undergoing EMT. Initiation of cushion tissue formation is dependent on calcineurin-mediated Nfatc signaling to repress VEGF expression in the myocardium underlying the site of prospective valve formation. This repression of Vegf is essential for EMT (Chang et al., 2004). Because Vegf expression is sensitive to oxygen deprivation, premature induction of Vegf expression by hypoxia could lead to defective cushion formation and heart development (Dor et al., 2001).

Expansion of the Cushion Mesenchyme and Transition from Expansion to Valve Formation

Atrioventricular cushion mesenchyme proliferates profusely during septation. While proliferation of the cushion mesenchyme is important for providing enough cushion mesenchyme for closure of the atrioventricular septum with enough remaining to create valve leaflets, it is also important to control the rate and location of proliferation in formation of the valve apparatus. Remodelling and maturation of the valve primordium is accompanied by decreased proliferation (Lincoln et al., 2004). Several models of hypoproliferation have been associated with septation defects while overproliferation models are associated with abnormal valvulogenesis.

Fgf4 promotes proliferative expansion of the cushion mesenchyme (Sugi et al., 2003). Fgf4 is found in the cushion mesenchymal cells prior to leaflet formation in chick embryos. Fgf receptor (Fgfr) 3 message is confined to the endocardial rim of the atrioventricular cushion pads while Fgfr2 is expressed in cushion mesenchyme; Fgfr1 is detected in endocardium, cushion mesenchyme, and myocardium (Fig. 9.7) (Sugi et al., 2003).

The ErbB signaling family plays a role in both cushion expansion and slowed proliferation associated with valve formation. The receptors in this family are type 1 tyrosine kinase transmembrane glycoproteins that include ErbB1 (also called epidermal growth factor Egf receptor), ErbB2, ErbB3, and ErbB4. ErbB ligands include Egf-like ligands and neuregulins. ErbB1, B2 and B3 are expressed by endocardium and cushion mesenchyme cells derived from endocardium (Erickson et al., 1997, Gassmann et al., 1995). Co-expression of ErbB1 or ErbB3 with ErbB2 induces high phosphorylation of ErbB2 (Chen et al., 2000). The ErbB1/B2 complex responds to a different set of ligands than ErbB2/B3 complex. Activation of the ErbB1/B2 complex decreases proliferation while activation of the ErbB2/B3 complex maintains proliferation. For example, during the

Figure 9.7. Expansion of the cardiac cushion mesenchyme in the atrioventricular canal.

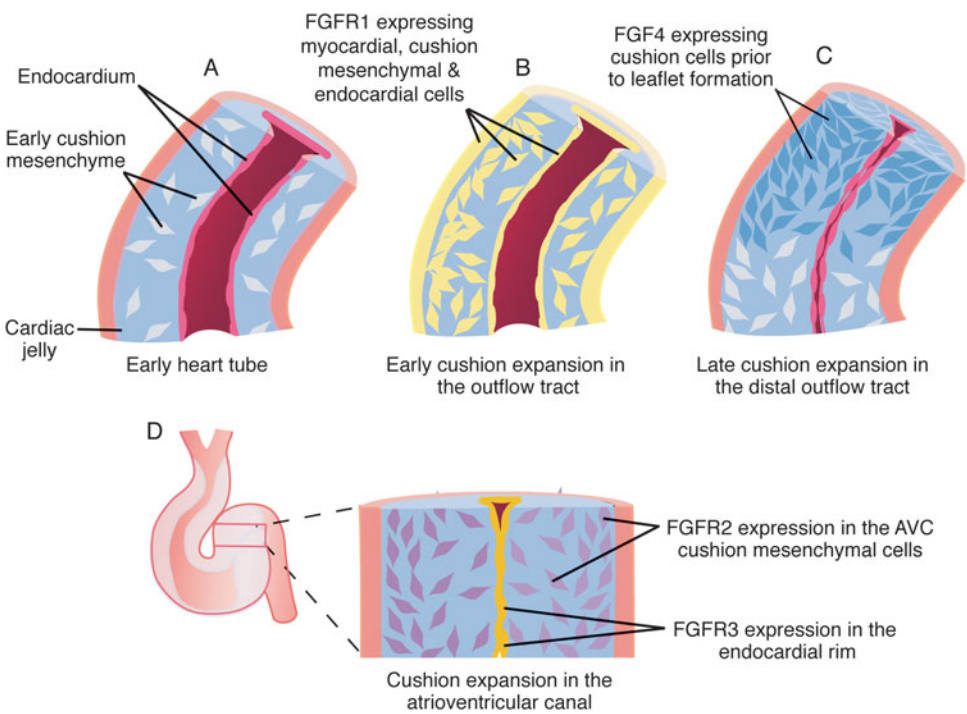

proliferative phase of cushion growth, hyaluronic acid or Neuregulin-1 activate the ErbB2/3 receptor complex which activates Ras. Activated Ras in turn activates the mitogen-activated protein kinase (Mapk) signaling cascade. Activated Mapk signaling maintains the cells in a proliferative phase. Lack of ErbB3 itself or neuregulin-1 results in hypoplasia of the cushion mesenchyme and atrioventricular canal defects (Camenisch et al., 2002, Erickson et al., 1997, Meyer and Birchmeier, 1995).

Activation of the ErbB1/B2 receptor complex leads to decreased proliferation. One ligand responsible for activation of ErbB1/B2 is heparin-binding epidermal growth factor-like growth factor (Hb-Egf). Hb-Egf is expressed as a transmembrane precursor that is cleaved at one or more sites in the extracellular domain to release soluble Hb-Egf growth factor. Tumor necrosis factor-alpha converting enzyme (Tace) is the enzyme that activates the Hb-Egf ligand (Fig. 9.8).

Targeted mutation of *Hb-Egf Tace* or *ErbB1* lead to enlarged, malformed atrioventricular and outflow valves (Chen et al., 2000, Iwamoto et al., 2003, Jackson et al., 2003). Early stages of cushion formation are unaffected so the problem appears to be in remodeling. With decreased Hb-Egf signaling via the ErbB1/B2 complex there is increased or prolonged proliferation of the valve primordia that is accompanied by prolonged Smad1/5/8 phosphorylation associated with increased Bmp signaling (Jackson et al., 2003). This suggests that ErbB1/B2 signaling is important for normal regulation of Bmp signaling (Jackson et al., 2003).

Loss of phospholipase C, a downstream effector of Egf and Ras signaling, also results in increased Smad1/5/8 phosphorylation and enlarged semilunar valves in mice (Tadano et al., 2005). Thus, Bmp inhibition is part of the process of valve elongation and remodeling. Consistent with this, mice lacking the inhibitory Smad6 have increased valve cell proliferation and lack of remodeling similar to *Hb-Egf* mutant mice (Galvin et al., 2000, Jackson et al., 2003).

Signaling pathways that use Ras are important in mediating the transition from cushion mesenchyme proliferation to remodeling the valve leaflets. Ras signaling is downregulated as the cushions are remodeled into the valve leaflets and this downregulation requires Nf1 (Gitler et al., 2003). Ectopic expression of activated Ras or loss or *Nf1* results in increased cushion proliferation. Mice lacking *Nf1* have severely defective cardiac cushion formation and valvulogenesis that are caused by increased proliferation, decreased cell death, and limited remodeling of both atrioventricular and outflow cushions. Nf1 protein includes a GTPase-activating (GAP) domain that promotes intrinsic GTPase activity of Ras-GTP, resulting in down-regulated Ras signaling. Endothelial-specific inactivation of *Nf1* causes hyperplasia of the endocardial cushions because of elevated Ras signaling in the *Nf1*-null endothelial cells and greater nuclear localization of the transcription factor Nfatc1 (Gitler et al., 2003). *Nf1* deficiency can be reproduced in culture by activation of Ras signaling pathways, and the *Nf1*-null mutant phenotype can be abrogated by inhibiting Ras (Lakkis and Epstein, 1998). These data suggest that Ras signaling is normally downregulated as endothelial cells mature into valve leaflets and that Nf1 is required for this downregulation.

The ErbB signaling involved in valvulogenesis is different for atrioventricular and semilunar valves. Reduction of ErbB1 preferentially affects semilunar valves (Chen et al., 2000; Sibilia et al., 2003). Mice lacking *ErbB3* show defects in both atrioventricular and semilunar valvulogenesis (Erickson et al., 1997; Gassmann et al., 1995). Therefore the upstream receptor tyrosine kinase regulators of Shp2 signaling in heart valvulogenesis

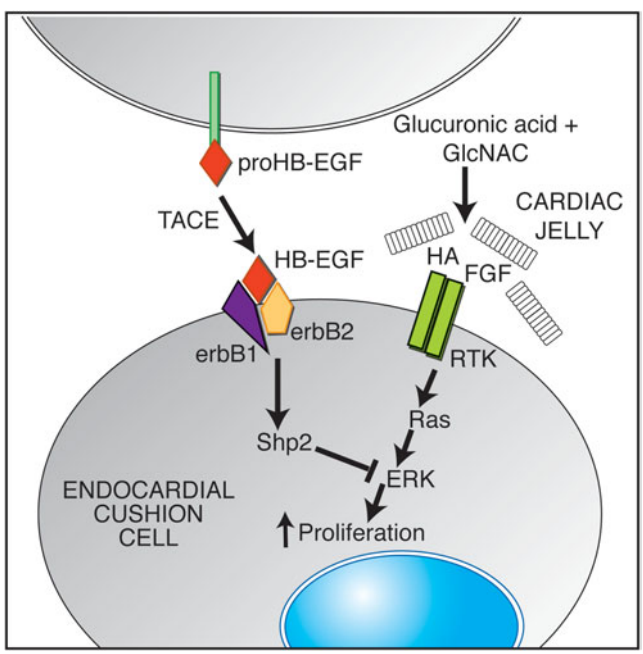

Figure 9.8. Model for ErbB signaling. Transmembrane precursor pro-HB-EGF is cleaved by TACE to HB-EGF, an ErbB1 ligand. When HB-EGF binds ErbB1 it heterodimerizes with ErbB2 which results in decreased proliferation of the cushion mesenchyme and BMP expression. Activation of ErbB2/3 heterodimers by hyaluronic acid increases proliferation of the cushion mesenchyme via Ras signaling. Hyaluronic acid is synthesized from glucuronic acid and *N*-acetylglucosamine (GlcNAc).

are Hb-Egf acting through ErbB1 in the semilunar valves and through ErbB3 in both sets of valves.

Expression of Noonan Syndrome Shp2 Q79R protein with gain-of-function causes increased proliferation which can be dampened by expression of dominant negative Mek1, which inhibits Mapk activation (Krenz et al., 2005; Lakkis and Epstein, 1998).

AV Valve Formation

AV valves include the valve leaflets and a connecting tensile apparatus which consists of both the chordae tendineae and their myotendinous junctions with the papillary muscles (Fig. 9.9). The function of the tensile apparatus is to maintain the valves closed during ventricular systole. The leaflets and tensile apparatus are formed mostly by a process of delamination of the inner layers of the inlet zone of the right ventricle.

The atrioventricular endocardial cushions fuse and condense into distinct mitral and tricuspid valve primordium which remodel to form the leaflets and supporting structures. The leaflets are comprised of three recognized layers in both the atrioventricular and semilunar valves. The layers in the atrioventricular valve leaflets are called the atrialis, the spongiosa and the fibrosa from the atrial to the ventricular sides. The same three layers are recognized in the semilunar valve leaflets but the atrialis layer is called the ventricularis layer in the semilunar valve leaflets (Lincoln et al., 2006). The septal leaflets or cusps of the mitral and tricuspid valves develop from the superior (dorsal) and inferior (ventral) atrioventricular cushions. The leaflets delaminate from the ventricular septal wall (de Lange et al., 2004). The mural leaflets are excavated from the myocardial wall by myocardial cell death, which frees the fibrous leaflets (de Lange et al., 2004).

A second wave of calcineurin/Nfat signaling is required in the endocardium to direct elongation and refinement of the cusps. This mechanism operates in both zebrafish and mouse, indicating a conserved role for calcineurin/Nfat signaling (Chang et al., 2004). During delamination of the valves, Bmp4 and Bmp6 mRNA are expressed at the ventricular side of the mitral valve, and Bmp4 mRNA is expressed at the ventricular side of the tricuspid valve; however, the function of these signaling molecules is not known (Fig. 9.6). Engineering of a Bmp type II receptor that lacks half of the ligand-binding domain in mice results in reduced signaling capability and absence of the semilunar valves but atrioventricular valve formation is normal (Delot et al., 2003). Thus, the signaling requirements for development of the atrioventricular and semilunar valves may be very different (Delot, 2003).

Early biochemical and ultrastructural studies demonstrated that heart valves are primarily composed of an organized matrix of connective tissue (Manasek, 1976). *Sox* genes directly regulate expression of type II collagen and aggrecan genes in chondrogenesis, and both collagen type II and aggrecan are present in the cushion tissue mesenchyme and developing valves of the developing chick heart (Ng et al., 1997; Swiderski et al., 1994). However, in the cushions only aggrecan expression correlates with that of Sox8 and Sox9, making it unclear what drives expression of the collagens in the cushions (Montero et al., 2002). Collagen types I, III, and V are also present in stage 18 cushion cells. Expression of both message and protein in the nascent atrioventricular valves decreases during the remodeling stages 22–45 (day 3.5–19); type II collagen protein is undetectable at stage 38 (day 12), while collagens I, III, and V persist in the valve regions. Distinct patterns of extracellular matrix molecule expression can be identified in the valve leaflets and supporting structures of the chicken mitral valve and both atrioventricular valves of the mouse. In the chick, the mural leaflet of the tricuspid valve is a muscular flap that is atypical of atrioventricular valves. It is predominantly unreactive with chondrogenic and tendon lineage markers. However, expression of type I collagen, type IIA collagen and tenascin can be seen in the septal leaflet as well as the atrial surface of the muscular tricuspid leaflet. Sox9, a major transcriptional regulator of collagen type IIA expression, is transiently expressed between E10.5 and 14.5 in the mouse (Rahkonen et al., 2003). Types I and II collagen and tenascin are present in all of the mitral leaflets but not in the chordae tendineae and myotendinous junctions (Lincoln et al., 2004). Fibulin-1, vitronectin, and fibronectin are concentrated in endocardial cushions at boundaries with the myocardium (Bouchey et al., 1996).

Elongation and remodeling of the primordia into mature valve structures is associated with regionalized cell proliferation of valve progenitor populations, while maturation of the valve primordia is accompanied by decreased proliferation (Lincoln et al., 2004). Using *Tie2-cre* transgenic mice bred with

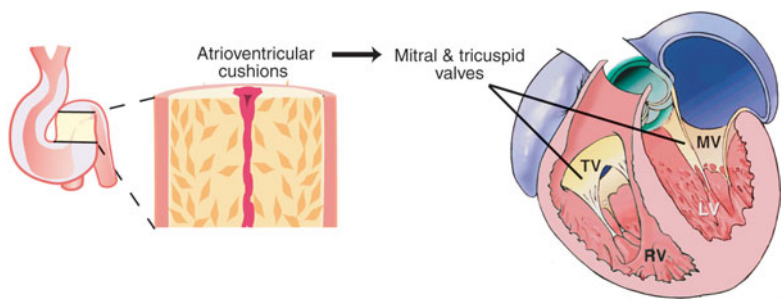

Figure 9.9. After expansion of the atrioventricular cushion mesenchyme, the cushion is remodeled to form the components of the mitral and tricuspid valve apparatus. TV, tricuspid valve; RV, right ventricle; MV, mitral valve; LV, left ventricle.

ROSA26R reporter mice has allowed an evaluation of the proportion of the valve apparatus derived from endocardial cells (Kisanuki et al., 2001). Endocardial cell progeny are located throughout the endocardial cushions of the atrioventricular canal at E12.5. The high levels of recombination observed at E12.5 in atrioventricular endocardial cushions and valve primordia are indicative of the extensive endocardial contributions to these structures. Extensive contributions of endocardially derived cells were detected in the mature valve leaflets, chordae tendineae, and myotendinous junctions, demonstrating their endothelial origins (Lincoln et al., 2004). Surprisingly the supporting valvuloseptal fibrous continuity that spans the ventricular septum between the septal leaflets of the mitral and tricuspid valves is of endocardial origin. No endothelial cells contribute to the muscular components of the atrial or ventricular septa. (Jiang et al., 2000; Kirby et al., 1983).

Cardiac Defects Associated with Cushion Tissue

Noonan Syndrome

Noonan syndrome is one of the most common genetic conditions associated with congenital heart defects (see also Chapter 15, Fig. 15.6). It includes atypical facies, developmental delay, and cognitive deficits, in addition to short stature. The most common heart defect is dysplastic pulmonary valve and atrioventricular septal defects. Mutation in the *PTPN11* gene (Q79R) is associated with 50% of Noonan syndrome patients. *PTPN11* encodes a ubiquitously expressed protein tyrosine phosphatase, Shp2 (src homology region2, phosphatase 2), which contains two Src homology domains (SH2) at the amino terminus and a protein tyrosine phosphatase (PTP) domain at the carboxyl terminus. Shp2 enhances Ras-activated signaling through ErbB1 receptors. In cultured cells, Shp2 activity is required for ErbB1 receptor-mediated activation of Mapk. In mice, an *ErbB1* hypomorphic allele in combination with heterozygous *Ptpn11* shows increased severity of valve malformations. Protein tyrosyl phosphatases like Shp2 attenuate positive signaling. The D61G and Q79R mutations found in Noonan syndrome show gain of function with increased phosphatase activity. Both of these mutations are associated with hyperproliferation of the valve tissue.

Atrioventricular Canal and Down Syndrome

Cx40(−/−)/*Cx43*(+/−) mice progeny have common atrioventricular junction with abnormal atrioventricular connection. Since both of these connexins are expressed by conduction myocardium, it is possible that early development of this specialized myocardium, which is derived from the atrioventricular canal, is affected such that this region does not develop normally (Kirchhoff et al., 2000). The idea that myocardial differentiation is involved in pathogenesis of this malformation is further supported by the fact that embryos lacking *Fog2* also have common atrioventricular canal. Fog2 is a Gata cofactor and is needed for normal expression of myocardial genes (Tevosian et al., 2000).

Endocardial cushion tissues are not only important in valve formation but also in atrial and ventricular septation. The inlet ventricular septum and atrial septum primum include atrioventricular cushion-derived tissue. Tissue from the inferior atrioventricular cushion merges with the muscular ventricular septum to form the membranous septum. The atrial septum primum is derived from atrial muscle but requires cushion tissue to fuse with the atrioventricular cushions. Thus defects in fusion of the primary atrial septum are considered to be atrioventricular cushion tissue defects (Webb et al., 1996, 1998).

The atrioventricular canal defect found in trisomy 21 (Down syndrome) is the best example of a primary atrial septum defect. Frequently the septal leaflet of the mitral valve is bicuspid. The *Down syndrome critical region 1* (*DSCR1*) gene has been identified on human chromosome 21 and is linked to the trisomy 21 phenotype, which includes abnormal development of the atrioventricular cushion tissue. This gene is also present on the syntenic region of mouse chromosome 16. During septal and valve development, *DSCR1* is expressed in the endocardium of the developing atrioventricular and semilunar valves, the muscular interventricular septum, and the ventricular myocardium. This gene contains an Nfat-rich calcineurin-responsive element adjacent to exon 4. Transgenic mice with the regulatory region of the *Dscr1* gene linked to *lacZ* show expression of the gene in the endocardium of the developing valves and aorticopulmonary septum of the heart. Expression in the developing valve endocardium co-localizes with Nfatc1. *DSCR1* expression is absent in *Nfatc1*-null valve endocardium, suggesting that Nfatc1 signaling is required for *DSCR1* expression (Lange et al., 2004).

Atrioventricular Valve Abnormalities

Accessory mitral valve tissue is a rare congenital malformation causing left ventricular outflow tract obstruction (Aoka et al., 2004). It can be associated with other malformations, including ventricular septal defect and cerebrovascular thrombolysis. The accessory valve tissue has been classified as: Type I is fixed and can be nodular (IA) or membranous (IB), while type II is mobile and pedunculated (IIA) or leaflet like (IIB). Type IIB is further subdivided as rudimentary chordae and developed chordae (Prifti et al., 2001).

Tricuspid Atresia

Tricuspid atresia accounts for 1%–3% of congenital cardiac disorders (Sade and Fyfe, 1990). It is characterized by agenesis of the tricuspid valve, which blocks regurgitation of blood into the right atrium from the right ventricle during ventricular

contraction. Tricuspid atresia is accompanied by an atrial and a ventricular septal defect (Rao, 1980). FOG2 is a multi-zinc-finger protein that is co-expressed with GATA4 and interacts with the N-terminal zinc finger of GATA4 to repress GATA4-dependent transcription (Lu et al., 1999; Svensson et al., 2000a; Tevosian et al., 2000). *Fog2*-deficient mice have tricuspid atresia with both atrial and ventricular septal defects (Svensson et al., 2000b).

Ebstein's Anomaly

This sequence of malformations includes malformed tricuspid valve leaflets, atrial septal defect or patent foramen ovale, and right ventricular outflow tract obstruction. Because of the malformed tricuspid valve, there is regurgitant flow into the right atrium. The tricuspid valve leaflets do not attach normally to the connective tissue valve annulus, and the effective orifice is displaced downward into the right ventricular cavity. Only the septal and posterior leaflets are displaced and divide the right ventricle into two portions. The inlet portion of the right ventricle is atrialized and has a thinner wall than normal, while the trabecular and outlet portions constitute the functional right ventricle. An atrial septal defect is present in more than one-third of hearts, and the majority of the remainder has a patent foramen ovale. The downward displacement of the septal tricuspid valve leaflet is associated with discontinuity of the central fibrous body and septal atrioventricular ring, thus creating a potential for accessory pathways for muscular atrioventricular connections and ventricular pre-excitation. A significant number of patients have increased fibrosis in the left ventricular wall and ventricular septum. The downward displacement of the leaflets in Ebstein's anomaly suggests that delamination from the inlet portion failed to occur (Frescura et al., 2000).

REFERENCES

al Moustafa, A. E., and L. E. Chalifour. 1993. Immortal cell lines isolated from heart differentiate to an endothelial cell lineage in the presence of retinoic acid. Cell Growth Differ. 4:841–847.

Aoka, Y., N. Ishizuka, Y. Sakomura, H. Nagashima, M. Kawana, A. Kawai, and H. Kasanuki. 2004. Accessory mitral valve tissue causing severe left ventricular outflow tract obstruction in an adult. Ann. Thorac. Surg. 77:713–715.

Armstrong, E. J., and J. Bischoff. 2004. Heart valve development: endothelial cell signaling and differentiation. Circ. Res. 95: 459–470.

Baldwin, H. S., H. M. Shen, H.-C. Yan, H. M. DeLisser, A. Chung, C. Mickanin, T. Trask, N. E. Kirschbaum, P. J. Newman, S. M. Albelda, and C. A. Buck. 1994. Platelet endothelial cell adhesion molecule-1 (PECAM-1/CD31): alternatively spliced, functionally distinct isoforms expressed during mammalian cardiovascular development. Development 120:2539–2553.

Bernanke, D. H., and R. R. Markwald. 1982. Migratory behavior of cardiac cushion tissue cells in a collagen-lattice culture system. Dev. Biol. 91:235–245.

Borg, T. K., D. S. Raso, and L. Terracio. 1990. Potential role of the extracellular matrix in postseptation development of the heart. Ann. NY Acad. Sci. 588:87–92.

Bouchey, D., W. S. Argraves, and C. D. Little. 1996. Fibulin-1, vitronectin, and fibronectin expression during avian cardiac valve and septa development. Anat. Rec. 244:540–551.

Boyer, A. S., I. I. Ayerinskas, E. B. Vincent, L. A. McKinney, D. L. Weeks, and R. B. Runyan. 1999. TGFβ2 and TGFβ3 have separate and sequential activities during epithelial-mesenchymal cell transformation in the embryonic heart. Dev. Biol. 208: 530–545.

Brown, C. B., A. S. Boyer, R. B. Runyan, and J. V. Barnett. 1999. Requirement of type III TGF-β receptor for endocardial cell transformation in the heart. Science 283:2080–2082.

Burch, G. H., M. A. Bedolli, S. McDonough, S. M. Rosenthal, and J. Bristow. 1995. Embryonic expression of tenascin-X suggests a role in limb, muscle, and heart development. Dev. Dyn. 203: 491–504.

Camenisch, T. D., D. G. M. Molin, A. Person, R. B. Runyan, A. C. Gittenberger-de Groot, J. A. McDonald, and S. E. Klewer. 2002. Temporal and distinct TGFb ligand requirements during mouse and avian endocardial cushion morphogenesis. Dev. Biol. 248:170–181.

Carmona, R., M. Gonzalez-Iriarte, D. Macias, J. M. Perez-Pomares, L. Garcia-Garrido, and R. Munoz-Chapuli. 2000. Immunolocalization of the transcription factor Slug in the developing avian heart. Anat. Embryol. 201:103–109.

Chang, C. P., J. R. Neilson, J. H. Bayle, J. E. Gestwicki, A. Kuo, K. Stankunas, I. A. Graef, and G. R. Crabtree. 2004. A field of myocardial-endocardial NFAT signaling underlies heart valve morphogenesis. Cell 118:649–663.

Chen, B. B., R. T. Bronson, L. D. Klaman, T. G. Hampton, J. F. Wang, P. J. Green, T. Magnuson, P. S. Douglas, J. P. Morgan, and B. G. Neel. 2000. Mice mutant for Egfr and Shp2 have defective cardiac semilunar valvulogenesis. Nat. Genet. 24:296–299.

Chen, X., T. K. Yeung, and Z. Wang. 2000. Enhanced drug resistance in cells coexpressing ErbB2 with EGF receptor or ErbB3. Biochem. Biophys. Res. Commun. 277:757–763.

Coffin, D. J., and T. J. Poole. 1988. Embryonic vascular development: immunohistochemical identification of the origin and subsequent morphogenesis of the major vessel primordia in quail embryos. Development 102:735–748.

Cohen-Gould, L., and T. Mikawa. 1996. The fate diversity of mesodermal cells within the heart field during chicken early embryogenesis. Dev. Biol. 177:265–273.

Crossin, K. L., and S. Hoffman. 1991. Expression of adhesion molecules during the formation and differentiation of the avian endocardial cushion tissue. Dev. Biol. 145:227–286.

de la Pompa, J. L., L. A. Timmerman, H. Takimoto, H. Yoshida, A. J. Elia, E. Samper, J. Potter, A. Wakeham, L. Marengere, B. L. Langille, G. R. Crabtree, and T. W. Mak. 1998. Role of the NF-ATc transcription factor in morphogenesis of cardiac valves and septum. Nature 392:182–186.

de Lange, F. J., A. F. Moorman, R. H. Anderson, J. Manner, A. T. Soufan, C. de Gier-de Vries, M. D. Schneider, S. Webb, M. J. van den Hoff, and V. M. Christoffels. 2004. Lineage and morphogenetic analysis of the cardiac valves. Circ. Res. 95:645–654.

Delorme, B., E. Dahl, T. Jarry-Guichard, J.-P. Briand, K. Willecke, D. Gros, and M. Th, veniau-Ruissy. 1997. Expression pattern of connexin gene products at the early developmental stages of the mouse cardiovascular system. Circ. Res. 81:423–437.

Delot, E. C. 2003. Control of endocardial cushion and cardiac valve maturation by BMP signaling pathways. Mol. Genet. Metabol. 80:27–35.

Delot, E. C., M. E. Bahamonde, M. X. Zhao, and K. M. Lyons. 2003. BMP signaling is required for septation of the outflow tract of the mammalian heart. Development 130:209–220.

Dor, Y., T. Camenisch, A. Itin, G. I. Fishman, J. A. McDonald, P. Carmeliet, and E. Keshet. 2001. A novel role for VEGF in endocardial cushion formation and its potential contribution to congenital heart defects. Development 128:1531–1538.

Eisenberg, C. A., and R. R. Markwald. 1997. Mixed cultures of avian blastoderm cells and the quail mesoderm cell line QCE-6 provide evidence for the pluripotentiality of early mesoderm. Dev. Biol. 191:167–181.

Erickson, S. L., K. S. O'Shea, N. Ghaboosi, L. Loverro, G. Frantz, M. Bauer, L. H. Lu, and M. W. Moore. 1997. ErbB3 is required for normal cerebellar and cardiac development: a comparison with ErbB2-and heregulin-deficient mice. Development 124: 4999–5011.

Frescura, C., A. Angelini, L. Daliento, and G. Thiene. 2000. Morphological aspects of Ebstein's anomaly in adults. Thorac. Cardiovasc. Surg. 48:203–208.

Galvin, K. M., M. J. Donovan, C. A. Lynch, R. I. Meyer, R. J. Paul, J. N. Lorenz, V. Fairchild-Huntress, K. L. Dixon, J. H. Dunmore, M. A. Gimbrone, Jr., D. Falb, and D. Huszar. 2000. A role for Smad6 in development and homeostasis of the cardiovascular system. Nat. Genet. 24:171–174.

Gassmann, M., F. Casagranda, D. Orioli, H. Simon, C. Lai, R. Klein, and G. Lemke. 1995. Aberrant neural and cardiac development in mice lacking the ErbB4 neuregulin receptor. Nature 378:390–394.

Gill, K. A., and N. P. Brindle. 2005. Angiopoietin-2 stimulates migration of endothelial progenitors and their interaction with endothelium. Biochem. Biophys. Res. Commun. 336:392–396.

Gitler, A. D., Y. Zhu, F. A. Ismat, M. M. Lu, Y. Yamauchi, L. F. Parada, and J. A. Epstein. 2003. Nf1 has an essential role in endothelial cells. Nat. Genet. 33:75–79.

Gittenberger-de Groot, A. C., M. P. F. M. Peeters, M. M. T. Mentink, R. G. Gourdie, and R. E. Poelmann. 1998. Epicardium-derived cells contribute a novel population to the myocardial wall and the atrioventricular cushions. Circ. Res. 82:1043–1052.

Graef, I. A., F. Chen, and G. R. Crabtree. 2001. NFAT signaling in vertebrate development. Curr. Opin. Genet. Dev. 11:505–512.

Iwamoto, R., S. A. Yamazaki, M. Asakura, S. Takashima, H. Hasuwa, K. Miyado, S. Adachi, M. Kitakaze, K. Hashimoto, G. Raab, D. Nanba, S. Higashiyama, M. Hori, M. Klagsbrun, and E. Mekada. 2003. Heparin-binding EGF-like growth factor and ErbB signaling is essential for heart function. Proc. Natl. Acad. Sci. USA 100:3221–3226.

Jackson, L. F., T. H. Qiu, S. W. Sunnarborg, A. Chang, C. Zhang, C. Patterson, and D. C. Lee. 2003. Defective valvulogenesis in HB-EGF and TACE-null mice is associated with aberrant BMP signaling. EMBO J. 22:2704–2716.

Jiang, X., D. H. Rowitch, P. Soriano, A. P. McMahon, and H. M. Sucov. 2000. Fate of the mammalian cardiac neural crest. Development 127:1607–1616.

Kanda, S., Y. Miyata, Y. Mochizuki, T. Matsuyama, and H. Kanetake. 2005. Angiopoietin 1 is mitogenic for cultured endothelial cells. Cancer Res. 65:6820–6827.

Kelley, C., H. Blumberg, L. I. Zon, and T. Evans. 1993. GATA-4 is a novel transcription factor expressed in endocardium of the developing heart. Development 118:817–827.

Kirby, M. L., T. F. Gale, and D. E. Stewart. 1983. Neural crest cells contribute to aorticopulmonary septation. Science 220:1059–1061.

Kirby, M. L., A. Lawson, H. Stadt, D. Kumiski, K. Wallis, E. McCraney, K. Waldo, Y. Li, and G. C. Schoenwolf. 2003. Hensen's node gives rise to the ventral midline of the foregut: implications for organizing head and heart development. Dev. Biol. 253:175–188.

Kirchhoff, S., J. S. Kim, A. Hagendorff, E. Thonnissen, O. Kruger, W. H. Lamers, and K. Willecke. 2000. Abnormal cardiac conduction and morphogenesis in connexin40 and connexin43 double-deficient mice. Circ. Res. 87:399–405.

Kisanuki, Y. Y., R. E. Hammer, J.-I. Miyazaki, S. C. Williams, J. A. Richardson, and M. Yanagisawa. 2001. Tie2-cre transgenic mice: a new model for endothelial cell-lineage analysis in vivo. Dev. Biol. 230:230–242.

Krenz, M., K. E. Yutzey, and J. Robbins. 2005. Noonan syndrome mutation Q79R in Shp2 increases proliferation of valve primordia mesenchymal cells via extracellular signal-regulated kinase 1/2 signaling. Circ. Res. 97:813–820.

Krug, E. L., R. B. Runyan, and M. R. Markwald. 1985. Protein extracts from early embryonic hearts initiate cardiac endothelial cytodifferentiation. Dev. Biol. 112:414–426.

Kumai, M., K. Nishii, K. Nakamura, N. Takeda, M. Suzuki, and Y. Shibata. 2000. Loss of connexin45 causes a cushion defect in early cardiogenesis. Development 127:3501–3512.

Kurihara, Y., H. Kurihara, H. Oda, K. Maemura, R. Nagai, T. Ishikawa, and Y. Yazaki. 1995. Aortic arch malformations and ventricular septal defect in mice deficient in endothelin-1. J. Clin. Invest. 96:293–300.

Lakkis, M. M., and J. A. Epstein. 1998. Neurofibromin modulation of ras activity is required for normal endocardial-mesenchymal transformation in the developing heart. Development 125: 4359–4367.

Lakkis, M. M., and J. A. Epstein. 1998. Neurofibromin modulation of ras activity is required for normal endocardial mesenchymal transformation in the developing heart. Development 125:4359–4367.

Lange, A. W., J. D. Molkentin, and K. E. Yutzey. 2004. DSCR1 gene expression is dependent on NFATc1 during cardiac valve formation and colocalizes with anomalous organ development in trisomy 16 mice. Dev. Biol. 266:346–360.

Lee, R. K. K., D. Y. R. Stainier, B. M. Weinstein, and M. C. Fishman. 1994. Cardiovascular development in the zebrafish. II. Endocardial progenitors are sequestered within the heart field. Development 120:3361–3366.

Liao, W., B. W. Bisgrove, H. Sawyer, B. Hug, B. Bell, K. Peters, D. J. Grunwald, and D. Y. R. Stainier. 1997. The zebrafish gene *cloche* acts upstream of a *flk-1* homologue to regulate endothelial cell differentiation. Development 124:381–389.

Liebner, S., A. Cattelino, R. Gallini, N. Rudini, M. Iurlaro, S. Piccolo, and E. Dejana. 2004. Beta-catenin is required for endothelial-mesenchymal transformation during heart cushion development in the mouse. J. Cell Biol. 166:359–367.

Lincoln, J., C. M. Alfieri, and K. E. Yutzey. 2004. Development of heart valve leaflets and supporting apparatus in chicken and mouse embryos. Dev. Dyn. 230:239–250.

Lincoln, J., A. W. Lange, and K. E. Yutzey. 2006. Hearts and bones: shared regulatory mechanisms in heart valve, cartilage, tendon, and bone development. Dev. Biol. 294:292–302.

Little CD and B. J. Rongish. 1995. The extracellular matrix during heart development. Experientia. 51:873–882.

Lough, J., and Y. Sugi. 2000. Endoderm and heart development. Dev. Dyn. 217:327–342.

Lu, J. R., T. A. McKinsey, H. Xu, D. Z. Wang, J. A. Richardson, and E. N. Olson. 1999. FOG-2, a heart- and brain-enriched cofactor for GATA transcription factors. Mol. Cell. Biol. 19:4495–44502.

Manasek, F. J. 1970. Sulfated extracellular matrix production in the embryonic heart and adjacent tissues. J. Exp. Zool. 174:415–439.

Manasek, F. J. 1976. Macromolecules of the extracellular compartment of embryonic and mature hearts. Circ. Res. 38:331–337.

Manasek, F. J., M. Reid, W. Vinson, J. Seyer, and R. Johnson. 1973. Glycosaminoglycan synthesis by the early embryonic chick heart. Dev. Biol. 35:332–348.

Markwald, R. R., T. P. Fitzharris, and W. N. Adams Smith. 1975. Structural analysis of endocardial cytodifferentiation. Dev. Biol. 42:160–180.

Markwald, R. R., R. B. Runyan, G. T. Kitten, F. M. Funderberg, D. H. Bernanke, and P. R. Brauer. 1984. Use of collagen gel cultures to study heart development: proteoglycan and glycoprotein interactions during the formation of endocardial cushion tissue. In: The Role of Extracellular Matrix in Development, ed. Tresltad, R., 323–350. New York: Alan R. Liss.

Mendler, M., S. G. Eich-Bender, L. Vaughan, K. H. Winterhalter, and P. Bruckner. 1989. Cartilage contains mixed fibrils of collagen types II, IX and XI. J. Cell Biol. 108:191–197.

Meyer, D., and C. Birchmeier. 1995. Multiple essential functions of neuregulin in development. Nature 378:386–390.

Mjaatvedt, C. H., E. L. Krug, and R. R. Markwald. 1991. An antiserum (ES1) against a particulate form of extracellular matrix blocks the transition of cardiac endothelium into mesenchyme in culture. Dev. Biol. 145:219–230.

Mollier, S. 1906. Die erste Anlage des Herzens bei den Wirbeltieren. In: Handbuch der vergleichnden und experimentellen Entwincklungslehre der Wilbertiere, ed. Hertwig, O., 1026–1051. Jena: Gustav Fisher.

Montero, J. A., B. Giron, H. Arrechedera, Y. C. Cheng, P. Scotting, J. Chimal-Monroy, J. A. Garcia-Porrero, and J. M. Hurle. 2002. Expression of *Sox8*, *Sox9* and *Sox10* in the developing valves and autonomic nerves of the embryonic heart. Mech. Dev. 118: 199–202.

Moore, C. S., C. H. Mjaatvedt, and J. D. Gearhart. 1998. Expression and function of activin beta A during mouse cardiac cushion tissue formation. Dev. Dyn. 212:548–562.

Nakajima, Y., T. Yamagishi, S. Hokari, and H. Nakamura. 2000. Mechanisms involved in valvuloseptal endocardial cushion formation in early cardiogenesis: roles of transforming growth factor (TGF)-beta and bone morphogenetic protein (BMP). Anat. Rec. 258:119–127.

Nemer, G., and M. Nemer. 2002. Cooperative interaction between GATA5 and NF-ATc regulates endothelial-endocardial differentiation of cardiogenic cells. Development 129:4045–4055.

Nemer, G., S. T. Qureshi, D. Malo, and M. Nemer. 1999. Functional analysis and chromosomal mapping of *Gata5*, a gene encoding a zinc finger DNA-binding protein. Mamm. Genome. 10:993–999.

Ng, L. J., S. Wheatley, G. E. Muscat, J. Conway-Campbell, J. Bowles, E. Wright, D. M. Bell, P. P. Tam, K. S. Cheah, and P. Koopman. 1997. SOX9 binds DNA, activates transcription, and coexpresses with type II collagen during chondrogenesis in the mouse. Dev. Biol. 183:108–121.

Noden, D. M. 1990. Origins and assembly of avian embryonic blood vessels. Ann. NY Acad. Sci. 236–249.

Person, A. D., S. E. Klewer, and R. B. Runyan. 2005. Cell biology of cardiac cushion development. Int. Rev. Cytol. 243:287–335.

Prifti, E., G. Frati, M. Bonacchi, V. Vanini, and S. Chauvaud. 2001. Accessory mitral valve tissue causing left ventricular outflow tract obstruction: case reports and literature review. J. Heart Valve Dis. 10:774–778.

Puri, M. C., J. Partanen, J. Rossant, and A. Bernstein. 1999. Interaction of the TEK and TIE receptor tyrosine kinases during cardiovascular development. Development 126:4569–4580.

Qu, R., M. M. Silver, and M. Letarte. 1998. Distribution of endoglin in early human development reveals high levels on endocardial cushion tissue mesenchyme during valve formation. Cell Tissue Res. 292:333–343.

Rahkonen, O., M. Savontaus, E. Abdelwahid, E. Vuorio, and E. Jokinen. 2003. Expression patterns of cartilage collagens and *Sox9* during mouse heart development. Histochem. Cell Biol. 120:103–110.

Ranger, A. M., M. J. Grusby, M. R. Hodge, E. M. Gravallese, F. C. De la Brousse, T. Hoey, C. Mickanin, H. S. Baldwin, and L. H. Glimcher. 1998. The transcription factor NF-ATc is essential for cardiac valve formation. Nature 392:186–190.

Rao, P. S. 1980. A unified classification for tricuspid atresia. Am. Heart J. 199:799–804.

Reiter, J. F., J. Alexander, A. Rodaway, D. Yelon, R. Patient, N. Holder, and D. Y. R. Stainier. 1999. *Gata5* is required for the development of the heart and endoderm in zebrafish. Genes Dev. 13:2983–2995.

Romano, L. A., and R. B. Runyan. 2000. Slug is an essential target of TGFá2 signaling in the developing chicken heart. Dev. Biol. 223:91–102.

Runyan, R. B., and R. R. Markwald. 1983. Invasion of mesenchyme into three-dimensional collagen gels: a regional and temporal analysis of interaction in embryonic heart tissue. Dev. Biol. 95:108–114.

Sade, R. M. and D. A. Fyfe. 1990. Tricuspid atresia: current concepts in diagnosis and treatment. Pediatr. Clin. North Am. 37:151–169.

Schubert, F., R. Mootoosamy, E. Walters, A. Graham, L. Tumiotto, A. Munsterberg, A. Lumsden, and S. Dietrich. 2002. Wnt6 marks sites of epithelial transformations in the chick embryo. Mech. Dev. 114:143–148.

Sibilia, M., B. Wagner, A. Hoebertz, C. Elliott, S. Marino, W. Jochum, and E. F. Wagner. 2003. Mice humanised for the EGF receptor display hypomorphic phenotypes in skin, bone and heart. Development 130:4515–4525.

Stalsberg, H. 1969. Regional mitotic activity in the precardiac mesoderm and differentiating heart tube in the chick embryo. Dev. Biol. 20:28–45.

Stalsberg, H., and R. L. DeHaan. 1969. The precardiac areas and formation of the tubular heart in the chick embryo. Dev. Biol. 19:128.

Sugi, Y., N. Ito, G. Szebenyi, K. Myers, J. F. Fallon, T. Mikawa, and R. R. Markwald. 2003. Fibroblast growth factor (FGF)-4 can induce proliferation of cardiac cushion mesenchymal cells during early valve leaflet formation. Dev. Biol. 258:252–263.

Sugi, Y., and R. R. Markwald. 1996. Formation and early morphogenesis of endocardial endothelial precursor cells and the role of endoderm. Dev. Biol. 175:66–83.

Sugi, Y., and R. R. Markwald. 2003. Endodermal growth factors promote endocardial precursor cell formation from precardiac mesoderm. Dev. Biol. 263:35–49.

Svensson, E.C., G. S. Huggins, F. B. Dardik, C. E. Polk, and J. M. Leiden. 2000a. A functionally conserved N-terminal domain of

the friend of GATA-2 (FOG-2) protein represses GATA4-dependent transcription. J. Biol. Chem. 275:20762–20769.

Svensson, E. C., G. S. Huggins, H. Lin H, C. Clendenin, F. Jiang, R. Tufts, F. B. Dardik, and J. M. Leiden. 2000b. A syndrome of tricuspid atresia in mice with a targeted mutation of the gene encoding Fog-2. Nat. Genet. 25:353–356.

Swiderski, R. E., K. J. Daniels, K. L. Jensen, and M. Solursh. 1994. Type II collagen is transiently expressed during avian cardiac valve morphogenesis. Dev. Dyn. 200:294–304.

Tadano, M., H. Edamatsu, S. Minamisawa, U. Yokoyama, Y. Ishikawa, N. Suzuki, H. Saito, D. Wu, M. Masago-Toda, Y. Yamawaki-Kataoka, T. Setsu, T. Terashima, S. Maeda, T. Satoh, and T. Kataoka. 2005. Congenital semilunar valvulogenesis defect in mice deficient in phospholipase C epsilon. Mol. Cell. Biol. 25:2191–2199.

Tevosian, S. G., A. E. Deconinck, M. Tanaka, M. Schinke, S. H. Litovsky, S. Izumo, Y. Fujiwara, and S. H. Orkin 2000. FOG-2, a cofactor for GATA transcription factors, is essential for heart morphogenesis and development of coronary vessels from epicardium. Cell 101:729–739.

Tian, H., S. L. McKnight, and D. W. Russell. 1997. Endothelial PAS domain protein 1 (EPAS1), a transcription factor selectively expressed in endothelial cells. Genes Dev. 11:72–82.

Timmerman, L. A., J. Grego-Bessa, A. Raya, E. Bertran, J. M. Perez-Pomares, J. Diez, S. Aranda, S. Palomo, F. McCormick, J. C. Izpisua-Belmonte, and J. L. de la Pompa. 2004. Notch promotes epithelial-mesenchymal transition during cardiac development and oncogenic transformation. Genes Dev. 18:99–115.

Walsh, E. C., and D. Y. Stainier. 2001. UDP-glucose dehydrogenase required for cardiac valve formation in zebrafish. Science 293:1670–1673.

Webb, S., R. H. Anderson, and N. A. Brown. 1996. Endocardial cushion development and heart loop architecture in the trisomy 16 mouse. Dev. Dyn. 206:301–309.

Webb, S., N. A. Brown, and R. H. Anderson. 1998. Formation of the atrioventricular septal structures in the normal mouse. Circ. Res. 82:645–656.

Wei, Y., and T. Mikawa. 2000. Fate diversity of primitive streak cells during heart field formation in ovo. Dev. Dyn. 219:505–513.

Wessels, A., and D. Sedmera. 2003. Developmental anatomy of the heart: a tale of mice and man. Physiol. Genom. 15:165–176.

Wunsch, A. M., C. D. Little, and R. R. Markwald. 1994. Cardiac endothelial heterogeneity defines valvular development as demonstrated by the diverse expression of JB3, an antigen of the endocardial cushion tissue. Dev. Biol. 165:585–601.

This page intentionally left blank

10

Epicardium and Coronary Vessel Development

During its early existence the wall of the tubular heart is composed of only two cellular layers, the myocardium and endocardium. These cellular layers are separated by an acellular cardiac jelly. The third cellular layer, the epicardium, develops mostly from an extracardiac population of cells called the proepicardium. The proepicardium spreads over the myocardial surface during looping, which is well after the heart begins to function. The proepicardium originates from the splanchnic mesoderm caudal to the attachment of the sinus venosus. Protrusions of cells form near the sinus venosus. The protrusions elongate to form fingerlike processes that touch the dorsal wall of the ventricle. From this initial contact the proepicardium invests all of the myocardium of the atria, atrioventricular canal, and ventricles in a single layer of epithelial cells called the epicardium. A completely separate source of cells derived from the splanchnic mesoderm of the ventral pharynx near the attachment of the outflow pole forms the epicardium of the outflow tract. The epicardium covering the atrioventricular canal and ventricles generates an extensive population of cells by epithelial–mesenchymal transformation. These cells form the coronary vasculature (endothelium and smooth muscle), blood progenitors, and fibroblasts (connective and cushion tissue). Under certain in vitro conditions, epicardially derived cells can be forced to adopt a myocardial cell lineage suggesting that these cells represent a type of multipotent stem cells.

Origin and Early Development of the Proepicardium

The term MYOEPICARDIUM was coined in 1906 by Mollier, who believed that the myocardial layer generated its epicardium (Mollier, 1906). Even though Kurkiewicz proposed as early as 1909 that the epicardium originated from an extracardiac source of mesenchyme, the term myoepicardium was in general use and is still found in embryology textbooks (Kurkiewicz, 1909). Studies by Manasek showed definitively that the epicardium did not originate from the myocardium, but the process of epicardial development was not well studied until the last part of the twentieth century (Manasek, 1969). We now know that there are two sources of extracardiac cells that form the epicardium. The best studied is the proepicardium, which originates from splanchnic mesenchyme near the inflow pole of the heart. The proepicardium generates the epicardium that covers the atria, atrioventricular canal, and ventricles. The epicardium covering the arterial pole does not originate from the proepicardium but is generated from a different source of splanchnic mesoderm near the outflow pole (Fig. 10.1).

The proepicardium in all vertebrate species examined begins as protrusions at the back of the pericardial cavity

Figure 10.1. The epicardium arises from two different sources. Most of the ventricles, atrioventricular junction, and atria are covered by epicardium derived from the proepicardium, which arises from splanchnic mesoderm near the inflow pole (*red*). The epicardium covering the conotruncus arises from splanchnic mesoderm near the outflow pole (*green*). RA, right atrium; RV, right ventricle; LA, left atrium; AVC, atrioventricular canal; LV, left ventricle.

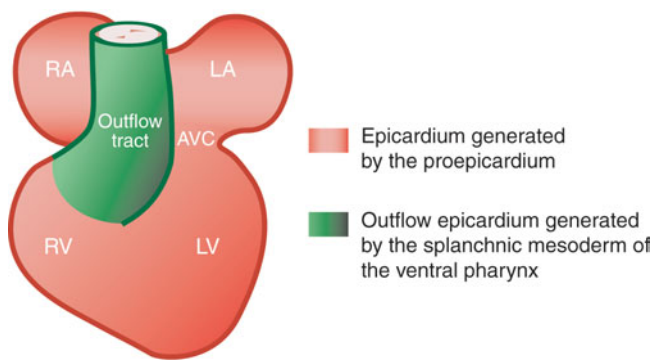

(Fig. 10.2) and crosses the coelom to reach the surface of the heart. In fish and rodents, cells from the splanchnic mesoderm in or near the SEPTUM TRANSVERSUM detach as free-floating, multicellular aggregates or vesicles that float across the PERICARDIAL COELOM and attach to the myocardium (Komiyama et al., 1987; Kuhn and Liebherr, 1988; Munoz-Chapuli et al., 1994). In mouse this occurs between gestation days 9 and 11 (Komiyama et al., 1987). In avian and amphibian embryos, a proepicardial bridge connects the proepicardial cells with the right atrioventricular myocardium across the pericardial coelom (Fig. 10.3). In the chick, this bridge develops on the surface of the sinus venosus and extends to the atrioventricular groove between stages 14 and 17 (Hiruma and Hirakow, 1989; Ho and Shimada, 1978; Manner, 1992; Nahirney et al., 2003; Shimada et al., 1981). The cellular bridge is constructed on an extracellular matrix bridge that appears at stage 14, crosses the coelomic cavity between the proepicardium and the myocardium, and disappears after the proepicardial cells contact the myocardial surface (Nahirney et al., 2003).

In either case, at each adhesion point, cells spread onto the myocardium to form a monolayer covering the myocardium (Fig. 10.3) (Hiruma and Hirakow, 1989; Ho and Shimada, 1978; Komiyama et al., 1996; Manasek, 1970; Manner, 1999). The first areas to be covered are the atrioventricular and CONOVENTRICULAR grooves with the ventricular surface quickly filled in. The atria and outflow tract are the last to be covered. This same pattern is true for epicardium that forms from vesicles in fish and mice. It is not clear how this stereotypical pattern is conserved, but it may be controlled by the spatiotemporal coordination of adhesion molecule expression (Wessels and Perez-Pomares, 2004). The surface of the heart is completely invested in epicardium in the mouse by E10.5, although the aorta is not completely covered until E11.5 (Moore et al., 1999).

The outflow epicardium originates near the outflow tract rather than the proepicardium (Gittenberger-de Groot et al., 2000; Perez-Pomares et al., 2003). An outflow epicardial sleeve originates from the pericardial coelomic epithelium in the vicinity of the aortic sac. The epicardial cells derived from the two different sources differ in their morphologic appearance, gene-expression profile, and in their ability to undergo epithelial-to-mesenchymal transformation (Perez-Pomares et al., 2003). The cells in the outflow epicardium have an elongated shape, while proepicardially derived cells have a rounded, polygonal shape. Both populations express cytokeratin and retinaldehyde dehydrogenase 2 (Raldh2).

Both the newly formed epicardium and the myocardium elaborate a rich subepicardial matrix consisting of collagens I, IV, V, and VI, fibronectin, flectin, fibulin-2, LAMININ, PROTEOGLYCANS, VITRONECTIN, FIBRILLIN-2, elastin, and tenascin-X (Fig. 10.4) (Wessels and Perez-Pomares, 2004). This matrix accumulates growth factors such as fibroblast growth factor

Figure 10.2. The proepicardium develops from protrusions of splanchnic mesoderm at the back of the pericardial cavity near the attachment of the inflow pole. The protrusions (*arrows*) elongate to span the coelom.

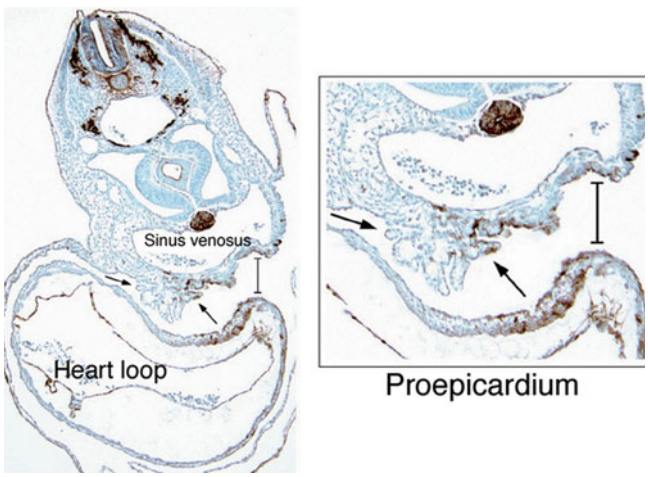

Figure 10.3. Initial contact of the proepicardium with the myocardium is followed by rapid spreading of the cells over the myocardium.

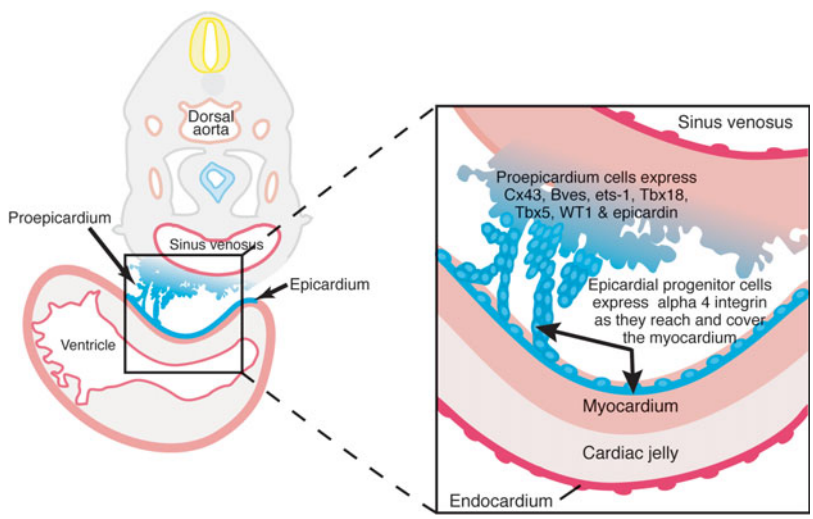

(Fgf) and vascular endothelial growth factor (Vegf) (Lavine et al., 2005; Tomanek et al., 1999). The atrioventricular groove accumulates more subepicardial matrix and generates more subepicardial cells than other regions of the heart (Wessels et al., 1996).

Some of the newly formed epicardial cells undergo epithelial-to-mesenchymal transformation. By this process of delamination, the epicardial monolayer generates a rich variety of cells that populate the developing heart (Fig. 10.5). While Hiruma and Hirakow noted blood island-like structures, which give rise to the capillaries of the coronary vascular plexus appearing in the subepicardial layer, it was Perez-Pomares et al. who originally showed in Syrian hamster and chick embryos that delamination of cells from the epicardium occurs by epithelial–mesenchymal transformation (Hiruma and Hirakow, 1989; Perez-Pomares et al., 1997). Epicardial cell tracing experiments using quail–chick chimeras have shown that epicardium-derived cells are not only the source of capillary endothelial cells but also interstitial myocardial fibroblasts, some cushion mesenchyme, and coronary vascular smooth muscle cells (Gittenberger-de Groot et al., 2000; Viragh and Challice, 1981). In addition to its function to provide these cells to the heart, studies that have inhibited epicardial outgrowth or caused absence of the epicardium by null genetic mutation show that myocardial growth is abnormal, indicating that the epicardium provides a factor needed for normal myocardial expansion (Kwee et al., 1995).

The precursors of the epicardium, as a migratory population, require integrins to move over the surface of the myocardium (Holly et al., 2000). Alpha 4 integrin is expressed in epicardial progenitor cells in the splanchnic mesoderm (Fig. 10.3) (Pinco et al., 2001). Alpha 4 integrins are cell surface receptors that mediate cell–extracellular matrix and cell–cell adhesivity by interacting with fibronectin and vascular cell adhesion molecule (Vcam)-1, respectively. Embryos that do not express α4-integrins fail to develop an epicardium and coronary vessels (Yang et al., 1995). In addition to its use during movement of the epicardium to cover the myocardium, α4-integrin is important in limiting epithelial-to-mesenchymal transformation of the epicardial cells (Dettman et al., 2003). Expression of α4-integrin by epicardial cells appears to be controlled by retinoic acid because embryos that are homozygous null for *Raldh2*, the gene coding for the major synthetic enzyme of retinoic acid, express no α4-integrins (Pinco et al., 2001; Xavier-Neto et al., 2000; Yang et al., 1995).

Figure 10.4. The epicardium overlies the myocardium with a rich subepicardial extracellular matrix between that provides the platform for epithelial-to-mesenchymal transformation of the epicardial cells.

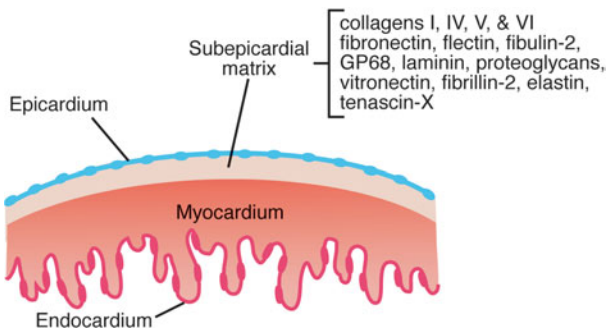

Epithelial–Mesenchymal Transformation of Epicardially Derived Cells

Once the epicardium has completely invested the myocardium, a subset of the cells delaminates from the epicardium into the subepicardial space. This results in a substantial population of mesenchymal epicardially derived cells (EPDCS), especially at the atrioventricular junction and over the prospective ventricles (Fig. 10.5) (Manner, 1999; Perez-Pomares et al., 1997).

Figure 10.5. Epicardial development from the proepicardium in a quail-chick chimera. (*A*) Shows the position of the proepicardium (protrusion of cells) from the right side. In *B* the chick proepicardium has been replaced by quail proepicardium (*black cells*). (*C*) The quail epicardium (black) covers the surface of the chick myocardium and produces cells (also black) that populate the subepicardial space or migrate into the myocardium. (From Manner, 1999, with permission.)

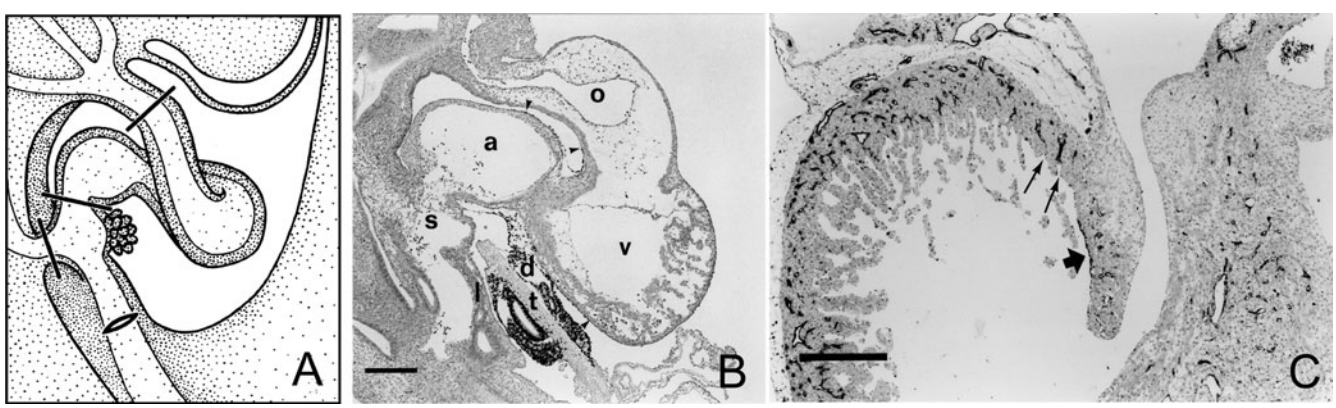

The delamination occurs between E11.5 and 12.5 in the mouse and stages 16–20 in the chick (Moore et al., 1999). The cells subsequently invade and migrate widely throughout the myocardium, populating the subendocardial space and atrioventricular cushions (Dettman et al., 1998; Gittenberger-de Groot et al., 1998; Manner, 1999; Mikawa and Fischman, 1992; Mikawa and Gourdie, 1996; Perez-Pomares et al., 2002). Fgfs and transforming growth factor beta (Tgfβ) promote and inhibit epithelial–mesenchymal transformation, respectively, and play a critical role in balancing the number of cells leaving the epithelial layer as mesenchymal cells (Morabito et al., 2001).

Cells of the epicardium express markers characteristic of three stages of development: epithelial, epithelial–mesenchymal transformation, and vascular differentiation. Proepicardial cells, located in the mesenchyme of the septum transversum, are uniformly positive for the epithelial cell marker, CYTOKERATIN (Landerholm et al., 1999). As the cells delaminate from the epicardial epithelium, they stop expressing cytokeratin and begin to express markers characteristic of migrating mesenchymal cells such as VIMENTIN. While they are in the subepicardial space they express both epithelial and mesenchymal markers.

Some factors are expressed initially in the splanchnic mesoderm and throughout the development of a continuous epicardial layer. These factors include Tbx18 and Tbx5, Wilms' tumor (Wt)1, and epicardin (Hatcher et al., 2000; Kraus et al., 2001; Moore et al., 1999; Robb et al., 1998). The function of Tbx18 in proepicardial development is currently unknown. *Tbx5*, a T-box transcription factor family member, is expressed in the proepicardium and continues to be expressed while the cells migrate over the surface of the myocardium. Expression ceases before the epicardial cells undergo epithelial–mesenchymal transformation. In the chick, retrovirus-mediated overexpression or antisense-mediated knockdown of Tbx5 prevents migration of the epicardial cells (Hatcher et al., 2004). *Wt1* is a tumor suppressor gene that encodes a zinc-finger transcription factor essential for the development of kidney, gonads, spleen, and adrenals. *Wt1*-null embryos lack all of these organs, and in addition, they fail to develop an epicardium. Without the epicardium the myocardium fails to grow resulting in heart failure between E13 and 15 (Moore et al., 1999). Wt1 protein is expressed from about stage 18 in the chick in specific areas of the splanchnic mesoderm. An invasion of Wt1-positive cells into the ventricular myocardium occurs from stage 26. Wt1 may function as a repressor of differentiation (Carmona et al., 2001). Finally, epicardin is a member of the basic helix–loop–helix (bHLH) transcription factor family that may function as a negative regulator of differentiation (Funato et al., 2003; Robb et al., 1998).

In the chick, myocardially produced Fgf family members 1, 2, and 7, and Bmp2 and 4 promote epithelial-to-mesenchymal transformation of Epdcs, while Tgfβ isoforms inhibit it (Morabito et al., 2001).

SLUG is a zinc-finger transcription factor, expressed by many cell types undergoing epithelial–mesenchymal transformation and is expressed prior to the epithelial–mesenchymal transformation by epicardial cells. In the chick, all epicardial cells are Slug-positive from their differentiation as epicardium until stage 24 (Carmona et al., 2000). The *C-ETS-1* PROTO-ONCOGENE codes for a transcription factor that activates some of the genes involved in degradation of extracellular matrices and cell migration. C-ets-1 is expressed in the proepicardium where it activates UROKINASE-TYPE PLASMINOGEN ACTIVATOR and MATRIX METALLOPROTEINASES. These factors play a crucial role in the mesenchymal transformation of the subepicardial mesenchyme (Macias et al., 1998). Fog2, a cofactor for Gata transcription factors, plays an unknown role in the transformation of epicardial cells (Crispino et al., 2001; Tevosian et al., 2000). Mice lacking Fog2 form an intact epicardial layer and express epicardium-specific genes normally. However, markers of cardiac vessel development do not appear subsequently, suggesting that there is a failure in epicardial epithelial–mesenchymal transformation (Tevosian et al., 2000). Transgenic re-expression of Fog2 in cardiomyocytes rescues the *Fog2*-null vascular phenotype, demonstrating that Fog2 function is required in the myocardium rather than the epicardium for coronary vessel development. Tenascin-X, a glycoprotein, is expressed in migrating epicardial cells and then is localized to the developing blood vessels and cardiac fibroblasts derived from the epicardium. It is most likely involved in cell-substrate adhesion needed for migration of the transformed cells (Burch et al., 1995).

Cells that have undergone epithelial–mesenchymal transformation invade the myocardium and undergo differentiation into coronary smooth muscle, endothelial cells, and subendocardial fibroblasts (Fig. 10.6). The cells are induced to various cell lineages by different factors. Vegf and Fgfs induce the cells toward hemangioblast cell lines that produce endothelial and hematopoietic cells. Pdgf and Tgfβ induce the cells toward myofibroblast lineages that become either fibroblasts or vascular smooth muscle cells (Fig. 10.7). Hypoxia may drive Vegf expression in the epicardium and underlying compact layer of the myocardium. Because the myocardium receives its oxygen from the ventricular lumen the subepicardial myocardium, which is distant from the lumen is thought to be more hypoxic than myocardium near the lumen; this gradient would then drive the transmural vascularization process (Tomanek et al., 1999).

That the endothelial cells forming the endothelial plexus arise from the epicardium was first shown using retroviral lineage tracing (Mikawa and Fischman, 1992). This was quickly confirmed in quail-to-chick chimeras (Poelmann et al., 1993). Even though there is no evidence that all of the coronary vascular endothelial cells are generated from the epicardium, this is generally held to be the case. The commitment of epicardially-derived cells into an endothelial lineage is controlled by Vegf and Fgf2 signaling (Tomanek et al., 1998, 2001).

Serum response factor (Srf) promotes expression of smooth muscle α-actin in the coronary vascular smooth muscle cells. Smooth muscle α-actin is the first smooth muscle gene to appear, after which the cells show rearrangement of

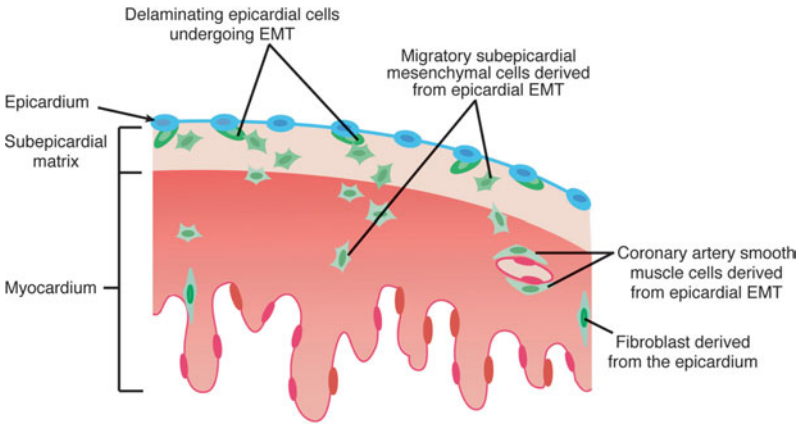

Figure 10.6. Migration of smooth muscle cells from the epicardium and formation of the smooth muscle tunica media of the coronary vessels.

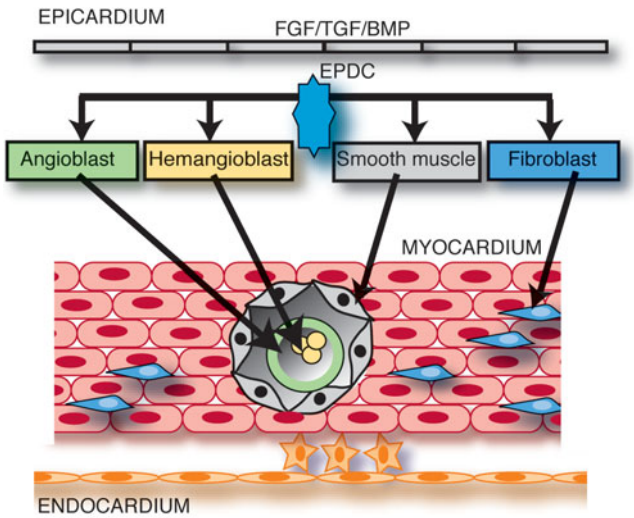

Figure 10.7. Proposed model of differentiation of epicardially-derived cells (EPDCs). BMPs and TGF-βs are involved in the induction of epithelial–mesenchymal transformation from the epicardium (*gray*). VEGF, FGF, PDGF, and TGFβ may play a role in the regulation of EPDC differentiation. VEGF and FGF induce the cells into angiogenic and hemangioblastic lineages. Hemangioblasts can differentiate as hematopoietic or endothelial cells. PDGF and TGFβ1 induce differentiation of EPDCs into fibroblast/smooth muscle lineages. The location of the various lineages with respect to the endocardium, myocardium, and epicardium is also indicated. (Adapted from Wessels and Perez-Pomares, 2004.)

cytoskeletal actin and form focal adhesions as they become motile. They begin to express other markers of smooth muscle differentiation including CAPSULIN, CALPONIN, SM22, and smooth muscle γ actin (Hidai et al., 1998; Landerholm et al., 1999). However, it is only later that smooth muscle myosin heavy chain can be detected (Landerholm et al., 1999). Capsulin, a bHLH-containing protein, is thought to be an ortholog of a *Drosophila* gene needed for differentiation of longitudinal visceral muscle. It can transactivate promoters that contain multiple E-boxes which are critical for transcription of genes needed for smooth muscle differentiation (Hidai et al., 1998).

BVES is a novel membrane protein expressed continuously by the proepicardium and the vascular smooth muscle derivatives (Wada et al., 2001). The bves protein accumulates at points of cell–cell contact and confers adhesive behavior to these cells. Neutralizing antibodies to bves inhibit migration of the vascular smooth muscle cells from the proepicardium (Wada et al., 2001).

A cell line has been developed from rat epicardium to study the characteristics of epicardial cells in culture. The cells express many of the markers of epicardium such as Wt1, Tbx18, Cx43, bves, and cytokeratins. The cells mimic epicardium in that they undergo epithelial–mesenchymal transformation in response to Egf or Fgfs and generate vascular elements including vascular smooth muscle (Wada et al., 2003). This cell line provides the potential to model development of the epicardium and its derivatives (Hatcher and Basson, 2003). Such modeling also provides the potential to develop artificial systems to generate new coronary arteries clinically. Interestingly, the cells form gap junctions with rat cardiomyocytes in culture, and the myocardial cells show increased expression of contractile proteins (Eid et al., 1992, 1994).

Epicardium Is Necessary for Myocardial Growth and Function

The epicardium is required for normal growth and maturation of the myocardium. If the epicardium fails to grow over the surface of the myocardium, as it does after certain genes have been deleted or if it is prevented mechanically, the embryo dies because of cardiac failure. This may be partly due to the absence of coronary vasculature, but there is also a direct trophic interaction of myocardium and epicardium that is necessary for myocardial growth. Without epicardium, the myocardium is thin and the ventricular septum fails to form properly.

In mouse embryos with null expression of *Wt1*, the proepicardium reaches the inflow end of the heart but never spreads to cover the atria, ventricles, and outflow myocardium (Moore et al., 1999). The myocardium fails to grow, and between E12.5 and 13.5, blood seeps into the pericardial cavity causing the embryos to die of heart failure.

α-4 Integrin and Vcam-1 are normally expressed in a reciprocal fashion in the epicardium and the underlying myocardium (Kwee et al., 1995). Vcam-1 is a cytokine-inducible cell surface protein capable of mediating adhesion to cells expressing α-4 integrins. In both α-4 integrin and Vcam-1 knockout mice, the embryos usually die early because the allantois fails to fuse with the chorion. Some embryos survive this but then die around E11.5–12.5 of cardiac failure with a phenotype similar to that of Wt1 because the epicardium and coronary vasculature fail to form (Yang et al., 1995). In both models, there is a reduction in the compact layer of the ventricular myocardium and an incomplete ventricular septum.

Retinoic acid signaling is important in the interaction of epicardium and myocardium to support myocardial growth. Interfering with retinoid signaling by genetic alteration of certain receptors (RXRα) or using retinoid receptor blockers causes a failure in formation of the compact zone even though the epicardium forms normally. Epicardial cells secrete Fgf9 that stimulates proliferation. The production of Fgf9 is induced by retinoic acid treatment and is inhibited by a retinoid receptor antagonist (Chen et al., 2002; Lavine et al., 2005). The Fgf signal is received by Fgf receptors (Fgfr) 1 and 2, which function redundantly in the myocardium. In the absence of retinoid or Fgf signaling, the myocardial cells undergo premature differentiation and fail to proliferate (Kastner et al., 1997; Lavine et al., 2005). In chick embryos where epicardial growth has been mechanically disrupted, the transmural pattern of myocyte proliferation is reduced along with expression of Fgf2 and Fgfr1 mRNA. The reduction is proportional to the extent of epicardial depletion (Pennisi et al., 2003).

Development of the Coronary Plexus

The formation of a functional coronary vasculature is essential for normal heart development. The coronary vasculature develops from an endothelial plexus that envelops the heart in the same temporospatial pattern as epicardium but with a delay accounted for by the epithelial-mesenchymal transformation and induction steps needed to generate endothelial cells. The plexus first assembles in the atrioventricular and ventricular-outflow tract junctions followed by the ventricles and atria. The outflow tract is the last to develop a "bulbar" plexus. Coronary circulation begins as venous sinusoids that connect with trabecular channels in the chick at stage 32. These trabecular channels connect with arterial vessels, producing a closed coronary circulatory system that is not completed until stage 41 (incubation day 14), long after septation is completed (Vrancken Peeters et al., 1997).

Construction of the coronary vasculature is by a mixture of vasculogenesis and angiogenesis (see Chapter 2). After the endothelial precursors are generated from the epicardium by epithelial–mesenchymal transformation and induced to be endothelial, they self-assemble, that is, undergo vasculogenesis. The plexus then grows by angiogenesis to provide circulation on a one-to-one basis with myocardial cells.

By stage 19 in the chick, epicardially derived cells populate the myocardium of the inner curvature. Migration into the myocardium appears to be restricted to the inner curvature between stages 19 and 22. The permissive myocardial environment expands to the atrioventricular canal, atrium, and ventricle at stages 23–24. Outflow tract myocardium is not permissive until stage 30 (Lie-Venema et al., 2005). This is a time when the outflow tract septum is well formed in the region of the truncus, and the conotruncal myocardium is being incorporated into the ventricles.

Differentiation of epicardially derived cells into vascular smooth muscle was also first reported based on retroviral lineage tracing and confirmed later using quail-to-chick chimeras (Mikawa and Fischman, 1992; Dettman et al., 1998; Gittenberger-de Groot et al., 1998). Endothelial cells may recruit and induce differentiation of the vascular smooth muscle.

The endothelial and vascular smooth muscle cells together form a coronary capillary plexus. As the myocardium develops, the nascent coronary capillary plexus displays a density gradient across the transmural axis of the myocardial wall, being higher on the outer, epicardial side than the inner, endocardial side (Tomanek et al., 1999). It has long been known that ectopic overexpression of FGFs in coronary vascular cell precursors promotes the formation and branching of coronary blood vessels in an autocrine manner, and recently this has led to the finding that a transmural FGF gradient correlates with the density of the capillary plexus (Hyer et al., 1999; Pennisi and Mikawa, 2005). Disruption of the gradient results in abnormal patterning in the density of the capillary plexus.

Development of the Coronary Stems and Coronary Sinus

The last step in coronary vascular development is ingrowth of multiple small vascular channels into the base of the aorta. The small vascular channels coalesce to form single coronary stems in the left and right coronary sinuses (Ando et al., 2004; Bogers et al., 1989; Waldo et al., 1990).

Many early investigations assumed the coronary stems actually sprouted from the aortic sinuses as capillary buds and that the endothelial buds then connected with the peritruncal ring (Aikawa and Kawano, 1982; Conte and Pellegrini, 1984; Hirakow, 1983; Hutchins et al., 1988).

However, this is not the case. The coronary artery ostia are present by about day 7 of chick development and these ostia are already connected via vascular channels with the peritruncal ring (Bogers et al., 1989). Each sinus receives multiple small vessels (Fig. 10.8) (Poelmann et al., 1993; Waldo et al., 1990). It was not clear from the early studies whether a single channel enlarges to form the coronary stem or if the multiple channels coalesce to form the stem. Recently, immunohistochemistry has shown that the multiple channels coalesce to form each coronary stem (Fig. 10.9) (Ando et al., 2004).

The origin of the smooth muscle tunics of the coronary stems is not known. However, disrupted patterning of the coronary stems is seen after secondary heart field ablation (Ward et al., 2005). In addition to producing myocardium, the secondary heart field generates smooth muscle at the base of the aorta (Waldo et al., 2005). Thus, it is possible, although still not shown, that the smooth muscle tunics of the coronary arteries derive from this region and this smooth muscle may be important in patterning the origins of the coronary arteries.

Figure 10.8. Left (LCA) and right coronary artery (RCA) development. *(A)* Multiple channels penetrate the aortic (Ao) wall in all of the aortic sinuses from the peritruncal ring. *(B)* Only the ones in the right and left sinuses survive and coalesce to form the main stems of the RCA and LCA. PT, pulmonary trunk; S, aorticopulmonary septum; g, cardiac ganglia. (From Waldo et al., 1990.)

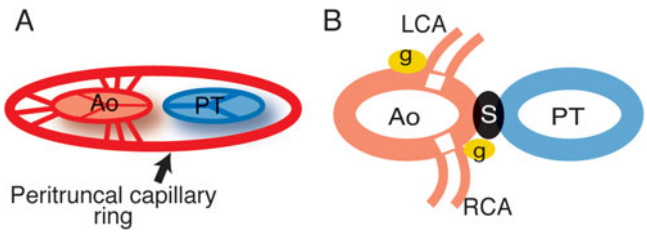

Figure 10.9. Confocal microscopic images of the developing small vessels penetrating the aorta at day 6 in the chick. At the onset of the formation of endothelial strands (*A*), QH1-positive endothelial progenitors (*arrows*) are seen in the aortic wall adjacent to the peritruncal ring (PR). At a later stage (*B*), QH1-positive cells (*arrowheads*) are connecting not only to the peritruncal ring but also to the aortic endothelium (E). LU, aortic lumen. (From Ando et al., 2004, with permission.)

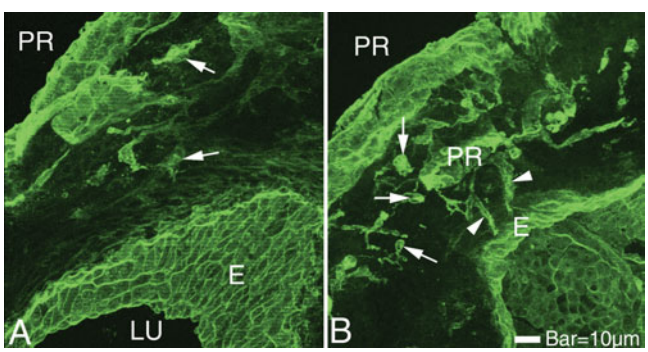

Coronary Artery Malformations

Congenital coronary artery anomalies occur in 0.2–1.2% of the general population (Angelini, 1989). Most of these anomalies do not cause myocardial ISCHEMIA, and they are often found incidentally during diagnosis and treatment of other diseases. Some are associated with poor myocardial PERFUSION (Reul et al., 2002).

Normal and anomalous coronary arteries have been classified by various criteria. A clinical classification has been proposed based on four classes of clinical significance: I—benign, II—relevant (related to myocardial ischemia), III—severe (related to sudden death), IV—critical (association of classes II and III with superimposed coronary artery disease) (Rigatelli et al., 2003). The classification most widely used is based on a report by the Society of Thoracic Surgeons–Congenital Heart Surgery Database Committee which classifies these anomalies in the following categories: (1) anomalous pulmonary origin, (2) anomalous aortic origin, (3) congenital atresia of the left main coronary artery, (4) coronary arteriovenous fistula, (5) coronary artery bridging, (6) coronary artery aneurysm, and (7) coronary stenosis. Of these, the 3 most common types of clinically significant coronary artery anomalies that are treated surgically are coronary arteriovenous fistula, anomalous pulmonary origin of the coronaries, and anomalous aortic origin of the coronaries (Dodge-Khatami et al., 2000).

Coronary Arteriovenous Fistulae

Coronary arteriovenous FISTULA describes a vessel that originates from a coronary artery and drains directly into a heart chamber, the pulmonary artery, the coronary sinus, or a pulmonary or central vein. This can occur in isolation or multiple times. The hemodynamic consequences depend on the site of drainage and the resistance in the fistula. Most fistulae originate from the right coronary artery and terminate in a right-sided heart chamber. However, fistulae can originate from the left coronary artery or any of its branches. A fistula may precipitate right- or left-heart volume overload, but it may also cause myocardial ischemia due to coronary artery steal, which results from preferential blood flow through the fistula (Reul et al., 2002).

Anomalous Pulmonary Origin

When one of the main coronary arteries originates from the pulmonary artery, myocardial perfusion is dependent on the extent of COLLATERAL CIRCULATION and, to a lesser degree, on the pulmonary vascular resistance. If a collateral network is not well established, patchy areas of ischemia and fibrosis develop, which interfere with ventricular function. This can lead to ventricular aneurysms and/or mitral REGURGITATION. If the collateral network is well developed by the time the pulmonary vascular resistance falls at birth, the region supplied

by the anomalous artery is perfused by collaterals. This is essentially a functional single coronary system. Blood flow in the anomalous artery can become reversed, and then preferential blood flow into the low-pressure pulmonary artery results in coronary steal, which again leads to myocardial ischemia (Reul et al., 2002).

Anomalous Aortic Origin

Anomalous origin of either the right or left coronary artery from the non-coronary aortic sinus is often completely asymptomatic; however, if this occurs in athletes, it can cause angina or sudden death. The proximal portion of the anomalous coronary artery frequently exits the aorta at an acute angle, which creates functional or actual stenosis of the artery. The proximal portion of the anomalous artery can also travel between the roots of the aorta and pulmonary artery. In this case, during exertion, the anomalous artery may be blocked by expansion of the pulmonary artery against the aorta. The proximal anomalous artery may tunnel through the wall of the aorta for a variable distance, resulting in narrowing of the lumen.

Single Coronary Artery

Single coronary artery is a rare anomaly that is associated with sudden cardiac death (Fig. 10.10). Usually the left main coronary stem originates from the proximal right coronary artery and passes posterior and inferior to the aortic root. Similar to problems with a coronary originating from the noncoronary sinus, the angle at the origin compromises coronary blood flow (Kuon and Ropers, 2004).

Figure 10.10. Image obtained by retrospectively gated multislice computed tomographic coronary angiography shows a single coronary artery originating from the right aortic sinus. *Left panel* shows a view from the apex. The left anterior descending coronary artery (LAD) courses in front of the pulmonary artery (PA). *Right panel* is a view from behind and cranial to the heart. The left circumflex coronary artery (LCX) courses behind the aorta (AO). Portions of the left atrium (LA) and right atrium (RA) have been electronically removed. LV, left ventricle; RCA, right coronary artery; RV, right ventricle. (From Deibler et al., 2004, with permission.)

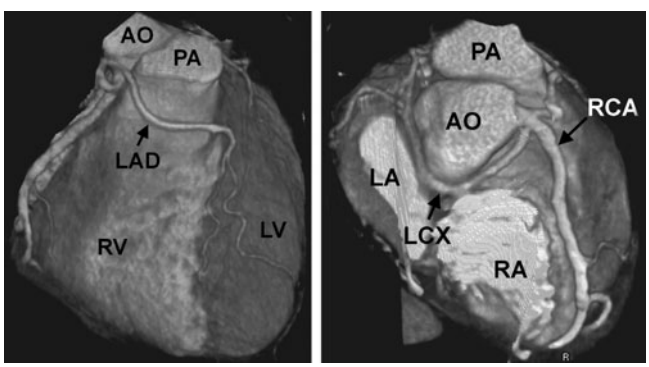

Double Left Anterior Descending Coronary Artery

Double left anterior descending coronary artery is a very rare anomaly that has been described in only five cases. In this case an anterior descending arises from both the left and right coronary arteries (Turhan et al., 2004).

REFERENCES

Aikawa, E., and J. Kawano. 1982. Formation of coronary arteries sprouting from the primitive aortic sinus wall of the chick embryo. Experientia 38:816–818.

Ando, K., Y. Nakajima, T. Yamagishi, S. Yamamoto, and H. Nakamura. 2004. Development of proximal coronary arteries in quail embryonic heart: multiple capillaries penetrating the aortic sinus fuse to form main coronary trunk. Circ. Res. 94:346–352.

Angelini, P. 1989. Normal and anomalous coronary arteries: definitions and classification. Am. Heart J. 117:418–434.

Bogers, A. J. J. C., A. C. Gittenberger-de Groot, R. E. Poelmann, and H. A. Huysmans. 1989. Development of the origin of the coronary arteries, a matter of ingrowth or outgrowth? Anat. Embryol. 180:437–441.

Burch, G. H., M. A. Bedolli, S. McDonough, S. M. Rosenthal, and J. Bristow. 1995. Embryonic expression of tenascin-X suggests a role in limb, muscle, and heart development. Dev. Dyn. 203:491–504.

Carmona, R., M. Gonzalez-Iriarte, D. Macias, J. M. Perez-Pomares, L. Garcia-Garrido, and R. Munoz-Chapuli. 2000. Immunolocalization of the transcription factor Slug in the developing avian heart. Anat. Embryol. 201:103–109.

Carmona, R., M. Gonzalez-Iriarte, J. M. Perez-Pomares, and R. Munoz-Chapuli. 2001. Localization of the Wilm's tumour protein WT1 in avian embryos. Cell Tissue Res. 303:173–186.

Chen, T. H., T. C. Chang, J. O. Kang, B. Choudhary, T. Makita, C. M. Tran, J. B. Burch, H. Eid, and H. M. Sucov. 2002. Epicardial induction of fetal cardiomyocyte proliferation via a retinoic acid-inducible trophic factor. Dev. Biol. 250:198–207.

Conte, G., and A. Pellegrini. 1984. On the development of the coronary arteries in human embryos, stages 14–19. Anat. Embryol. 169:209–218.

Crispino, J. D., M. B. Lodish, B. L. Thurberg, S. H. Litovsky, T. Collins, J. D. Molkentin, and S. H. Orkin. 2001. Proper coronary vascular development and heart morphogenesis depend on interaction of GATA-4 with FOG cofactors. Genes Dev. 15:839–844.

Deibler, A. R., R. S. Kuzo, M. Vohringer, E. E. Page, R. E. Safford, J. N. Patron, G. E. Lane, R. L. Morin, and T. C. Gerber. 2004. Imaging of congenital coronary anomalies with multislice computed tomography. Mayo Clin. Proc. 79:1017–1023.

Dettman, R. W., W. Denetclaw, Jr., C. P. Ordahl, and J. Bristow. 1998. Common epicardial origin of coronary vascular smooth muscle, perivascular fibroblasts, and intermyocardial fibroblasts in the avian heart. Dev. Biol. 193:169–181.

Dettman, R. W., S. H. Pae, C. Morabito, and J. Bristow. 2003. Inhibition of α4-integrin stimulates epicardial-mesencymal transformation and alters migration and cell fate of epicardially derived mesenchyme. Dev. Biol. 257:315–328.

Dodge-Khatami, A., C. Mavroudis, and C. L. Backer. 2000. Congenital heart surgery nomenclature and database project: anomalies of the coronary arteries. Ann. Thorac. Surg. 69:S270–297.

Eid, H., M. L. de Bold, J. H. Chen, and A. J. de Bold. 1994. Epicardial mesothelial cells synthesize and release endothelin. J. Cardiovasc. Pharmacol. 24:715–720.

Eid, H., D. M. Larson, J. P. Springhorn, M. A. Attawia, R. C. Nayak, T. W. Smith, and R. A. Kelly. 1992. Role of epicardial mesothelial cells in the modification of phenotype and function of adult rat ventricular myocytes in primary coculture. Circ. Res. 71:40–50.

Funato, N., K. Ohyama, T. Kuroda, and M. Nakamura. 2003. Basic helix-loop-helix transcription factor epicardin/capsulin/Pod-1 suppresses differentiation by negative regulation of transcription. J. Biol. Chem. 278:7486–7493.

Gittenberger-de Groot, A. C., M. P. F. M. Peeters, M. Bergwerff, M. M. T. Mentink, and R. E. Poelmann. 2000. Epicardial outgrowth inhibition leads to compensatory mesothelial outflow tract collar and abnormal cardiac septation and coronary formation. Circ. Res. 87:969–971.

Gittenberger-de Groot, A. C., M. P. F. M. Peeters, M. M. T. Mentink, R. G. Gourdie, and R. E. Poelmann. 1998. Epicardium-derived cells contribute a novel population to the myocardial wall and the atrioventricular cushions. Circ. Res. 82:1043–1052.

Hatcher, C. J., and C. T. Basson. 2003. Modeling development of the epicardium and coronary vasculature-In vitro veritas? Circ. Res. 92:477–479.

Hatcher, C. J., N. Y. S.-G. Diman, M.-S. Kim, D. Pennisi, Y. Song, M. M. Goldstein, T. Mikawa, and C. T. Basson. 2004. A role for tbx5 proepicardial cell migration during cardiogensis. Physiol. Genomics 18:129–140.

Hatcher, C. J., M. M. Goldstein, C. S. Mah, C. S. Delia, and C. T. Basson. 2000. Identification and localization of tbx5 transcription factor during human cardiac morphogenesis. Dev. Biol. 219:90–95.

Hidai, H., R. Bardales, R. Goodwin, T. Quertermous, and E. E. Quertermous. 1998. Cloning of capsulin, a basic helix-loop-helix factor expressed in progenitor cells of the pericardium and the coronary arteries. Mech. Dev. 73:33–43.

Hirakow, R. 1983. Development of the cardiac blood vessels in staged human embryos. Acta Anat. (Basel) 115:220–230.

Hiruma, T., and R. Hirakow. 1989. Epicardium formation of chick embryonic heart: computer-aided reconstruction, scanning, and transmission electron microscopic studies. Am. J. Anat. 184:129–138.

Ho, E., and Y. Shimada. 1978. Formation of the epicardium studied with the scanning electron microscope. Dev. Biol. 66:579–585.

Holly, S. P., M. K. Larson, and L. V. Parise. 2000. Multiple roles of integrins in cell motility. Exp. Cell Res. 261:69–74.

Hutchins, G. M., A. Kessler-Hanna, and G. W. Moore. 1988. Development of the coronary arteries in the embryonic human heart. Circulation 77:1250–1257.

Hyer, J., M. Johansen, A. Prasad, A. Wessels, M. L. Kirby, R. G. Gourdie, and T. Mikawa. 1999. Induction of Purkinje fiber differentiation by coronary arterialization. Proc. Natl. Acad. Sci. USA 96:13214–13218.

Kastner, P., N. Messaddeq, M. Mark, O. Wendling, J. M. Grondona, S. Ward, N. Ghyselinck, and P. Chambon. 1997. Vitamin A deficiency and mutations of RXRa, RXRb and RARa lead to early differentiation of embryonic ventricular cardiomyocytes. Development 124:4749–4758.

Komiyama, M., K. Ito, and Y. Shimada. 1987. Origin and development of the epicardium in the mouse embryo. Anat. Embryol. 176:183–189.

Komiyama, M., K. Ito, and Y. Shimada. 1996. Origin and development of epicardium in the mouse embryo. Anat. Embryol. 176:183–189.

Kraus, F., B. Haenig, and A. Kispert. 2001. Cloning and expression analysis of the mouse T-box gene *Tbx18*. Mech. Dev. 100: 83–86.

Kuhn, H.-J., and G. Liebherr. 1988. The early development of the epicardium in *Tupaia belangeri*. Anat. Embryol. 177:225–234.

Kuon, E., and D. Ropers. 2004. Single coronary artery—a rarity in the catheterization laboratory: case report and current review. Can. J. Cardiol. 20:647–651.

Kurkiewicz, T. 1909. O histogenezie miesna sercowego zwierzat kregowych-Zur Histogenese des Hersmuskels der Wilbertiere. Bull. Int. Acad. Sci. Cracovie 148–191.

Kwee, L., H. S. Baldwin, H. M. Shen, C. L. Stewart, C. Buck, C. A. Buck, and M. A. Labow. 1995. Defective development of the embryonic and extraembryonic circulatory systems in vascular cell adhesion molecule (VCAM-1) deficient mice. Development 121:489–503.

Landerholm, T. E., X. R. Dong, J. Lu, N. S. Belaguli, R. J. Schwartz, and M. W. Majesky. 1999. A role for serum response factor in coronary smooth muscle differentiation from proepicardial cells. Development 126:2053–2062.

Lavine, K. J., K. Yu, A. C. White, X. Zhang, C. Smith, J. Partanen, and D. M. Ornitz. 2005. Endocardial and epicardial derived FGF signals regulate myocardial proliferation and differentiation in vivo. Dev. Cell 8:85–95.

Lie-Venema, H., I. Eralp, S. Maas, A. C. Gittenberger-De Groot, R. E. Poelmann, and M. C. DeRuiter. 2005. Myocardial heterogeneity in permissiveness for epicardium-derived cells and endothelial precursor cells along the developing heart tube at the onset of coronary vascularization. Anat. Rec. 282:120–129.

Macias, D., J. M. Perez-Pomares, L. Garcia-Garrido, R. Carmona, and R. Munoz-Chapuli. 1998. Immunoreactivity of the ets-1 transcription factor correlates with areas of epithelial-mesenchymal transition in the developing avian heart. Anat. Embryol. 198: 307–315.

Manasek, F. J. 1969. Embryonic development of the heart. II. Formation of the epicardium. J. Embryol. Exp. Morphol. 22:333–348.

Manasek, F. J. 1970. Histogenesis of the embryonic myocardium. Am. J. Cardiol. 25:149–168.

Manner, J. 1992. The development of pericardial villi in the chick embryo. Anat. Embryol. (Berl.) 186:379–385.

Manner, J. 1999. Does the subepicardial mesenchyme contribute myocardioblasts to the myocardium of the chick embryo heart? A quail-chick chimera study tracing the fate of the epicardial primordium. Anat. Rec. 255:212–226.

Mikawa, T., and D. A. Fischman. 1992. Retroviral analysis of cardiac morphogenesis: discontinuous formation of coronary vessels. Proc. Natl. Acad. Sci. USA 89:9504–9508.

Mikawa, T., and R. G. Gourdie. 1996. Pericardial mesoderm generates a population of coronary smooth muscle cells migrating into the heart along with ingrowth of the epicardial organ. Dev. Biol. 174:221–232.

Mollier, S. 1906. Die erste Anlage des Herzens bei den Wirbeltieren. In: Handbuch der vergleichnden und experimentellen Entwincklungslehre der Wilbertiere, ed. Hertwig, O., 1026–1051. Jena: Gustav Fisher.

Moore, A. W., L. McInnes, J. Kreidberg, N. D. Hastie, and A. Schedl. 1999. YAC complementation shows a requirement for Wt1 in

the development of epicardium, adrenal gland and throughout nephrogenesis. Development 126:1845–1857.

Morabito, C. J., R. W. Dettman, J. Kattan, J. M. Collier, and J. Bristow. 2001. Positive and negative regulation of epicardial-mesenchymal transformation during avian heart development. Dev. Biol. 234:204–215.

Munoz-Chapuli, R., D. Macias, C. Ramos, V. de Andres, A. Gallego, and P. Navarro. 1994. Cardiac development in the dogfish (*Scyliorhinus canicula*): a model for the study of vertebrate cardiogenesis. Cardioscience 5:245–253.

Nahirney, P. C., T. Mikawa, and D. A. Fischman. 2003. Evidence for an extracellular matrix bridge guiding proepicardial cell migration to the myocardium of chick embryos. Dev. Dyn. 227:511–523.

Pennisi, D. J., V. L. T. Ballard, and T. Mikawa. 2003. Epicardium is required for the full rate of myocyte proliferation and levels of expression of myocyte mitogenic factors FGF2 and its receptor FGFR-1, but not for transmural myocardial patterning in the embryonic chick heart. Dev. Dyn. 228:161–172.

Pennisi, D. J., and T. Mikawa. 2005. Normal patterning of the coronary capillary plexus is dependent on the correct transmural gradient of FGF expression in the myocardium. Dev. Biol. 279: 378–390.

Perez-Pomares, J. M., D. Macias, L. Garcia-Garrido, and R. Munoz-Chapuli. 1997. Contribution of the primitive epicardium to the subepicardial mesenchyme in hamster and chick embryos. Dev. Dyn. 210:96–105.

Perez-Pomares, J. M., A. Phelps, M. Sedmerova, R. Carmona, M. Gonz lez-Iriarte, R. Munoz-Chapuli, and A. Wessels. 2002. Experimental studies on the spatiotemporal expression of WT1 and RALDH2 in the embryonic avian heart: a model for the regulation of myocardial and valvuloseptal development by epicardially-derived cells (EPDCs). Dev. Biol. 247:307–326.

Perez-Pomares, J. M., A. Phelps, M. Sedmerova, and A. Wessels. 2003. Epicardial-like cells on the distal arterial end of the cardiac outflow tract do not derive from the proepicardium but are derivatives of the cephalic pericardium. Dev. Biol. 227:56–68.

Pinco, K. A., S. Liu, and J. T. Yang. 2001. α4 integrin is expressed in a subset of cranial neural crest cells and in epicardial progenitor cells during early mouse development. Mech. Dev. 100:99–103.

Poelmann, R. E., A. C. Gittenberger-de Groot, M. M. T. Mentink, R. Bokenkamp, and B. Hogers. 1993. Development of the cardiac coronary vascular endothelium, studied with antiendothelial antibodies, in chicken-quail chimeras. Circ. Res. 73:559–568.

Reul, R. M., D. A. Cooley, G. L. Hallman, and G. J. Reul. 2002. Surgical treatment of coronary artery anomalies: report of a 37 1/2-year experience at the Texas Heart Institute. Tex. Heart Inst. J. 29:299–307.

Rigatelli, G., G. Docali, P. Rossi, D. Bovolon, D. Rossi, A. Bandello, G. Lonardi, and G. Rigatelli. 2003. Congenital coronary artery anomalies angiographic classification revisited. Int. J. Cardiovasc. Imaging 19:361–366.

Robb, L., L. Mifsud, L. Hartley, C. Biben, N. G. Copeland, D. J. Gilbert, N. A. Jenkins, and R. P. Harvey. 1998. Epicardin: a novel basic helix-loop-helix transcription factor gene expressed in epicardium, branchial arch myoblasts, and mesenchyme of developing lung, gut, kidney, and gonads. Dev. Dyn. 213:105–113.

Shimada, Y., E. Ho, and N. Toyota. 1981. Epicardial covering over myocardial wall in the chick embryo as seen with the scanning electron microscope. Scan. Elect. Microsc. II:275–280.

Tevosian, S. G., A. E. Deconinck, M. Tanaka, M. Schinke, S. H. Litovsky, S. Izumo, Y. Fujiwara, and S. H. Orkin. 2000. FOG-2, a cofactor for GATA transcription factors, is essential for heart morphogenesis and development of coronary vessels from epicardium. Cell 101:729–739.

Tomanek, R. J., K. Lotun, E. B. Clark, P. R. Suvarna, and N. Hu. 1998. VEGF and bFGF stimulate myocardial vascularization in embryonic chick. Am. J. Physiol. 274:H1620–H1626.

Tomanek, R. J., A. Ratajska, G. T. Kitten, X. P. Yue, and A. Sandra. 1999. Vascular endothelial growth factor expression coincides with coronary vasculogenesis and angiogenesis. Dev. Dyn. 215:54–61.

Tomanek, R. J., W. Zheng, K. G. Peters, P. N. Lin, J. S. Holifield, and P. R. Suvarna. 2001. Multiple growth factors regulate coronary embryonic vasculogenesis. Dev. Dyn. 221:265–273.

Turhan, H., R. Atak, A. R. Erbay, K. Senen, and E. Yetkin. 2004. Double left anterior descending coronary artery arising from the left and right coronary arteries: a rare congenital coronary artery anomaly. Heart Vessels 19:196–198.

Viragh, S., and C. E. Challice. 1981. The origin of the epicardium and the embryonic myocardial circulation in the mouse. Anat. Rec. 201:157–168.

Vrancken Peeters, M.-P. F. M., A. C. Gittenberger-de Groot, M. M. T. Mentink, J. E. Hungerford, C. D. Little, and R. E. Poelmann. 1997. The development of the coronary vessels and their differentiation into arteries and veins in the embryonic quail heart. Dev. Dyn. 208:338–348.

Wada, A. M., D. E. Reese, and D. M. Bader. 2001. Bves: prototype of a new class of cell adhesion molecules expressed during coronary artery development. Development 128:2085–2093.

Wada, A. M., T. K. Smith, M. E. Osler, D. E. Reese, and D. M. Bader. 2003. Epicardial/mesothelial cell line retains vasculogenic potential of embryonic epicardium. Circ. Res. 92:525–531.

Waldo, K. L., M. R. Hutson, C. C. Ward, M. Zdanowicz, H. A. Stadt, D. Kumiski, R. Abu-Issa, and M. L. Kirby. 2005. Secondary heart field contributes myocardium and smooth muscle to the arterial pole of the developing heart. Dev. Biol. 281:78–90.

Waldo, K. L., W. Willner, and M. L. Kirby. 1990. Origin of the proximal coronary artery stem and a review of ventricular vascularization in the chick embryo. Am. J. Anat. 188:109–120.

Wessels, A., M. W. M. Markman, J. L. M. Vermeulen, R. H. Anderson, A. F. M. Moorman, and W. H. Lamers. 1996. The development of the atrioventricular junction in the human heart. Circ. Res. 78:110–117.

Wessels, A., and J. M. Perez-Pomares. 2004. The epicardium and epicardially derived cells (EPDCs) as cardiac stem cells. Anat. Rec. 276:43–57.

Xavier-Neto, J., M. D. Shapiro, L. Houghton, and N. Rosenthal. 2000. Sequential programs of retinoic acid synthesis in the myocardial and epicardial layers of the developing avian heart. Dev. Biol. 219:129–141.

Yang, J. T., H. Rayburn, and R. O. Hynes. 1995. Cell adhesion events mediated by á4 integrins are essential in placental and cardiac development. Development 121:549–560.

11

Neural Crest, Great Arteries, and Outflow Septation

The neural crest is a population of multipotential cells that delaminate from the dorsal neural tube and migrate widely throughout the body. Based on the cells' axial level of origin from the neural tube, the neural crest is divided into cranial and trunk regions. Both cranial and trunk neural crest cells give rise to the peripheral nervous system and melanocytes. However, only cranial neural crest has the potential to give rise to "ECTOMESENCHYMAL" CELLS. Ectomesenchymal cells take part in development of a wide variety of structures in the head, neck, and heart. Because of the importance of neural crest-derived ectomesenchyme in heart development, a subregion of the cranial neural crest has been called "cardiac neural crest." Cardiac neural crest cells also support development and final patterning of the great arteries of the thorax. Neural crest cells are essential for modulating signaling in the caudal pharynx, which is important for normal development of the arterial pole of the heart (see Chapter 6). A subpopulation of cardiac neural crest cells migrates from the caudal pharynx into the cardiac outflow tract to form the aorticopulmonary septum, which divides the common arterial blood flow into pulmonary and systemic streams in animals with lungs. In addition to these roles of ectomesenchymal cells derived from neural crest, neural derivatives provide the innervation of the heart. Cardiac innervation is covered in Chapter 13.

Cardiac Neural Crest

Neural crest cells originate from the region of the neuroepithelium that borders the surface ectoderm. The neuroepithelium gives rise to the neural tube that forms the central nervous system. Crest cells are divided broadly into cranial and trunk based on their ability to give rise to ectomesenchyme: only cranial neural crest has this capacity. Cranial neural crest originates from the mid-diencephalon to somite 5, and trunk crest extends from somite 5 to the caudal tip of the neural tube (Fig. 11.1). Cardiac crest is a subdivision of the cranial crest. It originates in the neural folds spanning from the middle of the OTIC PLACODE to the caudal border of somite 3, corresponding to RHOMBOMERES 6, 7, and 8. The region of neural crest cells migrating to the heart was documented extensively using quail-chick chimeras and was called "cardiac neural crest," not because the cells migrated exclusively to the heart, but because they were found through ablation studies to be critical for normal heart development (Hutson and Kirby, 2003; Kirby et al., 1983, 1985). In some respects, the cardiac crest represents a transitional domain between the cranial and trunk regions of crest, because it shares some properties common to both regions. It generates ectomesenchyme like the cranial region of crest, and it lacks the ability for regeneration like trunk

Figure 11.1. The cardiac neural crest is the caudal part of the cranial crest. T, telencephalon; D, diencephalon; Mes, mesencephalon; Met, metencephalon; Mye, myelencephalon.

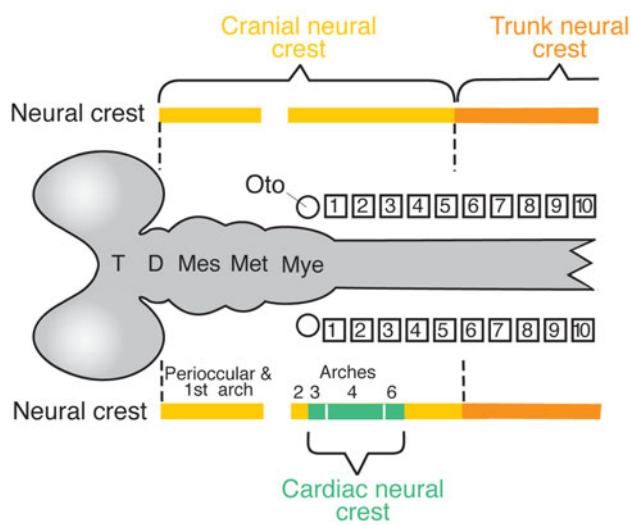

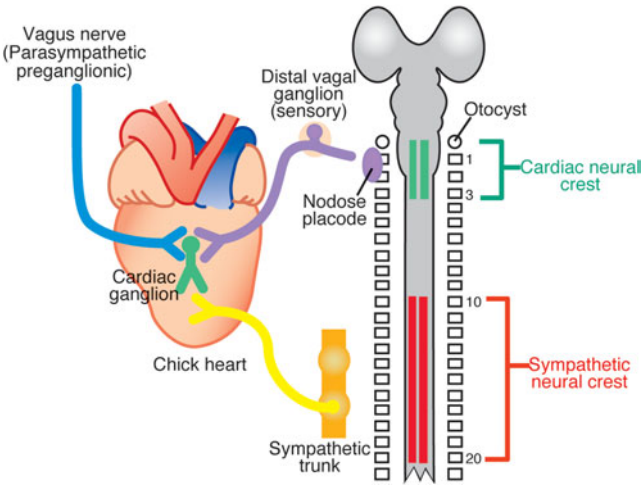

Figure 11.2. Derivatives of neural crest from two axial levels influence the heart. Cardiac neural crest (*green*) provides mesenchymal and neural elements. Trunk neural crest between somites 10 and 20 (*red*) provides the sympathetic innervation via the sympathetic trunks.

region of crest. Some of the pre-otic regions of crest are capable of remarkable feats of regeneration from the more ventral neural tube (Sechrist et al., 1995).

The cardiac neural crest provides all of the PARASYMPATHETIC INNERVATION to the heart (Fig. 11.2) (Kirby and Stewart, 1983). In addition, ectomesenchymal cells from the cardiac crest form the smooth muscle tunics of the great arteries and the connective tissue of glands in the neck—thymus, thyroid, and parathyroids (Bockman and Kirby, 1984; Jiang et al., 2002). Lastly, ectomesenchyme from the cardiac crest forms the aorticopulmonary septum that divides the outflow tract into systemic and pulmonary outlets (Kirby et al., 1983). Trunk neural crest provides sympathetic innervation but does not contribute to the structural development of the heart (Fig. 11.2).

Neural Crest Cell Migration

The neural crest cells migrate away from the neural tube in waves beginning around the time the neural tube closes. Cardiac neural crest cells require a wide variety of environmental signals in order to be specified, migrate, proliferate, differentiate, and survive. Specification of neural crest cells is dependent on signals from either the non-neural ectoderm, non-axial mesoderm, or both (LaBonne and Bronner-Fraser, 1999). One model of neural crest induction includes a double gradient of craniocaudal and mediolateral signaling (Aybar and Mayor, 2002). The craniocaudal gradient is formed by Wnt and Wnt inhibitors. The mediolateral gradient is formed by bone morphogenic protein (Bmp) signaling from the non-neural ectoderm. After neural tube closure, Bmps from the ectoderm, along with Wnts, fibroblast growth factor (Fgf), and retinoic acid from the node, are required for late induction of neural crest (Aybar and Mayor, 2002).

Although there is some discrepancy among the different animals used for study, neural crest specification generally involves the downregulation of Bmp signaling in the neural plate with an increase in Bmp signaling in the surface ectoderm, resulting in the activation of Slug in the cells at the border between the two tissues, which thus become specified as neural crest. Slug is a zinc finger transcription factor and one of the earliest markers expressed by neural crest cells. Other transcription factor families expressed by neural crest cells in the early specification/differentiation steps include PAX, FOX, Zic, SOX, and MEIS. Recent experiments suggest that neural crest specification may involve multiple successive inductions, with intermediate levels of Bmp signaling initiating the specification, and Wnt acting as a secondary signal (Garcia-Castro et al., 2002; Knecht and Bronner-Fraser, 2002).

In addition to a role in induction, Wnt signaling may also play a role in cardiac neural crest migration. Wnt1 is expressed in early migrating neural crest cells and is turned off as the cells migrate away from the neural tube. Mutations in the mouse *DISHEVELLED2* gene, another member of the Wnt signaling pathway, result in some of the same cardiac defects seen after cardiac neural crest ablation, including persistent truncus arteriosus (Hamblet et al., 2002). In these mutants, few neural crest cells are detected in the outflow tract and the pharyngeal arches. Dishevelled is thought to be involved in stabilizing microtubules needed to maintain cell polarity, an important feature in migrating cells.

Cardiac Neural Crest and Pharyngeal Patterning

Cardiac crest cells first migrate into the CIRCUMPHARYNGEAL RIDGE, where they pause while pharyngeal arches 3, 4 and 6 are formed (Figs. 11.3, 11.4, and 11.5). As each arch forms, the crest cells migrate in and surround the nascent aortic arch arteries that form from strands of endothelial cells initially attached to the pharyngeal endoderm (Fig. 11.6). Non-cardiac, cranial neural crest cells populate arches 1 and 2, where they mostly develop into skeletal elements in the arches. In contrast, the caudal arches (3, 4, and 6), which are populated by cardiac neural crest cells, are largely devoted to glandular and vascular development.

The parathyroid and thymus glands are generated from endoderm in the third pharyngeal pouch, and their development is dependent on an interaction of the neural crest and endoderm. The neural crest cells in arches 3 and 4 induce endoderm to form the glands. Communication is two way because neural crest patterning is influenced by signals from the endoderm (Ruhin et al., 2003). It appears that the Hox code carried by neural crest cells into the caudal arches is also important in patterning, as altering *Hox* gene expression in

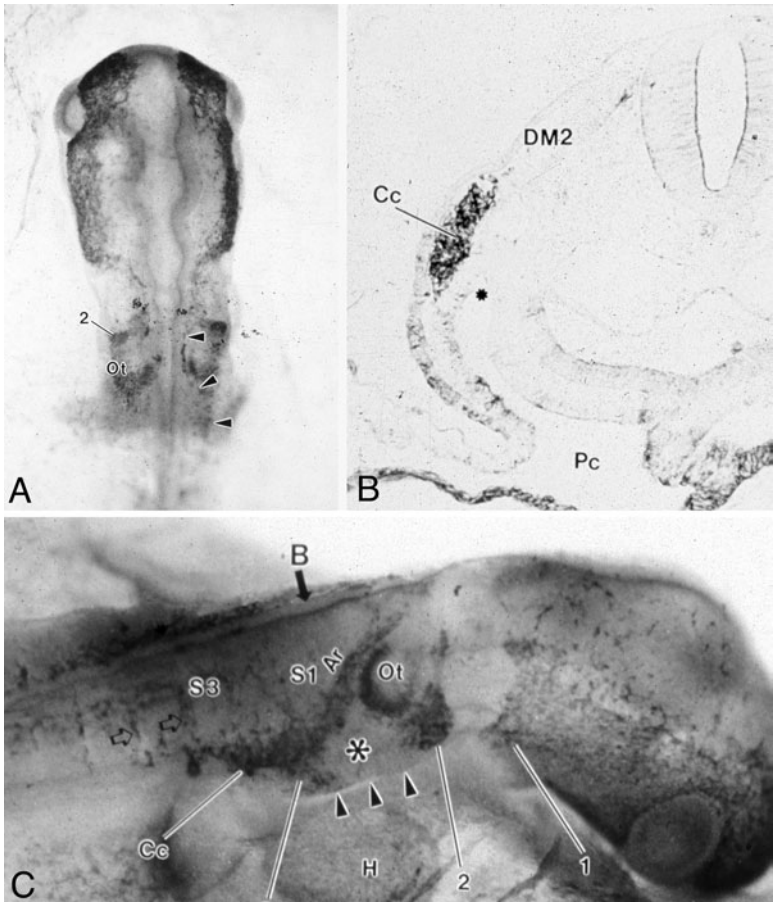

Figure 11.3. Cardiac neural crest cells, seen after neurofilament immunostaining, originate from the postotic rhombomeres and migrate from the neural tube to the circumpharyngeal ridge (*arrowheads* in *A* and dark cells in *C*). Some of the cells have already migrated into pharyngeal arch 3. The cells in the circumpharyngeal ridge will migrate into arches 4 and 6 as they form. *Asterisk* in *B* shows the position of arch 2. Ot, otocyst; Cc, circumpharyngeal crest; Da, Dorsal aorta; Ph, Pharynx; Pc, Pericardial cavity, S1, somite 1. (From Kuratani and Kirby, 1991, with permission.)

Figure 11.4. Migration of the cardiac neural crest to the circumpharyngeal ridge, caudal pharyngeal arches (3–6), and outflow tract depicted schematically. S1, S2, S3, S4, somites 1–4.

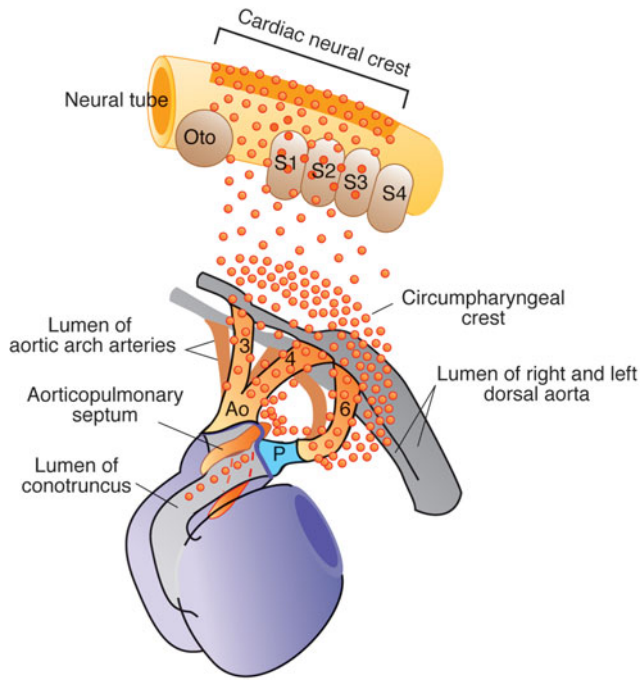

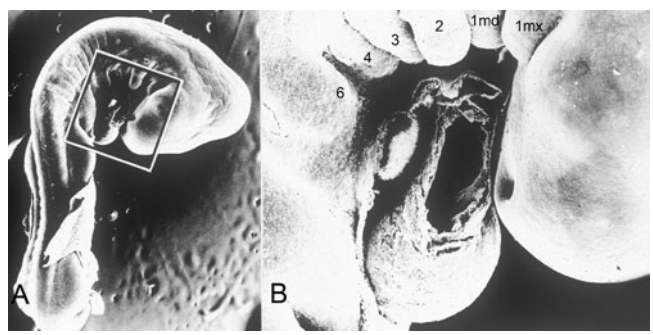

Figure 11.5. Scanning electron micrograph of the pharyngeal arches in a chick embryo. (*A*) Overview. The head is to the right. (*B*) Bulges are produced by cardiac neural crest in the pharyngeal arches. 1md, mandibular part of pharyngeal arch 1; 1mx, maxillary part of pharyngeal arch 1; 2–6, pharyngeal arches 2–6. (Courtesy of K. K. Sulik, Embryo Images at www.med.unc.edu/embryo_images/.)

neural crest cells before they migrate leads to abnormal patterning of the pharyngeal arches (Kirby et al., 1997).

The aortic arch arteries are a bilaterally paired series of arteries that connect the aortic sac ventrally with the initially paired dorsal aortas located dorsal to the foregut. These arteries

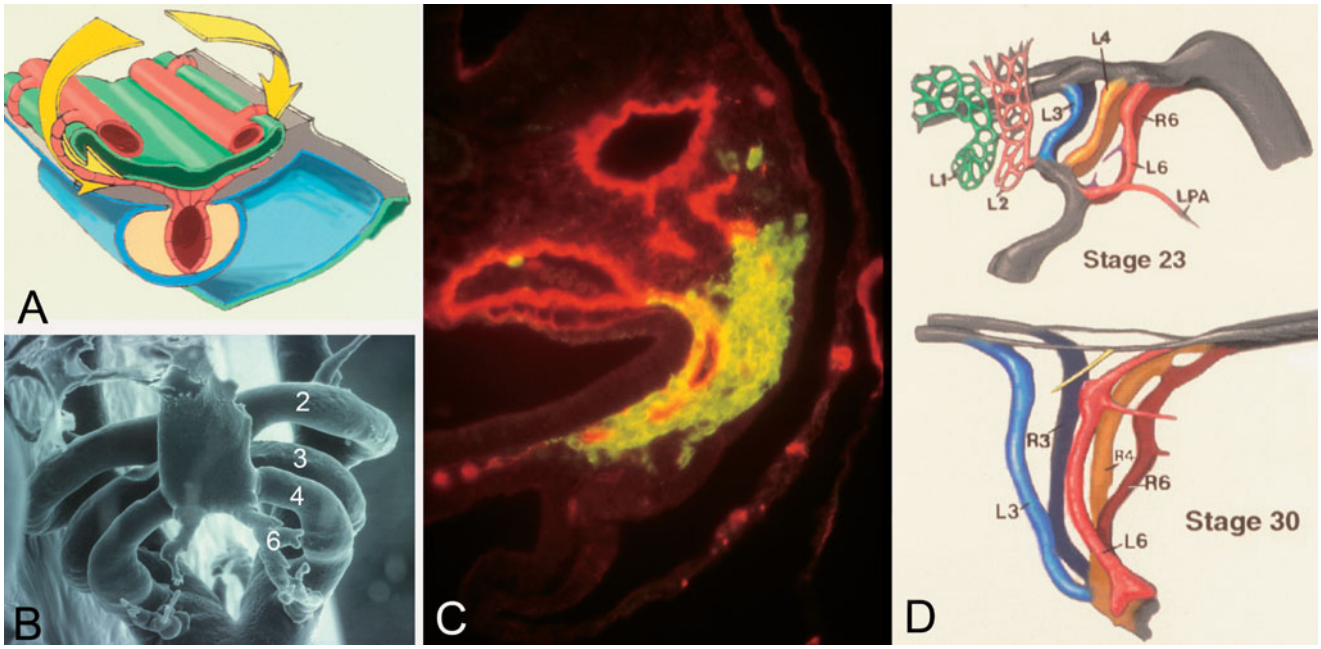

Figure 11.6. (*A*) Cardiac neural crest cells (*yellow arrows and yellow cells*) migrate into pharyngeal arches 3, 4, and 6 and surround the endothelial strands that will form the aortic arch arteries. (*B*) Aortic arch arteries form from cranial to caudal. Arch arteries 2, 3, and 4 are well formed with 6 in the process of forming. Arch artery 1 has already disappeared. (*C*) Neural crest cells (*yellow*) migrating into the third pharyngeal arch to surround the endothelial cells that will form arch artery 3 (*red*). (*D*) The aortic arch arteries seen from the side form in series and are bilaterally symmetrical. Neural crest cells are important in the remodeling from a bilaterally symmetrical series of arches to the asymmetric great arteries and form their smooth muscle tunics. (*B* from Bockman et al., 1987, with permission.)

develop from endothelial strands in the pharyngeal arches (Fig. 11.6). The interaction of crest cells with the aortic arch arteries is not necessary for formation of these arteries, but cardiac crest cells play an important role in repatterning of the initially bilaterally symmetrical arteries into the asymmetric great arteries (Fig. 11.6) (Bockman et al., 1987, 1989; Kirby et al., 1997; Waldo et al., 1996).

In fish, the aortic arch arteries remain bilaterally symmetrical gill arteries, and thus little remodeling is required to bring them to their mature pattern. However, in animals with divided pulmonary and systemic circulations, the caudal three aortic arch arteries are repatterned into the adult great arteries (see also Chapter 2). In avians and mammals, these include the common carotid, definitive aortic arch, and the ductus arteriosus. The repatterning steps that convert the bilaterally symmetrical aortic arch arteries to the great arteries are also dependent on the presence of neural crest cells in the caudal pharynx.

Endothelin signaling is thought to be involved in aortic arch artery patterning because mutations in the endothelin-1 (Et1) signaling pathway are associated with abnormal great artery development. The cognate receptor for Et1 ligand, called endothelin A (EtA), is expressed by neural crest cells in the pharyngeal arches (Clouthier et al., 1998, 2000, 2003; Morishima et al., 2003; Yanagisawa et al., 1998a,b). In addition, *EtA*-null ES cells are excluded from the walls of the aortic arch arteries, suggesting that neural crest cells require EtA to interact with the endothelium of the aortic arch arteries as they are forming (Clouthier et al., 2003). Little is known about the downstream effectors of endothelin signaling; however, the basic helix–loop–helix transcription factor Hand2 is one downstream effector of endothelin signaling in the pharyngeal arches. The Hand2 gene has an evolutionarily conserved enhancer with four homeodomain binding sites that are required for endothelin-activated activity in the pharyngeal arches. Dlx6, a member of the Distal-less family of homeodomain proteins, acts as an intermediary between endothelin signaling and Hand2 transcription (Charite et al., 2001). Unfortunately, we do not know the downstream effectors of Hand2 that allow an understanding of the neural crest–endothelial interactions for normal patterning and formation of the tunica media by the cardiac crest cells.

Haploinsufficiency for the transcriptional regulator Tbx1, by contrast, affects the initial growth and patterning of the arch arteries and is not associated with remodeling defects. Although there is no detectable defect in neural crest cells, the smooth muscle tunica media of the definitive aortic arch, which is derived from the fourth aortic arch artery, is reduced, suggesting that proliferation of the crest cells might be suboptimal (Kochilas et al., 2002; Lindsay et al., 2001; Morishima et al., 2003). Tbx1 is not expressed by the neural crest cells in the pharyngeal arches but rather by the pharyngeal endoderm, where it is an upstream regulator of endodermal Fgf8 expression (Yamagishi et al., 2003). Ectodermally expressed Fgf8 is necessary for initial development of the fourth aortic arch

artery because deletion of Fgf8 expression specifically from the pharyngeal ectoderm prevents development of the fourth arch arteries, which leads to interrupted arch. How Tbx1 expression relates to ectodermal Fgf8 expression is not known because Tbx1 is not co-expressed in the ectoderm with Fgf8 (Macatee et al., 2003).

Cardiac Neural Crest and Outflow Septation

Most of our knowledge of the distribution of cardiac neural crest cells in the heart comes from quail–chick chimeras. More recently, ADENOVIRAL and RETROVIRAL EXPRESSION VECTORS have been used to trace the cells, but because of the limited ability to confine these vectors to precise locations and abnormal cell death associated with them, the most reliable information is still from chimeras. Neural crest cells in chimeras rarely undergo cell death and are seen in the mature heart (Waldo et al., 1994). Retrovirally marked neural crest cells mostly die before the cardiovascular system is mature. The reason for this death is not known, but during the integration process, retroviruses can cause DNA damage that might result ultimately in cell death (Daniel et al., 2003).

In quail–chick chimeras, the cardiac neural crest cells are limited largely to the outflow tract. However, retrovirally labeled cells emigrate from the neural tube late and migrate to the inflow pole (Poelmann et al., 1998). These cells also die and their role in cardiovascular development remains to be elucidated.

After the cardiac neural crest cells migrate into arches 3, 4, and 6, they proliferate. A subset of the cells continues migrating into the cardiac outflow cushions (Fig. 11.4). The cushions themselves are ridges of mesenchyme that spiral into the outflow tract. The mesenchyme that populates the cushions migrates into the outflow tract from the pharynx. The neural crest cells follow these preformed cushions and collect as condensed cells in two columns or prongs centered in the distal or truncal outflow cushions (Fig. 11.7) (Waldo et al., 1998, 1999). The prongs are connected distally by a shelf of mesenchymal cells that protrude into the dorsal wall of the aortic sac. It is located between the origins of the fourth and sixth pairs of arch arteries and is thus correctly placed to separate the systemic from the pulmonary outflow (the fourth arch will become the arch of the aorta and the sixth arch will become the ductus arteriosus). The prongs end abruptly when they reach the proximal or conal portion of the outflow tract (Fig. 11.7). The prongs of condensed mesenchyme connected by the shelf of tissue in the aortic sac is called the aorticopulmonary septation complex (Waldo et al., 1998). This complex does not extend into the conus, where neural crest cells are dispersed subendocardially in no identifiable pattern.

Outflow septation occurs by three different mechanisms based on this initial configuration of neural crest cells (Waldo et al., 1998). The shelf protruding into the dorsal wall of the aortic sac provides the initial division between the systemic and pulmonary blood streams (Fig. 11.7). The shelf elongates into the distal outflow tract at the expense of the prongs. Because the prongs themselves spiral, the elongating shelf spirals. After the prongs are used in building the distal portion of the outflow septum in the aortic sac and truncus, the proximal outflow septum in the conus closes zipperlike from distal to proximal toward the ventricles. This appears to occur as the proximal (conal) cushions are myocardialized. MYOCARDIALIZATION takes place when invading myocardial cells cause the cushions to bulge into the lumen. The bulging cushions meet in the middle of the lumen. When they touch, the endocardium covering the cushions breaks down, allowing mixing of the underlying mesenchyme and myocardium and this brings about the fusion of the opposing cushions to form a septum (Fig. 11.7). Because the neural crest cells were subendocardial prior to the fusion, they now appear as a seam where the two cushions fused (Waldo et al., 1998, 1999). The process of myocardialization is induced by unidentified factors produced by the non-myocardial component of the outflow tract and can only be induced in the outflow myocardium during the period of outflow septation (Van den Hoff et al., 1999).

After division of the outflow tract, the mesenchyme that formed the truncal cushions is remodeled into an aortic and pulmonary semilunar valve. Each valve has three cusps or leaflets (Fig. 11.8). The cushions are comprised of mesenchyme, derived from the pharynx, from epithelial-mesenchymal transformation of the endocardium and from neural crest-derived ectomesenchyme (Fig. 11.9). While neural crest cells are located on the tips of the leaflets of the formed valves, their role in valve formation is not known. In the mouse, the earliest anlage of the valves can be seen at E11.5, as three pairs of ridges protruding into the lumen of the truncus. These early cusps consist of a core of mesenchymal tissue covered by the endocardium. From E12.5 to 14, excavation of the arterial face of the cusps results in thinning to the final shape (Fig. 11.9). The excavation process appears to be the result of selective growth of the free edges of the cusps due to an inductive interaction between the endocardium of the arterial face of the cusps and the underlying mesenchyme. The histogenesis of the cusps continues into the postnatal period (Hurle et al., 1980). In the chick, the formation of the valves begins between stages 26 and 29 from anlage consisting of three pyramidal shaped cusps formed by a core of loosely packed mesenchymal cells covered by a flattened endothelium. Between stages 30 and 35, the cusps are excavated on their distal face. The endothelium on the cushion invades the distal cushion by growing into it to create an arterial face. Cells are detached toward the bloodstream by cell death. Histogenesis of the valves occurs from stage 36 until hatching. During the histogenesis phase some myocardial cells invade the valvular tissue and a prominent fibrous layer is formed in the distal face of the cusps (Hurle, 1979).

Little is known about the factors that are involved in semilunar valve formation. Shear stress may play a role in remodeling the cushions to valve leaflets because interfering with blood flow alters endothelial morphology and causes malformation of the

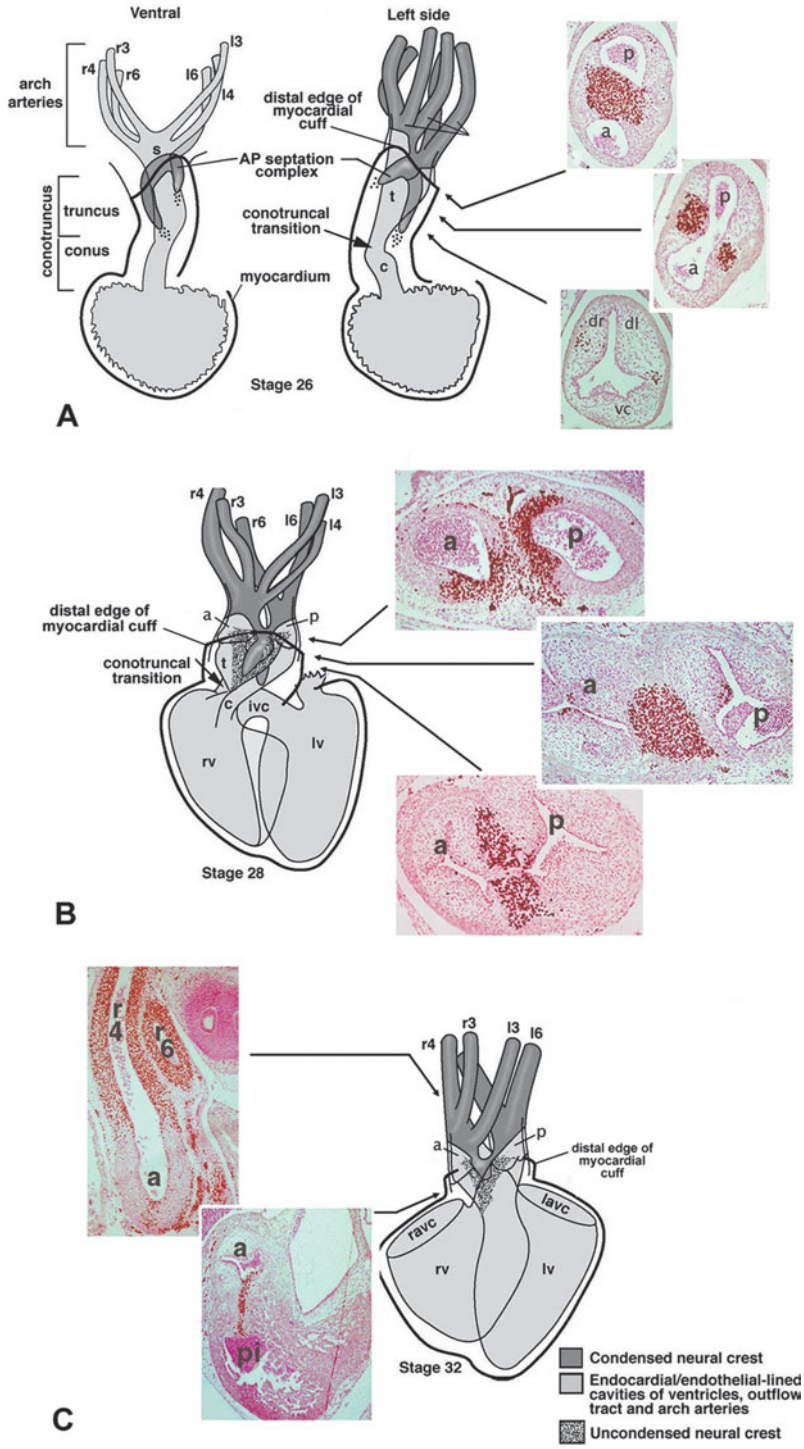

Figure 11.7. Schematic representation of outflow septation with accompanying histological sections of quail–chick chimeras to illustrate the position of neural crest cells during outflow septation. Quail cardiac neural crest cells are dark brown and chick cells are pink. (*A*) Position of the condensed mesenchyme (gray in the drawing and dark brown in the sections) of the aorticopulmonary septation complex. (*B*) The outflow myocardium has been partially incorporated into the right ventricle and the truncus divided at the level of the semilunar valves (a and p). (*C*) The conus after it has divided with a seam of neural crest cells remaining.
(From Waldo et al., 1998, with permission.)

aortic valve leaflets (Colvee and Hurle, 1983; Hurle and Colvee, 1983). Tenascin is present in zones specialized in bearing mechanical loads during semilunar valve formation (Garcia-Martinez et al., 1990). Nfatc1 is also required for formation of the outflow cushions and valves. Activation of Nfatc1 in human pulmonary valve endothelial cells is specific to vascular endothelial growth factor (Vegf) signaling through Vegf receptor 2. Vegf-induced Nfatc1 nuclear translocation is calcineurin dependent. Failure of nuclear translocation of Nfatc1 leads to reduced Vegf-induced human pulmonary valve endothelial cell proliferation (Johnson et al., 2003). During delamination of the valves, Bmp2, -4, and -6 mRNA are expressed at the vascular side of the forming semilunar valves (Somi et al., 2004). Engineering of a Bmp type II receptor that lacks half of the ligand-binding domain in mice results in reduced signaling capability and absent formation of the semilunar valves (Delot et al., 2003).

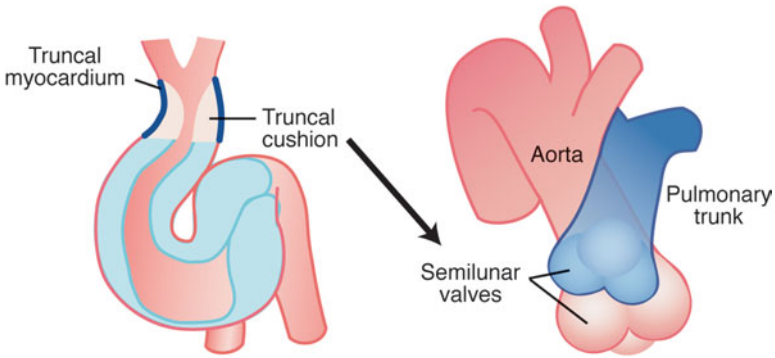

Figure 11.8. Remodeling of the distal or truncal outflow cushions to form the semilunar valves.

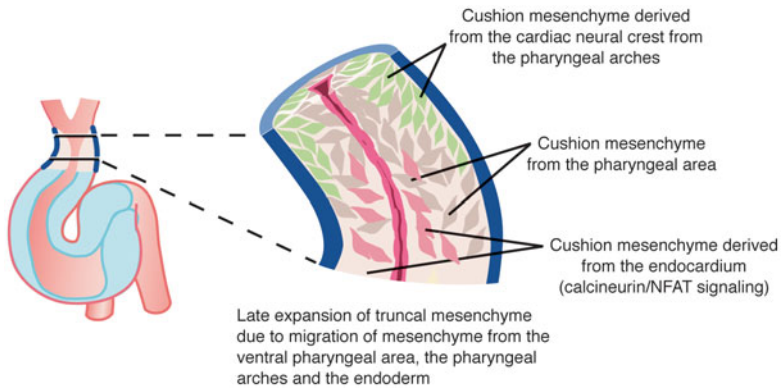

Figure 11.9. The distal outflow cushions are composed of mesenchyme from several different sources. These cushions are remodeled to form the semilunar valves.

In the pharynx, the aortic arch arteries are remodeled. In the chick the right and left aortic arch 3 become the right and left brachiocephalic arteries. In mouse and human, aortic arch arteries 3 form the common carotids. In the chick, the right fourth aortic arch artery becomes the aorta, while the left fourth aortic arch artery disappears. In mouse and human, the right fourth aortic arch artery becomes the base of the subclavian artery and the left fourth aortic arch artery becomes the arch of the aorta. In the chick, the sixth arch arteries become bilateral ductus arteriosus. In mouse and human, the left sixth aortic arch artery forms the ductus arteriosus and the right sixth aortic arch artery disappears (see Chapter 2).

After this remodeling is complete, the neural crest cells that have surrounded the arteries from the time they migrated into the pharyngeal arches now form a tunica media composed of vascular smooth muscle cells around each of the remodeled arteries (Le Lièvre and Le Douarin, 1975). However, these sheaths do not abut the myocardium. The most proximal walls of the aorta and pulmonary trunks are not covered by neural crest–derived tunics, leaving a gap. This gap of non-neural crest–derived smooth muscle cells is provided by cells from the secondary heart field that have interposed between the neural crest covering the artery that remains after repatterning and the outflow myocardium (Fig. 11.10; see also Fig. 6.11).

The pattern of migration and events in outflow septation appear to be very similar in mouse. Morris-Kay and colleagues used marking techniques in cultured rat embryos to show that neural crest cells did indeed migrate to the heart (Fukiishi and Morriss-Kay, 1992). However, a major advance for our understanding of mammalian cardiac neural crest came with transgenic methods that allowed the neural crest cells to be marked genetically. Lo and colleagues used a portion of the *Cx43* promoter driving *lacZ* to create a transgenic mouse with marked neural crest cells (Lo et al., 1997). Interestingly, the pattern of neural crest migration and participation in cardiovascular development reflected quail–chick chimeras very well (Lo et al., 1997, 1999; Waldo et al., 1999). Use of CRE RECOMBINASE (cre–lox) technology further refined the ability to track neural crest cells by cell lineage tracing in mouse embryos, and the most commonly used promoters to drive cre recombinase today are the *Wnt1cre, Pax3cre, P0cre, and PLEXINA2cre* (Fig. 11.11) (Brown et al., 2001; Jiang et al., 2000; Lee et al., 1997). While there are some differences in the patterns of labeled neural crest cells in these models (they have never been carefully compared), it is difficult to understand the precise differences and what they might mean. However, all of the models generally show the same cardiac neural crest patterns that were described for quail–chick chimeras.

Studies of cardiac neural crest in zebrafish embryos have shown that neural crest cells migrating into the heart may be capable of adopting a myocardial phenotype (Li et al., 2003; Sato and Yost, 2003). While the cardiac neural crest in zebrafish may originate from a slightly different axial level, its migration and final destination appear very similar to that in mouse and chick (Li et al., 2003). The fact that cardiac neural crest exists in the zebrafish is remarkable because the zebrafish cardiac

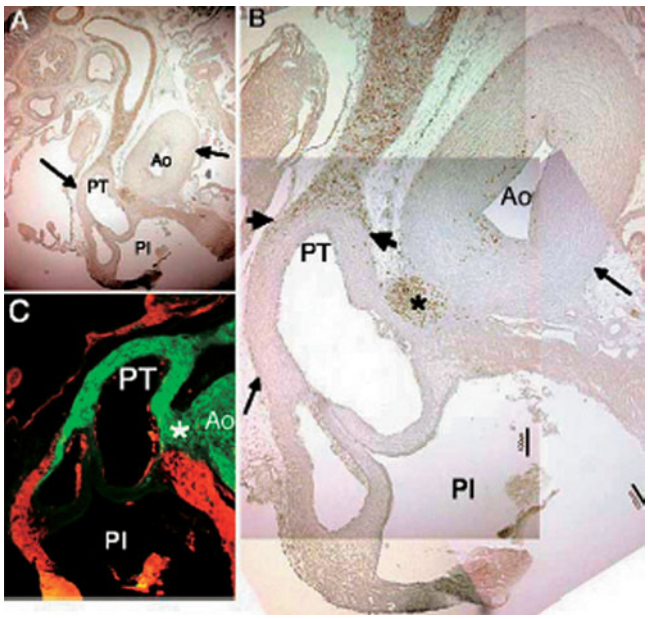

Figure 11.10. Smooth muscle at the base of the aorta and pulmonary trunk is not derived from cardiac neural crest. Day 11 quail-to-chick chimera stained with QCPN (quail cells—*brown*), MF20 (myocardium—*red*) and α-smooth muscle actin (smooth muscle—*green*). (*A*) A histological section of the pulmonary trunk (PT), pulmonary infundibulum (PI), and the proximal aorta (Ao). (*B*) A higher magnification of *A*. The proximal smooth muscle in the walls of the PT and Ao (*arrows*) are composed of non-cardiac neural crest cells, while the distal part of the PT is composed of neural crest cells. *Arrowheads* mark the transition. Remnant of the neural crest-derived aorticopulmonary (AP) septum (*). (*C*) The base of the PT and aorta consists of non-neural crest smooth muscle. (From Waldo et al., 2005, with permission.)

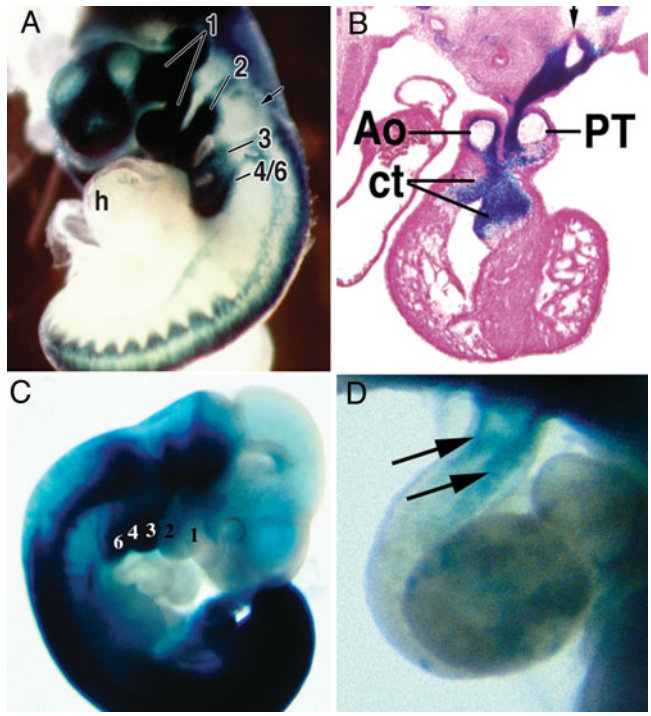

Figure 11.11. *Wnt1–cre* × *R26R* (*A* and *B*) and *Pax3–cre* × *R26R* (*C* and *D*) show cardiac neural crest in the pharynx and outflow tract (arrows) identical to the pattern of neural crest in quail–chick chimeras. Ao, aorta; PT, pulmonary trunk; ct, cushion tissue; h, heart; 1–6, pharyngeal arches (*Pax3–cre* from Epstein et al., 2000, with permission; *Wnt1–cre* from Jiang et al., 2000, with permission.)

output is directed to the gills, making septation of the outflow tract into pulmonary and systemic circulations unnecessary.

The Chick Ablation Model as a "Gold Standard" for Defects Caused by Cardiac Neural Crest

Ablation of the premigratory neural crest between the middle of the otic placode and somite 4 (Fig. 11.12) leads to a number of congenital defects that have provided much of our knowledge of cardiac neural crest function. The neural crest ablation model was the first reliable model of congenital heart defects in an experimental animal and has served as the "gold" standard for defining the pathogenesis of heart defects in other experimental models and in transgenic mice. Cardiac neural crest ablation leads to a number of cardiovascular and non-cardiovascular defects (Fig. 11.13). Non-cardiovascular phenotypes include hypoplasia or aplasia of the thymus, parathyroids, and occasionally the thyroid gland. This is thought to be due to a failure in interaction between the neural crest–derived mesenchyme and the pouch endoderm (Bockman and Kirby, 1984).

The cardiovascular phenotypes include three distinct components: (1) defective development of the cardiac outflow tract, (2) abnormal myocardial function, and (3) abnormal patterning of the great arteries.

Because conotruncal heart defects and thymic hypoplasia are part of the spectrum in several clinical syndromes, the speculation quickly was made that the "cardiac neural crest" was the embryogenic agent in the DiGeorge and velocardiofacial phenotypes (Kirby and Bockman, 1984; Van Mierop and Kutsche, 1986).

While several cardiac dysmorphologies have been reported after cardiac neural crest ablation, only those involving outflow or conotruncal defects are seen routinely, and these are the cardiac defects that have been investigated most thoroughly (Nishibatake et al., 1987). The morphological defects include complete absence of outflow septation (persistent truncus arteriosus, common trunk) and overriding aorta (Fig. 11.13). Overriding aorta is an alignment defect rather than a problem of septation and is linked with abnormal looping. In this defect the aorta overrides the ventricular septum such that blood entering the aorta is from both the right and left ventricles. The defect is always accompanied by a ventricular septal defect.

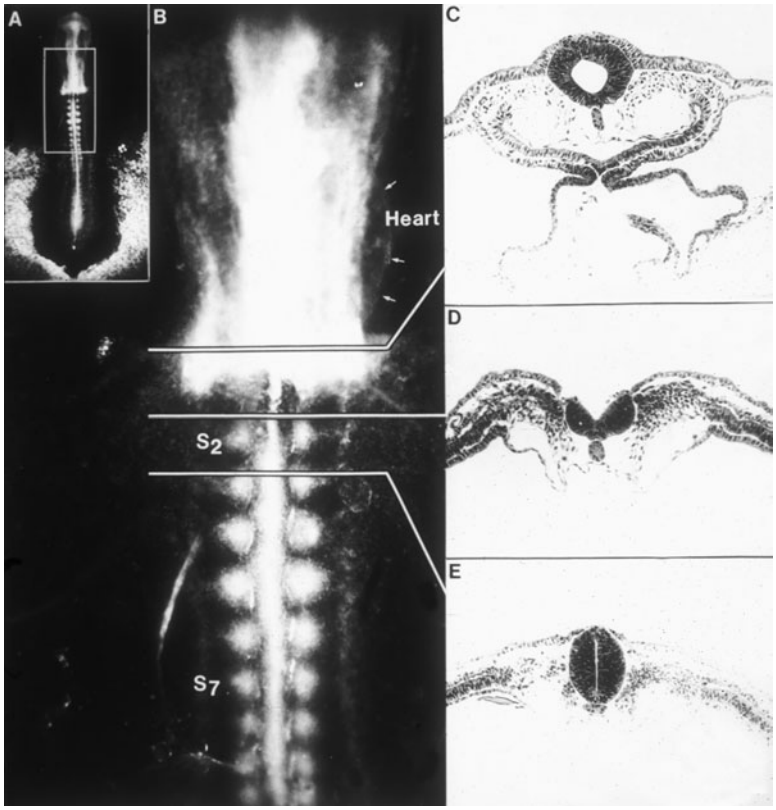

Figure 11.12. Cardiac neural crest ablation. *A* and *B* show a whole mount embryo at stage 11 that had the neural folds between the mid-otic placode and somite 3 ablated at stage 9. The notochord can be seen clearly where the neural folds were removed. *C–E* are transverse sections through the embryo at the levels indicated in B showing that only the neural folds and adjacent ectoderm have been removed. S_2, S_7, somites 2 and 7, respectively.

The early studies were definitive in showing that cardiac neural crest was physically responsible for generating or orchestrating outflow septation and that the cardiac phenotype produced directly by neural crest ablation was persistent truncus arteriosus (Kirby, 1987). However, embryogenesis of the other abnormalities, that is, abnormal myocardial function and looping, was more difficult to understand.

Myocardial Function and Looping are Compromised After Neural Crest Ablation

Myocardial dysfunction occurs before any sign of cardiac dysmorphogenesis in neural crest–ablated embryos (Farrell et al., 2001; Leatherbury et al., 1990). Ejection fraction is significantly depressed and the embryos that survive compensate by ventricular dilation, which maintains cardiac output in the normal range (Leatherbury et al., 1990; Tomita et al., 1991). Depressed contractility was hypothesized to be due to alterations in the aortic arch arteries, which are also affected by the ablation, but no changes in flow or pressure were ever found (Leatherbury et al., 1990). Even when aortic arch arteries are closed by laser ablation, no changes can be found in ventricular contractility (Kirby et al., unpublished data). The pattern of increased wall stress in the neural crest-ablated embryos is similar to that seen in humans with primary dilated cardiomyopathy (Leatherbury et al., 1990). These functional changes indicate that the myocardium is dysfunctional prior to the time when neural crest cells physically contact the heart. The underlying myocardial problems are depressed L-type calcium current, decreased calcium transient, excitation–contraction coupling, and calcium sensitivity of the contractile apparatus (Creazzo et al., 1998; Farrell et al., 2001).

In addition to primary myocardial dysfunction, looping is abnormal after neural crest ablation (Yelbuz et al., 2002). In fact, the outflow limb of the cardiac loop is shorter and straighter than normal and the trabeculated myocardium is seemingly pulled toward the point of outflow attachment to the pharynx (Fig. 11.14). This shortening is due to a failure of addition of myocardium to the outflow tract from the secondary heart field (Waldo et al., 2005). The cells that normally migrate from the secondary heart field proliferate rather than migrate and differentiate.

All of the cardiac defects caused by cardiac neural crest ablation can be rescued by replacing the cardiac neural crest (Fig. 11.15). Backtransplantation of cardiac crest that had been treated with control antisense or antisense RNA to *Hira,* a candidate DiGeorge gene, rescues myocardial function, arch artery patterning, and outflow alignment even though the embryos have persistent truncus arteriosus (Fig. 11.15) (Farrell et al., 1999). This was the first evidence that various portions of the cardiac neural crest–ablation phenotype could be separated and led to the idea that the ablation produces direct and indirect effects.

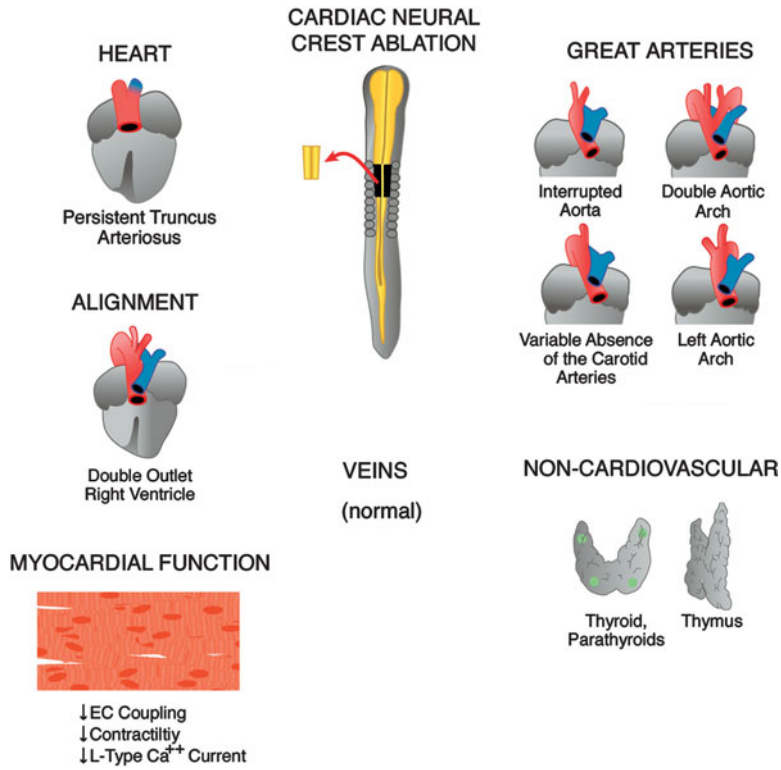

Figure 11.13. The morphological and functional consequences of cardiac neural crest ablation.

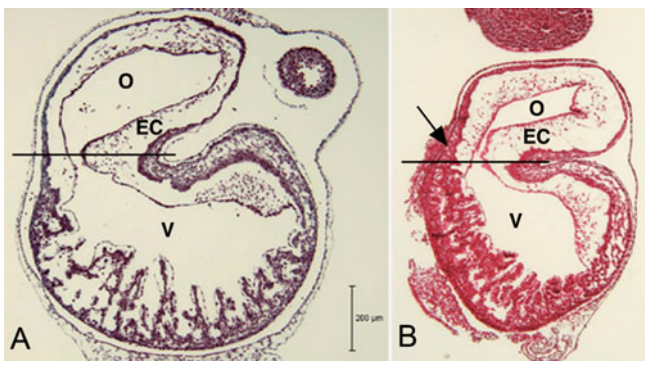

Figure 11.14. A and B show the position of the trabeculae which indicate the position of the right ventricular wall in a sham-operated embryo (A) and after neural crest ablation (B). The trabeculae are pulled into the outflow tract after neural crest ablation because of the shortened outflow tract. EC, endocardial cushion; V, ventricle; O, outflow tract. (Adapted from Yelbuz et al., 2002.)

Role of Neural Crest in Modulating Signaling in the Pharynx

The key to many of the early signs of primary myocardial dysfunction can be found in the pharynx. The onset of myocardial dysfunction coincides with the time when cardiac neural crest cells begin to migrate into pharyngeal arch 3 (Farrell et al., 2001; Waldo et al., 1996). The pharyngeal endoderm is a potent signaling center and is very important in early myocardial development. One of the signaling factors expressed by both the pharyngeal endoderm and ectoderm is Fgf8. The function of Fgf8 in the pharynx is still unknown, but it is one of the factors needed for initial induction of myocardial differentiation in the cardiogenic field. In the neural crest–ablated embryos, the ablation occurs too late to disrupt development of the myocardium that forms the initial heart tube. After neural crest ablation, elevated Fgf8 signaling can be measured in the pharynx during the time when the myocardium is being added from the secondary heart field (Fig. 11.16). Ablation of the secondary heart field itself results in malalignment of the outflow tract, that is, overriding aorta (Ward et al., 2005). After neural crest ablation, the excessive Fgf8 signaling can be neutralized by blocking antibodies or chemically inhibiting signaling with SU5402. Either of these treatments in neural crest–ablated embryos restores development of the myocardium from the secondary heart field. This leads to normal looping and normal outflow alignment (Hutson et al., 2005). By contrast, treatment of sham-operated embryos with either Fgf8 inhibitor also results in failure of myocardial development from the secondary heart field. The phenotype is similar to that of the *Fgf8* hypomorphic mouse that develops double outlet right ventricle and persistent truncus arteriosus (Abu-Issa et al., 2002; Frank et al., 2002). Fgf8, though not expressed by the neural crest, is thought to be a survival/proliferative factor for the neural crest cells as they migrate into the pharyngeal arches and the fact that persistent truncus arteriosus occurs in the hypomorphic mouse suggests that neural crest cells do not function normally to divide the outflow tract.

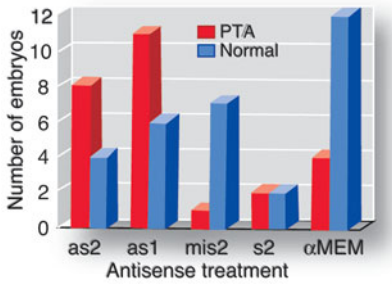

Hemodynamics in Backtransplanted Chick Embryos

Treatment	N	CO	HR (p<0.001)	EF (p=0.017)
αMEM	20	31±16	154±28	84±11
MIS	20	34±11	170±14	83±12
AS	23	41±18	166±23	84±9

Figure 11.15. After backtransplantation of premigratory cardiac neural crest the cells migrate in normal patterns. Treatment of premigratory neural crest with antisense to *Hira*, a DiGeorge candidate gene, results in persistent truncus arteriosus. Cardiac function and outflow alignment are normal even though the embryos have a severe outflow septation defect showing that cardiac function, outflow alignment, and outflow septation are under the control of different developmental processes related to neural crest cell function.

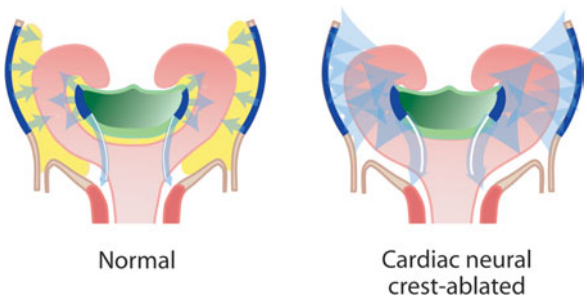

Figure 11.16. In a normal embryo (*left*) FGF8 (*blue*) is produced by the pharyngeal endoderm and ectoderm and neural crest cells (*yellow*) attenuate FGF8 signaling by an unknown mechanism. The FGF8 is excessive when neural crest does not arrive in the caudal pharynx (*right*) because of abnormal persistence of FGF8b isoform, suggesting an interaction between neural crest and the pharyngeal endoderm and/or ectoderm.

Phenocopies of the Cardiac Neural Crest Ablation in Mouse

Many genes have been associated with a neural crest ablation phenotype in transgenic and mutant mice (Bamforth et al., 2001; Brewer et al., 2002; Feiner et al., 2001). Two naturally occurring mutants, *Patch* and *Splotch*, show neural crest ablation phenotypes in a background of more severe abnormalities (Conway et al., 1997a–c; Epstein, 1996; Franz, 1989; Morrison-Graham et al., 1992). Homozygous Splotch embryos have myocardial dysfunction, similar to that seen after neural crest ablation, that causes embryonic lethality by 14.5 dpc (Fig. 11.17) (Conway et al., 1997c). They also have persistent truncus arteriosus, outflow malalignment, abnormally patterned aortic arch arteries, absent thymus, thyroid and parathyroids, SPINA BIFIDA, and abnormal pigmentation (Auerbach, 1954; Franz, 1989). *Pax3*, the gene mutated in *Splotch*, shows high expression in the dorsal neural tube and migrating cardiac neural crest cells. Expression diminishes as the cells populate arches 3, 4, and 6, and the cardiac outflow tract (Conway et al., 1997b; Epstein et al., 2000). Cre–lox technology has been used to fate map the *Pax3*-expressing cells in normal and Splotch mice. The neural crest cells migrate to the arches and outflow tract, but the cells are fewer in number than normal (Epstein et al., 2000). This suggests that *Pax3* is not necessary for migration of the cardiac neural crest but may play a role in expansion of the neural crest cell population. Therefore, as in the chick ablation model, a critical number of cardiac neural crest cells must reach the pharynx for control of pharyngeal signaling and then the outflow tract for proper septation. The paucity of neural crest cells in arches 3, 4, and 6 may phenocopy the failure of addition of the myocardium from the secondary heart field, as seen in the chick ablation model, resulting in the malalignment defects observed in the Splotch mouse (Conway et al., 2000; Yelbuz et al., 2002). Recently *Msx2*, a homeobox gene regulating Bmp signaling, has been shown to be a downstream effector of Pax3 (Kwang et al., 2002). Msx2 is upregulated in the Splotch mutant, and a loss of function *Msx2* mutation rescues the cardiac defect of the Splotch mutant embryos, as well as defects in the dorsal root ganglia, thymus, and thyroid (Kwang et al., 2002).

The advent of targeted knockouts in mouse led to the development of many models that recapitulate all or portions of the neural crest ablation phenotype in chick. The earliest knockout was of *Hoxa3*. The cardiac neural crest phenotype of this mouse is partial in that the glands derived from the third pharyngeal pouch are absent, and the third aortic arch artery is patterned abnormally (Chisaka and Capecchi, 1991; Kameda et al., 2002). However, the *Hoxa3* mutant mouse does not have any cardiac defects. It was later confirmed in chick that disrupted *Hox* expression is associated with abnormal patterning of the great arteries but not with outflow defects (Kirby et al., 1997).

Semaphorin 3C (Sema3C), one member of a family of secreted ligands that are important in axon guidance in the nervous system, is also important in the migration and targeting

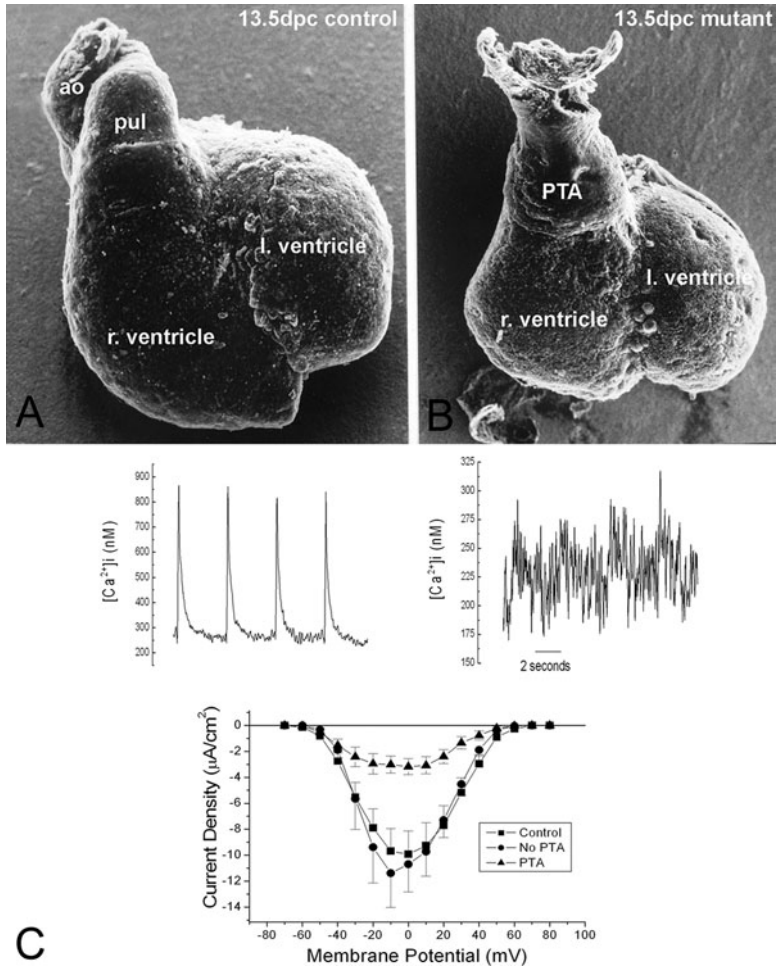

Figure 11.17. The phenotype of the Splotch mouse is similar to neural crest-ablation phenotype. (*A*) Normal outflow development in an E13.5 mouse. (*B*) Persistent truncus arteriosus (PTA) in a Splotch littermate. (*C*) Myocardial calcium transient (*upper graphs*) and L-type calcium current (*lower graph*). *Upper left panel* shows the calcium transient from a wild type E13.5 embryo as compared to the depressed transient in a Splotch homozygous mutant heart in the upper right panel. The lower panel illustrates a significant reduction in the L-type calcium current. (■) wild-type; (▽) Splotch mutant with PTA; (○) Splotch mutant without PTA. r. ventricle, right ventricle; l. ventricle, left ventricle; T, truncus; pul, pulmonary trunk; ao, aorta. (From Conway et al., 1997, with permission.)

of cardiac neural crest cells to the outflow tract. *Sema3C*-null mice have interrupted aortic arch and persistent truncus arteriosus (Fig. 11.18) (Feiner et al., 2001). However, other neural crest derivatives, like the dorsal root ganglia, are normal in Sema3C-null embryos, suggesting that Sema3C signaling is particularly important for cardiac neural crest. Sema3C is expressed in outflow myocardium. Semaphorins signal though a multimeric receptor complex Plexins and Neuropilin (Np)1 and/or Np 2. Plexin A2 is expressed specifically in the migratory as well as postmigratory cardiac neural crest derivatives in the outflow tract (Brown et al., 2001). The receptor complex of Np1 and PlexinA2 appears to be the functional receptor complex that signals the cardiac neural crest, as *Np1* nulls also have persistent truncus arteriosus and interrupted aortic arch (Kawasaki et al., 1999). Thus, it seems that cardiac neural crest cells are using guidance cues similar to those that axons use in the nervous system to target or guide themselves to the cardiac outflow tract.

Et1 is a paracrine factor thought to be important in patterning cardiac neural crest cell derivatives. Mutations or deletions of Et1, the endothelial converting enzyme (Ece1), or its receptor (EtA) result in aberrant patterning of the great vessels and the conotruncus in addition to defects in craniofacial patterning (Clouthier et al., 1998; Kurihara et al., 1994; Yanagisawa et al., 1998a,b). Ece1 is expressed in the pharyngeal ectoderm and in the arch artery endothelium, while the EtA receptor and Et1 ligand are expressed by the neural crest–derived pharyngeal mesenchyme as well as the ectoderm and endoderm (Clouthier et al., 1998; Kempf et al., 1998). Et signaling may play a role in patterning a subset of neural crest lineages. In chick, premigratory neural crest cells infected with a virus expressing the precursor protein for Et1 called preproEt1, undergo selective expansion of the adventitial cells but not the smooth muscle cells of the great arteries (Ballard and Mikawa, 2002). In *EtA*-null mice, the neural crest cells migrate but expression of several EtA-induced transcription factors, including goosecoid, Dlx2, Dlx3, Hand1, Hand2, and BARX1 are absent or reduced (Clouthier et al., 2000). EtA is a G-protein-coupled receptor. Double null mutation of $G\alpha_q$ and $G\alpha_{11}$ leads to a phenotype that is in all respects similar to the EtA-null phenotype, suggesting that these two subunits are responsible for downstream signaling from the EtA receptor (Ivey et al., 2003).

Tbx1 is a member of the T-box family of transcription factors related to brachyury, which is important in mesoderm formation. It is a candidate gene for the DIGEORGE phenotype and lies within the commonly deleted region of chromosome 22q11 associated with a large percentage of patients with DiGeorge

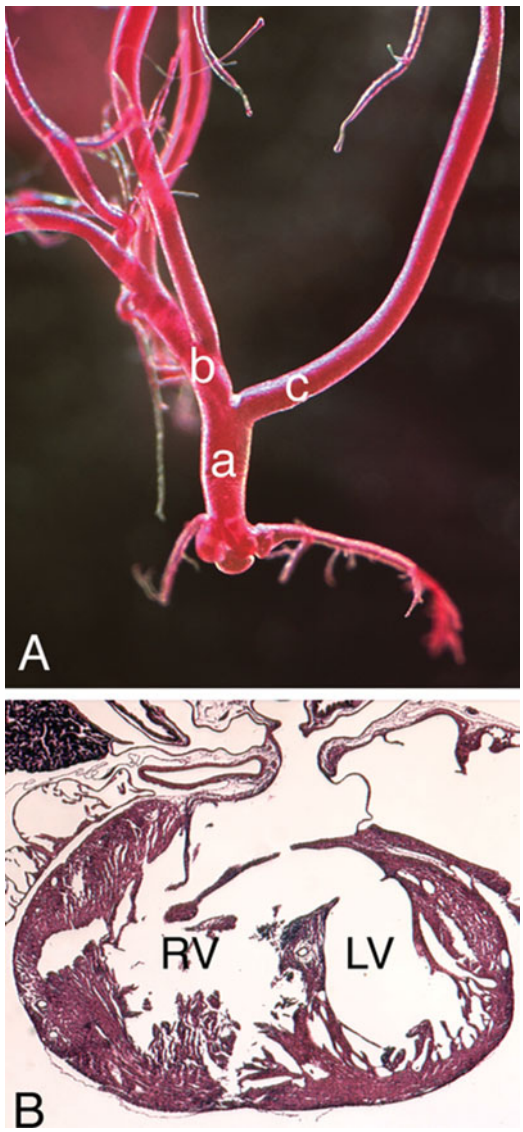

Figure 11.18. Semaphorin 3C null mutation in a mouse model with a phenotype similar to that seen after neural crest ablation. (*A*) Corrosion cast shows persistent truncus arteriosus and interrupted arch. (*B*) Large ventricular septal defect. a, aorta; b, right brachiocephalic; c, left carotid; LV, left ventricle; RV, right ventricle. (From Feiner et al., 2001, with permission.)

syndrome. *Tbx1* homozygous mutation causes multiple developmental defects, including cardiovascular, craniofacial, ear, thymus, and parathyroid defects. Mice haploinsufficient for Tbx1 have major defects in the growth and development of the aortic arch arteries, although outflow septation is normal, suggesting that the pharyngeal patterning is particularly sensitive for *Tbx1* dosage (Vitelli et al., 2002). At first glance one would predict from the phenotype that there is a primary defect in the cardiac neural crest cells, but Tbx1 is expressed in the pharyngeal endoderm and secondary heart field and not by neural crest cells. Tbx1 has been associated with proliferation of cells in the secondary heart field (Xu et al., 2004). *Tbx1* is at least one gene required for normal maturation of the aortic arches, and Tbx1 can rescue the cardiovascular defects in mice with a chromosomal microdeletion similar to the 22q11 microdeletion seen in many patients with DiGeorge syndrome. In addition, *Tbx1* mutations have been identified in humans with congenital heart defects (Yagi et al., 2003).

Foxc1 and Foxc2 are members of the forkhead family of transcription factors. These genes are also required for proper cardiovascular patterning. Foxc1 and Foxc2 have overlapping expression patterns in head mesoderm, endothelial, and mesenchymal cells of the developing heart, blood vessels, and somites. Embryos lacking *Foxc1* and/or *Foxc2* have COARCTATION of the aorta or interrupted aortic arch and ventricular septal defects (Iida et al., 1997; Kume et al., 2001; Winnier et al., 1999). In these animals, the arch vessels form and are initially patterned correctly, but the remodeling of the vessels, especially in the fourth arch, goes awry. The cardiovascular phenotype suggests that Foxc1 and Foxc2 play a part in the interactions between the aortic arch 4 endothelial cells and their surrounding cardiac neural crest cells.

The *Cx43* knockout has not been so straightforward to analyze. *Cx43* is a gap junction gene expressed by migrating neural crest cells. Gap junctions are intracellular junctions that allow the passage of signaling molecules, low molecular weight metabolites, and ions between cells. In addition, Cx43 has recently been shown to alter signaling in the Wnt pathway (Xu et al., 2001). *Cx43*-null mice die soon after birth because of right ventricular outflow obstruction, consisting of one or two pouches at the base of the pulmonary outflow (Reaume et al., 1995). This defect has never been seen in mice or chicks with neural crest ablation phenotypes. The migration rate and coupling of neural crest cells in *Cx43*-null embryos or in a dominant negative transgenic mouse (FC) are decreased. Thus, a reduced number of neural crest cells arrive in the heart. Overexpression of Cx43 specifically limited to neural crest cells results in an increased rate of migration and cell coupling, as well as increased neural crest cells in the outflow tract (Huang and Lo, 1998; Huang et al., 1998a,b; Xu et al., 2001). Interestingly, CMV43 mice, like the *Cx43*-null mice, have defects in the right ventricle and pulmonary outflow region although these defects are not identical to the knockout (Ewart et al., 1997; Huang and Lo, 1998; Huang et al., 1998b). Recent studies have shown that Cx43 is also essential for normal coronary vessel formation (Li et al., 2002). The endothelial cells and smooth muscle of the coronary vessels arise from the proepicardium, which undergoes an epithelial-mesenchymal transformation. The proepicardial cells also express Cx43, and these cells are functionally coupled. This suggests that the *Cx43*-null phenotype may have multiple underlying causes.

The transcriptional regulator Sox4 is not expressed in neural crest cells but in the non-neural crest–derived mesenchymal cells that populate the cushions of the outflow tract and atrioventricular canal. *Sox4*-null mice suffer from lack of fusion of the outflow cushions, causing persistent truncus arteriosus in some embryos and large infundibular septal defects in others (Ya et al., 1998).

Frizzled2, a receptor in the Wnt signal transduction pathway, is expressed in the cardiac neural crest–populated regions of the outflow tract (Van Gijn et al., 2001). Pitx2 is directly induced in neural crest cells in the outflow tract by the Wnt–Dsh–β–catenin signaling (Kioussi et al., 2002). In the absence of *Pitx2*, defective proliferation of the neural crest cells leads to persistent truncus arteriosus (Kioussi et al., 2002).

Retinoic Acid

Retinoic acid (RA), the biologically active form of vitamin A, is an important signaling molecule in development. Neural crest cells, among many other cell types, are primary targets of RA signaling. An excess or paucity of RA is teratogenic and induces cardiovascular, thyroid, and craniofacial malformations. The cardiovascular defects include persistent truncus arteriosus, interrupted aortic arch, and double outlet right ventricle, all characteristics of cardiac neural crest ablation. The RA signal is transduced by ligand-inducible nuclear receptors, retinoic acid receptors (RARs), and retinoic X receptors (RXRs). Active RA receptors are heterodimers of one RAR and one RXR. Each receptor type has three subtypes (α, β, and γ) encoded by separate genes. Cardiovascular defects are associated with signaling mediated by RARα1 and RARβ receptors. Mouse embryos lacking the α1 isoform of the RARα gene plus all isoforms of the RARβ have persistent truncus arteriosus (Lee et al., 1997). Interestingly, when the RARα1/RARβ-deficient mice are crossed with a *Wnt1–cre* mouse to lineage trace the neural crest, the number, migration, and terminal fate of the cardiac neural crest is normal, suggesting that surrounding tissues respond directly to RA signaling and then induce the neural crest cells to initiate aorticopulmonary septation (Jiang et al., 2002).

The conotruncal ridges form normally in RXRα/RARβ compound mutants but fail to fuse, apparently as a result of excessive apoptosis of mesenchymal cells. Many cardiomyocytes in the conotruncal wall of these mutants appear necrotic. Thus excessive cell death in the conotruncus is a potential cause of ventricular septal defects (Ghyselinck et al., 1998).

Cardiovascular Malformations Related to Cardiac Neural Crest

Persistent Truncus Arteriosus

Persistent truncus arteriosus (PTA) is an uncommon malformation that is found in only about 1% of patients with congenital heart malformations. PTA results from the absence of the outflow septum (Goor, 1972). In this defect, a single great artery arises from the base of the heart that supplies systemic, coronary, and pulmonary blood flow. The single vessel, with usually three or four valve leaflets, always occurs together with a ventricular septal defect. The various types of truncus are classified by the extent of deficiency of the septum. The two main classification systems used to describe the anatomy of PTA are those of Collett and Edwards or Van Praagh and Van Praagh (Collett and Edwards, 1949; Van Praagh and Van Praagh, 1965). The former classification depends on the morphological extent of deficiency of the outflow septum and does not require inferred embryologic processes, so it is presented here. In type I PTA, the aorta and pulmonary arteries arise from a common semilunar valve. This contrasts with type II PTA, in which the main pulmonary artery is absent, and the right and left pulmonary arteries arise from a common orifice in the back of the aortic wall. Type III PTA is characterized by one or both pulmonary arteries arising independently from either side of the common trunk. The pulmonary arteries arise from the thoracic aorta in type IV PTA. Eighty percent of children born with PTA die within the first year of life without surgical intervention (Williams et al., 1999). Clinical signs at presentation include congestive heart failure, cyanosis, respiratory infection or distress, failure to thrive, cardiac arrhythmias, and rarely, CLUBBING of fingers and toes. Associated cardiovascular anomalies include PATENT FORAMEN OVALE, right aortic arch, PATENT DUCTUS ARTERIOSUS, stenotic or hypoplastic pulmonary arteries, interrupted arch, aberrant right or left subclavian arteries, persistent left superior vena cava, and coronary artery anomaly. Most patients have PTA as part of a syndromic sequence, the most common being the DiGeorge syndrome (Williams et al., 1999).

DiGeorge Syndrome

The DiGeorge syndrome consists of a conotruncal malformation (Fig. 11.19), type B interrupted aortic arch, absent or hypoplastic thymus, craniofacial dysmorphology, and cognitive or behavioral disorders. It can also include absent or hypoplastic parathyroid and thyroid glands. A variant of the DiGeorge phenotype, called Sprintzen or velocardiofacial syndrome, also includes cleft palate. The DiGeorge syndrome was characterized originally as defective development of structures derived from the third and fourth pharyngeal pouches (Finley et al., 1977). After the discovery that neural crest provides the mesenchyme of the third, fourth, and sixth arches, as well as the outflow septum, the DiGeorge syndrome was recognized as resulting from defective development of the neural crest (Kirby and Bockman, 1984; Van Mierop and Kutsche, 1986). More recently, the phenotype has been linked to a microdeletion in chromosome 22q11. This has led to assignment of yet another name to the phenotype associated with chromosome 22q11 microdeletion which is CATCH22 (*C*ardiac defects, *A*bnormal facies, *T*hymic hypoplasia, *C*left palate, and *H*ypocalcemia). Identification of the chromosome 22 microdeletion subsequently led to the recognition of *Tbx1* as the gene that is most likely to underlie the phenotype, although is it generally recognized that the multiple forms of the phenotype are likely to involve modifier genes. Tbx1 is not expressed by cardiac neural crest cells until they begin to form the aorticopulmonary septation complex in the outflow tract. However, it is expressed in the pharyngeal endoderm and in the secondary heart field. Tbx1 expression in

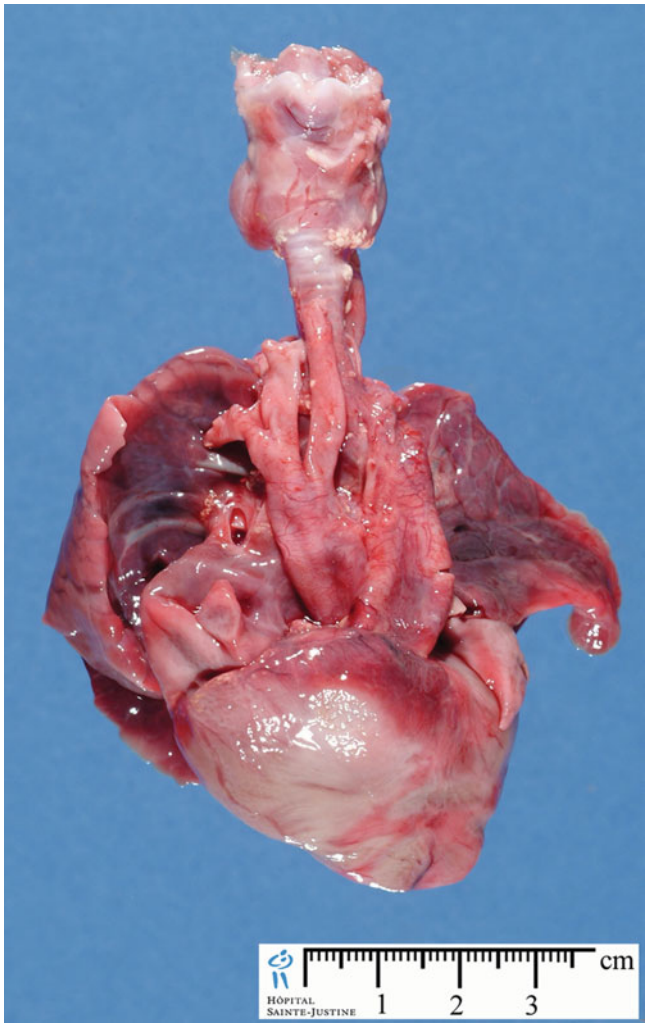

Figure 11.19. Thymic aplasia and right aortic arch in a human patient with DiGeorge syndrome. (Courtesy of humpath.com, with permission.)

the endoderm may control Fgf8 expression, which affects some aspect of neural crest development, perhaps proliferation (Yamagishi et al., 2003). Expression of Tbx1 in the secondary heart field has been linked with proliferation (Xu et al., 2004). The craniofacial and cognitive defects have been less well studied. It has become obvious that the cardiovascular components of this phenotype result from disrupted signaling and proliferation of target cell populations and are not caused by a single cell population. The characteristics of the syndrome are discussed more thoroughly in Chapter 15.

REFERENCES

Abu-Issa, R., G. Smyth, I. Smoak, K.-I. Yamamura, and E. Meyers. 2002. *Fgf8* is required for pharyngeal arch and cardiovascular development in the mouse. Development 129:4613–4625.

Auerbach, R. 1954. Analysis of the developmental effects of a lethal mutation in the house mouse. J. Exp. Zool. 127:305–329.

Aybar, M. J., and R. Mayor. 2002. Early induction of neural crest cells: lessons learned from frog, fish and chick. Curr. Opin. Genet. Dev. 12:452–458.

Ballard, V. L. T., and T. Mikawa. 2002. Constitutive expression of prepro endothelin in the cardiac neural crest selectively promotes expansion of the adventitia of the great vessels in vivo. Dev. Biol. 251:167–177.

Bamforth, S. D., J. Bragan‡a, J. J. Eloranta, J. N. Murdoch, F. I. R. Marques, K. R. Kranc, H. Farza, D. J. Henderson, H. C. Hurst, and S. Bhattacharya. 2001. Cardiac malformations, adrenal agenesis, neural crest defects and exencephaly in mice lacking Cited2, a new Tfap2 co-activator. Nat. Genet. 29:469–474.

Bockman, D. E., and M. L. Kirby. 1984. Dependence of thymus development on derivatives of the neural crest. Science 223:498–500.

Bockman, D. E., M. E. Redmond, and M. L. Kirby. 1989. Alteration of early vascular development after ablation of cranial neural crest. Anat. Rec. 225:209–217.

Bockman, D. E., M. E. Redmond, K. Waldo, H. Davis, and M. L. Kirby. 1987. Effect of neural crest ablation on development of the heart and arch arteries in the chick. Am. J. Anat. 180:332–341.

Brewer, S., X. B. Jiang, S. Donaldson, T. Williams, and H. M. Sucov. 2002. Requirement for AP-2α in cardiac outflow tract morphogenesis. Mech. Dev. 110:139–149.

Brown, C. B., L. Feiner, M. M. Lu, J. Li, X. K. Ma, A. L. Webber, L. Jia, J. A. Raper, and J. A. Epstein. 2001. PlexinA2 and semaphorin signaling during cardiac neural crest development. Development 128:3071–3080.

Charite, J., D. G. McFadden, G. Merlo, G. Levi, D. E. Clouthier, M. Yanagisawa, J. A. Richardson, and E. N. Olson. 2001. Role of *Dlx6* in regulation of an endothelin-1-dependent, *dHAND* branchial arch enhancer. Genes Dev. 15:3039–3049.

Chisaka, O., and M. R. Capecchi. 1991. Regionally restricted developmental defects resulting from targeted disruption of the mouse homeobox gene *hox-1.5*. Nature 350:473–479.

Clouthier, D. E., K. Hosoda, J. A. Richardson, S. C. Williams, H. Yanagisawa, T. Kuwaki, M. Kumada, R. E. Hammer, and M. Yanagisawa. 1998. Cranial and cardiac neural crest defects in endothelin-A receptor-deficient mice. Development 125:813–824.

Clouthier, D. E., S. C. Williams, R. E. Hammer, J. A. Richardson, and M. Yanagisawa. 2003. Cell-autonomous and nonautonomous actions of endothelin-A receptor signaling in craniofacial and cardiovascular development. Dev. Biol. 261:506–519.

Clouthier, D. E., S. C. Williams, H. Yanagisawa, M. Wieduwilt, J. A. Richardson, and M. Yanagisawa. 2000. Signaling pathways crucial for craniofacial development revealed by endothelin-A receptor-deficient mice. Dev. Biol. 217:10–24.

Collett, R. W., and J. E. Edwards. 1949. Persistent truncus arteriosus: a classification according to anatomic types. Surg. Clin. North Am. 29:1245–1270.

Colvee, E., and J. M. Hurle. 1983. Malformations of the semilunar valves produced in chick embryos by mechanical interference with cardiogenesis. An experimental approach to the role of hemodynamics in valvular development. Anat. Embryol. (Berl.) 168:59–71.

Conway, S. J., J. Bundy, J. Chen, E. Dickman, R. Rogers, and B. M. Will. 2000. Decreased neural crest stem cell expansion is responsible for the conotruncal heart defects within the Splotch (*Sp2H*)/*Pax3* mouse mutant. Cardiovasc. Res. 1:6176–6191.

Conway, S. J., R. E. Godt, C. J. Hatcher, L. Leatherbury, V. V. Zolotouchnikov, M. A. Brotto, A. J. Copp, M. L. Kirby, and T. L. Creazzo. 1997a. Neural crest is involved in development of abnormal myocardial function. J. Mol. Cell. Cardiol. 29:2675–2685.

Conway, S. J., D. J. Henderson, and A. J. Copp. 1997b. *Pax3* is required for cardiac neural crest migration in the mouse: evidence from the splotch (Sp2H) mutant. Development 124:505–514.

Conway, S. J., D. J. Henderson, M. L. Kirby, R. H. Anderson, and A. J. Copp. 1997c. Development of a lethal congenital heart defect in the splotch (*Pax3*) mutant mouse. Cardiovasc. Res. 36:163–173.

Creazzo, T. L., R. E. Godt, L. Leatherbury, S. J. Conway, and M. L. Kirby. 1998. Role of cardiac neural crest cells in cardiovascular development. Annu. Rev. Physiol. 60:267–286.

Daniel, R., G. Kao, K. Taganov, J. G. Greger, O. Favorova, G. Merkel, T. J. Yen, R. A. Katz, and A. M. Skalka. 2003. Evidence that the retroviral DNA integration process triggers an ATR-dependent DNA damage response. Proc. Natl. Acad. Sci. USA 100:4778–4783.

Delot, E. C., M. E. Bahamonde, M. X. Zhao, and K. M. Lyons. 2003. BMP signaling is required for septation of the outflow tract of the mammalian heart. Development 130:209–220.

Epstein, J. A. 1996. *Pax3*, neural crest and cardiovascular development. Trends Cardiovasc. Med. 6:255–261.

Epstein, J. A., J. Li, D. Lang, F. Chen, C. B. Brown, F. Z. Jin, M. M. Li, M. Thomas, E. C. J. Liu, A. Wessels, and C. W. Lo. 2000. Migration of cardiac neural crest cells in *Splotch* embryos. Development 127:1869–1878.

Ewart, J. L., M. F. Cohen, R. A. Meyer, G. Y. Huang, A. Wessels, R. G. Gourdie, A. J. Chin, S. M. J. Park, B. O. Lazatin, S. Villabon, and C. W. Lo. 1997. Heart and neural tube defects in transgenic mice overexpressing the *Cx43* gap junction gene. Development 124: 1281–1292.

Farrell, M. J., J. L. Burch, K. Wallis, L. Rowley, D. Kumiski, H. Stadt, R. E. Godt, T. L. Creazzo, and M. L. Kirby. 2001. FGF-8 in the ventral pharynx alters development of myocardial calcium transients after neural crest ablation. J. Clin. Invest. 107:1509–1517.

Farrell, M. J., H. Stadt, K. T. Wallis, P. Scambler, R. L. Hixon, R. Wolfe, L. Leatherbury, and M. L. Kirby. 1999. *HIRA*, a DiGeorge syndrome candidate gene, is required for cardiac outflow tract septation. Circ. Res. 84:127–135.

Feiner, L., A. L. Webber, C. B. Brown, M. M. Lu, L. Jia, P. Feinstein, P. Mombaerts, J. A. Epstein, and J. A. Raper. 2001. Targeted disruption of semaphorin 3C leads to persistent truncus arteriosus and aortic arch interruption. Development 128:3061–3070.

Finley, J. P., G. F. Collins, J. P. de Chadarevian, and R. L. Williams. 1977. DiGeorge syndrome presenting as severe congenital heart disease in the newborn. Can. Med. Assoc. J. 116:635–640.

Frank, D., L. Fotheringham, J. Brewer, L. Muglia, Tristani-Firouzi, M. Capecchi, and A. Moon. 2002. An *Fgf8* mouse mutant phenocopies human 22q11. deletion syndrome. Development 129: 4591–4603.

Franz, T. 1989. Persistent truncus arteriosus in the Splotch mutant mouse. Anat. Embryol. (Berl.) 180:457–464.

Fukiishi, Y., and G. M. Morriss-Kay. 1992. Migration of cranial neural crest cells to the pharyngeal arches and heart in rat embryos. Cell Tissue Res. 268:1–8.

Garcia-Castro, M. I., C. Marcelle, and M. Bronner-Fraser. 2002. Ectodermal Wnt function as a neural crest inducer. Science 297:848–851.

Garcia-Martinez, V., D. Sanchez-Quintana, and J. M. Hurle. 1990. Histogenesis of the semilunar valves: an immunohistochemical analysis of tenascin and type-I collagen distribution in developing chick heart valves. Cell Tissue Res. 259:299–304.

Ghyselinck, N. B., O. Wendling, N. Messaddeq, A. Dierich, C. Lampron, D. Decimo, S. Viville, P. Chambon, and M. Mark. 1998. Contribution of retinoic acid receptor beta isoforms to the formation of the conotruncal septum of the embryonic heart. Dev Biol. 198:303–318.

Goor, D. A. 1972. The development of isolated ventricular septal defect, persistent truncus arteriosus, A-V canal malformation, and transposition complexes. Cardiovasc. Clin. 4:149–174.

Hamblet, N. S., N. Lijam, P. Ruiz-Lozano, J. B. Wang, Y. S. Yang, Z. G. Luo, L. Mei, K. R. Chien, D. J. Sussman, and A. Wynshaw-Boris. 2002. *Dishevelled 2* is essential for cardiac outflow tract development, somite segmentation and neural tube closure. Development 129:5827–5838.

Huang, G. Y., E. S. Cooper, K. Waldo, M. L. Kirby, N. B. Gilula, and C. W. Lo. 1998a. Gap junction-mediated cell-cell communication modulates mouse neural crest migration. J. Cell Biol. 143: 1725–1734.

Huang, G. Y., A. Wessels, B. R. Smith, K. K. Linask, J. L. Ewart, and C. W. Lo. 1998b. Alteration in connexin 43 gap junction gene dosage impairs conotruncal heart development. Dev. Biol. 198: 32–44.

Hurle, J. M. 1979. Scanning and light microscope studies of the development of the chick embryo semilunar heart valves. Anat. Embryol. (Berl.) 157:69–80.

Hurle, J. M., and E. Colvee. 1983. Changes in the endothelial morphology of the developing semilunar heart valves. A TEM and SEM study in the chick. Anat. Embryol. 167:67–83.

Hurle, J. M., E. Colvee, and A. M. Blanco. 1980. Development of mouse semilunar valves. Anat. Embryol. (Berl.) 160:83–91.

Hutson, M. R., and M. L. Kirby. 2003. Neural crest and cardiovascular development: a 20-year perspective. Birth Defects Res. C Embryo Today 69:2–13.

Hutson, M. R., H. A. Stadt, J. Burch, T. L. Creazzo, and M. L. Kirby. 2006. Cardiac arterial pole alignment is sensitive to FGF8 signaling in the pharynx. Dev. Biol. 295:486–497.

Iida, K., H. Koseki, H. Kakinuma, N. Kato, Y. Mizutani-Koseki, H. Ohuchi, H. Yoshioka, S. Noji, K. Kawamura, Y. Kataoka, F. Ueno, M. Taniguchi, N. Yoshida, T. Sugiyama, and N. Miura. 1997. Essential roles of the winged helix transcription factor MFH-1 in aortic arch patterning and skeletogenesis. Development 124:4627–4638.

Ivey, K., B. Tyson, P. Ukidwe, D. G. McFadden, G. Levi, E. N. Olson, D. Srivastava, and T. M. Wilkie. 2003. Gxq and Gx11 proteins mediate endothelin-1.signaling in neural crest-derived pharyngeal arch mesenchyme. Dev. Biol. 255:230–237.

Jiang, X., B. Choudhary, E. Merki, K. Chien, R. Maxson, and H. M. Sucov. 2002. Normal fate and altered function of the cardiac neural crest cell lineage in retinoic acid receptor mutant embryos. Mech. Dev. 117:115–122.

Jiang, X., D. H. Rowitch, P. Soriano, A. P. McMahon, and H. M. Sucov. 2000. Fate of the mammalian cardiac neural crest. Development 127:1607–1616.

Johnson, E. N., Y. M. Lee, T. L. Sander, E. Rabkin, F. J. Schoen, S. Kaushal, and J. Bischoff. 2003. NFATc1 mediates vascular endothelial growth factor-induced proliferation of human pulmonary valve endothelial cells. J. Biol. Chem. 278:1686–1692.

Kameda, Y., T. Nishimaki, M. Takeichi, and O. Chisaka. 2002. Homeobox gene *Hoxa3* is essential for the formation of the carotid body in the mouse embryos. Dev. Biol. 247:197–209.

Kawasaki, T., T. Kitsukawa, Y. Bekku, Y. Matsuda, M. Sanbo, T. Yagi, and H. Fujisawa. 1999. A requirement for neuropilin-1 in embryonic vessel formation. Development 126:4895–4902.

Kempf, H., C. Linares, P. Corvol, and J.-M. Gasc. 1998. Pharmacological inactivation of the endothelin type A receptor in the early chick embryo: a model of mispatterning of the branchial arch derivatives. Development 125:4931–4941.

Kioussi, C., P. Briata, S. H. Baek, D. W. Rose, N. S. Hamblet, T. Herman, K. A. Ohgi, C. Lin, A. Gleiberman, J. Wang, V. Brault, P. Ruiz-Lozano, H. D. Nguyen, R. Kemler, C. K. Glass, A. Wynshaw-Boris, and M. G. Rosenfeld. 2002. Identification of a Wnt/Dvl/beta-Catenin → Pitx2 pathway mediating cell-type-specific proliferation during development. Cell 111:673–685.

Kirby, M. L. 1987. Cardiac morphogenesis: recent research advances. Pediatr. Res. 21:219–224.

Kirby, M. L., and D. E. Bockman. 1984. Neural crest and normal development: a new perspective. Anat. Rec. 209:1–6.

Kirby, M. L., T. F. Gale, and D. E. Stewart. 1983. Neural crest cells contribute to aorticopulmonary septation. Science 220:1059–1061.

Kirby, M. L., P. Hunt, K. T. Wallis, and P. Thorogood. 1997. Normal development of the cardiac outflow tract is not dependent on normal patterning of the aortic arch arteries. Dev. Dyn. 208: 34–47.

Kirby, M. L., and D. E. Stewart. 1983. Neural crest origin of cardiac ganglion cells in the chick embryo: identification and extirpation. Dev. Biol. 97:433–443.

Kirby, M. L., K. L. Turnage, and B. M. Hays. 1985. Characterization of conotruncal malformations following ablation of "cardiac" neural crest. Anat. Rec. 213:87–93.

Knecht, A. K., and M. Bronner-Fraser. 2002. Induction of the neural crest: a multigene process. Nat. Rev. Genet. 3:453–461.

Kochilas, L., S. Merscher-Gomez, M. M. Lu, V. Potluri, J. Liao, R. Kucherlapati, B. Morrow and J. A. Epstein. 2002. The role of neural crest during cardiac development in a mouse model of DiGeorge syndrome. Dev. Biol. 251:157–166.

Kume, T., H. Y. Jiang, J. M. Topczewska, and B. L. M. Hogan. 2001. The murine winged helix transcription factors, *Foxc1* and *Foxc2*, are both required for cardiovascular development and somitogenesis. Genes Dev. 15:2470–2482.

Kuratani, S. C., and M. L. Kirby. 1991. Initial migration and distribution of the cardiac neural crest in the avian embryo: an introduction to the concept of the circumpharyngeal crest. Am. J. Anat. 191:215–227.

Kurihara, Y., H. Kurihara, H. Suzuki, T. Kodama, K. Maemura, R. Nagai, H. Oda, T. Kuwaki, W.-H. Cao, N. Kamada, K. Jishage, Y. Ouchi, S. Azuma, Y. Toyoda, T. Ishikawa, M. Kumada, and Y. Yazaki. 1994. Elevated blood pressure and craniofacial abnormalities in mice deficient in endothelin-1. Nature 368: 703–710.

Kwang, S. J., S. M. Brugger, A. Lazik, A. E. Merrill, L. Y. Wu, Y. H. Liu, M. Ishii, F. O. Sangiorgi, M. Rauchman, H. M. Sucov, R. L. Maas, and R. E. Maxson, Jr. 2002. *Msx2* is an immediate downstream effector of *Pax3* in the development of the murine cardiac neural crest. Development 129:527–538.

LaBonne, C., and M. Bronner-Fraser. 1999. Molecular mechanisms of neural crest formation. Annu. Rev. Cell Dev. Biol. 15:81–112.

Le Lievre, C. S., and N. M. Le Douarin. 1975. Mesenchymal derivatives of the neural crest. Analysis of chimaeric quail and chick embryos. J. Embryol. Exp. Morphol. 34:125–154.

Leatherbury, L., H. E. Gauldin, K. L. Waldo, and M. L. Kirby. 1990. Microcinephotography of the developing heart in neural crest-ablated chick embryos. Circulation 81:1047–1057.

Lee, M. J., A. Brennan, A. Blanchard, G. Zoidl, Z. Dong, A. Tabernero, C. Zoidl, M. A. R. Dent, K. R. Jessen, and R. Mirsky. 1997. P0 is constitutively expressed in the rat neural crest and embryonic nerves and is negatively and positively regulated by axons to generate non-myelin-forming and myelin-forming Schwann cells, respectively. Mol. Cell. Neurosci. 8:336–350.

Lee, R. Y., J. M. Luo, R. M. Evans, V. Giguere, and H. M. Sucov. 1997. Compartment-selective sensitivity of cardiovascular morphogenesis to combinations of retinoic acid receptor gene mutations. Circ. Res. 80:757–764.

Li, W. E., K. Waldo, K. L. Linask, T. Chen, A. Wessels, M. S. Parmacek, M. L. Kirby, and C. W. Lo. 2002. An essential role for connexin43 gap junctions in mouse coronary artery development. Development 2031–2042.

Li, Y. X., M. Zdanowicz, L. Young, D. Kumiski, L. Leatherbury, and M. L. Kirby. 2003. Cardiac neural crest in zebratish embryos contributes to myocardial cell lineage and early heart function. Dev. Dyn. 226:540–550.

Lindsay, E. A., H. Su, M. Morishima, T. Huynh, T. Pramparo, V. Jurecic, G. Ogunrinu, H. F. Sutherland, P. J. Scambler, A. Bradley, and A. Baldini. 2001. *Tbx1* haploinsufficiency in the DiGeorge syndrome region causes aortic arch defects in mice. Nature 410:97–101.

Lo, C. W., M. F. Cohen, G. Y. Huang, B. O. Lazatin, N. Patel, R. Sullivan, C. Pauken, and S. M. J. Park. 1997. *Cx43* gap junction gene expression and gap junctional communication in mouse neural crest cells. Dev. Genet. 20:119–132.

Lo, C. W., K. L. Waldo, and M. L. Kirby. 1999. Gap junction communication and the modulation of cardiac neural crest cells. Trends Cardiovasc. Med. 9:63–69.

Macatee, T. L., B. P. Hammond, R. Benjamin, B. R. Arenkiel, L. Francis, D. U. Frank, and A. M. Moon. 2003. Ablation of specific expression domains reveals discrete functions of ectoderm- and endoderm-derived FGF8 during cardiovascular and pharyngeal development. Development 130:6361–6374.

Morishima, M., H. Yanagisawa, M. Yanagisawa, and A. Baldini. 2003. Ece1 and *Tbx1* define distinct pathways to aortic arch morphogenesis. Dev. Dyn. 228:95–104.

Morrison-Graham, K., G. C. Schatteman, T. Bork, D. F. Bowen-Pope, and J. A. Weston. 1992. A PDGF receptor mutation in the mouse (Patch) perturbs the development of a non-neuronal subset of neural crest-derived cells. Development 115:133–142.

Nishibatake, M., S. A. Kargas, H. J. Bruyere, and E. F. Gilbert. 1987. Cardiovascular malformations induced by bromodeoxyuridine in the chick embryo. Teratology 36:125–132.

Poelmann, R. E., T. Mikawa, and A. C. Gittenberger-de Groot. 1998. Neural crest cells in outflow tract septation of the embryonic chicken heart: differentiation and apoptosis. Dev. Dyn. 212: 373–384.

Reaume, A. G., P. A. de Sousa, S. Kulkarni, B. L. Langille, D. Zhu, T. C. Davies, S. C. Juneja, G. M. Kidder, and J. Rossant. 1995. Cardiac malformation in neonatal mice lacking connexin43. Science 267:1831–1834.

Ruhin, B., S. Creuzet, C. Vincent, L. Benouaiche, N. M. Le Douarin, and G. Couly. 2003. Patterning of the hyoid cartilage depends upon signals arising from the ventral foregut endoderm. Dev. Dyn. 228:239–246.

Sato, M., and H. J. Yost. 2003. Cardiac neural crest contributes to cardiomyogenesis in zebrafish. Dev. Biol. 257:127–139.

Sechrist, J., M. A. Nieto, R. T. Zamanian, and M. Bronner-Fraser. 1995. Regulative response of the cranial neural tube after neural fold ablation: spatiotemporal nature of neural crest regeneration and up-regulation of Slug. Development 121: 4103–4115.

Somi, S., A. A. M. Buffing, A. F. M. Moorman, and M. J. B. Van Den Hoff. 2004. Dynamic patterns of expression of BMP isoforms 2, 4, 5, 6, and 7 during chicken heart development. Anat. Rec. 279:636–651.

Tomita, H., D. M. Connuck, L. Leatherbury, and M. L. Kirby. 1991. Relation of early hemodynamic changes to final cardiac phenotype and survival after neural crest ablation in chick embryos. Circulation 84:1289–1295.

Van den Hoff, M. J. B., A. F. M. Moorman, J. M. Ruijter, W. H. Lamers, R. W. Bennington, R. R. Markwald, and A. Wessels. 1999. Myocardialization of the cardiac outflow tract. Dev. Biol. 212:477–490.

Van Gijn, M. E., W. M. Blankesteijn, J. F. M. Smits, B. Hierck, and A. C. Gittenberger-de Groot. 2001. *Frizzled 2* is transiently expressed in neural crest-containing areas during development of the heart and great arteries in the mouse. Anat. Embryol. (Berl.) 203:185–192.

Van Mierop, L. H. S., and L. M. Kutsche. 1986. Cardiovascular anomalies in DiGeorge syndrome and importance of neural crest as a possible pathogenetic factor. Am. J. Cardiol. 58:133–137.

Van Praagh, R., and S. Van Praagh. 1965. The anatomy of common aorticopulmonary trunk (truncus arteriosus communis) and its embryologic implications. Am J. Cardiol. 16:406–425.

Vitelli, F., M. Morishima, I. Taddei, E. A. Lindsay, and A. Baldini. 2002. *Tbx1* mutation causes multiple cadiovascular defects and disrupts neural crest and cranial nerve migratory pathways. Hum. Mol. Genet. 11:915–922.

Waldo, K., S. Miyagawa-Tomita, D. Kumiski, and M. L. Kirby. 1998. Cardiac neural crest cells provide new insight into septation of the cardiac outflow tract: aortic sac to ventricular septal closure. Dev. Biol. 196:129–144.

Waldo, K. L., M. R. Hutson, C. C. Ward, M. Zdanowicz, H. A. Stadt, D. Kumiski, R. Abu-Issa, and M. L. Kirby. 2005. Secondary heart field contributes myocardium and smooth muscle to the arterial pole of the developing heart. Dev. Biol. 281:78–90.

Waldo, K. L., M. R. Hutson, M. Zdanowicz, H. A. Stadt, J. Zdanowicz, and M. L. Kirby. 2005. Cardiac neural crest is necessary for normal addition of the myocardium to the arterial pole from the secondary heart field. Dev. Biol. 281:66–77.

Waldo, K. L., D. Kumiski, and M. L. Kirby. 1996. Cardiac neural crest is essential for the persistence rather than the formation of an arch artery. Dev. Dyn. 205:281–292.

Waldo, K. L., D. H. Kumiski, and M. L. Kirby. 1994. Association of the cardiac neural crest with development of the coronary arteries in the chick embryo. Anat. Rec. 239:315–331.

Waldo, K. L., C. W. Lo, and M. L. Kirby. 1999. Connexin 43 expression reflects neural crest patterns during cardiovascular development. Dev. Biol. 208:307–323.

Waldo, K. L., S. Miyagawa-Tomita, D. Kumiski, and M. L. Kirby. 1998. Cardiac neural crest cells provide new insight into septation of the outflow tract: aortic sac to ventricular septal closure. Dev. Biol. 196:129–144.

Ward, C., H. A. Stadt, M. R. Hutson, and M. L. Kirby. 2005. Ablation of the secondary heart field leads to tetralogy of Fallot and pulmonary atresia. Dev. Biol. 284:72–83.

Williams, J. M., M. de Leeuw, M. D. Black, R. M. Freedom, W. G. Williams, and B. W. McCrindle. 1999. Factors associated with outcomes of persistent truncus arteriosus. J. Am. Coll. Cardiol. 34:545–553.

Winnier, G. E., T. Kume, K. Y. Deng, R. Rogers, J. Bundy, C. Raines, M. A. Walter, B. L. M. Hogan, and S. J. Conway. 1999. Roles for the winged helix transcription factors MF1 and MFH1 in cardiovascular development revealed by nonallelic noncomplementation of null alleles. Dev. Biol. 213:418–431.

Xu, H., M. Morishima, J. N. Wylie, R. J. Schwartz, B. G. Bruneau, E. A. Lindsay, and A. Baldini. 2004. *Tbx1* has a dual role in the morphogenesis of the cardiac outflow tract. Development 131:3217–3227.

Xu, X., W. E. I. Li, G. Y. Huang, R. Meyer, T. Chen, Y. Luo, M. P. Thomas, G. L. Radice, and C. W. Lo. 2001. Modulation of mouse neural crest cell motility by N-cadherin and connexin 43 gap junctions. J. Cell Biol. 154:217–229.

Ya, J., M. W. Schilham, P. A. de Boer, A. F. Moorman, H. Clevers, and W. H. Lamers. 1998. Sox4-deficiency syndrome in mice is an animal model for common trunk. Circ. Res. 83:986–994.

Yagi, H., Y. Furutani, H. Hamada, T. Sasaki, S. Asakawa, S. Minoshima, F. Ichida, K. Joo, M. Kimura, S. Imamura, N. Kamatani, K. Momma, A. Takao, M. Nakazawa, N. Shimizu, and R. Matsuoka. 2003. Role of *TBX1* in human del22q11.2.syndrome. Lancet 362:1366–1373.

Yamagishi, H., J. Maeda, T. H. Hu, J. McAnally, S. J. Conway, T. Kume, E. N. Meyers, C. Yamagishi, and D. Srivastava. 2003. *Tbx1* is regulated by tissue-specific forkhead proteins through a common Sonic hedgehog-responsive enhancer. Genes Dev. 17:269–281.

Yanagisawa, H., R. E. Hammer, J. A. Richardson, S. C. Williams, D. E. Clouthier, and M. Yanagisawa. 1998a. Role of endothelin-1/endothelin-A receptor-mediated signaling pathway in the aortic arch patterning in mice. J. Clin. Invest. 102:22–33.

Yanagisawa, H., M. Yanagisawa, R. P. Kapur, J. A. Richardson, S. C. Williams, D. E. Clouthier, D. De Wit, N. Emoto, and R. E. Hammer. 1998b. Dual genetic pathways of endothelin-mediated intercellular signaling revealed by targeted disruption of endothelin converting enzyme-1 gene. Development 125: 825–836.

Yelbuz, T. M., K. L. Waldo, D. H. Kumiski, H. A. Stadt, R. R. Wolfe, L. Leatherbury, and M. L. Kirby. 2002. Shortened outflow tract leads to altered cardiac looping after neural crest ablation. Circulation 106:504–510.

12

Development of the Cardiac Pacemaking and Conduction System

It is important that the tubular heart and the four-chambered heart beat in a coordinated fashion to propel blood from the inflow to the outflow. In a straight heart tube, because the myocardium is electrically coupled, the solution is relatively straightforward. But, coordinated contractions are necessarily different in a tube versus a four-chambered heart. Thus, development of the pacemaking and conduction system represents one of the most intriguing processes in heart development. Coordinated cardiac contractions are regulated by impulses that originate at the sinoatrial (SA) NODE, located at the junction of the superior vena cava and right atrium. Impulses generated at this node spread through the atrial chamber myocardium, to initiate contraction of the atria. The impulse is also spread to the atrioventricular (AV) NODE, located in the base of the atrial septum at the junction of the atria and ventricles, and is the only conducting route from the atria to the ventricles. The main function of the AV node is to slow the impulse from the atrial to the ventricular myocardium. Transmission of an impulse directly from the atrial myocardium to the ventricular myocardium is prevented by a nonconducting band of connective tissue at the atrioventricular junction called the ANNULUS FIBROSIS. The impulse is delayed by the atrioventricular node to allow time for atrial contraction before ventricular excitation. After the slight delay the impulse is propagated rapidly via the atrioventricular (His) bundle to the BUNDLE BRANCHES located in the top of the ventricular septum. The bundle branches divide on either side of the ventricular septum into branches that terminate in a highly ramified network of PURKINJE FIBERS that will activate both ventricles simultaneously, beginning at the APEX. The impulse is transferred from the Purkinje network into the working ventricular myocardium.

Function of the Pacemaking and Conduction System in the Mature Heart

Myocardial cells are electrically coupled to form a syncytium by virtue of INTERCALATED DISCS that form between the ends of the cells (Fig. 12.1). Thus contraction that proceeds from inflow to outflow in a straight heart tube needs no paths of excitation. In the mature three- or four-chambered heart, blood must be efficiently propelled through the systemic and pulmonary circulations with a coordinated ventricular contraction that begins at the apex of the heart, and in a wringing fashion squeezes the blood into the aorta and pulmonary arteries. The electrical impulse that stimulates contraction is initiated in the SA node in the right atrium. For the contraction to begin at the apex, it is essential that the electrical impulse reach the apex of the ventricles before it can stimulate contraction of the myocardium at the base of the heart. In mammalian and avian species, this is accomplished by the specialized rapid ventricular conduction system extending from the AV node as the common His bundle which subsequently branches into right and left bundle branches in the ventricular septum. These major bundle branches send smaller branches throughout the ventricular myocardium (Fig. 12.2). The conduction system is comprised of bundles of specialized large diameter muscle fibers located in the subendocardium throughout the ventricles. These are called Purkinje fibers and they have a distinct morphology with respect to the working ventricular myocardium. Purkinje fibers are well-coupled with gap junctions and the large fiber diameter provides for a cable property that together with the gap junctions facilitates rapid impulse conduction. Propagation of

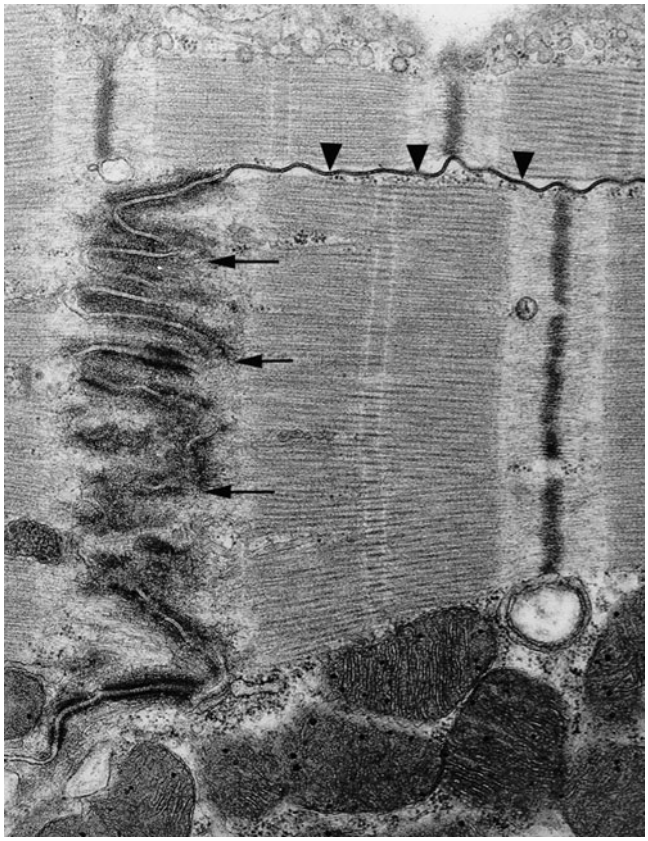

Figure 12.1. Myocardial cells are electrically coupled at intercalated discs (*arrows*), wavy junctions, which link the membranes at the ends of the myocardial cells in a region corresponding to the Z-line of the myofibrils. Gap junction plaques are located in the region of membrane indicated by the arrowheads. (From Severs, 2000, with permission.)

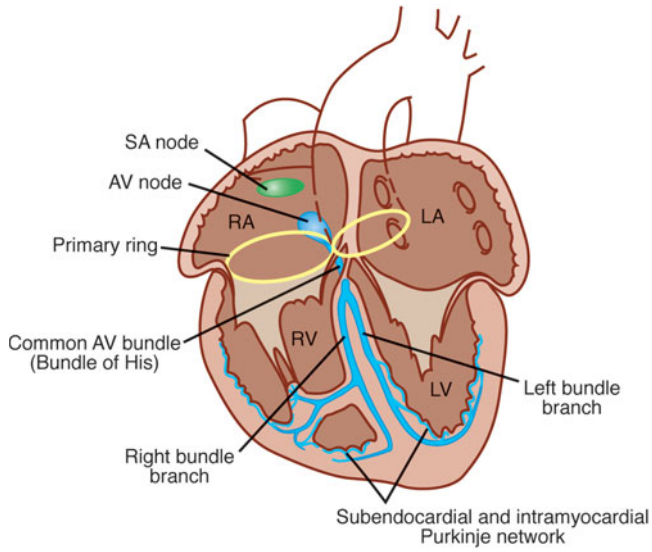

Figure 12.2. Diagram of the well-developed avian cardiac conduction system. The electrical impulse that controls the heart rate is initiated in the SA (sinoatrial) node. It proceeds via the atrial myocardium to the AV (atrioventricular) node, where it is delayed to allow time for atrial contraction. It is then propagated via the AV bundle into the right and left bundle branches and finally into the Purkinje network. This ensures that contraction begins at the apex and travels toward the base (AV junction) of the heart. (From Takabayashi-Suzuki et al., 2000, with permission.)

the impulse proceeds from the SA node through the atrium at about 0.1 to 1 m/sec and is greatly slowed while passing through the AV node to 0.01–0.05 m/sec (referred to as the AV delay). The impulse conduction in the ventricular system is very fast with a velocity of 2–4 m/sec in the His-Purkinje system versus 0.3–1.0 m/sec for the ventricular myocardium (Bers, 2001).

Functional development of the ventricular conduction system has been well investigated in recent years using optical mapping methods employing extracellular microelectrodes, photodiode arrays, or high-speed digital cameras together with voltage-sensitive fluorescent indicators (Chuck et al., 2004; Myers and Fishman, 2003; Rothenberg et al., 2004; Sedmera et al., 2003). Not surprisingly, the appearance of mature apex-to-base conduction in higher vertebrates parallels the anatomical development of the His–Purkinje system. Apex-to-base conduction is also present in vertebrates with two- or three-chambered hearts (e.g., zebrafish and Aftrican clawed toad), although it appears that rapid conduction in the ventricular trabeculae functions in place of a defined His–Purkinje system (Sedmera et al., 2003).

Morphological Identification of Components of the Pacemaking and Conduction System

The conduction tissue and nodes were originally recognized and defined by morphological criteria (Bozler, 1942; Goldenberg and Rothberger, 1936; Purkinje, 1845; Tawara, 1906). In fact, anatomical criteria still provide the standard for recognizing components of the cardiac conduction system (Anderson et al., 2004). The anatomical standards are now being augmented by molecular criteria, but these sometimes lead to incorrect conclusions. This is especially true in the developing conduction system, where the anatomical criteria do not apply until the heart is fairly mature.

The anatomical/histological criteria for identifying the nodes and conduction system are based on connective tissue isolation, histological features of the cells that distinguish them from working myocardium, the pattern of innervation, and expression of enzymes such as ACETYLCHOLINE ESTERASE (Anderson and Taylor, 1972; Hoover et al., 2004). The cells of the mature His–Purkinje system are distinguished from working myocardium because they are larger and have paler cytoplasm, a sheath of connective tissue, and different fiber orientation (Tawara, 1906). Because identification of a region or cell as part of the pacemaking and conduction system requires that all of these features are met, looking at a single

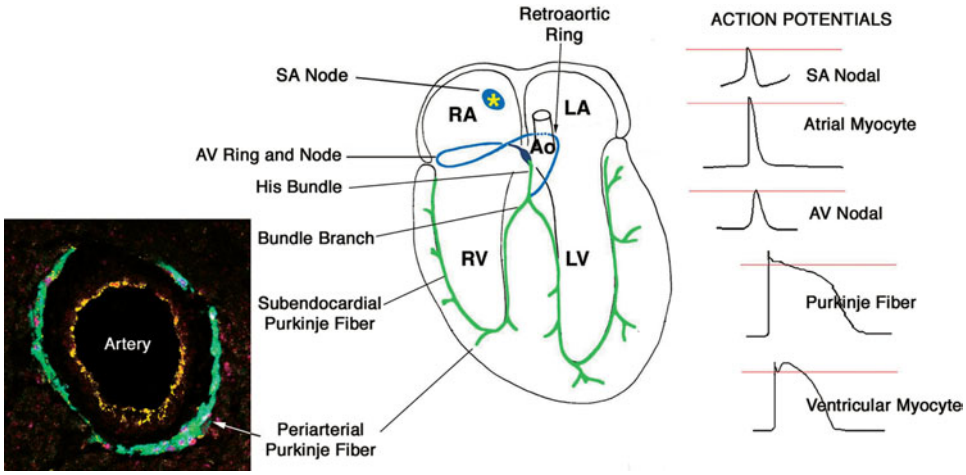

Figure 12.3. Components of the cardiac conduction system and action potentials from the myocardium. The drawing of the conduction system is based on Davies (1930). Periarterial Purkinje fibers (*green*) surround the coronary arteries in the chick. Ao, aorta; LA, left atrium; RA, right atrium; RV, right ventricle; LV, left ventricle. (Figure courtesy of R. Gourdie, MUSC, Charleston, SC.)

cell in isolation has never been a particularly useful measure of whether that cell is specialized for conduction.

While morphological criteria are still the standard, there are physiological and molecular characteristics that can be used along with these histological features to identify elements of the conduction system (Fig. 12.3) (Mikawa and Fischman, 1996). However, these characteristics are not so apparent in embryos, and so a battery of other molecular markers has been found and used. In the chick heart, Purkinje fibers form a cellular network in the subendocardium and penetrate the myocardium along the arterial beds (Davies, 1930; Gourdie et al., 1995; Lamers et al., 1991; Vassal-Adams, 1982). These cells express a conduction cell–specific gap junction (see later), and some proteins typically expressed by neurons and skeletal muscle cells include NF160 (neuronal intermediate filament), HNK-1, and PSA-NCAM (Alyonycheva et al., 1997; Chuck and Watanabe, 1997; de Groot et al., 1987; Gonzalez-Sanchez and Bader, 1985; Gorza et al., 1984, 1988; Gorza and Vitadello, 1989; Gourdie et al., 1999; Sartore et al., 1978; Wessels et al., 1992). It is not known why conduction system cells share expression of these genes with nervous tissues although it should not be surprising as both types of cells share some of their electrical properties. These cells only poorly express cardiac muscle specific myofibrillar proteins such as CARDIAC MYOSIN BINDING PROTEIN-C, which is essential for normal myocardial contractility (Bonne et al., 1995; Watkins et al., 1995).

A defining characteristic of embryonic cardiac muscle is that it can beat without any external stimulation and that the cells with the fastest intrinsic rate set the beat rate of the rest. The myocytes of the SA node have the most rapid beat rate and are thus the PACEMAKER. The mature node is distinguished by a rich network of nerve terminals representing both the sympathetic and parasympathetic divisions of the AUTONOMIC NERVOUS SYSTEM. The atrial myocytes that comprise the SA node are heterogeneous. There is a gradual change in the intrinsic properties of SA node cells from the center of the node to the periphery. This heterogeneity is important for the function of the SA node because it prevents HYPERPOLARIZATION of the SA node by the surrounding atrial muscle. It helps promote propagation of excitation from the SA node to the right atrial myocardium, and it provides a duration gradient of action potentials that protects the node from action potentials outside (Boyett et al., 2000).

Electrical activity is first seen at the seven-somite stage in chick, and contractions begin at the nine-somite stage. In the rat, action potentials and contractions have been measured at E9.5. The electrical impulse is generated at the inflow junction of the sinus venosus and atrium and propagated with uniform velocity through the epithelial myocytes via gap junctions, generating a caudal-to-cranial contraction wave that pushes blood from the inflow to the outflow (Kamino et al., 1981; Patten and Kramer, 1933). The SA node becomes morphologically distinct well after the heart begins to function. The node is located at the junction of the right COMMON CARDINAL VEIN with the wall of the right atrium (Viragh and Challice, 1980). SA nodal cells have elongated nuclei, moderate amounts of myofibrils, and abundant GLYCOGEN (Shimada et al., 2004). The cells are smaller than working atrial myocytes, have a spindle shape, and form bundles arranged in parallel along the CRISTA TERMINALIS (Shimada et al., 2004).

While there has been a great deal of controversy over whether specific SA to AV node conduction tracts exist, it is now well established that any preferential conduction through the atrial myocardium between the nodes depends on the nonuniform anisotropic arrangement of the working atrial myocardium (Spach and Kootsey, 1983). Insulated pathways through the atrial myocardium do not exist, so an atrial conduction system (as defined by Anderson) does not exist (Anderson et al., 2004).

The AV node, located at the base of the atrial septum, is a compact cluster of nodal cells that form a RETICULAR NETWORK. The cells are loosely organized and tend to intermingle with atrial myocytes in the upper part of the node. They become more regularly organized as they connect with the AV bundle. Cells of the AV node are smaller than working myocytes, are highly branched, have few myofibrils, are abundant in glycogen, and are insulated by connective tissue (Shimada et al., 2004). The major function of the AV node is to provide for a delay as

an electrical impulse is conducted from the atrial to the ventricular myocardium (de Jong et al., 1992; Lieberman and Paes de Carvalho, 1967).

The AV bundle (also called His bundle) originates at the posterior right atrial wall near the atrial septum and atrioventricular junction. It passes over the upper, fibrous margin of the ventricular septum and bifurcates near the base of the aorta into right and left bundle branches. The myocytes in the AV bundle and the Purkinje fibers are larger than those in the AV node, oval, and rich in glycogen and have sparse myofibrils distributed at the periphery of the cell (Shimada et al., 2004; Tawara, 1906).

The bundle branches terminate in Purkinje fibers, which are widely distributed in the myocardium. The Purkinje fibers are electrically coupled to myocardial cells by gap junctions. It is this arrangement of fast conducting fibers that accounts for base-to-apex excitation and ventricular contraction (Pennisi et al., 2002). The Purkinje fibers form a subepicardial reticulum (Shimada et al., 2004). These cells show great species-dependent variability. In general, they tend to be much larger than working myocytes or any other elements of the conduction system. They have abundant glycogen and only a few peripherally placed myofibrils (Shimada et al., 2004). Purkinje cells have large gap junctions.

Conduction Myocardium Arises from Working Myocardium

When the embryonic heart first begins to contract, it has no specialized conduction system. The expression of neuronal markers in the Purkinje fibers gave rise to the hypothesis that this tissue originated from neural crest (Filogamo and Peirone, 1995; Gorza et al., 1988). However, recent lineage analysis in chick embryos, employing retroviral cell tracing, showed persuasively that single contractile myocytes can generate daughter cells that include conducting cells near the perivascular regions of the coronary arteries (Cheng et al., 1999). The Purkinje fibers, AV node, AV bundle, and bundle branches are without doubt largely derived from myocytes (Gourdie et al., 1995). The Purkinje fibers differentiate within individual myocyte clones, suggesting that they are recruited from the working myocardium. Conduction cell differentiation occurs within individual myocyte clones that occupy only a segment of the myocardium (Gourdie et al., 1995).

In early development, the primitive heart tube is composed uniformly of small fusiform myocytes and there is no morphologically distinct region of conducting cells. Nonetheless, conduction of the contractile impulse begins with the primary pacemaker region located in the primitive atrium and presumably in the region of the future SA node. The primitive pacemaker comprises the fastest beating myocytes and the conduction impulse spreads sequentially and uniformly from this group of cells towards the primitive ventricle and outflow tract. Using a photodiode array, Kamino and colleagues identified the pacemaker activity in the primitive atrium just before folding of the precontractile cardiogenic region to form the heart tube (Fujii et al., 1981). In the chick embryo, optical mapping demonstrates gradual development of the conduction system in the trabeculae during secondary trabeculation of the ventricles. The process takes about 3 days from stages 21–31 (Chuck et al., 2004). Mature conduction from base to apex is apparent by stage 31 (Fig. 12.4). Cardiogenesis occurs more rapidly in mouse development and the transition from sequential base-to-apex conduction in the trabeculae to mature conduction occurs over a period of about 1 day (~E9.5–10.5) (Fig. 12.4) (Myers and Fishman, 2003).

Thus, as myocardial cells in the primary heart tube are proliferating and developing contractile properties and chamber-specific characteristics, they begin to segregate into both working or chamber myocardium and specialized myocardium of the conduction system (Fig. 12.5). One characteristic that distinguishes slow-conducting from fast-conducting myocardium lies in the potential for intercellular communication in these two types of myocardium (DeMello, 1982; DeHaan and Chen, 1990; Delorme et al., 1995). In slow-conducting myocardium, sparse gap junctions are responsible for the intercellular transfer of the depolarizing action potential (Van Kempen et al., 1991, 1996). Poor coupling of slow-conducting myocytes through gap junctions may be necessary to prevent the much larger fast-conducting working myocardium from overwhelming the pacing nodes. Once the working myocardium has differentiated, the low level of expression of the connexins in the nodes serves as a useful marker for delineating the INTERDIGITATION of the nodal and working myocardium (ten Velde et al., 1995).

Developing conductive myocardium co-expresses atrial and ventricular myosin heavy chain isoforms during a much longer developmental period than working myocardium, contributing to the idea that conduction myocardium retains a more undifferentiated phenotype than working myocardium. However, it could also be the most specialized because of its early removal from differentiation as working myocardium. Tracts of these co-expressing cells are now thought to provide pathways of preferential conduction (de Groot et al., 1988). Atrial and ventricular working myocardium differentiate as fast-conducting myocardium, while the inflow tract, atrioventricular canal, and outflow tract remain slow-conducting myocardium (de Jong et al., 1992). Subsequently, the SA and AV nodes develop from the slow-conducting myocardium of the inflow tract and atrioventricular canal, and the His bundle and bundle branches develop from the fast-conducting ventricular myocardium. The myocardium of the outflow tract is the least differentiated myocardium in the heart tube, perhaps because this myocardium is the last added to the heart tube (Paff, 1962; Waldo et al., 2001). This myocardium contracts very slowly, resulting in a sphincter-like closure that prevents regurgitation even in the absence of valves (Boucek et al., 1959). This BASE-TO-APEX activation pattern persists until just before septation (Fig. 12.4) (Chuck et al., 1997). During the final stages of outflow septation, the activation sequence is reversed to the apex-to-base pattern seen in the mature heart.

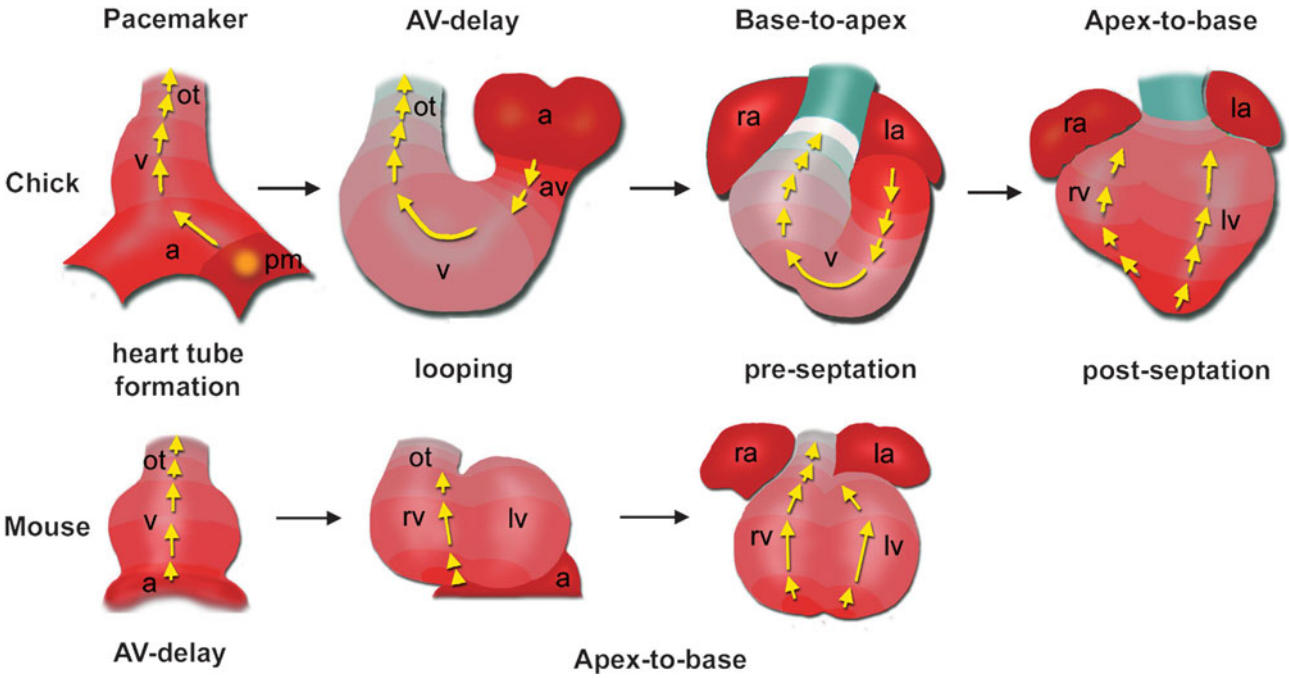

Figure 12.4. Electrical activation sequence at various stages of heart development in chick and mouse. Cardiomyocytes in the caudal heart tube are the first to become electrically active and become the "pacemaker." The activation sequence is altered from base-to-apex to apex-to-base earlier in the mouse heart than in the chick heart, where apex-to-base activation is concurrent with ventricular septation. The initial activation sequence is in the same direction as blood flow. The rate of impulse dissemination is represented by a color gradient with red being highest. a, atria; av, atrioventricular canal; la, left atrium; lv, left ventricle; ot, outflow tract; pm, pacemaker; ra, right atrium; rv, right ventricle; v, ventricle. (From Pennisi et al., 2002, with permission.)

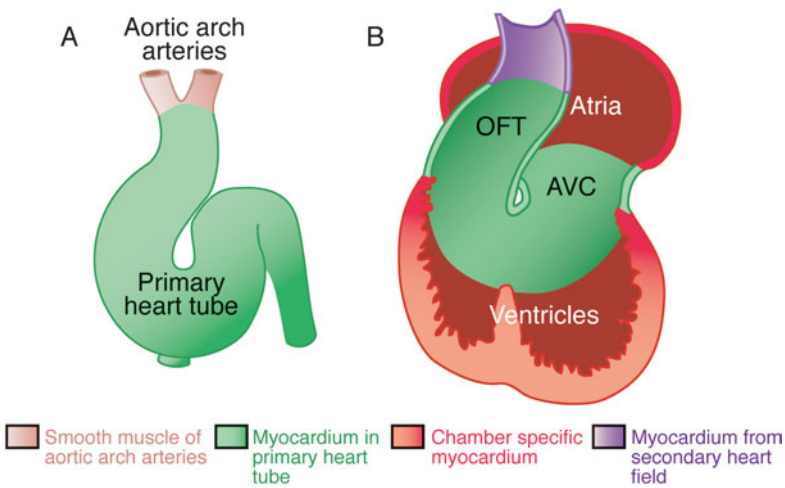

Figure 12.5. Development of the chamber myocardium from the heart tube. The conduction myocardium remains relatively undifferentiated as contractile cardiac muscle while specializing for electrical impulse generation.

This reversal is thought to be due to the onset of preferential conduction through the Purkinje network.

In the chick, the conduction myocardium develops in close spatial association with blood vessels. Differentiation of conduction myocardium may involve earlier commitment to nonproliferation than that of working myocytes (Gourdie et al., 1995). It is thought that the peripheral (i.e., the intramural Purkinje fiber network) and central components of the cardiac conduction system are derived from independent parent cells that are linked together to establish the integrated conduction system of the mature heart (Gourdie et al., 1995). In a recently described transgenic mouse, *lacZ* reporter gene expression delineates the developing cardiac conduction system, extending from the SA node to the Purkinje fibers. Optical mapping studies of the hearts from these mice demonstrate that the His–Purkinje system is functioning well before septation is complete, which explains why apex-to-base activation occurs in the mouse prior to septation (Rentschler et al., 2001).

Trabeculae have unusual conduction properties from their earliest appearance and are the precursors of the Purkinje

fibers of the conduction system (Moorman et al., 2000; Rentschler et al., 2002).

Connexins and Gap Junctions

Intercalated discs occur at the ends of cardiac muscle cells in a region corresponding to the Z-line of the myofibrils. The last Z-line of the myofibril within the cell is "replaced" by the intercalated disk of the cell membrane (Fig. 12.1). Gap junctions are found in the membrane between the intercalated discs (Fig. 12.1). The gap junctions are made from connexin proteins that form intercellular pores between myocardial cells (Fig. 12.6) (Willecke et al., 2002). Although 20 distinct connexin genes have been identified in the human genome, only three types, *connexin43* (*Cx43*), *Cx40*, and *Cx45*, are expressed in heart (Fig. 12.7). These three connexins have different conductive properties and join myocardial cells in an electrical SYNCYTIUM. Cx43 is abundant in atrial and ventricular working myocardium (Fig. 12.7) (Coppen et al., 1998; Davis et al., 1995; Fromaget et al., 1990; Saffitz et al., 1995). Cx40 has the largest CONDUCTANCE and is expressed in atrial tissue and the fast-conducting His–Purkinje system (Delorme et al., 1995; Gros and Jongsma, 1996). Cx45 is expressed in both primary myocardium and in the SA and slow-conducting AV node (Alcolea et al., 1999; Coppen et al., 1999; Kumai et al., 2000).

Six connexin proteins oligomerize to form a HEMICHANNEL (connexon) that migrates to the cell surface membrane and is incorporated at the periphery of junctional plaques (Fig. 12.6). A hemichannel in one cell combines with a corresponding hemichannel in an adjacent cell to form a complete gap junction channel (Gaietta et al., 2002; Laird et al., 1995). Colocalization of different connexin proteins in gap junction plaques can be seen immunohistochemically and probably reflects formation of HETEROMERIC GAP JUNCTION CHANNELS (Honjo et al., 2002; Kanter et al., 1993; Yeh et al., 1998). A major role of gap junctions in the myocardium is to enable rapid and coordinated electrical excitation, which is a prerequisite for normal rhythmic cardiac function. The junctions also facilitate intercellular exchange of small regulatory and signaling molecules. Diffusion of molecules with a molecular mass below 1000 Da occurs across gap junctions, but a role for this type of junctional communication in the cardiac conduction system is not known (Kumar and Gilula, 1996).

Cx40 and Cx43 appear after birth in the mouse ventricular conduction system (Van Kempen et al., 1995). Cx40 is found earlier than Cx43 and disappears when levels of Cx43 become more abundant because Cx43 suppresses Cx40 expression. The SA and AV nodes preferentially express Cx45 which is first seen in the myocardium of the AV canal, that is, in the early heart tube (Alcolea et al., 1999). It is not known whether the myocardium of the AV canal differentiates into AV node cells (Cheng et al., 1999). The rapidly conducting myocardium expresses high-conductance gap junction proteins, Cx43 and 45 (Pennisi et al., 2002).

Figure 12.6. Gap junctions are formed by connexons (*A*) that form channels by multimerizing (*B*). These are packed tightly in junctional plaques between intercalated discs. (Adapted from Kumar and Gilula, 1996 and Wei et al., 2004, courtesy of Cecilia Lo.)

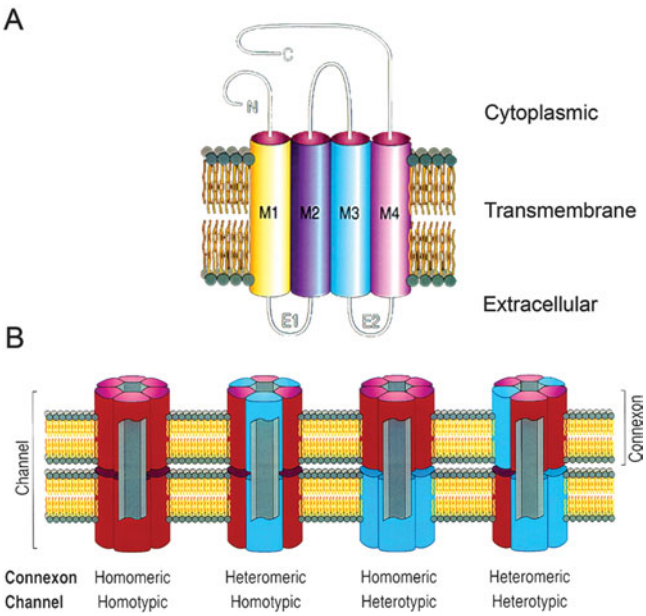

Figure 12.7. Connexins expressed in the heart. Cx45 is expressed in the AV node and bundle, Cx40 in the His–Purkinje system and Cx43 in the chamber or working myocardium.

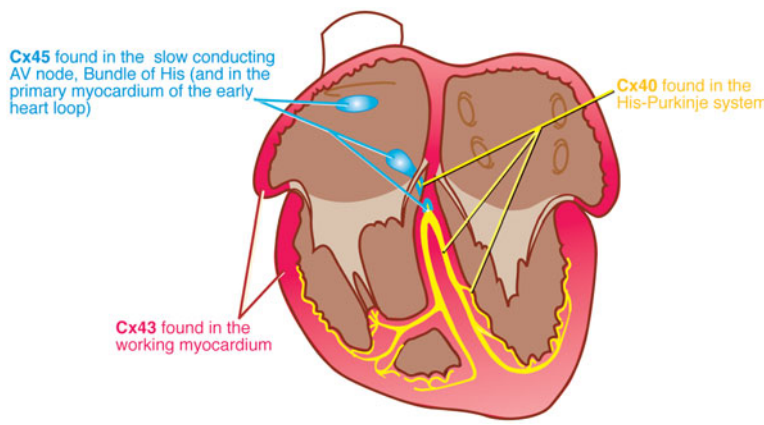

Recent work in the mouse has identified preferential expression of Cx30.2 in nodal tissue (Kreuzberg et al., 2005). Cx30.2 forms low conductance gap junction channels and these may in part account for the significant delay in conduction that occurs across the atrioventricular junction.

Cx45-null mice initiate heart contractions normally but die of heart failure at E10 (Kumai et al., 2000). The interpretation of this is somewhat confused by the fact that development of both the AV cushions and AV canal myocardium are compromised. *Cx40*-null mice have inducible atrial TACHYARRHYTHMIAS with partial AV block (Hagendorff et al., 1999; Kirchhoff et al., 1998; Simon et al., 1998; Tamaddon et al., 2000). Cx45 is co-expressed with Cx40 in the His bundle and Purkinje fibers and may compensate for the lack of Cx40 in these parts of the conduction system even though the channels made by these two connexins have very different functional properties. *Cx43*-null mice survive early development because of early expression of Cx45 and Cx40. These mice die at birth from right ventricular outflow obstruction caused by the presence of smooth muscle-lined pouches (Huang et al., 1998; Li et al., 2002). This phenotype is most likely due to malfunction of a non-myocardial cell population because cardiac myocyte-specific deletion of Cx43 does not result in the same phenotype. Instead, these mice develop spontaneous ventricular arrhythmias around 2 months postnatally, which result in sudden death (Gutstein et al., 2001). Compound heterozygous mice lacking normal levels of Cx40 and Cx43 show cardiac conduction abnormalities. The electrocardiograms of these animals suggest that the effects of these two connexins are additive in the conduction myocardium of the ventricle but not the atrium (Kirchhoff et al., 2000). These animals also have a common atrioventricular canal suggesting that specification/differentiation of the conduction myocardium in the atrioventricular canal is important for normal morphological development and septation.

Ion Channels in the Developing Conduction System

Ion channels have been thoroughly discussed in Chapter 5. Only two ion channel proteins have been identified as being differentially expressed at a higher level in the conduction system. Both are potassium channel related. The first is minK, which is an essential accessory subunit associated with KvLQT1, a voltage-gated potassium channel. MinK is expressed throughout the heart but has been shown to be very highly expressed in the mouse conduction system (Kupershmidt et al., 1999). KvLQT1 itself is highly expressed in all regions of the heart and in humans, inherited mutations in this channel lead to long QT syndrome (discussed further, below) (Kreuzberg et al., 2005). The prolongation of the QT interval implies that repolarization of the ventricular myocardium takes longer than normal. The potassium current carried by KvLQT1 channels is referred to by physiologists as the delayed rectifier current, I_{Ks}. I_{Ks} contributes to repolarization of the action potential and loss of function results in prolongation of the action potential.

The second potassium ion channel protein that has been shown to be highly expressed in the mouse and chick embryonic ventricular conduction system is Task1 (Fig. 12.8) (Graham et al., 2006). Task1 (KCNK3 in the human genome) is a two-pore domain background potassium channel that is active as an outward current throughout the cardiac action potential. As an almost pure potassium background current, its activity tends to stabilize the resting membrane potential near the equilibrium potential for potassium (~ -90 mV). Unlike most markers of the conduction system, the expression pattern for Task1 is remarkably similar in both mouse and chick embryonic heart. Initially in the early tubular heart, expression is uniform. In the ventricles, expression gradually becomes restricted to the trabecular myocardium and subsequently to the His–Purkinje conduction system. Expression remains high in the atrium. Task1 has several unique properties that suggest it may be an important modulator of conduction system activity. It is sensitive to extracellular pH in the normal physiological range ($K_{D(pH)} = 7.3$, Hill coefficient ≈ 1.5–2.0; Morton et al., 2003; O'Connell et al., 2002). This suggests that the channel may act as a pH sensor for acidosis.

Figure 12.8. Immunofluorescent staining of Task-1 in the chick embryo. Task-1 preferentially marks the ventricular conduction systems of the chick and mouse embryonic heart. (From Graham et al., 2006, with permission.)

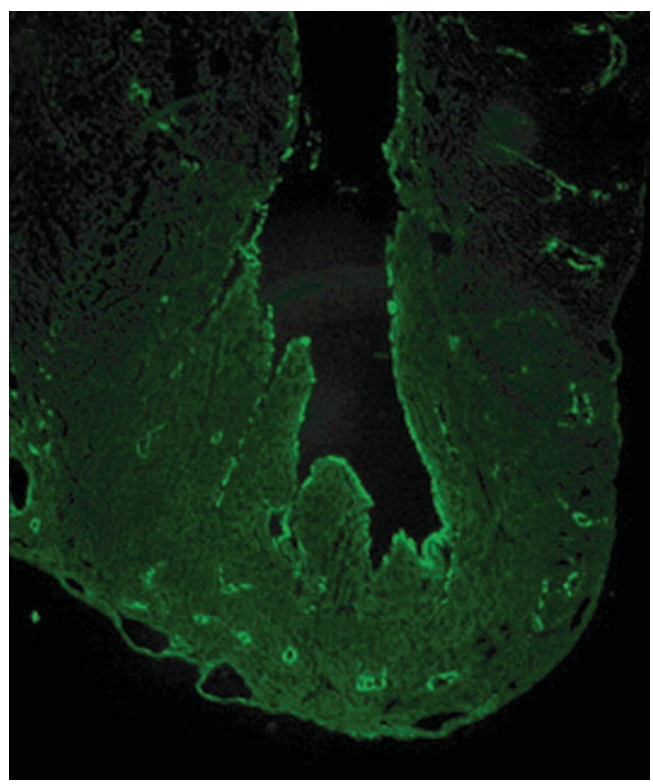

Task1 is also inhibited by hypoxia and appears to serve as an O_2 sensor. Importantly, Task1 activity is inhibited by receptor-mediated cell signaling mechanisms that increase phospholipase-C and protein kinase activity (Bayliss et al., 2003). The latter suggests that its activity may be inhibited by α-adrenergic and/or muscarinic receptor stimulation by the autonomic nervous system. However, whether Task1 plays a significant role in regulation of ventricular conduction remains to be determined.

Induction and Differentiation of the Conduction Myocardium

The primary heart tube is composed of slow-conducting myocardium that Moorman and colleagues have called "primary" myocardium to distinguish it from "working" or fully differentiated chamber myocardium (Moorman and Lamers, 1994). In the chick, the conduction velocity remains about 1 cm/sec in the outflow myocardium, while it increases 20-fold in the prospective ventricles to about 20 cm/sec between days 2 and 7 of incubation. Transmembrane potentials of outflow and atrioventricular canal myocytes slowly rise, while the upstroke velocity in atrial and ventricular myocardium increases 8- to 13-fold. Repolarization of the outflow myocardium finishes at the start of the next cycle. As the chamber myocardium is specified and differentiates into working myocardium, it is separated by a band of slow-conducting primary myocardium in the AV canal, which serves to delay conduction from the atria to the ventricles (Fig. 12.9) (Moorman et al., 1998). The rapidly conducting "working" myocardium is thought by some investigators to represent more advanced myocardial differentiation. The slowly conducting myocardial zones appear to be essential for the function of the embryonic heart because alternating segments of slow and fast conduction are necessary for consecutive contraction of the tubular heart. The prolonged peristaltic contraction in the atrioventricular canal and outflow tract provides a one-way sphincteric function prior to the development of mature valves (de Jong et al., 1992). Sequential activation of the atria and ventricles with an AV delay is reflected in the development of an adult-type electrocardiogram (Paff et al., 1968; Van Mierop, 1967). The fast conduction system, represented by the ventricular conduction system because it develops from ventricular myocardium, includes the AV bundle, bundle branches, and Purkinje fibers, and these are the last to differentiate (Moorman et al., 1998). In the chick the maturation of this part of the conduction system correlates with the switch from base-to-apex activation to apex-to-base activation (Chuck et al., 1997).

In the mouse, Tbx3 is expressed in the nodes, the internodal regions, and the cardiac conduction system in the mature heart and functions to repress transcription of chamber-specific genes in the regions from which the components of the central conduction system are subsequently formed (Fig. 12.10)

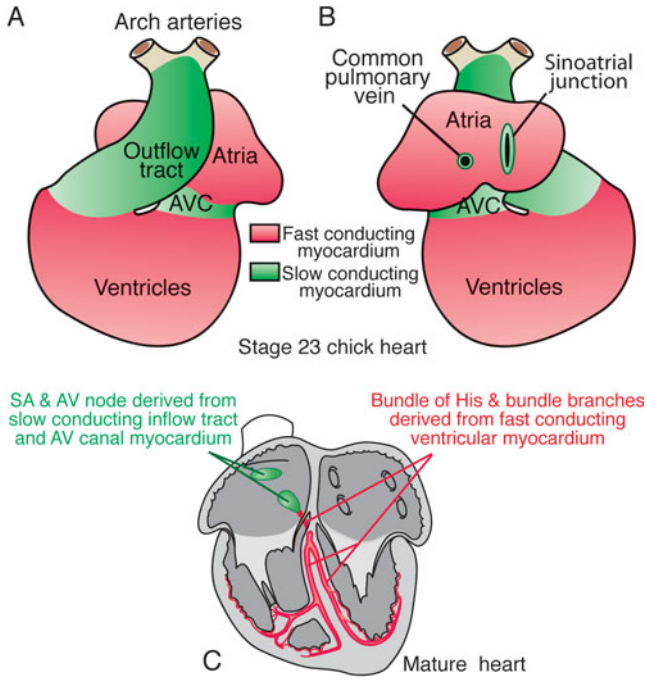

Figure 12.9. Fast- and slow-conducting myocardium in the developing heart tube and in the cardiac conduction system.

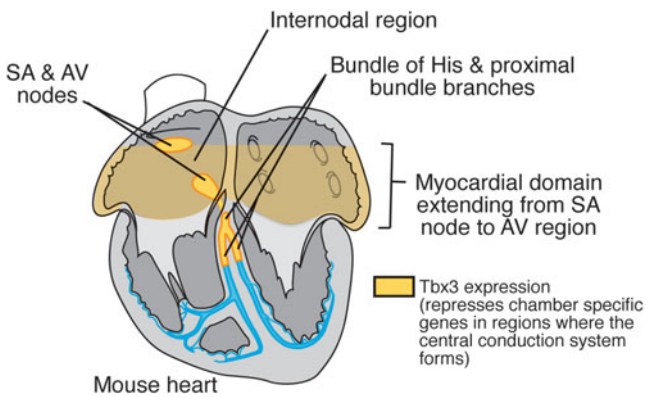

Figure 12.10. Inhibitory role of Tbx3 in formation of the central conduction system.

(Hoogaars et al., 2004). During cardiac development, Tbx3 is expressed from the time of looping in an uninterrupted myocardial domain that extends from the SA node to the AV canal (Fig. 12.10). Expression of chamber-type myocardial markers is specifically absent from this Tbx3 expression domain. These regions also correlate with NF160 staining in the rabbit heart, blue labeling in the various mouse models with galactosidase-marked conduction myocardium, and Gln2 expression in the human heart (Fig. 12.11) (Moorman et al., 1998; Rentschler et al., 2001; Rothenberg et al., 2005). NF160 actually labels all the components of the rabbit conduction system simultaneously and throughout development, but unfortunately, this global conduction system marker is unique to the rabbit (Rothenberg et al., 2005).

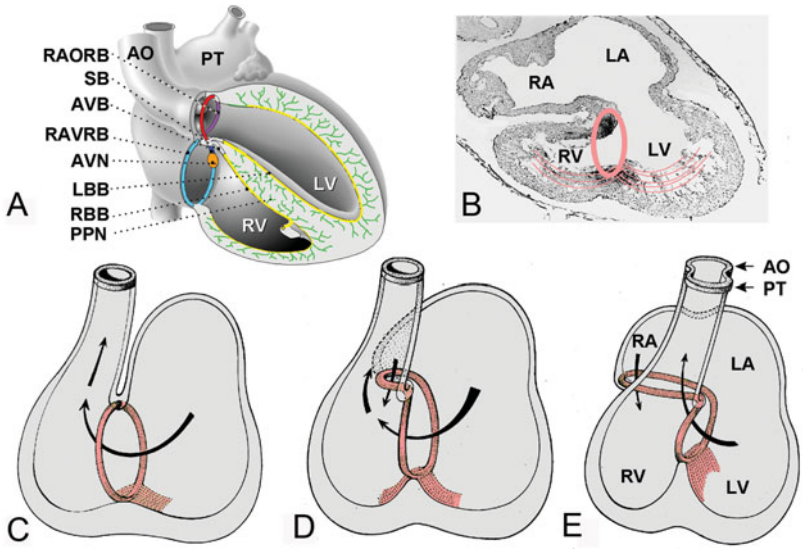

Figure 12.11. The AV bundle, bundle branches, and Purkinje cells are presaged by GlN2 expression (*red* in *B*) in a ring of interventricular myocardium shown in *C*, *D*, and *E*. (*A*) Drawing of the ventricular conduction system. (*B*) Section of a 5-week human heart immunostained for GlN2 (*red*) that identifies the developing conduction system. (*C–E*) are drawings representing the development of the AV bundle and bundle branches based on reconstructions of GlN2 expression in developing human heart at 5 (*C*), 6 (*D*), and 7 (*E*) weeks of development. RAORB, retroaortic root branch; SB, septal branch; RAVRB, right atrioventricular ring bundle; LBB and RBB, left and right bundle branches, respectively; LA, left atrium; LV, left ventricle; RA, right atrium; RV, right ventricle; AO, aorta; and PT, pulmonary trunk. (From Moorman et al., 1998, with permission.)

As the AV bundle, bundle branches and Purkinje fibers differentiate, some of the proteins typically found in working myocardium for instance cardiac myosin binding protein C fails to be upregulated in the conduction myocardium (Takebayashi-Suzuki et al., 2000, 2001). By contrast, proteins expressed in neural tissues, such as neurofilaments and central nervous system-associated glycoproteins, and skeletal muscle are upregulated (Gonzalez-Sanchez and Bader, 1985; Gorza et al., 1994; Sartore et al., 1978). Conduction myocardium begins to express specific sets of ion channels, connexins, and transcription factors, including upregulated Nkx2.5 (Takebayashi-Suzuki et al., 2001; Thomas et al., 2001). In the chick, the most terminal Purkinje fibers of the conduction system associate intimately with coronary arteries (Gourdie et al., 2003). Markers of the Purkinje fibers in the chick include neurofilament EAP300, Cx42, atrial myosin heavy chain, and slow muscle myosin heavy chain. All of these markers are virtually undetectable in mouse E13 ventricular myocytes, suggesting that they are not present and/or functional.

In the chick, myocytes traced from the tubular heart are capable of differentiating into periarterial Purkinje fibers near the coronary arteries almost until hatching (Gourdie et al., 1995). These periarterial Purkinje fibers are not seen in mammalian hearts where the Purkinje fibers are subendocardial rather than intramyocardial (Moorman et al., 1998). Purkinje fibers differentiate from a subset of contractile myocytes (Cheng et al., 1999; Gourdie et al., 1995). In the chick, suppression or enhancement of coronary arterial branching is associated with a decrease or increase in Purkinje fiber differentiation, respectively (Fig. 12.12) (Hyer et al., 1999). The endothelium at these sites may provide instructive cues as inhibition of intramural coronary arterial development or ectopic arterial development in the developing heart results in suppression or ectopic Purkinje fiber differentiation, respectively (Gourdie et al., 1998, 1999; Hyer et al., 1999; Mikawa and Fischman, 1996). Endocardial and/or endothelial cells can induce and/or maintain conduction myocytes (Pennisi et al., 2002).

In the chick, when base-to-apex activation is replaced by apex-to-base activation at 5–7 days of incubation, the cardiac conduction system expresses increased Wnt11 relative to the surrounding myocardium (Bond et al., 2003). Expression continues to increase until incubation day 14 when Wnt11 is downregulated. Wnt7a is expressed at elevated levels in cells adjacent to the ventricular endocardium along the interventricular septum and tips of the trabeculae at incubation day 10. These sites correlate with the spatiotemporal distribution of Cx40, a marker for the subendocardial and periarterial conduction fibers (Bond et al., 2003).

Endothelin, a growth factor secreted by endothelial cells, promotes expression of Purkinje fiber markers in the chick (Gourdie et al., 1998, Kanzawa et al., 2002, Takebayashi-Suzuki et al., 2001, Takebayashi-Suzuki et al., 2000). The activating factor for endothelin-1, endothelin converting enzyme (Ece)1, is localized to the endocardium and endothelium, suggesting that endothelial/endocardial cells produce endothelin, while endothelinA receptor is expressed throughout the ventricular myocardium (Fig. 12.13) (Mikawa and Gourdie, 1996, Rychter and Ostadal, 1971). Forced coexpression of Ece1 and the endothelin-1 precursor called preproET-1 into working myocytes is sufficient to convert embryonic myocytes into Purkinje fibers (Takebayashi-Suzuki et al., 2001). No conversion of myocytes to Purkinje fibers is induced by Fgf, Pdgf, Vegf, ANGIOTENSIN II, or INSULIN-LIKE GROWTH FACTOR I (Pennisi et al., 2002). A subset of genes which is expressed by Purkinje fibers is not induced by endothelin, suggesting that other factors are necessary for Purkinje fiber induction (Mikawa et al., 2003).

Neuregulin-1 has been suggested as a factor important for conduction system development in the mouse although it is also present in the chick (Ford et al., 1999; Hertig et al., 1999; Rentschler et al., 2002). Neuregulin is expressed by the embryonic endocardium, and its receptors, erbB2 and erbB4, are

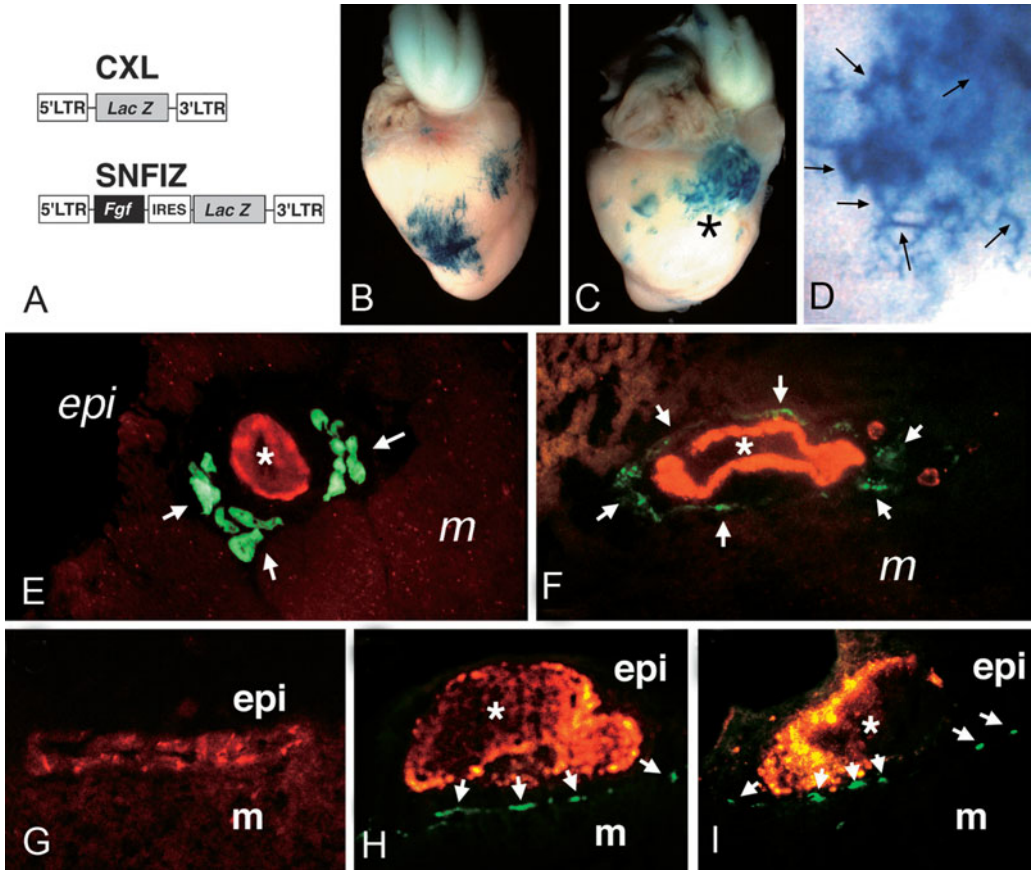

Figure 12.12. Forced expression of FGF in the chick heart leads to hypervascularization which in turn increases Purkinje cell density. (*A*) Proviral construct that expresses only β-galactosidase (CXL)or β-galactosidase with FGF4 (SNFIZ). (*B*) Heart expressing only β-galactosidase (*blue*). (*C*) Heart expressing both β-galactosidase and FGF4. (*D*) vessels (*arrows*) induced by ectopic FGF4 expression. Ectopic induction of Purkinje fibers at FGF-induced sites of hypervascularization. E–I cryosections double-labeled with an antibody that recognizes Purkinje fibers (*green*) and β-galactosidase (*red*) or smooth muscle (*red*) antibodies. Periarterial Purkinje fibers (*green*) in ventricular myocardium (m) of an E18 chick (*E*) and adult (*F*) chicken are shown for comparison with arterial smooth muscle (*red*). (*G*) no Purkinje fibers are induced in the myocardium subjacent to epicardial cells (*red*) infected with control B-gal virus. (*H* and *I*) Induced Purkinje fibers (*green, arrows*) in myocardium adjacent to blood vessels induced by ectopic FGF4. *Asterisks* mark the lumen of the artificially formed vessels. Epi, epicardium. (From Hyer et al., 1999, with permission.)

expressed by the embryonic myocardium (Rentschler et al., 2002). Exogenously delivered neuregulin-1 induces excessive trabeculae and upregulates Purkinje fiber differentiation (Hertig et al., 1999; Rentschler et al., 2002). Because deletion of *neuregulin* and its *ErbB receptors* genes are lethal very early in development, it has not been possible to test genetically whether they are involved in conduction myocardium induction (Armstrong and Bischoff, 2004; Schroeder et al., 2003). Murine embryonic cardiomyocyte cultures induced with endothelin-1 and/or neuregulin-1 showed that cardiomyogenesis and cardiac conduction system-specific markers, such as Nkx2.5, Gata4, Irx4, Cx40, Cx45, Hf-1b, and MinK, were up-regulated in the presence of either growth factor. Immunofluorescence analysis showed that endothelin-1 or neuregulin-1 increased the number of cells expressing the Purkinje fiber-specific marker Cx40. Interestingly, endothelin-1 and neuregulin-1 treatment together did not have an additive effect in inducing conduction myocardium (Patel and Kos, 2005).

An essential and frequently overlooked component of conduction system development is establishing the electrical discontinuity at the atrioventricular junction (Fig. 12.14). In the embryonic heart tube, the atrioventricular myocardium is electrically coupled. If this persisted, the atrioventricular delay and the mature ventricular activation sequence would not be possible. The separation between atrial and ventricular myocardium at the atrioventricular junction in the developing human heart is established by the incorporation of nonmyocardial tissue at the atrioventricular sulcus with the atrioventricular cushions tissue. The separation of atrial and ventricular myocardium in human embryos starts at about 7 weeks and is completed around the 12th week of development leaving the atrioventricular bundle as the only myocardial continuity between atrial and ventricular myocardium (Wessels et al., 1996). There is still controversy about whether accessory pathways grow later or are remnants of incomplete separation from abnormal development, and the most recent

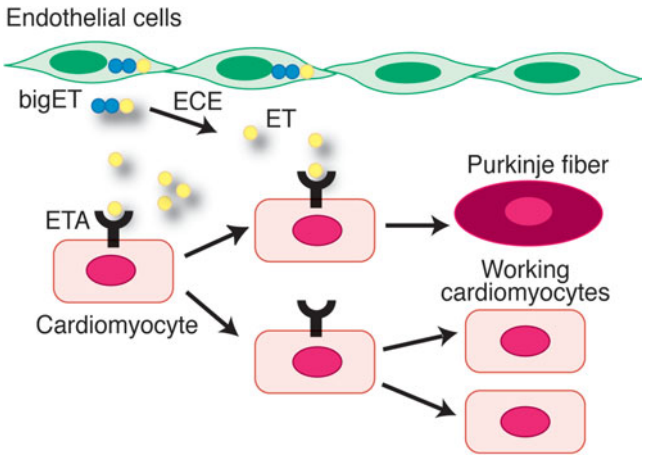

Figure 12.13. Proposed model for endothelin induction of Purkinje fibers. Endothelin-converting enzyme-1 (ECE)-expressing endothelial cells convert endothelin precursor (bigET) into mature endothelin (ET) which induces differentiation of the Purkinje fibers via endothelin receptors (ETR) on cardiomyocytes. (Adapted from Takebayashi-Suzuki et al., 2000.)

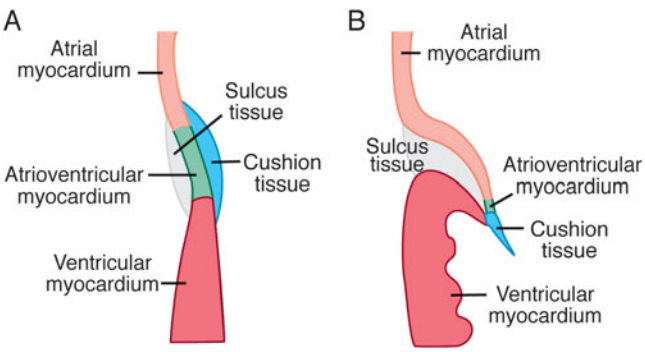

Figure 12.14. Diagrammatic representation of the atrioventricular junction showing development of myocardial discontinuity. (Adapted from Wessels et al., 1996.)

evidence suggests that these pathways may be reestablished after birth (Patel et al., 2003).

Development of the Electrocardiogram

In avian embryos, a pacemaker is first established in the inflow tract at the straight heart tube stage (Hirota et al., 1983; Van Mierop, 1967). In the chick embryo, a pacemaker differentiates around 25–35 h of incubation; this corresponds to E7.5 in the mouse (Kamino et al., 1981), (Gourdie et al., 2003). The currents and channels that function to begin electrical activity and pacemaking are under intense investigation. From the onset of function, a cranial-to-caudal axis is established both for pacemaker dominance and for intrinsic beat (Satin et al., 1988). Polarity along this axis, with the leading pacemaker being most posterior, maintains a unidirectional wave of

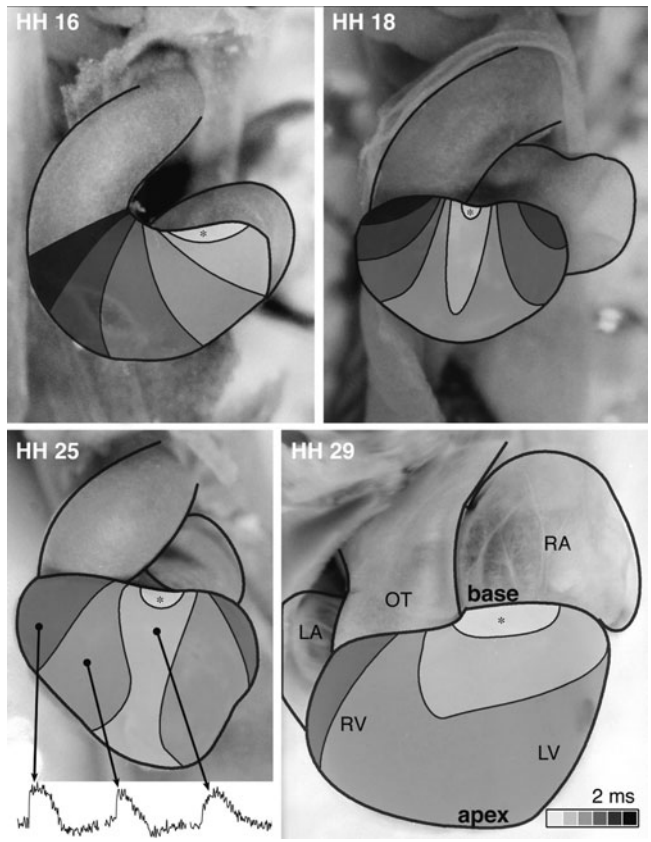

Figure 12.15. Optical mapping generates electrical activation maps of anterior surface of the embryonic ventricles. Note the preferential anterior conduction pathway typically present at stages 17/18 and 24/25. (From Sedmera et al., 2004, with permission.)

contraction. This unidirectional wave is essential to the successful maintenance of properly coordinated blood flow. The genetic underpinnings of the cranial-to-caudal axis of contraction are unknown. However, transplantation and optical mapping experiments have shown that the polarity along this axis of contraction is not fixed and can adapt to a new position (DeHaan, 1967; Kamino et al., 1988).

A SINUSOIDAL ELECTROCARDIOGRAM can be obtained from the linear heart tube before either separation of the atrial and ventricular myocardium and before the conduction system cells can be distinguished (Hoff Ebbe et al., 1939; Paff et al., 1968; Seidl et al., 1981). After working myocardium begins to differentiate the presence of a mixture of primary myocardium, which retains conduction properties, and the more highly differentiated working chamber myocardium leads to an impulse that is generated at the inflow end of the heart and delayed by a ring of atrioventricular primary myocardium that causes atrioventricular delay (Moorman and Christoffels, 2003). The primary myocardium lacks gap junctions characterized by Cx40 and never expresses atrial natriuretic factor, both characteristics of working myocardium (Anderson et al., 2004). Tbx2 and -3 are expressed in cells that do not transform into working myocardium (Habets et al., 2002; Hoogaars et al., 2004).

The preseptation chick heart initiates an electrical impulse in the region below the left atrium, and excitation spreads toward the apex and outflow tract, called base-to-apex activation (Fig. 12.15) (Chuck et al., 1997; Sedmera et al., 2004). As the final steps in septation occur, activation appears first at the apex with rapid spread toward the base of the ventricles, called apex-to-base activation. This shift in activation sequence suggests that the onset of His-Purkinje function is coordinated with septation; however, septation is not coordinated with the shift to apex-to-base conduction in the mouse and rabbit.

In mouse, the thinner myocardium and earlier maturation of the central conduction system allows activation from the apex prior to ventricular septation (Rentschler et al., 2001). This is also true in the rabbit, where the presence of collagen in the AV junction coincides with the appearance of an AV interval on the electrocardiogram (Rothenberg et al., 2004).

Genetic Models of Conduction System Development

Studying the conduction system during development has been problematic because of the lack of markers of the differentiating conduction myocardium. Genetically engineered mice with reporter genes marking the conduction myocardium are now available and have provided a wealth of information about the developing conduction system. The transgenic lines to date are *CCS–lacZ*, *MinK–lacZ*, *Gata6–lacZ*, *troponin I–lacZ*, and *Cx40–EGFP* (Davis et al., 2001; Di Lisi et al., 2000; Kupershmidt et al., 1999; Miquerol et al., 2004; Rentschler et al., 2001).

The *CCS–lacZ* transgene appears to label the entire cardiac pacemaking and conduction system throughout development, although there is controversy as to whether excess, nonconduction system tissue is also being labeled (Anderson et al., 2004). The only other marker that completely labels this system is NF-160 in the rabbit. The *CCS–lacZ* mouse line is a transgenic line with an ENGRAILED (En)-2 enhancer driving *lacZ* inserted into a site near an endogenous promoter that drives this specific expression. The endogenous gene has not been identified. *CCS–lacZ* transgene is expressed in the SA node, left and right venous valve leaflets septum spurium, right and left atrioventricular ring, His bundle, bundle branches, right ventricular moderator band, left atrium and in the posterior wall surrounding the pulmonary venous orifice. The cells in the pulmonary venous orifice are continuous with cells in the left venous valve leaflet in the right atrium. *LacZ*-positive tissue also can be identified in BACHMANN'S BUNDLE, running retro-aortically between the right atrium and left atrium (Jongbloed et al., 2004). Electrophysiological correlation of labeled cells in the atrium and histological correlation with other markers have not been performed.

The *MinK–lacZ* mouse was created by replacing the *MinK* gene with a nuclear-targeted LACZ REPORTER CONSTRUCT (Kupershmidt et al., 1999). The MinK protein co-assembles with KvLqt1 to form a slowly activating, delayed rectifier K current that has a role in cardiac repolarization (Barhanin et al., 1996; Sanguinetti et al., 1996). Expression is initially seen in mice at E8–9 along the dorsal wall of the newly formed heart tube and subsequently in the inner curvature (Kondo et al., 2003). By E10.5, discrete rings of galactosidase expression are found at the atrioventricular junction along with expression at the intersection of the crest of the developing interventricular septum, the inferior endocardial cushion, and the caudal wall of the outflow tract; some expression is also found in the subendocardial trabeculations. By E11.5–12.5, the AV node is visible as an invagination of the atrioventricular ring into the inferior atrioventricular cushion and is colocalized with an extension of the crest of the interventricular septum. Rings of expression at these stages surround both the outflow tract and the atrioventricular canal. The conduction system attains its adult pattern concurrent with the completion of septation at E13.5 (Kondo et al., 2003).

The cardiac-specific chicken *Gata6* enhancer was used to drive *lacZ* expression in the AV canal myocardium during early development. It appears later in the atrioventricular junction, node, His bundle, and bundle branches. *Gata6*-driven deletion of the *Alk3* gene, which codes for the Bmp type Ia receptor caused deletion of *Alk3* just in the AV canal. These mice have ventricular preexcitation (Davis et al., 2001).

The cardiac *troponin I–lacZ* transgene is expressed in atrioventricular canal myocardium early in development. Later β-galactosidase positive cells are found in the atrioventricular node and in the lower rim of both right and left atria. Because this is not a lineage marker, it is unclear whether the cells in the atrioventricular node and lower atria are descendants of the atrioventricular canal myocardium, but the common expression suggests that this might be the case (Di Lisi et al., 2000).

Because Cx40 is expressed in the conduction system, it is possible to use its promoter to drive expression of enhanced green fluorescent protein (Egfp) to map the earliest precursors. Egfp signal was seen in the coronary arteries, the atria, the atrioventricular node, and the His–Purkinje system. An interesting result of this study is that the His–Purkinje system was found to be asymmetrical. Only one fascicle makes up the right bundle branch, while there are about 20 on the left. In addition, the density of the Purkinje fibers in the ventricles is low on the right and high on the left. The profiles of the electrical activation patterns recorded on the right and left sides of the interventricular septum are also asymmetrical (Miquerol et al., 2004).

Dysrhythmias and Other Conduction System Dysfunctions

Atrioventricular Conduction Disease

AV conduction disease occurs when conduction is slowed or blocked anywhere along the conduction system pathways

(Benson, 2004). Conduction is classified by the extent of block, that is, first, second, or third degree, and where the block occurs. This is based on the PR interval on the electrocardiogram. The PR interval is measured from the onset of the P-wave to the onset of the QRS complex. First-degree AV block is the mildest form of block and is seen as prolongation of the PR interval, while third degree block is the most severe, and no atrial impulses conduct to the ventricle. Thus the QRS complex occurs independent of the P-wave entirely (Benson, 2004). In second-degree block, some atrial impulses are conducted to the ventricle while others are not. In type 1 second-degree block the PR interval becomes progressively prolonged before the failure of conduction occurs while in type 2 second-degree block, the block occurs without any prolongation of the PR interval (Benson, 2004). These two types indicate the anatomic site of the block. Type 1 second-degree block occurs because of dysfunction at the AV node while type 2 is a block at the distal His–Purkinje system (Benson, 2004). Congenital AV block in the absence of cardiac malformation is usually found in maternal autoimmune disease, particularly autoantibodies to SSA/Ro and/or SSB/La ribonucleoproteins associated with neonatal lupus syndrome (Buyon et al., 1998; Moak et al., 2001). AV block can be detected between 16 and 24 weeks of gestation.

AV conduction disturbance is frequently seen in patients with neuromuscular diseases, although it also occurs in isolation idiopathically (Benson, 2004). The association of single gene mutations with AV conduction disease indicates that it is genetically heterogeneous. AV conduction abnormalities are also seen in association with congenital heart defects. Heterozygous mutations in *NKX2.5* are identified as a cause of AV conduction disease as well as several cardiac malformations, including atrial septal defect, ventricular septal defect, tetralogy of Fallot, and tricuspid valve abnormalities including Ebstein malformation (Benson et al., 1999; Goldmuntz et al., 2002; McElhinney et al., 2002; Schott et al., 1998; Watanabe et al., 2002). However, AV block in humans can be caused by *NKX2.5* mutation without structural malformations (Benson et al., 1999). Ventricular restricted knockout of *Nkx2.5* in mice results in progressive AV block (Pashmforoush et al., 2004). In humans, *NKX2.5* mutation causes AV node conduction delay that progressively worsens to second- or third-degree block (Benson et al., 1999). *TBX5* mutations are also associated with a similar progressive AV conduction disease, but the functional relationship of the two genes is not known (Basson et al., 1997).

Recent experimental evidence in mice that are heterozygous null for *Nkx2.5* have conduction defects that correlate with cellular hypoplasia (Jay et al., 2004). The His bundle is thin and hypoplastic with low-amplitude depolarization, and the Purkinje fibers are much reduced in number. This hypocellular Purkinje network can explain the prolonged QRS duration seen in these mice. Furthermore, MinK–galactosidase-positive cells are never present in the AV region of *Nkx2.5*-null embryos, suggesting that Nkx2.5 is needed to establish the AV node.

Wolff–Parkinson–White Syndrome

Wolff–Parkinson–White syndrome is characterized by a congenitally existing accessory conduction pathway between the atria and ventricles that causes pre-excitation of the ventricles. Wolff–Parkinson–White syndrome has recently been identified as a glycogen storage disease. It is a familial arrhythmogenic disease characterized by ventricular preexcitation, atrial fibrillation, tachyarrhythmias, progressive conduction system disease, and cardiac hypertrophy. It occurs in 0.1–0.3% of the population, causes considerable morbidity, and may cause sudden death. The syndrome is an autosomal dominant disorder and has been linked to a mutation in the γ-2 regulatory subunit (PRKAG2) of AMP-activated protein kinase (AMPK). These observations confirm an important functional role of AMPK in the regulation of ion channels specific to cardiac tissue (Gollob et al., 2001). In mice, Prkag2 mutations cause formation of vacuoles filled with glycogen-associated granules within myocytes that disrupt the annulus fibrosis which is necessary for isolating atria from ventricles (Arad et al., 2003). Accumulation of glycogen-associated granules engorges the myocytes, causing pre-excitation.

Long QT Syndrome (LQTS)

Long QT syndrome is characterized by an extended delay between the QRS complex and the T wave on the electrocardiogram which can lead to sudden death. Inherited forms of LQTS are predominantly autosomal dominant, although less common autosomal recessive forms exist and typically result in more severe phenotypes. Romano–Ward syndrome is typically autosomal dominant and predominantly heterozygous, although some more severe homozygous forms exist (Wang et al., 1996). Romano–Ward syndrome is distinguishable from Jervell Lange–Nielsen syndrome, because the latter is autosomal recessive and always accompanied by hearing loss (Chen et al., 1999). Long QT syndrome results from mutations in genes coding for proteins that underlie the myocardial action potential: ion channels, accessory subunits, and associated modulatory proteins. To date, five genes have been implicated in Na^+ and K^+ channel linked LQTS (Table 12.1 and Fig. 12.16) (Clancy and Kass, 2005). Mutations in the cardiac voltage-gated sodium channel α-subunit gene (*SCN5A*) result in persistent sodium current which delays repolarization. Delayed repolarization leads to a distinctive polymorphic ventricular tachycardia called torsades de pointes.

Brugada Syndrome

Brugada syndrome was first characterized in 1992 as syncopal episodes and/or resuscitated sudden death in patients with a structurally normal heart and right bundle branch block with ST segment elevation in electrocardiogram leads V1 to V3. The disease has an autosomal dominant pattern of transmission in 50% of the familial cases. Several different mutations

Table 12.1.
Na^+ and K^+ Channel LQT-Associated Genes and Proteins. I_{Na}, Fast Voltage-Gated Na^+ Channel; I_{Ks}, Slowly Activating Component of the Delayed Rectifier K^+ Current; I_{Kr}, Rapidly Activating Component of the Delayed Rectifier K^+ Current

Type	LQTS1	LQTS2	LQTS3	LQTS5	LQTS6
Gene	*KCNQ1*	*KCNH2 (hERG)*	*SCN5A*	*KCNE1*	*KCNE2*
Protein	KCNQ1, KvLQT1, α-subunit of I_{Ks}	HERG or α-subunit of I_{Kr}	$Na_v1.5$ or α-subunit of I_{Na}	KCNE1, MinK or β-subunit is I_{Ks}	MiRP1 or β-subunit of I_{Kr}

From Clancy and Kass (2005), with permission.

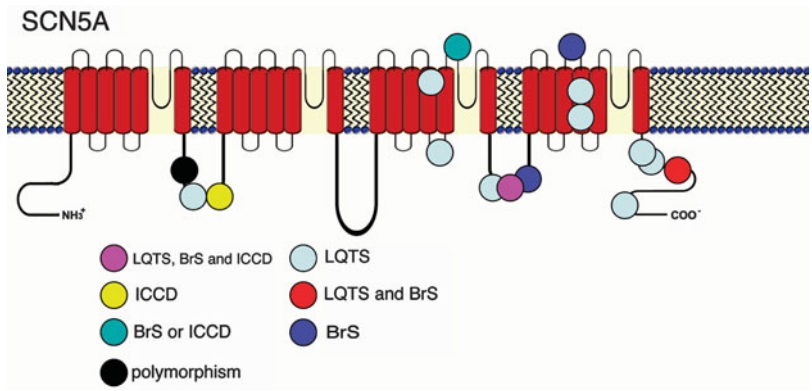

Figure 12.16. Diagram of the voltage-gated cardiac Na^+ channel (NaV1.5). Mutations of this channel at the sites indicated lead to the LQT3 form of long QT syndrome (LQTS), Brugada syndrome (BrS), and isolated cardiac conduction disorder (ICCD) or mixed combinations of disorders. (From Clancy and Kass, 2005, with permission.)

have been identified that affect the structure, function, and trafficking of the sodium channel (Brugada et al., 2005). One of these is mutation in the cardiac voltage-gated sodium channel α-subunit gene (*SCN5A*) described for long QT syndrome. *SCN5A* mutations associated with Brugada syndrome reduce sodium current, which alters transmural myocardial voltage gradients. This causes ventricular fibrillation. *SCN5A* mutations are also associated with AV block.

REFERENCES

Alcolea, S., M. Theveniau-Ruissy, T. Jarry-Guichard, I. Marics, E. Tzouanacou, J. P. Chauvin, J. P. Briand, A. F. Moorman, W. H. Lamers, and D. B. Gros. 1999. Downregulation of connexin 45 gene products during mouse heart development. Circ. Res. 84:1365–1379.

Alyonycheva, T., L. Cohen-Gould, C. Siewert, D. A. Fischman, and T. Mikawa. 1997. Skeletal muscle-specific myosin binding protein-H is expressed in Purkinje fibers of the cardiac conduction system. Circ. Res. 80:665–672.

Anderson, R. H., V. M. Christoffels, and A. F. Moorman. 2004. Controversies concerning the anatomical definition of the conduction tissues. Anat. Rec. 280:8–14.

Anderson, R. H., and I. M. Taylor. 1972. Development of atrioventricular specialized tissue in human heart. Br. Heart J. 34:1205–1214.

Arad, M., I. P. Moskowitz, V. V. Patel, F. Ahmad, A. R. Perez-Atayde, D. B. Sawyer, M. Walter, G. H. Li, P. G. Burgon, C. T. Maguire, D. Stapleton, J. P. Schmitt, X. X. Guo, A. Pizard, S. Kupershmidt, D. M. Roden, C. I. Berul, C. E. Seidman, and J. G. Seidman. 2003. Transgenic mice overexpressing mutant PRKAG2 define the cause of Wolff–Parkinson–White syndrome in glycogen storage cardiomyopathy. Circulation 107:2850–2856.

Armstrong, E. J., and J. Bischoff. 2004. Heart valve development: endothelial cell signaling and differentiation. Circ. Res. 95: 459–470.

Barhanin, J., F. Lesage, E. Guillemare, M. Fink, M. Lazdunski, and G. Romey. 1996. K(V)LQT1 and lsK (minK) proteins associate to form the I(Ks) cardiac potassium current. Nature 384:78–80.

Basson, C. T., D. R. Bachinsky, R. C. Lin, T. Levi, J. A. Elkins, J. Soults, D. Grayzel, E. Kroumpouzou, T. A. Traill, J. Leblanc-Straceski, B. Renault, R. Kucherlapati, J. G. Seidman, and C. E. Seidman. 1997. Mutations in human cause limb and cardiac malformation in Holt-Oram syndrome. Nat. Genet. 15:30–34.

Bayliss, D. A., J. E. Sirois, and E. M. Talley. 2003. The TASK family: two-pore domain background K^+ channels. Mol. Interv. 3: 205–219.

Benson, D. W. 2004. Genetics of atrioventricular conduction disease in humans. Anat. Rec. 280:934–939.

Benson, D. W., G. M. Silberbach, A. Kavanaugh-McHugh, C. Cottrill, Y. Zhang, S. Riggs, O. Smalls, M. C. Johnson, M. S. Watson, J. G. Seidman, C. E. Seidman, J. Plowden, and J. D. Kugler. 1999. Mutations in the cardiac transcription factor *NKX2.5* affect diverse cardiac developmental pathways. J. Clin. Invest. 104: 1567–1573.

Bers, D. M. 2001. Excitation-Contraction Coupling and Cardiac Contractile Force. Norwell, MA: Kluwer Academic.

Bond, J., D. Sedmera, J. Jourdan, Y. H. Zhang, C. A. Eisenberg, L. M. Eisenberg, and R. G. Gourdie. 2003. Wnt11 and Wnt7a are up-regulated in association with differentiation of cardiac conduction cells in vitro and in vivo. Dev. Dyn. 227:536–543.

Bonne, G., L. Carrier, J. Bercovici, C. Cruaud, P. Richard, B. Hainque, M. Gautel, S. Labeit, M. James, J. Beckmann, J. Weissenbach, H.-P. Vosberg, M. Fiszman, M. Komajda, and K. Schwartz. 1995.

Cardiac myosin binding protein-C gene splice acceptor site mutation is associated with familial hypertrophic cardiomyopathy. Nat. Genet. 11:438–440.

Boucek, R. J., W. P. Murphy, and G. H. Paff. 1959. Electrical and mechanical properties of chick embryo heart chambers. Circ. Res. 7:787–793.

Boyett, M. R., H. Honjo, and I. Kodama. 2000. The sinoatrial node, a heterogeneous pacemaker structure. Cardiovasc. Res. 47:658–687.

Bozler, E. 1942. The initiation of impulses in cardiac muscle. Am. J. Physiol. 138:273–282.

Brugada, P., R. Brugada, C. Antzelevitch, and J. Brugada. 2005. The Brugada syndrome. Arch. Mal Coeur Vaiss. 98:115–122.

Buyon, J. P., R. Hiebert, J. Copel, J. Craft, D. Friedman, M. Katholi, L. A. Lee, T. T. Provost, M. Reichlin, L. Rider, A. Rupel, S. Saleeb, W. L. Weston, and M. L. Skovron. 1998. Autoimmune-associated congenital heart block: demographics, mortality, morbidity and recurrence rates obtained from a national neonatal lupus registry. J. Am. Coll. Cardiol. 31:1658–1666.

Chen, Q., D. Zhang, R. L. Gingell, A. J. Moss, C. Napolitano, S. G. Priori, P. J. Schwartz, E. Kehoe, J. L. Robinson, E. Schulze-Bahr, Q. Wang, and J. A. Towbin. 1999. Homozygous deletion in KVLQT1 associated with Jervell and Lange-Nielsen syndrome. Circulation 99:1344–1347.

Cheng, G., W. H. Litchenberg, G. J. Cole, T. Mikawa, R. P. Thompson, and R. G. Gourdie. 1999. Development of the cardiac conduction system involves recruitment within a multipotent cardiomyogenic lineage. Development 126:5041–5049.

Chuck, E. T., D. M. Freeman, M. Watanabe, and D. S. Rosenbaum. 1997. Changing activation sequence in the embryonic chick heart—implications for the development of the His-Purkinje system. Circ. Res. 81:470–476.

Chuck, E. T., K. Meyers, D. France, T. L. Creazzo, and G. E. Morley. 2004. Transitions in ventricular activation revealed by two-dimensional optical mapping. Anat. Rec. 280:990–1000.

Chuck, E. T., and M. Watanabe. 1997. Differential expression of PSA-NCAM and HNK-1 epitopes in the developing cardiac conduction system of the chick. Dev. Dyn. 209:182–195.

Clancy, C. E., and R. S. Kass. 2005. Inherited and acquired vulnerability to ventricular arrhythmias: cardiac Na^+ and K^+ channels. Physiol. Rev. 85:33–47.

Coppen, S. R., E. Dupont, S. Rothery, and N. J. Severs. 1998. Connexin45 expression is preferentially associated with the ventricular conduction system in mouse and rat heart. Circ. Res. 82:232–243.

Coppen, S. R., N. J. Severs, and R. G. Gourdie. 1999. Connexin45 (α6) expression delineates an extended conduction system in the embryonic and mature rodent heart. Dev. Genet. 24:82–90.

Davies, F. 1930. The conducting system of the bird's heart. J. Anat. 64:129–146.

Davis, D. L., A. V. Edwards, A. L. Juraszek, A. Phelps, A. Wessels, and J. B. E. Burch. 2001. A GATA-6 gene heart-region-specific enhancer provides a novel means to mark and probe a discrete component of the mouse cardiac conduction system. Mech. Dev. 108:105–119.

Davis, L. M., M. E. Rodefeld, K. Green, E. C. Beyer, and J. E. Saffitz. 1995. Gap junction protein phenotypes of the human heart and conduction system. J. Cardiovasc. Electrophysiol. 6:813–822.

de Groot, I. J. M., E. Sanders, S. D. Visser, W. H. Lamers, F. de Jong, J. A. Los, and A. F. M. Moorman. 1987. Isomyosin expression in developing chicken atria: a marker for the development of conductive tissue? Anat. Embryol. 176:515–523.

de Groot, I. J. M., A. Wessels, S. Viragh, W. H. Lamers, and A. F. M. Moorman. 1988. The relation between isomyosin heavy chain expression patterns and the architecture of sinoatrial nodes in chicken, rat and human embryos. In: Sarcomeric and Non-Sarcomeric Muscles: Basic and Applied Research Prospects for the 90's., ed. Carraro, U., 305–310. Padova, Italy: Unipress Padova.

de Jong, F., T. Opthof, A. A. Wilde, M. J. Janse, R. Charles, W. H. Lamers, and A. F. Moorman. 1992. Persisting zones of slow impulse conduction in developing chicken hearts. Circ. Res. 71:240–250.

de Jong, F., T. Opthof, A. A. M. Wilde, M. J. Janse, R. Charles, W. H. Lamers, and A. F. M. Moorman. 1992. Persisting zones of slow impulse conduction in developing chicken hearts. Circ. Res. 71:240–250.

De Mello, W. C. 1982. Intercellular communication in cardiac muscle. Circ. Res. 51:1–9.

DeHaan, R. L. 1967. Development of form in the embryonic heart. An experimental approach. Circulation 36:821–833.

DeHaan, R. L., and Y. H. Chen. 1990. Development of gap junctions. Ann. NY Acad. Sci. 588:164–173.

Delorme, B., E. Dahl, T. Jarry-Guichard, I. Marics, J.-P. Briand, K. Willecke, D. Gros, and M. Th, veniau-Ruissy. 1995. Developmental regulation of connexin 40 gene expression in mouse heart correlates with the differentiation of the conduction system. Dev. Dyn. 204:358–371.

Di Lisi, R., C. Sandri, D. Franco, S. Ausoni, A. F. M. Moorman, and S. Schiaffino. 2000. An atrioventricular canal domain defined by cardiac troponin I transgene expression in the embryonic myocardium. Anat. Embryol. 202:95–101.

Filogamo, G., and S. M. Peirone. 1995. Ontogenesis of the structural elements of the heart. Cardioscience 6:19–23.

Ford, B. D., J. A. Loeb, and G. D. Fischbach. 1999. Neuregulin stimulates DNA synthesis in embryonic chick heart cells. Dev. Biol. 214:139–150.

Fromaget, C., A. El Aoumari, E. Dupont, J. P. Briand, and D. Gros. 1990. Changes in the expression of connexin 43, a cardiac gap junctional protein, during mouse heart development. J. Mol. Cell. Cardiol. 22:1245–1258.

Fujii, S., A. Hirota, and K. Kamino. 1981. Optical indications of pacemaker potential and rhythm generation in early embryonic chick heart. J. Physiol. 312:253–263.

Gaietta, G., T. J. Deerinck, S. R. Adams, J. Bouwer, O. Tour, D. W. Laird, G. E. Sosinsky, R. Y. Tsien, and M. H. Ellisman. 2002. Multicolor and electron microscopic imaging of connexin trafficking. Science 296:503–507.

Goldenberg, M., and C. J. Rothberger. 1936. Uber des Elektrogramm der spezifischen Herz-muskulature. Pfl¸gers Arch. 237:295–306.

Goldmuntz, E., E. Geiger, and D. W. Benson. 2002. Nkx2.5 mutations in patients with tetralogy of fallot. Circulation 104:2565–2568.

Gollob, M. H., M. S. Green, A. S. Tang, T. Gollob, A. Karibe, A. S. Ali Hassan, F. Ahmad, R. Lozado, G. Shah, L. Fananapazir, L. L. Bachinski, and R. Roberts. 2001. Identification of a gene responsible for familial Wolff–Parkinson–White syndrome. N. Engl. J. Med. 344:1823–1831.

Gonzalez-Sanchez, A., and D. Bader. 1985. Characterization of a myosin heavy chain in the conductive system of the adult and developing chicken heart. J. Cell Biol. 100:270–275.

Gorza, L., S. Schiaffino, and M. Vitadello. 1988. Heart conduction system: a neural crest derivative? Brain Res. 457:360–366.

Gorza, L., S. Vettore, and M. Vitadello. 1994. Molecular and cellular diversity of heart conduction system myocytes. Trends Cardiovasc. Med. 4:153–159.

Gorza, L., and M. Vitadello. 1989. Distribution of conduction system fibers in the developing and adult rabbit heart revealed by an antineurofilament antibody. Circ. Res. 65:360–369.

Gourdie, R. G., B. S. Harris, J. Bond, C. Justus, K. W. Hewett, T. X. O'Brien, R. P. Thompson, and D. Sedmera. 2003. Development of the cardiac pacemaking and conduction system. Birth Defects Res. C Embryo Today 69:46–57.

Gourdie, R. G., S. Kubalak, and T. Mikawa. 1999. Conducting the embryonic heart: Orchestrating development of specialized cardiac tissues. Trends Cardiovasc. Med. 9:18–26.

Gourdie, R. G., T. Mima, R. P. Thompson, and T. Mikawa. 1995. Terminal diversification of the myocyte lineage generates Purkinje fibers of the cardiac conduction system. Development 121:1423–1431.

Gourdie, R. G., Y. Wei, D. Kim, S. C. Klatt, and T. Mikawa. 1998. Endothelin-induced conversion of embryonic heart muscle cells into impulse-conducting Purkinje fibers. Proc. Natl. Acad. Sci. USA 5:6815–6818.

Graham, V., H. Zhang, S. Willis, and T. L. Creazzo. 2006. Expression of a two-pore domain K^+ channel (TASK-1) in developing avian and mouse ventricular conduction systems. Dev. Dyn. 235:143–151.

Gros, D. B., and H. J. Jongsma. 1996. Connexins in mammalian heart function. Bioessays 18:719–730.

Gutstein, D. E., G. E. Morley, H. Tamaddon, D. Vaidya, M. D. Schneider, J. Chen, K. R. Chien, H. Stuhlmann, and G. I. Fishman. 2001. Conduction slowing and sudden arrhythmic death in mice with cardiac-restricted inactivation of connexin43. Circ. Res. 88:333–339.

Habets, P. E. M. H., A. F. M. Moorman, D. E. W. Clout, M. A. Van Roon, M. Lingbeek, M. van Lohuizen, M. Campione, and V. M. Christoffels. 2002. Cooperative action of *Tbx2* and *Nkx2.5* inhibits ANF expression in the atrioventricular canal: implications for cardiac chamber formation. Genes Dev. 16:1234–1246.

Hagendorff, A., B. Schumacher, S. Kirchhoff, B. Luderitz, and K. Willecke. 1999. Conduction disturbances and increased atrial vulnerability in Connexin40-deficient mice analyzed by transesophageal stimulation. Circulation 99:1508–1515.

Hertig, C. M., S. W. Kubalak, Y. B. Wang, and K. R. Chien. 1999. Synergistic roles of neuregulin-1 and insulin-like growth factor-I in activation of the phosphatidylinositol 3-kinase pathway and cardiac chamber morphogenesis. J. Biol. Chem. 274:37362–37369.

Hirota, A., T. Sakai, S. Fujii, and K. Kamino. 1983. Initial development of conduction pattern of spontaneous action potential in early embryonic precontractile chick heart. Dev. Biol. 99:517–523.

Hoff Ebbe, M., T. Kramer, C, D. B. Delafield, and B. M. Patten. 1939. The development of the electrocardiogram of the embryonic heart. Am. Heart J. 17:470–488.

Honjo, H., M. R. Boyett, S. R. Coppen, Y. Takagishi, T. Opthof, N. J. Severs, and I. Kodama. 2002. Heterogeneous expression of connexins in rabbit sinoatrial node cells: correlation between connexin isotype and cell size. Cardiovasc. Res. 53:89–96.

Hoogaars, W. M., A. Tessari, A. F. Moorman, P. A. de Boer, J. Hagoort, A. T. Soufan, M. Campione, and V. M. Christoffels. 2004. The transcriptional repressor *Tbx3* delineates the developing central conduction system of the heart. Cardiovasc. Res. 62:489–499.

Hoover, D. B., C. E. Ganote, S. M. Ferguson, R. D. Blakely, and R. L. Parsons. 2004. Localization of cholinergic innervation in guinea pig heart by immunohistochemistry for high-affinity choline transporters. Cardiovasc. Res. 62:112–121.

Huang, G. Y., A. Wessels, B. R. Smith, K. K. Linask, J. L. Ewart, and C. W. Lo. 1998. Alteration in connexin 43 gap junction gene dosage impairs conotruncal heart development. Dev. Biol. 198:32–44.

Hyer, J., M. Johansen, A. Prasad, A. Wessels, M. L. Kirby, R. G. Gourdie, and T. Mikawa. 1999. Induction of Purkinje fiber differentiation by coronary arterialization. Proc. Natl. Acad. Sci. USA 96:13214–13218.

Hyer, J., M. Johansen, A. Prasad, A. Wessels, M. L. Kirby, R. G. Gourdie, and T. Mikawa. 1999. Induction of Purkinje fiber differentiation by coronary arterialization. Proc. Natl. Acad. Sci. USA 96:13214–13218.

Jay, P. Y., B. S. Harris, C. T. Maguire, A. Buerger, H. Wakimoto, M. Tanaka, S. Kupershmidt, D. M. Roden, T. M. Schultheiss, T. X. O'Brien, R. G. Gourdie, C. I. Berul, and S. Izumo. 2004. *Nkx2–5* mutation causes anatomic hypoplasia of the cardiac conduction system. J. Clin. Invest. 113:1130–1137.

Jongbloed, M. R., M. J. Schalij, R. E. Poelmann, N. A. Blom, M. L. Fekkes, Z. Wang, G. I. Fishman, and A. C. Gittenberger-De Groot. 2004. Embryonic conduction tissue: a spatial correlation with adult arrhythmogenic areas. J. Cardiovasc. Electrophysiol. 15:349–355.

Kamino, K., A. Hirota, and S. Fujii. 1981. Localization of pacemaking activity in early embryonic heart monitored using voltage-sensitive dye. Nature 290:595–597.

Kamino, K., H. Komuro, and T. Sakai. 1988. Regional gradient of pacemaker activity in the early embryonic chick heart monitored by multisite optical recording. J. Physiol. 402:301–314.

Kanter, H. L., J. G. Laing, S. L. Beau, E. C. Beyer, and J. E. Saffitz. 1993. Distinct patterns of connexin expression in canine Purkinje fibers and ventricular muscle. Circ. Res. 72:1124–1131.

Kanzawa, N., C. P. Poma, K. Takebayashi-Suzuki, K. G. Diaz, J. Layliev, and T. Mikawa. 2002. Competency of embryonic cardiomyocytes to undergo Purkinje fiber differentiation is regulated by endothelin receptor expression. Development 129:3185–3194.

Kirchhoff, S., J. S. Kim, A. Hagendorff, E. Thonnissen, O. Kruger, W. H. Lamers, and K. Willecke. 2000. Abnormal cardiac conduction and morphogenesis in connexin40 and connexin43 double-deficient mice. Circ. Res. 87:399–405.

Kirchhoff, S., E. Nelles, A. Hagendorff, O. Kruger, O. Traub, and K. Willecke. 1998. Reduced cardiac conduction velocity and predisposition to arrhythmias in connexin40-deficient mice. Curr. Biol. 8:299–302.

Kondo, R. P., R. H. Anderson, S. Kupershmidt, D. M. Roden, and S. M. Evans. 2003. Development of the cardiac conduction system as delineated by *minK–lacZ*. J. Cardiovasc. Electrophysiol. 14:383–391.

Kreuzberg, M. M., G. Sohl, J. S. Kim, V. K. Verselis, K. Willecke, and F. F. Bukauskas. 2005. Functional properties of mouse connexin30.2 expressed in the conduction system of the heart. Circ. Res. 96:1169–1177.

Kumai, M., K. Nishii, K. Nakamura, N. Takeda, M. Suzuki, and Y. Shibata. 2000. Loss of connexin45 causes a cushion defect in early cardiogenesis. Development 127:3501–3512.

Kumar, N. M., and N. B. Gilula. 1996. The gap junction communication channel. Cell 84:381–388.

Kupershmidt, S., T. Yang, M. E. Anderson, A. Wessels, K. D. Niswender, M. A. Magnuson, and D. M. Roden. 1999. Replacement by

homologous recombination of the *minK* gene with *lacZ* reveals restriction of *minK* expression to the mouse cardiac conduction system. Circ. Res. 84:146–152.

Laird, D. W., M. Castillo, and L. Kasprzak. 1995. Gap junction turnover, intracellular trafficking, and phosphorylation of connexin43 in brefeldin A-treated rat mammary tumor cells. J. Cell Biol. 131:1193–1203.

Lamers, W. H., F. De Jong, I. J. DeGroot, and A. F. Moorman. 1991. The development of the avian conduction system, a review. Eur. J. Morphol. 29:233–253.

Li, W. E. I., K. Waldo, K. L. Linask, T. Chen, A. Wessels, M. S. Parmacek, M. L. Kirby, and C. W. Lo. 2002. An essential role for connexin43 gap junctions in mouse coronary artery development. Development 129:2031–2042.

Lieberman, M., and A. Paes de Carvalho. 1967. Effect of locally applied acetylcholine on the embryonic cardiac action potential. Experientia 23:539–540.

McElhinney, D. B., I. D. Krantz, L. Bason, D. A. Piccoli, K. M. Emerick, N. B. Spinner, and E. Goldmuntz. 2002. Analysis of cardiovascular phenotype and genotype-phenotype correlation in individuals with a *JAG1* mutation and/or Alagille syndrome. Circulation 106:2567–2574.

Mikawa, T., and D. A. Fischman. 1996. The polyclonal origin of myocyte lineages. Annu. Rev. Physiol. 58:509–521.

Mikawa, T., and R. G. Gourdie. 1996. Pericardial mesoderm generates a population of coronary smooth muscle cells migrating into the heart along with ingrowth of the epicardial organ. Dev. Biol. 174:221–232.

Mikawa, T., R. G. Gourdie, K. Takebayashi-Suzuki, N. Kanzawa, J. Hyer, D. J. Pennisi, C. P. Poma, M. Shulimovich, K. G. Diaz, J. Layliev, and A. Prasad. 2003. Induction and patterning of the Purkinje fibre network. Novartis Found. Symp. 250:142–153; discussion 153–156, 276–279.

Miquerol, L., S. Meysen, M. Mangoni, P. Bois, H. V. van Rijen, P. Abran, H. Jongsma, J. Nargeot, and D. Gros. 2004. Architectural and functional asymmetry of the His–Purkinje system of the murine heart. Cardiovasc. Res. 63:77–86.

Moak, J. P., K. S. Barron, T. J. Hougen, H. B. Wiles, S. Balaji, N. Sreeram, M. H. Cohen, A. Nordenberg, G. F. Van Hare, R. A. Friedman, M. Perez, F. Cecchin, D. S. Schneider, R. A. Nehgme, and J. P. Buyon. 2001. Congenital heart block: development of late-onset cardiomyopathy, a previously underappreciated sequela. J. Am. Coll. Cardiol. 37:238–242.

Moorman, A. F., and V. M. Christoffels. 2003. Cardiac chamber formation: development, genes, and evolution. Physiol. Rev. 83: 1223–1267.

Moorman, A. F. M., F. de Jong, M. M. F. J. Denyn, and W. H. Lamers. 1998. Development of the cardiac conduction system. Circ. Res. 82:629–644.

Moorman, A. F. M., and W. H. Lamers. 1994. Molecular anatomy of the developing heart. Trends Cardiovasc. Med. 4:257–264.

Moorman, A. F. M., C. A. Schumacher, P. A. J. de Boer, J. Hagoort, K. Bezstarosti, M. J. B. Van den Hoff, G. T. M. Wagenaar, J. M. J. Lamers, F. Wuytack, V. M. Christoffels, and J. W. T. Fiolet. 2000. Presence of functional sarcoplasmic reticulum in the developing heart and its confinement to chamber myocardium. Dev. Biol. 223:279–290.

Morton, M. J., A. D. O'Connell, A. Sivaprasadarao, and M. Hunter. 2003. Determinants of pH sensing in the two-pore domain K(+) channels TASK-1 and -2. Pflugers Arch. 445:577–583.

Myers, D. C., and G. I. Fishman. 2003. Molecular and functional maturation of the murine cardiac conduction system. Trends Cardiovasc. Med. 13:289–295.

O'Connell, A. D., M. J. Morton, and M. Hunter. 2002. Two-pore domain K^+ channels-molecular sensors. Biochim. Biophys. Acta 1566:152–161.

Paff, G. H. 1962. Simultaneous electrocardiograms and myograms of the isolated atrium, ventricle and conus of the embryonic chick heart. Anat. Rec. 142:73–80.

Paff, G. H., R. J. Boucek, and T. C. Harrell. 1968. Observations on the development of the electrocardiogram. Anat. Rec. 160:575–582.

Pashmforoush, M., J. T. Lu, H. Chen, T. S. Amand, R. Kondo, S. Pradervand, S. M. Evans, B. Clark, J. R. Feramisco, W. Giles, S. Y. Ho, D. W. Benson, M. Silberbach, W. Shou, and K. R. Chien. 2004. Nkx2–5 pathways and congenital heart disease; loss of ventricular myocyte lineage specification leads to progressive cardiomyopathy and complete heart block. Cell 117:373–386.

Patel, R., and L. Kos. 2005. Endothelin-1 and Neuregulin-1 convert embryonic cardiomyocytes into cells of the conduction system in the mouse. Dev. Dyn. 233:20–28.

Patel, V. V., M. Arad, I. P. Moskowitz, C. T. Maguire, D. Branco, J. G. Seidman, C. E. Seidman, and C. I. Berul. 2003. Electrophysiologic characterization and postnatal development of ventricular pre-excitation in a mouse model of cardiac hypertrophy and Wolff–Parkinson–White syndrome. J. Am. Coll. Cardiol. 42: 942–951.

Patten, B. M., and T. Kramer. 1933. The initiation of contraction in the embryonic chick heart. Am. J. Anat. 53:349–375.

Pennisi, D. J., S. Rentschler, R. G. Gourdie, G. I. Fishman, and T. Mikawa. 2002. Induction and patterning of the cardiac conduction system. Int. J. Dev. Biol. 46:765–775.

Purkinje, J. 1845. Mikroskopisch-neurologische Beobachtungen. Arch. Anat. Physiol. Wiss. Med. 12:281–295.

Rentschler, S., D. M. Vaidya, H. Tamaddon, K. Degenhardt, D. Sassoon, G. E. Morley, J. Jalife, and G. I. Fishmann. 2001. Visualization and functional characterization of the developing murine cardiac conduction system. Development 128:1785–1792.

Rentschler, S., J. Zander, K. Meyers, D. France, R. Levine, G. Porter, S. A. Rivkees, G. E. Morley, and G. I. Fishman. 2002. Neuregulin-1 promotes formation of the murine cardiac conduction system. Proc. Natl. Acad. Sci. USA 99:10464–10469.

Rothenberg, F., I. R. Efimov, and M. Watanabe. 2004. Functional imaging of the embryonic pacemaking and cardiac conduction system over the past 150 years: technologies to overcome the challenges. Anat. Rec. 280:980–989.

Rothenberg, F., V. P. Nikolski, M. Watanabe, and I. R. Efimov. 2005. Electrophysiology and anatomy of embryonic rabbit hearts before and after septation. Am. J. Physiol. 288:H344–H351.

Rychter, Z., and B. Ostadal. 1971. Mechanism of the development of coronary arteries in chick embryos. Folia Morphol. 19:113–124.

Saffitz, J. E., L. M. Davis, B. J. Darrow, H. L. Kanter, J. G. Laing, and E. C. Beyer. 1995. The molecular basis of anisotropy: role of gap junctions. J. Cardiovasc. Electrophysiol. 6:498–510.

Sanguinetti, M. C., M. E. Curran, A. Zou, J. Shen, P. S. Spector, D. L. Atkinson, and M. T. Keating. 1996. Coassembly of K(V)LQT1 and minK (IsK) proteins to form cardiac I(Ks) potassium channel. Nature 384:80–83.

Sartore, S., S. Pierobon-Bormioli, and S. Schiaffino. 1978. Immunohistochemical evidence for myosin polymorphism in the chicken heart. Nature 274:82–83.

Satin, J., S. Fujii, and R. L. DeHaan. 1988. Development of cardiac beat rate in early chick embryos is regulated by regional cues. Dev. Biol. 129:103–113.

Schott, J. J., D. W. Benson, C. T. Basson, W. Pease, G. M. Silberbach, J. P. Moak, B. J. Maron, C. E. Seidman, and J. G. Seidman. 1998. Congenital heart disease caused by mutations in the transcription factor *NKX2–5*. Science 281:108–111.

Schroeder, J. A., L. F. Jackson, D. C. Lee, and T. D. Camenisch. 2003. Form and function of developing heart valves: coordination by extracellular matrix and growth factor signaling. J. Mol. Med. 81:392–403.

Sedmera, D., M. Reckova, M. R. Bigelow, A. Dealmeida, C. P. Stanley, T. Mikawa, R. G. Gourdie, and R. P. Thompson. 2004. Developmental transitions in electrical activation patterns in chick embryonic heart. Anat. Rec. 280:1001–1009.

Sedmera, D., M. Reckova, A. deAlmeida, M. Sedmerova, M. Biermann, J. Volejnik, A. Sarre, E. Raddatz, R. A. McCarthy, R. G. Gourdie, and R. P. Thompson. 2003. Functional and morphological evidence for a ventricular conduction system in zebrafish and *Xenopus* hearts. Am. J. Physiol. 284:H1152–H1160.

Seidl, W., M. Schulze, G. Steding, and D. Kluth. 1981. A few remarks on the physiology of the chick embryo heart (*Gallus gallus*). Folia Morphol. 29:581.

Severs, N. J. 2000. The cardiac muscle cell. Bioessays 22:188–199.

Shimada, T., H. Kawazato, A. Yasuda, N. Ono, and K. Sueda. 2004. Cytoarchitecture and intercalated disks of the working myocardium and the conduction system in the mammalian heart. Anat. Rec. 280:940–951.

Simon, A. M., D. A. Goodenough, and D. L. Paul. 1998. Mice lacking connexin40 have cardiac conduction abnormalities characteristic of atrioventricular block and bundle branch block. Curr. Biol. 8:295–298.

Spach, M. S., and J. M. Kootsey. 1983. The nature of electrical propagation in cardiac muscle. Am. J. Physiol. 244:H3–H22.

Takebayashi-Suzuki, K., L. B. Pauliks, Y. Eltsefon, and T. Mikawa. 2001. Purkinje fibers of the avian heart express a myogenic transcription factor program distinct from cardiac and skeletal muscle. Dev. Biol. 234:390–401.

Takebayashi-Suzuki, K., M. Yanagisawa, R. G. Gourdie, N. Kanzawa, and T. Mikawa. 2000. In vivo induction of cardiac Purkinje fiber differentiation by coexpression of preproendothelin-1 and endothelin converting enzyme-1. Development 127:3523–3532.

Tamaddon, H. S., D. Vaidya, A. M. Simon, D. L. Paul, J. Jalife, and G. E. Morley. 2000. High-resolution optical mapping of the right bundle branch in connexin40 knockout mice reveals slow conduction in the specialized conduction system. Circ. Res. 87:929–936.

Tawara, S. 1906. Das reizleitungs-system des Saugetierherzens. Gustv. Fischer, Jena.

ten Velde, I., B. de Jonge, E. E. Verheijck, M. J. van Kempen, L. Analbers, D. Gros, and H. J. Jongsma. 1995. Spatial distribution of connexin43, the major cardiac gap junction protein, visualizes the cellular network for impulse propagation from sinoatrial node to atrium. Circ. Res. 76:801–811.

Thomas, P. S., H. Kasahara, A. M. Edmonson, A. Izumo, M. H. Yacoub, P. J. Barton, and R. G. Gourdie. 2001. Elevated expression of *Nkx-2.5* in developing myocardial conduction cells. Anat. Rec. 263:307–313.

Van Kempen, M. J., J. L. Vermeulen, A. F. Moorman, D. Gros, D. L. Paul, and W. H. Lamers. 1996. Developmental changes of connexin40 and connexin43 mRNA distribution patterns in the rat heart. Cardiovasc. Res. 32:886–900.

Van Kempen, M. J. A., C. Fromaget, D. Gros, A. F. M. Moorman, and W. H. Lamers. 1991. Spatial distribution of connexin43, the major cardiac gap junction protein, in the developing and adult rat heart. Circ. Res. 68:1638–1651.

Van Kempen, M. J. A., I. ten Velde, A. Wessels, P. W. Oosthoek, D. Gros, H. J. Jongsma, A. F. M. Moorman, and W. H. Lamers. 1995. Differential connexin distribution accommodates cardiac function in different species. Microsc. Res.Tech. 31:420–436.

Van Mierop, L. H. S. 1967. Location of pacemaker in chick embryo heart at the time of initiation of heartbeat. Am. J. Physiol. 212:407–415.

Vassal-Adams, P. R. 1982. The development of the atrioventricular bundle and its branches in the avian heart. J. Anat. 134:169–183.

Viragh, S., and C. E. Challice. 1980. The development of the conduction system in the mouse embryo heart. Dev. Biol. 80:28–45.

Waldo, K. L., D. H. Kumiski, K. T. Wallis, H. A. Stadt, M. R. Hutson, D. H. Platt, and M. L. Kirby. 2001. Conotruncal myocardium arises from a secondary heart field. Development 128:3179–3188.

Wang, Q., M. E. Curran, I. Splawski, T. C. Burn, J. M. Millholland, T. J. VanRaay, J. Shen, K. W. Timothy, G. M. Vincent, T. de Jager, P. J. Schwartz, J. A. Towbin, A. J. Moss, D. L. Atkinson, G. M. Landes, T. D. Connors, and M. T. Keating. 1996. Positional cloning of a novel potassium channel gene: *KVLQT1* mutations cause cardiac arrhythmias. Nat. Genet. 12:17–23.

Watanabe, Y., D. W. Benson, S. Yano, T. Akagi, M. Yoshino, and J. C. Murray. 2002. Two novel frameshift mutations in *NKX2.5* result in novel features including visceral inversus and sinus venosus type ASD. J. Med. Genet. 39:807–811.

Watkins, H., R. Anan, D. A. Coviello, P. Spirito, J. G. Seidman, and C. E. Seidman. 1995. A de novo mutation in á-tropomyosin that causes hypertrophic cardiomyopathy. Circulation 91: 2302–2305.

Wei, C. J., X. Xu, and C. W. Lo. 2004. Connexins and cell signaling in development and disease. Annu. Rev. Cell Dev. Biol. 20: 811–838.

Wessels, A., M. W. M. Markman, J. L. M. Vermeulen, R. H. Anderson, A. F. M. Moorman, and W. H. Lamers. 1996. The development of the atrioventricular junction in the human heart. Circ. Res. 78:110–117.

Wessels, A., J. L. M. Vermeulen, F. J. Verbeek, S. Viragh, F. Kalman, W. H. Lamers, and A. F. M. Moorman. 1992. Spatial distribution of "tissue-specific" antigens in the developing human heart and skeletal muscle III. An immunohistochemical analysis of the distribution of the neural tissue antigen G1N2 in the embryonic heart; implications for the development of the atrioventricular conduction system. Anat. Rec. 232:97–111.

Willecke, K., J. Eiberger, J. Degen, D. Eckardt, A. Romualdi, M. Guldenagel, U. Deutsch, and G. Sohl. 2002. Structural and functional diversity of connexin genes in the mouse and human genome. J. Biol. Chem. 383:725–737.

Yeh, H. I., S. Rothery, E. Dupont, S. R. Coppen, and N. J. Severs. 1998. Individual gap junction plaques contain multiple connexins in arterial endothelium. Circ. Res. 83:1248–1263.

13

Innervation of the Developing Heart

The heart has both AFFERENT (sensory) and EFFERENT (motor) innervation (Fig. 13.1). The motor innervation is part of the autonomic nervous system, which provides efferent information to all of the viscera. Because of the integration of signals that is now recognized in the AUTONOMIC GANGLIA, there has been a tendency to include the afferent nerves as part of the autonomic nervous system; however, this discussion maintains the classical separation, and the sensory innervation is considered as separate from the autonomic motor innervation.

Sensory or afferent innervation of the heart is provided by terminals of afferent neurons located in the nodose ganglia and various dorsal root ganglia. These cells bring sensory information from the heart to the central nervous system (CNS), where they form reflex loops with motor neurons that effect changes in heart rate and/or force of contraction.

All motor or autonomic output from the CNS is via PREGANGLIONIC to POSTGANGLIONIC neural relay. The preganglionic neurons are located in the BRAINSTEM or SPINAL CORD, and they synapse on postganglionic neurons located in the periphery. The locations of the preganglionic neurons in the CNS and the postganglionic peripheral ganglia identify whether they constitute the parasympathetic or sympathetic division of the autonomic nervous system.

In the parasympathetic division of autonomic innervation, the preganglionic neurons are located in the brainstem. Their axons travel via the vagus nerve to the postganglionic neurons located in CARDIAC GANGLIA in or near the heart. The sympathetic preganglionic neurons are located in the INTERMEDIOLATERAL CELL COLUMN in the thoracic spinal cord and connect with postganglionic neurons located in the lower cervical/upper thoracic sympathetic chain which is situated next to the vertebral column (paravertebral).

All of the preganglionic neurons of both autonomic divisions use ACETYLCHOLINE as their major neurotransmitter while the postganglionic neurons are distinguished by using

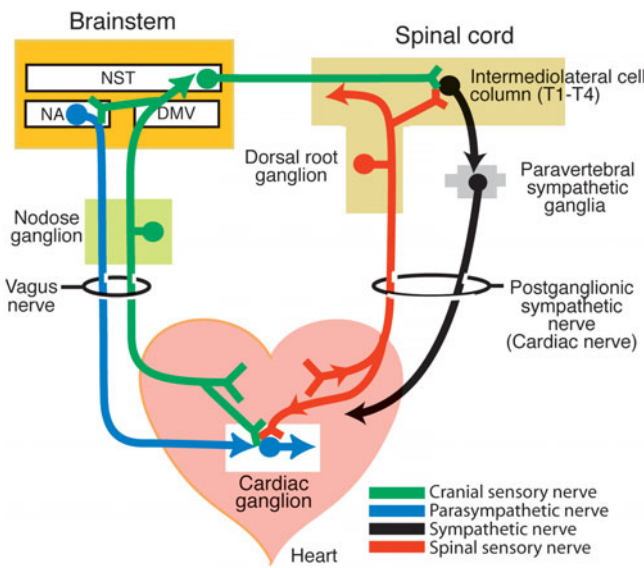

Figure 13.1. Schematic of the general plan of the innervation of the heart. Direction of the impulse is indicated by the arrow. Sensory (afferent) terminals located in the heart and great vessels have their cell bodies in the nodose ganglia (*green*) and travel with the vagus nerves to the nucleus of the solitary tract in the brainstem. A second set of sensory nerves (*red*) have their cell bodies in the dorsal root ganglia. Their processes travel with the cardiac nerves to their cell bodies located in the dorsal root ganglia and from there to the spinal cord. The motor (efferent) innervation is represented by parasympathetic and sympathetic divisions of the autonomic nervous system. The parasympathetic preganglionic neurons (*blue*) originate in the brainstem (DMV, dorsal motor nucleus of the vagus and nucleus ambiguus) and travel via the vagus nerves to the cardiac ganglia located in the heart. The preganglionic nerves synapse on postganglionic nerves (*blue*) that slow the heart beat. The preganglionic sympathetic neurons (*black*) are located in the spinal cord. These synapse on postganglionic neurons located in the paravertebral sympathetic chain ganglia *(black)*. The postganglionic nerves travel to the heart via the cardiac nerves and increase the beat rate and force of myocardial contraction.

separate transmitters. The parasympathetic postganglionic neurons use acetylcholine and are called cholinergic. These neurons exert TONIC CONTROL over heart rate to slow it. The sympathetic postganglionic neurons use NOREPINEPHRINE, a CATECHOLAMINE, and are called ADRENERGIC. These neurons increase heart rate and force of contraction.

The development of this complex system of cardiac control is largely unexplored. A few general statements can be made regarding development. First, all of the autonomic postganglionic neurons derive from the neural crest; second, innervation of the heart is slow to develop and mature, and in most animals it is not fully functional until well after birth. The onset of parasympathetic activity precedes that of sympathetic activity in all species examined thus far. As a consequence, the parasympathetic–cholinergic control becomes functional and plays a role in cardiac function earlier than the sympathetic–adrenergic neural control. However, it has recently been recognized that the heart itself synthesizes norepinephrine/epinephrine (catecholamines) and is susceptible to control by circulating catecholamines, which may substitute for the late-appearing sympathetic adrenergic innervation.

Sensory Innervation

Cardiac sensory nerve endings can be functionally divided into two main groups based on whether they are associated with vagal (parasympathetic) or sympathetic nerves (Fig. 13.1). Afferent axons in the vagus have their cell bodies located in the nodose ganglia. These nerves provide sensory information to control both sympathetic and parasympathetic visceral motor reflexes. They exert tonic inhibition on sympathetic activity via γ-aminobutyric acid (GABAergic) and glutamine (glutamatergic) synapses (Crick, 2000; Evans et al., 2003).

Afferent axons associated with sympathetic nerves have their cell bodies located in the dorsal root ganglia, and these fibers do not have any tonic influence over either sympathetic or parasympathetic activity but may be more important for registering pain, such as that associated with ischemia as in ANGINA (Hua et al., 2004). Some of the afferent fibers connect directly with sympathetic postganglionic neurons in the STELLATE GANGLIA (Crick, 2000).

Both of these afferent systems send collaterals that connect directly with parasympathetic postganglionic neurons or interneurons in the cardiac ganglia that interface with the parasympathetic neurons. These mediate local reflex control of parasympathetic activity.

The nodose ganglia are the distal ganglia of the vagus nerve and are derived from the nodose placodes on days 2–5 of incubation in the chick (d'Amico-Martel, 1982). Cell death is characteristic of all sensory ganglia, and the loss of half of the neurons in the nodose ganglia occurs between embryonic days E5 and 20. At the same time, neuron cell bocy and ganglion size increases. The neurons continue to increase in size until 2 weeks after hatching, when they reach their adult size. MYELINATION is first seen on incubation day 15. Unlike in the dorsal root ganglia, the number of neurons in the nodose ganglia increases by 62% after hatching (d'Amico-Martel, 1982, Harrison et al., 1994).

The NEUROTROPHINS—nerve growth factor (NGF), brain-derived neurotrophic factor (BDNF), neurotrophin-3 (Nt3) and neurotrophin-4 (Nt4)—are crucial target-derived factors controlling the survival of peripheral sensory neurons during the embryonic period of programmed cell death (Fig. 13.2). The neurotrophins that support nodose ganglion neurons during development are Bdnf, Nt3, and Nt4. Both Nt3 and Nt4 are crucial during the period of ganglion formation, whereas Bdnf acts later in development. Thus, most of the nodose ganglion neurons depend on more than one neurotrophin that act in a complementary as well as a collaborative manner in a developmental sequence (ElShamy and Ernfors, 1997).

The sensory neurons of the nodose ganglion were thought to develop independently of Ngf, which is required for survival of most peripheral neurons. However, the number of neurons in the nodose ganglia undergoing apoptosis is elevated, and the Ngf receptor tyrosine kinase called TRKA is decreased in the nodose ganglia of *Ngf*-null embryos. In vitro, the viability of nodose neurons is supported by Bdnf, and only a minor proportion is affected by Ngf (Forgie et al., 2000). These results suggest that the afferent neurons include at least two subpopulations of neurons.

Figure 13.2. Neurotrophins and their receptors. Primary receptor interactions are shown by *solid arrows*. Weaker or secondary interactions are shown by *dashed arrows*. All four neurotrophin ligands bind to the low-affinity receptor (p75), which does not have obvious signaling capability.

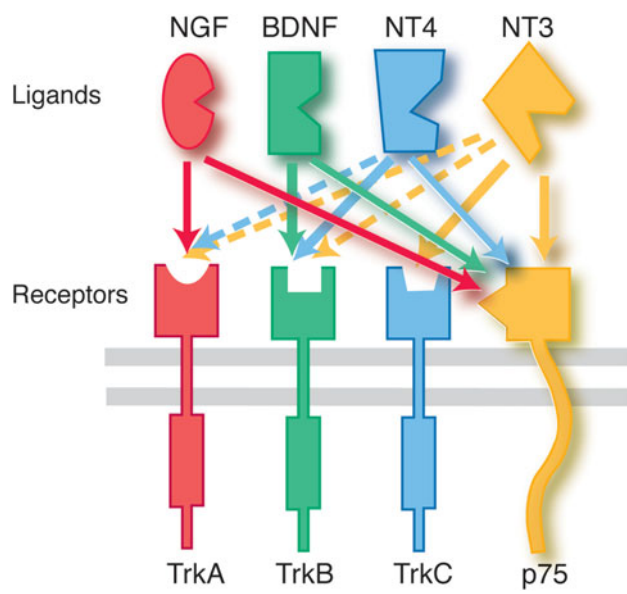

The central processes of the nodose sensory neurons travel via the bilateral vagus nerves to the brainstem. The NUCLEUS OF THE SOLITARY TRACT is the major terminus for visceral sensory input in the brainstem and from there information is relayed to the preganglionic motor nuclei (Fig. 13.1). The development of these processes has been examined in the rat. At 12dpc, labeled vagal sensory neurons are present in the nodose ganglia, and a few sensory axons project into the dorsolateral medulla. Central sensory processes become increasingly prevalent between 13dpc and 14dpc but remain restricted to the SOLITARY TRACT. The nucleus of the solitary tract becomes visible as a distinct cluster of cells by about 17dpc, and by 19dpc all the subnuclei are discernible. There is a delay of 48 h between the ingrowth of afferents to the nucleus of the solitary tract and the first appearance of synapses. The earliest synapses are simple, symmetrical membrane thickenings first apparent at 17dpc. SYNAPTIC VESICLES are not apparent until 19dpc. Synaptic glomeruli, which are a characteristic feature of afferent input to the adult nucleus of the solitary tract, develop sometime after birth (Zhang and Ashwell, 2001). Acetylcholinesterase activity appears at 15dpc to 17dpc and is distributed in the adult pattern by E19 (Zhang and Ashwell, 2001). Central integration of vagal afferent input matures slightly earlier in the sheep than the rat and is intact in fetal and newborn sheep (Merrill et al., 1999).

The sensory terminals connect, directly or indirectly, with the vagal preganglionic parasympathetic neurons located also in the brainstem. Vagal motor neurons are first seen at 13dpc, clustered within a region corresponding to the NUCLEUS AMBIGUUS. Direct vagovagal, sensorimotor interaction appears at 16dpc. By 18dpc, the vagal nuclei appear remarkably mature (Rinaman and Levitt, 1993).

The sympathetic afferent fibers that travel with the sympathetic nerves are the processes of neurons located in the dorsal root ganglia. These neurons are mostly NOCICEPTIVE, or pain sensing fibers, and use SUBSTANCE P as their primary neurotransmitter. While a few collaterals connect directly with postganglionic sympathetic or parasympathetic neurons in the peripheral ganglia to mediate direct reflexes, most feed information into the dorsal horn of the spinal cord. The fibers are activated by focal coronary artery occlusion and are thought to mediate perception of angina.

Development of Parasympathetic Innervation and the Cardiac Plexus

Preganglionic cardiac parasympathetic neurons originate in the external division of the nucleus ambiguus located in the medulla oblongata (Fig. 13.1). The DORSAL VAGAL MOTOR COMPLEX, which is important in gastrointestinal neural control, provides relatively weak input to the cardiac ganglia. Parasympathetic nerves exit the lateral medulla at the same planes as their cells of origin. All of the preganglionic neurons form during early embryonic life, and no new vagal motor neurons are added during fetal or postnatal development (Hopkins et al., 1984). The preganglionic neurons connect with their postganglionic relays in the cardiac ganglia, located on the surface of the heart or in nerve plexuses near it (Gabella, 1976).

The cardiac ganglia are distributed widely (Fig. 13.3). They surround the sinoatrial node and the roots of the venae cavae and pulmonary veins, and they are scattered on the posterior atrial wall, in the posterior atrioventricular groove, in the interatrial septum, near the atrioventricular node, and in the atrial appendages (Calaresu and St Louis, 1967; King and Coakley, 1958; Kuntz, 1934; Mitchell, 1956; Moravec and Moravec, 1987; Moravec et al., 1986; Roberts et al., 1989; Sato, 1954; Smith, 1971; Tcheng, 1951; Woollard, 1926; Yuan et al., 1994). In addition, cardiac ganglia are associated with the origins of both right and left coronary arteries in the human, dog, and chicken (Armour and Hopkins, 1990; Waldo et al., 1994; Yuan et al., 1994). The majority of atrial ganglia are situated in the subepicardial connective tissue. Two independent sets of ganglia selectively control sinoatrial rate and atrioventricular conduction (Gatti et al., 1995). Cardiac rate is controlled by neurons located in the ganglia near the sinoatrial node, while conduction is controlled by a separate set of ganglia located at the junction of the inferior vena cava and the

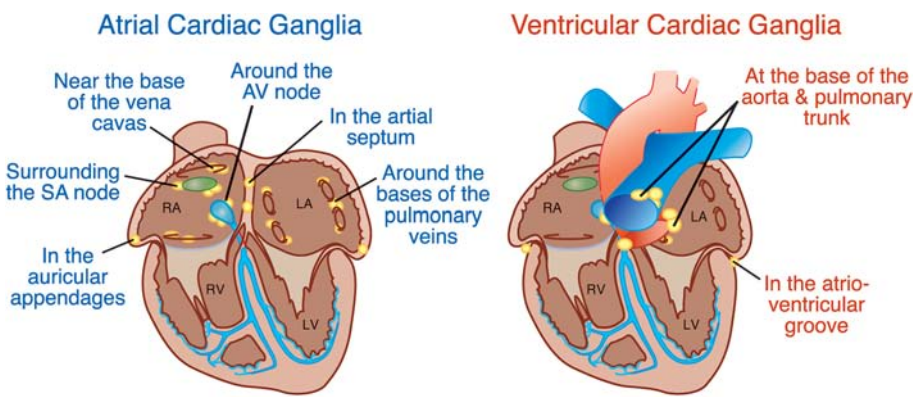

Figure 13.3. Distribution of the parasympathetic cardiac ganglia in the atria and ventricles.

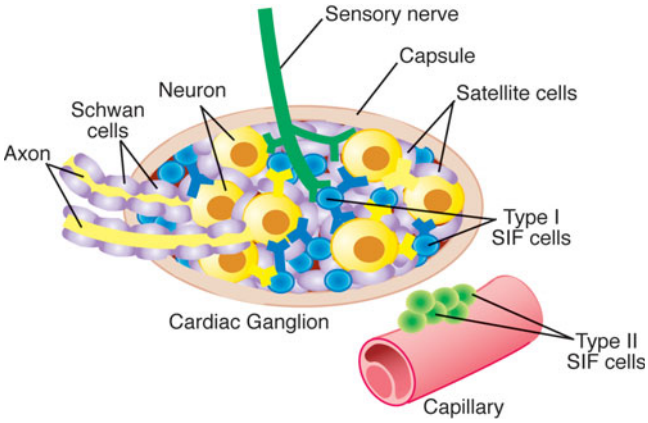

Figure 13.4. The various cell types and their interactions in the cardiac ganglia. Type I SIF cells function as small interneurons in the parasympathetic cardiac ganglia while type II SIF cells are located in clusters near capillaries and function as paracrine signaling centers.

left atrium. Ventricular innervation is much sparser and arises from ganglia located in the plexus surrounding the roots of the aorta and pulmonary trunk.

The structural integrity of the ganglia and their constituent neurons is dependent on constant stimulation from the vagus nerve (Tay et al., 1984). The structure of the cardiac ganglia and the composition of cells they contain varies from species to species (Anderson and Smith, 1971; Calaresu and St Louis, 1967; Janes et al., 1986; King and Coakley, 1958; Kirby et al., 1980; Kuntz, 1934; McMahan and Purves, 1976; Mitchell et al., 1953; Papka, 1976; Yuan et al., 1994). The atrial cardiac ganglia contain an average of 30 neurons (Fig. 13.4). Typically the ganglia consist of principal neurons (postganglionic parasympathetic), SATELLITE CELLS, and SMALL INTENSIVELY FLUORESCENT (SIF) cells whose processes are confined to the ganglia and act as interneurons (Ellison and Hibbs, 1976; McMahan and Purves, 1976). The principal neurons send motor information to cardiomyocytes. The SIF cells are distinguished from principal cells by the presence of numerous granular vesicles seen via the electron microscope. They are interposed between pre- and postganglionic parasympathetic neurons and between direct afferent fibers and the postganglionic neurons (Dail and Barton, 1983). SIF cells display TYROSINE HYDROXYLASE immunoreactivity (Horackova and Armour, 1995). From the general morphology of the cells, two types of SIF cells exist: type 1 cells have processes, and type 2 cells are without processes and are thus thought to function as paracrine cells. The type 1 SIF cells project axons to principal neurons within the cardiac ganglia (Horackova and Armour, 1995). Clusters of type 2 cells are often in close proximity to capillaries. SIF cells are present in the heart of non-vertebrate chordates (CYCLOSTOMES) even though the heart is not innervated nor are there cardiac ganglia. In amphibians and mammals, SIF cells become integrated within the cardiac ganglia as they appear (Taxi et al., 1983).

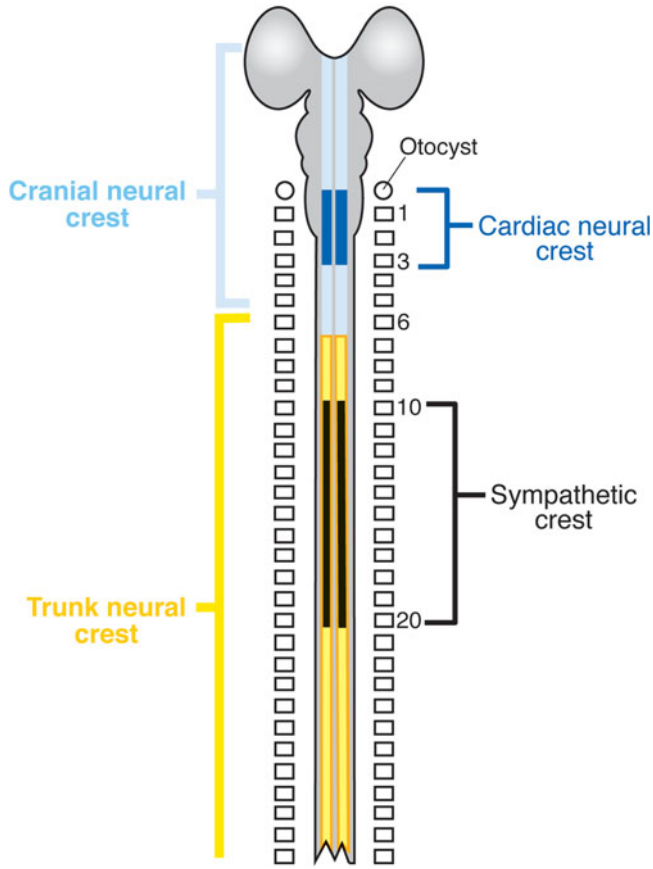

Figure 13.5. All of the peripheral neurons and supporting cells of both divisions of the autonomic nervous system that innervate the heart are derived from neural crest. The parasympathetic peripheral nerves are from the cardiac neural crest located between the otocyst and somite 4, and the sympathetic peripheral nerves are from neural crest originating adjacent to somites 10–20.

The primary neurotransmitter used by the parasympathetic neurons in the cardiac ganglia is acetylcholine. However, neurons containing SOMATOSTATIN, substance P, CALCITONIN GENE-RELATED PEPTIDE, VASOACTIVE INTESTINAL PEPTIDE, and NEUROPEPTIDE Y can also be found, indicating that sympathetic, sensory, and intrinsic neurons modify the parasympathetic activity in the heart. This suggests that cardiac ganglia serve as integrators of convergent neuronal activity rather than simple relays (Steel et al., 1994, 1996; Tay and Wong, 1992). The various neuropeptide modulators may act presynaptically to modulate neurotransmitter release or directly at neuroeffector terminals within the heart. Despite the morphological and biochemical similarities found among the cardiac ganglia in various locations in the heart, there are clear differences in functionality among these ganglia (Selyanko, 1992).

Most of the studies of the development of the cardiac ganglia have been performed in chicks, rabbits, pigs, rats, and humans. All of the postganglionic autonomic neurons are derived from the neural crest (Fig. 13.5). Those that populate the cardiac ganglia originate from the cardiac neural crest,

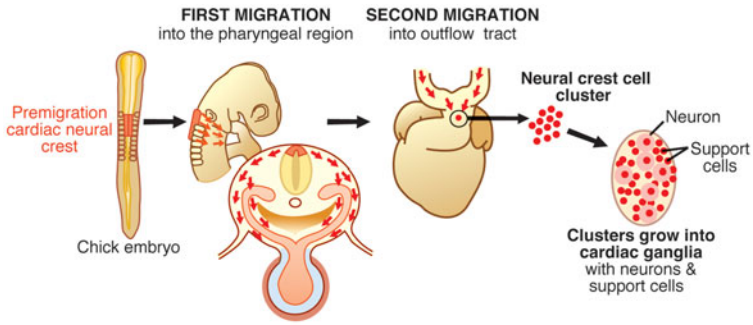

Figure 13.6. The parasympathetic cardiac ganglia originate from the premigratory neural crest cells located between the mid-otic placode and somite 3, also called the cardiac neural crest. These cells migrate dorsolaterally through the pharyngeal arches and into the heart where they form clusters over the entire surface of the heart and along all of the coronary blood vessels. The cells in the clusters differentiate as neurons and supporting cells.

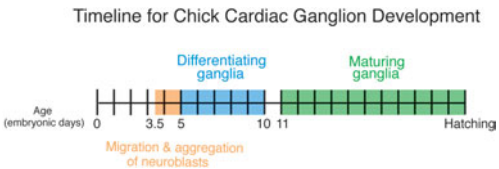

Figure 13.7. Major events in development of the parasympathetic cardiac ganglia in the chick.

which is located between the otic placodes and somite 4. In addition to providing the cardiac ganglia with neurons and satellite and SCHWANN CELLS, the cardiac crest also provides ectomesenchymal cells that are necessary for septation of the outflow tract of the heart (see Chapter 11) (Keating and Sanguinetti, 1996; Kirby et al., 1983).

During the first stage of parasympathetic neural development, the cells that become principal neurons of the cardiac ganglia migrate from their origin. They carry information regarding their neuraxial level of origin, which may be important in establishing communication with central nuclei. These cells are contacted by preganglionic fibers, and a decision of which neurotransmitter to synthesize is made based on the peripheral structure innervated (Shvalev and Sosunov, 1989).

The development of the cardiac ganglia in the chicken starts with migration and aggregation of the neural crest precursors on E3.5–5 (Fig. 13.6). The neural crest precursors seem to follow motor axons of the vagus into the heart, where they form small aggregates around the outflow tract. The cells enter the arterial pole via the arterial cardiac vagal branches and the venous pole via cardiac vagal branches that travel with the superior vena cava (Kirby et al., 1980; Verberne et al., 1998). A few supporting cells can be seen intermingled with the axons of the vagus or neuroblasts. Differentiating ganglia can be seen on E5–10, and mature ganglia are first seen at E11. Maturation continues until hatching (Kirby et al., 1980). In the differentiating phase, most of the neuronal population is composed of neuroblasts that have globular or bell-shaped perikarya. The supporting cells are more numerous. Dividing and dying neuroblasts are intermixed. Immature neurons form the largest population of neuronal elements in the ganglia from 11 days to hatching. In maturing ganglia, the PERIKARYA adopt a more typical appearance and are ovoid, becoming larger and rounder, with their nuclei located in an eccentric position. Numerous small satellite cells are present, and axodendritic synapses are more prominent. Axonal synapses can be identified by mid-incubation. The satellite cells are more numerous and are smaller than neurons. SIF cells can be identified as early as E6, and they show processes by day 7 (Enemar et al., 1965). Ultrastructurally, small clusters of SIF cells can be seen close to the cardiac ganglia but separated by processes of supporting cells (Kirby et al., 1980). More details are known about development of the cardiac parasympathetic innervation in the chick than in other species although the developmental sequence in chick appears to be representative of other species examined (Fig. 13.7).

In rabbits, from 18 dpf, the cardiac ganglia consist of parasympathetic postganglionic neurons, supporting cells, and SIF cells (Fig. 13.4). The neurons receive afferent input from synaptic terminals with small clear vesicles, typical of most cholinergic terminals, and small dense-core vesicles, typical of adrenergic terminals. These adrenergic terminals are probably part of an inhibitory system in the ganglia. The SIF cells receive afferent input from cholinergic type synaptic terminals and terminate on parasympathetic postganglionic neurons that are thought to be reciprocal synapses that modulate transmission through these neurons (Papka, 1976).

The cardiac ganglia in newborn rats are relatively immature and undergo extensive development in the first 3 postnatal weeks (Horackova et al., 2000). In the first two postnatal weeks, 2 main subpopulations of intrinsic neurons can be found. One subpopulation is located in the atrial septum and a second around the origin of the superior vena cava. Tyrosine hydroxylase–immunoreactive neurons, which are most likely SIF cells, are the most abundant. The postganglionic parasympathetic neurons, which are CHOLINE ACETYLTRANSFERASE–immunoreactive, are less abundant. The ganglia become more numerous and begin to be seen around the origins of the inferior vena cava and the pulmonary veins and in both atrial walls close to the atrioventricular junction. Extrinsic innervation is established during the third week. Two types of tyrosine hydroxylase–positive neurons are present in the cardiac ganglia: one co-expresses neuropeptide Y, and a second non-neuropeptide Y-expressing cell that lacks processes. These cells

are embedded in small clusters in the ganglia. The number of choline acetyltransferase–positive neurons increases, and they become surrounded by a rich network of cholinergic VARICOSE NERVE FIBERS, some of which originate extrinsically. Another population of relatively small ganglia are positive for vasoactive intestinal polypeptide and substance P (Horackova et al., 2000).

In human development, cardiac ganglia have been seen from 7 weeks of gestation, which is before complete development of septation (Gordon et al., 1993).

Development of the Sympathetic–Adrenal Axis

Both sympathetic postganglionic neurons and CHROMAFFIN cells that form the adrenal medulla in avian embryos arise from a common bipotential precursor that initially expresses neuronal traits (Vogel and Weston, 1990).

Preganglionic sympathetic motor neurons arise in the ventral ventricular zone and migrate radially into the ventral horn of the developing spinal cord, where they form a single motor column (Phelps et al., 1991). The autonomic motor neurons subsequently become separated from the somatic motor neurons and are displaced dorsally into the intermediolateral cell column that will become their permanent location. They become progressively more multipolar (Markham and Vaughn, 1991).

The postganglionic sympathetic innervation of the heart arises from the paravertebral sympathetic chains and is derived from the trunk neural crest region (Fig. 13.5) (Kirby, 1993). In the chick, the neurons of the sympathetic trunk arise from the trunk neural crest adjacent to somites 10–20. Tyrosine hydroxylase, a rate-limiting enzyme in catecholamine biosynthesis, appears at stage 18 in sympathetic trunk precursors near the dorsal aorta; clusters of catecholamine-positive cells then appear bilateral to the aorta at about 3.5 days of incubation or stages 20–22 (Allan and Newgreen, 1977; Ernsberger et al., 2000; Kirby and Gilmore, 1976). If the catecholamine pool is enhanced, the cells can be observed at stage 18 (Allan and Newgreen, 1977). The appearance of catecholamine-synthesizing enzymes is preceded by the transcription factor called chick achaete scute homolog (Cash) and can be detected at stage 15 (Ernsberger et al., 1995). By day 4, the aggregates are continuous cords that are designated the PRIMARY SYMPATHETIC TRUNKS. The sympathetic ganglia, like the dorsal root ganglia and ventral spinal roots, require the normal rostrocaudal alternation of somitic mesoderm for segmental morphogenesis. The migrating neural crest cells, which contribute to both the dorsal root ganglia and primary sympathetic chain, are partitioned between these two types of ganglia by rostral somitic mesoderm (Goldstein and Kalcheim, 1991).

At 4.5–5 days (stage 25), the secondary or permanent paravertebral trunks begin to form and cell processes are first seen. Secondary trunk formation is essentially complete by stage 28, at which time the primary trunks become discontinuous. The secondary trunks develop RAMI COMMUNICANTES, the proximal and distal connections to the ventral nerve roots (Kirby and Gilmore, 1976). Axons sprout from the principal ganglion cells along the entire length of the trunks by days 6–8. The thoracic cardiac nerve is first seen leaving the trunk in the lower cervical-upper thoracic regions at day 7–7.5. On day 9, the sympathetic terminals make contact with the vagus. While they can be seen in the outflow region and atria on day 10, they do not reach the ventricles until day 11 (Kirby et al., 1980; Kirby and Stewart, 1986). As for parasympathetic cardiac innervation, more details are known about development of the sympathetic cardiac innervation in the chick than in other species although the developmental sequence appears to be the same for other species that have been examined (Fig. 13.8).

In the mouse, a primary sympathetic chain is also formed by ventral migration of the sympathoadrenal lineage of neural

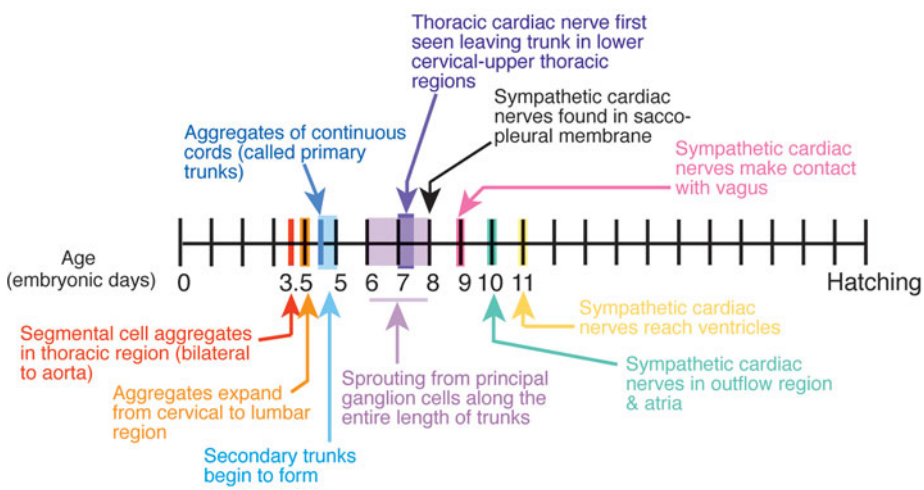

Figure 13.8. Major events in development of the sympathetic innervation of the heart in the chick embryo.

crest cells. Neuregulin-1/ErbB2/ErbB3 signaling are important in the migration of these cells (Britsch et al., 1998). Transcriptional regulators, including mouse achaete scute homolog (MASH1), PHOX2A, and Phox2b are expressed by these progenitors in response to Bmp secreted from the dorsal aorta (Ernsberger et al., 2000; Groves et al., 1995; Guillemot et al., 1993; Pattyn et al., 1997; Schneider et al., 1999; Tiveron et al., 1996). These genes play a role in promoting expression of tyrosine hydroxylase and dopamine β-hydroxylase (Guillemot et al., 1993; Pattyn et al., 1999). Growth of sympathetic nerves is mostly along blood vessels, suggesting that blood vessels regulate guidance of the nerves. Sympathetic neuroblasts also develop into chromaffin cells that form the adrenal medulla. In the chick, stages in development of adrenal medullary cells have been identified by the expression of various proteins. The earliest are permanent markers (CHROMOGRANIN-A, chromogranin-B, tyrosine hydroxylase, and GALANIN), followed by a set showing progressively increased expression until day 10 of development (dopamine-β-hydroxylase, proprotein convertase 2, somatostatin, and met-enkephalin), and finally, late-appearing markers (secretogranin II, neuropeptide Y, PHENYLETHANOLAMINE-*N*-METHYLTRANSFERASE, and NEURON-SPECIFIC ENOLASE) (Sanchez-Montesinos et al., 1996).

The adrenal medulla consists of a large population of chromaffin cells, which lack neuronal processes, and ganglion cells with typical neuronal morphology. In humans these two major cell types can be distinguished in the developing adrenal medulla as large cells with pale nuclei and ill-defined cytoplasm, which are present from 9 weeks gestation, and clusters of small cells, present from 14 weeks, respectively. The large cells express chromogranin A, SYNAPTOPHYSIN, and tyrosine hydroxylase, characteristic of adult chromaffin cells, while the small cells express neurofilament and tyrosine hydroxylase, typical of ganglion cells in the adult adrenal medulla. Late in development, the large cells are surrounded by clusters of ganglion cells (Molenaar et al., 1990). In the pig, migrating neural crest cells invade the fetal cortex and form cords that become the centers of proliferation and differentiation of the chromaffin cells (Chumasov et al., 2003).

Mash1 is necessary for the development of chromaffin cells. Most adrenal medullary cells in *Mash1*-null mice identified by Phox2b immunoreactivity fail to express tyrosine hydroxylase and are thus unable to synthesize catecholamines. The cells in *Mash1*-null mice do not contain chromaffin granules and have a neuroblast-like phenotype (Huber et al., 2002). In addition, most of the cells in the adrenal medulla die by birth. GLUCOCORTICOIDS were thought to be essential for suppressing neuronal commitment, thus channeling neural crest cells toward the chromaffin phenotype. However, mice deficient for a functional glucocorticoid receptor possess the full complement of adrenal chromaffin cells at birth, suggesting that signals other than glucocorticoid hormones may be important in triggering chromaffin cell differentiation (Schober et al., 2000).

Function of Growth Factors in Autonomic Development

The development of sympathetic neurons and adrenal chromaffin cells involves a series of steps, each having different responsiveness to growth factors and glucocorticoids (Anderson, 1997). Fgfs, Bmps, and neurotrophins are important modulators in development of the autonomic lineages. Fgfs and Bmps influence neuronal fate decisions, while neurotrophin responsiveness appears relatively late in differentiation and modulates cell survival and growth (Anderson, 1997).

Neurotrophins are a family of factors required for the survival of all peripheral neurons during development (Enomoto et al., 2001). The neurotrophins include Ngf, Bdnf, Nt4, and Nt3 (Fig. 13.2). Tissues engineered to express high levels Ngf or Nt3 show increased sympathetic and sensory fibers (Albers et al., 1996; Hassankhani et al., 1995). Ngf and Nt3 appear to influence sympathetic neurons late in development via TrkA receptors because the initial projections of sympathetic axons occur normally in *TrkA*-deficient mice (Fagan et al., 1996; Francis and Landis, 1999; Wyatt et al., 1997).

Sympathetic neural development depends on a cascade of neurotrophic factors. Nt3 appears to be important during sympathetic maturation postnatally, as postnatal homozygous Nt3 mutants lose half of the neurons in the superior cervical ganglia by abnormally high apoptosis (ElShamy et al., 1996). The fact that only half of the neurons are affected indicates that there are subpopulations of neurons that are differentially dependent on this factor. TrkA appears at E13.5, and is necessary for survival of sympathetic neurons after E15.5 and for proper innervation of the target (Fagan et al., 1996).

The glial cell line-derived neurotrophic factor (GDNF) family of neurotrophic factors includes Gdnf, neurturin, artemin, and persephin. These factors signal through a receptor complex composed of the RET TYROSINE KINASE and Gdnf family receptors (Gfr)α-glycosylphosphatidylinositol-linked cell surface binding proteins. Four members of the Gfrα family act as preferential receptors for the four ligands (Baloh et al., 1998a,b; Enomoto et al., 2001; Kotzbauer et al., 1996; Lin et al., 1993; Milbrandt et al., 1998). Ret deficiency affects normal migration and initiation of sympathetic axonal growth. Ret and artemin are the receptor and ligand essential for early sympathetic neuron differentiation (Enomoto et al., 2001).

Neuregulin is an Egf-like growth and differentiation factor that signals through the ErbB family of tyrosine kinase receptors. Mice with targeted mutations in the *erbB2*, *erbB3*, or *neuregulin-1* genes have hypoplasia of the primary sympathetic ganglion chain. Neuregulin-1 is expressed as neural crest cells first appear, and mutant mice lack the precursor cell pool forming the primary sympathetic ganglion chain (Britsch et al., 1998).

Ciliary neurotrophic factor (Cntf) and its receptor are expressed in the developing embryonic chick heart and may be involved in parasympathetic synapse formation. Cntf and

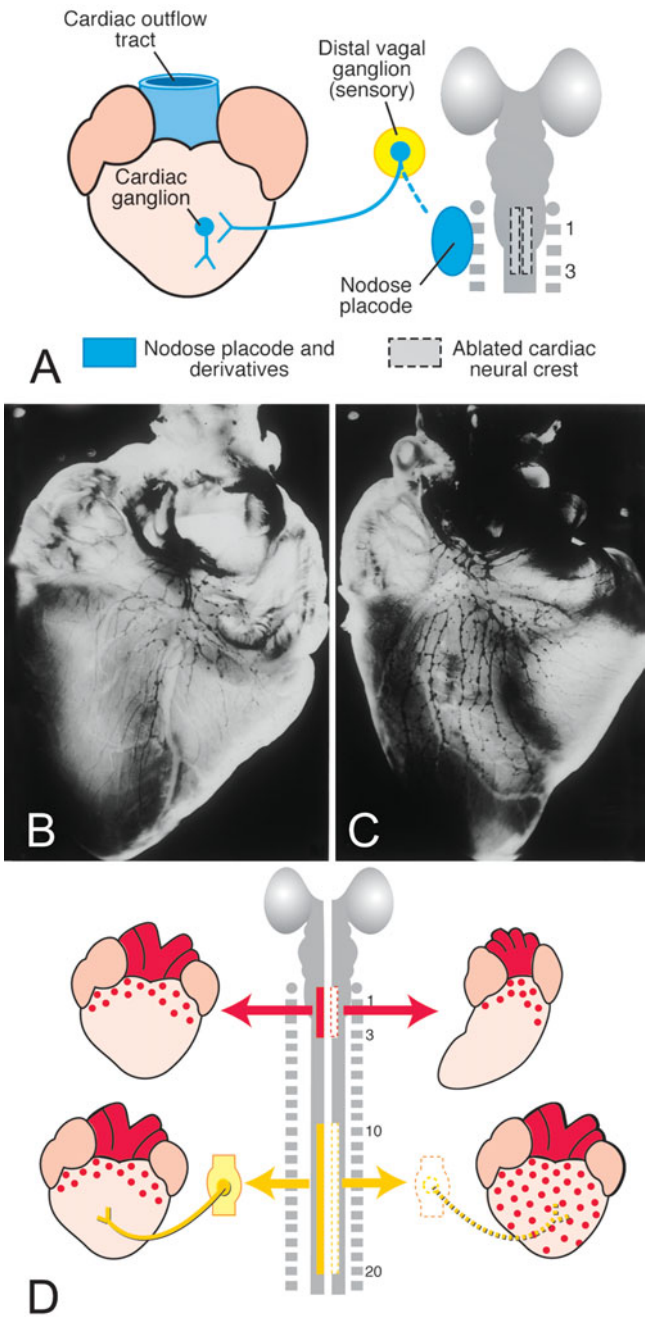

Figure 13.9. Plasticity of the developing autonomic nervous system and competition for growth factors can be seen after removal of the neural progenitors. (*A*) If the premigratory neural crest that contributes to the cardiac ganglia is ablated, the ganglia still develop but from neuronal precursors that originate in the nodose placodes. (*B*) Acetylcholinesterase histochemistry on whole-mount E12 chick heart showing normal cardiac ganglia development (*black dots*) and (*C*) dramatic expansion of the ganglia after sympathetic neural crest ablation. (*D*) Summary of the results after removal of neural crest progenitors of the cardiac autonomic innervation. (Adapted from Kirby et al., 1987.)

Cntf receptor mRNA levels are highest at E11–13, which corresponds to the period of parasympathetic cardiac ganglia expansion in chick atria. Levels of atrial Cntf receptor mRNA are higher in atria than in ventricle, corresponding to the higher degree of parasympathetic innervation occurring in atria. Treatment of isolated atria or cultured atrial myocytes with recombinant Cntf causes phosphorylation and nuclear translocation of STAT3 (Signal Transducers and Activators of Transcription), a transcriptional activator. One of the downstream targets that is upregulated by Cntf signaling is muscarinic receptors. Indeed, there appears to be an interaction of Cntf and muscarinic activity because Cntf receptor expression in the atrium is increased or decreased by simulation or inhibition of muscarinic receptors, respectively (Wang and Halvorsen, 1998).

Several studies have shown that there is competition for neurotrophins in the peripheral nervous system and that this competition is important in determining the richness of end-organ innervation. In the absence of sympathetic innervation to the heart, the cholinergic cardiac plexus increases dramatically due to both hypertrophy and hyperplasia of the ganglion cells as well as their terminals (Fig. 13.9). The additional cells are an expansion of the normal population of cholinergic neurons in the heart rather than from some extra source (Kirby et al., 1987). This suggests that there is competition for growth factors by the nerve terminals in the heart to induce and/or maintain normal autonomic innervation. Interestingly, if the parasympathetic neural progenitors are removed, they are reconstituted from the nodose placodes (Kirby, 1988).

Genetic Control of Autonomic Neurogenesis

The genes that regulate neurogenesis are not specifically linked to innervation of the developing heart. However, their identification and characterization in neuronal development has important implications for the developing cardiac ganglia. The destiny of each cell is determined by the temporal and spatial activation of a gene and how it is controlled by transcription factors (Kern et al., 1995).

Recent studies show that several helix-loop-helix (HLH) transcription factors play an essential role in neural development. In *Drosophila* an HLH-containing proneural gene called *achaete-scute* is important in neurogenesis (Fig. 13.10). Mammalian (*Mash*) and chick (*Cash*) homologs mentioned previously, are important in development of all autonomic neurons. Targeted mutation in *Mash1* blocks development of sympathetic and parasympathetic neurons. The *Mash1*-null mutant mouse has no autonomic nervous system and dies at birth. Supporting cells are not affected in the autonomic ganglia, but there is a partial reduction in size of the adrenal chromaffin cell population. Undifferentiated neural crest-derived precursors are present in their appropriate location and subsequently disappear. Mash1 protein is expressed by some sensory neurons, but its level of expression is less than and later than its expression by the autonomic sublineages. Because sensory neurons are not affected by the absence of *Mash1*, this suggests that Mash1 expression is restricted to the

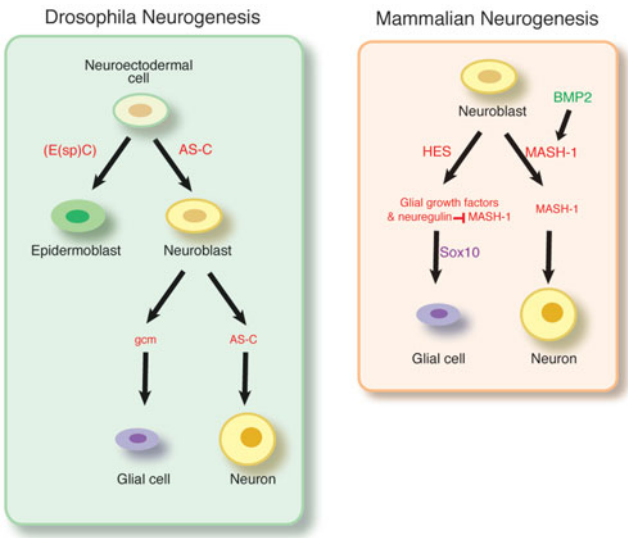

Figure 13.10. Function of the *achaete-scute* (AS-C) family of neurogenic genes in *Drosophila* and mammalian neurogenesis.

autonomic sublineage early in development (Guillemot et al., 1993; Wang and Kirby, 1995).

The precursors of the sensory lineages express neurogenin-1 and -2. Neurogenin-1 activates expression of NeuroD, a basic HLH transcriptional regulator, and downstream neuronal elements such as N-tubulin in neural crest-derived sensory neurons of the dorsal root ganglia. Neurogenin-2 is expressed in placode-derived sensory neurons, that is, the nodose ganglion neurons (Anderson, 1997).

Little is known about the factors that control Mash1 expression in neural crest cells. The Ret receptor may activate Mash1 expression (Anderson, 1994). In the rat, Mash1 and Ret are co-expressed in the cardiac ganglia. Retinoic acid treatment downregulates both and disrupts the differentiation of cardiac neural crest cells into neurons by regulating the expression of the homeodomain transcriptional regulator Phox2a (Shoba et al., 2002). After RA treatment, the population of cells expressing Phox2a is reduced in the cardiac ganglia.

Bmp2 induces Mash1 and neurogenesis in neural crest stem cells (Shah et al., 1996). Endothelial cells of the dorsal aorta may be a source of signals that influence the differentiation of neural crest-derived autonomic neurons in the sympathetic sublineage that forms the primary sympathetic trunks (Groves et al., 1995; Stern et al., 1991).

Negative regulation of Mash1 also appears to be important in the decision between neuronal and support/Schwann cell fate. In neural crest stem cell cultures, glial growth factors inhibit the induction of Mash1. In vertebrate peripheral nervous system, neuregulin, a member of the Egf-Tgfα superfamily, controls the choice between neuronal and support cell lineages (Anderson, 1995). In the presence of these factors, cells that would become neurons choose a support/Schwann cell fate (Shah et al., 1994).

Sox10 is expressed by neural crest cells and is required early for maintaining the cells in an undifferentiated state. As the neurons begin to differentiate, Sox10 is necessary for differentiation of the Schwann cells throughout the peripheral nervous system (Fig. 13.11) (Britsch et al., 2001). In the heart, the progressive development of the cardiac plexus can be visualized by Sox10. This process starts by day 6 of incubation, progressing in the following days. The Sox10 expression persists in Schwann cells and is lost in the cardiac neurons (Montero et al., 2002). A role for Sox10 in the control of the cardiac innervation has been suggested by the association of alterations in the autonomic control of heart dynamics in humans haploinsufficient for Sox10 (Korsch et al., 2001).

Neurotransmitter Development and Onset of Cardiac Neurohumoral Responses

The neurotransmitters used by autonomic postganglionic neuroblasts are determined partially by the local environment. Parasympathetic neurons express acetylcholine from early differentiation. Early sympathetic neuroblasts express a large repertoire of neuroactive substances, and the expression of these becomes restricted further during development as the neuroblasts mature. Almost all sympathetic neurons express a primary neurotransmitter, norepinephrine, and peptides that modulate signaling. Factors that regulate development of these co-transmitters in sympathetic neurons are unknown. Two thirds of the neuronal clones derived from sympathetic neurons isolated before they have preganglionic input or contact their peripheral target express neuropeptide Y, which shows that cell lineage plays a role in peptide identity (Hall and MacPhedran, 1995).

Acetylcholine

Whole-organ acetylcholinesterase histochemistry shows the development and location of the cardiac ganglia and subepicardial plexuses in the chick heart first on days 7 and 8 of incubation. The appearance of acetylcholine itself is difficult to study, but an indication of it is high-affinity choline uptake which is a neural property (Wetzel and Brown, 1983). High-affinity choline uptake can first be measured on day 7 of incubation, after which it increases rapidly to reach a peak at days 10–12 of incubation (Kirby and Stewart, 1983). The fact that acetylcholinesterase and high affinity choline uptake appear concurrently indicates the onset of nerve ingrowth from the parasympathetic innervation. Cholinergic neuroeffector transmission begins on day 12 of incubation; however, pretreatment with a drug that causes early accumulation of acetylcholine causes allows transmission to begin prematurely on day 10, indicating that synapses are present and functional but that acetylcholine has to accumulate to a certain level before the parasympathetic terminals can release enough to elicit a response (Pappano, 1977).

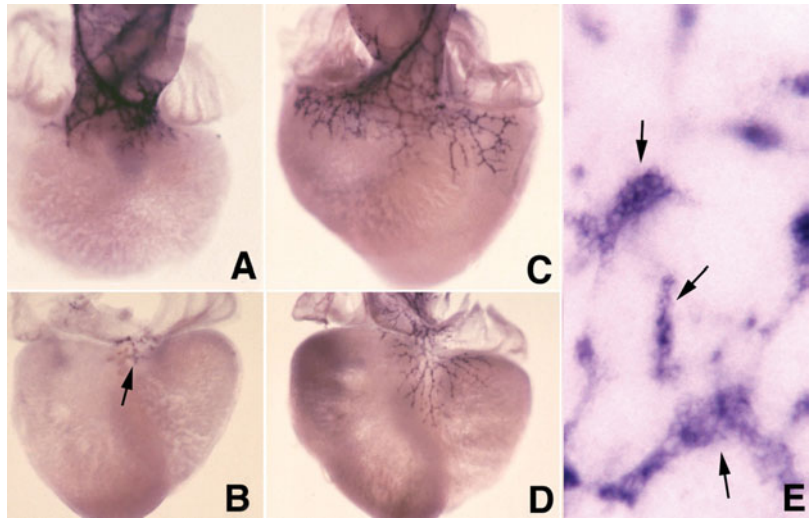

Figure 13.11. Sox 10 expression illustrates development of the cardiac ganglia in the chick. Panels *A* and *C* are frontal views of the heart at days 6 and 8 of incubation showing the nerves running from the arterial pole and spreading over the surface of the ventricles. Panels *B* and *D* are complementary views of the diaphragmatic face of the same heart. Panel *E* is a high magnification of the labeling pattern showing that transcripts are distributed in a dotted pattern (*arrows*) that corresponds with the glial cells accompanying the autonomic nerves. (From Montero et al., 2002, with permission.)

Catecholamines

Tyrosine hydroxylase-immunoreactive nerve fibers are scarce at birth in rat heart but increase rapidly during the first 2 postnatal weeks, reaching approximately adult levels by the third week. The fibers are first seen in the atrial chambers and later in the ventricular free wall, starting from the subepicardial myocardium. The fibers last appear in the atrial appendages and interventricular septum (Nyquist-Battie et al., 1994). Tyrosine hydroxylase–expressing neurons are not found in the cardiac ganglia (Nyquist-Battie et al., 1994)

In the chick, specific neuronal uptake of tritiated norepinephrine, a measure of innervation, can be detected on E11 in the atria. The highest tyrosine hydroxylase activity and norepinephrine concentration occur on E7, which is well before the arrival of sympathetic nerves in the heart. The norepinephrine concentration is particularly low on E10–13, when the sympathetic nerves begin to arborize in the heart. Because tyrosine hydroxylase activity is present in the heart before the arrival of sympathetic innervation and after sympathectomy, the catecholamines in the heart are thought to be synthesized by a population of myocardial cells (Stewart and Kirby, 1985). A more recent study has shown that the adrenergic biosynthetic enzymes are expressed early by myocardial cells interspersed throughout the myocardium. By E11.5, they are localized to regions of the sinoatrial and atrioventricular nodes. Gradually expression decreases in these regions but increases along the crest of the interventricular septum, where the bundle of His is located (Ebert and Thompson, 2001). The role of these extraneuronally produced catecholamines is not known, but the heart does have receptors and responds to exogenously applied catecholamines well before functional innervation is established. In the frog, extraneuronally produced catecholamines are thought to have a paracrine function in cardiac control. Catecholamines and their synthetic enzymes, tyrosine hydroxylase, dopamine β-hydroxylase, and phenylethanolamine *N*-methyltranferase, are found in the noninnervated *Xenopus* larval heart, which synthesizes and stores catecholamines in the myocardium (Kloberg and Fritsche, 2002).

In all the animals studied, maturation of the sympathetic innervation of the heart and onset of function is very late in fetal or postnatal development. In the chick, it is just prior to hatching and in most mammals maturation of the sympathetic nervous system is postnatal. However, it is a common theme that cardiac β-adrenergic receptors and catecholamine sensitivity are present well before birth. In the chick embryo, catecholamines applied prior to functional innervation cause tachycardia.

In 9.5 dpc mouse hearts, β-adrenergic agonists increase the spontaneous beating rate, slope of the pacemaker potential and action potential duration with decreased maximum upstroke velocity. L-type Ca^{2+} channel currents are modulated by β-adrenergic receptors probably via a cAMP-dependent pathway (Liu et al., 1999). Prolonged activation of β-adrenergic receptors by isoproterenol causes an increase in muscarinic acetylcholine receptor number and muscarinic responsiveness in chick myocardial cells because of an increase in muscarinic receptor mRNA levels (Jackson and Nathanson, 1995).

These results suggest that catecholamines can alter transcriptional activity of some genes. It was initially reported that sympathetic denervation of the heart led to no significant alterations in heart growth (Bareis et al., 1981). However, when pieces of embryonic heart were cultured in the anterior eye chamber to determine the effect on growth in the absence of normal hemodynamic load, the growth and beating rate, which are normally modulated by ocular autonomic neurons that grow into the graft, are compromised after sympathetic denervation of the eye (Tucker and Gautier, 1990). This suggests that sympathetic innervation plays a role in cardiac growth. Functional α_2-adrenergic receptors are present in the fetal rat heart, where they have been shown to influence development of

the actin cytoskeleton (Porter et al., 2003). Isoproterenol, a β-adrenergic agonist, stimulates c-fos expression in the developing rat heart. The expression of c-fos is associated with trophic activation of genes involved in both cell differentiation and cell growth. Interestingly, repeated administration of isoproterenol to neonatal rats does not elicit cardiac hypertrophy, as it would in adult rats (Slotkin et al., 1995).

Adenosine

Adenosine is a nucleoside produced by all cells as a metabolite of ATP (Olah and Stiles, 1995; Pelleg and Belardinelli, 1993; Tucker and Linden, 1993). ATP serves as a co-transmitter within the sympathetic nervous system and is also released from endothelium and aggregating thrombocytes. Extracellular adenosine activates PURINERGIC RECEPTORS that couple with G proteins to initiate intracellular signaling. Adenosine receptors are among the earliest G protein-coupled receptors expressed in the mammalian heart and are present well before sympathetic innervation develops and matures. This suggests that there is an extraneuronal source for adenosine signaling (Cothran et al., 1995). In fact, fetal plasma levels of adenosine are very high, and this may be the source of purinergic receptor ligands (Sawa et al., 1991).

The adenosinergic system is the earliest functionally responsive system in the heart. In rat at 8.0 dpc and older, adenosine receptor activation decreases heart rate (Porter and Rivkees, 2001). Between 9 and 12 dpc, adenosine agonists potently downregulate heart rate by a G protein-mediated mechanism that alters cAMP, ATP-dependent kinase, L-type calcium, sodium, and chloride channels, and consequently the pacemaker current (Hofman et al., 1997). Treatment of embryos with adenosine receptor agonist causes ventricular hypoplasia via decreased cell proliferation (Zhao and Rivkees, 2001).

Adenosine is generated by enzymatic degradation of ATP. It acts at the axon terminal to inhibit norepinephrine release from sympathetic nerve endings and causes vasodilatation of smooth muscle via endothelium-dependent and endothelium-independent actions. Adenosine also has important antiarrhythmic properties and prevents some of the deleterious sequelae of ischemia. In humans, adenosine evokes a sympathoexcitatory reflex mediated by chemically sensitive receptors and afferent nerves in the heart. This reflex may be active during exercise and ischemia (Rongen et al., 1997).

Somatostatin

Somatostatin is first seen in chick embryos at E11. It is fully developed in E16 to 17 embryos. Somatostatin is present in postganglionic neurons, and while somatostatin-immunoreactive fibers form a rich plexus in atrial and ventricular myocardium, they are not seen in the vessel walls as are many of the other neuropeptides (Corvetti et al., 1988). Somatostatin immunoreactivity can be localized in humans at 10 weeks of gestation to cell bodies in cardiac ganglia, as well as to nerve fibers, indicating an intrinsic origin for this nerve subpopulation (Gordon et al., 1993).

Substance P

Substance P is also first seen in chick embryos at E11 and is fully developed by E16–17, which is about the time that adrenergic innervation becomes functional. Substance P-immunoreactive fibers are densest in nerve bundles and in isolated fibers in the myocardium, pericardium, and vessel walls. It is also seen in the cardiac ganglia (Corvetti et al., 1988).

The onset of substance P-immunoreactive innervation in human fetuses at 18–24 weeks of gestation suggests that the sensory afferent innervation lags significantly behind autonomic innervation. However, as noted previously, the autonomic innervation appears in the heart long before it becomes functional (Gordon et al., 1993).

Calcitonin Gene-Related Peptide

It is unclear whether calcitonin gene-related peptide (Cgrp) is primarily expressed by sensory innervation in the heart or if it is also in the autonomic neurons. In the fetal puppy and rat, Cgrp appears with a burst of immunoreactivity during the neonatal and early perinatal period; however, the amount of Cgrp immunoreactivity decreases during maturation (Kuncova and Slavikova, 2000; Shoba and Tay, 2000; Ursell et al., 1991). The extramural coronary arteries, sinoatrial and atrioventricular nodes show high Cgrp reactivity, although the cardiac ganglia are not positive for Cgrp, indicating an extrinsic, sensory origin of these fibers (Shoba and Tay, 2000; Ursell et al., 1991).

In the mouse, nitric oxide synthase (NOS) and Cgrp are co-expressed by the sensory innervation of the heart. Co-expression is found from 19 dpc in the mouse in both the cardiac ganglia and nerve fibers. A considerable proportion of sensory Cgrp-immunopositive fibers are also immunoreactive for Nos (Shoba and Tay, 2000). The late onset of Cgrp appearance in mammals suggests that sensory innervation of the heart is later than autonomic innervation. Furthermore, mice lacking Cgrp expression demonstrate no obvious phenotypic differences from their wild-type littermates, suggesting that Cgrp is not involved in any obvious aspect of cardiac development (Lu et al., 1999).

Cgrp immunoreactive innervation can be found at 18–24 weeks of human gestation, which is after autonomic innervation develops (Gordon et al., 1993).

Vasoactive Intestinal Peptide

Vasoactive intestinal peptide (Vip) can be immunolocalized in the chick embryo at E11 but continues to accumulate until E16–17. VIP is seen mostly in single fibers traveling along the walls of the coronary vessels and in the pericardium. Some VIP immunoreactive neurons can be seen in the cardiac ganglia and these may represent local sensory feedback loops (Corvetti et al., 1988).

In puppies aged 1–6 weeks, Vip concentration is higher in the coronary arteries than in the myocardium (Kralios et al., 1999). Vip is present in rat atria at postnatal day 1. The levels increase in the right atrium between postnatal days 10 and 25, remain high at postnatal day 45, but decline after that. In the mature heart, the peptide levels are significantly higher in the left than in the right atrium, but the significance of this differential expression is not known (Kuncova and Slavikova, 2000).

Vip-immunoreactive nerves appear in human atria at 10–12 weeks of gestation. These neuropeptide-containing terminals appear to be of extrinsic origin because they are not found in the cardiac ganglia at these ages (Gordon et al., 1993).

Neuropeptide Y

Neuropeptide Y (Npy) is a 36-amino-acid peptide found in the heart, postganglionic sympathetic nerves that innervate cardiac blood vessels, cardiac ganglia, endocardium, and myocardium (Palmiter et al., 1998). Fibers containing Npy synapse on postganglionic parasympathetic neurons in the cardiac ganglia. In fact, it is the most abundant peptide in the heart. Nerve activation and ischemia promote release of Npy, which causes vasoconstriction and smooth muscle cell proliferation, and recent studies have shown that Npy is a potent growth and angiogenic factor (Pons et al., 2004; Zukowska-Grojec et al., 1998). Npy acts through multiple G protein–coupled receptors to elicit a range of effects.

In puppies aged 1–6 weeks, Npy concentration is higher in the coronary arteries than in the myocardium, suggesting advanced innervation (Kralios et al., 1999). The Npy-mediated, sympathetic–parasympathetic interaction develops rapidly in the postnatal puppy and is fully expressed by 1 month of age. This developmental change is likely the result of maturation of sympathetic nervous system function after birth (Rios et al., 1996).

During rat development, Npy can be seen in the nodes and perinodal areas at 16 dpc. By postnatal day 7 it is also seen in the valves and ventricles. It increases through the first 3 weeks of postnatal life and then remains stable through adulthood (Palmiter et al., 1998). Npy immunoreactivity is also localized to a large proportion of the intrinsic cardiac ganglia from 16 days of gestation onwards, with a progressive increase in the number of neuronal cell bodies per ganglia with age (Shoba and Tay, 2000).

In the mouse, double-label immunohistochemistry shows co-localization of Npy with ventricular and atrial noradrenergic nerves, but it is also expressed by non-noradrenergic nerves in atria (Nyquist-Battie et al., 1994). The interatrial septum and atrial walls have a higher density of Npy than tyrosine hydroxylase–immunoreactive fibers. Npy-producing neurons are also detected in intrinsic ganglia (Nyquist-Battie et al., 1994).

At 10 weeks of human gestation, Npy is found in the major subpopulation of peptide-containing nerves, with the highest density in the atria decreasing in the ventricles (Gordon et al., 1993)

Npy is needed for increased myocardial Ca^{2+} current density at birth (Palmiter et al., 1998, Protas et al., 2003). Cultured myocardial cells show an increase in L-type Ca^{2+} current ($I_{Ca,L}$) density when they are co-cultured with sympathetic nerves. The increased current is blocked by antibodies to Npy. Myocytes from *Npy*-null neonatal mice fail to increase the density of $I_{Ca,L}$. Both $I_{Ca,L}$ density and action potential duration are significantly greater in adult wild-type than in Npy-null myocytes, whereas $I_{Ca,L}$ density is equivalent in neonatal wildtype and *Npy*-null myocytes. Together these results suggest that Npy does not influence $I_{Ca,L}$ prenatally, but the postnatal increase in $I_{Ca,L}$ density is entirely Npy dependent (Protas et al., 2003).

In addition to altering myocyte function, Npy is as angiogenic as Fgf2. At low concentrations it promotes vessel sprouting, adhesion, migration, proliferation, and capillary tube formation by endothelial cells. Endothelial cells express Npy receptors and the enzyme that cleaves the Npy propeptide to form an angiogenic isoform. Because sympathetic nerves are also a major source of Npy, both endothelium and sympathetic nerves may be important in angiogenesis during development (Zukowska-Grojec et al., 1998).

Onset of Neural Control of Heart Function

The autonomic innervation to the heart exerts profound influence on cardiac physiology. Stimulation by the sympathetic system acts to increase the rate and force of contraction while parasympathetic stimulation serves to antagonize the effects of sympathetic nerves. In the normal heart, there is a balance between these opposing elements. These effects of cholinergic and adrenergic stimulation are achieved primarily by modulation of ion channel activity and sarcoplasmic reticulum function in cardiac myocytes. Much is known regarding the cellular mechanisms and these details have been reviewed extensively (Higgins, 1983; Robinson, 1996; van der Heyden et al., 2005; Vanoli et al., 1998). To facilitate understanding of developmental changes, a brief synopsis of autonomic effects on adult cardiac myocytes is provided here.

Stimulation of β-adrenergic receptors by catecholamines acts on several effector mechanisms via G-protein coupling with adenylate cyclase and subsequent elevation of cyclic adenosine monophosphate (cAMP). The increase in the beat frequency is due primarily to an increase in the magnitude of the repolarizing K^+ delayed rectifier current combined with an increase in I_f (see Chapter 5). The increase in I_K increases the rate of repolarization and thereby shortens the action potential while an increase in I_f increases the rate of diastolic depolarization. In addition, there is an increase in peak systolic tension due largely to an increase in the activity of L-type Ca^{2+} channels. Increased influx from sarcolemmal L-type channels has an amplifying effect because this Ca^{2+} triggers further release from the sarcoplasmic reticulum. In addition,

cAMP-dependent phosphorylation of the sarcoplasmic reticulum protein phospholamban, enhances uptake by the sarcoplasmic reticulum Ca^{2+}-ATPase thereby increasing sarcoplasmic reticulum Ca^{2+} stores and consequently, the amount of Ca^{2+} released with each beat.

Muscarinic acetylcholine receptor stimulation from parasympathetic nerves directly antagonizes the effects of catecholamines and sympathetic stimulation by a G protein–dependent mechanism that inhibits adenylate cyclase. The result is reduced elevation of cytosolic Ca^{2+} and a subsequent decrease in contractility. In addition, cholinergic stimulation, again through a G protein–dependent mechanism, activates a background K^+ channel that produces a hyperpolarizing membrane current. The effect of this current is to reduce the beat frequency by slowing the rate of diastolic depolarization. The acetylcholine activated background K^+ channel does not appear to be present in ventricular myocytes.

In the developing heart, the onset of parasympathetic innervation precedes sympathetic innervation. This has been best characterized in the chick embryo. In the chick, postganglionic parasympathetic neurons and nerve fibers are detected in the heart at about E4 and the system becomes functional at around E11. This is halfway through the gestation period for the chicken (22 days). Sympathetic fibers are detected at about day 9 and the system is functional by day 16 (Kirby et al., 1989; Pappano et al., 1982). Interestingly, adrenergic and cholinergic receptors and their associated effector mechanisms are present in cardiac myocytes well before autonomic nerve fibers can be found innervating the heart. It is not known why these autonomic receptor-mediated effector mechanisms are present before there is functional innervation. The level of circulating catecholamines in the embryo may be high from endocrine-like secretion of catecholamines from the developing adrenal medulla and sympathetic chain ganglia (Kirby et al., 1989; Mulder et al., 2000; Pappano et al., 1982; Portbury et al., 2003). These circulating catecholamines increase during periods of embryo hypoxia and it has been proposed that they mitigate the bradycardia and other effects of hypoxia on cardiac function (Mulder et al., 2000; Portbury et al., 2003). The uterine environment as well as the avian egg is constitutively hypoxic which is compensated in part by high-affinity hemoglobin and high hematocrit. In addition, mammalian fetuses nearer to term are subjected to regular episodes of hypoxia due to periodic maternal uterine contractures. In avian species, O_2 tension is relatively low with respect to ambient air and the embryos are thought to be susceptible to small changes in ambient O_2 because of restricted diffusion across the egg shell and underlying membrane.

The level of autonomic innervation in the human at birth has been recently documented and has been found to be very similar to the adult pattern and density (Chow et al., 1995). Sympathetic fibers are found throughout the atrial and ventricular myocardium. Parasympathetic fibers are found throughout the atria but there is a paucity of fibers in the ventricles. This observation is consistent with an absence of muscarinic acetylcholine receptor activated background K^+ channels in ventricular myocytes that has been seen in other species (Satoh et al., 1990).

The onset of cardiac sympathetic function in the mammalian ventricle during early postnatal life is associated with alterations in Na^+, L-type Ca^{2+}, pacemaker, inward rectifier and transient outward K^+ currents caused by sustained activation of myocardial Npy receptors, α-adrenergic receptors, and β-adrenergic receptors (Qu and Robinson, 2004).

In human heart, muscarinic receptor-mediated cholinergic and β-adrenergic receptor–mediated responses are elicited soon after the initiation of the heart beat, during the fourth and fifth weeks of gestation, respectively (Fig. 13.12). The maximum cardiac response to all these agonists becomes stronger as development continues. However, because the cardiac nerves have not developed at this time, this does not represent the onset of neural control of the heart. Formation of morphological and functional control by the autonomic innervation occurs in the human heart well after the appearance of the reactivity to autonomic transmitters. Muscarinic–cholinergic innervation is established at 10–12 weeks of gestation, and adrenergic transmission is found at 13–14 weeks. By 15–17 weeks, tachycardia can be elicited by atropine, indicating that there is tonic control of heart rate by the parasympathetic nerves. Bradycardia can be elicited by β-blockers in weeks 23–28, suggesting that sympathetic innervation is functional. This seems to follow the general pattern that the parasympathetic–cholinergic control of the developing heart is functional earlier than sympathetic–adrenergic neural control (Papp, 1988).

Figure 13.12. Events in innervation and onset of neural control during human heart development.

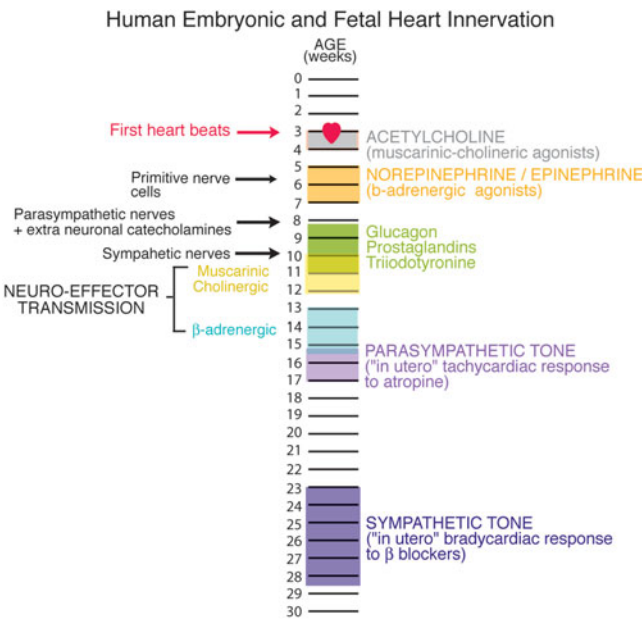

The onset of cardiac sympathetic function in puppies occurs in the first 6 postnatal weeks. There is nonuniform maturation of the cardiac nerves coupled with localized distribution of the nerves, which is the basis for regional sympathetic imbalance and arrhythmiogenesis in early life (Kralios and Millar, 1978). Isolated rat sinoatrial node cells and ventricular myocytes are supersensitive to norepinephrine and acetylcholine. The sinoatrial node cells remain sensitive to both norepinephrine and acetylcholine after the development of innervation but ventricular cells are significantly less sensitive to norepinephrine and acetylcholine. Thus, neurotrophic modulation is not homogeneous throughout the myocardium and may be dependent on the specific myocardial cell innervated (Atkins and Marvin, 1989).

β-Adrenergic receptors play a major role in the postnatal modulation of cardiac rhythm, rate, and repolarization by the sympathetic nervous system at all ages, while α-adrenergic receptors are much less important (Cua et al., 1997). In the mouse, the β_1-adrenergic receptor is primarily responsible for sympathetic regulation of both cardiac heart rate (chronotropy) and force of contraction (inotropy). In contrast, during fetal development α-adrenergic stimulation increases heart rate. Co-culture of fetal myocardium with adrenergic nerves changes the response of myocardial cells to α-adrenergic agonists from excitation to inhibition (Drugge et al., 1985). In the rat, adrenergic stimulation causes modest increases in heart rates beginning at 9.0 dpc. Muscarinic activation decreases heart rates only after 13 dpc (Porter and Rivkees, 2001).

Embryonic chickens rely primarily on adrenergic control of cardiovascular function, with no contribution from the parasympathetic nervous system (Crossley and Altimiras, 2000). Muscarinic antagonists have no effect on heart rate, while β-adrenergic antagonists cause bradycardia.

Congenital Disorders Involving Cardiac Innervation

Autonomic dysfunction may result from diseases that affect primarily either the CNS or the peripheral autonomic nervous system. The most common pathogenesis of disturbed autonomic function in CNS diseases is degeneration of the intermediolateral cell columns or damage to the descending pathways that synapse on the intermediolateral cell column. Both lead to progressive autonomic failure (McLeod and Tuck, 1987).

The peripheral autonomic nervous system may be damaged in isolation in the acute and subacute autonomic NEUROPATHIES or in association with a generalized peripheral neuropathy. The peripheral neuropathies most likely to cause severe autonomic disturbance are those in which small myelinated and unmyelinated fibers are damaged in the baroreflex afferents, the vagal efferents to the heart, or the sympathetic efferent pathways to the mesenteric vascular bed. Acute demyelination of the sympathetic and parasympathetic nerves in the GUILLAIN-BARRÉ SYNDROME may also cause acute autonomic dysfunction (McLeod and Tuck, 1987).

Many disease states known as DYSAUTONOMIAS are the consequence of impaired autonomic interactions (Garson et al., 1990). Familial dysautonomia and SUDDEN INFANT DEATH SYNDROME (SIDS) are the most frequently mentioned (Taylor and Marcus, 1990). Long QT syndrome was for many years thought to be due to imbalanced sympathetic and parasympathetic stimulation of the heart, and even though recent molecular genetic studies indicate that the syndrome results from mutations in genes encoding cardiac myocyte ion channels, the therapy for Long QT includes left cervical sympathectomy and administration of β-adrenergic receptor antagonists (Keating and Sanguinetti, 1996).

Familial Dysautonomia

Familial dysautonomia (also known as Riley-Day syndrome) is a disorder affecting people of Ashkenazi Jewish descent. It is the best known and most frequently occurring of congenital sensory neuropathies and is characterized by widespread sensory and variable autonomic dysfunction. The gene underlying this disease has been mapped to a 0.5-cM region on chromosome 9q31. The ethnic bias is due to a founder effect, with more than 99.5% of disease alleles sharing a common ancestral haplotype. One of the genes in this locus, *IKBKAP*, harbors two mutations that can cause familial dysautonomia. The major HAPLOTYPE mutation is located in the donor splice site of INTRON 20 and can result in skipping of exon 20 in the mRNA of patients with familial dysautonomia. The mutation associated with the minor haplotype is a missense mutation in exon 19, which is predicted to disrupt a potential phosphorylation site (Slaugenhaupt et al., 2001).

Patients with familial dysautonomia have an increased risk of sudden death. In some patients with familial dysautonomia, sympathetic cardiac dysfunction is indicated by prolongation of corrected QT (QTc) interval (Hilz et al., 1998). Stress tests show that patients with familial dysautonomia have a reduced cardiac parasympathetic response, most likely caused by efferent parasympathetic dysfunction (Hilz et al., 1999).

All familial dysautonomia patients have abnormal ORTHOSTATIC BLOOD PRESSURE, heart rate responses, and cardiac tone. QTc prolongation indicates an underlying sympathetic dysfunction. Heart rate variability suggests that some familial dysautonomia patients have abnormalities in parasympathetic, as well as sympathetic, cardiac tone (Axelrod et al., 1997).

Sudden Infant Death Syndrome

Although the description of the mechanisms responsible for sudden infant death syndrome (SIDS) is still far from complete, it appears to involve both arousal responses and cardiac autonomic controls during sleep–wake processes (Kahn et al., 2002). Both hypocellularity of the motor vagal nuclei and

delayed vagal maturation have been associated with SIDS (Becker and Zhang, 1996; Macchi et al., 2002).

Innervation Disorders that Accompany Other Congenital Disease

Individuals with Down syndrome but not congenital heart disease exhibit reduced heart rate and blood pressure responses to isometric handgrip exercise and cold pressor testing, which is consistent with autonomic dysfunction. Autonomic dysfunction may partially explain chronotropic incompetence observed during maximal treadmill exercise in these individuals (Fernhall and Otterstetter, 2003).

Increased heart rate, reduced variability in heart rate, and elevated levels of norepinephrine and RENIN are significant predictors of clinical symptoms such as tachypnea in infants with congenital cardiac malformations. Heart rate variability is a noninvasive measure of autonomic nervous system activity. The heart rate variability is reduced in congestive heart failure and in children with congenital heart disease. Propranolol reduces the presumed autonomic imbalance in infants with heart failure due to congenital heart disease (Buchhorn et al., 2002).

REFERENCES

Albers, K. M., T. N. Perrone, T. P. Goodness, M. E. Jones, M. A. Green, and B. M. Davis. 1996. Cutaneous overexpression of NT-3 increases sensory and sympathetic neuron number and enhances touch dome and hair follicle innervation. J. Cell Biol. 134:487–497.

Allan, I. J., and D. F. Newgreen. 1977. Catecholamine accumulation in neural crest cells and the primary sympathetic chain. Am. J. Anat. 149:413–421.

Anderson, D. J. 1994. Stem cells and transcription factors in the development of the mammalian neural crest. FASEB J. 8:707–713.

Anderson, D. J. 1995. A molecular switch for the neuron-glia developmental decision. Neuron 15:1219–1222.

Anderson, D. J. 1997. Cellular and molecular biology of neural crest cell lineage determination. TIG 13:276–280.

Anderson, R. H., and R. B. Smith. 1971. Feline ventricular ganglion cells. Nature 231:155–160.

Armour, J. A., and D. A. Hopkins. 1990. Activity of in situ canine ventricular neurons. Am. J. Physiol. 258:H326-336.

Atkins, D. L., and W. J. Marvin, Jr. 1989. Chronotropic responsiveness of developing sinoatrial and ventricular rat myocytes to autonomic agonists following adrenergic and cholinergic innervation in vitro. Circ. Res. 64:1051–1062.

Axelrod, F. B., D. Putman, D. Berlin, and M. Rutkowski. 1997. Electrocardiographic measures and heart rate variability in patients with familial dysautonomia. Cardiology 88:133–140.

Baloh, R. H., A. Gorodinsky, J. P. Golden, M. G. Tansey, C. L. Keck, N. C. Popescu, E. M. Johnson, Jr., and J. Milbrandt. 1998a. GFRalpha3 is an orphan member of the GDNF/neurturin/persephin receptor family. Proc. Natl. Acad. Sci. USA 95:5801–5806.

Baloh, R. H., M. G. Tansey, P. A. Lampe, T. J. Fahrner, H. Enomoto, K. S. Simburger, M. L. Leitner, T. Araki, E. M. Johnson, Jr., and J. Milbrandt. 1998b. Artemin, a novel member of the GDNF ligand family, supports peripheral and central neurons and signals through the GFRalpha3-RET receptor complex. Neuron 21:1291–1302.

Bareis, D. L., R. E. Morgan, C. Lau, and T. A. Slotkin. 1981. Maturation of sympathetic neurotransmission in the rat heart. IV. Effects of guanethidine-induced sympathetectomy on neonatal development of synaptic vesicles, synaptic terminal function and heart growth. Dev. Neurosci. 4:15–24.

Becker, L. E., and W. Zhang. 1996. Vagal nerve complex in normal development and sudden infant death syndrome. Can. J. Neurol. Sci. 23:24–33.

Britsch, S., D. E. Goerich, D. Riethmacher, R. I. Peirano, M. Rossner, K. A. Nave, C. Birchmeier, and M. Wegner. 2001. The transcription factor *Sox10* is a key regulator of peripheral glial development. Genes Dev. 15:66–78.

Britsch, S., L. Li, S. Kirchhoff, F. Theuring, V. Brinkmann, C. Birchmeier, and D. Riethmacher. 1998. The ErbB2 and ErbB3 receptors and their ligand, neuregulin-1, are essential for development of the sympathetic nervous system. Genes Dev. 12:1825–1836.

Buchhorn, R., M. Hulpke-Wette, J. Nothroff, and T. Paul. 2002. Heart rate variability in infants with heart failure due to congenital heart disease: reversal of depressed heart rate variability by propranolol. Med. Sci. Monit. 8:CR661–666.

Calaresu, F. R., and A. J. St Louis. 1967. Topography and numerical distribution of intracardiac ganglion cells in the cat. J. Comp. Neurol. 131:55–66.

Chow, L. T. C., S. S. M. Chow, R. H. Anderson, and J. A. Gosling. 1995. The innervation of the human myocardium at birth. J. Anat. 187:107–114.

Chumasov, E. I., M. Z. Atagimov, V. I. Sokolov, and V. G. Seliverstova. 2003. [Development of adrenal chromaffin tissue]. Morfologiia 123:68–73.

Corvetti, G., L. Andreotti, and L. S. Daneo. 1988. Chick peptidergic innervation: localization and development. Bas. Appl. Histochem. 32:485–493.

Cothran, D. L., T. R. Lloyd, H. Taylor, J. Linden, and G. P. Matherne. 1995. Ontogeny of rat myocardial A1 adenosine receptors. Biol. Neonate 68:111–118.

Crick, S. J., Sheppard, M. N., and Anderson, R.H. 2000. Nerve supply of the heart. In: The Nervous System and the Heart, ed. Ter Horst, G. J., 3–54. Totowa, NJ: Humana.

Crossley, D. I., and J. Altimiras. 2000. Ontogeny of cholinergic and adrenergic cardiovascular regulation in the domestic chicken (*Gallus gallus*). Am. J. Physiol. 279:1091.

Cua, M., A. Shvilkin, P. Danilo, Jr., and M. R. Rosen. 1997. Developmental changes in modulation of cardiac repolarization by sympathetic stimulation: the role of beta- and alpha-adrenergic receptors. J. Cardiovasc. Electrophysiol. 8:865–871.

d'Amico-Martel, A. 1982. Temporal patterns of neurogenesis in avian cranial sensory and autonomic ganglia. Am. J. Anat. 163:351–372.

Dail, W. G., and S. Barton. 1983. Structure and organization of mammalian sympathetic ganglia. In Autonomic Ganglia, ed. Elfin, L. G. New York: John Wiley & Sons.

Drugge, E. D., M. R. Rosen, and R. B. Robinson. 1985. Neuronal regulation of the development of the à-adrenergic chronotropic response in the rat heart. Circ. Res. 57:415–423.

Ebert, S. N., and R. P. Thompson. 2001. Embryonic epinephrine synthesis in the rat heart before innervation: association with

pacemaking and conduction tissue development. Circ. Res. 88:117–124.

Ellison, J. P., and R. G. Hibbs. 1976. An structural study of mammalian cardiac ganglia. J. Mol. Cell. Cardiol. 8:89–101.

ElShamy, W. M., and P. Ernfors. 1997. Brain-derived neurotrophic factor, neurotrophin-3, and neurotrophin-4 complement and cooperate with each other sequentially during visceral neuron development. J. Neurosci. 17:8667–8675.

ElShamy, W. M., S. Linnarsson, K.-F. Lee, R. Jaenisch, and P. Ernfors. 1996. Prenatal and postnatal requirements of NT-3 for sympathetic neuroblast survival and innervation of specific targets. Development 122:491–500.

Enemar, A., and B. Falck. 1965. Observations on the appearance of norepinephrine in the sympathetic nervous system of the chick embryo. Dev. Biol. 11:268–283.

Enomoto, H., P. A. Crawford, A. Gorodinsky, R. O. Heuckeroth, E. M. Johnson, Jr., and J. Milbrandt. 2001. RET signaling is essential for migration, axonal growth and axon guidance of developing sympathetic neurons. Development 128:3963–3974.

Ernsberger, U., H. Patzke, J. P. Tissier-Seta, T. Reh, C. Goridis, and H. Rohrer. 1995. The expression of tyrosine hydroxylase and the transcription factors *cPhox-2* and *Cash-1*: evidence for distinct inductive steps in the differentiation of chick sympathetic precursor cells. Mech. Dev. 52:125–136.

Ernsberger, U., E. Reissmann, I. Mason, and H. Rohrer. 2000. The expression of dopamine beta-hydroxylase, tyrosine hydroxylase, and *Phox2* transcription factors in sympathetic neurons: evidence for common regulation during noradrenergic induction and diverging regulation later in development. Mech. Dev. 92:169–177.

Evans, C., S. Baxi, R. Neff, P. Venkatesan, and D. Mendelowitz. 2003. Synaptic activation of cardiac vagal neurons by capsaicin sensitive and insensitive sensory neurons. Brain Res. 979:210–215.

Fagan, A. M., H. Zhang, S. Landis, R. J. Smeyne, I. Silos-Santiago, and M. Barbacid. 1996. TrkA, but not TrkC, receptors are essential for survival of sympathetic neurons in vivo. J. Neurosci. 16:6208–6218.

Fernhall, B., and M. Otterstetter. 2003. Attenuated responses to sympathoexcitation in individuals with Down syndrome. J. Appl. Physiol. 94:2158–2165.

Forgie, A., F. Kuehnel, S. Wyatt, and A. M. Davies. 2000. In vivo survival requirement of a subset of nodose ganglion neurons for nerve growth factor. Eur. J. Neurosci. 12:670–676.

Francis, N. J., and S. C. Landis. 1999. Cellular and molecular determinants of sympathetic neuron development. Annu. Rev. Neurosci. 22:541–566.

Gabella, G. 1976. Structure of the Autonomic Nervous System. New York: John Wiley & Sons.

Garson, A. J., J. T. Bricker, and D. G. McNamara. 1990. The Science and Practice of Pediatric Cardiology. Philadelphia: Lea & Febiger.

Gatti, P. J., T. A. Johnson, I. K. Jordan, W. Coleman, and V. J. Massari. 1995. The physiological and anatomical demonstration of functionally selective parasympathetic ganglia located in discrete fat pads on the feline myocardium. J. Auton. Nerv. Syst. 51:255–259.

Goldstein, R. S., and C. Kalcheim. 1991. Normal segmentation and size of the primary sympathetic ganglia depend upon the alternation of rostrocaudal properties of the somites. Development 112:327–334.

Gordon, L., J. M. Polak, G. J. Moscoso, A. Smith, D. M. Kuhn, and J. Wharton. 1993. Development of the peptidergic innervation of human heart. J. Anat. 183:131–140.

Groves, A. K., K. M. George, J.-P. Tissier-Seta, J. D. Engel, J.-F. Brunet, and D. J. Anderson. 1995. Differential regulation of transcription factor gene expression and phenotypic markers in developing sympathetic neurons. Development 121:887–901.

Guillemot, F., L.-C. Lo, J. E. Johnson, A. Auerbach, D. J. Anderson, and A. L. Joyner. 1993. Mammalian *achaete-scute* homolog 1 is required for the early development of olfactory and autonomic neurons. Cell 75:463–476.

Hall, A. K., and S. E. MacPhedran. 1995. Multiple mechanisms regulate sympathetic neuronal phenotype. Development 121:2361–2371.

Harrison, T. A., H. A. Stadt, and M. L. Kirby. 1994. Developmental characteristics of the chick nodose ganglion. Dev. Neurosci. 16:67–73.

Hassankhani, A., M. E. Steinhelper, M. H. Soonpaa, E. B. Katz, D. A. Taylor, A. Andrade-Rozental, S. M. Factor, J. J. Steinberg, L. J. Field, and H. J. Federoff. 1995. Overexpression of NGF within the heart of transgenic mice causes hyperinnervation, cardiac enlargement, and hyperplasia of ectopic cells. Dev. Biol. 169:309–321.

Higgins, D. 1983. The ontogeny of the response of the avian embryo heart to autonomic neurotransmitters and to neurotransmitter-like drugs. Pharmacol. Ther. 20:53–77.

Hilz, M. J., E. H. Kolodny, I. Neuner, B. Stemper, and F. B. Axelrod. 1998. Highly abnormal thermotests in familial dysautonomia suggest increased cardiac autonomic risk. J. Neurol. Neurosurg. Psychiatry 65:338–343.

Hilz, M. J., B. Stemper, P. Sauer, U. Haertl, W. Singer, and F. B. Axelrod. 1999. Cold face test demonstrates parasympathetic cardiac dysfunction in familial dysautonomia. Am. J. Physiol. 276:R1833–1839.

Hofman, P. L., K. Hiatt, M. C. Yoder, and S. A. Rivkees. 1997. A1 adenosine receptors potently regulate heart rate in mammalian embryos. Am. J. Physiol. 273:R1374–1380.

Hopkins, D. A., P. M. Gootman, N. Gootman, S. M. Di Russo, and M. E. Zeballos. 1984. Brainstem cells of origin of the cervical vagus and cardiopulmonary nerves in the neonatal pig (*Sus scrofa*). Brain Res. 306:63–72.

Horackova, M., and J. A. Armour. 1995. Role of peripheral autonomic neurons in maintaining adequate cardiac function. Cardiovasc. Res. 30:326–335.

Horackova, M., J. Slavikova, and Z. Byczko. 2000. Postnatal development of the rat intrinsic cardiac nervous system: a confocal laser scanning microscopy study in whole-mount atria. Tissue Cell 32:377–388.

Hua, F., B. A. Ricketts, A. Reifsteck, J. L. Ardell, and C. A. Williams. 2004. Myocardial ischemia induces the release of substance P from cardiac afferent neurons in rat thoracic spinal cord. Am. J. Physiol. 286:H1654–1664.

Huber, K., B. Bruhl, F. Guillemot, E. N. Olson, U. Ernsberger, and K. Unsicker. 2002. Development of chromaffin cells depends on MASH1 function. Development 129:4729–4738.

Jackson, D. A., and N. M. Nathanson. 1995. Subtype-specific regulation of muscarinic receptor expression and function by heterologous receptor activation. J. Biol. Chem. 270:22374–22377.

Janes, R. D., J. C. Brandys, D. A. Hopkins, D. E. Johnstone, D. A. Murphy, and J. A. Armour. 1986. Anatomy of human extrinsic cardiac nerves and ganglia. Am. J. Cardiol. 57:199–309.

Kahn, A., T. Sawaguchi, A. Sawaguchi, J. Groswasser, P. Franco, S. Scaillet, I. Kelmanson, and B. Dan. 2002. Sudden infant deaths: from epidemiology to physiology. Forensic Sci. Int. 130 Suppl:S8–20.

Keating, M. T., and M. C. Sanguinetti. 1996. Molecular genetics insights into cardiovascular disease. Science 272:681–685.

Kern, M. J., E. A. Argao, and S. S. Potter. 1995. Homeobox genes and heart development. Trends Cardiovasc. Med. 5:47–54.

King, T. S., and J. B. Coakley. 1958. The intrinsic nerve cells of the cardiac atria of mammals and man. J. Anat. 92:353–376.

Kirby, M. L. 1988. Nodose placode contributes autonomic neurons to the heart in the absence of cardiac neural crest. J. Neurosci. 8:1089–1095.

Kirby, M. L. 1993. Cellular and molecular contributions of the cardiac neural crest to cardiovascular development. Trends Cardiovasc. Med. 3:18–23.

Kirby, M. L., D. C. Conrad, and D. E. Stewart. 1987. Increase in the cholinergic cardiac plexus in sympathetically aneural hearts. Cell Tissue Res. 247:489–496.

Kirby, M. L., T. L. Creazzo, and J. L. Christiansen. 1989. Chronotropic responses of chick hearts to field stimulation following various neural crest ablations. Circ. Res. 65:1547–1554.

Kirby, M. L., T. F. Gale, and D. E. Stewart. 1983. Neural crest cells contribute to aorticopulmonary septation. Science 220:1059–1061.

Kirby, M. L., and S. A. Gilmore. 1976. A correlative histofluorescence and light microscopic study of the formation of the sympathetic trunks in chick embryos. Anat. Rec. 186:437–450.

Kirby, M. L., J. W. McKenzie, and T. A. Weidman. 1980. Developing innervation of the chick heart: a histofluorescence and light microscopic study of sympathetic innervation. Anat. Rec. 196:333–340.

Kirby, M. L., and D. E. Stewart. 1983. Neural crest origin of cardiac ganglion cells in the chick embryo: identification and extirpation. Dev. Biol. 97:433–443.

Kirby, M. L., and D. E. Stewart. 1986. Development of the ANS innervation to the avian heart. In: Developmental Neurobiology of the Autonomic Nervous System., ed. Gootman, P., 135–158. Clifton, NJ: Humana Press.

Kirby, M. L., T. A. Weidman, and J. W. McKenzie. 1980. An ultrastructural study of the cardiac ganglia in the bulbar plexus of the developing chick heart. Dev. Neurosci. 3:174–184.

Kloberg, A. J., and R. Fritsche. 2002. Catecholamines are present in larval *Xenopus laevis*: a potential source for cardiac control. J. Exp. Zool. 292:293–303.

Korsch, E., J. Steinkuhle, M. Massin, S. Lyonnet, and R. L. Touraine. 2001. Impaired autonomic control of the heart by *SOX10* mutation. Eur. J. Pediatr. 160:68–69.

Kotzbauer, P. T., P. A. Lampe, R. O. Heuckeroth, J. P. Golden, D. J. Creedon, E. M. Johnson, Jr., and J. Milbrandt. 1996. Neurturin, a relative of glial-cell-line-derived neurotrophic factor. Nature 384:467–470.

Kralios, F. A., N. Cluff, F. L. Anderson, G. R. Hanson, and A. C. Kralios. 1999. Postnatal development of peptidergic innervation of the canine heart. J. Mol. Cell. Cardiol. 31:215–225.

Kralios, F. A., and C. K. Millar. 1978. Functional developmental of cardiac sympathetic nerves in newborn dogs: evidence for asymmetrical development. Cardiovasc. Res. 12:547–554.

Kuncova, J., and J. Slavikova. 2000. Vasoactive intestinal polypeptide and calcitonin gene-related peptide in the developing rat heart atria. Auton. Neurosci. 83:58–65.

Kuntz, A. 1934. Autonomic Nervous System. Philadelphia: Lea & Febiger.

Lin, L. F., D. H. Doherty, J. D. Lile, S. Bektesh, and F. Collins. 1993. GDNF: a glial cell line-derived neurotrophic factor for midbrain dopaminergic neurons. Science 260:1130–1132.

Liu, W., K. Yasui, A. Arai, K. Kamiya, J. Cheng, I. Kodama, and J. Toyama. 1999. Beta-adrenergic modulation of L-type Ca^{2+}-channel currents in early-stage embryonic mouse heart. Am. J. Physiol. 276:H608–613.

Lu, J. T., Y. J. Son, J. Lee, T. L. Jetton, M. Shiota, L. Moscoso, K. D. Niswender, A. D. Loewy, M. A. Magnuson, J. R. Sanes, and R. B. Emeson. 1999. Mice lacking alpha-calcitonin gene-related peptide exhibit normal cardiovascular regulation and neuromuscular development. Mol. Cell. Neurosci. 14:99–120.

Macchi, V., R. Snenghi, R. De Caro, and A. Parenti. 2002. Monolateral hypoplasia of the motor vagal nuclei in a case of sudden infant death syndrome. J. Anat. 200:195–198.

Markham, J. A., and J. E. Vaughn. 1991. Migration patterns of sympathetic preganglionic neurons in embryonic rat spinal cord. J. Neurobiol. 22:811–822.

McLeod, J. G., and R. R. Tuck. 1987. Disorders of the autonomic nervous system: Part 1. Pathophysiology and clinical features. Ann. Neurol. 21:419–430.

McMahan, U. J., and D. Purves. 1976. Visual identification of two kinds of nerve cells and their synaptic contacts in a living autonomic ganglion of the mudpuppy (*Necturus maculosus*). J. Physiol. 254:405–425.

Merrill, D. C., J. L. Segar, O. J. McWeeny, and J. E. Robillard. 1999. Sympathetic responses to cardiopulmonary vagal afferent stimulation during development. Am. J. Physiol. 277:H1311–1316.

Milbrandt, J., F. J. de Sauvage, T. J. Fahrner, R. H. Baloh, M. L. Leitner, M. G. Tansey, P. A. Lampe, R. O. Heuckeroth, P. T. Kotzbauer, K. S. Simburger, J. P. Golden, J. A. Davies, R. Vejsada, A. C. Kato, M. Hynes, D. Sherman, M. Nishimura, L. C. Wang, R. Vandlen, B. Moffat, R. D. Klein, K. Poulsen, C. Gray, A. Garces, E. M. Johnson, Jr., et al. 1998. Persephin, a novel neurotrophic factor related to GDNF and neurturin. Neuron 20:245–253.

Mitchell, G. A. G. 1956. Cardiovascular Innervation. Edinburgh: E & S Livingstone.

Mitchell, G. A. G., R. Brown, and F. B. Cookson. 1953. Ventricular nerve cells in mammals. Nature 172:812.

Molenaar, W. M., V. M. Lee, and J. Q. Trojanowski. 1990. Early fetal acquisition of the chromaffin and neuronal immunophenotype by human adrenal medullary cells. An immunohistological study using monoclonal antibodies to chromogranin A, synaptophysin, tyrosine hydroxylase, and neuronal cytoskeletal proteins. Exp. Neurol. 108:1–9.

Montero, J. A., B. Giron, H. Arrechedera, Y. C. Cheng, P. Scotting, J. Chimal-Monroy, J. A. Garcia-Porrero, and J. M. Hurle. 2002. Expression of *Sox8, Sox9* and *Sox10* in the developing valves and autonomic nerves of the embryonic heart. Mech. Dev. 118: 199–202.

Moravec, J., and M. Moravec. 1987. Intrinsic nerve plexus of mammalian heart: morphological basic of cardiac rhythmic activity. Int. Rev. Cytol. 106:89–148.

Moravec, M., A. Courtalon, and J. Moravec. 1986. Intrinsic neurosecretory neurons of the rat atrioventricular junction: possibility of local neuromuscular feed back loops. J. Mol. Cell. Cardiol. 18:357–367.

Mulder, A. L., J. M. Golde, A. A. Goor, D. A. Giussani, and C. E. Blanco. 2000. Developmental changes in plasma catecholamine

concentrations during normoxia and acute hypoxia in the chick embryo. J. Physiol. 527 Pt 3:593–599.

Mulder, G. B., N. Manley, J. Grant, K. Schmidt, W. P. Zeng, C. Eckhoff, and L. Maggio-Price. 2000. Effects of excess vitamin A on development of cranial neural crest-derived structures: a neonatal and embryologic study. Teratology 62:214–226.

Nyquist-Battie, C., P. K. Cochran, S. A. Sands, and B. M. Chronwall. 1994. Development of neuropeptide Y and tyrosine hydroxylase immunoreactive innervation in postnatal rat heart. Peptides 15:1461–1469.

Olah, M. E., and G. L. Stiles. 1995. Adenosine receptor subtypes: characterization and therapeutic regulation. Annu. Rev. Pharmacol. Toxicol. 35:581–606.

Palmiter, R. D., J. C. Erickson, G. Hollopeter, S. C. Baraban, and M. W. Schwartz. 1998. Life without neuropeptide Y. Recent Prog. Horm. Res. 53:163–199.

Papka, R. E. 1976. Studies of cardiac ganglia in pre- and postnatal rabbits. Cell Tissue Res. 175:17–35.

Papp, J. G. 1988. Autonomic response and neurohumoral control in the human early antenatal heart. Basic Res. Cardiol. 83:2–9.

Pappano, A. J. 1977. Ontogenetic development of autonomic neuroeffector transmission and transmitter reactivity in embryonic and fetal hearts. Pharmacol. Rev. 29:3–33.

Pappano, A. J., P. M. Hartigan, and M. D. Coutu. 1982. Acetylcholine inhibits positive inotropic effect of cholera toxin in ventricular muscle. Am. J. Physiol. 243:H434-441.

Pattyn, A., X. Morin, H. Cremer, C. Goridis, and J. F. Brunet. 1997. Expression and interactions of the two closely related homeobox genes *Phox2a* and *Phox2b* during neurogenesis. Development 124:4065–4075.

Pattyn, A., X. Morin, H. Cremer, C. Goridis, and J. F. Brunet. 1999. The homeobox gene *Phox2b* is essential for the development of autonomic neural crest derivatives. Nature 399:366–370.

Pelleg, A., and L. Belardinelli. 1993. Cardiac electrophysiology and pharmacology of adenosine: basic and clinical aspects. Cardiovasc. Res. 27:54–61.

Phelps, P. E., R. P. Barber, and J. E. Vaughn. 1991. Embryonic development of choline acetyltransferase in thoracic spinal motor neurons: somatic and autonomic neurons may be derived from a common cellular group. J. Comp. Neurol. 307:77–86.

Pons, J., E. W. Lee, L. Li, and J. Kitlinska. 2004. Neuropeptide Y: multiple receptors and multiple roles in cardiovascular diseases. Curr. Opin. Invest. Drugs 5:957–962.

Portbury, A. L., R. Chandra, M. Groelle, M. K. McMillian, A. Elias, J. R. Herlong, M. Rios, S. Roffler-Tarlov, and D. M. Chikaraishi. 2003. Catecholamines act via a beta-adrenergic receptor to maintain fetal heart rate and survival. Am. J. Physiol. 284: H2069–2077.

Porter, A. C., S. P. Svensson, W. D. Stamer, J. J. Bahl, J. G. Richman, and J. W. Regan. 2003. Alpha-2 adrenergic receptors stimulate actin organization in developing fetal rat cardiac myocytes. Life Sci. 72:1455–1466.

Porter, G. A., Jr., and S. A. Rivkees. 2001. Ontogeny of humoral heart rate regulation in the embryonic mouse. Am. J. Physiol. 281: R401–407.

Protas, L., A. Barbuti, J. Qu, V. O. Rybin, R. D. Palmiter, S. F. Steinberg, and R. B. Robinson. 2003. Neuropeptide Y is an essential in vivo developmental regulator of cardiac ICa,L. Circ. Res. 93:972–979.

Qu, J., and R. B. Robinson. 2004. Cardiac ion channel expression and regulation: the role of innervation. J. Mol. Cell. Cardiol. 37:439–448.

Rinaman, L., and P. Levitt. 1993. Establishment of vagal sensorimotor circuits during fetal development in rats. J. Neurobiol. 24: 641–659.

Rios, R., A. Stolfi, P. H. Campbell, and A. S. Pickoff. 1996. Postnatal development of the putative neuropeptide-Y-mediated sympathetic–parasympathetic autonomic interaction. Cardiovasc. Res. 31 Spec No: E96–103.

Roberts, L. A., G. R. Slocum, and D. A. Riley. 1989. Morphological study of the innervation pattern of the rabbit sinoatrial node. Am. J. Anat. 185:74–88.

Robinson, R. B. 1996. Autonomic receptor—effector coupling during post-natal development. Cardiovasc. Res. 31 Spec. No:E68–76.

Rongen, G. A., J. S. Floras, J. W. Lenders, T. Thien, and P. Smits. 1997. Cardiovascular pharmacology of purines. Clin. Sci. (Lond) 92:13–24.

Sanchez-Montesinos, I., J. A. Merida-Velasco, J. Espin-Ferra, and L. Scopsi. 1996. Development of the sympathoadrenal system in the chick embryo: an immunocytochemical study with antibodies to pan-neuroendocrine markers, catecholamine-synthesizing enzymes, proprotein-processing enzymes, and neuropeptides. Anat. Rec. 245:94–101.

Sato, H. 1954. Innervation of the heart dog. Tohoku J. Exp. Med. 39:343–356.

Satoh, E., T. Yanagisawa, and N. Taira. 1990. Specific antagonism by glibenclamide of negative inotropic effects of potassium channel openers in canine atrial muscle. Jpn. J. Pharmacol. 54: 133–141.

Sawa, R., H. Asakura, and G. G. Power. 1991. Changes in plasma adenosine during simulated birth of fetal sheep. J. Appl. Physiol. 70:1524–1528.

Schneider, C., H. Wicht, J. Enderich, M. Wegner, and H. Rohrer. 1999. Bone morphogenetic proteins are required in vivo for the generation of sympathetic neurons. Neuron 24:861–870.

Schober, A., K. Krieglstein, and K. Unsicker. 2000. Molecular cues for the development of adrenal chromaffin cells and their preganglionic innervation. Eur. J. Clin. Invest. 30 (Suppl 3):87–90.

Selyanko, A. A. 1992. Membrane properties and firing characteristics of rat cardiac neurons in vitro. J. Auton. Nerv. Syst. 39:181–189.

Shah, N. M., A. K. Groves, and D. J. Anderson. 1996. Alternative neural crest cell fates are instructively promoted by TGFb superfamily members. Cell 85:331–343.

Shah, N. M., M. A. Marchionni, I. Isaacs, P. Stroobant, and D. J. Anderson. 1994. Glial growth factor restricts mammalian neural crest stem cells to a glial fate. Cell 77:349–360.

Shoba, T., S. T. Dheen, and S. S. Tay. 2002. Retinoic acid influences *Phox2* expression of cardiac ganglionic cells in the developing rat heart. Neurosci. Lett. 321:41–44.

Shoba, T., and S. S. W. Tay. 2000. Nitrergic and peptidergic innervation in the developing rat heart. Anat. Embryol. (Berl.) 201:491–500.

Shvalev, V. N., and A. A. Sosunov. 1989. Electron microscopic study of cardiac ganglia in human fetuses. J. Auton. Nerv. Syst. 26:1–9.

Slaugenhaupt, S. A., A. Blumenfeld, S. P. Gill, M. Leyne, J. Mull, M. P. Cuajungco, C. B. Liebert, B. Chadwick, M. Idelson, L. Reznik, C. Robbins, I. Makalowska, M. Brownstein, D. Krappmann, C. Scheidereit, C. Maayan, F. B. Axelrod, and J. F. Gusella. 2001. Tissue-specific expression of a splicing mutation in the *IKBKAP* gene causes familial dysautonomia. Am. J. Hum. Genet. 68: 598–605.

Slotkin, T. A., S. E. Lappi, and F. J. Seidler. 1995. Beta-adrenergic control of c-fos expression in fetal and neonatal rat tissues: relationship to

cell differentiation and teratogenesis. Toxicol. Appl. Pharmacol. 133:188–195.

Smith, R. B. 1971. Intrinsic innervation of the avian heart. Acta Anat. (Basel) 79:112–119.

Steel, P. A., E. C. Aromataris, and B. M. Riederer. 1996. Endogenous opioid peptides in parasympathetic, sympathetic and sensory nerves in the guinea-pig heart. Cell Tissue Res. 284:331–339.

Steel, P. A., L. Gibbins, J. L. Morris, and B. Mayer. 1994. Multiple populations of neuropeptides-containing intrinsic neurons in the guinea-pig heart. Neuroscience 62:241–250.

Stern, C. D., K. B. Artinger, and M. Bronner-Fraser. 1991. Tissue interactions affecting the migration and differentiation of neural crest cells in the chick embryo. Development 113:207–216.

Stewart, D. E., and M. L. Kirby. 1985. Endogenous tyrosine hydroxylase activity in the developing chick heart: a possible source of extraneuronal catecholamines. J. Mol. Cell. Cardiol. 17:389–398.

Taxi, J., M. Derer, and A. Domich. 1983. Morphology and histophysiology of SIF cells in the autonomic ganglia. In: Autonomic Ganglia., ed. Elfvin, L. G., New York: John Wiley & Sons.

Tay, S. S. W., and W. C. Wong. 1992. Immunocytochemical localization of substance P-like nerves in the cardiac ganglia of the monkey (*Macaca fascicularis*). J. Anat. 180:239–245.

Tay, S. S. W., W. C. Wong, and E. A. Ling. 1984. An ultrastructural study of the neuronal changes in the ganglia of the monkey (*Macaca fascicularis*) following unilateral vagotomy. J. Anat. 138:67–80.

Taylor, A. A., and B. Marcus. 1990. Interactions of the nervous system and the heart. In: The science and practice of pediatric cardiology. ed. Garson, A. J., J. T. Bricker, and D. G. McNamara, Philadelphia: Lea & Febiger.

Tcheng, K. T. 1951. Innervation of the dog's heart. Am. Heart J. 41:512–524.

Tiveron, M.-C., M.-R. Hirsch, and J.-F. Brunet. 1996. The expression pattern of the transcription factor *Phox2* delineates synaptic pathways of the autonomic nervous system. J. Neurosci. 16:7649–7660.

Tucker, A. L., and J. Linden. 1993. Cloned receptors and cardiovascular responses to adenosine. Cardiovasc. Res. 27:62–67.

Tucker, D. C., and C. H. Gautier. 1990. Role of sympathetic innervation in cardiac development in oculo. Ann. NY Acad. Sci. 588:120–130.

Ursell, P. C., C. L. Ren, and P. Danilo, Jr. 1991. Anatomic distribution of autonomic neural tissue in the developing dog heart: II. Nonadrenergic noncholinergic innervation by calcitonin gene-related peptide-immunoreactive tissue. Anat. Rec. 230:531–538.

van der Heyden, M. A., T. J. Wijnhoven, and T. Opthof. 2005. Molecular aspects of adrenergic modulation of cardiac L-type Ca^{2+} channels. Cardiovasc. Res. 65:28–39.

Vanoli, E., D. Cerati, and R. F. Pedretti. 1998. Autonomic control of heart rate: pharmacological and nonpharmacological modulation. Basic Res. Cardiol. 93 Suppl 1:133–142.

Verberne, M. E., A. C. Gittenberger-de Groot, and R. E. Poelmann. 1998. Lineage and development of the parasympathetic nervous system of the embryonic chick heart. Anat. Embryol. (Berl) 198:171–184.

Vogel, K. S., and J. A. Weston. 1990. The sympathoadrenal lineage in avian embryos. I. Adrenal chromaffin cells lose neuronal traits during embryogenesis. Dev. Biol. 139:1–12.

Waldo, K. L., D. H. Kumiski, and M. L. Kirby. 1994. Association of the cardiac neural crest with development of the coronary arteries in the chick embryo. Anat. Rec. 239:315–331.

Wang, S., and M. L. Kirby. 1995. Expression pattern of chick *achaete-scute* homologue (CASH) associated with mid-embryogenesis (stages 23 to 28). Roux's Arch. Dev. Biol. 205:1–9.

Wang, X., and S. W. Halvorsen. 1998. Reciprocal regulation of ciliary neurotrophic factor receptors and acetylcholine receptors during synaptogenesis in embryonic chick atria. J. Neurosci. 18:7372–7380.

Wetzel, G. T., and J. H. Brown. 1983. Relationships between choline uptake, acetylcholine synthesis and acetylcholine release in isolated rat atria. J. Pharmacol. Exp. Ther. 226:343–348.

Woollard, H. H. 1926. The innervation of the heart. J. Anat. 60:345–373.

Wyatt, S., L. G. Pinon, P. Ernfors, and A. M. Davies. 1997. Sympathetic neuron survival and TrkA expression in NT3-deficient mouse embryos. EMBO J. 16:3115–3123.

Yuan, B.-X., J. L. Ardell, D. A. Hopkins, A. M. Losier, and J. A. Armour. 1994. Gross and microscopic anatomy of the canine intrinsic cardiac nervous system. Anat. Rec. 239:75–87.

Zhang, L. L., and K. W. Ashwell. 2001. The development of cranial nerve and visceral afferents to the nucleus of the solitary tract in the rat. Anat. Embryol. (Berl.) 204:135–151.

Zhang, L. L., and K. W. Ashwell. 2001. Development of the cyto- and chemoarchitectural organization of the rat nucleus of the solitary tract. Anat. Embryol. (Berl.) 203:265–282.

Zhao, Z., and S. A. Rivkees. 2001. Inhibition of cell proliferation in the embryonic myocardium by A1 adenosine receptor activation. Dev. Dyn. 221:194–200.

Zukowska-Grojec, Z., E. Karwatowska-Prokopczuk, W. Rose, J. Rone, S. Movafagh, H. Ji, Y. Yeh, W. T. Chen, H. K. Kleinman, E. Grouzmann, and D. S. Grant. 1998. Neuropeptide Y: a novel angiogenic factor from the sympathetic nerves and endothelium. Circ. Res. 83:187–195.

This page intentionally left blank

14 Co-authored with Fred Schachat

Evolutionary Developmental Biology of the Heart

Our ignorance of the laws of variation is profound. Not in one case out of a hundred can we pretend to assign any reason why this or that part differs, more or less, from the same part in the parents. But whenever we have the means of instituting a comparison, the same laws appear to have acted in producing the lesser differences between varieties of the same species, and the greater differences between species of the same genus—Charles Darwin, Origin of Species, 1859

The evolution of multicellularity and complex body plans in metazoans was accompanied by the simultaneous development of a cardiovascular system to serve cellular nutrition, gas–fluid–ion exchange, and general physiological homeostasis (Opitz and Clark, 2000). Circulatory systems are a requirement for increasing body size. Small creatures obtain nourishment and eliminate waste by diffusion, but as body size increases, circulation is needed for these functions. Because the circulatory system is composed of soft tissue, it is unlikely that we will ever have direct evidence of heart development from the fossil record. Nevertheless, when enough similarities accumulate between even vastly divergent organisms and morphology of the "heart," it is possible to speculate whether the heart arose only once in evolutionary history or multiple times as in the case of photosensitive cells (Gerhart and Kirschner, 1997). Evolutionary developmental biology is focused on discovering how genes and epigenetic factors coordinate development to produce phenotypes. A central concept emerging from comparative studies of developmental genes and their interactions is that genes have been co-opted for different functional roles as evolution proceeds.

Almost all body plans can be broken down into morphological modules, and until the second half of the twentieth century, the evidence for evolution was based on morphological homology of these modules. However, this constrained view of change precludes inclusion of many non-morphological factors including genetic and epigenetic regulation. The advent of the genomic era and elucidation of transcriptional cassettes and signaling pathways that can also be seen as modules allow inclusion of this broadened concept of modules as substrates of evolutionary change. Modular organization allows generation of complexity, developmental robustness, and evolutionary flexibility or evolvability. Modules exist in time and space, and the divergence of modules and replicated modules is an important feature of evolution. Modular development addresses the genetic basis of "EXAPTATION" in which a module that evolves for one adaptive reason is later used for some other role. In the case of genes, they are co-opted not individually but as interacting networks. Co-option of these networks allows formation of new structural or functional modules. This is unlikely to happen on a piecemeal basis, with one gene at a time being co-opted from the original to the new function. If a gene whose product acts at a particular point in an interaction cascade can be expressed at an ectopic location, then the whole cassette downstream would be expressed in the new location too (Arthur, 2002). This chapter addresses whether "hearts" have arisen multiple times in evolution and how the concept of modules can be used to understand increasing complexity in vertebrate heart morphology and function in evolution and development. Chapter 15 will again use the concept of modules to explore how they might underlie the pathogenesis of syndromic traits.

The Unitary Origin Hypothesis

Many factors lean positively toward a unitary origin of the heart. The circulatory systems of most arthropods and many worms are open. They generally consist of a single, open-ended, muscular tube that slowly pumps the interstitial fluid (hemolymph) around the body. *Drosophila*, the fruit fly, has probably been the most thoroughly studied of the invertebrates. The *Drosophila* dorsal vessel is widely considered the genetic and morphological homolog of the vertebrate heart and there are many similarities in development and genetic history. In *Drosophila* the precursor cells of the dorsal vessel are specified from bilateral progenitor fields in the dorsal mesoderm. The cells form two single rows that migrate dorsally along the ectoderm to meet at the midline, where they form a linear vessel (Fig. 14.1). Inductive signals activate distinct combinations of transcriptional regulators needed for

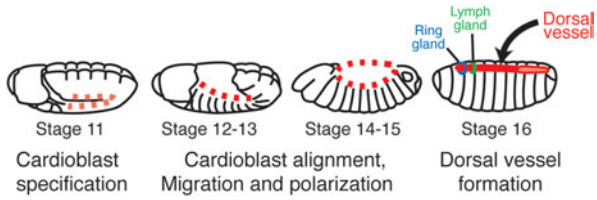

Figure 14.1. Steps in *Drosophila* dorsal vessel (heart) development. Cardioblasts that form the dorsal vessel are shown in red. (Adapted from Cripps and Olson, 2002.)

appropriate cardioblast (considered the myocardial homolog) differentiation. Movement of hemolymph is in a posterior-to-anterior direction similar to that in the vertebrate heart. There is a distinct anterior–posterior polarity in that the posterior region has a large lumen and three pairs of valve-like ostia, and the anterior outflow region has a smaller lumen. The homeodomain-containing transcription factor *tinman* can be replaced by the vertebrate homolog *Nkx2.5*, although *tinman* is essential for differentiation of the cardioblasts while *Nkx2.5* is not required for myocardial cell differentiation. Both cardioblasts and pericardial cells develop from the tinman-positive cardiogenic mesoderm, as do myocardial and pericardial cells in vertebrate heart development. Similar to Nkx2.5, tinman requires at least one partner to generate cardioblasts. Pannier, a Gata family member, is one of these partners, as is D-Mef2. Induction of cardioblasts requires BMP signaling by a family member called Dpp, which induces both tinman and pannier (Sorrentino et al., 2005). The *Drosophila* heart is patterned along the craniocaudal axis by differential gene expression in cardial cells that presage the chamber-specific gene expression observed in vertebrates. For example, ostial cells in the fly that line the inflow of hemolymph into the heart tube specifically express the fly orthologue of Coup-tfII, which is necessary for atrial formation in the mouse.

Similarities can also be found in one of the simplest chordates, *Ciona intestinalis*, commonly known as the sea squirt. It has a heart consisting of a single layered myoepithelial U-shaped tube surrounded by a single layer of pericardial coelom. The initial stages of heart development are similar to those in vertebrate heart development. At the 110-cell stage, the heart lineage is represented by two cells near the vegetal pole. After gastrulation, the heart precursors are four large bilaterally paired cells. These cells migrate ventrally to fuse along the midline and a subset of the cells forms the heart tube (Davidson and Levine, 2003). This story is remarkably similar to that for vertebrates where bilateral fields of mesodermal cells are set aside during and after gastrulation, the cells fuse at the midline, and a subset of them forms a heart tube.

However, a major difference in the *Ciona* myoepithelial tube and *Drosophila* dorsal vessel as compared to the vertebrate heart is the absence of endocardial/endothelial cells to separate the intravascular compartment. These invertebrate "hearts" also lack an epicardium that provides a panoply of cells to all vertebrate hearts.

What is most striking in heart evolution is the contrast between the apparent evolutionary conservation of the genetic regulatory processes and the diversity in construction and form of the heart in evolution (or phylogeny). In its most direct form, the unitary origin hypothesis postulates that the "heart tube" was present in the basal bilaterian (the cenancestor of protostomes and deuterostomes) and that the heart tube contains the functional, morphological, and genetic blueprint that establishes the foundation for the evolution of all deuterostome hearts. In chordates, the argument for a unitary origin is supported by the commonality of position, function—propulsion of a circulatory fluid and the periodic autonomous contractions of heart tubes and hearts—and embryological origin. In its most assertive form, it suggests that the underlying plan for a four-chambered vertebrate heart is present in the four "contractile" segments of the ventral hemal vessel of amphioxus the living descendent of ancestral chordates (Bone et al., 1995).

This construction of the unitary origin hypothesis as applied to chordates necessitates the "discovery" of four cardiac chamber precursors in all chordates and vertebrates. Consequently, in addition to the two-chambered systemic heart of fish, the non-contractile sinus venous and the conus arteriosus are considered heart chambers. The difficulty with this proposition is that it contradicts the functional morphology of *Branchiostoma* and basal fishes, and appears to suggest that evolution is a prescient process (Bone et al., 1995). However, there are less expansive arguments for a unitary origin of the chordate heart that suggest the similarity of the pumping activity of a muscular tube and expression of tinman homologs in primitive heart tubes imply the heart tube specifies the foundation for later patterning and modular additions that led to the evolution of the vertebrate myocardium and its chambers (Fig. 14.3) (Fishman and Olson, 1997).

Although in the absence of either a fossil record or the presence of intermediates in heart evolution, this more restricted argument can be challenged on the basis of retrospective bias, it seems compelling, if it is limited to heart evolution within Chordates.

Clearly, many issues need to be resolved in evaluating the unitary model in respect to chordate heart evolution, but the most immediate are: (1) assessing the likelihood that the basal bilaterian and the basal chordate had "heart tubes" such as those that arise during the development of the vertebrate heart; (2) considering whether the design of successful vascular pumps is substantially constrained; and (3) determining whether there are strict limits on the emergence of additional vascular pumps.

Innovation in the Evolution of the Vertebrate Heart

The nearly universal presence of a propulsive heart tube in PROTOSTOMES and DEUTEROSTOMES coupled with the expression of members of the tinman family of transcription factors

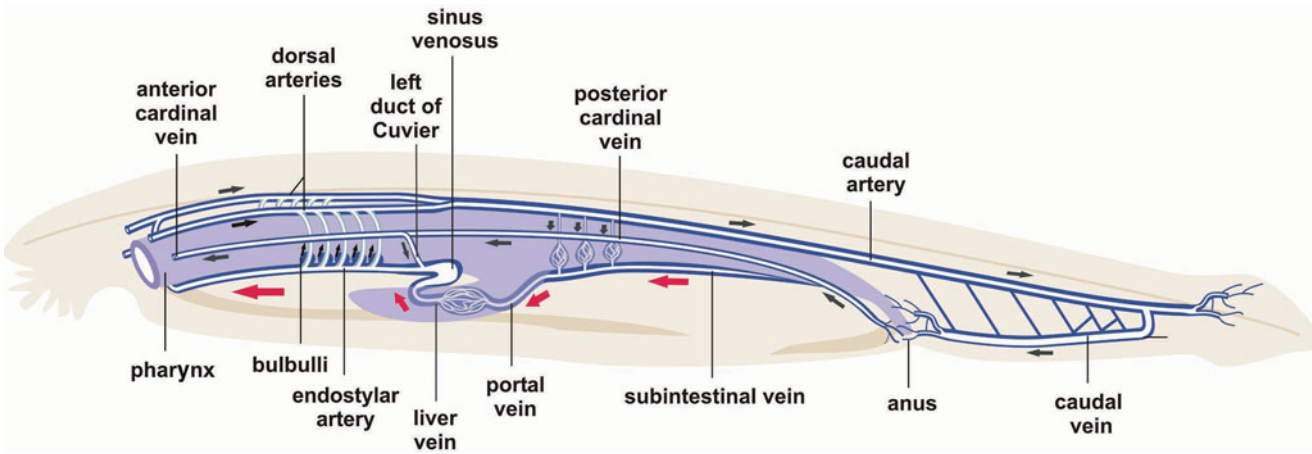

Figure 14.2. The major vessels of *Branchiostoma*. The four contractile ventral vessels proposed for *Branchiostoma*, the subintestinal vein, the portal vein, the liver vein, and the endostylar artery, are shown with *red arrows* indicating the direction of flow. (From Simoes-Costa et al., 2005, with permission.)

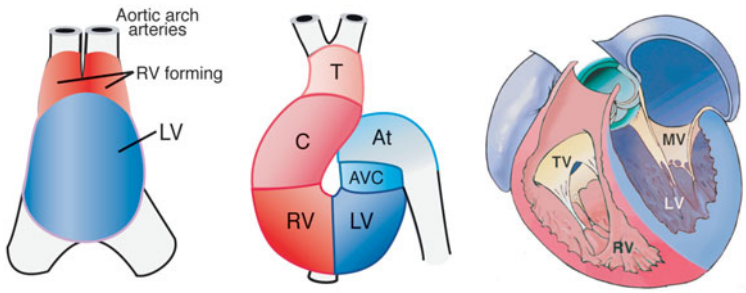

Figure 14.3. The modular evolution of the heart. A suggested pathway for the evolution of the multichambered vertebrate heart by patterning and modular addition to the "primitive" heart tube. LV, left ventricle; RV, right ventricle; At, atrium; AVC, atrioventricular canal; C, conus; T, truncus; TV, tricuspid valve; MV, mitral valve.

during its formation generates strong inferences that (1) the heart tube originated in the cenancestor of protostomes and deuterostomes and (2) the evolutionary transition from heart tube to the multichambered vertebrate heart was the result of adaptive transformations of this "primitive" heart tube. While these inferences seem parsimonious, they may overemphasize morphological and molecular homologies and ignore the likelihood of independent events in the evolution of chordate and vertebrate hearts (Cartmill, 1979; Cracraft, 2005; Gans and Northcutt, 1983). Their emphasis on similarities inferred to be primitive for all protostomes and deuterostomes obscures significant functional, morphological, and developmental differences that are unique to vertebrate hearts. In particular, studies on the descendants of basal chordates and fish suggest that the vertebrate heart is the result of a variety of evolutionary excursions that are not explained by a scenario in which a primitive heart tube undergoes a continuous and progressive series of adaptations to yield the vertebrate four-chambered heart.

If there are vertebrate innovations in the evolution of the heart, they likely include:

1. The origin of endocardium/endothelium and, with it, the evolution of a new mechanism for the generation of a cardiac conducting system.
2. Co-opting the tinman family of transcription factors to specify positional information for the placement or formation of new circulatory pump elements or modules (as Pax6 is universally co-opted as a selector gene in photoreceptor formation).
3. Generation of completely novel vertebrate cardiomyocytes.
4. A change in the role of the initial vertebrate heart tube, which likely was so deeply canalized for its function that a new organ capable of the propulsive circulation characteristic of the multi-chambered vertebrate heart evolved.

Did Either the Basal Bilaterian or the Basal Chordate Have a "Heart Tube"?

The argument for a unitary origin of the heart in chordates is generally based on the assumption that a heart tube was present in the CENANCESTOR of bilaterian, but Erwin and Davidson call this assumption into question (Erwin and Davidson, 2002; Fishman and Olson, 1997). They argue that there is no evidence from either the geological or molecular record to support the claim that the pre-Cambrian cenancestor of protostomes

and deuterostomes possessed a complex circulatory system. Moreover, they propose a solution to the "*pax* conundrum" in which the association of a regulatory gene family with the development of evolutionarily nonhomologous organs is explained by positing that the initial role for such genes was to regulate cell-specific proteins that were utilized in those organs (Davidson, 2001). Thus, in the case of visual systems, the initial role of *pax* genes was not to control the formation of photoreceptor organs themselves, but to regulate photoreceptor pigment expression; and the role of *tinman* genes in heart organogenesis is an elaboration of their initial role in the regulation of contractile protein expression. Thus, both the fossil and molecular evidence leads them to conclude that the heart tube arose independently in different CLADES and is homoplastic.

With respect to chordates, functional morphology and genetic studies suggest that there are difficulties with supposing a unique origin for the "heart tube" even within Chordata. This may not be surprising as Gans and Northcutt suggested that the evolution of a powerful circulatory system was a key innovation—such as the development of the head, neural crest, and gills—in the evolution from BENTHIC chordates to predatory vertebrates (Gans and Northcutt, 1983). In amphioxus, the living chordate descendent of ancestral vertebrates, the tissues that compose the propulsive ventral veins and their development are fundamentally different from those of the vertebrate heart. Instead of an endothelium and a surrounding myocardium composed of striated muscle, there is only a single layer of "myoepithelial" cells that form around lumens that initially traversed a connective tissue extracellular matrix (Rahr, 1981; Stach, 1998). Moreover, despite the image of four contractile ventral vessels in Fig. 14.2, it is likely that most, if not all, of the pulsatile activity of these vessels is the result of contraction of the body or contractile activity in the associated coelomic mesothelium, rather than the independent contractions by the myoepithelial cells that comprise the vessel wall so again, not homologous (Nielsen, 2001; Rahr, 1981; Ruppert, 1997; Stach, 1998). In addition, initial studies on myosin expression in the branchial basket and its associated vessels suggest that a non-muscle myosin, rather than an ancestor of the cardiac-like striated muscle myosins is expressed in these vessels (Schachat, Song, and Park, unpublished data). These observations create difficulties for the unitary origin model of the heart tube that suggest it was intrinsically contractile and with the difference in tissue composition of the putative amphioxus "heart tube," a role for tinman in regulating gene expression that is specific to the heart.

How Many Ways Can a Vascular Pump Evolve?

To understand how many ways a vascular pump can be generated, it is necessary to consider the biomechanical and material constraints on its design. In a biological system, the free energy that drives circulatory flow can arise from net fluid production (such as occurs in spermatogenesis to propel spermatozoa out of the seminiferous tubules), from osmosis (generated by a differential in osmolyte concentration), and from differential pressure (generated by a either ciliary action or contractile activity coupled to elastic recoil).

Critical physical constraints involving dimensionless numbers, such as those that govern the ratio of vessel diameters at sites of bifurcation and the rate of fluid flow to diffusion, are determinative features in circulatory systems (Vogel, 2003; Vogel and Calvert, 1992). Perhaps the simplest example of such a constraint is the use of tubular vessels with circular cross sections to minimize the ratio of vessel surface area to volume and wall turbulence. Because either ciliary motion or muscle contraction can be used to generate differential pressure in biological systems, and ciliary action is inconsistent with minimizing turbulence in a high flow system, the successful biological design for a system of blood circulatory vessels seems to involve a muscular pump, or as described for amphioxus, a vessel that is mechanically linked to an external contractile pump.

Is It Difficult for Vascular Pumps to Evolve in Chordates?

This question is best answered by considering the functional morphology and diversity of chordate circulatory systems. The observations on *Branchiostoma*, as well as Erwin and Davidson's argument for independent evolution of the heart tube in all phyla, argue strongly that hearts have evolved independently (and are therefore not phylogenetically homologous) in all metazoan phyla and perhaps even within the phylum Chordata (Erwin and Davidson, 2002). In all cases, the design of these hearts is constrained by both biomechanics and the biological substrates available for their construction. But examination of the diversity of "auxiliary" hearts in chordates and the basal fish indicate that these constraints do not require a unitary origin for vascular pumps, a single mechanism for their emergence, or even a prolonged dependence on some "primitive" form of a heart tube within a phylum. New hearts (and multiple hearts) evolved in response to changing selective pressures. The evolution of these multiple hearts enabled biological systems to explore the fitness landscape of coordinated gene expression, regulation, and tissue organization consistent with the biological and biophysical constraints on heart design.

The Hearts of Hagfish

The circulatory system of the hagfish *Myxine glutinosa* exemplifies the diversity and complexity of basal chordate and fish circulatory pumps. *Myxine* possess a two-chambered branchial or systemic heart and three or four auxiliary hearts (Fig. 14.2).

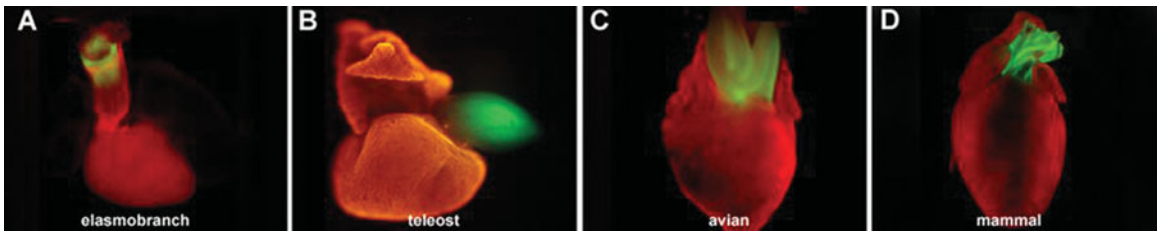

Figure 14.4. Conserved development of the arterial pole shown by a nitric oxide indicator DAF-2DA that identifies the smooth muscle (green) immediately distal to the myocardium at the arterial pole in all vertebrates examined. Myocardium is stained with MF20 (*red*).

The multiplicity of hearts is physiologically essential because the hagfish has an exceptionally low pressure circulatory system, and it uses the series of in-line auxiliary vascular pumps to boost blood pressure. The two chambered branchial heart propels blood to the ventral aorta and, via lateral branches of the aorta, to the gill pouches at low pressure to avoid damaging the extensive and delicate capillary network responsible for respiratory gas exchange. In the gill pouches, blood flow is boosted prior to its entry into the systemic circulation by the periodic contraction of two layers of extrinsic striated muscle that surround each gill pouch. Following passage of blood through the cranial vessels, blood pressure is boosted by the action of the cardinal heart, which like the gill hearts is composed of extrinsic striated muscle, to propel it through the inferior jugular and cardinal veins. The third auxiliary heart system is the caudal heart, which is similar to the caudal hearts of teleosts. The caudal heart is composed of two sacs, separated by a median caudal cartilage. Each of the chambers is compressed by a thin sheet of muscle that is attached to the fin skeleton and distinct from the myomeric muscle. When one chamber of the caudal heart is compressed, blood is propelled across a semilunar valve (to prevent retrograde flow) into the caudal vein; and the other chamber expands drawing in blood from the subcutaneous sinus. Although the caudal heart is composed of striated muscle, like the gill and cardinal hearts, the muscle is not extrinsic to the circulatory system. Rather it is activated by spinal motor nerves when the hagfish is at rest, and inactive when the fish is swimming and contractions of the myomeric muscle are sufficient to propel the caudal circulation. The final pump in series is the single-chambered portal heart that is composed of autonomously beating cardiac muscle that propels blood through the hepatic portal network and on to the sinus venous of the systemic heart.

There are several interesting aspects of this primitive circulatory system: first, the two aneural autonomously beating hearts (the branchial and portal hearts) are in close proximity, suggesting that autonomously beating hearts may be restricted to a ventral branchial location where more derived vertebrate hearts develop. The location of these cardiac muscle pumps may reflect the positional expression of tinman. In addition, the single-chambered aneural portal heart shows that hearts composed of "true" cardiomyocytes did not need to have multiple chambers.

Second, the atrium of the branchial heart appears to be an evagination of the ventricle that generates an atrial chamber that is unlike most atria because it is neither thinner walled nor smaller than the ventricle, though it does initiate the heart beat. Thus, the hagfish atrium may not have arisen in the same way that modern atria do.

Third, with regard to the speculation that auxiliary hearts were evolutionary excursions that enabled novel gene combinations to be explored for use in cardiac function, the myosin heavy chain expressed in the atria and ventricle of the systemic heart and that of the caudal heart appears to be identical and homologous with vertebrate slow/cardiac myosins, while the myosin heavy chain in the gills is homologous with the striated muscle myosin expressed in vertebrate jaw muscle (Schachat, Song, Long, and Koob, unpublished data).

In conclusion, it appears that the development of vascular pumps occurs in response to physiological demand, though hearts with "true" myocardial cells may only develop in a ventral branchial location.

Hearts in Skates

Skates are elasmobranchs, a clade composed of the living descendants of the most basal vertebrates, and their circulatory system, like that of the hagfish, is informative with regard to the evolution of the vertebrate cardiovascular system. They possess a two-chambered systemic heart, as well as a caudal heart, and during embryonic development, before the caudal heart appears, they use a specialized tail pump appendage that propels sea water to perfuse the encased embryo with oxygen (Long and Koob, 1997; Zimmer, 1999).

The embryonic tail pump appendage is the only part of the myomeric muscle that expresses a myosin heavy chain homologous to the vertebrate slow/cardiac myosin. This slow/cardiac myosin heavy chain isoform is also expressed in adult atrium. But the ventricle expresses an entirely different myosin heavy chain that is homologous to the vertebrate "slow-tonic" myosin heavy chain, which is found only in skate extraocular muscle (Schachat, Song, Long, and Koob, unpublished data).

Lastly, the hearts of skates, like those of other elasmobranchs, Chimaeriformes, and primitive bony fish, possess a vessel, the conus arteriosus, that conducts blood from the ventricle to the aorta. The conus is an awkward outflow vessel,

comprised of an elastic fibrous connective tissue surrounded by what has been described as cardiac muscle, with three internal valves that act to prevent retrograde flow. The reason for the redundancy of the valves is unclear, and its muscular wall does not appear to contribute significantly to blood flow following ventricular systole (Satchell, 1991). Because the conus arteriosus is not present in more derived bony fish, it has been considered a region of a primitive heart that is lost in evolution, but its complex structure is highly suggestive of the kind of initial adaptations that might have been selected for in the evolution of a primitive "heart tube" to a more powerful heart (Satchell, 1991). The surrounding cardiac muscle would have provided more propulsive force than the kind of contractile cells associated with the amphioxus contractile vessels; the slightly rigid elastic wall would have provided for elastic recoil following a systolic contraction; and the valves would have prevented retrograde flow. These features, coupled with the incorporation of the conus arteriosus into the ventricle, lead to the inference that this highly canalized structure may have been the endpoint in experiment in heart design that was unable to meet the circulatory demands of predatory vertebrates that required the emergence of a multichambered heart. If this speculation is correct, vertebrate evolution required a successor to the "heart tube" that likely drew on the selective excursions of auxiliary hearts to generate new combinations of contractile proteins, organized into new genetic modules that provided a selective advantage for the pump that now drives vertebrate circulatory systems.

The Vertebrate Dilemma: How to Evolve a Four-Chambered Heart from a Tube Invested in Myocardium

The speculation so far has landed us on the side of the uniqueness (non-homology) of the vertebrate heart, which first appears as a myocardium-covered endothelial tube in elasmobranchs. The problem then becomes to allow the flexibility for this simple tube to respond to the progressively urgent demands of altering a gill-breathing animal to a land animal with lungs and the requirement for a partially divided circulation, and finally from a ectothermic or cold-blooded (fish, amphibians, reptiles) to a endothermic or warm-blooded (birds and mammals) animal, requiring a four-chambered heart with fully divided pulmonary and systemic circulations. The most likely substrate for this transition is modules.

Modules

The modular construction of the vertebrate heart may play a major role in its adaptive evolution from a two-chambered to a four-chambered heart. Wagner and Mezey have defined three different types of modules: developmental, genetic process, and variational modules (Wagner and Mezey, 2003). A developmental module is a semi-autonomous part of the embryo that can form all or mostly outside its normal context. This type of developmental autonomy allows for temporal dissociation or heterochrony between different body parts. It also allows deployment of the same developmental module in different parts of the body or organ, or heterotopy. Genetic process modules are genetic networks used in different developmental contexts. These modules are also context insensitive. However, while developmental modules work at the multicellular level, genetic process modules use subcellular molecular machines. This makes them functionally individualized. Variational modules are based on the relationship between genetic variation and phenotypic variation, that is, specification of which genetic differences give rise to which phenotypes. The evolutionary importance of variational modules is in their relation to patterns of natural selection and their response to selection. These modules act as independent units of phenotypic evolution. For discussing the evolutionary developmental biology of the heart, we will define the following modules: (1) developmental modules include the morphological modules that comprise the various defined regions and chambers, cell lineage modules, and functional modules; (2) genetic process modules include transcriptional and signaling modules; and (3) variational modules include changes in gene expression and transcriptional targets in hearts from a variety of species.

It is possible to think of modules as existing at several levels in the developing heart, from the whole organ to combinations of its constituent chambers and developmental parts. Once the heart tube forms, it is attached to the body only at the inflow and outflow regions, with the body of the tube developing relatively independently of other structures. Thus, much of the growth and morphogenesis of the heart is in an environment of its own making and physically separated from the main body axis. However, limiting our consideration of modules to the morphological might detract from a wider consideration of the modular nature of other features that are equally important in understanding the evolutionary developmental history of the heart.

Morphological Modules

Morphological modules build on concepts such as "morphogenetic field" (Nelson, 2004). In development of a module, the first step is to establish the boundaries of the module, next the identity of the module, and finally the polarity of the module (Carroll, 2005). The module is then subdivided into submodules which are in turn divided again into submodules. For example, establishing the segments in *Drosophila* first requires the delimitation of parasegments. This is done using gradients of transcriptional regulators that define poles and axes. The gradients allow finer and finer definition of the anterior–posterior and dorsoventral coordinates. These coordinates lead to expression of transcriptional regulators that define the

identity of the module. The parasegments recombine to form definitive segments.

A similar series of steps can be envisioned in development of the heart. First, the heart field is established in the splanchnic mesoderm based on translation of the body axes: craniocaudal, dorsoventral and right–left polarity. As the heart field is converted into a semi-autonomous heart tube new polarities are established that allow subcompartmentalization within the heart tube into new modules. While the craniocaudal axis of the body remains the craniocaudal axis of the heart tube, the dorsoventral and right–left body axes are reinterpreted in the heart tube as right–left and dorsoventral, respectively. The initial modules in the heart tube are the inflow limb and outflow limbs which are created by looping. The inflow limb becomes subdivided into atrium, atrioventricular canal, and left ventricle while the outflow limb is subdivided into right ventricle and conotruncus. Finally, the left and right atria and ventricles are established as modules. Within the ventricles the myocardium is divided into trabeculae and compact myocardium and the conduction myocardium is distinguished from the working myocardium. Each of these new morphological units represents a module, and thus, modular morphological development in the heart represents successive subdivisions to delineate the definitive modules of the heart. Morphological evolution can affect development of the "field" module or any of the ensuing submodules independently without necessarily affecting the whole organism or organ.

The outflow tract is divided into systemic and pulmonary circuits by septation, which depends on a co-opted extracardiac population of cells from the neural crest (Kirby et al., 1983). In addition to the physical process of septation, a new problem arises with the divided outflow tract, which is to align the outflow vessels with the appropriate ventricles. To do this the outflow tract shortens and rotates in order to bring the aorta into its correct alignment with the left ventricular outflow and the pulmonary trunk in correct alignment with the right ventricular outflow. Elimination of specific foci of myocytes in the distal outflow coincides with the shortening and rotation (Watanabe et al., 1998). During outflow septation, the myocardium of the distal outflow is retracted into the ventricular myocardium and this remodeling process involves cell death in specific foci. The remodeling and cell death are necessary for correct alignment of the aorta and pulmonary trunk with the ventricles (Watanabe et al., 1998, 2001). During this process, the distal myocardium becomes slightly hypoxic, which triggers cell death. Exposing embryos to hyperoxia during this critical stage prevents the cell death and causes improper shortening and/or rotation of the outflow tract which results in incorrect alignment of the aorta and pulmonary trunk with the ventricles (Sugishita et al., 2004a,b). Is it possible that this hypoxia may be a driving force not only in the developmental appearance of outflow septation but also in the evolutionary appearance of divided systemic and pulmonary blood streams. With the development of lungs, deoxygenated blood is carried to the lungs via the pulmonary outflow, which results in lower oxygen tension in the outflow tract causing slight hypoxia. Hypoxia in the outflow tract would then be a trigger for separation of the two outflow streams.

Cell Lineage Modules

The cell lineage modules most obviously used in building a heart are endocardium, myocardium, epicardium, and neural crest. The invertebrates and amphioxus lack both endocardium and neural crest (Holland et al., 2004). However, in amphioxus and ascidians, a gene called *AmphiFoxD*, has been found that is homologous to those expressed by vertebrate neural crest cells. During amphioxus development, the neural plate is bordered by cells that express genes involved in vertebrate neural crest induction. However, the cells lack the ability to delaminate, migrate, and differentiate into the plethora of cell types generated by neural crest cells in vertebrates (Trainor et al., 2003; Yu et al., 2002).

The general patterns of cranial neural crest migration from dorsal neural tube to ventral branchial arches are conserved throughout vertebrates, with cells migrating in identifiable streams. In agnathans and gnathostomes, neural crest cells arising from the mid-hindbrain are able to migrate caudally while those from the caudal hindbrain can migrate both rostrally and caudally. Further, neural crest cells originating from different axial levels can populate the same arch. This is distinct from teleosts and the other vertebrates, where there is strict delineation of the neural crest streams from the hindbrain and almost no mixing in the branchial/pharyngeal arches (McCauley and Bronner-Fraser, 2003; Suzuki and Kirby, 1997).

Interestingly, the smooth muscle that invests the arterial trunk(s) shows conservation of nitric oxide signaling in vertebrate hearts with undivided pulmonary circulation and those with divided pulmonary circulation (Fig. 14.5) (Grimes and Kirby, unpublished). The significance of this is not known but it indicates that this cell lineage may be conserved throughout the vertebrates.

Functional Modules

Warm-blooded (endothermic) vertebrates such as birds and mammals have a high resting metabolic rate that enables them to maintain a constant body temperature. Endotherms use more oxygen and need more fuel than cold-blooded (ectothermic) vertebrates, such as fish, lizards, and frogs. Ectotherms have lower body temperatures that fluctuate with environmental temperature. Endotherms have a capacity for prolonged strenuous activity that is unattainable by ectotherms. In addition endotherms have four-chambered hearts divided such that oxygenated blood coming from the lungs (a pulmonary functional module) is separated from the deoxygenated blood arriving from the rest of the body (a systemic functional module). The three-chambered heart of most reptiles and amphibians allows controlled mixing of pulmonary and systemic blood, which is important in diving, where

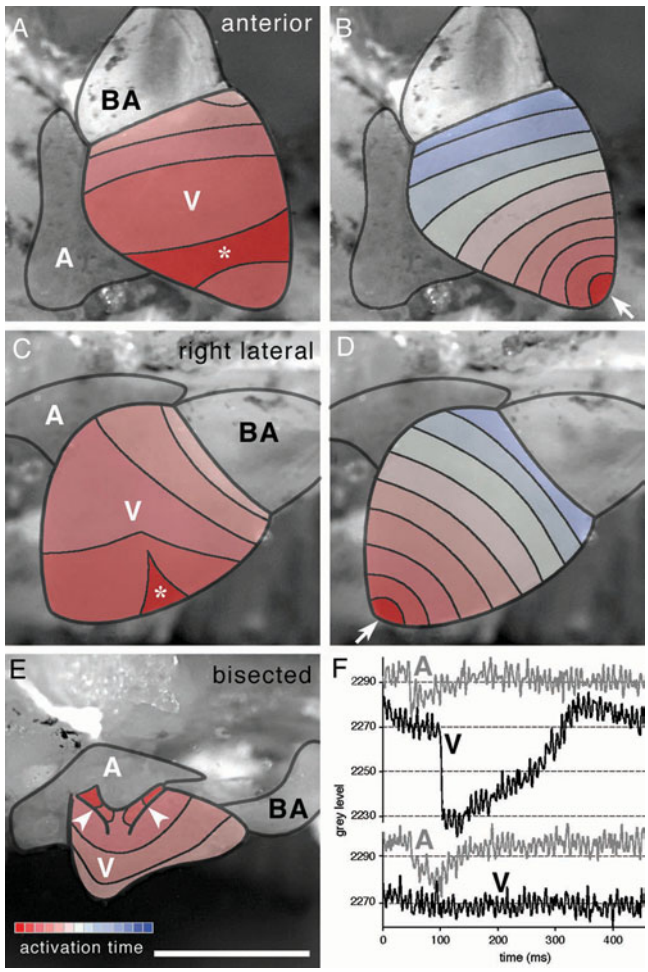

Figure 14.5. Optical mapping of the zebrafish heart shows activation sequence is base-to-apex in the ventricle. *(A–D)* show that activation begins at the apex of the ventricle and proceeds toward the bulbus arteriosus in a normal heart. *(E)* After bisection of the conduction system activation begins at the atrioventricular junction rather than at the ventricular apex. *(F)* shows the timing delay between the atrial and ventricular activation indicating a delay at the atrioventricular junction. A, atrium; V, ventricle; BA, bulbus arteriosus. (Courtesy of D. Sedmera.)

shunting blood from the lungs accelerates the transition to a lower metabolic rate, increasing the time between breaths.

Another type of functional module is the cardiac pacemaking and conduction system which is poorly developed in teleosts and becomes highly specialized in land animals with multichambered hearts. In the chordate heart, each myocardial cell has pacemaking properties since each is autorhythmic and poorly coupled, features that are prerequisite for slow conduction and there is peristaltic propulsion of blood with the inflow region of the heart functioning as a dominant pacemaker (Moorman and Christoffels, 2003). The first sign of a functional conduction system has been reported in zebrafish. A wave of excitation spreads uniformly through the ventricle and is delayed at the AV junction. Ventricular activation begins at the apex of the ventricle. This implies that a conduction system exists in zebrafish even though no discernible specialized conduction cells can be found. Trabecular bands with polysialic acid neural cell adhesion molecule (Ps-ncam) staining are continuous between the atrioventricular canal and the apex of the ventricle. Ps-ncam is the most reliable marker of the His—Purkinje system in avian hearts. Thus, in zebrafish, the ventricular trabeculae are thought to provide a functional equivalent of the chick and mammalian His—Purkinje system (Sedmera et al., 2003). There are fine myocardial tracts at the atrioventricular junction that connect the two chambers, and these are insulated by a wedge of connective tissue reminiscent of the break in myocardial continuity at the atrioventricular junction in vertebrates with more complex hearts.

Moorman and Christoffels propose that the embryonic vertebrate tubular heart consists of poorly coupled pacemaker-like cardiac muscle cells, with the highest pacemaker activity at the venous pole, causing unidirectional peristaltic contraction waves. In the embryonic vertebrate heart, ventricular chambers differentiate ventrally and atrial chambers dorsally. The developing chamber myocardium displays high proliferative activity and begins to be well coupled with low pacemaker activity, permitting fast conduction and efficient contraction. These myocytes are also referred to as working myocardium. Some of the myocardium from the original tube is set aside from this pool of working myocardium as slowly proliferating pacemaker-like myocardium that is barredfrom differentiating into chamber myocardium as the atrial and ventricular chambers develop. When the trabecular myocardium develops in the ventricles, it proliferates slowly and ultimately contributes to the ventricular conduction system (Moorman and Christoffels, 2003).

Transcriptional Modules

Transcriptional modules have been very informative in facilitating our understanding of the relationship of invertebrate and vertebrate hearts. Transcriptional modules evolve and are used to establish morphological, cell lineage, and functional modules. In the case of the heart, most of the transcriptional modules that we know and understand best promote development of the cardiomyocyte cell lineage. The transcriptional modules used in myogenesis from all the animals that have been studied include Nk domain containing tinman and tinman-related Nkx transcriptional regulators; Mads box proteins such as Mef2; Gata factors; basic helix–loop–helix transcriptional regulators such as the Hand proteins; T-box transcription factors such as Tbx5 and -20; homeodomain transcription factors such as Isl1. The transcriptional modules form large transcriptional complexes.

Even though these transcriptional modules have been co-opted for development of cardiomyocyte lineage development (Fig. 14.6), this does not in any way indicate a direct ancestral relationship of the cardioblasts in *Drosophila*, myoepithelial

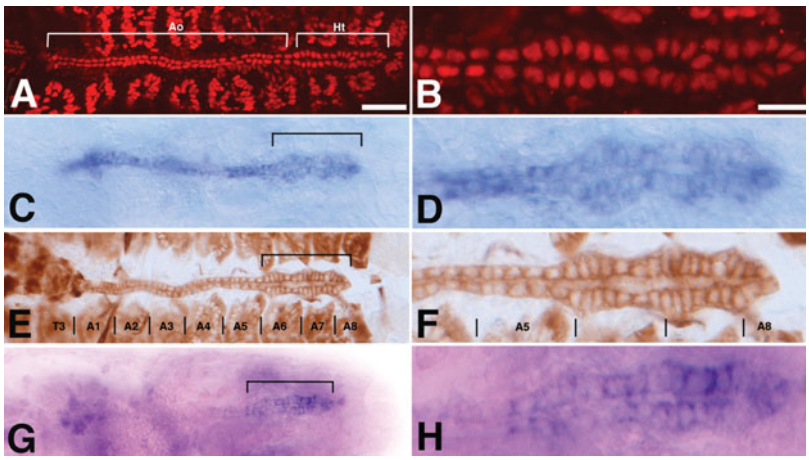

Figure 14.6. Stage 16 *Drosophila* embryos stained with various markers for transcriptional control. (*A* and *B*) Mef2 protein accumulation in the muscle cells of the embryo. The dorsal vessel consisted of two parallel rows of cells at the dorsal midline. Note that the distance between the two rows of Mef2-positive nuclei is greater in the "heart" (Ht) compared to the "aorta" (Ao). (*C* and *D*) Hand transcripts. (*E* and *F*) Myosin heavy chain (Mhc) protein in the cardial cells of the dorsal vessel. All pictures are dorsal views oriented with anterior toward the left. In *C* and *E*, the location of the "heart" is bracketed. (From Lovato et al., 2002, with permission.)

cells in basal chordates such as hagfish, and myocardial cells found in vertebrates as discussed earlier.

Nk Family

One of the earliest transcription factors expressed in all animals with contractile vascular cells is the Nk family (Bodmer, 1993; Schultheiss et al., 1995). Loss of *tinman* expression in *Drosophila* causes a complete failure of myocardial development, but in the mouse null expression of *Nkx2.5* does not ablate early development of myocardial cells, and heart development continues until looping. It is currently thought from molecular and cell marking studies that Nkx2.5 is specifically required for left ventricular chamber development (Brand, 2003; Lyons et al., 1995; Redkar et al., 2001; Yamagishi et al., 2001). The difference in absolute requirement for tinman versus non-requirement for Nkx2.5 supports the argument that these "muscle" cells are not homologous. Injection of dominant-negative Nkx2.3 or Nkx2.5 constructs with point mutations blocks heart formation in *Xenopus* mimicking the *tinman* (*Nkx2.5*-null) phenotype in *Drosophila* (Fu et al., 1998; Grow and Krieg, 1998). Because the myocardial genes are promoted by large stable complexes that still function, although poorly, without one of the components such as Nkx2.5, mutant or dominant negative proteins may be more detrimental in disrupting function of the multimeric complexes in transcriptional regulation (Brand, 2003).

Gata Family

Vertebrate and invertebrate Gata factors also act in multiprotein complexes to either activate or repress transcription. Several of their protein partners are members of the same families across multiple species. For example, different members of the NK homeodomain family interact with Gata family members to promote differentiation of cardiomyocytes, smooth muscle cells and endoderm. A single *Gata* gene, called *pannier*, is required for dorsal vessel development in *Drosophila* (Gajewski et al., 1999). Pannier works synergistically with tinman. Ectopic coexpression of pannier and tinman results in a spatial expansion of cardioblast gene expression. Pannier is represented by three *Gata* gene products, Gata-4, -5, and -6, in vertebrate hearts (Molkentin, 2000). Gata4 appears to be the most important in regulating myocardial gene expression. Null expression of *Gata4* in the mouse leads to a reduction in the cardiac myocyte pool (Kuo et al., 1997; Molkentin et al., 1997). Gata4 expression is also required in the visceral endoderm for fusion of the bilateral heart fields in the ventral midline (Narita et al., 1997). Gata5 plays a role in endocardial differentiation and is also required for endoderm formation in zebrafish and *Xenopus* (Nemer and Nemer, 2002; Reiter et al., 2001; Weber et al., 2000). Mutation of *Gata5* (called *faust*) in the zebrafish is associated with cardia bifida and a reduction in cardiomyocytes (Reiter et al., 2001). Overexpression of Gata5 in zebrafish embryos causes ectopic Nkx2.5 expression and subsequent formation of ectopic myocardium (Reiter et al., 1999). Nkx3.2, a smooth muscle transcriptional activator interacts synergistically interacts with Gata6 to transactivate smooth muscle genes, including *Sm22a*, *caldesmon,* and *α1-integrin* (Nishida et al., 2002).

T-box Family

The encoded T-domain proteins are members of a rapidly growing and highly conserved family of transcription factors that share a region of homology with the DNA-binding domain (T-domain) of the mouse *brachyury* (or *T*) gene product. *Brachyury* is the founding member of the family. It is a naturally occurring dominant mutation in mice who have a short tail phenotype (hence *T*). In homozygous mice it has profound effects on gastrulation (Herrmann and Kispert, 1994).

The T-box gene family is very important for heart development, with many T-box transcription factors, including Tbx1, -2, -5, -18, and -20, expressed in the developing heart and/or heart fields. The T-box proteins interact in large transcriptional complexes with Gata4 and Nkx2.5 (Fan et al., 2003a,b;

Garg et al., 2003; Hiroi et al., 2001; Plageman and Yutzey, 2005). Mutations of T-box genes are associated with several different cardiac malformations (Table 14.1). Downstream targets of T-box transcription factors include Nppa, Cx40, Cx43, Tbx5, and Fgf10 (Agarwal et al., 2003; Bruneau et al., 2001; Christoffels et al., 2004; Hiroi et al., 2001; Hoogaars et al., 2004; Xu et al., 2004).

An amphioxus T-box gene, *AmphiTbx1/10*, is orthologous to vertebrate *Tbx1* and *Tbx10*. AmphiTbx1/10 is first expressed in branchial arch endoderm and mesoderm of developing neurulae. Branchial expression is restricted to the first three branchial arches, and disappears by 4 days of development. Tbx1/10-mediated branchial arch endoderm and mesoderm patterning functions predate the origin of neural crest but were later co-opted as *Tbx1* during the evolution of developmental programs regulating branchial neural crest (Mahadevan et al., 2004).

Tbx2 is known primarily as a transcriptional repressor (Carreira et al., 1998; Chen et al., 2004). One of the repressed targets is Cx43, which is important in developing cardiomyocytes for gap junctional coupling of the cells (Chen et al., 2004). *Tbx2* is expressed in the zebrafish heart at 2–3 dpf (Ruvinsky et al., 2000). In *Xenopus* Tbx2 is expressed in the branchial arches and heart at comparable stages (Hayata et al., 1999). The most detailed study of Tbx2 expression has been done in chick. Tbx2 expression is detected in a crescent in the chick at stage 5. However, at this stage the crescent of expression is in the endoderm rather than in the cardiogenic mesenchyme. By stage 8, Tbx2 is seen in the cardiogenic mesenchyme. Its expression in the myocardium declines as fusion of the heart tube begins at stage 10 and it is maintained only in the caudal heart. As the heart loops Tbx2 expression becomes limited to the atrioventricular canal myocardium (Yamada et al., 2000). A role for Tbx2 in chamber specification has been discussed in Chapter 8. Tbx2 expression overlaps with both Bmp2 and Bmp4 during all stages of heart development. Application of Bmp2 protein selectively activates Tbx2 and Tbx3 expression in non-cardiogenic embryonic tissue, and the Bmp antagonist Noggin downregulates Tbx2 expression. In *Bmp2*-null mice, Tbx2 is not expressed suggesting that Tbx2 expression is regulated by Bmp2 signaling during early cardiogenesis (Yamada et al., 2000).

In *Drosophila* a gene designated *Tb66F2* and also called *Dorsocross1* has been found to be similar to *Tbx3*. It is expressed in a subset of cardioblasts that do not express tinman (Lo and Frasch, 2001). Tb66F2 may work as a repressor similar to mammalian Tbx3 (Ryan and Chin, 2003). In mouse heart, Tbx3 is expressed throughout development in the sinoatrial node, internodal myocardium, atrioventricular node,

Table 14.1.
Expression and Function of T-box Genes in the Developing heart

Species/Gene	Expressed	Cardiovascular null phenotype
Drosophila		
Org-1 (tbx1)	Visceral mesoderm	Not reported
Dorsocross1-3 (tbx6)	Cardiogenic mesoderm	No dorsal vessel
H15 (tbx20)	Cardioblasts; dorsal vessel	Not reported
Zebrafish		
Van gogh (tbx1)	Pharynx	Aortic arch anomalies
Heartstrings (tbx5)	Heart, forelimb	Thin hypomorphic heart
Tbx18	Heart, somites	Not reported
hrT (tbx20)	Lateral plate mesoderm; heart	Thin hypomorphic heart (morphant)
Mouse		
Tbx1	Heart, outflow tract, pharynx	Aortic arch anomalies, PTA
Tbx2	Heart, limbs	Not reported
Tbx3	Heart, conduction system	No reported cardiac defects
Tbx5	Heart, atria, forelimbs	Hypomorphic posterior heart tube
Tbx18	Epicardium, somites	No reported cardiac defects
Tbx20	Primitive heart, cushions	Not reported
Human		Haploinsufficiency
TBX1	Not reported	DiGeorge (22q11del)Syndrome (IAA, OFT anomalies)
TBX3	Not reported	Ulnar mammary syndrome (no reported heart defects)
TBX5	Atria, forelimbs	Holt-Oram syndrome (ASD, conduction disease)

Abbreviations are outflow tract (OFT); persistent truncus arteriosus (PTA); interrupted aortic arch (IAA); atrial septal defect (ASD). From Plageman and Yutzey (2005), with permission.

bundle, and proximal bundle branches from E8.5. Because it is expressed only in conduction myocardium, Tbx3 may serve to repress gene expression typical of chamber or working myocardium (Hoogaars et al., 2004). Because no conduction myocardium homolog has been identified in *Drosophila*, it is not possible to speculate on whether the function of this gene is conserved.

Tbx4 has been reported to be expressed in the sinus venosus and atrium in the developing mouse heart at E12.5 (Chapman et al., 1996). However, in the chick Tbx4 is expressed in the outflow tract particularly in the tissue surrounding the aortic sac (Krause et al., 2004). Thus, while the transcriptional function of this gene may be conserved, its function in terms of cell lineage is not conserved even within animals with four-chambered hearts.

Tbx5 is required for correct development of the atria in mammals and in zebrafish. The cardiac expression patterns of Tbx5 in zebrafish, *Xenopus*, chick, and mouse are extremely similar: transcripts are first found in the lateral plate mesoderm and then in the sinus venosus, atrium, and primitive ventricle, that is, the inflow limb of the developing heart (Bruneau et al., 1999; Chapman et al., 1996; Garrity et al., 2002; Horb and Thomsen, 1999; Liberatore et al., 2000; Yamada et al., 2000). In chick and mouse, there is little or no expression in the right ventricle, while in human heart development, Tbx5 expression persists after ventricular septation in both right and left ventricles (Hatcher et al., 2000). In human heart development, Tbx5 illustrates the sensitivity of phenotype to gene dosage because patients with extra copies of *TBX5* have some of the features of Holt-Oram syndrome (see Chapter 15) (Vaughan and Basson, 2000). Tbx5 promotes normal expression of Nkx2.5, which is also a Tbx5 binding partner, and two genes expressed in the atrium, *Nppa* (atrial natriuretic factor) and *Cx40*. The expression of all of these is reduced when *Tbx5* is not expressed in heterozygous or homozygous null embryos (Bruneau et al., 2001; Hiroi et al., 2001). In *Xenopus*, injection of a hormone-inducible dominant negative Tbx5 results in failure of heart development (Horb and Thomsen, 1999). However, in zebrafish with a recessive mutation caused by a premature stop codon after the T-box DNA binding domain of *Tbx5*, called *heartstrings*, the heart shows bradycardia and a failure to loop (Garrity et al., 2002). While this truncated protein can bind DNA, it lacks a carboxy-terminal domain that has been shown to regulate transcriptional activator activity (Hiroi et al., 2001). Ectopic overexpression of Tbx5 caused by treatment with retinoic acid inhibits normal growth of the ventricular wall (Hatcher et al., 2001; Liberatore et al., 2000).

Tbx12 is an alternately spliced product of the *Tbx20* gene (Carson et al., 2000; Iio et al., 2001; Kraus et al., 2001). Cardiac expression of Tbx12/20 is first seen in the cardiogenic fields (Carson et al., 2000). After formation of the heart tube, it is expressed throughout the myocardium and to a lesser extent in the endocardium. It continues to be expressed during looping, chamber specification, and septation in most myocardial cells, including the outflow tract. Tbx12/20 expression in neonatal myocardium is stronger in the atria than in the ventricles. The *Tbx20* gene in zebrafish is called *hrT*. HrT has been shown to regulate Tbx5 expression. Zebrafish embryos with diminished hrT function, produced by injection of dominant negative hrT, lack circulation and have abnormal hearts. In *Drosophila*, *H15* is thought to be a *Tbx20* ortholog. It is expressed in the cardiac primordia and is maintained as these cells form cardioblast cells at the dorsal midline during dorsal vessel formation (Griffin et al., 2000).

Signaling Modules

Induction is the process by which a cell or tissue influences the fate of another cell or tissue. Competence is the ability to respond to an inductive signal and is a subset of that cell's or tissue's potency (Slack, 1991). Induction can occur by direct cell-to-cell contact or from a distance. Induction at a distance most likely involves a diffusible factor or morphogen, which is a long-range signaling molecule that acts in a concentration-dependent manner. Signaling at a distance can also occur by a cell relay mechanism or long cytoplasmic projections (Vincent and Perrimon, 2001).

Signaling molecules usually impart specification and determination of cells and tissues, while other factors, such as the transcriptional regulators discussed above, are required for imparting identity. Genes that impart identity are referred to as selector genes (Garcia-Bellido, 1975). Patterning of the heart involves an interaction between signaling pathways and selector proteins (Fig. 14.7). There is evidence from *Drosophila* that signaling pathways and selector proteins have the same target genes (Affolter and Mann, 2001; Guss et al., 2001). The combinatorial action of signaling molecules and selector proteins brings about a set of structural proteins and enzymes that are characteristic for the cell type induced.

Bone Morphogenetic Protein

Bone morphogenetic protein (Bmp) has a highly conserved role in heart development. Several members of the Bmp family are expressed in anterior endoderm and/or cardiogenic mesoderm. Multiple cardiac-restricted transcription factors are induced by Bmp2 with distinct kinetics. Expression of tinman in *Drosophila* is dependent on Bmp signaling. In the chick, zebrafish, *Xenopus,* and mouse, Bmp produced by the anterior endoderm induces myocardial differentiation (Andree et al., 1998; Brand, 2003; Kishimoto et al., 1997; Lough and Sugi, 2000; Schultheiss et al., 1997; Shi et al., 2000). Noggin, which binds Bmps with high affinity, prevents myocardial differentiation (Schlange et al., 2000). *Bmp2*-null mice have abnormal heart development even though myocardial specification of cardiac mesoderm occurs normally, and in double mutants of *Bmp5* and *Bmp7*, cardiac morphogenesis is severely delayed (Solloway and Robertson, 1999; Zhang and Bradley, 1996).

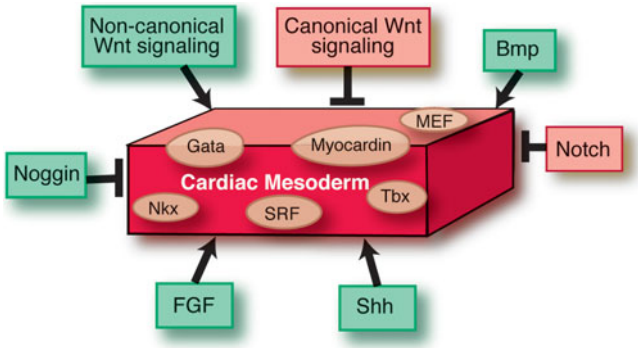

Figure 14.7. Overview of the signaling pathways and transcriptional regulators (*tan*) involved in cardiogenic induction. Positive signals (*green*) mostly from the endoderm act as inducers of cardiac mesoderm formation. Inhibitory signals (*pink*) are mainly from the mesoderm.

Smads are intracellular effectors of Bmp signaling and at least one Smad functions as a transcriptional regulator. The *tinman* enhancer has multiple Smad binding sites. Ectodermal Dpp, the *Drosophila* Bmp equivalent, maintains tinman expression in the cardioblasts (Frasch, 1995, Xu et al., 1998). Moreover, in the vertebrate *Nkx2.5* promoter, several Smad binding sites are present within the enhancer that drives expression in the cardiac crescent and in the outflow tract (Liberatore et al., 2002; Lien et al., 2002). Thus, the observed function of Dpp in *Drosophila*, which maintains tinman expression, seems evolutionarily conserved and is also utilized in vertebrate heart formation (Brand, 2003).

Wnt

Wingless (wg), the *Drosophila* homolog of Wnt, is required along with Dpp for tinman expression (Wu et al., 1995). However, in frog, chick, and mouse, inhibition of canonical Wnt signaling through β-catenin appears to be important for heart formation. Ectopic expression of Wnt1 in the heart field blocks myocardial differentiation and induces blood formation (Marvin et al., 2001). Crescent is a protein that competes with the Wnt receptor and inhibits Wnt signaling. It is expressed in anterior endoderm during gastrulation and may be the factor needed to inhibit Wnt signaling through β-catenin. Explants of caudal lateral mesendoderm or paraxial mesoderm can be induced to form myocardium by Crescent or other Wnt antagonists expressed by the neural tube (Schneider and Mercola, 2001; Tzahor and Lassar, 2001). Tissue-specific knockout of β-catenin from the endoderm results in differentiation of myocardium from the endoderm in gastrulating mice embryos, suggesting that canonical Wnt signaling through β-catenin may be involved in the separation of endodermal and mesodermal cell lineages (Lickert et al., 2002).

Wnt11 is a non-canonical Wnt that signals independently of β-catenin and can inhibit signaling through the canonical Wnt pathway (Pandur et al., 2002). It is expressed in the mesoderm caudal to the heart field and can induce cardiogenesis in caudal non-cardiogenic mesoderm in the chick embryo (Eisenberg and Eisenberg, 1999). Wnt11 activates protein kinase C (PKC) and CamKII in a G-protein–dependent manner (Kuhl et al., 2000). Treatment of the P19 cell line with Wnt11 conditioned medium causes the cells to differentiate as cardiomyocytes (Pandur et al., 2002). The initial heart field may therefore be defined by the presence of Bmp2 and the inhibition of the canonical Wnt pathway through the combined action of endoderm-localized Wnt antagonist and mesoderm-derived Wnt11 (Brand, 2003).

Fibroblast Growth Factor

Fgf8 is expressed in the cardiogenic mesoderm in mouse, chick, and zebrafish (Alsan and Schultheiss, 2002; Crossley and Martin, 1995; Reifers et al., 2000). In the zebrafish *Fgf8* mutant *acerebellar* (*ace*), neither Nkx2.5 nor Gata4 is expressed, and ventricular morphogenesis is abnormal (Reifers et al., 2000). Fgf8 is expressed in the pharyngeal endoderm and can substitute for pharyngeal endoderm to induce cardiac mesoderm (Alsan and Schultheiss, 2002). Null mutation of *Fgf8* is early embryo lethal, precluding analysis of myocardiogenesis; however, an Fgf8 hypomorphic mouse affects addition of the outflow limb (right ventricle, conus and truncus) to the heart tube (Abu-Issa et al., 2002; Meyers and Martin, 1999). A combination of Bmp2 and Fgf4 can stimulate heart formation from non-cardiogenic mesoderm, while neither can do so alone (Barron et al., 2000). Fgf and Bmp signaling appear to act synergistically to drive myocardial lineage differentiation. In *Drosophila*, an Fgf receptor called heartless, is required for the mesodermal cell spreading necessary to position the mesoderm under inducing ectoderm to form cardioblasts (Beiman et al., 1996; Gisselbrecht et al., 1996; Shishido et al., 1997). If this receptor is mutated, the dorsal vessel does not develop, hence the name of the mutant is heartless.

Notch

Notch signaling may be involved in establishing subpopulations within the Nkx2.5-positive cardiogenic mesoderm. Notch signaling in *Drosophila* is required for the inhibition of cardiogenesis (Han and Bodmer, 2003). Active Notch signaling is required when a dividing mesenchymal cell undergoes asymmetric cell division to two daughter cells with different cell fates, that is, pericardial cell versus cardioblast. Cells that undergo symmetric division in which both progenitors give rise to a single type of myocardial-only or pericardial-only cell are unaffected by Notch signaling (Han and Bodmer, 2003). If Notch signaling is induced throughout the cardiogenic mesoderm in *Drosophila*, there is an absence of myocardial precursors accompanied by an increase in the number of pericardial cells, leading to the absence of the myocardial dorsal vessel, the *Drosophila* equivalent of a heart. By contrast, overexpression of a Notch antagonist results in the complete absence of

pericardial fates. Notch signaling inhibits myocardial differentiation in a subset of Nkx2.5-expressing cells in the *Xenopus* cardiogenic mesenchyme (Rones et al., 2000). Fate mapping shows that this subset does not contribute to the embryonic heart tube but may contribute to the pericardium. However, this subset has not been fate-mapped to stages following heart tube formation and is therefore not ruled out as a cell population contributing to heart development and morphogenesis.

In conclusion, the existence of highly conserved developmental-genetic regulatory modules in the evolution of the vertebrate heart is an example of process homology in a system that has undergone dramatic adaptive changes in construction and form during phylogeny (Cracraft, 2005).

REFERENCES

Abu-Issa, R., G. Smyth, I. Smoak, K.-I. Yamamura, and E. Meyers. 2002. Fgf8 is required for pharyngeal arch and cardiovascular development in the mouse. Development 129:4613–4625.

Affolter, M., and R. Mann. 2001. Development. Legs, eyes, or wings—selectors and signals make the difference. Science 292:1080–1081.

Agarwal, P., J. N. Wylie, J. Galceran, O. Arkhitko, C. Li, C. Deng, R. Grosschedl, and B. G. Bruneau. 2003. Tbx5 is essential for forelimb bud initiation following patterning of the limb field in the mouse embryo. Development 130:623–633.

Alsan, B. H., and T. M. Schultheiss. 2002. Regulation of avian cardiogenesis by *Fgf8* signaling. Development 129:1935–1943.

Andree, B., D. Duprez, B. Vorbusch, H. H. Arnold, and T. Brand. 1998. BMP-2 induces ectopic expression of cardiac lineage markers and interferes with somite formation in chicken embryos. Mech. Dev. 70:119–131.

Arthur, W. 2002. The emerging conceptual framework of evolutionary developmental biology. Nature 415:757–764.

Barron, M., M. Gao, and J. Lough. 2000. Requirement for BMP and FGF signaling during cardiogenic induction in non-precardiac mesoderm is specific, transient, and cooperative. Dev. Dyn. 218:383–393.

Beiman, M., B. Z. Shilo, and T. Volk. 1996. Heartless, a *Drosophila* FGF receptor homolog, is essential for cell migration and establishment of several mesodermal lineages. Genes Dev. 10:2993–3002.

Bodmer, R. 1993. The gene *tinman* is required for specification of the heart and visceral muscles in *Drosophila*. Development 118: 719–729.

Bone, Q., N. B. Marshall, and J. H. S. Blaxter. 1995. Biology of Fishes. Glasgow: Blackie Academic and Professional.

Brand, T. 2003. Heart development: molecular insights into cardiac specification and early morphogenesis. Dev. Biol. 258:1–19.

Bruneau, B. G., M. Logan, N. Davis, T. Levi, C. J. Tabin, J. G. Seidman, and C. E. Seidman. 1999. Chamber-specific cardiac expression of *Tbx5* and heart defects in Holt-Oram syndrome. Dev. Biol. 211:100–108.

Bruneau, B. G., G. Nemer, J. P. Schmitt, F. Charron, L. Robitaille, S. Caron, D. A. Conner, M. Gessler, M. Nemer, C. E. Seidman, and J. G. Seidman. 2001. A murine model of Holt-Oram syndrome defines roles of the T-box transcription factor *Tbx5* in cardiogenesis and disease. Cell 106:709–721.

Carreira, S., T. J. Dexter, U. Yavuzer, D. J. Easty, and C. R. Goding. 1998. Brachyury-related transcription factor *Tbx2* and repression of the melanocyte-specific TRP-1 promoter. Mol. Cell. Biol. 18:5099–5108.

Carroll, S. B. 2005. Endless Forms Most Beautiful. The New Science of Evo Devo and the Making of the Animal Kingdom. New York: W. W. Norton.

Carson, C. T., E. R. Kinzler, and B. A. Parr. 2000. *Tbx12*, a novel T-box gene, is expressed during early stages of heart and retinal development. Mech. Dev. 96:137–140.

Cartmill, M. 1979. The volar skin of Primates: its frictional characteristics and their functional significance. Am. J. Phys. Anthropol. 50:497–510.

Chapman, D. L., N. Garvey, S. Hancock, M. Alexiou, S. I. Agulnik, J. J. Gibson-Brown, J. Cebra-Thomas, R. J. Bollag, L. M. Silver, and V. E. Papaioannou. 1996. Expression of the T-box family genes, *Tbx1-Tbx5*, during early mouse development. Dev. Dyn. 206:379–390.

Chen, J. R., B. Chatterjee, R. Meyer, J. C. Yu, J. L. Borke, C. M. Isales, M. L. Kirby, C. W. Lo, and R. J. Bollag. 2004. *Tbx2* represses expression of Connexin43 in osteoblastic-like cells. Calcif. Tissue Int. 74:561–573.

Christoffels, V. M., W. M. H. Hoogaars, A. Tessari, D. E. W. Clout, A. F. M. Moorman, and M. Campione. 2004. T-Box transcription factor *tbx2* represses differentiation and formation of the cardiac chambers. Dev. Biol. 229:763–770.

Cracraft, J. 2005. Phylogeny and evo-devo: characters, homology, and the historical analysis of the evolution of development. Zoology (Jena) 108:345–356.

Cripps, R. M., and E. N. Olson. 2002. Control of cardiac development by an evolutionarily conserved transcriptional network. Dev. Biol. 246:14–28.

Crossley, P. H., and G. R. Martin. 1995. The mouse *Fgf8* gene encodes a family of polypeptides and is expressed in regions that direct outgrowth and patterning in the developing embryo. Development 121:439–451.

Davidson, B., and M. Levine. 2003. Evolutionary origins of the vertebrate heart: specification of the cardiac lineage in Ciona intestinalis. Proc. Natl. Acad. Sci. USA 100:11469–11473.

Davidson, E. H. 2001. Genomic Regulatory Systems. Development and Evolution. San Diego: Academic Press.

Eisenberg, C. A., and L. M. Eisenberg. 1999. WNT11 promotes cardiac tissue formation of early mesoderm. Dev. Dyn. 216:45–58.

Erwin, D. H., and E. H. Davidson. 2002. The last common bilaterian ancestor. Development 129:3021–3032.

Fan, C., M. A. Duhagon, C. Oberti, S. Chen, Y. Hiroi, I. Komuro, P. I. Duhagon, R. Canessa, and Q. Wang. 2003. Novel *TBX5* mutations and molecular mechanism for Holt-Oram syndrome. J. Med. Genet. 40:e29.

Fan, C., M. Liu, and Q. Wang. 2003. Functional analysis of *TBX5* missense mutations associated with Holt-Oram syndrome. J. Biol. Chem. 278:8780–8785.

Fishman, M. C., and E. N. Olson. 1997. Parsing the heart: genetic modules for organ assembly. 91:153–156.

Frasch, M. 1995. Induction of visceral and cardiac mesoderm by ectodermal Dpp in the early Drosophila embryo. Nature 374:464–467.

Fu, Y., W. Yan, T. J. Mohun, and S. M. Evans. 1998. Vertebrate *tinman* homologues *XNkx2-3* and *XNkx2-5* are required for heart formation in a functionally redundant manner. Development 125:4439–4449.

Gajewski, K., N. Fossett, J. D. Molkentin, and R. A. Schulz. 1999. The zinc finger proteins Pannier and GATA4 function as cardiogenic factors in *Drosophila*. Development 126:5679–5688.

Gans, C., and R. G. Northcutt. 1983. Neural crest and the origin of the vertebrates: a new head. Science 220:268–274.

Garcia-Bellido, A. 1975. Genetic control of wing disc development in Drosophila. Ciba Found. Symp.29:161–182.

Garg, V., I. S. Kathiriya, R. Barnes, M. K. Schluterman, I. N. King, C. A. Butler, C. R. Rothrock, R. S. Eapen, K. Hirayama-Yamada, K. Joo, R. Matsuoka, J. C. Cohen, and D. Srivastava. 2003. *GATA4* mutations cause human congenital heart defects and reveal an interaction with *TBX5*. Nature 424:443–447.

Garrity, D. M., S. Childs, and M. C. Fishman. 2002. The heartstrings mutation in zebrafish causes heart/fin *Tbx5* deficiency syndrome. Development 129:4635–4645.

Gerhart, J., and M. Kirschner. 1997. Cells, Embryos, and Evolution. Malden, MA: Blackwell.

Gisselbrecht, S., J. B. Skeath, C. Q. Doe, and A. M. Michelson. 1996. heartless encodes a fibroblast growth factor receptor (DFR1/ DFGF- R2) involved in the directional migration of early mesodermal cells in the *Drosophila* embryo. Genes Dev. 10: 3003–3017.

Griffin, K. J. P., J. Stoller, M. Gibson, S. Chen, D. Yelon, D. Y. R. Stainier, and D. Kimelman. 2000. A conserved role for H15-related T-box transcription factors in zebrafish and *Drosophila* heart formation. Dev. Biol. 218:235–247.

Grow, M. W., and P. A. Krieg. 1998. *Tinman* function is essential for vertebrate heart development: elimination of cardiac differentiation by dominant inhibitory mutants of the tinman-related genes, *XNkx2-3* and *XNkx2-5*. Dev. Biol. 204:187–196.

Guss, K. A., C. E. Nelson, A. Hudson, M. E. Kraus, and S. B. Carroll. 2001. Control of a genetic regulatory network by a selector gene. Science 292:1164–1167.

Han, Z., and R. Bodmer. 2003. Myogenic cells fates are antagonized by Notch only in asymmetric lineages of the *Drosophila* heart, with or without cell division. Development 130:3039–3051.

Hatcher, C. J., M. M. Goldstein, C. S. Mah, C. S. Delia, and C. T. Basson. 2000. Identification and localization of *TBX5* transcription factor during human cardiac morphogenesis. Dev. Dyn. 219:90–95.

Hatcher, C. J., M.-S. Kim, C. S. Mah, M. M. Goldstein, B. Wong, T. Mikawa, and C. T. Basson. 2001. *TBX5* transcription factor regulates cell proliferation during cardiogenesis. Dev. Biol. 230:177–188.

Hayata, T., H. Kuroda, A. Eisaki, and M. Asashima. 1999. Expression of *Xenopus* T-box transcription factor, *tbx2* in *Xenopus* embryo. Dev. Genes Evol. 209:625–628.

Herrmann, B. G., and A. Kispert. 1994. The T genes in embryogenesis. Trends Genet. 10:280–286.

Hiroi, Y., S. Kudoh, K. Monzen, Y. Ikeda, Y. Yazaki, R. Nagai, and I. Komuro. 2001. *Tbx5* associates with *Nkx2-5* and synergistically promotes cardiomyocyte differentiation. Nat. Genet. 28:276–280.

Holland, L. Z., V. Laudet, and M. Schubert. 2004. The chordate amphioxus: an emerging model organism for developmental biology. Cell Mol. Life Sci. 61:2290–2308.

Hoogaars, W. M., A. Tessari, A. F. Moorman, P. A. de Boer, J. Hagoort, A. T. Soufan, M. Campione, and V. M. Christoffels. 2004. The transcriptional repressor *Tbx3* delineates the developing central conduction system of the heart. Cardiovasc. Res. 62:489–499.

Horb, M. E., and G. H. Thomsen. 1999. *Tbx5* is essential for heart development. Development 126:1739–1751.

Iio, A., M. Koide, K. Hidaka, and T. Morisaki. 2001. Expression pattern of novel chick T-box gene, *Tbx20*. Dev. Genes Evol. 211: 559–562.

Kirby, M. L., T. F. Gale, and D. E. Stewart. 1983. Neural crest cells contribute to normal aorticopulmonary septation. Science 220: 1059–1061.

Kishimoto, Y., K. H. Lee, L. Zon, M. Hammerschmidt, and S. Schulte-Merker. 1997. The molecular nature of zebrafish swirl: BMP2 function is essential during early dorsoventral patterning. Development 124:4457–4466.

Kraus, F., B. Haenig, and A. Kispert. 2001. Cloning and expression analysis of the mouse T-box gene *Tbx20*. Mech. Dev. 100: 87–91.

Krause, A., W. Zacharias, T. Camarata, B. Linkhart, E. Law, A. Lischke, E. Miljan, and H. G. Simon. 2004. *Tbx5* and *Tbx4* transcription factors interact with a new chicken PDZ-LIM protein in limb and heart development. Dev. Biol. 273:106–120.

Kuhl, M., L. C. Sheldahl, M. Park, J. R. Miller, and R. T. Moon. 2000. The Wnt/Ca^{2+} pathway: a new vertebrate Wnt signaling pathway takes shape. TIG 16:279–283.

Kuo, C. T., E. E. Morrisey, R. Anandappa, K. Sigrist, M. M. Lu, M. S. Parmacek, C. Soudais, and J. M. Leiden. 1997. *GATA4* transcription factor is required for ventral morphogenesis and heart tube formation. Genes Dev. 11:1048–1060.

Liberatore, C. M., R. D. Searcy-Schrick, E. B. Vincent, and K. E. Yutzey. 2002. *Nkx-2.5* gene induction in mice is mediated by a *smad* consensus regulatory region. Dev. Biol. 244:243–256.

Liberatore, C. M., R. D. Searcy-Schrick, and K. E. Yutzey. 2000. Ventricular expression of *tbx5* inhibits normal heart chamber development. Dev. Biol. 223:169–180.

Lickert, H., S. Kutsch, B. Kanzier, Y. Tamai, M. Taketo, and R. Kemler. 2002. Fomation of multiple hearts in mice following deletion of B-catenin in the embryonic endoderm. Dev. Cell 3:171–181.

Lien, C. L., J. McAnally, J. A. Richardson, and E. N. Olson. 2002. Cardiac-specific activity of an *Nkx2-5* enhancer requires an evolutionarily conserved smad binding site. Dev. Biol. 244:257–266.

Lo, P. C., and M. Frasch. 2001. A role for the COUP-TF-related gene seven-up in the diversification of cardioblast identities in the dorsal vessel of *Drosophila*. Mech. Dev. 104:49–60.

Long, J. H. J., and T. J. Koob. 1997. Ventilating the skate egg capsule: the transitory tail pump of embryonic little skates (Raja erinacea). Bull. Mt. Des. Is. Bio. Lab. 36:117–119.

Lough, J., and Y. Sugi. 2000. Endoderm and heart development. Dev. Dyn. 217:327–342.

Lovato, T. L., T. P. Nguyen, M. R. Molina, and R. M. Cripps. 2002. The Hox gene abdominal-A specifies heart cell fate in the *Drosophila* dorsal vessel. Development 129:5019–5027.

Lyons, I., L. Parsons, L. Hartley, R. Li, J. E. Andrews, L. Robb, and R. P. Harvey. 1995. Myogenic and morphogenetic defects in the heart tubes of murine embryos lacking the homeo box gene *Nkx2-5*. Genes Dev. 9:1654–1666.

Mahadevan, N. R., A. C. Horton, and J. J. Gibson-Brown. 2004. Developmental expression of the amphioxus *Tbx1/10* gene illuminates the evolution of vertebrate branchial arches and sclerotome. Dev. Genes Evol. 214:559–566.

Marvin, M. J., G. Di Rocco, A. Gardiner, S. M. Bush, and A. B. Lassar. 2001. Inhibition of Wnt activity induces heart formation from posterior mesoderm. Genes Dev. 15:316–327.

McCauley, D. W., and M. Bronner-Fraser. 2003. Neural crest contributions to the lamprey head. Development 130:2317–2327.

Meyers, E. N., and G. R. Martin. 1999. Differences in left–right axis pathways in mouse and chick: functions of FGF8 and SHH. Science 285:403–406.

Molkentin, J., Q. Lin, S. Duncan, and E. Olson. 1997. Requirement of the transcription factor *GATA4* for heart tube formation and ventral morphogenesis. Genes Dev. 11:1061–1072.

Molkentin, J. D. 2000. The zinc finger-containing transcription factors *GATA-4,-5,* and*-6* - ubiquitously expressed regulators of tissue-specific gene expression. J. Biol. Chem. 275:38949–38952.

Moorman, A. F., and V. M. Christoffels. 2003. Cardiac chamber formation: development, genes, and evolution. Physiol. Rev. 83:1223–1267.

Narita, N., M. Bielinska, and D. B. Wilson. 1997. Wild-type endoderm abrogates the ventral developmental defects associated with *GATA-4* deficiency in the mouse. Dev. Biol. 189:270–274.

Nelson, C. 2004. Selector genes and the genetic control fo developmental modules. In: Modularity in Development and Evolution, ed. Schlosser, G. and G. P. Wagner, 17–33. Chicago: University of Chicago.

Nemer, G., and M. Nemer. 2002. Cooperative interaction between *GATA5* and NF-ATc regulates endothelial-endocardial differentiation of cardiogenic cells. Development 129:4045–4055.

Nielsen, C. 2001. Animal Evolution. Oxford: Oxford University Press.

Nishida, W., M. Nakamura, S. Mori, M. Takahashi, Y. Ohkawa, S. Tadokoro, K. Yoshida, K. Hiwada, K. Hayashi, and K. Sobue. 2002. A triad of serum response factor and the GATA and NK families governs the transcription of smooth and cardiac muscle genes. J. Biol. Chem. 277:7308–7317.

Opitz, J. M., and E. B. Clark. 2000. Heart development: an introduction. Am. J. Med. Genet. 97:238–247.

Pandur, P., M. Lasche, L. M. Eisenberg, and M. Kuhl. 2002. Wnt-11 activation of a non-canonical Wnt signalling pathway is required for cardiogenesis. Nature 418:636–641.

Plageman, T. F. J., and K. E. Yutzey. 2005. Differential expression and function of *Tbx5* and *Tbx20* in cardiac development. J. Biol. Chem. 279:19026–19034.

Rahr, H. 1981. The ultrastructure of the blood vessels of *Branchiostoma lanceolatum* (Pallas) (Cephalochordata). 1. Relations between blood vessels, epithelia, basal laminae, and "connective tissue." Zoomorphology 97:53–74.

Redkar, A., M. Montgomery, and J. Litvin. 2001. Fate map of early avian cardiac progenitor cells. Development 128:2269–2279.

Reifers, F., E. C. Walsh, S. L. ger, D. Y. R. Stainier, and M. Brand. 2000. Induction and differentiation of the zebrafish heart requires fibroblast growth factor 8 (fgf8/acerebellar). Development 127:225–235.

Reiter, J. F., J. Alexander, A. Rodaway, D. Yelon, R. Patient, N. Holder, and D. Y. Stainier. 1999. *Gata5* is required for the development of the heart and endoderm in zebrafish. Genes Dev. 13:2983–2995.

Reiter, J. F., Y. Kikuchi, and D. Y. R. Stainier. 2001. Multiple roles for *Gata5* in zebrafish endoderm formation. Development 128:125–135.

Rones, M. S., K. A. McLaughlin, M. Raffin, and M. Mercola. 2000. Serrate and Notch specify cell fates in the heart field by suppressing cardiomyogenesis. Development 127:3865–3876.

Ruppert, E. E. 1997. Cephalochordata (Acrania). In: Microscopic Anatomy of Invertebrates, ed. Harrison, F. W. and E. E. Ruppert, 349–504. New York: Wiley-Liss.

Ruvinsky, I., A. C. Oates, L. M. Silver, and R. K. Ho. 2000. The evolution of paired appendages in vertebrates: T-box genes in the zebrafish. Dev. Genes Evol. 210:82–91.

Ryan, K., and A. J. Chin. 2003. T-box genes and cardiac development. Birth Defects Res. C Embryo Today 69:25–37.

Satchell, G. H. 1991. Physiology and Form of Fish Circulation. Cambridge: Cambridge University Press.

Schlange, T., B. Andre, H. H. Arnold, and T. Brand. 2000. BMP2 is required for early heart development during a distinct time period. Mech. Dev. 91:259–270.

Schneider, V. A., and M. Mercola. 2001. Wnt antagonism initiates cardiogenesis in *Xenopus laevis.* Genes Dev. 15:304–315.

Schultheiss, T. M., J. B. E. Burch, and A. B. Lassar. 1997. A role for bone morphogenetic proteins in the induction of cardiac myogenesis. Genes Dev. 11:451–462.

Schultheiss, T. M., S. Xydas, and A. B. Lassar. 1995. Induction of avian cardiac myogenesis by anterior endoderm. Development 121: 4203–4214.

Sedmera, D., M. Reckova, A. deAlmeida, M. Sedmerova, M. Biermann, J. Volejnik, A. Sarre, E. Raddatz, R. A. McCarthy, R. G. Gourdie, and R. P. Thompson. 2003. Functional and morphological evidence for a ventricular conduction system in zebrafish and *Xenopus* hearts. Am. J. Physiol. 284:H1152–1160.

Shi, Y., S. Katsev, C. Cai, and S. Evans. 2000. BMP signaling is required for heart formation in vertebrates. Dev. Biol. 224:226–237.

Shishido, E., N. Ono, T. Kojima, and K. Saigo. 1997. Requirements of DFR1/heartless, a mesoderm-specific *Drosophila* FGF-receptor, for the formation of heart, visceral and somatic muscles, and ensheathing of longitudinal axon tracts in CNS. Development 124:2119–2128.

Simoes-Costa, M. S., M. Vasconcelos, A. C. Sampaio, R. M. Cravo, V. L. Linhares, T. Hochgreb, C. Y. Yan, B. Davidson, and J. Xavier-Neto. 2005. The evolutionary origin of cardiac chambers. Dev. Biol. 277:1–15.

Slack, J. M. W. 1991. From Egg to Embryo. Cambridge: Cambridge University Press.

Solloway, M. J., and E. J. Robertson. 1999. Early embryonic lethality in *Bmp5;Bmp7* double mutant mice suggests functional redundancy within the 60A subgroup. Development 126:1753–1768.

Sorrentino, R. P., K. M. Gajewski, and R. A. Schulz. 2005. *GATA* factors in *Drosophila* heart and blood cell development. Semin. Cell Dev. Biol. 16:107–116.

Stach, T. 1998. Coelomic cavities may function as a vascular system in amphioxus larvae. Biol. Bull. 195:260–263.

Sugishita, Y., D. W. Leifer, F. Agani, M. Watanabe, and S. A. Fisher. 2004a. Hypoxia-responsive signaling regulates the apoptosis-dependent remodeling of the embryonic avian cardiac outflow tract. Dev. Biol. 273:285–296.

Sugishita, Y., M. Watanabe, and S. A. Fisher. 2004b. Role of myocardial hypoxia in the remodeling of the embryonic avian cardiac outflow tract. Dev. Biol. 267:294–308.

Suzuki, H. R., and M. L. Kirby. 1997. Absence of neural crest cell regeneration from the postotic neural tube. Dev. Biol. 184:222–233.

Trainor, P. A., K. R. Melton, and M. Manzanares. 2003. Origins and plasticity of neural crest cells and their roles in jaw and craniofacial evolution. Int. J. Dev. Biol. 47:541–553.

Tzahor, E., and A. B. Lassar. 2001. Wnt signals from the neural tube block ectopic cardiogenesis. Genes Dev. 15:255–260.

Vaughan, C. J., and C. T. Basson. 2000. Molecular determinants of atrial and ventricular septal defects and patent ductus arteriosus. Am. J. Med. Genet. 97:304–309.

Vincent, S., and N. Perrimon. 2001. Developmental biology. Fishing for morphogens. Nature 411:533, 535–536.

Vogel, S. 2003. Comparative Biomechanics. Life's Physical World. Princeton, NJ: Princeton University Press.

Vogel, S., and R. A. Calvert. 1992. Vital Circuits: On Pumps, Pipes, and the Workings of Circulatory Systems. Oxford: Oxford University Press.

Wagner, G. P., and J. G. Mezey. 2003. The role of genetic architecture constraints in the origin of variational modularity. In: Modularity in Development and Evolution, ed. Schlosser, G. and G. P. Wagner, 338–358. Chicago: University of Chicago.

Watanabe, M., A. Choudhry, M. Berlan, A. Singal, E. Siwik, S. Mohr, and S. A. Fisher. 1998. Developmental remodeling and shortening of the cardiac outflow tract involves myocyte programmed cell death. Development 125:3809–3820.

Watanabe, M., A. Jafri, and S. A. Fisher. 2001. Apoptosis is required for the proper formation of the ventriculo-arterial connections. Dev. Biol. 240:274–288.

Weber, H., C. E. Symes, M. E. Walmsley, A. R. F. Rodaway, and R. K. Patient. 2000. A role for *GATA5* in *Xenopus* endoderm specification. Development 127:4345–4360.

Wu, X., K. Golden, and R. Bodmer. 1995. Heart development in *Drosophila* requires the segment polarity gene wingless. Dev. Biol. 169:619–628.

Xu, H., M. Morishima, J. N. Wylie, R. J. Schwartz, B. G. Bruneau, E. A. Lindsay, and A. Baldini. 2004. *Tbx1* has a dual role in the morphogenesis of the cardiac outflow tract. Development 131:3217–3227.

Xu, X., Z. Yin, J. B. Hudson, E. L. Ferguson, and M. Frasch. 1998. Smad proteins act in combination with synergistic and antagonistic regulators to target Dpp responses to the *Drosophila* mesoderm. Genes Dev. 12:2354–2370.

Yamada, M., J. P. Revelli, G. Eichele, M. Barron, and R. J. Schwartz. 2000. Expression of chick *Tbx-2, Tbx-3*, and *Tbx-5* genes during early heart development: evidence for BMP2 induction of *Tbx2*. Dev. Biol. 228:95–105.

Yamagishi, H., C. Yamagishi, O. Nakagawa, R. P. Harvey, E. N. Olson, and D. Srivastava. 2001. The combinatorial activities of *Nkx2.5* and *dHAND* are essential for cardiac ventricle formation. Dev. Biol. 289:190–203.

Yu, J. K., N. D. Holland, and L. Z. Holland. 2002. An amphioxus winged helix/forkhead gene, AmphiFoxD: insights into vertebrate neural crest evolution. Dev. Dyn. 225:289–297.

Zhang, H., and A. Bradley. 1996. Mice deficient for BMP2 are nonviable and have defects in amnion/chorion and cardiac development. Development 122:2977–2986.

Zimmer, C. 1999. At the Water's Edge: Fish With Fingers, Whales With Legs, and How Life Came Ashore but Then Went Back to Sea. New York: Touchstone.

15

Some New Insights into the Embryogenesis of Heart Malformations in the Context of Syndromes

While the figures vary from region to region, a reasonable estimate of the incidence of birth defects is 6.7 per 100,000 (Yang et al., 1997). Of these, 50% are cardiovascular. Not all, but many of these cardiovascular defects occur as part of a syndrome or association of defects. The defects most frequently associated with cardiovascular malformations are in craniofacial structures, but they can also include limbs or other internal organs such as the kidneys. Research is very rapidly identifying genetic linkages with these syndromes, but the pathogenic processes that link a gene to a phenotype are still largely unknown. After describing many of the syndromes that contain cardiovascular malformations as a major characteristic of the phenotype, the genesis of some of these syndromes is discussed in light of our recent insights into modules that were presented in Chapter 14.

Clinically Identified Syndromes with Cardiovascular Malformations

Alagille Syndrome

Alagille syndrome is an autosomal dominant disorder characterized by developmental abnormalities of the heart, liver, eye, skeleton, and kidney. Heart defects are seen in more than 95% of Alagille syndrome patients, and these usually involve stenosis of the pulmonary trunk or arteries, or tetralogy of Fallot (Krantz et al., 1999). Pulmonary stenosis and tetralogy of Fallot are both associated with abnormal addition of myocardium and/or smooth muscle cells to the arterial pole from the secondary heart field (Ward et al., 2005). However, the cause of the more distal pulmonary stenosis is completely unknown. The other clinical manifestations of Alagille syndrome include CHOLESTASIS caused by intrahepatic bile duct underdevelopment, abnormal vertebrae, eye defects, and facial dysmorphism. These defects are the basis for the clinical diagnosis. Several other consistent clinical findings have been reported, although not with as high a frequency as the main manifestations (Emerick et al., 1999). Intracranial bleeding due to vascular anomalies causes significant morbidity and mortality (Emerick et al., 1999). Vascular anomalies have been noted from some of the earliest descriptions of this syndrome (Alagille et al., 1987; Watson and Miller, 1973). An alternative name for the syndrome is arteriohepatic dysplasia, which recognizes the vascular contribution. Pulmonary artery involvement is a hallmark feature of the condition and one of the most common manifestations (Emerick et al., 1999). However, the aorta, renal, celiac, superior mesenteric, and subclavian arteries can also be abnormal (reviewed by Kamath et al., 2004).

Point mutations and microdeletions of a gene known as *Jagged1* (*JAG1* in human gene terminology), located on chromosome 20p12, are associated with Alagille syndrome. Jagged1 is a ligand in the Notch signaling pathway discussed in Chapter 2 (Li, L. et al., 1997). In cardiovascular development, it is expressed in both the heart and pharyngeal region (Loomes et al., 1999). Notch signaling is important in remodeling the venous system, vascular branching and maintenance, and maintaining the smooth muscle coat. It may also suppress differentiation of cardiomyocytes (Chapter 3) and this is essential for the correct specification of myocardial and nonmyocardial cell fates during differentiation of the primary heart fields (Rones et al., 2000).

Currently, *JAG1* mutations have been identified in only 60%–70% of individuals with clinically diagnosed Alagille syndrome, suggesting that the phenotype may be produced by other mutations (Spinner et al., 2001). However, there is currently no evidence suggesting a second locus for the disorder, and the inability to identify a mutation in the 30% of individuals without a *JAG1* mutation is thought to be because of technical limitations in testing this fairly large gene.

(Brachmann-)Cornelia-de Lange

This syndrome is characterized by developmental delay, limb abnormalities, growth restriction, hearing loss, internal organ involvement, and atypical facial appearance with MICROCEPHALY, excessive body hair and confluent eyebrows, thick eyelashes, low frontal hairline, upturned nose, long PHILTRUM, thin lips, mandibular or maxillary receding jaw, and low-set ears. Cardiac anomalies are reported in 14%–28% of cases. They are most commonly ventricular septal defect, atrial septal defect, pulmonary stenosis, tetralogy of Fallot, mitral atresia, stenosis or coarctation of the aorta, atrioventricular septal defect, or single ventricle.

Cornelia-de Lange syndrome is a rare malformation syndrome, although mildly affected patients seem to be rather common. The genetic basis of the syndrome and the reasons for its phenotypic variability are still unknown. One report of a patient with mild manifestation of the syndrome had asymmetric growth of half of the body and irregularly shaped skin pigmentation, which had not been reported previously but is associated with genetic mosaicism in other conditions. Thus, the suggestion has been made that the syndrome is possibly the result of mosaicism for a somatic mutation or submicroscopic deletion (Zankl et al., 2003). This would also explain the heterogeneity of the heart defects seen, as they are not united by any single developmental process.

Campomelic Dysplasia

This is a frequently lethal skeletal malformation syndrome characterized by congenital bowing of the femur and tibia, club foot (talipes), hypoplastic scapulae, 11 pairs of ribs, small jaw, and small chest. One third of the patients have heart malformations that include ventricular septal defect, atrial septal defect, and tetralogy of Fallot. Three quarters of males with campomelic dysplasia have partial to complete sex reversal. Most individuals die as neonates from pulmonary hypoplasia. This condition is caused by heterozygous mutation in *SOX9*, located on 17q24 (Foster and Graves, 1994; Kwok et al., 1995; Wagner et al., 1994). SOX9 is a transcriptional regulator containing a DNA binding HMG MOTIF that is capable of directing nuclear import and DNA bending. It is required along with *SRY*, the male sex determining gene, to activate testis-forming genes, repress ovary-forming genes, or both (Harley et al., 2003). It is also important in a cascade of genes expressed in the decision to make bone or cartilage (Eames et al., 2004).

In the heart, Sox9 is expressed during epithelial–mesenchymal transformation to form the cushion tissue (Chapter 9). In *Sox9*-null mutants, endocardial cushions are markedly hypoplastic, and Nfatc1 is ectopically expressed in that it is not restricted to endothelial cells. *Sox9*-deficient endocardial mesenchymal cells fail to express ErbB3, which is required for endocardial cushion cell differentiation and proliferation (Akiyama et al., 2004). While defective development of cushion tissue might explain the atrial and ventricular septal defects, it is likely that abnormal development of the secondary heart field underlies the tetralogy of Fallot, and there is no currently known association of Sox9 with development of the secondary heart field.

CHARGE

CHARGE is an acronym for Coloboma (or gap) in the iris or retina, Heart defects, Atresia of the nasal passages, Retardation of both mental and somatic development, Genital anomalies, and Ear abnormalities or deafness (Pagon et al., 1981). Atresia of the nasal passages (choanae) or coloboma are obligatory for the diagnosis, but two of the other features must also be present. This syndrome shares many characteristics with VACTERL association and Goldenhar syndrome (see later). It is estimated that the incidence is 1:12,000 (Kallen et al., 1999, Khadilkar et al., 1999). The cardiac anomalies include conotruncal malformations (32%), tetralogy of Fallot (26%), atrioventricular septal defect (19%), patent ductus arteriosus (17%), right or left outflow anomaly (14%), aortic arch malformation (6%), atrial septal defect (6%), and ventricular septal defect (3%) (Williams, 2005).

The pathogenesis of CHARGE syndrome is unknown although several hypothetical mechanisms have been proposed. These include exposure to teratogens; intrauterine insult during days 35–45 of pregnancy; and generalized disturbance of the mesoderm and/or neural crest (Meter and Weaver, 1996; Oley et al., 1988; Siebert et al., 1985; Van Warburg, 1982; Wright et al., 1986). Some evidence points to a genetic cause, as several patients who have been reported with the CHARGE phenotype have chromosomal abnormalities and show autosomal dominant inheritance of a mild CHARGE phenotype (Mitchell et al., 1985a,b). Other evidence for genetic transmission of the syndrome includes concordance in monozygotic twins and triplets (Blake et al., 1989; Oley et al., 1988; Tellier et al., 1998).

Some patients have been shown to have mutations or deletions in a chromodomain helicase DNA-binding gene (*CHD*)*7* located on chromosome 8q12 (Vissers et al., 2004). CHD7 regulates expression or repression of cassettes of other genes by altering chromatin structure. The changes in chromatin structure are stable changes that can be maintained throughout subsequent cell division and differentiation (Cavalli and Paro, 1998). CHD7 is expressed in tissues commonly involved in CHARGE syndrome, although some expression can be detected in all tissues. The highest expression is in the brain, kidney, and skeletal muscle (Nagase et al., 2000). However, only about 60% of CHARGE patients tested have identifiable mutations in the *CHD7* gene, which again suggests that CHARGE syndrome has heterogeneous etiologies (Williams, 2005). Clues to the function of CHD7 are obtained from the POLYCOMB PROTEINS, which are other members of this chromatin remodeling family of genes that provide "epigenetic memory." Polycomb-M33-deficient mice show poor growth, early mortality, multiple skeletal anomalies, and proliferation defects in several cell

types (Core et al., 1997). The skeletal malformations are homeotic in nature and imply dysregulation of *Hox* genes. These changes are similar to those seen in null mutants for *mel-18* and *bmi-1*, two other members of the Polycomb group genes (Akasaka et al., 1996; Alkema et al., 1995; van der Lugt et al., 1994). This implies potential interaction between these genes in the regulation of *Hox* complexes in mice. *Hox* genes of the bithorax complex, which is controlled by the polycomb genes, are important in *Drosophila* heart tube development (Perrin et al., 2004). Interaction of polycomb and xbmi-1 proteins in *Xenopus* shows that the same types of multimeric polycomb gene complexes are also formed in vertebrates (Reijnen et al., 1995).

DiGeorge, Velocardiofacial (Sphrintzen), Conotruncal Anomaly Face, Opitz GBBB, Cayler and CATCH-22

The DiGeorge phenotype appears to result from deficiencies at a multitude of genetic loci. The most well studied has been HEMIZYGOUS INTERSTITIAL DELETION of 22q11 (Fig. 15.1), which is the most common microdeletion resulting in a syndrome (Funke et al., 1999). It occurs in about 1:4000 live births (Yagi et al., 2003). However, other loci are associated with the phenotype. Even so, the 22q11 microdeletion is associated with 40%–90% of patients with the phenotype depending on the center reporting the study. The cardiovascular malformations include interrupted arch and other malformations of the great arteries (Fig. 15.2) (60%–90% of patients), persistent truncus arteriosus (40%–50%), pulmonary atresia (27%), tetralogy of Fallot (26%–35%), and ventricular septal defect (16%–17%). Transposition of the great arteries, atrial septal defect, double outlet right ventricle, tricuspid atresia, and double aortic arch are seen in a small percentage of DiGeorge patients (1%–2%) (Iserin et al., 1998;) Marino et al., 2001; Volpe et al., 2003). Extracardiac anomalies include absent thymus (28%), hypocalcemia (hypoplastic parathyroid glands) (21%), oropalatal abnormalities such as VELOPHARYNGEAL INSUFFICIENCY and cleft soft palate (14%), immunologic deficiencies (12%), and abnormalities in the central nervous system (12%), renal tract (12%), gastrointestinal system (7%), and skeleton (7%). Patients with this deletion are also likely to have abundant or unruly scalp hair; narrow palpebral fissures; and a laterally "built-up" nose (Ravnan et al., 1996). The microdeletion is always associated with at least one non-cardiac anomaly (Marino et al., 2001). Linkage of the 22q11 deletion with the phenotype is complicated by the association of other syndromes with the deletion. A small subgroup of patients with VACTERL association (see later) have the 22q11 deletion (Digilio et al., 1999). To make things even more complicated, a few individuals without any of the clinical signs of DiGeorge syndrome have been found with the 22q11 microdeletion (Iserin et al., 1998). This suggests that a plethora of modifying genes are involved in development of the phenotype.

Figure 15.1. 22q11 deletion is visualized by fluorescence in situ hybridization (FISH) using a probe to the deleted region (*red dots*) and a second probe to chromosome 22 in (*green dots*). As can be seen from this preparation of metaphase chromosomes, there are 2 chromosomes 22 (four green dots) but only one set has the 22q11 region (two red dots). (From Chen et al., 2005, with permission.)

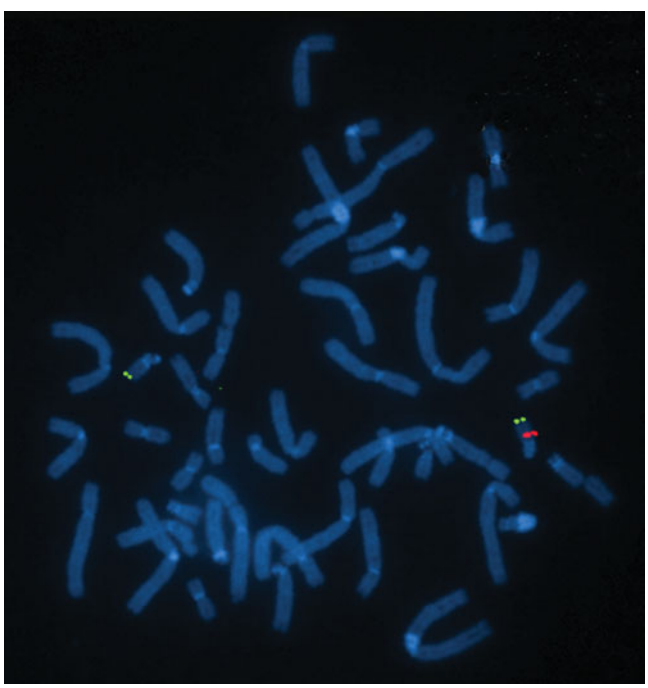

Figure 15.2. Magnetic resonance imaging of the great arteries in a DiGeorge patient. Left aortic arch with an isolated right subclavian artery (RSCA). Volume rendering with shaded surface display from the coronal view (top) and the right anterior oblique view (bottom) showing connection of the RSCA to the vertebral artery (VA) and no communication with the innominate artery (IA). (From Johnson et al., 2005, with permission.)

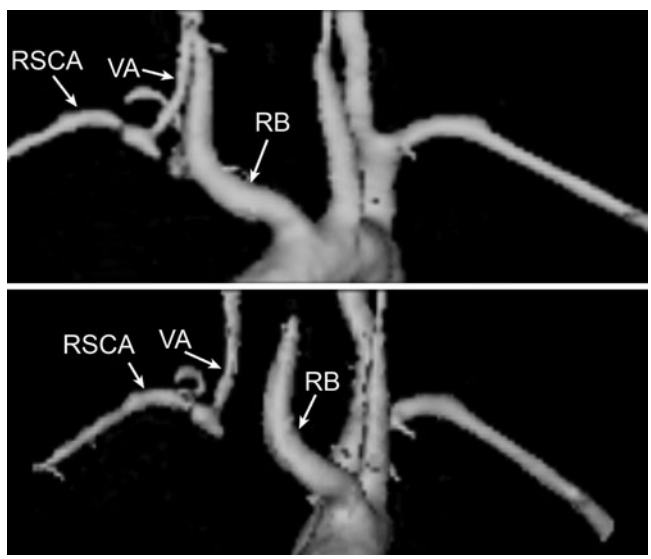

Diagnosis of 22q11.2 deletion is made by fluorescence in situ hybridization (FISH) using a probe specific to the deleted region or, alternatively, polymerase chain reaction (PCR) (Driscoll, 2001). Several genes and microdeletions have been tested to determine if an animal model of the syndrome can be made. One of the candidate genes, *Hira* is expressed in the neural crest and in neural crest-derived tissues. Functional attenuation of *Hira* in the chick cardiac neural crest results in persistent truncus arteriosus, one characteristic of DiGeorge syndrome, but does not affect the development of the aortic arch, a major characteristic of the syndrome (Farrell et al., 1999). Interruption of the aortic arch is found in an engineered mouse model that mimics the microdeletion found on chromosome 22q11 (Lindsay et al., 1999). By adding successive genes back into this mouse, *Tbx1* was identified as the gene with primary responsibility for this phenotype. Indeed, null expression of *Tbx1* alone is associated with persistent truncus arteriosus and interrupted arch (Lindsay et al., 2001). A *TBX1* mutation has now been described in two unrelated patients with DiGeorge phenotype, and a family without the 22q11.2 deletion. One is diagnosed with sporadic conotruncal anomaly face syndrome/velocardiofacial syndrome and one with sporadic DiGeorge syndrome. Three patients from a single family have *TBX1* mutation associated with conotruncal anomaly face syndrome/velocardiofacial syndrome (Yagi et al., 2003).

Sonic hedgehog is necessary for Tbx1 expression, and Tbx1 expression appears to be required for endodermal expression of *Fgf8* (Garg et al., 2001; Vitelli et al., 2002; Yamagishi et al., 2003). Null expression of Fgf8 also mimics many aspects of the phenotype, suggesting that abnormal Fgf8 signaling may be a major effector linking the genotype with the phenotype (Abu-Issa et al., 2002; Frank et al., 2002; Vitelli et al., 2002). Neural crest ablation in chick embryos also produces a DiGeorge-like phenotype, and neural crest was thought for many years to be the major cell population affected (Kirby and Bockman, 1984; Van Mierop and Kutsche, 1984). It is now thought that neural crest development is not normal, but this is secondary rather than causative. Tbx1 is also expressed in the secondary heart field, and the *Tbx1*-null mouse shows reduced proliferation of the cells in the secondary heart field that should add myocardium to the arterial pole of the heart (Xu et al., 2004). This abnormality could lead to the conotruncal anomalies seen in these syndromes but it also does not explain the interrupted arch phenotype.

Several other genes are candidates for the phenotype based on animal models with phenotypes resembling the DiGeorge phenotype. The naturally occurring mutation in the *Pax3* gene found in the Splotch mouse shows some aspects of the phenotype, including persistent truncus arteriosus; variations in the patterning of the great arteries; and reduced or aplastic thymus, parathyroid, and ultimobranchial bodies. However, this mouse also has significant other phenotypic variations, such as cranioschisis, that are not found in patients with the 22q11 deletion (Conway et al., 1997; Epstein, 1996; Franz, 1989).

Down—Trisomy 21

The major phenotypic features of Down syndrome are mental retardation and hypotonia. Congenital heart defects are present only in a subset of patients, and the types of defects vary widely. The major defects seen are atrioventricular septal defect, ventricular septal defect, isolated secundum atrial septal defect, and tetralogy of Fallot (Freeman et al., 1998). Down syndrome is usually caused by the presence of an extra chromosome 21 (Fig. 15.3), but a subset of the diagnostic features may be caused by trisomy limited to region 21q22.3 (Baptista et al., 2000; Korenberg et al., 1994).

Increased adhesiveness of mesenchymal cells in the atrioventricular cushions has been proposed as the pathogenetic

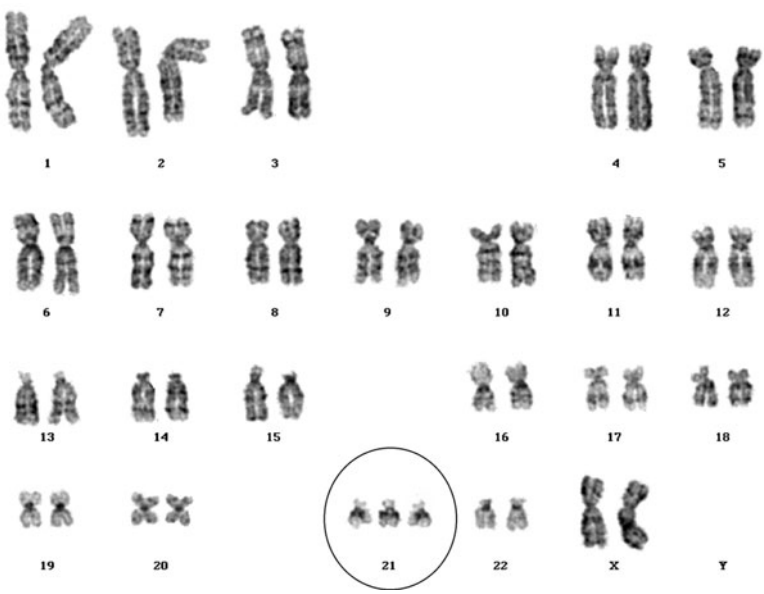

Figure 15.3. Chromosome analysis shows trisomy 21 (circled). (From Antonarakis et al., 2004, with permission.)

mechanism leading to the heart defects. Indeed, all of the associated heart defects seem to involve abnormal development of the mesenchymal cells generated by epithelial–mesenchymal transformation of the endocardium in the atrioventricular canal (Kurnit et al., 1985). Several of the genes in the 21q22 region are cell adhesion molecules. One of these genes called *Down syndrome cell adhesion molecule* (*DSCAM*), is expressed in the heart during cardiac development (Barlow et al., 2001). A closely related cell adhesion molecule, neural cell adhesion molecule (Ncam), is associated with increased adhesiveness when overexpressed, suggesting that DSCAM might mediate increased adhesiveness, which potentially causes the atrioventricular cushions to be smaller or otherwise abnormal (Paoloni-Giacobino et al., 1997). In addition, some collagens are expressed on chromosome 21. Genetic variation in the *COLLAGEN6A1*, also on chromosome 21, shows some linkage with heart defects (Davies et al., 1995). One other gene that is not a cell adhesion molecule itself but could alter cell adhesivity through other mechanisms is *DSCR1* (down syndrome critical region 1). It is overexpressed in brain and heart of Down syndrome individuals (Fuentes et al., 1995, 2000). The DSCR1 gene product interacts with CALCINEURIN A. Overexpression of this gene inhibits calcineurin-dependent gene transcription through the inhibition of Nfat translocation to the nucleus (Fuentes et al., 2000). Translocation of Nfat to the nucleus is an important step in epithelial-mesenchymal transformation and formation of the atrioventricular cushion tissue (Nishii et al., 2001).

Ellis-van Creveld (Chondroectodermal Dysplasia)

This is a relatively rare, autosomal recessive skeletal dysplasia characterized by short limbs, short ribs, postaxial polydactyly, and cardiac and renal anomalies with dysplastic nails and teeth. It is caused by mutations in *EVC* and *EVC2* on chromosome 4p16 (Ruiz-Perez et al., 2003). The cardiac defects are common atrium, atrioventricular septal defect, or both, atrial septal defect, ventricular septal defect and situs inversus. *EVC* and *EVC2* lie in a head-to-head configuration that is conserved from fish to man. The defects caused by mutation in either gene are phenotypically indistinguishable (Ruiz-Perez et al., 2003). The functions of the *EVC/EVC2* genes are at present unknown.

Holt-Oram Syndrome

Holt-Oram syndrome is a heart–hand malformation syndrome linked to point mutations in the *TBX5* gene (Basson et al., 1997; Li, Q. et al., 1997). It segregates in an autosomal dominant transmission, indicating haploinsufficiency, and it occurs in at least 1/100,000 live births (McDermott et al., 2005). The syndrome is characterized by upper limb anomalies involving the radial or thumb side of the wrist and hand (Fig. 15.4) and congenital heart defects. The upper limb deformity may affect the hands unilaterally or bilaterally but in the case of bilateral malformations, it affects the two sides differently to give asymmetric hand malformations. The most common cardiovascular abnormalities associated with Holt-Oram phenotype include atrial septal defects (usually of the ostium secundum type), muscular ventricular septal defects with abnormal trabeculation, and cardiac conduction disease, which can occur regardless of the presence of structural heart defects (Basson et al., 1997; Bruneau et al., 1999; Li, Q. et al., 1997; McDermott et al., 2005). Mutations in *TBX5* are associated with 70% of Holt-Oram patients.

Tbx5 is uniformly expressed throughout the cardiogenic fields in amphibian, chick, and mammalian embryos (Bruneau et al., 1999; Hatcher et al., 2000; Horb and Thomsen, 1999). As the heart loop forms, Tbx5 expression continues in the presumptive left ventricle but is excluded from the right ventricle, right part of the ventricular septum and outflow tract. The trabeculae, both superior and inferior vena cavae, and the atrial side of the atrioventricular valves also express high levels of Tbx5 (Bruneau et al., 1999; Hatcher et al., 2000). This expression pattern is maintained during the rest of heart development.

The actual pathogenetic mechanism of the cardiac phenotype is still unclear but recent data suggest that Tbx5 can act to arrest myocardial proliferation and thus may modulate myocardial growth (Hatcher et al., 2001). Cx40 deficiency may account for the skeletal malformations in Holt-Oram syndrome, as Tbx5 promotes expression of Cx40 in limb bones and a 50% reduction in either Tbx5 or Cx40 produces bone abnormalities, demonstrating their crucial control over skeletal development. Tbx5 via Cx40 also controls expression of

Figure 15.4. Two types of upper limb malformations. (*A*) Typical upper limb malformation of Holt-Oram syndrome is evident in the left hand with absent thumb and malformation of the wrist, causing disarticulation of the carpal bones with the radius bone. These are typical preaxial ray malformations associated with *TBX5* mutation. (*B*) For comparison, the left hand of an individual with a postaxial ulnar ray malformation (associated with ulnar–mammary syndrome caused by mutations in *TBX3*). The thumb and radial ray are normal. However, digits 4 and 5 are absent. (From McDermott et al., 2005, with permission.)

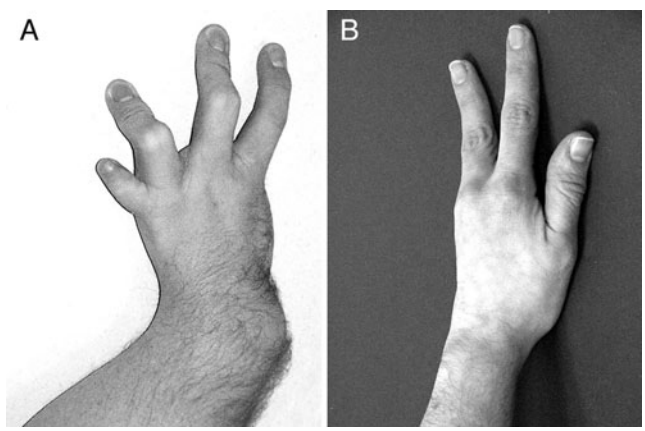

Sox9, a factor essential for chondrogenesis and skeletal growth (Pizard et al., 2005).

Heterozygous *Tbx5*-null mice phenocopy some attributes of the human Holt-Oram syndrome. However, 50%–80% of perinatal mortality of the heterozygous mutant mice is dependent on genetic background, and since death in early infancy is not a characteristic of Holt-Oram syndrome, the mouse model is not a perfect representation of the human disease. However, the *Tbx5* heterozygous null mice that survive beyond the perinatal period do tend to have large ostium secundum atrial septal defects. Heterozygotes that die in the perinatal period have membranous or muscular ventricular septal defect in addition to atrial septal defects (Bruneau et al., 2001). These mice also have conduction system abnormalities, involving both the sinoatrial and atrioventricular nodes. The conduction system abnormalities mimic those described for human Holt-Oram syndrome (Hatcher et al., 2001). Homozygous null *Tbx5* mice die at E10.5 with severely hypoplastic sinus venosus, atrium, and presumptive left ventricle and a failure of looping by E8.5 (Bruneau et al., 2001). Atrial septation is never initiated, and no atrioventricular cushions can be seen.

Kabuki

Kabuki is a traditional form of Japanese theater in which the eyebrows are made up to express the role. Patients with this syndrome have faces characteristic of the made-up actors (Fig. 15.5). Caucasian children have an oriental look (Schrander-Stumpel et al., 2005). This characteristic face occurs in 100% of the patients and is frequently associated with cleft palate or bifid uvula, abnormal dentition, and dysplastic ears. The most constant feature is long palpebral fissures together with eversion of the lateral part of the lower eyelid and arched eyebrows that are sparse or notched in the lateral one third. Depressed/flat nasal tip is also a frequent finding (Schrander-Stumpel et al., 2005). Other features include skeletal anomalies (90%), including short fingers with abnormal fingerprints (95%), and the presence of fetal fingertip pads, mild to moderate mental retardation (over 90%), and pre- or postnatal growth deficiency (70%). Congenital heart defects are a cardinal feature and are seen in 32%–58% of children with the syndrome (Wessels et al., 2002). The defects include coarctation of the aorta or atrial or ventricular septal defect. There is a tendency for male preponderance in patients with coarctation of the aorta. There is an overlap between cardiac malformations seen in Kabuki syndrome and those of Turner syndrome, leading to the suggestion that the syndrome is X-linked (Digilio et al., 2001). Even so, the etiology of the syndrome is not known, and a diagnostic laboratory test is not available. A recent report shows 8p22–8p23.1 duplication in six patients with the syndrome (Milunsky and Huang, 2003). However, this duplication was not found in a separate cohort of 28 patients (Miyake et al., 2004).

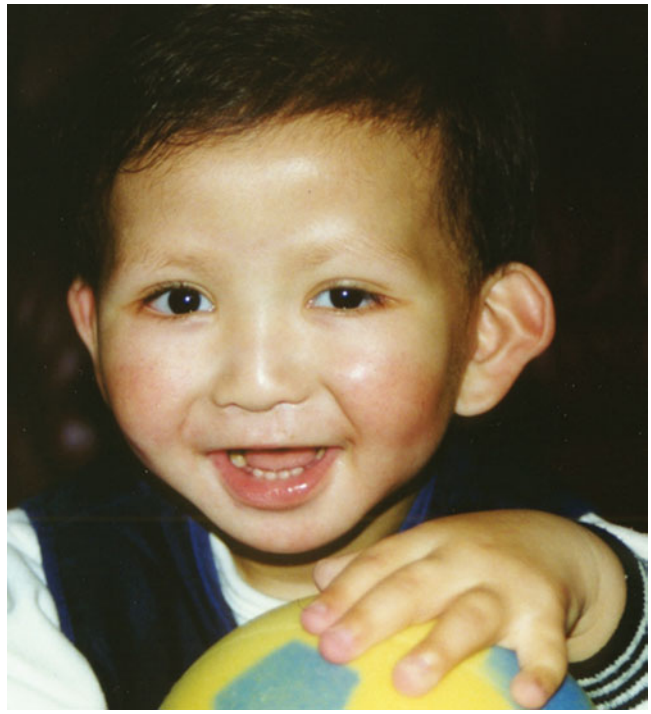

Figure 15.5. Two- and a half-year-old boy with Kabuki syndrome. Note the short fifth finger on both hands, with the top part turned inside, rather large slightly malformed ears, and arched eyebrows. (Photo courtesy of F. Faase www.iwriteiam.nl/Andy.html and Prof. dr. Connie Schrander-Stumpel, clinical geneticist, Maastricht, the Netherlands.)

Neurofibromatosis Type 1 (von Recklinghausen Neurofibromatosis)

Neurofibromatosis type 1 or von Recklinghausen neurofibrosis is a genetic disorder that occurs in 1 of 4000 neonates. Patients are characterized by benign and malignant tumors and also have cardiovascular defects, including pulmonary valvular stenosis and vascular abnormalities. The *NF1* gene is mutant in this disease. Nf1 suppresses Ras signaling in endothelial cells. Oversignaling by the ras pathway in the outflow endocardium results in hyperactivation of Nfat and excessive production of cushion mesenchyme in the conal and truncal cushions, which is most likely the cause of pulmonary stenosis (Gitler et al., 2003).

Noonan

This syndrome occurs in 0.5–1:1000 births (Noonan, 1968). Noonan syndrome is an inherited autosomal dominant disease (Tartaglia et al., 2001, 2002, 2003, 2004). However, it is genetically heterogeneous, with nearly 50% of cases caused by gain-of-function mutations in *PTPN11* on chromosome 12, the gene encoding the protein tyrosine phosphatase SHP2 (Jongmans et al., 2005; Weiss et al., 2004). The defining features

Figure 15.6. Typical facial features and multiple naevi on the back of an adult patient with Noonan syndrome. (From Jongmans et al., 2005, with permission.)

are short stature, slight facial dysmorphism, and webbed neck (Fig. 15.6). Congenital heart defects occur in about 60% of cases. The heart defects include left ventricular hypertrophy, pulmonary stenosis, atrial septal defect, and dysplastic pulmonary valve. It is not known how hyperfunctional SHP2 causes these defects. However, it is known that SHP2 is a cytoplasmic Src-homology 2 domain-containing protein tyrosine phosphatase that plays an important role in intracellular signaling during development (Tartaglia and Gelb, 2005).

Ritscher-Schinzel (Cranio-Cerebello-Cardiac, 3C)

Clinical features of 3C syndrome include craniofacial anomalies (abnormally large head with prominent forehead and occiput, enlarged parietal foramina, wide-set eyes, down-slanting palpebral fissures, ocular colobomas, depressed nasal bridge, narrow or cleft palate, and low-set ears), cerebellar malformations, and cardiac defects. Cardiac defects include ventricular septal defect, atrial septal defect, tetralogy of Fallot, double outlet right ventricle, hypoplastic left heart, aortic stenosis, pulmonary stenosis, and valvular anomalies (Leonardi et al., 2001). Several patients and families have been identified with deletions of a 1.3 Mb critical region of chromosome 6p25. However, specific deletions or disease-causing mutations have not been identified in this minimal critical region (Descipio et al., 2005).

Short Rib-Polydactyly

This classification defines a group of lethal skeletal dysplasias inherited as an autosomal recessive. It is distinguished by thoracic hypoplasia, short ribs, short limbs, and extra fingers. There are four variants of the syndrome, types I–IV; however, only type I (Saldino-Noonan syndrome) is associated with cardiac anomalies, which are present in 50% of patients (Pajkrt et al., 2004). The cardiac anomalies include atrioventricular septal defect, persistent left superior vena cava, complete situs inversus, transposition of the great arteries, coarctation of the aorta, hypoplastic right or left heart, and ventricular septal defect (Pajkrt et al., 2004). No etiologies have been proposed.

Smith-Lemli-Opitz Syndrome

Smith-Lemli-Opitz syndrome was first recognized in 1964 (Smith et al., 1964). Patients are characterized by developmental delay and mild to major, even lethal dysmorphic features that include extra fingers, cataracts, renal anomalies, ambiguous genitalia in males, and severe malformation of the forebrain. Cardiac anomalies occur in about 40% of cases (Pajkrt et al., 2004). The most common cardiac defects are atrioventricular septal defect, atrial septal defect, patent ductus arteriosus, and ventricular septal defect. Tetralogy of Fallot, aortic stenosis or coarctation, hypoplastic left heart syndrome, pulmonary stenosis, or tricuspid atresia are found in a few patients (Lin et al., 1997; Winter et al., 1985). This is an autosomal recessive syndrome resulting from a mutation in the *7-DEHYDROCHOLESTEROL REDUCTASE* gene on 11q13 (Wassif et al., 1998; Waterham et al., 1998), causing abnormal cholesterol biosynthesis that results in hypocholesterolemia with elevated 7-dehydrocholesterol. The high levels of 7-dehydrocholesterol are thought to be teratogenic (Clayton, 1998).

Smith-Magenis Syndrome

Smith-Magenis syndrome is characterized by mental retardation, sleep dysfunction with inverted circadian rhythm of melatonin, hyperactivity, repetitive motions, self-hugging, and self-injurious behaviors (Chen et al., 1996; Smith et al., 1986; Stratton et al., 1986). Patients commonly have short stature, broad face, midface

hypoplasia, bowed or tented upper lip, ocular abnormalities, middle ear and laryngeal abnormalities, hoarse voice, curved spine, hearing loss, signs of peripheral neuropathy, and hypercholesterolemia (Chen et al., 1996; Smith et al., 2002). Less common malformations include cleft palate, renal, or urinary tract anomalies, thyroid dysfunction, immune system dysfunction, seizures, and congenital heart defects (Chen et al., 1996; Smith et al., 2002). A variety of structural heart defects have been identified, including various septal defects, valvular abnormalities, and tetralogy of Fallot (Greenberg et al., 1996). Total anomalous pulmonary venous return was reported in two patients with the syndrome (Myers and Challman, 2004).

Smith-Magenis syndrome is due to a microdeletion of chromosome17p11.2. Haploinsufficiency of the retinoic acid-induced 1 gene (*RAI1*), located in the deleted region, may be responsible for the behavioral, neurological, otolaryngological, and craniofacial aspects of Smith-Magenis syndrome but heart and renal defects are most likely due to hemizygosity of other genes in the 17p11.2 region (Myers and Challman, 2004; Slager et al., 2003). Null mutation of Rai1 in the mouse results in craniofacial anomalies reminiscent of Smith-Magenis syndrome (Bi et al., 2005).

Trisomy 18 (Edward Syndrome)

Trisomy 18 occurs in approximately 1 in 6000 liveborn infants. About 95% of conceptuses with trisomy 18 are thought to die in embryonic or fetal life and only 5%–10% of those born survive beyond the first year. Trisomy 18 is caused by the presence of an extra copy or partial copy of chromosome 18. More than 90% of infants with Trisomy 18 syndrome have a complete extra copy. The extra chromosome is usually maternal. Infants with trisomy 18 are recognized by their small size at birth, prominent occiput, short eyelid fissures, small mouth and jaw, external ear variations, clenched fist with index finger overlapping the third and fifth finger overlapping the 4th, small fingernails, underdeveloped or altered thumbs, short sternum, club feet and extra skin at the back of the neck. They show severe psychomotor retardation, severe growth retardation, and microcephaly. More than 90% of children with trisomy 18 have a congenital heart malformation. The malformations include ventricular and/or atrial septal defect patent ductus arteriosus, double outlet right ventricle, hypoplastic left heart and valve dysplasia usually of the aortic and pulmonary semilunar valves (Carey, 2005).

VACTERL Association

VACTER is an acronym for Vertebral defects, Anal atresia, Cardiac anomalies, Tracheoesophageal fistula with Esophageal atresia, and Renal dysplasia (Quan and Smith, 1973). Limb defects were later noted, and the acronym VACTERL was coined (Kaufman, 1973; Nora and Nora, 1975; Temtamy and Miller, 1974). Other common findings include ear abnormalities, facial clefting, and genitourinary anomalies. The presence of two or more of these anomalies allows clinical diagnosis to be made, and a majority of patients have only two or three of the anomalies associated with this disease. Fewer than 1% of patients have five or more of the anomalies (Khoury et al., 1983). The foregut and hindgut anomalies, limb and foregut anomalies, vertebral and hindgut anomalies, and vertebral and foregut anomalies have the highest association rates (Khoury et al., 1983). Nearly half of patients diagnosed with tracheoesophageal fistula have other features of VACTERL association. The cardiac anomalies that occur as part of this constellation of defects are not well described.

The exact cause of VACTERL association is currently unknown. It affects approximately 1 in 5000 live births (Rittler et al., 1996). More than 1000 cases have been reported in the medical literature (Botto et al., 1997; Khoury et al., 1983; Rittler et al., 1996; Weaver et al., 1986). Around 12% of the affected fetuses are stillborn, and about 48% of the babies born with the syndrome die within the first year of life (Khoury et al., 1983; Rittler et al., 1996). There are very few reported cases of familial occurrence of VACTERL association (Auchterlonie and White, 1982; Czeizel and Ludanyi, 1985; McMullen et al., 1996; Nezarati and McLeod, 1999). Thus, the etiology is currently thought to be multifactorial with significant environmental influences.

A mouse model of VACTERL syndrome has been reported by mutation of *Gli2* and/or *Gli3*, members of the hedgehog signaling pathway (Fig. 15.7). *Gli* genes encode transcription factors used in hedgehog signaling. Shh signaling plays critical roles in the development of both the foregut and hindgut. This suggests that defective hedgehog signaling may play a role in development of the VACTERL phenotype (Kim et al., 2001a,b).

Williams-Beuren Syndrome

Williams-Beuren syndrome is characterized by elf-like facial features, mental retardation, mild growth deficiency, supravalvular aortic stenosis, and anomalies of the aorta and renal arteries (Gosch and Pankau, 1994; Pankau et al., 1992, 1996, 1997; Partsch et al., 1999; Wessel et al., 1994). Coronary artery anomalies also occur and may lead to sudden death, although no information is available defining the risk of sudden death in Williams-Beuren syndrome (Bird et al., 1996; Imashuku et al., 2000; Suarez-Mier and Morentin, 1999; Imashuku et al., 2000; Wessel et al., 2004). Williams-Beuran syndrome is associated with a microdeletion on chromosome 7, but hemizygosity at the *ELASTIN* (*ELN*) locus in the region of the microdeletion may account for the cardiovascular portion of the phenotype (Johnson et al., 1995). Mental retardation and hypercalcemia, which are also associated with the syndrome, are more likely to be caused by other genes flanking the elastin gene on chromosome 7 (Meng et al., 1998). *LIMK1*, one of the flanking genes, is deleted in all instances of Williams-Beuren syndrome where the elastin gene is deleted. Isolated cases of supravalvular aortic stenosis are usually accompanied by elastin deletion without a *LIMK1* deletion (Wu et al., 1998).

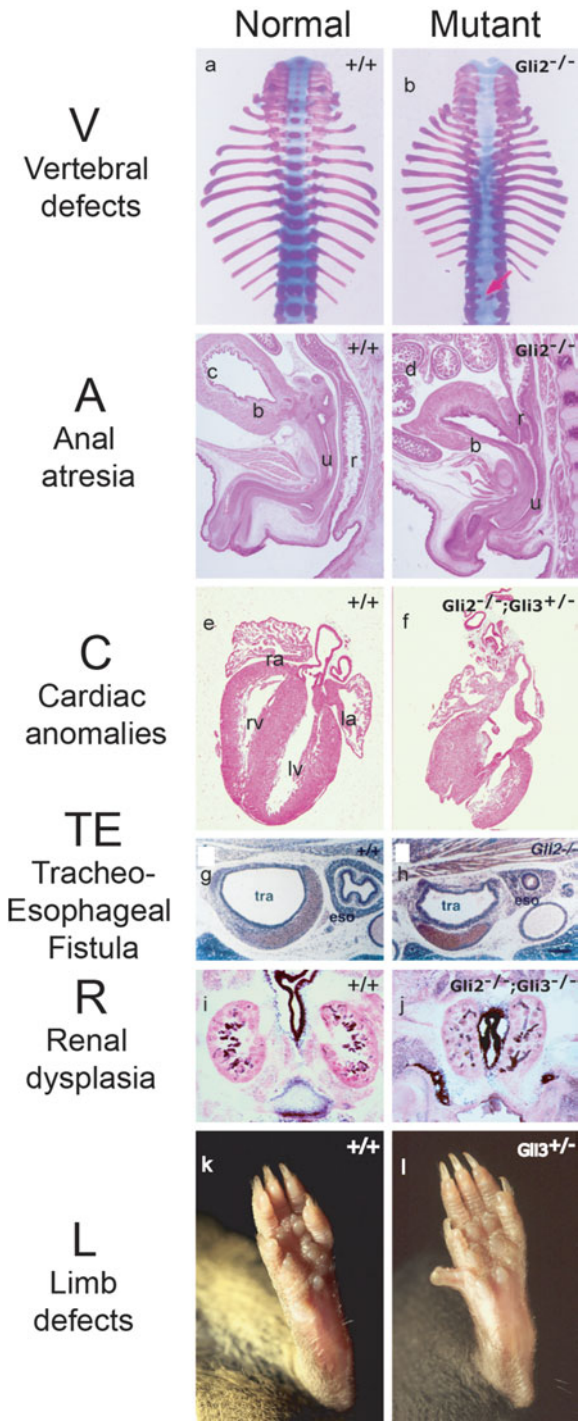

Figure 15.7. Mouse model of VACTERL association caused by disrupting members of the sonic hedgehog signaling pathway. (From Kim et al., 2001, with permission.)

Syndromes Caused by Teratogens

Anticonvulsant Syndromes

Epilepsy is a common neurological disorder in women who become pregnant, and fetuses exposed to anticonvulsants in utero have an increased risk of malformations (Jick and Terris, 1997). Characteristic dysmorphic features and malformations occur with fetal exposure to anti-epileptic drugs including phenytoin, valproate, and carbamazepine. The phenotype includes typical facial features, neural tube defects, genital, musculoskeletal, and cardiac defects. Behavioral disorders include autism and hyperactivity (Moore et al., 2000). Cardiac defects occur in about 25% and include ventricular septal defect, atrial septal defect, pulmonary stenosis, and aortic stenosis (Kozma, 2001).

Fetal Alcohol Syndrome

Maternal alcohol use during pregnancy can lead to fetal alcohol syndrome (FAS), which is characterized by growth retardation, craniofacial malformations, heart and neural defects. Paternal abuse of alcohol can also lead to cognitive and behavioral abnormalities that include learning and memory deficits, hyperactivity, and poor stress tolerance (Abel, 2004). The cellular and molecular mechanisms responsible for ethanol teratogenicity remain unknown but the phenotype suggests that neural crest cell development is perturbed. Research suggests that cranial neural crest cells are eliminated by ethanol-induced apoptosis (Cartwright and Smith, 1995b). Ethanol exposure enhances cell death within areas populated by cranial neural crest cells, particularly in the craniofacial mesenchyme. This neural crest cell death can be rescued by treatment of the embryos with sonic hedgehog (Ahlgren et al., 2002).

Genetic background is a major risk factor for fetal alcohol syndrome in mice and chick models (Cartwright and Smith, 1995a; Ogawa et al., 2005). In mouse models, alcohol treatment specifically compromises development of the heart and neural tube in one strain of mice, whereas it specifically decreases the number of somites and the development of pharyngeal arches in a separate strain. This unique pattern of vulnerability in specific organs suggests a significant genetic influence that may be more important in severity of the phenotype than the amount or timing of maternal alcohol ingestion (Ogawa et al., 2005).

Vitamin A Teratogenesis (Retinopathy)

Hypervitaminosis A, caused by treatment with the active (all-*trans*) form of retinoic acid was one of the earliest teratogenic models of heart defects (Wilson and Warkany, 1950). Retinoic acid exposure is associated with dextroposed aorta and a wide diversity of abnormal patterning of the great arteries (Bouman et al., 1997; Gruber et al., 1996; Mendelsohn et al., 1994; Tran and Sucov, 1998). Some insight has been gained by null mutation of combinations of retinoid acid (RAR) and/or retinoid X (RXR) receptors in mice. Depending on the combination of receptor mutations, selective defects can be obtained in specific cardiovascular structures. Certain combinations of the isoforms control cell maturation. Premature maturation of the myocardium occurs in double mutants, which leads to severe hypoplasia of the ventricles (Kastner et al., 1997; Lee et al., 1997). However,

the pathogenic mechanism for other heart defects seen in retinoic acid teratogenesis is currently not known. Retinoic acid serves as an endogenous signaling molecule in many normal aspects of cardiovascular development which have been noted in many other chapters.

Modules as Substrates Linking Genotype to Phenotype

As can be seen from these descriptions, some syndromes affect adjacent regions of the body, but most MALFORMATION SEQUENCES involve development in widely separated body regions at very different times in development. What are the shared factors that allow these seemingly heterogeneous defects? Any hypothesis about the pathogenesis of a syndrome with multiple components should meet three criteria: (1) it must explain all of the malformations associated with the syndrome; (2) it must explain why certain anomalies are not associated with the syndrome; and (3) it should predict anomalies that could be associated with the syndrome but have not yet been described. In the end, there must be molecular confirmation of the proposed mechanism (Williams, 2005). In the last chapter, the idea of modules was introduced as a concept that is important in evolution. Modules are semi-autonomous units that can take the form of morphological fields, gene regulation networks, signaling, cell types, and so forth. As introduced in Chapter 14, this broad concept of modular development provides a substrate for understanding how gradual changes can take place in evolution by affecting these semi-autonomous units without compromising the viability of the organism as a whole. This same concept of modules is useful in understanding how certain sequences of malformations might occur. Obviously, the majority of malformation sequences are not based in single morphological modules, since they affect multiple parts of the body. There is one noted exception discussed in the next section, the cardiocraniofacial field. The other modules that should be considered as effectors of malformation sequences are functional, cell lineage, transcriptional, and signaling.

In producing a sequence of malformations, the only requirements for the module are that it is common to all aspects of the sequence and that it is subject to the same error in all the morphological modules, that is, developmental fields that are affected in the sequence of malformations. For example, a transcriptional or signaling module might contain a mutant component that disrupts the function of an entire network in all the fields where it is normally expressed and where the defect is seen. So long as the mutation is a germ line mutation, the analysis is straightforward. However, some syndromes and/or heart defects are suspected to be somatic mutations resulting in mosaicism, and then the search for causation becomes infinitely more complicated.

A good example of a somatic cell mutation that affects a cell lineage module is found with *NKX2–5* mutations. *NKX2–5* mutations have been found in the hearts of patients with diseased heart tissues, while the mutations are not present in normal, unaffected heart tissue of the same patient. This indicates that the mutations are somatic and, further, that the cells comprising the heart are mosaic. Similar mutations have been found in Down syndrome patients with cardiac malformations (Reamon-Buettner and Borlak, 2004). In this case, a cell lineage module has most likely been affected by malfunction of a transcriptional module.

A simpler example of a germ line mutation in a transcriptional module can be nicely illustrated using the Holt-Oram syndrome. In this syndrome, patients have a familial history of congenital heart defects and preaxial radial ray upper limb defects (Fig. 15.4). In about 70% of cases, the malformations in this syndrome are strongly linked with mutations in *TBX5*, a well-characterized transcriptional regulator that is expressed in both of the morphological modules affected, i.e., the myocardium and the mesenchyme that forms the forelimb bud. Transcriptional regulators can dramatically affect development by altering cassettes of downstream targets within a particular morphological module without affecting other modules.

The mutations in the *TBX5* gene associated with heart and hand defects, affect the ability of the TBX5 protein to activate transcription, bind DNA or interact with other transcriptional complexes or proteins. The best studied are missense mutations in the T-box (Basson et al., 1997; Li, Q. et al., 1997; Muller and Herrmann, 1997). The mutant protein is unable to activate the *Nppa* promoter because of reduced ability both to bind DNA and interact with Gata4 or Nkx2.5 (Fan et al., 2003a,b; Garg et al., 2003; Hiroi et al., 2001; Plageman and Yutzey, 2004). However, failure to activate the *Nppa* promoter, while it might affect heart development, probably does not affect hand development.

The heart and hand both arise from lateral plate mesoderm, but at vastly different times and places in the embryo; thus different morphological modules are subject to incorrect development.

In the limb, Tbx5 functions downstream of Wnt signaling to regulate *Fgf10,* which, in turn, maintains Tbx5 expression and initiates and maintains Fgf8 expression during forelimb outgrowth. (Ng et al., 2002; Takeuchi et al., 2003). In the chick, misexpression of dominant-negative forms of Tbx5 causes disruption of the anterior limb mesenchyme and the structures that are derived from this region of the limb bud. The most common phenotype is absence of the radius and anterior digits, that is, thumb and forefinger. This is associated with downregulation of Fgf10 and Fgf8 in the anterior limb (Rallis et al., 2003). Thus, Tbx5 expressed in its forelimb module downregulates proliferation, possibly through regulation of growth factors, in the case of the forelimb Fgf8 and Fgf10 (Rallis et al., 2003).

Does Tbx5 perform a similar function in the heart? Several of the T-box transcription factors control proliferation in the heart, and in fact Tbx5 has been shown to control proliferation of myocardial cells in vitro and in chick hearts with mosaic expression of Tbx5 in vivo. Immunohistochemical studies of

human hearts also demonstrated that TBX5 expression is inversely related to cellular proliferation (Cai et al., 2005; Hatcher et al., 2001). However, no cell cycle components have been shown to be directly affected by Tbx5 as a transcriptional regulator, so it may be the case that proliferation is modulated via growth factor signaling, and the Fgf family would be a prime candidate for regulation of myocardial proliferation. Indeed, Tbx5 activates the mouse *Fgf10* promoter in the heart by means of a single T-box binding element in transfected nonmyocardial cells (Agarwal et al., 2003; Xu et al., 2004).

This illustrates for two different diseases, one associated with somatic mosaicism and one with germline mutation, how the concept of modules can be used to explain all of the malformations associated with the syndrome. It further explains why certain other anomalies are not associated with the syndrome, that is, malformations do not occur where the mutant genes are not expressed. The third criterion that it should predict anomalies that could be associated with the syndrome but have not yet been described is easily applied by investigation of the other morphological modules where Tbx5 is expressed. Indeed, Tbx5 was recently found to be expressed in the human retina. Recognition of this novel expression domain was quickly followed by the discovery of ocular malformations in two unrelated families with mutations in the *TBX5* gene (Gruenauer-Kloevekorn and Froster, 2003).

Face, Brain, and Heart as a Morphological Module

While most sequences of malformations found in syndromes are not part of a single morphological module, the DiGeorge or velocardiofacial syndrome involves abnormal development of the face, brain and heart. Abnormal brain development is inferred from the abnormal behavioral characteristics of patients with diagnosed DiGeorge syndrome, although it should be emphasized that no congenital structural abnormality of the brain has yet been identified.

Development of the heart, brain and face can be understood best when they are considered initially as a single "cardiocraniofacial" morphological module. Because the DiGeorge phenotype affects each of the components in this initial module, it is most likely that abnormal development is based in the morphological module. The cardiocraniofacial module, comprised initially of neural ectoderm, definitive endoderm and lateral plate mesoderm, is subdivided during subsequent development into the less global morphological modules of heart, brain, and face, which in turn are subdivided many more iterations (Fig. 15.8). A morphological module in this context is a spatial domain in which every part has a stage determined by the state of neighboring parts, so the whole has a specific relational structure (Goodwin, 1990). Both genes and the environment set the values of parameters that establish the module and sustain its characteristic growth and subdivision. Therefore, genetic and environmental factors do not primarily cause the module because they do not define modules but only realize or stabilize some of the possibilities of the module. What governs the transformation of morphological modules and defines the set of possible forms during development? The development of the module is dependent on contingent interaction and temporal sequence, that is, networks and dialogue (Goodwin, 2002; Oyama, 1994). How does a single gene or set of genes, which probably do not set up the module, govern the developmental possibilities of the module? Generally, a module has an organizing center and, in the case of the cardiocraniofacial module, the organizing center appears to be the foregut endoderm, which extends from the prechordal plate (an arguably endodermal structure) to the anterior intestinal portal. The endoderm, via movement of the anterior intestinal portal, allows the bilateral heart fields to merge into a midline heart tube that actually covers the region that will become the face. The heart tube is displaced caudally as the pharyngeal arches form and establish the components that will develop into a face and neck. The same endoderm induces myocardial differentiation from the cardiogenic fields. The mesendodermal prechordal plate, which gives rise to the midline ventral endoderm, induces formation of the forebrain.

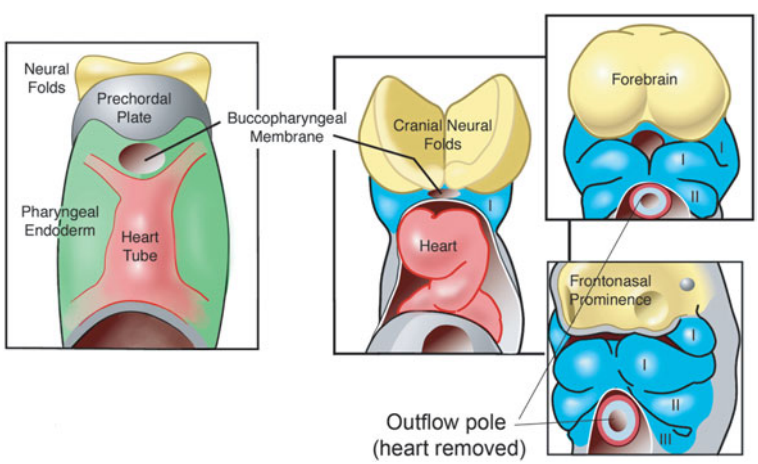

Figure 15.8. Development of the cardiocraniofacial field as envisioned in a human embryo.

After formation of the foregut pocket, the endoderm orchestrates patterning of the pharyngeal pouches and arches.

Several sequences of malformations may be cardiocraniofacial module defects, including DiGeorge, velocardiofacial, retinoid embryopathy, and fetal alcohol. The varied outcomes of a single gene deletion, a chromosomal microdeletion or an environmental insult on the module results from perhaps only slight modifications in the dialogue among components of the field. Again a gene mutation affecting a transcriptional or a signaling module, could alter the dialogue between cells in the module, which would subtly destabilize elements of the module. Because the endoderm appears to be the organizer for the field, any alteration in its capacity as a signaling center has the potential to lead to alterations in development throughout the module.

For example, the DiGeorge phenotype has been linked to absence or mutations in *TBX1*. It has been shown in experimental animals that Tbx1 is expressed by the endoderm and that it controls expression of Fgf8 in the pharyngeal endoderm at a time when critical patterning and differentiation events are occurring in the pharyngeal arches, which contains neural crest, pharyngeal pouches, secondary heart field, and forebrain. A reduction of this important signaling component would lead to abnormal development along the entire module. The insult would be limited to a brief but critical time period. While we do not yet know the details of such an insult, the data point to failure of a transcriptional module leading to failure of a signaling module within the cardiocraniofacial morphological module.

REFERENCES

Abel, E. 2004. Paternal contribution to fetal alcohol syndrome. Addict. Biol. 9:127–133; discussion 135–136.

Abu-Issa, R., G. Smyth, I. Smoak, K.-I. Yamamura, and E. Meyers. 2002. Fgf8 is required for pharyngeal arch and cardiovascular development in the mouse. Development 129:4613–4625.

Agarwal, P., J. N. Wylie, J. Galceran, O. Arkhitko, C. Li, C. Deng, R. Grosschedl, and B. G. Bruneau. 2003. *Tbx5* is essential for forelimb bud initiation following patterning of the limb field in the mouse embryo. Development 130:623–633.

Ahlgren, S. C., V. Thakur, and M. Bronner-Fraser. 2002. Sonic hedgehog rescues cranial neural crest from cell death induced by ethanol exposure. Proc. Natl. Acad. Sci. USA 99:10476–10481.

Akasaka, T., M. Kanno, R. Balling, M. A. Mieza, M. Taniguchi, and H. Koseki. 1996. A role for *mel-18*, a Polycomb group-related vertebrate gene, during the anteroposterior specification of the axial skeleton. Development 122:1513–1522.

Akiyama, H., M. C. Chaboissier, R. R. Behringer, D. H. Rowitch, A. Schedl, J. A. Epstein, and B. de Crombrugghe. 2004. Essential role of *Sox9* in the pathway that controls formation of cardiac valves and septa. Proc. Natl. Acad. Sci. USA 101:6502–6507.

Alagille, D., A. Estrada, M. Hadchouel, M. Gautier, M. Odievre, and J. P. Dommergues. 1987. Syndromic paucity of interlobular bile ducts (Alagille syndrome or arteriohepatic dysplasia): review of 80 cases. J. Pediatr. 110:195–200.

Alkema, M. J., M. T. van der Lugt, R. C. Bobeldijk, A. Berns, and M. van Lohuizen. 1995. Transformation of axial skeleton due to overexpression of *bmi-1* in transgenic mice. Nature 374:724–727.

Antonarakis, S. E., R. Lyle, E. T. Dermitzakis, A. Reymond, and S. Deutsch. 2004. Chromosome 21 and down syndrome: from genomics to pathophysiology. Nat. Rev. Genet. 5:725–738.

Auchterlonie, I. A., and M. P. White. 1982. Recurrence of the VATER association within a sibship. Clin. Genet. 21:122–124.

Baptista, M. J., U. L. Fairbrother, C. M. Howard, M. J. Farrer, G. E. Davies, D. Trikka, K. Maratou, A. Redington, G. Greve, P. R. Njolstad, and A. M. Kessling. 2000. Heterotrisomy, a significant contributing factor to ventricular septal defect associated with Down syndrome? Hum. Genet. 107:476–482.

Barlow, G. M., X. N. Chen, Z. Y. Shi, G. E. Lyons, D. M. Kurnit, L. Celle, N. B. Spinner, E. Zackai, M. J. Pettenati, A. J. Van Riper, M. J. Vekemans, C. H. Mjaatvedt, and J. R. Korenberg. 2001. Down syndrome congenital heart disease: a narrowed region and a candidate gene. Genet. Med. 3:91–101.

Basson, C. T., D. R. Bachinsky, R. C. Lin, T. Levi, J. A. Elkins, J. Soults, D. Grayzel, E. Kroumpouzou, T. A. Traill, J. Leblanc-Straceski, B. Renault, R. Kucherlapati, J. G. Seidman, and C. E. Seidman. 1997. Mutations in human cause limb and cardiac malformation in Holt-Oram syndrome. Nat. Genet. 15:30–34.

Bi, W., T. Ohyama, H. Nakamura, J. Yan, J. Visvanathan, M. J. Justice, and J. R. Lupski. 2005. Inactivation of Rai1 in mice recapitulates phenotypes observed in chromosome engineered mouse models for Smith-Magenis syndrome. Hum. Mol. Genet. 14:983–995.

Bird, L. M., G. F. Billman, R. V. Lacro, R. L. Spicer, L. K. Jariwala, H. E. Hoyme, R. Zamora-Salinas, C. Morris, D. Viskochil, M. J. Frikke, and M. C. Jones. 1996. Sudden death in Williams syndrome: report of ten cases. J. Pediatr. 129:926–931.

Blake, K. D., J. M. Ratcliffe, and R. K. Wyse. 1989. CHARGE association in two monozygous triplets. Int. J. Cardiol. 25:339–341.

Botto, L. D., M. J. Khoury, P. Mastroiacovo, E. E. Castilla, C. A. Moore, R. Skjaerven, O. M. Mutchinick, B. Borman, G. Cocchi, A. E. Czeizel, J. Goujard, L. M. Irgens, P. A. Lancaster, M. L. Martinez-Frias, P. Merlob, A. Ruusinen, C. Stoll, and Y. Sumiyoshi. 1997. The spectrum of congenital anomalies of the VATER association: an international study. Am. J. Med. Genet. 71:8–15.

Bouman, H. G. A., M. L. A. Broekhuizen, A. M. J. Baasten, A. C. Gittenberger-de Groot, and A. C. G. Wenink. 1997. Stereological study of stage 34 chicken hearts with looping disturbances after retinoic acid treatment: disturbed growth of myocardium and atrioventricular cushion tissue. Anat. Rec. 248:242–250.

Bruneau, B. G., M. Logan, N. Davis, T. Levi, C. J. Tabin, J. G. Seidman, and C. E. Seidman. 1999. Chamber-specific cardiac expression of *Tbx5* and heart defects in Holt-Oram syndrome. Dev. Biol. 211:100–108.

Bruneau, B. G., G. Nemer, J. P. Schmitt, F. Charron, L. Robitaille, S. Caron, D. A. Conner, M. Gessler, M. Nemer, C. E. Seidman, and J. G. Seidman. 2001. A murine model of Holt-Oram Syndrome defines roles of the T-box transcription factor *Tbx5* in cardiogenesis and disease. Cell 106:709–721.

Cai, C. L., W. Zhou, L. Yang, L. Bu, Y. Qyang, X. Zhang, X. Li, M. G. Rosenfeld, J. Chen, and S. Evans. 2005. T-box genes coordinate regional rates of proliferation and regional specification during cardiogenesis. Development 132:2475–2487.

Carey, J. 2005. Trisomy 18 Facts. Support Organization for Trisomy 18, 13 and Related Disorders. http://www.trisomy.org/html/trisomy_18_facts.htm. Accessed July 24, 2006.

Cartwright, M. M., and S. M. Smith. 1995a. Increased cell death and reduced neural crest cell numbers in ethanol-exposed embryos: partial basis for the fetal alcohol syndrome phenotype. Alcohol Clin. Exp. Res. 19:378–386.

Cartwright, M. M., and S. M. Smith. 1995b. Stage-dependent effects of ethanol on cranial neural crest cell development: partial basis for the phenotypic variations observed in fetal alcohol syndrome. Alcohol Clin. Exp. Res. 19:1454–1462.

Cavalli, G., and R. Paro. 1998. Chromo-domain proteins: linking chromatin structure to epigenetic regulation. Curr. Opin. Cell Biol. 10:354–360.

Chen, R. M., J. R. Lupski, F. Greenberg, and R. A. Lewis. 1996. Ophthalmic manifestations of Smith-Magenis syndrome. Ophthalmology 103:1084–1091.

Chen, Y. F., P. L. Kou, S. J. Tsai, K. F. Chen, H. H. Chan, C. M. Chen, and H. S. Sun. 2005. Computational analysis and refinement of sequence structure on chromosome 22q11.2 region: application to the development of quantitative real-time PCR assay for clinical diagnosis. Genomics 7:290–297.

Clayton, P. T. 1998. Disorders of cholesterol biosynthesis. Arch. Dis. Child 78:185–189.

Conway, S. J., D. J. Henderson, M. L. Kirby, R. H. Anderson, and A. J. Copp. 1997. Development of a lethal congenital heart defect in the *splotch* (*Pax3*) mutant mouse. Cardiovasc. Res. 36:163–173.

Core, N., S. Bel, S. J. Gaunt, M. Aurrand-Lions, J. Pearce, A. Fisher, and M. Djabali. 1997. Altered cellular proliferation and mesoderm patterning in Polycomb-M33-deficient mice. Development 124: 721–729.

Czeizel, A., and I. Ludanyi. 1985. An aetiological study of the VACTERL-association. Eur. J. Pediatr. 144:331–337.

Davies, G. E., C. M. Howard, M. J. Farrer, M. M. Coleman, L. B. Bennett, L. M. Cullen, R. K. H. Wyse, J. Burn, R. Williamson, and A. M. Kessling. 1995. Genetic variation in the COL6A1 region is associated with congenital heart defects in trisomy 21 (Down's syndrome). Ann. Hum. Genet. 59:253–269.

Descipio, C., L. Schneider, T. L. Young, N. Wasserman, D. Yaeger, F. Lu, P. G. Wheeler, M. S. Williams, L. Bason, L. Jukofsky, A. Menon, R. Geschwindt, A. E. Chudley, J. Saraiva, A. A. Schinzel, A. Guichet, W. E. Dobyns, A. Toutain, N. B. Spinner, and I. D. Krantz. 2005. Subtelomeric deletions of chromosome 6p: molecular and cytogenetic characterization of three new cases with phenotypic overlap with Ritscher-Schinzel (3C) syndrome. Am. J. Med. Genet. 134:3–11.

Digilio, M. C., B. Marino, P. Bagolan, A. Giannotti, and B. Dallapiccola. 1999. Microdeletion 22q11 and oesophageal atresia. J. Med. Genet. 36:137–139.

Digilio, M. C., B. Marino, A. Toscano, A. Giannotti, and B. Dallapiccola. 2001. Congenital heart defects in Kabuki syndrome. Am. J. Med. Genet. 100:269–274.

Driscoll, D. A. 2001. Prenatal diagnosis of the 22q11.2 deletion syndrome. Genet. Med. 3:14–18.

Eames, B. F., P. T. Sharpe, and J. A. Helms. 2004. Hierarchy revealed in the specification of three skeletal fates by *Sox9* and *Runx2*. Dev. Biol. 274:188–200.

Emerick, K. M., E. B. Rand, E. Goldmuntz, I. D. Krantz, N. B. Spinner, and D. A. Piccoli. 1999. Features of Alagille syndrome in 92 patients: frequency and relation to prognosis. Hepatology 29:822–829.

Epstein, J. A. 1996. *Pax3*, neural crest and cardiovascular development. Trends Cardiovasc. Med. 6:255–261.

Fan, C., M. A. Duhagon, C. Oberti, S. Chen, Y. Hiroi, I. Komuro, P. I. Duhagon, R. Canessa, and Q. Wang. 2003. Novel TBX5 mutations and molecular mechanism for Holt-Oram syndrome. J. Med. Genet. 40:e29.

Fan, C., M. Liu, and Q. Wang. 2003. Functional analysis of *TBX5* missense mutations associated with Holt-Oram syndrome. J. Biol. Chem. 278:8780–8785.

Farrell, M. J., H. Stadt, K. T. Wallis, P. Scambler, R. L. Hixon, R. Wolfe, L. Leatherbury, and M. L. Kirby. 1999. *HIRA*, a DiGeorge syndrome candidate gene, is required for cardiac outflow tract septation. Circ. Res. 84:127–135.

Foster, J. W., and J. A. Graves. 1994. An *SRY*-related sequence on the marsupial X chromosome: implications for the evolution of the mammalian testis-determining gene. Proc. Natl. Acad. Sci. USA 91:1927–1231.

Frank, D., L. Fotheringham, J. Brewer, L. Muglia, Tristani-Firouzi, M. Capecchi, and A. Moon. 2002. An *Fgf8* mouse mutant phenocopies human 22q11 deletion syndrome. Development 129: 4591–4603.

Franz, T. 1989. Persistent truncus arteriosus in the Splotch mutant mouse. Anat. Embryol. (Berl) 180:457–464.

Freeman, S. B., L. F. Taft, K. J. Dooley, K. Allran, S. L. Sherman, T. J. Hassold, M. J. Khoury, and D. M. Saker. 1998. Population-based study of congenital heart defects in Down syndrome. Am. J. Med. Genet. 80:213–217.

Fuentes, J. J., M. A. Pritchard, A. M. Planas, A. Bosch, I. Ferrer, and X. Estivill. 1995. A new human gene from the Down syndrome critical region encodes a proline-rich protein highly expressed in fetal brain and heart. Hum. Mol. Genet. 4:1935–1944.

Fuentes, J. J., L. Genesca, T. J. Kingsbury, K. W. Cunningham, M. Perez-Riba, X. Estivill, and S. de la Luna. 2000. DSCR1, overexpressed in Down syndrome, is an inhibitor of calcineurin-mediated signaling pathways. Hum. Mol. Genet. 9:1681–1690.

Funke, B., L. Edelmann, N. McCain, R. K. Pandita, J. Ferreira, S. Merscher, M. Zohouri, L. Cannizzaro, A. Shanske, and B. E. Morrow. 1999. Der(22) syndrome and velo-cardio-facial syndrome/DiGeorge syndrome share a 1.5-Mb region of overlap on chromosome 22q11. Am. J. Hum. Genet. 64:747–758.

Garg, V., I. S. Kathiriya, R. Barnes, M. K. Schluterman, I. N. King, C. A. Butler, C. R. Rothrock, R. S. Eapen, K. Hirayama-Yamada, K. Joo, R. Matsuoka, J. C. Cohen, and D. Srivastava. 2003. *GATA4* mutations cause human congenital heart defects and reveal an interaction with *TBX5*. Nature 424:443–447.

Garg, V., C. Yamagishi, T. H. Hu, I. S. Kathiriya, H. Yamagishi, and D. Srivastava. 2001. *Tbx1*, a DiGeorge syndrome candidate gene, is regulated by Sonic hedgehog during pharyngeal arch development. Dev. Biol. 235:62–73.

Gitler, A. D., Y. Zhu, F. A. Ismat, M. M. Lu, Y. Yamauchi, L. F. Parada, and J. A. Epstein. 2003. *Nf1* has an essential role in endothelial cells. Nat. Genet. 33:75–79.

Goodwin, B. C. 1990. Structuralism in biology. Sci. Prog. 74:227–244.

Goodwin, B. C. 2002. The causes of biological form. In: Causes of Development, ed. G. Butterworth and P. Bryant, 49–63. New York: Harvester Wheatsheaf.

Gosch, A., and R. Pankau. 1994. Social-emotional and behavioral adjustment in children with Williams-Beuren syndrome. Am. J. Med. Genet. 53:335–339.

Greenberg, F., R. A. Lewis, L. Potocki, D. Glaze, J. Parke, J. Killian, M. A. Murphy, D. Williamson, F. Brown, R. Dutton, C. McCluggage, E. Friedman, M. Sulek, and J. R. Lupski. 1996. Multi-disciplinary

clinical study of Smith-Magenis syndrome (deletion 17p11.2). Am. J. Med. Genet. 62:247–254.

Gruber, P., S. W. Kubalak, T. Pexieder, H. M. Sucov, R. M. Evans, and K. R. Chien. 1996. RXRα deficiency confers genetic susceptibility to aortic sac, conotruncal, atrioventricular cushion, and ventricular muscle defects. J. Clin. Invest. 98:1332–1343.

Gruenauer-Kloevekorn, C., and U. G. Froster. 2003. Holt-Oram syndrome: a new mutation in the *TBX5* gene in two unrelated families. Ann. Genet. 46:19–23.

Harley, V. R., M. J. Clarkson, and A. Argentaro. 2003. The molecular action and regulation of the testis-determining factors, SRY (sex-determining region on the Y chromosome) and *SOX9* [SRY-related high-mobility group (HMG) box 9]. Endocr. Rev. 24:466–487.

Hatcher, C. J., M. M. Goldstein, C. S. Mah, C. S. Delia, and C. T. Basson. 2000. Identification and localization of *TBX5* transcription factor during human cardiac morphogenesis. Dev. Dyn. 219:90–95.

Hatcher, C. J., M.-S. Kim, C. S. Mah, M. M. Goldstein, B. Wong, T. Mikawa, and C. T. Basson. 2001. *TBX5* transcription factor regulates cell proliferation during cardiogenesis. Dev. Biol. 230:177–188.

Hiroi, Y., S. Kudoh, K. Monzen, Y. Ikeda, Y. Yazaki, R. Nagai, and I. Komuro. 2001. *Tbx5* associates with *Nkx2–5* and synergistically promotes cardiomyocyte differentiation. Nat. Genet. 28:276–280.

Horb, M. E., and G. H. Thomsen. 1999. *Tbx5* is essential for heart development. Development 126:1739–1751.

Imashuku, S., S. Hayashi, K. Kuriyama, S. Hibi, Y. Tabata, and S. Todo. 2000. Sudden death of a 21-year-old female with Williams syndrome showing rare complications. Pediatr. Int. 42:322–324.

Iserin, L., P. De Lonlay, G. Viot, D. Sidi, J. Kachaner, A. Munnich, S. Lyonnet, M. Vekemans, and D. Bonnet. 1998. Prevalence of the microdeletion 22q11 in newborn infants with congenital conotruncal cardiac anomalies. Eur. J. Pediatr. 157:881–884.

Jick, S. S., and B. Z. Terris. 1997. Anticonvulsants and congenital malformations. Pharmacotherapy 17:561–564.

Johnson, M. C., R. M. Payne, J. W. Grant, and A. W. Strauss. 1995. The genetic basis of paediatric heart disease. Ann. Med. 27: 289–300.

Johnson, T. R., E. Goldmuntz, D. M. McDonald-McGinn, E. H. Zackai, and M. A. Fogel. 2005. Cardiac magnetic resonance imaging for accurate diagnosis of aortic arch anomalies in patients with 22q11.2 deletion. Am. J. Cardiol. 96:1726–1730.

Jongmans, M., E. A. Sistermans, A. Rikken, W. M. Nillesen, R. Tamminga, M. Patton, E. M. Maier, M. Tartaglia, K. Noordam, and I. van der Burgt. 2005. Genotypic and phenotypic characterization of Noonan syndrome: new data and review of the literature. Am. J. Med. Genet. 134:165–170.

Kallen, K., E. Robert, P. Mastroiacovo, E. E. Castilla, and B. Kallen. 1999. CHARGE Association in newborns: a registry-based study. Teratology 60:334–343.

Kamath, B. M., N. B. Spinner, K. M. Emerick, A. E. Chudley, C. Booth, D. A. Piccoli, and I. D. Krantz. 2004. Vascular anomalies in Alagille syndrome: a significant cause of morbidity and mortality. Circulation 109:1354–1358.

Kastner, P., N. Messaddeq, M. Mark, O. Wendling, J. M. Grondona, S. Ward, N. Ghyselinck, and P. Chambon. 1997. Vitamin A deficiency and mutations of RXRα, RXRβ and RARα lead to early differentiation of embryonic ventricular cardiomyocytes. Development 124:4749–4758.

Kaufman, R. L. 1973. Birth defects and oral contraceptives. Lancet 1:1396.

Khadilkar, V. V., F. J. Cameron, and R. Stanhope. 1999. Growth failure and pituitary function in CHARGE and VATER associations. Arch. Dis. Child 80:167–170.

Khoury, M. J., J. F. Cordero, F. Greenberg, L. M. James, and J. D. Erickson. 1983. A population study of the VACTERL association: evidence for its etiologic heterogeneity. Pediatrics 71:815–820.

Kim, J., P. Kim, and C. C. Hui. 2001. The VACTERL association: lessons from the Sonic hedgehog pathway. Clin. Genet. 59:306–315.

Kim, P. C. W., R. Mo, and C. C. Hui. 2001. Murine models of VACTERL syndrome: role of sonic hedgehog signaling pathway. J. Pediatr. Surg. 36:381–383.

Kirby, M. L., and D. E. Bockman. 1984. Neural crest and normal development: a new perspective. Anat. Rec. 209:1–6.

Korenberg, J. R., X. N. Chen, R. Schipper, Z. Sun, R. Gonsky, S. Gerwehr, N. Carpenter, C. Daumer, P. Dignan, C. Disteche, et al. 1994. Down syndrome phenotypes: the consequences of chromosomal imbalance. Proc. Natl. Acad. Sci. USA 91:4997–5001.

Kozma, C. 2001. Valproic acid embryopathy: report of two siblings with further expansion of the phenotypic abnormalities and a review of the literature. Am. J. Med. Genet. 98:168–175.

Krantz, I. D., R. Smith, R. P. Colliton, H. Tinkel, E. H. Zackai, D. A. Piccoli, E. Goldmuntz, and N. B. Spinner. 1999. *Jagged1* mutations in patients ascertained with isolated congenital heart defects. Am. J. Med. Genet. 84:56–60.

Kurnit, D. M., J. F. Aldridge, R. Matsuoka, and S. Matthysse. 1985. Increased adhesiveness of trisomy 21 cells and atrioventricular canal malformations in Down syndrome: a stochastic model. Am. J. Med. Genet. 20:385–399.

Kwok, C., P. A. Weller, S. Guioli, J. W. Foster, S. Mansour, O. Zuffardi, H. H. Punnett, M. A. Dominguez-Steglich, J. D. Brook, I. D. Young, et al. 1995. Mutations in *SOX9*, the gene responsible for Campomelic dysplasia and autosomal sex reversal. Am. J. Hum. Genet. 57:1028–1036.

Lee, R. Y., J. M. Luo, R. M. Evans, V. Giguere, and H. M. Sucov. 1997. Compartment-selective sensitivity of cardiovascular morphogenesis to combinations of retinoic acid receptor gene mutations. Circ. Res. 80:757–764.

Leonardi, M. L., G. S. Pai, B. Wilkes, and R. R. Lebel. 2001. Ritscher-Schinzel cranio-cerebello-cardiac (3C) syndrome: report of four new cases and review. Am. J. Med. Genet. 102:237–242.

Li, L. H., I. D. Krantz, Y. Deng, A. Genin, A. B. Banta, C. C. Collins, M. Qi, B. J. Trask, W. L. Kuo, J. Cochran, T. Costa, M. E. M. Pierpont, E. B. Rand, D. A. Piccoli, L. Hood, and N. B. Spinner. 1997. Alagille syndrome is caused by mutations in human *Jagged1*, which encodes a ligand for *Notch1*. Nat. Genet. 16:243–251.

Li, Q. Y., R. A. Newbury-Ecob, J. A. Terrett, D. I. Wilson, A. R. J. Curtis, C. H. Yi, T. Gebuhr, P. J. Bullen, S. C. Robson, T. Strachan, D. Bonnet, S. Lyonnet, I. D. Young, J. A. Raeburn, A. J. Buckler, D. J. Law, and J. D. Brook. 1997. Holt-Oram syndrome is caused by mutations in *TBX5*, a member of the Brachyury (T) gene family. Nat. Genet. 15:21–29.

Lin, A. E., H. H. Ardinger, R. H. Ardinger, Jr., C. Cunniff, and R. I. Kelley. 1997. Cardiovascular malformations in Smith-Lemli-Opitz syndrome. Am. J. Med. Genet. 68:270–278.

Lindsay, E. A., A. Botta, V. Jurecic, S. Caratinni-Rivera, Y.-C. Cheah, H. M. Rosenblatt, A. Bradley, and A. Baldini. 1999. Congenital heart disease in mice deficient for the DiGeorge syndrome region. Nature 401:379–383.

Lindsay, E. A., H. Su, M. Morishima, T. Huynh, T. Pramparo, V. Jurecic, G. Ogunrinu, H. F. Sutherland, P. J. Scambler, A. Bradley, and

A. Baldini. 2001. *Tbx1* haploinsufficiency in the DiGeorge syndrome region causes aortic arch defects in mice. Nature 410:97–101.

Loomes, K. M., L. A. Underkoffler, J. Morabito, S. Gottlieb, D. A. Piccoli, N. B. Spinner, H. S. Baldwin, and R. J. Oakey. 1999. The expression of *Jagged1* in the developing mammalian heart correlates with cardiovascular disease in Alagille syndrome. Hum. Mol. Genet. 8:2443–2449.

Marino, B., M. C. Digilio, A. Toscano, S. Anaclerio, A. Giannotti, C. Feltri, M. A. de Ioris, A. Angioni, and B. Dallapiccola. 2001. Anatomic patterns of conotruncal defects associated with deletion 22q11. Genet. Med. 3:45–48.

McDermott DA, Bressan MC, He J, Lee JS, Aftimos S, Brueckner M, Gilbert F, Graham GE, Hannibal MC, Innis JW, Pierpont ME, Raas-Rothschild A, Shanske AL, Smith WE, Spencer RH, St John-Sutton MG, van Maldergem L, Waggoner DJ, Weber M, Basson CT. McDermott, D. A., M. C. Bressan, J. He, J. S. Lee, S. Aftimos, M. Brueckner, F. Gilbert, G. E. Graham, M. C. Hannibal, J. W. Innis, M. E. Pierpont, A. Raas-Rothschild, A. L. Shanske, W. E. Smith, R. H. Spencer, M. G. St John-Sutton, L. van Maldergem, Waggoner, M. Weber, and C. T. Basson. 2005. *TBX5* genetic testing validates strict clinical criteria for Holt-Oram syndrome. Pediatr. Res. 58:981–986.

McMullen, K. P., P. S. Karnes, C. R. Moir, and V. V. Michels. 1996. Familial recurrence of tracheoesophageal fistula and associated malformations. Am. J. Med. Genet. 63:525–528.

Mendelsohn, C., D. Lohnes, D. Decimo, T. Lufkin, M. LeMeur, P. Chambon, and M. Mark. 1994. Function of the retinoic acid receptors (RARs) during development (II) Multiple abnormalities at various stages of organogenesis in RAR double mutants. Development 120:2749–2771.

Meng, X., X. Lu, Z. Li, E. D. Green, H. Massa, B. J. Trask, C. A. Morris, and M. T. Keating. 1998. Complete physical map of the common deletion region in Williams syndrome and identification and characterization of three novel genes. Hum. Genet. 103: 590–599.

Milunsky, J. M., and X. L. Huang. 2003. Unmasking Kabuki syndrome: chromosome 8p22–8p23.1 duplication revealed by comparative genomic hybridization and BAC-FISH. Clin. Genet. 64:509–516.

Mitchell, J. A., S. L. Davenport, M. A. Hefner, and M. M. Shei. 1985. Use of an expert model to test diagnostic criteria in CHARGE syndrome. J. Med. Syst. 9:425–436.

Mitchell, J. A., J. Giangiacomo, M. A. Hefner, J. W. Thelin, and J. M. Pickens. 1985. Dominant CHARGE association. Ophthalmol. Paediatr. Genet. 6:271–276.

Miyake, N., N. Harada, O. Shimokawa, H. Ohashi, K. Kurosawa, T. Matsumoto, Y. Fukushima, T. Nagai, V. Shotelersuk, K. Yoshiura, T. Ohta, T. Kishino, N. Niikawa, and N. Matsumoto. 2004. On the reported 8p22–8p23.1 duplication in Kabuki make-up syndrome (KMS) and its absence in patients with typical KMS. Am. J. Med. Genet. 128:170–172.

Moore, S. J., P. Turnpenny, A. Quinn, S. Glover, D. J. Lloyd, T. Montgomery, and J. C. Dean. 2000. A clinical study of 57 children with fetal anticonvulsant syndromes. J. Med. Genet. 37: 489–497.

Muller, C. W., and B. G. Herrmann. 1997. Crystallographic structure of the T domain-DNA complex of the Brachyury transcription factor. Nature 389:884–888.

Myers, S. M., and T. D. Challman. 2004. Congenital heart defects associated with Smith-Magenis syndrome: two cases of total anomalous pulmonary venous return. Am. J. Med. Genet. 131:99–100.

Nagase, T., R. Kikuno, K. I. Ishikawa, M. Hirosawa, and O. Ohara. 2000. Prediction of the coding sequences of unidentified human genes. XVI. The complete sequences of 150 new cDNA clones from brain which code for large proteins in vitro. DNA Res. 7:65–73.

Nezarati, M. M., and D. R. McLeod. 1999. VACTERL manifestations in two generations of a family. Am. J. Med. Genet. 82:40–42.

Ng, J. K., Y. Kawakami, D. B. scher, A. Raya, T. Itoh, C. M. Koth, C. R. Esteban, J. Rodr¡guez-Le¢n, D. M. Garrity, M. C. Fishman, and J. C. I. Belmonte. 2002. The limb identity gene *Tbx5* promotes limb initiation by interacting with *Wnt2b* and *Fgf10*. Development 129:5161–5170.

Nishii, K., M. Kumai, and Y. Shibata. 2001. Regulation of the epithelial–mesenchymal transformation through gap junction channels in heart development. Trends Cardiovasc. Med. 11:213–218.

Noonan, J. A. 1968. Hypertelorism with Turner phenotype. A new syndrome with associated congenital heart disease. Am. J. Dis. Child 116:373–380.

Nora, A. H., and J. J. Nora. 1975. A syndrome of multiple congenital anomalies associated with teratogenic exposure. Arch. Environ. 30:17–21.

Ogawa, T., M. Kuwagata, J. Ruiz, and F. C. Zhou. 2005. Differential teratogenic effect of alcohol on embryonic development between C57BL/6 and DBA/2 mice: a new view. Alcohol Clin. Exp. Res. 29:855–863.

Oley, C. A., M. Baraitser, and D. B. Grant. 1988. A reappraisal of the CHARGE association. J. Med. Genet. 25:147–156.

Oyama, S. 1994. Rethinking development. In: Handbook of Psychological Anthropology, ed. Bock, P. K., 185–196. Westport, CT: Greenwood.

Pagon, R. A., J. M. Graham, Jr., J. Zonana, and S. L. Yong. 1981. Coloboma, congenital heart disease, and choanal atresia with multiple anomalies: CHARGE association. J. Pediatr. 99:223–227.

Pajkrt, E., B. Weisz, H. V. Firth, and L. S. Chitty. 2004. Fetal cardiac anomalies and genetic syndromes. Prenat. Diagn. 24:1104–1115.

Pankau, R., C. J. Partsch, A. Gosch, H. C. Oppermann, and A. Wessel. 1992. Statural growth in Williams-Beuren syndrome. Eur. J. Pediatr. 151:751–755.

Pankau, R., C. J. Partsch, A. Gosch, M. Winter, and A. Wessel. 1997. Picture of the month. William-Beuren syndrome. Arch. Pediatr. Adolesc. Med. 151:203–204.

Pankau, R., C. J. Partsch, M. Winter, A. Gosch, and A. Wessel. 1996. Incidence and spectrum of renal abnormalities in Williams-Beuren syndrome. Am. J. Med. Genet. 63:301–304.

Paoloni-Giacobino, A., H. M. Chen, and S. E. Antonarakis. 1997. Cloning of a novel human neural cell adhesion molecule gene (*NCAM2*) that maps to chromosome region 21q21 and is potentially involved in Down syndrome. Genomics 43:43–51.

Partsch, C. J., G. Dreyer, A. Gosch, M. Winter, R. Schneppenheim, A. Wessel, and R. Pankau. 1999. Longitudinal evaluation of growth, puberty, and bone maturation in children with Williams syndrome. J. Pediatr. 134:82–89.

Perrin, L., B. Monier, R. Ponzielli, M. Astier, and M. Semeriva. 2004. *Drosophila* cardiac tube organogenesis requires multiple phases of *Hox* activity. Dev. Biol. 272:419–431.

Pizard, A., P. G. Burgon, D. L. Paul, B. G. Bruneau, C. E. Seidman, and J. G. Seidman. 2005. Connexin 40, a target of transcription factor *tbx5,* patterns wrist, digits, and sternum. Mol. Cell Biol. 25: 5073–5083.

Plageman, T. F. J., and K. E. Yutzey. 2004. Differential expression and function of *Tbx5* and *Tbx20* in cardiac development. J. Biol. Chem. 279:19026–19034.

Quan, L., and D. W. Smith. 1973. The VATER association. Vertebral defects, Anal atresia, T-E fistula with esophageal atresia, radial and renal dysplasia: a spectrum of associated defects. J. Pediatr. 82:104–107.

Rallis, C., B. G. Bruneau, J. Del Buono, C. E. Seidman, J. G. Seidman, S. Nissim, C. J. Tabin, and M. P. Logan. 2003. *Tbx5* is required for forelimb bud formation and continued outgrowth. Development 130:2741–2751.

Ravnan, J. B., E. Chen, M. Golabi, and R. V. Lebo. 1996. Chromosome 22q11.2 microdeletions in velocardiofacial syndrome patients with widely variable manifestations. Am. J. Med. Genet. 66: 250–256.

Reamon-Buettner, S. M., and J. Borlak. 2004. Somatic *NKX2–5* mutations as a novel mechanism of disease in complex congenital heart disease. J. Med. Genet. 41:684–690.

Reijnen, M. J., K. M. Hamer, J. L. den Blaauwen, C. Lambrechts, I. Schoneveld, R. van Driel, and A. P. Otte. 1995. Polycomb and *bmi-1* homologs are expressed in overlapping patterns in *Xenopus* embryos and are able to interact with each other. Mech. Dev. 53:35–46.

Rittler, M., J. E. Paz, and E. E. Castilla. 1996. VACTERL association, epidemiologic definition and delineation. Am. J. Med. Genet. 63:529–536.

Rones, M. S., K. A. McLaughlin, M. Raffin, and M. Mercola. 2000. Serrate and Notch specify cell fates in the heart field by suppressing cardiomyogenesis. Development 127:3865–3876.

Ruiz-Perez, V. L., S. W. Tompson, H. J. Blair, C. Espinoza-Valdez, P. Lapunzina, E. O. Silva, B. Hamel, J. L. Gibbs, I. D. Young, M. J. Wright, and J. A. Goodship. 2003. Mutations in two nonhomologous genes in a head-to-head configuration cause Ellis-van Creveld syndrome. Am. J. Hum. Genet. 72:728–732.

Schrander-Stumpel, C. T., L. Spruyt, L. M. Curfs, T. Defloor, and J. J. Schrander. 2005. Kabuki syndrome: clinical data in 20 patients, literature review, and further guidelines for preventive management. Am. J. Med. Genet. 132:234–243.

Siebert, J. R., J. M. Graham, and C. MacDonald. 1985. Pathologic features of the CHARGE association: support for involvement of the neural crest. Teratology 31:331–336.

Slager, R. E., T. L. Newton, C. N. Vlangos, B. Finucane, and S. H. Elsea. 2003. Mutations in RAI1 associated with Smith-Magenis syndrome. Nat. Genet. 33:466–468.

Smith, A. C., A. L. Gropman, J. E. Bailey-Wilson, O. Goker-Alpan, S. H. Elsea, J. Blancato, J. R. Lupski, and L. Potocki. 2002. Hypercholesterolemia in children with Smith-Magenis syndrome: del (17) (p11.2p11.2). Genet. Med. 4:118–125.

Smith, A. C., L. McGavran, J. Robinson, G. Waldstein, J. Macfarlane, J. Zonona, J. Reiss, M. Lahr, L. Allen, and E. Magenis. 1986. Interstitial deletion of (17) (p11.2p11.2) in nine patients. Am. J. Med. Genet. 24:393–414.

Smith, D. W., L. Lemli, and J. M. Opitz. 1964. A newly diagnosed syndrome of multiple congenital anomalies. J. Pediatr. 64: 210–217.

Spinner, N. B., R. P. Colliton, C. Crosnier, I. D. Krantz, M. Hadchouel, and M. Meunier-Rotival. 2001. Jagged1 mutations in alagille syndrome. Hum. Mutat. 17:18–33.

Stratton, R. F., W. B. Dobyns, F. Greenberg, J. B. DeSana, C. Moore, G. Fidone, G. H. Runge, P. Feldman, G. S. Sekhon, R. M. Pauli, et al. 1986. Interstitial deletion of (17) (p11.2p11.2): report of six additional patients with a new chromosome deletion syndrome. Am. J. Med. Genet. 24:421–432.

Suarez-Mier, M. P., and B. Morentin. 1999. Supravalvular aortic stenosis, Williams syndrome and sudden death. A case report. Forensic Sci. Int. 106:45–53.

Takeuchi, J. K., K. Koshiba-Takeuchi, T. Suzuki, M. Kamimura, K. Ogura, and T. Ogura. 2003. *Tbx5* and *Tbx4* trigger limb initiation through activation of the *Wnt/Fgf* signaling cascade. Development 130:2729–2739.

Tartaglia, M., and B. D. Gelb. 2005. Noonan syndrome and related disorders: genetics and pathogenesis. Annu. Rev. Genom. Hum. Genet. 6:45–68.

Tartaglia, M., K. Kalidas, A. Shaw, X. Song, D. L. Musat, I. van der Burgt, H. G. Brunner, D. R. Bertola, A. Crosby, A. Ion, R. S. Kucherlapati, S. Jeffery, M. A. Patton, and B. D. Gelb. 2002. *PTPN11* mutations in Noonan syndrome: molecular spectrum, genotype-phenotype correlation, and phenotypic heterogeneity. Am. J. Hum. Genet. 70:1555–1563.

Tartaglia, M., S. Martinelli, G. Cazzaniga, V. Cordeddu, I. Iavarone, M. Spinelli, C. Palmi, C. Carta, A. Pession, M. Arico, G. Masera, G. Basso, M. Sorcini, B. D. Gelb, and A. Biondi. 2004. Genetic evidence for lineage-related and differentiation stage-related contribution of somatic *PTPN11* mutations to leukemogenesis in childhood acute leukemia. Blood 104:307–313.

Tartaglia, M., E. L. Mehler, R. Goldberg, G. Zampino, H. G. Brunner, H. Kremer, I. Van der Burgt, A. H. Crosby, A. Ion, S. Jeffery, K. Kalidas, M. A. Patton, R. S. Kucherlapati, and B. D. Gelb. 2001. Mutations in *PTPN11*, encoding the protein tyrosine phosphatase SHP-2, cause Noonan syndrome. Nat. Genet. 29:465–468.

Tartaglia, M., C. M. Niemeyer, A. Fragale, X. Song, J. Buechner, A. Jung, K. Hahlen, H. Hasle, J. D. Licht, and B. D. Gelb. 2003. Somatic mutations in *PTPN11* in juvenile myelomonocytic leukemia, myelodysplastic syndromes and acute myeloid leukemia. Nat. Genet. 34:148–150.

Tellier, A. L., V. Cormier-Daire, V. Abadie, J. Amiel, S. Sigaudy, D. Bonnet, P. de Lonlay-Debeney, M. P. Morrisseau-Durand, P. Hubert, J. L. Michel, D. Jan, H. Dollfus, C. Baumann, P. Labrune, D. Lacombe, N. Philip, M. LeMerrer, M. L. Briard, A. Munnich, and S. Lyonnet. 1998. CHARGE syndrome: report of 47 cases and review. Am. J. Med. Genet. 76:402–409.

Temtamy, S. A., and J. D. Miller. 1974. Extending the scope of the VATER association: definition of the VATER syndrome. J. Pediatr. 85:345–349.

Tran, C. M., and H. M. Sucov. 1998. The *RXR*α gene functions in a non-cell-autonomous manner during mouse cardiac morphogenesis. Development 125:1951–1956.

van der Lugt, N. M., J. Domen, K. Linders, M. van Roon, E. Robanus-Maandag, H. te Riele, M. van der Valk, J. Deschamps, M. Sofroniew, M. van Lohuizen, and A. Berns. 1994. Posterior transformation, neurological abnormalities, and severe hematopoietic defects in mice with a targeted deletion of the *bmi-1* proto-oncogene. Genes Dev. 8:757–769.

Van Meter, T. D., and D. D. Weaver. 1996. Oculo-auriculo-vertebral spectrum and the CHARGE association: clinical evidence for a common pathogenetic mechanism. Clin. Dysmorphol. 5:187–196.

Van Mierop, L. H. S., and L. M. Kutsche. 1984. Interruption of the aortic arch and coarctation of the aorta: pathogenetic relations. Am. J. Cardiol. 54:829–834.

Vissers, L. E., C. M. van Ravenswaaij, R. Admiraal, J. A. Hurst, B. B. de Vries, I. M. Janssen, W. A. van der Vliet, E. H. Huys, P. J. de Jong, B. C. Hamel, E. F. Schoenmakers, H. G. Brunner, J. A. Veltman, and A. G. van Kessel. 2004. Mutations in a new member of the chromodomain gene family cause CHARGE syndrome. Nat. Genet. 36:955–957.

Vitelli, F., I. /Taddei, M. Morishima, E. Meyers, E. Lindsay, and A. Baldini. 2002. A genetic link between *Tbx1* and fibroblast growth factor signaling. Development 129:4605–4611.

Volpe, P., M. Marasini, G. Caruso, A. Marzullo, A. L. Buonadonna, P. Arciprete, S. Di Paolo, G. Volpe, and M. Gentile. 2003. 22q11 deletions in fetuses with malformations of the outflow tracts or interruption of the aortic arch: impact of additional ultrasound signs. Prenat. Diagn. 23:752–757.

Wagner, T., J. Wirth, J. Meyer, B. Zabel, M. Held, J. Zimmer, J. Pasantes, F. D. Bricarelli, J. Keutel, E. Hustert, V. Wolf, N. Tommerup, W. Schempp, and G. Scherer. 1994. Autosomal sex reversal and campomelic dysplasia are caused by mutations in and around the SRY-related gene *SOX9*. Cell 79:1111–1120.

Warburg, M. 1982. Diagnostic precision in microphthalmos and coloboma of heterogeneous origin. Birth Defects Orig. Artic. Ser. 18:31–50.

Ward, C., H. Stadt, M. Hutson, and M. L. Kirby. 2005. Ablation of the secondary heart field leads to tetralogy of Fallot and pulmonary atresia. Dev. Biol. 284:72–83.

Wassif, C. A., C. Maslen, S. Kachilele-Linjewile, D. Lin, L. M. Linck, W. E. Connor, R. D. Steiner, and F. D. Porter. 1998. Mutations in the human sterol delta7-reductase gene at 11q12–13 cause Smith-Lemli-Opitz syndrome. Am. J. Hum. Genet. 63:55–62.

Waterham, H. R., F. A. Wijburg, R. C. Hennekam, P. Vreken, B. T. Poll-The, L. Dorland, M. Duran, P. E. Jira, J. A. Smeitink, R. A. Wevers, and R. J. Wanders. 1998. Smith-Lemli-Opitz syndrome is caused by mutations in the 7-dehydrocholesterol reductase gene. Am. J. Hum. Genet. 63:329–338.

Watson, G. H., and V. Miller. 1973. Arteriohepatic dysplasia: familial pulmonary arterial stenosis with neonatal liver disease. Arch. Dis. Child. 48:459–466.

Weaver, D. D., C. L. Mapstone, and P. L. Yu. 1986. The VATER association. Analysis of 46 patients. Am. J. Dis. Child 140:225–229.

Weiss, G., Y. Confino, A. Shemer, and H. Trau. 2004. Cutaneous manifestations in the cardiofaciocutaneous syndrome, a variant of the classical Noonan syndrome. Report of a case and review of the literature. J. Eur. Acad. Dermatol. Venereol. 18:324–327.

Wessel, A., V. Gravenhorst, R. Buchhorn, A. Gosch, C. J. Partsch, and R. Pankau. 2004. Risk of sudden death in the Williams-Beuren syndrome. Am. J. Med. Genet. 127:234–237.

Wessel, A., R. Pankau, D. Kececioglu, W. Ruschewski, and J. H. Bursch. 1994. Three decades of follow-up of aortic and pulmonary vascular lesions in the Williams-Beuren syndrome. Am. J. Med. Genet. 52:297–301.

Wessels, M. W., A. S. Brooks, J. Hoogeboom, M. F. Niermeijer, and P. J. Willems. 2002. Kabuki syndrome: a review study of three hundred patients. Clin. Dysmorphol. 11:95–102.

Williams, M. S. 2005. Speculations on the pathogenesis of CHARGE syndrome. Am. J. Med. Genet. 133:318–325.

Wilson, J. G., and J. Warkany. 1950. Cardiac and aortic arch anomalies in offspring of vitamin A deficient rats correlated with similar human anomalies. Pediatrics 5:708–725.

Winter, R., W. Rosenkranz, H. Hofmann, H. Zierler, H. Becker, and M. Borkenstein. 1985. Prenatal diagnosis of campomelic dysplasia by ultrasonography. Prenat. Diagn. 5:1–8.

Wright, C. G., O. E. Brown, W. L. Meyerhoff, and J. C. Rutledge. 1986. Auditory and temporal bone abnormalities in CHARGE association. Ann. Otol. Rhinol. Laryngol. 95:480–486.

Wu, Y. Q., V. R. Sutton, E. Nickerson, J. R. Lupski, L. Potocki, J. R. Korenberg, F. Greenberg, M. Tassabehji, and L. G. Shaffer. 1998. Delineation of the common critical region in williams syndrome and clinical correlation of growth, heart defects, ethnicity, and parental origin. Am. J. Med. Genet. 78:82–89.

Xu, H., M. Morishima, J. N. Wylie, R. J. Schwartz, B. G. Bruneau, E. A. Lindsay, and A. Baldini. 2004. *Tbx1* has a dual role in the morphogenesis of the cardiac outflow tract. Development 131:3217–3227.

Xu, H., M. Morishima, J. N. Wylie, R. J. Schwartz, B. G. Bruneau, E. A. Lindsay, and A. Baldini. 2004. *Tbx1* has a dual role in the morphogenesis of the cardiac outflow tract. Development 131:3217–3227.

Yagi, H., Y. Furutani, H. Hamada, T. Sasaki, S. Asakawa, S. Minoshima, F. Ichida, K. Joo, M. Kimura, S. Imamura, N. Kamatani, K. Momma, A. Takao, M. Nakazawa, N. Shimizu, and R. Matsuoka. 2003. Role of *TBX1* in human del22q11.2 syndrome. Lancet 362:1366–1373.

Yamagishi, H., J. Maeda, T. H. Hu, J. McAnally, S. J. Conway, T. Kume, E. N. Meyers, C. Yamagishi, and D. Srivastava. 2003. *Tbx1* is regulated by tissue-specific forkhead proteins through a common Sonic hedgehog-responsive enhancer. Genes Dev. 17:269–281.

Yang, Q. H., M. J. Khoury, and D. Mannino. 1997. Trends and patterns of mortality associated with birth defects and genetic diseases in the United States, 1979–1992: an analysis of multiple-cause mortality data. Genet. Epidemiol. 14:493–505.

Zankl, A., A. Rampa, and A. Schinzel. 2003. Brachmann-de Lange syndrome (BDLS) with asymmetry and skin pigmentary anomalies: a result of mosaicism for a putative bdls gene mutation? Am. J. Med. Genet. 118:358–361.

This page intentionally left blank

16

Myocardial Stem Cells

Adult cardiomyocytes are considered to be postmitotic, and the heart is thought to possess a relatively constant number of myocytes from just after birth to adulthood and into senescence. It has been proposed that cardiomyocytes can be replenished endogenously by proliferation of a small population of adult myocytes or regeneration by differentiation of stem cell progenitors endogenous to the heart. Because neither acute insult, such as that caused by ischemia, nor chronic disease, represented by cardiomyopathy, is associated with significant cardiomyocyte regeneration, these processes are most likely relatively inefficient. On the other hand, during the last 10 years it has been recognized that myocytes might be recruited from several extracardiac stem cell populations. However, these processes are insufficient to overcome cardiomyocyte death in the acutely or chronically damaged heart. Thus, current stem cell research is directed toward repopulating myocardium from engineered stem cell populations introduced into damaged heart muscle. The most promising stem cells are embryonic stem (ES) cells because of their multipotentiality; however, because of political controversy over the production and use of human stem cells, the complication of rejection, and the potential for formation of teratomas by ES cells, a great deal of attention is focused on autologous or host-derived adult stem cells.

Self-Renewal by Myocardial Cells or Myocardial Stem Cells

The adult heart myocardium has been considered terminally differentiated and as such incapable of regeneration. Cardiac remodeling, rather than myocardial replacement, is the normal response to ischemic insult. The remodeling includes cardiomyocyte hypertrophy, loss of myocytes through cell death, and progressive collagen replacement or fibrosis which ultimately culminates in poor ventricular function and heart failure. A limited population of cardiomyocytes at the border of the infarct region seem to have the ability to proliferate and regenerate myocardium after injury. Ki67, a marker for dividing cells, is positive at 1 day after an infarction, reaching a peak after 3 days and subsequently declining. The appearance of dividing nuclei is somewhat delayed, increasing after 3 days and peaking on day 5. Few Ki67-positive cells and dividing nuclei can be seen in the nonischemic myocardium (Yuasa et al., 2004).

This is in contrast to zebrafish, in which 20% of the myocardium of the adult heart is replaced 2 months after resection of the ventricle (Poss et al., 2002). Regeneration occurs through proliferation of myocardial cells at the leading epicardial edge of the new myocardium. A mitotic checkpoint kinase called Mps1 is a critical regulator of the cell cycle that appears to be important in this regeneration, as zebrafish with a mutation in this gene fail to regenerate myocardium and instead form scars. However, regeneration of this type is still not an option in mammals for recovery from myocardial injury.

De novo myocytes in an injured heart may originate from a proliferatory endogenous stem cell population or by fusion of myocytes with cells capable of proliferation. Myocytes near a myocardial injury may fuse with other proliferative cells to reenter the cell cycle. When cardiomyocytes are co-cultured with a proliferative non-cardiomyocyte population, such as endothelial cells or cardiac fibroblasts, they have been reported to fuse, retaining their cardiomyocyte phenotype but at the same time reentering the cell cycle. Transplanted endothelial cells or skeletal muscle–derived stem cells are thought to fuse with cardiomyocytes in vivo. In other studies, skeletal muscle–derived stem cells differentiate into skeletal myocytes that do not couple with endogenous cardiomyocytes (Abraham et al., 2005; Hutcheson et al., 2000). As Ki67-positive cells express both cardiomyocyte and endothelial lineage markers, fusion with other proliferative cell populations may occur in the injured heart (Matsuura et al., 2004). It is known that endothelial

progenitor cells migrate to ischemic myocardium where they induce neovascularization, preventing myocardial remodeling and fibrosis. These cells could provide the proliferative population needed for fusion. Thus, the presence of capillaries produced by these endothelial cells improves cardiac function and reduces myocardial cell death at the same time as inducing proliferation by the endogenous cardiomyocytes (Schuster et al., 2004).

Intracoronary injection of cardiac stem cells after myocardial injury, on the other hand, has been reported to significantly decrease the size of the infarcted region by limiting remodeling and preserving ventricular function. The new myocytes suspected to be produced by cardiac stem cells, have diploid DNA content and only two chromosomes 12, suggesting that the myocardial regeneration is not necessarily due to cell fusion (Dawn et al., 2005).

Although most adult myocytes are terminally differentiated, several investigators have proposed that there a small subpopulation of cycling myocytes produced by the differentiation of cardiac stem-like cells. It is unclear where these stem cells originate, as they may be set aside from progenitors during heart development. Alternatively, they may be generated elsewhere and take up residence in the heart secondarily. These are recognized by expression of sets of stem cell markers or the capability of cells isolated from the heart to form multiple cell lineages in culture (Beltrami et al., 2003; Kajstura et al., 1998; Quaini et al., 2002).

Sca1-Positive Cells

A population of Stem cell antigen (Sca)-1-positive cells can be isolated from the adult heart. These cells do not express cardiac structural genes or Nkx2.5 and represent a potential stem cell population (Oh et al., 2004). When the Sca-1-positive cells are isolated, they show features of stem cells: when they are exposed to oxytocin or 5′-azacytidine, a cytosine analogue that promotes cellular differentiation, they express cardiac transcription factors Nkx2.5 and Gata4 and contractile proteins including αMhc; develop sarcomeres; and begin to beat spontaneously. The beating cells increase their beat rate when exposed to isoproterenol (Matsuura et al., 2004). Interestingly if the Sca-1-positive cells are *Alk3*-null, they fail to express some of these markers. If the isolated Sca-1-positive cells are administered intravenously after myocardial injury, the cells home to the injured myocardium and differentiate as cardiomyocytes, with and without fusing with host cardiomyocytes (Oh et al., 2003).

A subpopulation of the cardiac Sca-1-positive cells has been further characterized as being c-kit-negative, CD45-negative and CD34-negative. Some stem cells are characterized by the ability to expel a Hoechst nuclear dye. The Hoechst dye excluding fraction in cardiac stem cells is 93% positive for Sca-1, which differs from bone marrow side population stem cells by lacking c-kit and CD45. When engineered to express green fluorescent protein (Gfp) and injected into wild-type blastocyst-stage embryos, in about one third of the resulting chimeras, the cells are found in the left ventricle and atria in about one third of the resulting chimeras. The cells home to ischemic regions when injected intravenously and generate cardiomyocytes in the peri-infarcted zone but are absent in the central portion of the infarcted region (Oh et al., 2004). The new cardiomyocytes represent a combination of fusion products with host cardiomyocytes and unfused cells.

C-kit-Positive Cells

A second subpopulation of intracardiac stem cells has slightly different stem cell surface antigens that include c-kit (stem cell factor receptor) and Mdr1 (Anversa and Nadal-Ginard, 2002b; Quaini et al., 2002). It is not clear if these cells are Sca-1-positive (Beltrami et al., 2003). During myocardial ischemia, there is a rapid induction of stem cell factor, the ligand for c-kit, which potentially activates these c-kit-positive stem cells to produce new myocardial cells (Beltrami et al., 2001; Frangogiannis et al., 1998). In culture c-kit-positive cells that are isolated from adult rat heart show self-renewal and are multipotent because they can differentiate as myocytes or smooth muscle or endothelial cells. When injected into ischemic hearts, this population proliferates and reconstitutes well-differentiated myocardium (Beltrami et al., 2003).

Isl-1-Positive Cells

Another population of potential intracardiac stem cells unrelated to the Sca-1-positive stem cells is Isl-1-positive myocardial progenitors. These cells are found in postnatal rat, mouse, and human myocardium, and they can be grown as stem cells in culture. When cultured with neonatal myocytes, the cells differentiate a mature cardiomyocyte phenotype without fusing with the preexisting myocytes. They are functional in that they show myocardial-type calcium transients and action potentials (Laugwitz et al., 2005).

Adult Extracardiac Stem Cells

Female hearts transplanted into male hosts show a significant number of Y-positive myocytes and coronary vessels suggesting seeding of the transplanted heart with host stem cells (Quaini et al., 2002). There are discrepancies in the literature about the degree of mosaicism in such hearts (Anversa and Nadal-Ginard, 2002a; Glaser et al., 2002; Laflamme et al., 2002; Muller et al., 2002). Homing of bone marrow cells into the myocardium of normal and dystrophic female mice, who received Y-chromosome-positive bone marrow transplants from congenic male donor mice has been detected, showing that cardiac muscle cells can be regenerated by recruitment of circulating bone marrow–derived cells (Bittner et al., 1999; Murry et al., 2004).

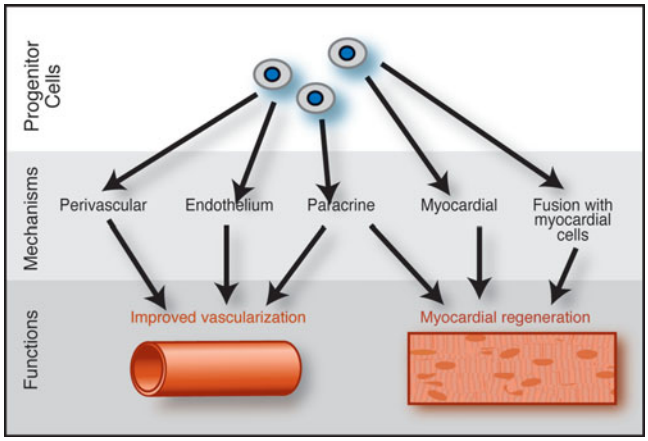

Figure 16.1. Progenitor cells may improve functional recovery of infarcted or failing myocardium by various potential mechanisms, including direct or indirect improvement of neovascularization. Paracrine factors released by progenitor cells may inhibit cardiac apoptosis, affect remodeling, or enhance endogenous repair (e.g., by tissue-resident progenitor cells). Differentiation into cardiomyocytes may contribute to cardiac regeneration. The extent to which these different mechanisms are active may critically depend on the cell type and setting, such as acute or chronic injury. (Adapted from Dimmeler et al., 2005.)

The stem cells that generated the cardiac myocytes may have originated from a variety of places because adult stem cells are found in many mature tissues. Bone marrow and skeletal muscle stem cells are well known self-regenerating cells. They also have the plasticity to generate cell lineages different from those within the organ from which the cells were harvested. Both types of stem cells have been used in recent years to assess their therapeutic potential for myocardial regeneration (Fig. 16.1). However, of all the populations of bone marrow–derived cells, only the mesenchymal stem cells have been shown to differentiate into cardiomyocytes in vitro (Heng et al., 2004). An additional stem cell source is derived from the adult liver which is known for its regenerative capacity and has also provided a stem cell line that shows potential for myocardial repair (Malouf et al., 2001). A final cell type that has been found promising as stem cells is adipocytes. Recent evidence suggests that adult-derived stem cells, like their embryonic counterparts, are pluripotent. These simple, undifferentiated and uncommitted cells are able to respond to signals from their host tissue microenvironment and differentiate, producing progeny that display a phenotype characteristic of the mature cells of that tissue (Heng et al., 2004).

Bone Marrow– and Peripheral Blood–Derived Stem Cells

Bone marrow has been used most frequently as a source of stem cells for clinical cardiac repair (Dimmeler et al., 2005). Stem cells derived from bone marrow are classified into four categories: hematopoietic, endothelial, mesenchymal, and multipotent. Separation of these cell types is important, as engraftment of unsorted cells into infarcted myocardium leads to hematopoietic rather than myocardial differentiation. When the cells are placed outside the infarcted region, they have been reported in some cases to differentiate as cardiomyocytes exclusively through cell fusion (Nygren et al., 2004).

Cardiomyogenic Stem Cells

Cardiomyogenic cells can be isolated from bone marrow–derived stem cells. When noncardiomyocytes are eliminated from a mixture of bone marrow–derived stem cells and expanded in culture, 6%–24% express myocardial genes (Hattan et al., 2005). All of these cells begin to beat spontaneously and express cardiomyocyte-specific genes. Direct cell–cell interaction with cardiomyocytes and soluble signaling molecules are important factors for differentiation of bone marrow cells into cardiomyocytes (Fukuhara et al., 2003; Rangappa et al., 2003). Transplanted into the left ventricle of adult mouse hearts, the cells survive and are oriented parallel to host cardiomyocytes. When male mice–derived c-kit-positive bone marrow cells, expressing green fluorescent protein are implanted in a female heart, they efficiently differentiate into myocytes and coronary vessels with no detectable differentiation into hematopoietic lineages. However, even though some stem cells exert a paracrine effect on the growth behavior of surviving myocardium in a lesion, the bone marrow stem cells do not have this capability. Differentiated cardiomyocytes, coronary arterioles and capillaries are generated independently of any cell fusion (Kajstura et al., 2005).

Hematopoietic Stem Cells

Hematopoietic stem cells are lineage (Lin)-negative, c-Kit-positive, Sca1-positive, and express low but significant levels of Thyl.1 (Thy1.1lo). These have been designated KTLS cells (Shizuru et al., 2005). When Lin-negative, c-Kit-positive bone marrow cells, expressing Gfp, were transplanted into a heart damaged by infarction, they occupied about 70% of the infarcted region as early as 9 days after transplantation and produced proliferating myocytes and vascular structures, that is, cardiomyocytes, endothelial, and smooth muscle cells. The cardiomyocytes expressed cardiac transcription factors Mef2, Gata4, and Nkx2.5; and the gap junction gene, Cx43. Mortality, infarct size, left ventricular cavity dilation and diastolic wall stress were all significantly reduced (Davani et al., 2005; Orlic et al., 2001).

Side Population

A "side population" of hematopoietic stem cells, defined by its ability to expel Hoechst nuclear dye, is CD34-negative, c-Kit-positive, and Sca-1-positive. These cells express the full range of hematopoietic lineages, and their classification as a subpopulation is questionable. This population was used in one study to repair infarcted myocardium and endothelial

cells in mice (Jackson et al., 2001). However, this plasticity of hematopoietic cells has not been reproduced by other investigators who have found only hematopoietic cells after they were introduced into the injured heart (Balsam et al., 2004; Murry et al., 2004).

Mesenchymal Stem Cells

Mesenchymal stem cells are a rare population of multipotent non-hematopoietic stem cells. They are CD34-negative and CD45-negative. Normally they form the stroma for bone marrow. The cells have the ability to differentiate into chondrocytes, osteoblasts, adipocytes, and fibroblasts (Jiang et al., 2002). The bone marrow stem cell population that regenerates myocardium is most likely mesenchymal stem cells (Kawada et al., 2004). Mesenchymal stem cells differentiate into cardiomyocytes after 5-azacytidine treatment if they are cocultured with cardiomyocytes or if they are grown on medium containing insulin, dexamethasone, and ascorbic acid. The cells form beating myocytes connected by intercalated discs. They express many cardiomyocyte transcription factors, including Nkx2.5 and Gata4, as well as Nppa, and α and β myosin heavy chain contractile proteins that are associated with organized sarcomeres. In addition, they exhibit sinus node-like and ventricular action potentials. Myofibrillar proteins are detected early in the cells, with cardiac troponin I, sarcomeric tropomyosin, and cardiac titin among the first expressed. Some cells develop cross-striated myofibrils characterized by α-actinin-positive Z bands after four or five passages in culture (Makino et al., 1999; Shim et al., 2004.)

In one study, human mesenchymal stem cells isolated from bone marrow aspirate were labeled with *lacZ*/β-galactosidase and injected into the left ventricle of adult SCID mice. At 4 days after the injection, none of the engrafted cells expressed myogenic markers but a small number of cells surviving past 1 week slowly adopted characteristics of the surrounding host cardiomyocytes. The cells showed expression of desmin, β-myosin heavy chain (βMhc), α-actinin, cardiac troponin T, and phospholamban at levels comparable to those of the host cardiomyocytes. In addition, the contractile proteins formed sarcomeres (Toma et al., 2002).

Peripheral Blood

Use of adult peripheral blood stem cells generated in the bone marrow would greatly simplify the process of obtaining cells for homografting. In one study, CD34-positive cells isolated from adult peripheral blood differentiated into cardiomyocytes, mature endothelial cells, and smooth muscle cells in vivo. The differentiation was augmented significantly by local tissue injury (Yeh et al., 2003).

Even with these encouraging results, the findings from different studies are controversial because different studies have shown completely opposite results. Endothelial progenitor cells are one of the subpopulations of mononuclear cells in the peripheral blood. These cells express vascular endothelial growth factor (Vegf) receptor 2, CD34, and CD133 (Davani et al., 2005). In some studies, they do not differentiate either in vitro or in vivo into cardiomyocytes. However, in other studies, they differentiate as endothelial cells in culture, and they home to ischemic regions of myocardium where they contribute to neovascularization in vivo. It is this increased circulation in the ischemic region, and not augmentation of the cardiomyocyte population in the region, that is suggested to improve left ventricular function and decrease myocyte cell death (Asahara et al., 1999; Kawamoto et al., 2001; Kocher et al., 2001). In another study, labeled epithelial progenitor cells that were co-cultured with rat cardiomyocytes for 6 days showed an increase in cell length and size to a cardiomyocyte-like morphology. About 10% of these cells express Mef2, Nppa, α-actinin, and cardiac troponin I. They show partial sarcomeric organization and develop functional gap junctions. The cells have calcium transients that are synchronized with adjacent rat cardiomyocytes. Evidently the physical presence of cardiomyocytes is a prerequisite for their differentiation as cardiomyocytes because they do not differentiate when they are exposed to cardiomyocyte-conditioned medium but they do when co-cultured with paraformaldehyde-fixed cardiomyocytes (Badorff et al., 2003).

Skeletal Muscle Stem Cells

Skeletal muscle stem cells, also known as satellite cells, were the first autologous adult stem cells proposed for clinical evaluation (Dimmeler et al., 2005). These cells reside in the basal lamina of adult skeletal muscles. They are undifferentiated and proliferation-competent cells that can regenerate damaged skeletal muscle fibers. Skeletal myoblasts have several potential advantages for cardiac therapy. They are resistant to ischemia, can be harvested as autologous cells, expanded and modified in vitro, and differentiate efficiently into adult skeletal muscle (Chiu et al., 1995; el Oakley et al., 1998; Taylor et al., 1998). Furthermore, autologous skeletal myoblasts can regenerate viable striated tissue within cryodamaged myocardium (Atkins et al., 1999). However, when co-cultured with cardiac myocytes, they couple but fail to form a nexus with the cardiac myocytes. This failure to form junctions potentially underlies problems related to ventricular arrhythmias in patients following introduction of skeletal muscle stem cells into the heart (Abraham et al., 2005).

Adult rat satellite cells, tagged in vitro with bromodeoxyuridine, have been grafted into normal hearts of syngeneic rats. The grafted cells form multinucleated, striated myofibrils that express the fast skeletal myosin heavy chain characteristic of a mature skeletal muscle phenotype. None of the grafts express cardiac markers or the intercalated disk proteins N-cadherin or Cx43, suggesting that neither cardiac contractile properties nor electromechanical coupling occur (Reinecke et al., 2002). Thus, skeletal satellite cells are not appropriate for myocardial differentiation without some preliminary differentiation in vitro. Stem cells from embryonic avian and neonatal rat skeletal

muscle differentiate into several mesodermal phenotypes in culture with dexamethasone treatment. However, there is also a population of non-satellite cells in adult murine skeletal muscle that progress under standard cell culture conditions to autonomously beating cardiomyocytes. If the cells are marked and injected intravascularly after acute myocardial infarction, they home to the heart and begin to differentiate without fusing to the host myocardial cells. Three months later, the cells were identified as striated muscle restricted to the region of the cardiac infarct (Winitsky et al., 2005).

Skeletal muscle cell grafting gives rise to a subpopulation of skeletal–cardiac hybrid cells with a currently unknown phenotype. Because myoblasts are disposed to fuse with other myoblasts during development, they are likely to fuse easily with cardiomyocytes. When neonatal rat cardiomyocytes are labeled with *lacZ*/β-galactosidase and green fluorescent protein (Gfp) and cocultured with unlabeled C2C12 myoblasts, a small population of skeletal myotubes expressing *lacZ* and GFP appear. Grafting of β-galactosidase-expressing C2C12 myoblasts into normal nude mouse hearts results in cells at the graft–host interface that express both β-galactosidase and cardiac-specific myosin light chain (Mlc)2v. Skeletal muscle cells have been constructed to express *Cre* when the cells fuse. If these are cocultured with myoblasts from *floxed–lacZ* reporter mice, the *lacZ* is activated, indicating fusion of the skeletal and cardiac myoblasts. Finally, *floxed–lacZ* skeletal myoblasts grafted into normal hearts of *αMHC-Cre*-positive mice show β-galactosidase expression, again indicating fusion of the skeletal myoblasts with host cardiomyocytes (Reinecke et al., 2004).

Skeletal muscle cells can differentiate into cardiomyocytes if they are in direct cell-to-cell contact with contracting cardiomyocytes. Cocultured skeletal muscle cells, isolated from transgenic mice expressing Gfp-positive skeletal muscle cells and cocultured with cardiomyocytes isolated from neonatal rats, express cardiac-specific markers, such as cardiac troponin T, Nppa, Nkx2.5, and Gata4. At their junctions with neighboring cardiomyocytes, the Gfp-positive cells express cadherin and Cx43. The cells show spontaneous action potentials that are blocked by treatment with nifedipine or cultured in Ca^{2+}-free medium. Interestingly, blocking calcium transients with these treatments also inhibits the skeletal muscle cells from expressing cardiac-specific proteins (Iijima et al., 2003). However, even though the skeletal myoblasts appear to be coupled via gap junctions with cardiac myoblasts they do not form normal electrically coupled junctions (Abraham et al., 2005).

Direct injection of autologous skeletal myoblasts into the region around injured myocardium has been performed during coronary bypass surgery and by subendocardial injection in the catheterization laboratory. Both approaches appear to improve function significantly. Nonetheless, ventricular arrhythmias occur quite frequently in the first week after myoblast injection suggesting that the skeletal myoblast-derived cells do not form appropriate contacts and disrupt normal myocardial electrical activation. In contrast, bone marrow–derived stem cells can be delivered to the injured myocardium by injection or by bone marrow stimulation, and while the incidence of ventricular arrhythmia does not seem to increase, the magnitude of functional improvement is marginal (Bick-Forrester et al., 2004).

Adipose Tissue

Adipose-derived adult stem cells are negative for CD31, CD34, CD106, and Vcam-1, and positive for fetal liver kinase (Flk1). The cells can be induced to differentiate into osteogenic and adipogenic lineages in vitro. They also have characteristics of endothelial progenitor cells when cultured with Vegf. The PI3 kinase inhibitor Ly294002 blocks differentiation of the cells into endothelial cells in vitro. The cells can be expanded in culture without senescence for more than 20 population doublings; they may be a potential source of endothelial cells for cellular pro-angiogenic therapies. In vivo, these cells can differentiate into endothelial cells that contribute to angiogenesis in hindlimb ischemia models (Cao et al., 2005).

Human adipose tissue stem cells demonstrate cardiomyocyte properties following transient exposure to cardiomyocyte extract. The cells express sarcomeric α-actinin, desmin, cardiac troponin I, and Cx43. They form binucleated, striated cells, beat spontaneously, express nuclear lamin A/C, a marker of terminally differentiated cells, and show increased cell cycle length (Gaustad et al., 2004).

Adult mesenchymal stem cells can be isolated from adipose tissue. Treatment with 5-azacytidine induces the cells to become binucleated and extend cytoplasmic processes to adjacent cells. At 2 weeks, 20%–30% of the cells have increased in size and form a ball-like appearance, and after 3 weeks they began to beat spontaneously. The cells show immunostaining for myosin heavy chain, α-actinin, and troponin-I (Rangappa et al., 2003).

Liver-Derived Stem Cells

An adult liver stem cell line (WBF344) was established from a single cloned epithelial cell isolated from a normal adult male rat liver. The cell line has been genetically modified to express β-galactosidase and Gfp. When these cells are co-cultured with dissociated rat or mouse neonatal cardiac cells, they express cardiac-specific proteins, develop a sarcoplasmic reticulum, and show myofibril and sarcomere formation. The cells beat rhythmically and have calcium transients. Coupling but not fusion with the adjacent established cardiomyocytes is important for myocardial differentiation (Muller-Borer et al., 2004), When the cells are transplanted into the hearts of female nude mice, they can be identified in their host tissues by the presence of a rat Y-chromosome–specific repetitive DNA sequence and by either β-galactosidase or Gfp expression. They differentiate in vivo into cardiomyocytes ranging from 20 to 110 um in length. The larger cells contain well-organized sarcomeres and myofibrils and form intercalated disks and gap junctions with their host myocytes (Malouf et al., 2001).

Embryonic Stem Cells

Embryonic stem (ES) cells are harvested from early embryos and grown in clonal cell lines in culture conditions that maintain their undifferentiated status (Fig. 16.2). These cells differentiate in vivo into all cell lineages and in vitro into many cell types depending on the culture conditions. Expression of cardiomyocyte molecular markers by ES cells as they differentiate into cardiomyocytes follows steps that recapitulate those of the in vivo differentiation of embryonic cardiomyocytes. Messenger RNA and proteins are expressed for the transcription factors Gata4 and Nkx2.5 first, followed by those for Nppa, Z-disk titin, α-actinin, myomesin, M band titin, myosin heavy chains, α-actin, cardiac troponin T (cTnT), myosin light chain (Mlc)2v, the Na^+–Ca^{2+} exchanger (NCX), and phospholamban (Doetschman et al., 1985; Loscalzo, 2004). In vitro the cells form structural and electromechanical connections with cardiomyocytes (Kehat et al., 2004). The cells gradually change from small and spherical to larger rod-shaped cells with recognizable myofibrils (Guan et al., 1999; Hescheler et al., 1997; Maltsev et al., 1993, 1994).

There is a time-dependent expression of ion channels (Abi-Gerges et al., 2000; Maltsev et al., 1993, 1994). ES cells that develop into cardiomyocytes begin to manifest spontaneous contractile activity by days 10–12 in culture and also develop into a functional syncytium through which waves of depolarization are propagated as spontaneous contractility becomes increasingly coordinated (Loscalzo, 2004). The expression of multiple connexins is differentially regulated during cardiomyocyte differentiation of ES cells (Oyamada et al., 1996). Transcripts for Cx43 and Cx45 with evidence of functional coupling can be detected in undifferentiated ES cells and in embryoid bodies before and after the appearance of beating cardiomyocytes. In contrast, Cx40 transcripts are not present in undifferentiated ES cells until beating starts.

Electrophysiological properties during the differentiation process indicate that the beat frequency of the preparation increases concomitant with a decrease of the action potential duration and rise time. The increase of conduction velocity is coincident with an increase in expression of Cx43 gap junction channels. After 4 weeks in culture, the cells begin to exhibit electrophysiological characteristics of the sinoatrial node, atrial, or ventricular myocytes. The cells respond to adrenergic stimulation from the first day of spontaneous beating but are not sensitive to cholinergic agonists until 4 days (Banach et al., 2003; Maltsev et al., 1999).

ES cells have the potential to acquire chamber specific myocardial properties. The cells heterogeneously express cTnI, Mlc2v, and Nppa. Treatment of the embryoid bodies with retinoic acid increases the percentage of Mlc2v-negative, atrial natriuretic peptide–positive cells and atrial-specific genes (Hidaka et al., 2003). Action potential recordings confirm the ability of the cells to differentiate into region-specific atrial, ventricular, and pacemaker cells (Hescheler et al., 1997; Maltsev et al., 1994). These different cell types are arranged in clusters rather than randomly distributed (Metzger et al., 1996; Miller-Hance et al., 1993). The cells are capable of developing into pacemaking cells. When human ES cells were placed in a pig heart with complete atrioventricular block they formed a rate-responsive pacemaker (Kehat et al., 2004).

One of the drawbacks to using human ES cells is that they are derived mainly from surplus embryos from in vitro fertilization, which means that they are allogenic and may provoke rejection by the host. A second drawback that has recently been alleviated is the need to destroy the conceptus to harvest the ES cells. However, new strategies are being developed to create ES cells from transplantation of an autologous epithelial cell nucleus into an ovum from which the haploid nucleus has been removed. The ES cells can be obtained from the multicellular clone which would be autologous with the nucleus of the donor. It is now possible to remove one cell from an eight-cell embryo without destroying the embryo. The single cell can be expanded and maintained as an ES cell line. A second technique involves harvest of human oocytes and replacing the nucleus with a donor nucleus. This technique has the advantage of allowing creation of an autogeneic ES cell line (Hwang et al., 2005).

In addition to these ethical concerns, ES cells have additional drawbacks, such as increased cell death due to ischemia when cardiomyocytes derived from ES cells are grafted into normal myocardium; and the potential for human ES cells to form teratomas in immunocompromised individuals (Gearhart, 1998; Thomson et al., 1998; Weissman, 2002; Zhang et al., 2001).

Figure 16.2. Embryonic stem (ES) and embryonic heart induction. ES cells are obtained from the inner cell mass of the blastocyst embryo which normally gives rise to an embryo with three germ layers during gastrulation. The ES cells are maintained as undifferentiated cells. For differentiation as cardiomyocytes they are cultured as embryoid bodies and induced with various factors. Induction probably recapitulates signaling that is normally produced by the endoderm during embryonic development. (From Foley and Mercola, 2004, with permission.)

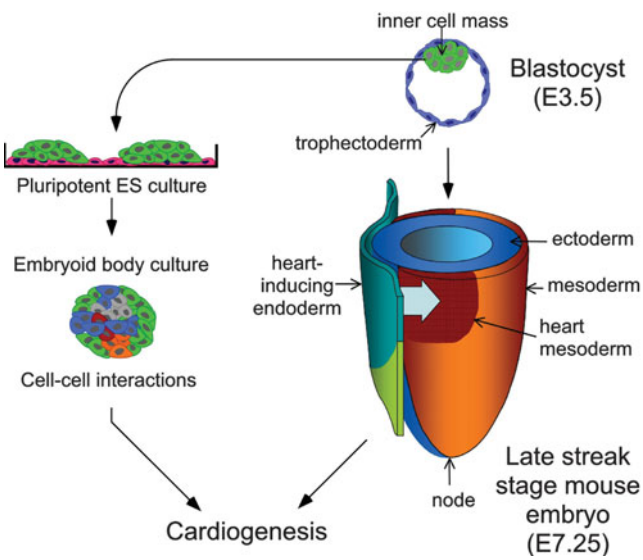

Stem Cell Homing

Homing is a multistep process that includes adhesion to activated endothelium or matrix, transmigration through the endothelium and invasion of the target tissue (Fig. 16.3). The mechanisms involved in stem cell homing to sites of injury are not well understood. It is known that a chemokine called stromal cell-derived factor-1 (Sdf1) mediates homing of stem cells to bone marrow by binding to receptors on circulating cells. Sdf1 and its receptor Cxcr4 are expressed in complementary patterns during embryonic organogenesis and guide stem cells to sites of rapid vascular expansion. They are also expressed in the adult cardiomyocytes. Sdf1 gene expression is regulated by hypoxia inducible factor (Hif)1, a hypoxia-induced transcription factor in endothelial cells. Thus, Sdf1 is expressed in ischemic tissue in direct proportion to reduced oxygen tension. Hif1-induced Sdf1 expression increases the adhesion, migration and homing of circulating progenitor cells to ischemic tissue; and blockade of Sdf1 in ischemic tissue prevents progenitor cell recruitment to sites of injury (Ceradini et al., 2004). Whether this system of homing can be engineered to improve homing of stem cells to ischemic myocardium is under investigation.

Figure 16.3. Mobilization and homing of stem cells. After intravascular delivery or mobilization from bone marrow, progenitor cells are targeted to the sites of injury by multiple signals. Homing is mediated by a multistep process including the initial adhesion, transmigration, and invasion. Molecular mechanisms contributing to these individual steps are indicated but likely vary depending on the cell type and model. (From Dimmeler et al., 2005, with permission.)

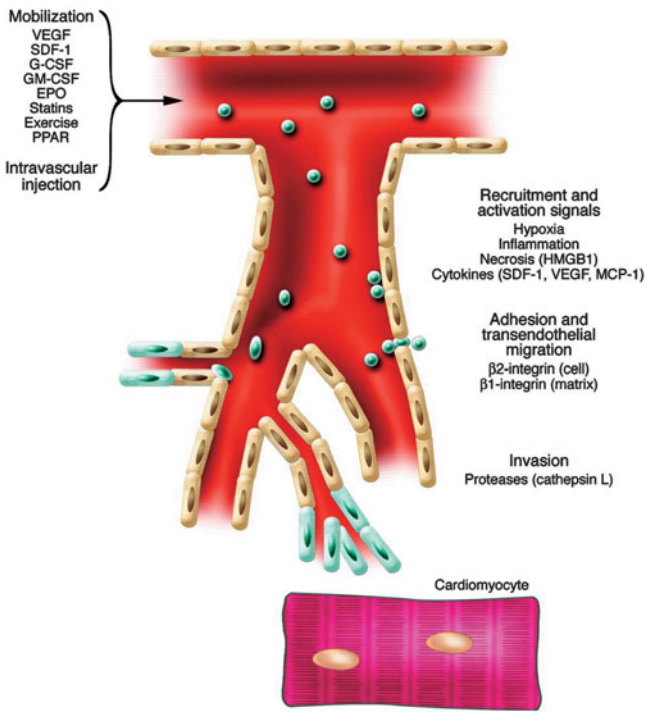

Clinical Trials

There are still many challenges to restoring cardiac function using stem cell therapy (Fig. 16.4). Cells that potentially restore cardiac function do so by several different mechanisms. These include incorporation as perivascular cells and differentiation as endothelial cells. Both of these features improve the chance and amount of neovascularization, which is important for endogenous cardiac regeneration. The other major mechanisms include differentiation of stem cells to a cardiac phenotype and fusion with cardiomyocytes to promote proliferation of a normally non-proliferative population (Fig. 16.5). Both the improvement of vascularization and regeneration of cardiomyocytes are benefited by production of paracrine factors.

Some of the consequences that still remain to be resolved in clinical repair of damaged hearts include: long-term fate of transplanted stem cells; ability of the transplanted cells to find

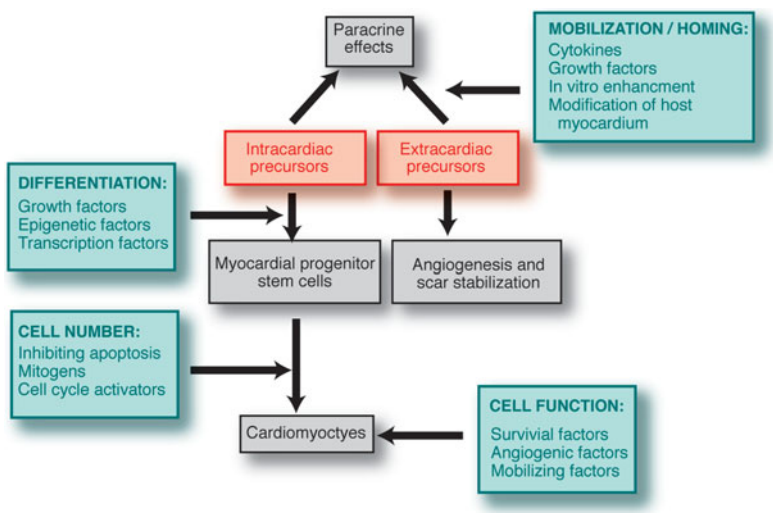

Figure 16.4. Current challenges for cell-based therapy in cardiac repair include identifying the origins of the novel cardiac progenitor and stem cells found within the heart, pinpointing the biologically active cells from bone marrow and other mixed populations, optimizing cell mobilization and homing, augmenting grafted cells' survival, defining the cues for cardiac differentiation, promoting donor cell proliferation, and exploiting cell therapy as a platform for secretory signals. (Adapted from Dimmeler et al., 2005.)

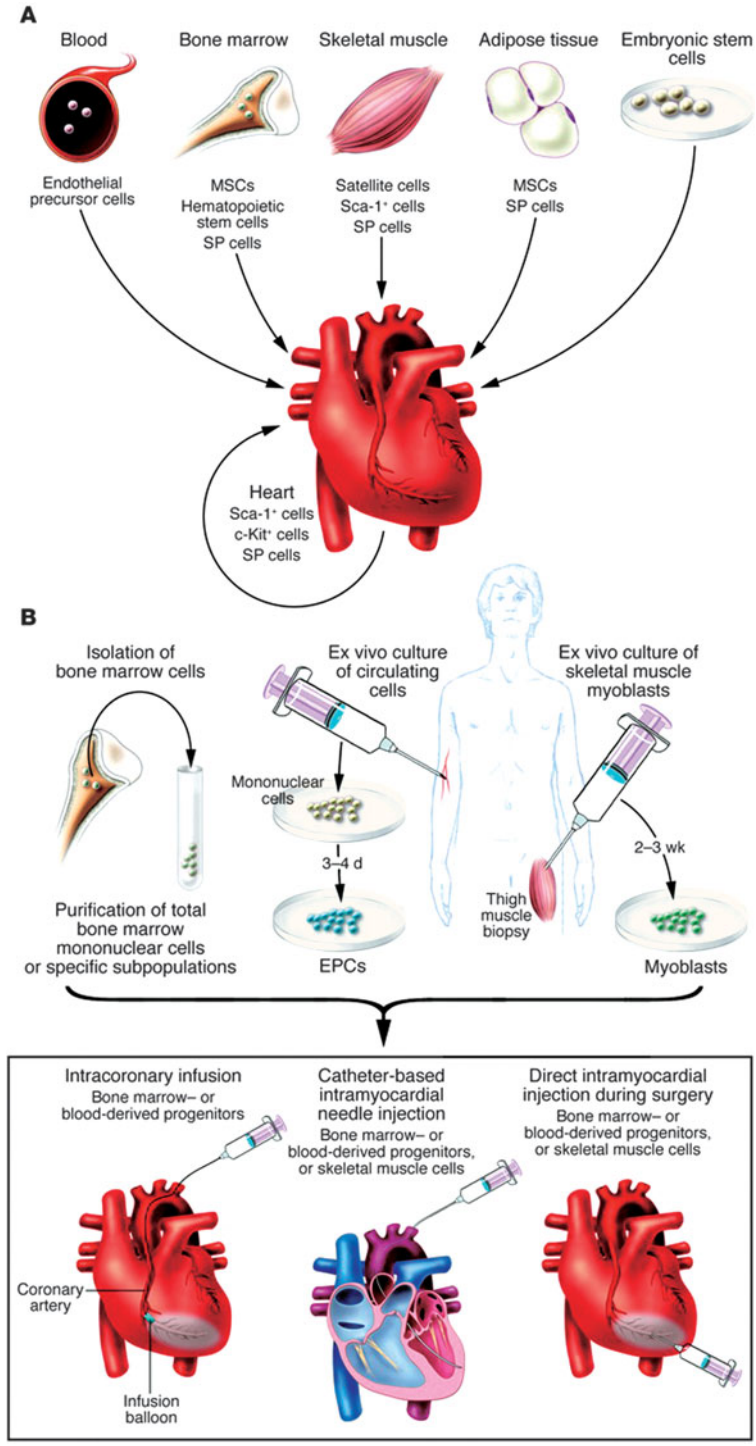

Figure 16.5. Summary of the sources of cells for cardiac repair, and routes of their administration. (*A*) Cells in current human trials include skeletal myoblasts, bone marrow, ES cells, adipose tissue, circulating (endothelial) progenitor cells and endogenous cardiac stem cells. (*B*) The cells are harvested from various locations and expanded in vitro prior to reintroduction into the heart. (*C*) Current trials use intracoronary, intramuscular, or direct injection during cardiac surgery. (From Dimmeler et al., 2005, with permission.)

an adequate myocardial environment to support their own differentiation; potency of the exogenous cells to transdifferentiate into cardiac cells; and angiogenesis needed to support regenerated myocytes (Quaini et al., 2004).

Bone marrow and circulating progenitor cells have been used in several clinical trials with promising results (Dimmeler et al., 2005). All of the published trials have similar results at 4–6 months after cell implantation. Generally about a million cells are implanted into the peri-infarct border zone during coronary artery bypass. Patients show slight improvement in global left ventricular ejection fraction, significantly reduced end-systolic left ventricular volumes and improved perfusion in the damaged region of myocardium. Even when different numbers of cells are infused the improvements are nearly identical. One of the first randomized, controlled trials for bone marrow engraftment involved 60 patients with myocardial

infarction who received autologous bone marrow cells by either intracoronary infusion or standard chemotherapy. At 6 months, the patients with the bone marrow infusion showed improved left ventricular function (Wollert et al., 2004).

One trial in which skeletal muscle–derived progenitor cells were injected directly into the scarred region of the left ventricle showed global and regional improvement in function, but patients receiving this therapy experienced life-threatening arrhythmias possible due to the lack of electrical coupling of skeletal muscle to the neighboring cardiomyocytes (Leobon et al., 2003; Smits et al., 2003).

Mobilizing endogenous stem cells has been considered by administering cytokines such as granulocyte colony stimulating factor and stem cell factor. Both cause increased release of stem cells from bone marrow into peripheral blood. If the cells can be induced to home to the myocardium and differentiate as cardiomyocytes, this could be the least invasive and perhaps safest of the therapies for improving cardiac function after injury. Administration of cytokines to mice prior to and after myocardial injury decreased the ischemic area by 40%, and cardiac function was improved along with survival (Orlic et al., 2001). However, a similar protocol tried in baboons enhanced the perfusion of the damaged myocardium but had little effect on myocardial repair (Norol et al., 2003).

Chronic Ischemic Heart Failure

In a phase I clinical trial of 10 patients with a left ventricular ejection fraction of less than 35%, an akinetic postinfarction scar, and indication for coronary artery bypass grafting, about 900 million autologous skeletal myoblast cells were injected into the scar during bypass grafting. At 10 months, contraction and viability were improved but ventricular arrhythmias developed between 11–22 days posttransplantation (Menasche et al., 2003). These results led to the requirement that patients enrolled in this trial have an implantable cardiovascular defibrillator.

In a series of non-randomized studies, CD133-positive bone marrow cells injected into the infarct border during coronary bypass showed improved myocardial perfusion with no accompanying episodes of ventricular arrhythmias but these resulted in little effect on ventricular contractility (Stamm et al., 2003). However, results with bone marrow–derived cells are in some cases at odds. Delivery of bone marrow mononuclear cells that are CD34- and CD45-positive by transendocardial catheter resulted in improved left ventricular function in one study (Perin et al., 2003). In a separate study with a similar protocol, the patients had decreased anginal episodes with no evidence of arrhythmias but also no improvement in left ventricular function (Tse et al., 2003).

Acute Myocardial Infarction

Cells have been administered to patients by transendocardial catheters, intravenous delivery, and local administration into the ischemic area during open heart surgery. Intravenous delivery is the easiest route, but because many cells are eliminated in the lungs, only a low percentage reaches the injured myocardium, necessitating the injection of a large number of cells. Transendocardial catheter-based cell administration is safe, but requires a high concentration of cells injected directly into the vessels supplying the target area (Strauer et al., 2002). The high pressures used for delivery of the cell solution may induce arrhythmias (Wollert et al., 2004). Local administration of the transplanted cells may be preferable to intravenous delivery; however, cells implanted into an ischemic area during open heart surgery cause arrhythmias (Menasche et al., 2001).

A group of patients who received autologous bone marrow–derived mononuclear cells isolated by Ficoll density separation, cultured overnight and administered by high-pressure infusion into an infarcted artery was compared to a group that received standard care. The stem cell group demonstrated reduced infarct size and increased stroke volume without an altered ejection fraction (Strauer et al., 2002). In an uncontrolled experiment, patients with percutaneous coronary intervention with stent implantation for acute myocardial infarction received autologous bone marrow–derived mononuclear cells, and after 6 months there was a significant increase in ejection fraction; but left ventricular diastolic volume was not different from patients who did not receive the transplant, indicating no improvement of ventricular remodeling (Wollert et al., 2004).

The idea that the diseased heart can be repaired by endogenous or extracardiac stem cells has revolutionized our thinking about cardiac repair. While the clinical trials are still too few to be definitive, they hold great promise. Large, randomized trials with carefully constructed control groups will be invaluable in making progress toward heart repair.

REFERENCES

Abi-Gerges, N., G. J. Ji, Z. J. Lu, R. Fischmeister, J. Hescheler, and B. K. Fleischmann. 2000. Functional expression and regulation of the hyperpolarization activated non-selective cation current in embryonic stem cell-derived cardiomyocytes. J. Physiol. 523 Pt 2:377–389.

Abraham, M. R., C. A. Henrikson, L. Tung, M. G. Chang, M. Aon, T. Xue, R. A. Li, B. O'Rourke, and E. Marban. 2005. Antiarrhythmic engineering of skeletal myoblasts for cardiac transplantation. Circ. Res. 97:159–167.

Anversa, P., and B. Nadal-Ginard. 2002a. Cardiac chimerism: methods matter. Circulation 106:e129–31; author reply e129–131.

Anversa, P., and B. Nadal-Ginard. 2002b. Myocyte renewal and ventricular remodelling. Nature 415:240–243.

Asahara, T., H. Masuda, T. Takahashi, C. Kalka, C. Pastore, M. Silver, M. Kearne, M. Magner, and J. M. Isner. 1999. Bone marrow origin of endothelial progenitor cells responsible for postnatal vasculogenesis in physiological and pathological neovascularization. Circ. Res. 85:221–228.

Atkins, B. Z., C. W. Lewis, W. E. Kraus, K. A. Hutcheson, D. D. Glower, and D. A. Taylor. 1999. Intracardiac transplantation of skeletal myoblasts yields two populations of striated cells in situ. Ann. Thorac. Surg. 67:124–129.

Badorff, C., R. P. Brandes, R. Popp, S. Rupp, C. Urbich, A. Aicher, I. Fleming, R. Busse, A. M. Zeiher, and S. Dimmeler. 2003. Transdifferentiation of blood-derived human adult endothelial progenitor cells into functionally active cardiomyocytes. Circulation 107:1024–1032.

Balsam, L. B., A. J. Wagers, J. L. Christensen, T. Kofidis, I. L. Weissman, and R. C. Robbins. 2004. Haematopoietic stem cells adopt mature haematopoietic fates in ischaemic myocardium. Nature 428:668–673.

Banach, K., M. D. Halbach, P. Hu, J. Hescheler, and U. Egert. 2003. Development of electrical activity in cardiac myocyte aggregates derived from mouse embryonic stem cells. Am. J. Physiol. 284: H2114–H2123.

Beltrami, A. P., L. Barlucchi, D. Torella, M. Baker, F. Limana, S. Chimenti, H. Kasahara, M. Rota, E. Musso, K. Urbanek, A. Leri, J. Kajstura, B. Nadal-Ginard, and P. Anversa. 2003. Audult cardiac stem cells are multipotent and support myocardial regeneration. Cell 114:763–776.

Beltrami, A. P., K. Urbanek, J. Kajstura, S. M. Yan, N. Finato, R. Bussani, B. Nadal-Ginard, F. Silvestri, A. Leri, C. A. Beltrami, and P. Anversa. 2001. Evidence that human cardiac myocytes divide after myocardial infarction. N. Engl. J. Med. 344: 1750–1757.

Bick-Forrester, J., M. S. Lee, R. R. Makkar, and J. S. Forrester. 2004. Partial restoration of myocardial function and perfusion by cell therapy following myocardial infarction. Curr. Opin. Cardiol. 19:631–637.

Bittner, R. E., C. Schofer, K. Weipoltshammer, S. Ivanova, B. Streubel, E. Hauser, M. Freilinger, H. Hoger, A. Elbe-Burger, and F. Wachtler. 1999. Recruitment of bone–marrow–derived cells by skeletal and cardiac muscle in adult dystrophic mdx mice. Anat. Embryol. (Berl) 199:391–396.

Cao, Y., Z. Sun, L. Liao, Y. Meng, Q. Han, and R. C. Zhao. 2005. Human adipose tissue-derived stem cells differentiate into endothelial cells in vitro and improve postnatal neovascularization in vivo. Biochem. Biophys. Res. Commun. 332:370–379.

Ceradini, D. J., A. R. Kulkarni, M. J. Callaghan, O. M. Tepper, N. Bastidas, M. E. Kleinman, J. M. Capla, R. D. Galiano, J. P. Levine, and G. C. Gurtner. 2004. Progenitor cell trafficking is regulated by hypoxic gradients through HIF-1 induction of SDF-1. Nat. Med. 10:858–864.

Chiu, R. C., A. Zibaitis, and R. L. Kao. 1995. Cellular cardiomyoplasty: myocardial regeneration with satellite cell implantation. Ann. Thorac. Surg. 60:12–18.

Davani, S., F. Deschaseaux, D. Chalmers, P. Tiberghien, and J. P. Kantelip. 2005. Can stem cells mend a broken heart? Cardiovasc. Res. 65:305–316.

Dawn, B., A. B. Stein, K. Urbanek, M. Rota, B. Whang, R. Rastaldo, D. Torella, X. L. Tang, A. Rezazadeh, J. Kajstura, A. Leri, G. Hunt, J. Varma, S. D. Prabhu, P. Anversa, and R. Bolli. 2005. Cardiac stem cells delivered intravascularly traverse the vessel barrier, regenerate infarcted myocardium, and improve cardiac function. Proc. Natl. Acad. Sci. USA 102:3766–3771.

Dimmeler, S., A. M. Zeiher, and M. D. Schneider. 2005. Unchain my heart: the scientific foundations of cardiac repair. J. Clin. Invest. 115:572–583.

Doetschman, T. C., H. Eistetter, M. Katz, W. Schmidt, and R. Kemler. 1985. The in vitro development of blastocyst-derived embryonic stem cell lines: formation of visceral yolk sac, blood islands and myocardium. J. Embryol. Exp. Morph. 87:27–45.

el Oakley, R. M., N. J. Brand, P. B. Burton, M. C. McMullen, G. B. Adams, M. C. Poznansky, P. J. Barton, and M. H. Yacoub. 1998. Efficiency of a high-titer retroviral vector for gene transfer into skeletal myoblasts. J. Thorac. Cardiovasc. Surg. 115:1–8.

Foley, A., and M. Mercola. 2004. Heart induction: embryology to cardiomyocyte regeneration. Trends Cardiovasc. Med. 14:121–125.

Frangogiannis, N. G., J. L. Perrard, L. H. Mendoza, A. R. Burns, M. L. Lindsey, C. M. Ballantyne, L. H. Michael, C. W. Smith, and M. L. Entman. 1998. Stem cell factor induction is associated with mast cell accumulation after canine myocardial ischemia and reperfusion. Circulation 98:687–698.

Fukuhara, S., S. Tomita, S. Yamashiro, T. Morisaki, C. Yutani, S. Kitamura, and T. Nakatani. 2003. Direct cell-cell interaction of cardiomyocytes is key for bone marrow stromal cells to go into cardiac lineage in vitro. J. Thorac. Cardiovasc. Surg. 125:1470–1480.

Gaustad, K. G., A. C. Boquest, B. E. Anderson, A. M. Gerdes, and P. Collas. 2004. Differentiation of human adipose tissue stem cells using extracts of rat cardiomyocytes. Biochem. Biophys. Res. Commun. 314:420–427.

Gearhart, J. 1998. New potential for human embryonic stem cells. Science 282:1061–1062.

Glaser, R., M. M. Lu, N. Narula, and J. A. Epstein. 2002. Smooth muscle cells, but not myocytes, of host origin in transplanted human hearts. Circulation 106:17–19.

Guan, K., D. O. Furst, and A. M. Wobus. 1999. Modulation of sarcomere organization during embryonic stem cell-derived cardiomyocyte differentiation. Eur. J. Cell Biol. 78:813–823.

Hattan, N., H. Kawaguchi, K. Ando, E. Kuwabara, J. Fujita, M. Murata, M. Suematsu, H. Mori, and K. Fukuda. 2005. Purified cardiomyocytes from bone marrow mesenchymal stem cells produce stable intracardiac grafts in mice. Cardiovasc. Res. 65:334–344.

Heng, B. C., H. Haider, E. K. Sim, T. Cao, and S. C. Ng. 2004. Strategies for directing the differentiation of stem cells into the cardiomyogenic lineage in vitro. Cardiovasc. Res. 62:34–42.

Hescheler, J., B. K. Fleischmann, S. Lentini, V. A. Maltsev, J. Rohwedel, A. M. Wobus, and K. Addicks. 1997. Embryonic stem cells: a model to study structural and functional properties in cardiomyogenesis. Cardiovasc. Res. 36:149–162.

Hidaka, K., J. K. Lee, H. S. Kim, C. H. Ihm, A. Iio, M. Ogawa, S. Nishikawa, I. Kodama, and T. Morisaki. 2003. Chamber-specific differentiation of *Nkx2.5*-positive cardiac precursor cells from murine embryonic stem cells. FASEB J. 17:740–742.

Hutcheson, K. A., B. Z. Atkins, M. T. Hueman, M. B. Hopkins, D. D. Glower, and D. A. Taylor. 2000. Comparison of benefits on myocardial performance of cellular cardiomyoplasty with skeletal myoblasts and fibroblasts. Cell Transplant. 9:359–368.

Hwang, W. S., S. I. Roh, B. C. Lee, S. K. Kang, D. K. Kwon, S. Kim, S. J. Kim, S. W. Park, H. S. Kwon, C. K. Lee, J. B. Lee, J. M. Kim, C. Ahn, S. H. Paek, S. S. Chang, J. J. Koo, H. S. Yoon, J. H. Hwang, Y. Y. Hwang, Y. S. Park, S. K. Oh, H. S. Kim, J. H. Park, S. Y. Moon, and G. Schatten. 2005. Patient-specific embryonic stem cells derived from human SCNT blastocysts. Science 308:1777–1783.

Iijima, Y., T. Nagai, M. Mizukami, K. Matsuura, T. Ogura, H. Wada, H. Toko, H. Akazawa, H. Takano, H. Nakaya, and I. Komuro. 2003. Beating is necessary for transdifferentiation of skeletal muscle-derived cells into cardiomyocytes. FASEB J. 17:1361–1363.

Jackson, K. A., S. M. Majka, H. Wang, J. Pocius, C. J. Hartley, M. W. Majesky, M. L. Entman, L. H. Michael, K. K. Hirschi, and M. A. Goodell. 2001. Regeneration of ischemic cardiac muscle

and vascular endothelium by adult stem cells. J. Clin. Invest. 107:1395–1402.

Jiang, Y., B. N. Jahagirdar, R. L. Reinhardt, R. E. Schwartz, C. D. Keene, X. R. Ortiz-Gonzalez, M. Reyes, T. Lenvik, T. Lund, M. Blackstad, J. Du, S. Aldrich, A. Lisberg, W. C. Low, D. A. Largaespada, and C. M. Verfaillie. 2002. Pluripotency of mesenchymal stem cells derived from adult marrow. Nature 418:41–49.

Kajstura, J., A. Leri, N. Finato, C. Di Loreto, C. A. Beltrami, and P. Anversa. 1998. Myocyte proliferation in end-stage cardiac failure in humans. Proc. Natl. Acad. Sci. USA 95:8801–8805.

Kajstura, J., M. Rota, B. Whang, S. Cascapera, T. Hosoda, C. Bearzi, D. Nurzynska, H. Kasahara, E. Zias, M. Bonafe, B. Nadal-Ginard, D. Torella, A. Nascimbene, F. Quaini, K. Urbanek, A. Leri, and P. Anversa. 2005. Bone marrow cells differentiate in cardiac cell lineages after infarction independently of cell fusion. Circ. Res. 96:127–137.

Kawada, H., J. Fujita, K. Kinjo, Y. Matsuzaki, M. Tsuma, H. Miyatake, Y. Muguruma, K. Tsuboi, Y. Itabashi, Y. Ikeda, S. Ogawa, H. Okano, T. Hotta, K. Ando, and K. Fukuda. 2004. Nonhematopoietic mesenchymal stem cells can be mobilized and differentiate into cardiomyocytes after myocardial infarction. Blood 104:3581–3587.

Kawamoto, A., H. C. Gwon, H. Iwaguro, J. I. Yamaguchi, S. Uchida, H. Masuda, M. Silver, H. Ma, M. Kearney, J. M. Isner, and T. Asahara. 2001. Therapeutic potential of ex vivo expanded endothelial progenitor cells for myocardial ischemia. Circulation 103:634–637.

Kehat, I., L. Khimovich, O. Caspi, A. Gepstein, R. Shofti, G. Arbel, I. Huber, J. Satin, J. Itskovitz-Eldor, and L. Gepstein. 2004. Electromechanical integration of cardiomyocytes derived from human embryonic stem cells. Nat. Biotechnol. 22:1282–1289.

Kocher, A. A., M. D. Schuster, M. J. Szabolcs, S. Takuma, D. Burkhoff, J. Wang, S. Homma, N. M. Edwards, and S. Itescu. 2001. Neovascularization of ischemic myocardium by human bone–marrow–derived angioblasts prevents cardiomyocyte apoptosis, reduces remodeling and improves cardiac function. Nat. Med. 7:430–436.

Laflamme, M. A., D. Myerson, J. E. Saffitz and C. E. Murry. 2002. Evidence for cardiomyocyte repopulation by extracardiac progenitors in transplanted human hearts. Circ. Res. 90:634–640.

Laugwitz, K. L., A. Moretti, J. Lam, P. Gruber, Y. Chen, S. Woodard, L. Z. Lin, C. L. Cai, M. M. Lu, M. Reth, O. Platoshyn, J. X. Yuan, S. Evans, and K. R. Chien. 2005. Postnatal isl1+ cardioblasts enter fully differentiated cardiomyocyte lineages. Nature 433:647–653.

Leobon, B. I. Garcin, P. Menasche, V. T. Vilquin, E. Audinat, S. Charpak. 2003. Myoblasts transplanted into rat infarcted myocardium are functionally isolated from their host. Proc. Natl. Acad. Sci. U.S.A. 100:7808–7811.

Loscalzo, J. 2004. Stem cells and regeneration of the cardiovascular system: facts, fictions, and uncertainties. Blood Cells Mol. Dis. 32:97–99.

Makino, S., K. Fukuda, S. Miyoshi, F. Konishi, H. Kodama, J. Pan, M. Sano, T. Takahashi, S. Hori, H. Abe, J. Hata, A. Umezawa, and S. Ogawa. 1999. Cardiomyocytes can be generated from marrow stromal cells in vitro. J. Clin. Invest. 103:697–705.

Malouf, N. N., W. B. Coleman, J. W. Grisham, R. A. Lininger, V. J. Madden, M. Sproul, and P. A. Anderson. 2001. Adult-derived stem cells from the liver become myocytes in the heart in vivo. Am. J. Pathol. 158:1929–1935.

Maltsev, V. A., G. J. Ji, A. M. Wobus, B. K. Fleischmann, and J. Hescheler. 1999. Establishment of á-adrenergic modulation of L-type Ca^{2+} current in the early stages of cardiomyocyte development. Circ. Res. 84:136–145.

Maltsev, V. A., J. Rohwedel, J. Hescheler, and A. M. Wobus. 1993. Embryonic stem cells differentiate in vitro into cardiomyocytes representing sinusnodal, atrial and ventricular cell types. Mech. Dev. 44:41–50.

Maltsev, V. A., A. M. Wobus, J. Rohwedel, M. Bader, and J. Hescheler. 1994. Cardiomyocytes differentiated in vitro from embryonic stem cells developmentally express cardiac-specific genes and ionic currents. Circ. Res. 75:233–244.

Matsuura, K., T. Nagai, N. Nishigaki, T. Oyama, J. Nishi, H. Wada, M. Sano, H. Toko, H. Akazawa, T. Sato, H. Nakaya, H. Kasanuki, and I. Komuro. 2004. Adult cardiac Sca-1-positive cells differentiate into beating cardiomyocytes. J. Biol. Chem. 279:11384–11391.

Matsuura, K., H. Wada, T. Nagai, Y. Iijima, T. Minamino, M. Sano, H. Akazawa, J. D. Molkentin, H. Kasanuki, and I. Komuro. 2004. Cardiomyocytes fuse with surrounding noncardiomyocytes and reenter the cell cycle. J. Cell Biol. 167:351–363.

Menasche, P., A. A. Hagege, M. Scorsin, B. Pouzet, M. Desnos, D. Duboc, K. Schwartz, J. T. Vilquin, and J. P. Marolleau. 2001. Myoblast transplantation for heart failure. Lancet 357:279–280.

Menasche, P., A. A. Hagege, J. T. Vilquin, M. Desnos, E. Abergel, B. Pouzet, A. Bel, S. Sarateanu, M. Scorsin, K. Schwartz, P. Bruneval, M. Benbunan, J. P. Marolleau, and D. Duboc. 2003. Autologous skeletal myoblast transplantation for severe postinfarction left ventricular dysfunction. J. Am. Coll. Cardiol. 41:1078–1083.

Metzger, J. M., W.-I. Lin, and L. C. Samuelson. 1996. Vital staining of cardiac myocytes during embryonic stem cell cardiogenesis in vitro. Circ. Res. 78:547–552.

Miller-Hance, W. C., M. LaCorbiere, S. J. Fuller, S. M. Evans, G. Lyons, C. Schmidt, J. Robbins, and K. R. Chien. 1993. In vitro chamber specification during embryonic stem cell cardiogenesis. Expression of the ventricular myosin light chain-2 gene is independent of heart tube formation. J. Biol. Chem. 268:25244–25252.

Muller-Borer, B. J., W. E. Cascio, P. A. Anderson, J. N. Snowwaert, J. R. Frye, N. Desai, G. L. Esch, J. A. Brackham, C. R. Bagnell, W. B. Coleman, J. W. Grisham, and N. N. Malouf. 2004. Adult-derived liver stem cells acquire a cardiomyocyte structural and functional phenotype ex vivo. Am. J. Pathol. 165:135–145.

Muller, P., P. Pfeiffer, J. Koglin, H. J. Schafers, U. Seeland, I. Janzen, S. Urbschat, and M. Bohm. 2002. Cardiomyocytes of noncardiac origin in myocardial biopsies of human transplanted hearts. Circulation 106:31–35.

Murry, C. E., M. H. Soonpaa, H. Reinecke, H. Nakajima, H. O. Nakajima, M. Rubart, K. B. Pasumarthi, J. I. Virag, S. H. Bartelmez, V. Poppa, G. Bradford, J. D. Dowell, D. A. Williams, and L. J. Field. 2004. Haematopoietic stem cells do not transdifferentiate into cardiac myocytes in myocardial infarcts. Nature 428:664–668.

Norol, F., P. Merlet, R. Isnard, P. Sebillon, N. Bonnet, C. Cailliot, C. Carrion, M. Ribeiro, F. Charlotte, P. Pradeau, J. F. Mayol, A. Peinnequin, M. Drouet, K. Safsafi, J. P. Vernant, and F. Herodin. 2003. Influence of mobilized stem cells on myocardial infarct repair in a nonhuman primate model. Blood 102:4361–4368.

Nygren, J. M., S. Jovinge, M. Breitbach, P. Sawen, W. Roll, J. Hescheler, J. Taneera, B. K. Fleischmann, and S. E. Jacobsen. 2004. Bone–marrow–derived hematopoietic cells generate cardiomyocytes

at a low frequency through cell fusion, but not transdifferentiation. Nat. Med. 10:494–501.

Oh, H., S. B. Bradfute, T. D. Gallardo, T. Nakamura, V. Gaussin, Y. Mishina, J. Pocius, L. H. Michael, R. R. Behringer, D. J. Garry, M. L. Entman, and M. D. Schneider. 2003. Cardiac progenitor cells from adult myocardium: homing, differentiation, and fusion after infarction. Proc. Natl. Acad. Sci. USA 100:12313–12318.

Oh, H., X. Chi, S. B. Bradfute, Y. Mishina, J. Pocius, L. H. Michael, R. R. Behringer, R. J. Schwartz, M. L. Entman, and M. D. Schneider. 2004. Cardiac muscle plasticity in adult and embryo by heart-derived progenitor cells. Ann. NY Acad. Sci. 1015:182–189.

Orlic, D., J. Kajstura, S. Chimenti, I. Jakoniuk, S. M. Anderson, B. Li, J. Pickel, R. McKay, B. Nadal-Ginard, D. M. Bodine, A. Leri, and P. Anversa. 2001. Bone marrow cells regenerate infarcted myocardium. Nature 410:701–705.

Oyamada, Y., K. Komatsu, H. Kimura, M. Mori, and M. Oyamada. 1996. Differential regulation of gap junction protein (connexin) genes during cardiomyocytic differentiation of mouse embryonic stem cells in vitro. Exp. Cell Res. 229:318–326.

Perin, E. C., H. F. Dohmann, R. Borojevic, S. A. Silva, A. L. Sousa, C. T. Mesquita, M. I. Rossi, A. C. Carvalho, H. S. Dutra, H. J. Dohmann, G. V. Silva, L. Belem, R. Vivacqua, F. O. Rangel, R. Esporcatte, Y. J. Geng, W. K. Vaughn, J. A. Assad, E. T. Mesquita, and J. T. Willerson. 2003. Transendocardial, autologous bone marrow cell transplantation for severe, chronic ischemic heart failure. Circulation 107:2294–2302.

Poss, K. D., L. G. Wilson, and M. T. Keating. 2002. Heart regeneration in zebrafish. Science 298:2188–2190.

Quaini, F., K. Urbanek, A. P. Beltrami, N. Finato, C. A. Beltrami, B. Nadal-Ginard, J. Kajstura, A. Leri, and P. Anversa. 2002. Chimerism of the transplanted heart. N. Engl. J. Med. 346:5–15.

Quaini, F., K. Urbanek, G. Graiani, C. Lagrasta, R. Maestri, M. Monica, A. Boni, F. Ferraro, R. Delsignore, G. Tasca, A. Leri, J. Kajstura, E. Quaini, and P. Anversa. 2004. The regenerative potential of the human heart. Int. J. Cardiol. 95 (Suppl 1): S26–S28.

Rangappa, S., J. W. Entwistle, A. S. Wechsler, and J. Y. Kresh. 2003. Cardiomyocyte-mediated contact programs human mesenchymal stem cells to express cardiogenic phenotype. J. Thorac. Cardiovasc. Surg. 126:124–132.

Rangappa, S., C. Fen, E. H. Lee, A. Bongso, and E. K. Sim. 2003. Transformation of adult mesenchymal stem cells isolated from the fatty tissue into cardiomyocytes. Ann. Thorac. Surg. 75:775–779.

Reinecke, H., E. Minami, V. Poppa, and C. E. Murry. 2004. Evidence for fusion between cardiac and skeletal muscle cells. Circ. Res. 94:e56–60.

Reinecke, H., V. Poppa, and C. E. Murry. 2002. Skeletal muscle stem cells do not transdifferentiate into cardiomyocytes after cardiac grafting. J. Mol. Cell. Cardiol. 34:241–249.

Schuster, M. D., A. A. Kocher, T. Seki, T. P. Martens, G. Xiang, S. Homma, and S. Itescu. 2004. Myocardial neovascularization by bone marrow angioblasts results in cardiomyocyte regeneration. Am. J. Physiol. 287:H525–H532.

Shim, W. S., S. Jiang, P. Wong, J. Tan, Y. L. Chua, Y. S. Tan, Y. K. Sin, C. H. Lim, T. Chua, M. Teh, T. C. Liu, and E. Sim. 2004. Ex vivo differentiation of human adult bone marrow stem cells into cardiomyocyte-like cells. Biochem. Biophys. Res. Commun. 324:481–488.

Shizuru, J. A., R. S. Negrin, and I. L. Weissman. 2005. Hematopoietic stem and progenitor cells: clinical and preclinical regeneration of the hematolymphoid system. Annu. Rev. Med. 56:509–538.

Smits, P. C., R. J. van Geuns, D. Poldermans, M. Bountioukos, E. E. Onderwater, C. H. Lee, A. P. Maat, and P. W. Serruys. 2003. Catheter-based intramyocardial injection of autologous skeletal myoblasts as a primary treatment of ischemic heart failure: clinical experience with six-month follow-up. J. Am. Coll. Cardiol. 42:2063–2069.

Stamm, C., B. Westphal, H. D. Kleine, M. Petzsch, C. Kittner, H. Klinge, C. Schumichen, C. A. Nienaber, M. Freund, and G. Steinhoff. 2003. Autologous bone-marrow stem-cell transplantation for myocardial regeneration. Lancet 361:45–46.

Strauer, B. E., M. Brehm, T. Zeus, M. Kostering, A. Hernandez, R. V. Sorg, G. Kogler, and P. Wernet. 2002. Repair of infarcted myocardium by autologous intracoronary mononuclear bone marrow cell transplantation in humans. Circulation 106: 1913–1918.

Taylor, D. A., B. Z. Atkins, P. Hungspreugs, T. R. Jones, M. C. Reedy, K. A. Hutcheson, D. D. Glower, and W. E. Kraus. 1998. Regenerating functional myocardium: improved performance after skeletal myoblast transplantation. Nat. Med. 4:929–933.

Thomson, J. A., J. Itskovitz-Eldor, S. S. Shapiro, M. A. Waknitz, J. J. Swiergiel, V. S. Marshall, and J. M. Jones. 1998. Embryonic stem cell lines derived from human blastocysts. Science 282:1145–1147.

Toma, C., M. F. Pittenger, K. S. Cahill, B. J. Byrne, and P. D. Kessler. 2002. Human mesenchymal stem cells differentiate to a cardiomyocyte phenotype in the adult murine heart. Circulation 105:93–98.

Tse, H. F., Y. L. Kwong, J. K. Chan, G. Lo, C. L. Ho, and C. P. Lau. 2003. Angiogenesis in ischaemic myocardium by intramyocardial autologous bone marrow mononuclear cell implantation. Lancet 361:47–49.

Weissman, I. L. 2002. Stem cells—scientific, medical, and political issues. N. Engl. J. Med. 346:1576–1579.

Winitsky, S. O., T. V. Gopal, S. Hassanzadeh, H. Takahashi, D. Gryder, M. A. Rogawski, K. Takeda, Z. X. Yu, Y. H. Xu, and N. D. Epstein. 2005. Adult murine skeletal muscle contains cells that can differentiate into beating cardiomyocytes in vitro. PLoS Biol. 3:e87.

Wollert, K. C., G. P. Meyer, J. Lotz, S. Ringes-Lichtenberg, P. Lippolt, C. Breidenbach, S. Fichtner, T. Korte, B. Hornig, D. Messinger, L. Arseniev, B. Hertenstein, A. Ganser, and H. Drexler. 2004. Intracoronary autologous bone-marrow cell transfer after myocardial infarction: the BOOST randomised controlled clinical trial. Lancet 364:141–148.

Yeh, E. T., S. Zhang, H. D. Wu, M. Korbling, J. T. Willerson, and Z. Estrov. 2003. Transdifferentiation of human peripheral blood CD34+ -enriched cell population into cardiomyocytes, endothelial cells, and smooth muscle cells in vivo. Circulation 108: 2070–2073.

Yuasa, S., K. Fukuda, Y. Tomita, J. Fujita, M. Ieda, S. Tahara, Y. Itabashi, T. Yagi, H. Kawaguchi, Y. Hisaka, and S. Ogawa. 2004. Cardiomyocytes undergo cells division following myocardial infarction is a spatially and temporally restricted event in rats. Mol. Cell. Biochem. 259:177–181.

Zhang, M., D. Methot, V. Poppa, Y. Fujio, K. Walsh, and C. E. Murry. 2001. Cardiomyocyte grafting for cardiac repair: graft cell death and anti-death strategies. J. Mol. Cell. Cardiol. 33:907–921.

Appendix I

Comparable Stages of Development of the Major Species Used in Discussion of Heart Development

Chick	Mouse	Human	Major common feature
Hamburger-Hamilton Stage/ Incubation time	Theiler Stage/ Days of gestation	Carnegie Stage/ Days of gestation	
3/12–13h	10/6.5–7.75d		Intermediate streak
4/18–19h		6/13–15d	Definitive streak
5/19–22h	11/7.25–8d	7/15–17d	Head process
6/23–25h		8/17–19d	Head fold
7/23–26h	12/8d	9/19–21d	1 somite
8/26–29h			4 somites
9/29–33h		10/22–23 (week4)	6–8 somites
10/33–38h	13/8–8.5d		9–11 somites
11/40–45h	14/8.5–9d	11/23–26	12–14 somites
12–13/45–52h	15/9d		15–20 somites
14/50–53h		12/26–20	20–25 somites
15–16/50–56h	16/10–10.25d		25–30 somites
17–18/52–72h	17/10.25–10.5d	13/28–32 (week 5)	30–35 somites
19/3–3.5d	18/10.5–11d	14/31–35	35–40 somites
20/3–3.5d	19/11–11.5d		40–43 somites
21–22/3.5–4d	20/11.5–12d	15/35–38	43–48 somites
23/4d		16/37–42 (week 6)	48–52 somites
24–26/4.5d	21/12–12.5d	17/42–44	52–55 somites
27–29/5–6.5d	12.5–13d	18/44–48 (week 7)	60 somites
30–32/6.5–7.5d	13.5d	19/48–51	
33–34/7.5–8d	22/14d	20/51–53 (week 8)	Heart septation completed
35/8.5–9d		21/53–54	
36/10d		22–23/54–60	
37/11d			
38/12d			
39/13d			
40/14d			
41/15d			
42/16d			
43/17d			
44/18d			
45/19–20d			
46/20–21/newly hatched chick	19d/Newborn mouse	40 weeks/newborn baby	

This page intentionally left blank

Glossary

Acerebellar Also called *Ace*, a mutant zebrafish with decreased expression of Fgf8 that lacks a cerebellum and has heart defects

Acetylcholine A neurotransmitter

Acetylcholinesterase An enzyme that degrades the neurotransmitter acetylcholine

Action potential (AP) A momentary change in electrical potential on the surface of a nerve or muscle cell that takes place when it is stimulated

Activin A signaling factor in the Tgf family

Adenosine A nucleoside produced as a metabolite of ATP that serves as a co-transmitter in the sympathetic nervous system

Adenoviral expression vector An engineered adenovirus that is usually replication incompetent and carries a gene that can be visualized to show what cells the adenovirus has infected. These expression vectors are used for cell tracing

Adherens junction A particular type of connection between two epithelial cells

Adrenergic Nerves that use the catecholamines norepinephrine and epinephrine as neurotransmitters

Afferent innervation Nerves that carry sensory information from the periphery to the central nervous system

Akt/Pkp Akt1/Pkb is the focal point for survival signals from growth and survival factor receptors, transduced via the P13-kinase pathway

Alagille syndrome An autosomal dominant genetic disorder that affects the liver, heart, and blood vessels

Alk Activin-like kinase receptor. The type 1 Tgfβ receptor

Allele One member of a pair or series of genes that occupy a specific position on a specific chromosome

Allosterically coupled Many proteins contain distinct interacting coupled receptor sites for two or more drug types. Binding to one receptor site can facilitate binding of another class of drugs to a separate site or conversely, be inhibitory. An excellent example is the α1 subunit of the L-type calcium channel where binding of the drug diltiazem to the α1 benzothiazepine receptor increases the affinity (decreases K_D) and the number of detectable receptor binding sites (B_{max}) for dihydropyridines (e.g., nifedipine) by about two- and threefold, respectively. In this case, it appears that binding of benzodiazepines stabilize a high-affinity receptor binding state for the dihydropyridines

Amhc1 Chick atrial myosin heavy chain 1; myocardial contractile protein expressed specifically by ventricular myocardium

Amnion A thin, tough, membranous sac that encloses the embryo or fetus of a mammal, bird, or reptile. It is filled with a serous fluid in which the embryo is suspended

Aneurysm A localized widening of an artery, vein, or the heart

Anf (Nppa) Atrial natriuretic factor; a peptide hormone coded by the *Nppa* gene. It is produced by the right atrium and stimulates the excretion of sodium and water by the kidneys and helps regulate blood pressure. During development, the expression of Anf is global throughout the myocardium and becomes restricted to the atria and then right atrium. It is used as a marker for progressive atrial chamber specification

Ang Angiopoietin; a growth factor that specifically promotes remodeling and stabilization of blood vessels

Angina Pain or discomfort due to lack of oxygen to the myocardium

Angioblast A cell with the potential to become an endothelial cell

Angiogenesis Sprouting of a new vessel from a preexisting vessel

Angiotensin A factor that causes vasoconstriction and activates production of aldosterone

Annulus fibrosis The fibrous rings around the heart valves where the valve leaflets merge with the heart muscle

Anomalous pulmonary venous drainage Some or all of the pulmonary veins drain to a location other than the left atrium

Anterior heart field A confusing term originally proposed by M. V. de la Cruz to indicate the myocardium added to the outflow tract after initial cardiac tube formation. It now means either (1) the most medial part of the cardiogenic fields that gives rise to the myocardium of the right ventricle, conus, and truncus; or (2) the area surrounding the attachment of the outflow tract to the pharynx that gives rise to the myocardium of the conus and truncus

Anterior intestinal portal An opening that marks the caudal extent of the foregut

Antisense oligomers Nucleotide sequences that are designed to specifically recognize portions of messenger RNA that block translation of the RNA to protein

Aorta Major arterial trunk carrying blood from the left ventricle

Aortic arch arteries Bilaterally paired series of arteries, numbered 1, 2, 3, 4, and 6, in birds and mammals that develop craniocaudally during heart development that carry blood from the aortic sac to the dorsal aortas. Aortic arch arteries 1 and 2 disappear while 3, 4, and 6 are remodeled into the great arteries

Aortic sac Collecting and distribution point for all the blood leaving the embryonic heart

Aortic sinuses The space at the base of the aorta just distal to the semilunar valve leaflets

Aorticopulmonary septation complex Condensed mesenchymal structure formed by cells derived from cardiac neural crest that septates the aortic sac and truncus

Aorticopulmonary septum The septum formed in the aortic sac by the aorticopulmonary septation complex

Apex The tip and most caudal part of the heart formed by the left ventricle

Apex-to-base activation The sequence of electrical activation in the heart after a mature conduction system is established

Apoptosis Programmed cell death

Arrhythmias An irregularity in the rhythm of the heartbeat

Arterial pole The point of junction of the myocardium and smooth muscle at the ventriculoarterial junction in the embryo and at the semilunar valves in the mature heart

Ascending limb The outflow limb of the looped heart consisting of the right ventricle, conus, and truncus

Asymmetry The left–right disposition of certain organs including the heart, lungs, stomach, liver, and spleen

Atresia Absence of a normal opening or vessel

Atrial appendage Also called auricle; an earlike flap on each atrium that is formed from myocardium in the initial heart tube

Atrial isomerism A condition in which the right and left atria, which are normally morphologically distinct, appear similar

Atrial septal defect A hole in the partition between the right and left atria that allows mixing of oxygenated and unoxygenated blood

Atrioventricular bundle Also called atrioventricular bundle of His or bundle of His; part of the conduction system found on the crest of the ventricular septum

Atrioventricular canal Part of the heart tube that joins the developing atria and ventricles

Atrioventricular canal defects Deficiency or absence of a partition in the atrioventricular canal to divide it into right and left channels

Atrioventricular conduction block A block in the conduction system at the atrioventricular junction that results in contraction of the atria without subsequent contraction of the ventricles

Atrioventricular cushions Bulges into the lumen of the atrioventricular canal that are caused by mesenchymal cells that populate the cardiac jelly

Atrioventricular groove Also called coronary sulcus; a groove on the outer surface of the heart marking the division between the atria and the ventricles

Atrioventricular septum (septum intermedium) The septum formed in the atrioventricular canal by fusion of the atrioventricular cushions. The septum divides the single atrioventricular canal into right and left canals

Autonomic ganglia Clusters of neurons near the vertebral column (paravertebral) or in the organs innervated, that control smooth and cardiac muscle

Autonomic nervous system The portion of the peripheral nervous system that regulates involuntary body functions, including those of the heart

Autonomous Not controlled by other cells or by outside forces

Autophosphorylation Phosphorylation of a protein when it makes a complex with a second protein

Autosome A chromosome that is not one of the sex chromosomes

AV node A cluster of specialized cardiomyocytes at the base of the right side of the atrial septum that acts as an electrical relay station for electrical impulses passing from the atria to the ventricles

Bachmann's bundle A group of specialized fibers connecting the right and left atria that appears similar to the atrioventricular node and the His–Purkinje conduction system but without any insulating tissue

Barx Homeodomain protein that regulates transcription of cell adhesion molecules (Cams)

Base-to-apex activation The sequence of electrical activation of the myocardium prior to septation and development of a mature conduction system

Bdnf Brain-derived neurotrophic factor; a neurotrophic factor that regulates neuronal growth, survival, and function during development

Benthic chordates Chordates that live on the bottom of the sea or lakes that are not predatory

Benzothiazepines A class of L-type calcium channel blockers that includes the clinically used drug, diltiazem. This class of drugs has potent cardiovascular effects including decreased heart rate and coronary vasodilatation

bHLH Basic helix–loop–helix; a protein motif found in many transcription factors. The HLH domain directs dimerization with other proteins and the basic region recognizes specific DNA sequences

Bicuspid aortic valve An aortic semilunar valve with only two cusps instead of the normal three

Bifid uvula The small, cone shaped tissue at the back of the soft palate is split into two parts

Bifurcation division into two branches

Bipotential Having the ability to develop in two different directions

Blastocyst A thin-walled hollow structure in early embryonic development that contains a cluster of cells called the inner cell mass, which give rise to all the cells in the embryo. The outer layer of cells gives rise to the placenta and other supporting tissues needed for fetal development within the uterus

Blastoderm A general term for all three germ layers of the embryo

Blood islands Clusters of cells that can form endothelial cells and blood cells

BMP Bone morphogenetic protein, designated numerically, several growth factors in the Tgf family

Bmper Bone morphogenetic protein-binding endothelial cell precursor-derived regulator

Brachiocephalic vein Vein formed by the union of the internal jugular and subclavian veins

Bradycardia Slower than normal heart rate

Brainstem The part of the brain that merges with the spinal cord. It consists of the medulla oblongata, midbrain, and pons, and houses the nerve centers of the head as well as the centers for respiration and heart control

Brugada syndrome An inherited form of cardiac arrhythmia with a typical electrocardiographic pattern of ST segment elevation in leads V1 to V3, and incomplete or complete right bundle branch block. This syndrome causes sudden death

Buccopharyngeal membrane A thin membrane that forms just caudal to the developing forebrain and becomes a septum between the primitive mouth and pharynx

Bulboventricular fold The cardiac loop is sometimes referred to as the bulboventricular loop. The bulboventricular fold is the point of greatest convexity of the looped heart

Bulbus Also known as bulbus arteriosus; a nebulous term that has been used to indicate right ventricle or other parts of the outflow limb of the looped heart tube

Bundle branches Tracts of specialized myocardial cells that carry impulses from the AV node down the interventricular septum

Bves Blood vessel epicardial substance; a membrane protein that functions in adhesion by the proepicardium, epicardium, and in the vascular smooth muscle derived from the epicardium

Cadherin A group of proteins expressed on the surface of cells that are important in cell adhesion to other cells

Calcineurin A protein phosphatase also known as protein phosphatase 2B (PP2B) that activates Nfat

Calcitonin gene-related peptide Cgrp; a peptide hormone used as a neurotransmitter in the autonomic nervous system

Calcium channels—L-type Voltage-gated calcium channels that have a higher threshold or more positive membrane potential for activation than T-type calcium channels. These channels are an absolute requirement for cardiac excitation-contraction coupling and may play some role in pacemaking. The α1 subunits contain allosterically coupled receptor binding sites for dihydropyridine, benzothiazepine, and phenylalkylamine classes of calcium channel blockers used clinically and are frequently referred to as dihydropyridine receptors. The three known isoforms are α1S, α1C and α1D (CaV1.1, CaV1.2 and CaV1.3, respectively in human genome nomenclature; see Table 5.1). α1C and α1D are found in heart. α1S is a skeletal muscle isoform

Calcium channels—T-type Voltage-gated calcium channels that have a lower threshold or more negative membrane potential for activation than L-type calcium channels. They are found in cardiac cells that are capable of spontaneous beating but are absent in mature ventricular myocytes. Of the three known isoforms, α1G and α1H are found in relatively high abundance in nodal cells, atrial myocytes, and Purkinje fibers and are believed to have a role in pacemaking. α1I is considered a brain isoform. In human genome nomenclature the isoforms are referred to as CaV3.1, CaV3.2, and CaV3.3, respectively (see Table 5.1)

Calcium-induced calcium release CICR; release of intracellular stored calcium in response to a calcium transient or wave

Calcium transient The waves of increasing and decreasing calcium caused by rhythmic electrical impulses that generate the heart beat

Calmodulin A ubiquitous calcium-binding protein of eukaryotic cells that mediates a variety of cellular responses to calcium

Calponin A smooth muscle-specific protein that binds actin, tropomyosin, and calmodulin that is involved in contraction; interaction of the protein with actin inhibits actomyosin Mg-ATPase activity

Calsequestrin A calcium-binding protein located on the inner membrane surface of the sarcoplasmic reticulum that serves to chelate and store calcium ions

Canonical Wnt signaling Intracellular signaling by a Wnt family member through β-catenin

Capsulin A bHLH transcription factor involved in coronary vascular smooth muscle differentiation

Cardia bifida a condition in which the bilateral cardiogenic fields do not fuse in the midline resulting in formation of two hearts

Cardiac ganglia Clusters of parasympathetic postganglionic neurons located in and around the heart

Cardiac jelly Acellular gelatinous matrix secreted by the myocardium and separating it from the endocardium in early heart development

Cardiac myosin binding protein C Also called cardiac MyBP-C; a protein that is arrayed transversely in sarcomere A-bands and binds myosin heavy chain in thick filaments and titin in elastic filaments. Phosphorylation of MyBP-C appears to modulate contraction

Cardinal veins The veins in vertebrate embryos, which are located on each side of the vertebral column and return the blood to the sinus venosus

Cardiocraniofacial field The field of cells that encompasses the region where the forebrain, face and heart develop

Cardiogenic fields Bilateral regions of cells in the anterolateral mesoderm that give rise to myocardial and most endocardial cells of the heart tube

Cardiomyopathy A general diagnostic term designating primary myocardial disease, often of obscure or unknown etiology

CarG box SRF binding site in the promoter regions of many cardiac genes

Caronte A secreted protein that mediates the Shh-dependent induction of left-specific genes in the lateral plate mesoderm. Caronte is induced by Shh and repressed by Fgf8. It activates the expression of Nodal by antagonizing a repressive activity of Bmp

Caspase An enzyme that is responsible for the breakdown of the cell during apoptosis by cleaving numerous cellular proteins. Caspase is synthesized as inactive procaspase that is later activated by proteolytic cleavage into an active caspase

Catecholamine Any of a group of amines derived from catechol that have important physiological effects as neurotransmitters and hormones and include epinephrine, norepinephrine, and dopamine

Catenins A versatile family of proteins that are important in transcriptional regulation, cell signaling, and cell adhesion

Cavernous angiomas Benign connective tissue tumors caused by abnormal proliferation of endothelial cells resulting in malformations of the vasculature

CCS-lacZ An insert in an unknown locus of the *engrailed-2* promoter element

Cell fate The cell lineage a cell will adopt if it is left in place

Cell lineage The general type of cell, that is, myocardial, endocardial, that an undifferentiated cell develops into

Cenancestor The most recent common ancestor of the taxa under consideration

Central veins Superior and inferior vena cava

C-ets-1 A gene expressed in the epicardium that codes for a transcription factor that activates some of the genes involved in degradation of extracellular matrices and cell migration. This gene has the potential to transform into an oncogene and is thus known as a proto-oncogene

Chamber Collecting point for blood

Champ Heart restricted helicase that negatively regulates cell proliferation

Channelopathy A disease caused by mutation of a gene that encodes a defective ion channel

Channels Intravascular conduits

Chemoattractant A molecule that attracts a migrating cell

Chimera An animal composed of tissue derived from two different animals usually from different species

Chisel A 9-kDa cytoskeletal protein with an unknown function used as a marker for the working myocardium of the atria and ventricles

Cholestasis Failure of bile to flow from the liver through the bile ducts

Choline acetyltransferase An enzyme that synthesizes acetylcholine

Cholinergic The designation of nerves that use acetylcholine as their neurotransmitter

Chordae tendinea Bands of connective tissue that connect the ventricular papillary muscles with the edges of the valve leaflets to prevent regurgitation of blood into the atria during ventricular contraction

Chorioallantoic graft Grafting an explanted piece of tissue onto the extraembryonic vasculature of a well-developed chick embryo at 8 or 9 days of incubation

Chromaffin cells Cells that store epinephrine as in the adrenal medulla

Chromogranin Any of a group of acidic polypeptides that are the major soluble protein constituents of the secretory granules of the chromaffin cells of the adrenal medulla

Cilia Fine hairlike projections from certain cells that sweep in unison to move fluid and particles

Circumpharyngeal ridge A longitudinal bulge over pharyngeal arches 3, 4, and 6 where cardiac neural crest cells pause in their migration while the arches are forming

Clade A related group of animals with a common ancestor

Clone A group of cells that originated from a single progenitor cell

Clubbing Enlargement of the ends of fingers and toes resulting from chronic cyanosis

CNTF Ciliary neurotrophic factor; a neurocytokine needed for synapse formation in the parasympathetic gangia

Coalignment The cardiogenic cells in the primitive streak are ordered in the same way as the cells in the heart tube

Coarctation Narrowing or constriction of a blood vessel, especially of the aorta

Cold pressor testing Placing the test subject's hand in cold water while testing heart function

Collagen Fibrous protein found in connective tissue

Collateral circulation Secondary channels that carry the major supply of blood after obstruction of the principal vessel

Coloboma A gap in the iris

Commitment Consignment of a cell to a particular fate

Common atrioventricular canal Deficiency or absence of atrioventricular septal tissue immediately above and/or below the normal level of the AV valves. The AV valves are abnormal

Common cardial vein Part of the embryonic venous system; formed by the junction of the anterior and posterior cardinal veins that drain the body wall and form one set of the major return channels to the heart

Compact zone The outer layer of myocardium

Complex II Succinate dehydrogenase (part of the electron transport chain)

Complex IV Cytochrome *c* oxidase (COX) (part of the electron transport chain)

Concentric hypertrophy Growth of the ventricular wall without overall enlargement, that is, the walls become thicker and the lumen is diminished

Conductance The measure of ease with which something conducts electricity

Conotruncal defects or malformations Congenital defects of the arterial pole that include, but are not limited to dextroposed aorta, tetralogy of Fallot, double outlet right ventricle, and transposition of the great arteries

Conotruncus The outflow tract or conus and truncus designated as a unit

Conoventricular groove an external indentation that marks the junction of the prospective right ventricular and conal myocardium

Contractile apparatus The unique structure in myocardial cells formed from specific proteins that is responsible for myocardial shortening

Conus (conus arteriosus) The proximal part of the embryonic outflow tract beyond the presumptive right ventricle. Also designates the smooth walled portion of the right ventricular outflow tract in the heart after septation

Convergence Craniocaudal movement of the outflow and inflow limbs toward each other

Coronary sinus A large vein that collects all the venous blood from the coronary vasculature and conducts it into the right atrium. Coronary sinuses of the aorta are located just above the right and left semilunar valve cusps and are the site of origin of the right and left coronary arteries, respectively

Coronary vasculature All of the blood vessels that nourish the heart

Couplons Basic units of excitation-contraction coupling responsible for calcium-induced calcium release in the heart. They are comprised of a cluster of surface membrane (sarcolemma) L-type calcium channels (dihydropyridine receptors) directly overlying a terminal dilation of the sarcoplasmic reticulum containing a dense cluster of calcium release channels (ryanodine receptors). This is a stable structure such that only a few nanometers of cytoplasmic space separate the calcium channel from the release channel in the membrane of the sarcoplasmic reticulum

Coup-tfII Chicken ovalbumin upstream promoter-transcription factor II; an orphan receptor involved in mesenchymal–epithelial interactions in development. In the Coup-tfII null mouse the atria and sinus venosus fail to develop

Cranial neural folds The edges of the neural plate in the head that roll up to form the neural tube which will become the brain

Cranial neural plate The midline cranial ectoderm that will become the brain

Cre recombinase A site-specific, bacteriophage P1-derived recombinase enzyme that cuts at loxP-tagged sites in DNA causing gene specific recombination. A method for introducing genetic modifications into specific genes by homologous recombination

Crescent An inhibitor of canonical Wnt signaling

Crista terminalis A vertical crest on the interior wall of the right atrium that lies to the right of the sinus of the vena cava and separates this from the remainder of the right atrium

Cristae The multiply folded inner membrane of a cell's mitochondrion that are fingerlike projections. The walls of the cristae are the site of ATP production

Cryptic A member of the EGF–CFC family of membrane-associated proteins associated with right-left patterning

C-terminus The extremity of a protein or polypeptide terminated by an amino acid with a free carboxyl group (COOH)

Cx Connexin; a family of proteins that form gap junctions

Cyanosis Bluish discoloration of the skin or mucous membranes caused by lack of oxygen in the blood

Cyclic AMP responsive element (Creb) The DNA target site (ATGACGTCAT) for transcription factors whose activities are regulated by cyclic AMP

Cyclostomes A class of primitive elongated freshwater fishes characteristically having a jawless sucking mouth with rasping teeth

Cysteine knot A secondary structure in a protein in which an embedded ring is formed by two disulfide bonds and a connecting backbone segment is threaded by a third disulfide bond

Cytokeratin A universal marker for epithelial cells

Cytokinesis Division of the cytoplasm during cell division

Delamination The process of detachment of a cell from an epithelial cell layer to become mesenchymal

Depolarization Change in membrane potential to a more positive potential

Desmin A protein that is important in maintaining the cytoskeleton in a muscle cell

Determination A second level of commitment to a particular cell lineage after specification

Deuterostomes Animals in which the first opening that appears in the embryo becomes the anus while the mouth appears at the other end of the digestive system as opposed to protostomes in which the mouth form first. The major groups of deuterostomes are chordates and echinoderms

Dextrocardia The heart loops to the left rather than the right and is subsequently located in the right side of the chest rather than in its normal location on the left

Diastolic potential Hyperpolarized membrane potential between action potentials. The maximum diastolic potential is the most negative potential reached during in the cardiac cycle. For sinoatrial cells this is about −50 to −60 mV and for ventricular cells it is approximately −85 mV

Differentiation Structural adaptation of a cell to perform a particular function

DiGeorge phenotype A congenital sequence of defects characterized by immunodeficiency, abnormal facies, conotruncal heart defects, hypocalcemia caused by hypoplasia or absence of the parathyroids, and increased susceptibility to infections

Dihydropyridine A potent class of L-type calcium channel antagonists and agonists (e.g., nifedipine and bay K8644, respectively). The antagonists are used clinically as coronary and systemic vasodilators particularly in the treatment of angina

Diploid Animals that have two of each chromosome

Discordance abnormal connection between the heart and inflow or outflow vessels

Dishevelled A segment polarity gene that plays a role in the signal transduction pathway mediated by multiple Wnt genes. It appears to be involved in controlling microtubule stability that is important in regulating cell polarity

Dissecting aorta A condition in which bleeding occurs into the wall of the aorta

Distal outflow tract Truncus arteriosus

Dkk Dickkopf, an inhibitor of canonical Wnt signaling

Dlx Distalless; a family of homeodomain-containing proteins that function as transcriptional regulators. The *Dlx* genes are distributed in pairs on the same chromosomes that contain hox clusters

Dominant negative A mutation that produces a protein that interacts with and/or interferes with the function of a wild-type protein

Dorsal aorta In the embryo, these are initially bilaterally paired and traverse the length of the embryo. During development, remodeling produces a single dorsal aorta that becomes the thoracic and abdominal aorta

Dorsal mesocardium The splanchnic mesoderm that connects the myocardial tube to the pericardial cavity

Dorsal vagal motor complex Anatomically and functionally integrated combination of the nucleus of the solitary tract, area postrema, and the dorsal vagal motor nucleus that form a neural network regulating the respiratory, gastrointestinal, and cardiovascular systems

DORV Double outlet right ventricle; a condition in which both the aorta and the pulmonary trunk receive their blood from the right ventricle

Double inlet left ventricle DILV; a condition in which both the right and left atria are connected to the left ventricle

Down syndrome A syndrome caused by triple copies of material on chromosome 21 characterized by atrial septal defects, slowed growth, abnormal facial features, and mental retardation

dV/dT The first derivative of voltage with respect to time. In electrically excitable cells, this term refers to the rate of change in membrane potential (mV/sec) usually in reference to the initial upstroke of the action potential

Dysautonomia Disruption of the function of the autonomic nervous system

Dysmorphic altered appearance

Ebstein malformation Also called Ebstein anomaly; abnormal tricuspid valve marked by a downward displacement of the septal and posterior leaflets into the cavity of the right ventricle

Ece Endothelial converting enzyme; an enzyme that cleaves active endothelin from a precursor protein

Ectomesenchyme Mesenchymal cells derived from the cranial neural crest that take part in development of many structural elements in the head, neck, and heart

Ectopic Anything that is in a place it is not usually found

Efferent innervation Nerves that originate in the central nervous system or in peripheral clusters of neurons that control muscles

Egf–cfc A family cell-associated glycoprotein co-receptors for Tgf-β-related proteins Nodal and Vg1. All Egf–cfc proteins

contain a consensus *O*-linked fucosylation site within the Egf-like motif that is necessary for their ability to function as co-receptors

Egfp Enhanced green fluorescent protein; a reporter that makes cells that express it fluoresce green. Expression can be driven by specific promoters to mark specific cells or to determine whether a particular cell expresses a particular gene by engineering the promoter for the gene to drive Egfp expression

Elasmobranch Fish with a cartilaginous, non-bony skeleton (sharks, skates, and rays)

Elastin A protein that recoils like a spring in connective tissue and accounts for the elasticity of blood vessels

Embolism The obstruction of a blood vessel by something that travels through the bloodstream, lodges, and blocks flow

Embryoid body A ball of embryonic stem cells that have been grown in hanging drop cultures rather than on feeder layers that keep the cells undifferentiated. Differentiation begins in the embryoid bodies and they develop beating foci of myocardial cells

Endocardial cushions Bulges into the lumen of the heart tube at the atrioventricular canal and in the conotruncus. The bulges are caused by mesenchymal cells populating the cardiac jelly

Endocardium Single layer of squamous epithelial cells that line the heart

Endoderm One of the three germ layers that forms during gastrulation. The endoderm forms the lining of the digestive tract including the foregut and pharynx that are involved in formation

Endoglin The type II Tgfβ receptor

Endothelial cell A cell that lines a blood vessel

Engrailed A transcription factor that specifies compartment boundaries

Enkephalin Naturally occurring opiate pentapeptides

EPDC Epicardially derived cells; consist of some cushion mesenchyme, coronary endothelial cells, coronary vascular smooth muscle and cardiac fibroblasts

Eph Receptor tyrosine kinases that respond to ephrins

Ephrin A soluble or membrane-attached growth factor important in blood vessel remodeling. Ephrin is unusual because it can act as either the ligand or the receptor so signaling can be bidirectional

Epiblast The layer of the embryo that generates all of the germ layers during gastrulation

Epicardin A bHLH transcription factor involved in epithelial–mesenchymal interactions that may play a role as a negative regulator in one or more subsets of epicardially derived cell types

Epicardium Outer epithelial covering over the myocardium that generates all the connective tissue, endothelial and smooth muscle cells to form the coronary vasculature

Epithelial–mesenchymal transformation The process of converting an epithelial cell to a mesenchymal cell. Epithelial cells are usually bound in sheets of cells while mesenchymal cells can migrate widely and differentiate into several cell types

Epithelium Any layer of cells that is polarized and has cell–cell junctions

Epitope A site on a protein that is recognized by an antibody

ErbB Several receptor tyrosine kinases designated 1–4, that bind neuregulin

Erk Extracellular signal-regulated kinase, one of the intracellular enzymes that is part of the phosphorylation cascade initiated by growth factor signaling

ES cells Embryonic stem cells; totipotent cells obtained from blastula stage embryos and grown on feeder cells that maintain their totipotency

Et1 Endothelin-1; a growth factor that interacts with the endothelin receptor A (EtA)

EtA Endothelin receptor A; a tyrosine kinase transmembrane receptor for endothelin ligands

Exaptation An evolutionary process in which a given adaptation is first naturally selected for, and subsequently used by the organism for something other than its original, intended purpose

Excitation–contraction coupling EC coupling; the processes that links excitation of a myocardial cell with subsequent contraction

Explant Cutting a particular tissue out of an embryo to study it in isolation from its normal environment

Expression profile The set of genes that a cell expresses

Extracardiac cells Cells that originate outside the cardiogenic mesoderm that subsequently migrate into the heart

Familial recurrence Appearing in several members of a family

Fate map Determining what a cell becomes by labeling it and following it through development to see what it differentiates into in an embryo

Fgf Fibroblast growth factor. A large family of growth factors

Fibrillin An extracellular matrix protein that forms an intricate lattice in which cells are embedded to build tissues. Fibrillin becomes part of small threadlike filaments called microfibrils, which in turn help build elastic fibers. Elastic fibers are essential for the function of flexible structures such as blood vessels, the lungs, and skin. Mutations in the fibrillin1 gene cause Marfan syndrome

Fibroelastosis Excessive production of collagenous and elastic fibrous tissue

Fibronectin One of the proteins in the extracellular matrix that binds integrins and is necessary for cell migration

Fibulin A protein that belongs to a family of extracellular proteins expressed in the basement membranes of blood vessels.

One of the fibulins may be essential for the polymerization of elastin, a major component in the walls of blood vessels

Field A region or area of an embryo that can be identified as a discrete unit

Filopodia Processes extended by a cell during migration

Fistulae An abnormal passage, opening, or connection

FK binding proteins (FKBP) A class of proteins that bind the immunosuppressant drugs, FK-506 and rapamycin. In cardiomyocytes, FKBP-12.6 is associated with each of the four subunits of the cardiac ryanodine receptor (calcium release channels in the sarcoplasmic reticulum). FKBP-506 appears necessary for coordinated gating. In the presence of FK-506 or rapamycin, FKBP-12.6 dissociates from the release channel resulting in increased activity and the appearance of subconducting states

Flectin An extracellular matrix protein that is associated with heart looping

Flk Also known as Vegf receptor 2

Floating head Mutation in the floating head locus of zebrafish that results in the absence of the notochord

Flt Also known as Vegf receptor 1

Foci Pleural of focus. The origin or center

Fog Friend of gata; large family of zinc finger-containing proteins that interact with Gata transcription factors

Forebrain The most cranial part of the developing nervous system

Foregut pocket The cranial part of the pharynx that is formed by the endoderm folding downwards

Fossa ovalis An oval depression seen on the right side of the atrial septum that is a remnant of the foramen ovale which allows oxygenated blood to pass from the right to the left atrium during fetal life. The foramen ovale closes at birth leaving the fossa ovalis

Fox A family of transcription factors of the winged helix type

Frizzled The receptor for canonical Wnt signaling

Frontonasal prominence Bulge in the middle of the developing face that will form the forehead and nose

Frzb Frizbee; a competitive inhibitor of canonical wnt signaling

$G_{\alpha q}/G_{\alpha 11}$ Members of the Gq family of G-proteins that transduce signals from receptors to the phosphatidyl-inositol-specific phospholipase C. In neural crest cells these Gq family members may transduce signals from the EtA receptor

Gabaergic Neurons that use gamma-aminobutyric acid as a neurotransmitter. Gaba is an amino acid neurotransmitter that is the major inhibitory transmitter in the brain

Galanin A neurotransmitter in the peripheral nervous system expressed in the adrenal medulla

Ganglion A cluster of neurons outside of the central nervous system

Gastrulation An event in early development that results in creation of three germ layers and three axes. The germ layers produced are called ectoderm, mesoderm, and endoderm and these will form the embryo. The three axes are craniocaudal (head–tail); dorsoventral (back–front) and right–left

Gata A family of transcription factors. Gata4, -5 and -6 are expressed in the heart

Gdnf Cell line-derived neurotrophic factor; a subgroup in the Tgfβ superfamily. These factors promote neuron survival and exert their effects through specific receptors

Germ layers Three layers that are created by gastrulation in the early embryo called ectoderm, mesoderm and endoderm. These layers subsequently develop into the adult organism

Gfr Gdnf family receptors; glycosyl-phosphatidylinositol–linked, cell surface receptors. Four receptor subtypes, termed Gfr-α-1 to 4, are currently recognized

Glucocorticoids Hormones released from the adrenal cortex that affect carbohydrate metabolism and have powerful anti-inflammatory actions

Glutaminergic Neurons that use glutamic acid as a transmitter. Glutamic acid is an amino acid that serves as a neurotransmitter

Glycogen The storage form of glucose found in conduction and nodal myocytes

Goosecoid A homeobox transcriptional regulator expressed specifically in the organizer and in neural crest

Great arteries Aorta, pulmonary trunk, brachiocephalic, and carotid arteries

Gridlock Also known as *grl*. A gene identified by a mutation in zebrafish. The gene is a downstream target of Notch signaling that is expressed in the dorsal aorta. If the gene is downregulated, the dorsal aorta disappears because the endothelial cells differentiate as a vein

Gsk3β Glycogen synthase kinase 3β; a protein kinase that phosphorylates β-catenin, preparing it for destruction

Guillain-Barré syndrome An acute disease that produces fever and nerve inflammation resulting in bilateral weakness or paralysis, most commonly in the legs and feet

H^+/K^+ transporter A membrane pump that exchanges protons (H^+) for potassium ions (K^+)

Hand A family of basic helix–loop–helix (bHLH) transcription factors

Haploinsufficient A condition in which one of the two copies of a gene in a diploid animal has a mutation that produces abnormal development

Haplotype A set of closely linked alleles, genes or DNA polymorphisms, inherited as a unit

Has2 Hyaluronic acid synthase 2; an enzyme needed for production of hyaluronic acid needed for development of the myocardial trabeculae and cardiac cushions

Hd Heart defect; a mutant mouse with disrupted versican gene that has a hypoplastic right ventricle

Head process The part of the notochord that first extends from the node toward the head

Hemangioblast A cell that can develop as an endothelial cell or a blood (hematopoietic) cell

Hematoblast A cell that develops into a hematopoietic cell

Hemichannel Connexon; the half of a gap junction channel composed of connexins formed by one cell that joins with a hemichannel in another cell to make the gap junction

Hemizygous interstitial deletion A region of DNA in one chromosome is missing

Hereditary hemorrhagic telangiectasia A disorder characterized by abnormal arteriovenous shunts

Hes Hairy/Enhancer of Split. A basic helix–loop–helix transcription factor that is a downstream target of Notch signaling. Hes represses transcription to suppress specific cell fates in the signaled cell

Heteromeric gap junctions Made of at least two different connexins

Heterotopic transplantation Moving cells from their normal position in the embryo to an alternate position to see what they can differentiate into

Heterozygous A condition in a diploid animal in which the two alleles of a particular gene are different

Hif Hypoxia inducible factor; a protein that is induced by hypoxia

hLamp Heart-specific lectin-associated matrix protein. A membrane glycoprotein that is associated with epithelial–mesenchymal transformation and cardiac looping

HMG motif A highly conserved DNA binding motif found in proteins that regulate transcription in a variety of genes

HNK1 Human natural killer cell antibody that recognizes many migrating cells including chick neural crest cells and secondary heart field cells

Holt-Oram syndrome A genetic syndrome associated with *TBX5* mutations and characterized by the combination of heart disease, usually atrial septal defect, and malformations of the upper limb

Homeostasis A constant state

Homodimers Complex of two identical proteins

Homogeneous All of the same or similar kind

Homozygous An animal with two identical copies of a gene

Hox code The combination of *hox* genes expressed in a particular segment or region. The *hox* genes comprise four clusters of paralogous or similar genes each located and regulated together on different chromosomes

Hrt Hairy related transcription factor family of proteins activated by Notch signaling

hrT Zebrafish homolog of *Tbx20*

Hyperpolarization An increase in the electrical potential difference across a cell membrane that makes it harder for the cell to fire or experience a depolarization

Hypoblast The lower layer of a chick embryo before gastrulation

Hypochord A transitory rod-like structure that develops under the notochord in the trunk region of fish and amphibian embryos

Hypomorphic A mutation that reduces, but does not completely eliminate, the function of a gene

Hypoplastic having fewer cells than normal

$I_{Ca,L}$ L-type calcium current. The primary source of trigger calcium for calcium-induced calcium release from the sarcoplasmic reticulum. See also Calcium channels—L-type

$I_{Ca,T}$ T-type calcium current. Found in cardiomyocytes capable of spontaneous beating. Absent in adult ventricle. See also Calcium channels—T-type

Idiopathic Something that occurs without an identified cause

I_f (funny current) One of the voltage gated membrane currents involved in pacemaking with the unusual property of being activated during repolarization of the action potential. There are four channel isoforms (HCN1–4 in the human genome) and their activity is increased by binding cAMP

I_{K1} Inward rectifier potassium current. Maintains the resting membrane potential near the potassium equilibrium potential (~90 mV). Absent in all early embryonic cardiomyocytes and in nodal pacemaking cells. Strongly expressed in mature ventricular myocytes

I_{Kr} Rapid delayed rectifier repolarizing potassium current

I_{Ks} Slow delayed rectifier repolarizing potassium current

Induction The initiation of a cell into a new more differentiated state

Inflow pole The region of the heart tube that receives venous blood

Infundibulum The smooth-walled portion of the right ventricle just below the pulmonary valve

Ingression Movement of the cells into the primitive streak to populate the endoderm or mesoderm

Inotropic Having to do with the strength of a heart beat. A negative inotropic effect is one that decreases the strength of the contraction while a positive inotropic effect is one that increases the strength of contraction

Insulin-like growth factor Igf; polypeptide growth factors with high sequence similarity to insulin

Integrin Transmembrane proteins consisting of α- and β-subunits that recognize and bind proteins in the extracellular matrix

Intercalated disc An undulating double membrane separating adjacent cells in cardiac muscle fibers. It holds the myofibrils together and permits easy transfer of an electrical potential.

Interdigitation Interlocking or interface between different cell types

Intermediolateral cell column A grossly identifiable column of neurons in the thoracic spinal cord located between the dorsal and ventral horns. The neurons in this column are the preganglionic sympathetic neurons

Interrupted arch Also designated IAA. The aortic arch which usually connects the ascending and descending aorta is missing

Intersegmental vessels Vessels that originate from the dorsal aorta and run between each pair of somites

Intron The DNA base sequence interrupting the protein coding sequence of a gene. The intron sequence is transcribed into RNA but is cut out of the message before it is translated into protein

***Inv* mouse** Mouse with a disruption in the inversin gene locus that has offspring with situs inversus

Ion channel An integral membrane protein that provides for the regulated transport of a specific ions across a membrane. Voltage-gated ion channels are activated by an electrical potential in the membrane

Irx Iroquois, a family of transcription factors containing homeodomain DNA binding motifs

Ischemia Insufficient blood supply

Isl1 Islet1. A LIM/homeodomain-containing transcription factor expressed in the cardiogenic mesoderm

Isoform Different versions of any protein that are made usually by the same gene

***Iv* mouse** A mouse line with a mutation in *left–right dynein* whose offspring have situs inversus

Ivemark syndrome Visceroatrial heterotaxia

Jagged One of the ligands for the Notch receptor

JB3 An antibody that recognizes a fibrillin-like antigen in the extracellular matrix of the cardiogenic mesoderm and endothelial/endocardial cells

Jekyll A zebrafish mutant with a mutation in *uridine 5′-diphosphate (UDP)-glucose dehydrogenase* a gene needed for production of hyaluronic acid, heparin sulfate, and chondroitin sulfate. The Jekyll mutant is unable to form an atrioventricular valve

Jervell Lange-Nielsen syndrome A form of long QT syndrome that is accompanied by deafness

Jnk cJun N-terminal kinase, an enzyme activated by some signaling molecules including non-canonical Wnts

Jumonji A gene expressed during heart development that participates in negative regulation of cell proliferation by repressing cyclinD1 expression

Junctional plaque Concentration of gap junctions in a region of the cell membrane where cells are in close apposition

Juvenile polyposis A disorder in which polyps develop throughout the gastrointestinal tract in the first decade or two of life

Kartagener's syndrome Situs inversus, recurrent respiratory infections caused by immotile bronchial cilia with chronic sinusitis, male infertility, and bronchiectasis

KIF A family of kinesin-like motor proteins

KvLqt1 A potassium channel protein coded for by the gene *KCNQ1*. Mutation in the gene can lead to a defective protein and several forms of inherited arrhythmias as long QT syndrome, short QT syndrome, and familial atrial fibrillation

LacZ The gene that codes for the enzyme β-galactosidase. β-galactosidase converts a number of colorless substrates to blue precipitate. It is inserted into a gene whose promoter directs its expression which is used to determine if a particular gene is expressed by a particular cell

Laminin Large, extracellular, noncollagenous glycoprotein with antigenic properties. It is localized in the basement membrane and functions to bind epithelial cells to the basement membrane

Lateral plate mesoderm The most lateral of the mesoderm germ layer that splits into two layers called splanchnic and somatic. The heart develops from the splanchnic layer and the body wall is formed by the somatic layer. The pericardial cavity is created by the split

Left ventricle Systemic ventricle that pumps oxygenated blood to the body

Left–right dynein a motor protein that is required for motility of the cilia that establish the left–right axis

Lefty A signaling factor in the Tgfβ superfamily that is essential for left–right axis determination

Ligand any molecule that binds a receptor

Limk Limb domain containing kinase; a serine protein kinase with two amino-terminal LIM motifs that induces stabilization of F-actin structures in transfected cells. This kinase plays a central role in regulating cell motility and morphogenesis by modulating the stability of actin cytoskeletal structures

Long QT syndrome A cardiac conduction system abnormality characterized by an extended delay in ventricular repolarization, which can lead to sudden death

Looping The process of converting a straight heart tube to a looped tube. Looping always occurs to the right

Lumen The inside of the tube or channel formed by endothelial or endocardial cells

Mads MCM1, agamous, deficiens, serum response factor; a member of the Mads box family of transcription factors

Malformation sequence A recurring pattern of congenital defects associated with a syndrome

Map kinase mitogen-activated protein kinase that is part of the intracellular cascade activated by growth factor signaling

Mash1 Mouse achaete-scute homolog 1; a transcription factor that is required for sympathetic postganglionic nerve differentiation

Matrix Denotes all the substances found outside of cells

Matrix metalloproteinase A group of enzymes that can break down proteins, such as collagen, that are normally found in the extracellular matrix. These enzymes need zinc or calcium cofactors to work properly. They are important in the subepicardial space for epithelial-mesenchymal transformation

Mediastinal mesenchyme The mesenchyme in the ventral midline of the thorax

Mef2 A transcription factor required for myocardial development

Meis Myeloid ecotropic leukemia virus integration site a transcriptional regulator that forms multimeric complexes together with vertebrate Hox proteins and can in addition function as a post-transcriptional regulator of protein levels of certain other transcription factors

Membrane potential The electrical potential inside a cell membrane measured relative to the fluid just outside; it is negative under resting conditions and becomes positive during an action potential

Membranous septum Last part of the ventricular septum to be closed from cushion tissue that fills in the opening left between the crest of the interventricular muscular septum and the atrioventricular mesenchymal septum

Mesenchymal-to-epithelial transformation The conversion of a mesenchymal cell to an epithelial cell

Mesenchyme Loose connection of undifferentiated cells that do not form cell–cell junctions or have any polarity

Mesendoderm Early midline cells in the head that have characteristics of both endoderm and mesoderm

Mesp1 Mesoderm posterior 2 gene. A gene that encodes a basic helix–loop–helix-containing protein expressed in all mesodermal cells

Mfh Mesenchyme fork head gene. A transcription factor with a conserved winged helix DNA-binding domain. Mfh1 is expressed in cephalic neural crest and mesenchymal cells in the prechordal region. It is associated with interrupted aortic arch

Mhc1A Myosin heavy chain1A; contractile protein expressed by mouse atrial myocardial cells

Mhc1V Myosin heavy chain 1V; contractile protein expressed by mouse ventricular myocardial cells

Microcephaly A condition, present at birth, in which the head is much smaller than normal for an infant of that age and gender

Migration Active movement of a cell from one place to another

MinK A protein that associates with KvLqt1 to form a delayed rectifier potassium channel

Mitogen Any stimulus that activates cell proliferation

Mitral valve A bicuspid atrioventricular valve between the left atrium and left ventricular

Mlc Myosin light chain. A contractile protein expressed in muscle cells

M-line Also called M band. One of the identifiable components of a sarcomere consisting of a fine dark band in the center of the H band in the myofibrils of striated muscle fibers

Module A semiautonomous, identifiable unit

Morphogen Any of various chemicals in embryonic tissue that influence the movement and organization of cells during morphogenesis by forming a concentration gradient

Msx MS type homeobox-containing gene; expressed during development in many mesenchymal cells

Mural The wall of a blood vessel

Myelination The process of insulating neuronal processes with myelin, a fatty sheath that allows efficient conduction of nerve impulses

Myocardial troughs An intermediate stage in formation of the myocardial tube from the flat cardiogenic plates

Myocardialization Migration of cardiomyocytes into a cushion or septum to replace the resident tissue with muscle

Myocardin Transcriptional activator expressed in vascular smooth muscle and myocardium

Myocardium The contractile cells that form the heart

MyoD A transcriptional master gene needed for skeletal muscle differentiation

Myoepicardium An incorrect name for the myocardium of the initial cardiac tube

Myofibrillogenesis The process of making the contractile proteins, myofibrils, in a muscle cell

Myomesin Protein found in the M line of the sarcomere

Myosin heavy chain Mhc; a protein with a globular head and filamentous tail that is a major determinant of contractile ATPase activity and the velocity of shortening in living muscle

Myosin light chain Mlc; accessory proteins that affect contractility by being phosphorylated

Neonatal lupus syndrome Neonatal lupus erythematosus (NLE) is a rare disorder caused by the transplacental passage of maternal autoantibodies. Maternal autoantibodies against Ro (SSA), La (SSB), and/or U1-ribonucleoprotein (U1-RNP) are passively transported across the placenta causing the disease

Neural crest A cellular band between the neural ectoderm and surface ectoderm that gives rise to cells that migrate throughout the body and form the peripheral nervous system, pigment cells and provide mesenchyme for face and heart development

Neural plate The midline ectoderm that will become the central nervous system

Neuregulin Also called heuregulin; a growth factor necessary for development of trabeculae and valves

Neuron-specific enolase A marker for neuroendocrine differentiation

Neuropathy An abnormal and usually degenerative state of the nervous system or nerves

Neuropeptide Y A 36-amino-acid peptide neurotransmitter found in the autonomic nervous system that augments the vasoconstrictor effects of noradrenergic neurons

Neuropilins Transmembrane proteins that act as co-receptors for Vegf and semaphorins

Neurotrophins A family of growth factors in the brain that encourage neuron differentiation and survival

Neurula An embryo at the stage in vertebrate development during which the neural plate closes to form the central nervous system

Nf160 A neuronal intermediate filament found in conduction cells

Nfat Nuclear factor of activated T-cells; a transcription factor located in the cytoplasm that translocates to the nucleus by calcium stimulation

Ngf Nerve growth factor; a naturally occurring neurotrophin required for growth and survival of certain neurons

Nke NK element; sequences in the control regions of genes that bind Nkx transcription factors

Nkx A family of genes encoding an Nk domain-containing transcription factor. Nkx2.5 is expressed in early myocardium where it regulates expression of many myocardial genes. It is expressed in a number of other tissues

No tail A zebrafish mutation in the *Brachyury* gene that causes the notochord not to form

Nociceptive Neurons that register pain

Nodal A signaling factor in the Tgfβ superfamily

Node Also called primitive node and Hensen's node. A local thickening of the blastoderm at the cephalic end of the primitive streak

Nodose ganglia The distal ganglia associated with the vagus nerve (cranial nerve X)

Noggin a soluble factor that inhibits Bmp

Noncompaction A condition in which the ventricular myocardium is loosely compacted with prominent ventricular trabeculations and deep intertrabecular recesses

Norepinephrine A neurotransmitter and a hormone released by the sympathetic nervous system and adrenal gland that increases heart rate and contractility as part of the fight-or-flight response

Nos Nitric oxide synthase; an enzyme needed for synthesis of nitric oxide

Notch Transmembrane receptor that usually inhibits differentiation of the cell when activated

Notochord A midline rod characteristic of all chordates formed from midline mesoderm that is generated by the node

Nppa Natriuretic peptide precursor a; the precursor peptide for atrial natriuretic factor (Anf)

Nt Neurotrophin; a family of structurally similar growth factors that regulate growth and differentiation

Nucleus ambiguus A cluster of neurons located in the medulla that mediates motor responses carried by the glossopharyngeal (IX) and vagus (X) cranial nerves

Nucleus of the solitary tract Region of the brainstem containing neuron cell bodies that receive most of the sensory information from the visceral organs and tongue

Oligomerize An association of multiple proteins

Orifice An aperture or hole that opens into a cavity

Orthostatic blood pressure Standing blood pressure

Otic placode Sn ectodermal thickening at the level of pharyngeal arch 2 that forms the inner ear

Outflow pole The region of the heart tube where arterial blood passes back into the body

Outflow septum Partition in the arterial pole or outflow tract that divides the systemic from the pulmonary blood streams

Overriding aorta A condition in which the aorta is not wedged between the tricuspid and mitral valves and overrides the ventricular septum to receive part of its blood from the right ventricle

P0 A glycoprotein expressed abundantly in peripheral nerves in the Schwann cell lineage. The gene is expressed in multipotent neural crest cells and its promoter has been used to drive Cre expression to specifically mark neural crest cells

Pacemaker The sinus node which controls heart rate via the conduction system

Pacemaker cells Any cells that set the rate of myocardial depolarization and hence contraction

Pacemaking and conduction system Consists of the sinoatrial and atrioventricular nodes and specialized myocardial cells that generate and propagate the electrical impulse in the heart

Papillary muscles Small bulges of myocardium in the ventricles that are attached to the valve leaflets by chordae tendinea

PAPVC Partial anomalous pulmonary venous connection; a condition in which one or more of the pulmonary veins empties into something other than the left atrium

Parasympathetic cardiac ganglia Clusters of postganglionic neurons surrounded by support cells in the heart that function to slow the heart rate

Parasympathetic nervous system A major division of the autonomic nervous system that regulates contraction of smooth and cardiac muscle in the viscera

Paraxial mesoderm The mesoderm lying adjacent to the neural tube that is partitioned into somites

Parietal pericardium The outer layer of the pericardium, which is a thin sac of tissue that surrounds the heart and is separated from it by pericardial fluid

Patch A mouse mutant with non-functional platelet-derived growth factor receptor-α (*Pdgfrα*) gene. The gene is normally expressed in the mesenchyme of multiple organs during embryonic development and is involved in cell proliferation, differentiation, migration, and apoptosis in many tissues

Patent ductus arteriosus Failure of the ductus arteriosus to close at birth

Patent foramen ovale A type of atrial septal defect

Pax A family of transcription factors containing both a homeodomain and a paired domain

Pdgf Platelet-derived growth factor. One of the growth factors important in development of the walls of the blood vessels

Pentalogy of Fallot A congenital heart defect with all of the features of tetralogy of Fallot in addition to an atrial septal defect

Perfusion Delivery of blood to a tissue

Pericardial coelom The cavity formed by splitting of the somatic and splanchnic layers of the lateral plate mesoderm that surrounds the heart

Perikarya Neuron cell bodies

Perivascular The cells that hang out around blood vessels

Perlecan A sulfate proteoglycan expressed in mesenchymal tissues during development. Perlecan binds growth factors and interacts with various extracellular matrix proteins and cell adhesion molecules

Pharyngeal arches Mesenchymal struts covered by ectoderm and lined by endoderm in the lateral pharynx

Phenylalkamines A potent class of calcium channel blockers that includes the clinically used drug, verapamil. These compounds slow the heart rate and force of contraction. Other effects include systemic and coronary vasodilation and slowing of conduction through the atrioventricular node

Phenylethanolamine-*N*-methyl transferase The enzyme that converts norepinephrine to epinephrine

Philtrum Two slight ridges in the skin that run from the nose to the upper lip

Phospholamban Accessory protein that inhibits calcium uptake by the sarcoplasmic reticulum Ca^{2+}-ATPase unless phosphorylated by protein kinase A activated in response to β-adrenergic stimulation

Phospholipase C An intracellular enzyme that is important in interpreting growth factor signal

Phox2 Transcription factor needed in a cell for catecholamine synthesis

PI3K Phosphoinositide-3 kinase, binds to phosphorylated protein tyrosine kinases and acts as an adapter to associate signaling components with the cell membrane

Pitx2 A transcription factor that is expressed on the left side of the embryo and serves as a marker of structures derived from the mesoderm on the left side

Pleuripotential Having the ability to differentiate into multiple cell lineages

Plexin A receptor for semaphorin. Plexin–semaphorin signaling are used in axon pathfinding, endothelial cell and neural crest migration

P_o The probability that an ion channel will be open to allow passage of ions

Polycomb proteins A group of chromatin remodeling proteins. Changes in chromatin effected by these proteins can be transmitted to daughter cells at cell division providing for a type of "epigenetic memory"

Postganglionic neurons Motor neurons located in peripheral autonomic ganglia that relay information from preganglionic neurons originating in the central nervous system to organs

Potential Potency, all of the possible cell types that a cell might differentiate into

Prechordal plate Midline mesendodermal tissue that originates from the node and induces the forebrain to form from the neural plate

Preganglionic neurons Neurons that originate in the central nervous system and synapse on motor neurons in peripheral autonomic ganglia that innervate an organ

Primary atrial septum The septum that divides the single atrium into right and left atria

Primary sympathetic trunks A transitory column of norepinephrine-producing cells dorsolateral to the dorsal aorta that disappears when the secondary permanent sympathetic trunk forms paravertebrally

Primary ventricular foramen The passageway between the nascent left and right ventricles. The passage is made smaller by growth of the ventricular septum; however, it never closes because it allows left ventricular continuity with the aortic vestibule which develops partly from the conus

Primitive streak A faint line on the dorsal surface of the embryo formed by movement of cells from the top or epiblast layer into the embryo to form the mesoderm and endoderm. The streak denotes the craniocaudal axis of the embryo

Primordium Basic cell type that differentiates into definitive cell lineages

Proepicardium Tissue originating in the extracardiac mesenchyme near the sinus venosus that forms most of the epicardium

Progenitor A cell that will become a particular cell over the course of development

Proliferation Division of a cell into two daughter cells

Prongs Condensed mesenchyme derived from neural crest that guides formation of the aorticopulmonary (outflow) septum

Proteoglycans Any of various mucopolysaccharides that are bound to protein chains in covalent complexes and occur in the extracellular matrix of connective tissue

Proteolytic cleavage Digestion of a protein

Proto-oncogene A gene having the potential for change into an active oncogene that can cause a cell to develop into a tumor cell. Many proto-oncogenes are used in normal development

Protostomes A taxon of animals characterized by development of the mouth at the site of the blastopore with the anus forming as a second opening. The protostomes, deuterostomes, and a few smaller phyla comprise the bilateria or animals with bilateral symmetry and three germ layers

Proximal outflow tract Conus arteriosus

Psa-ncam Polysialated neural cell adhesion molecule; an antigen expressed by some cells in the conduction system

Pseudotruncus A condition in which the pulmonary valve fails to develop and the arterial pole is represented by a single artery, the aorta

PTA Persistent truncus arteriosus, also called common trunk or truncus; a congenital cardiovascular deformity resulting from the failure of the septum between the aorta and pulmonary trunk to develop and characterized by a common pulmonary and systemic arterial trunk opening from both ventricles

Pulmonary hypertension Elevated blood pressure in the pulmonary arteries from constriction of the blood vessels in the lungs

Pulmonary pit A dimple in the back of the left ventricle between the right and left pulmonary ridges where the ostium of the pulmonary vein will form

Pulmonary sinuses The spaces just distal to the semilunar valve leaflets at the base of the pulmonary trunk

Pulmonary trunk Major arterial trunk carrying blood from the right ventricle

Purinergic receptors Receptors that bind adenosine and activate G-proteins to initiate intracellular signaling

Purkinje fibers Specialized myocardial cells or fibers that propagate an electrical impulse to the myocardium

RA *See* Retinoic acid

Raldh Retinaldehyde dehydrogenase; the rate limiting enzyme in RA production

Rami communicantes Connections of the sympathetic ganglia with the spinal nerves

Rar Retinoic acid receptor; a family of nuclear receptor proteins that alter transcription when bound to retinoic acid

Rbpjκ A transcription factor that is activated by Notch signaling

Receptor tyrosine kinase A protein in a cell membrane that responds to a specific growth factor signals by initiating a cascade of tyrosine phosphorylations inside the cell

Regurgitation Reflux of blood through a valve that doesn't close properly

Renin An enzyme produced by the kidney. Renin is released into the bloodstream by the kidneys to regulate blood pressure

Replication-incompetent retrovirus Retrovirus that has been genetically altered so it is unable to replicate

Repolarization The change in membrane potential that returns the membrane potential to a negative value after the depolarization phase of an action potential has just previously changed the membrane potential to a positive value

Ret A tyrosine kinase receptor important in sympathetic axonal growth

Reticular network A diffuse network of fine muscle fibers

Retinoic acid A product of vitamin A that binds Rars and Rxrs and controls cell division and differentiation through gene expression

Retroviral expression vector A replication incompetent retrovirus that expresses a gene that can be visualized

Retroviral labeling Use of a replication incompetent retrovirus that has been modified to express a gene that makes a protein that can either be visualized by itself, such as green fluorescent protein, or a protein that functions in an enzymatic reaction that makes a visible product such as lacZ which makes β-galactosidase

Rho GTPases A family of intracellular proteins involved in cell signaling

Rhombomere The identified segments of the hindbrain or rhombencephalon

Ribonucleoprotein A nucleoprotein that contains RNA, or ribonucleic acid

Rieger syndrome an autosomal dominant condition characterized by a variable combination of eye and dental anomalies, and umbilical hernia

Right ventricle The pulmonary ventricle that pumps deoxygenated blood to the lungs

Robo A receptor called roundabout that mediates slit signaling

Romano–Ward syndrome An autosomal dominant form of long QT syndrome

Rxr Retinoid-X receptor; a family of nuclear receptors that heterodimerize with Rars and several other receptors that bind DNA to alter gene transcription

Ryanodine receptor A class of calcium channels located in the membrane of the sarcoplasmic reticulum

SA node Also called sinoatrial node or sinus node; a small group of specialized cardiomyocytes located in the posterior wall of the right atrium that act as a pacemaker by generating at regular intervals the electric impulses that underlie heartbeat

Sarcomere Repeating subunit from which the myofibrils of striated muscle are built

Sarcoplasmic reticulum SR; a membrane network within the cytoplasm of muscle cells involved in the synthesis, modification, and transport of cellular materials and storage of

calcium that is released in response to a calcium transient for contraction

Satellite cells The cells in a ganglion that associate with the neuronal cell bodies

Schwann cells Cells derived from the neural crest that produce myelin on peripheral nerve processes

Scl Also known as Tal1, a member of the helix–loop–helix family of transcription factors found in endothelial precursors

Secondary atrial septum Septum secundum; a fold of myocardium that forms late in development that reinforces the primary atrial septum and allows blood flow between the right and left atria until the primary and secondary septa fuse at birth

Sema Semaphorin; a family of secreted and transmembrane proteins that serve as repulsive signals in endothelial, neural crest, and axonal development

Semilunar valves Leaflets of endocardium and connective tissue shaped like a half moon, located between the aorta and the left ventricle and between the pulmonary artery and the right ventricle

Septum spurium Cranial fusion of the right and left leaflets of the sinoatrial valve

Septum transversum Mesoderm near the sinus venosus where the liver forms. The proepicardium originates from the epithelial lining of the body cavity

SERCA Sarco/endoplasmic reticulum Ca^{2+}-ATPase. Refills the calcium stores after the heart beat

Serrate One of the ligands that activates Notch signaling

Shh Sonic hedgehog, one of the members of the hedgehog family of signaling molecules

Shunt A direct conduit between two blood vessels

SIDS Sudden infant death syndrome; unexplained, sudden death of an infant before 1 year of age

Sif cells Small intensely fluorescent cells; catecholaminergic cells found in the cardiac ganglia that act as interneurons or paracrine secretory neurons

Sinoatrial junction The junction of the sinus venosus with the atrium during early heart development

Sinoatrial valve A valve with two leaflets, right and left, that prevents blood from flowing retrograde from the atrium to the sinus venosus

Sinus A channel for passage of blood that does not have the tunics or coats found in the wall of an ordinary blood vessel

Sinus venosus The collection point for all the veins entering the heart during early development

Sinusoid Large thin-walled capillary-like blood vessel

Sinusoidal electrocardiogram A uniform wave that is generated by a single frequency

Situs Refers to the location of organs in the body. Situs solitus is the term used for normal placement of the asymmetric organs (lungs, liver, spleen, heart)

Situs inversus The term used for mirror-image placement of the asymmetric organs

Situs solitus Normal left–right placement of the organs

Slit A growth factor that guides migrating cells

Slow MyHC Slow myosin heavy chain; a contractile protein expressed in atrial myocardium

Slug A zinc-finger transcription factor expressed by prior to the epithelial–mesenchymal transformation by epicardial cells

SM22 A 22-kDa protein expressed by smooth muscle cells that physically associates with cytoskeletal actin filament bundles

Smad Intracellular effectors of the Bmp growth factors

Smoothened The receptor for hedgehog signaling

Sodium–calcium exchanger Ncx or Na–Ca exchanger; a membrane channel that exchanges sodium and calcium between the cell and the extracellular compartments

Solitary tract A slender compact bundle of primary sensory fibers in the brainstem made up of the central sensory processes of the vagus, glossopharyngeal, and facial nerves. The nerves convey information from stretch receptors and chemoreceptors in the walls of the cardiovascular, respiratory, and intestinal tracts and impulses generated by the receptor cells of the taste buds in the tongue

Somatic mesoderm The outer layer of lateral plate mesoderm after it splits. The somatic mesoderm forms the body wall

Somatostatin An inhibitory polypeptide used as a neurotransmitter by some neurons

Sox A family of transcription regulators defined by the mammalian testis-determining gene *Sry* and widely expressed during embryogenesis

Specification One of the early steps in commitment of a cell to develop in a particular lineage

Spina bifida A congenital defect in which the neural tube has not closed normally

Spina vestibuli Mesenchyme that extends from the mediastinum and covers the leading edge of the primary atrial septum

Spinal cord Part of the central nervous system consisting of a column of nerve tissue that runs from the base of the skull down the back. Nerves originating from the spinal cord carry most messages between the brain and the rest of the body and nerves originating in the periphery mostly relay information into the spinal cord

Splanchnic mesoderm The inner layer of mesoderm created by splitting of the lateral plate mesoderm

Splotch Mutant mouse with a dysfunctional *Pax3* gene

Sprintzen syndrome Also called velocardiofacial syndrome and VCFS; a congenital sequence of defects similar to the DiGeorge

syndrome, that is, characterized by immunodeficiency, abnormal facies, conotruncal heart defects, hypocalcemia caused by hypoplasia or absence of the parathyroids, and increased susceptibility to infections. Cleft palate is added to these defects

Srf Serum response factor. A transcription factor especially important in myocardial and smooth muscle development that binds to the serum response element (Sre) in the promoter-enhancer region of many genes

Ssa/Ro Sjogren's syndrome A antigen; a ribonucleoprotein that is attacked by an autoantibody that binds the surface of fetal conduction cardiomyocytes causing conduction abnormalities

Ssb/La Sjögren's syndrome B antigen; see Ssa/Ro

Stat Signal transducers and activators of transcription; a cytoplasmic transcriptional activator that translocates to the nucleus when a cell is stimulated with Cntf

Stellate ganglia Large ganglia located bilaterally near the first thoracic vertebra in the paravertebral sympathetic chain

Stenosis An abnormal constriction or narrowing

Su5402 A chemical that inhibits FGF signaling through FGF receptor 1

Subendocardium The space between the endocardium and myocardium that contains connective tissue and Purkinje fibers

Substance P A neurotransmitter that is found in sensory neurons that respond to pain

Suppressor of Hairless Also called SuH. A cofactor needed for notch transcriptional activity

Sympathectomy Mechanical or chemical destruction of the nerves in the sympathetic nervous system

Sympathetic nervous system The part of the autonomic nervous system originating in the thoracic and lumbar regions of the spinal cord that modulates "fight or flight" responses and otherwise generally inhibits or opposes the physiological effects of the parasympathetic nervous system

Sympathetic paravertebral ganglia A bilateral chain of neurons and their supporting cells located near the vertebral column. These cells innervate the viscera and cause an increase in heart rate and contraction force

Synaptic vesicles Membrane-bound compartments in neurons that contain neurotransmitters and are released when the neurons are electrically activated

Synaptophysin A protein found on the synaptic vesicle membrane

Syncytium A group of cells that behave as if they were a single cell

Syndecans A proteoglycan found in the extracellular matrix

Systole The portion of the cardiac cycle in which the heart muscle contracts, forcing the blood into the arterial vessels

Tachyarrhythmia Abnormally rapid heart beat

TAPVC Total anomalous pulmonary venous connection; a condition in which all of the pulmonary veins do not return blood to the left atrium

Tausig–Bing anomaly Congenital heart defect that includes double outlet right ventricle with pulmonary artery overriding the ventricular septal defect

Tbe Binding site in the promoter region of certain genes for *Tbx* transcription factors

Tbx A family of transcription factors that bind DNA via a T-box binding motif

TCF/LEF Transcription factors that are activated by canonical Wnt signaling

Telangiectasia Permanent enlargement of blood vessels causing redness in the skin or mucous membranes

Teleost Bony fish

Tenascin A protein found in the extracellular matrix that is associated with cell motility

Teratogen A substance that can cause birth defects

Terminal cisternae Dilated blind ending region of the sarcoplasmic reticulum and site of calcium release during excitation–contraction coupling. *See* also Couplons

Tetralogy of Fallot Also called TOF; a compound congenital heart defect with overriding aorta, pulmonary stenosis, ventricular septal defect, and hypertrophied right ventricular wall

Tetraploid embryo An embryo made by combining cells from a mutant embryo with cells from a second embryo that have been forced to be tetraploid, that is, have four of each chromosome rather than two as are found in diploid cells. Tetraploid cells can form only the extraembryonic tissues of an embryo and are frequently used with mutant diploid cells that cannot make normal placental components

Tetrodotoxin TTX; toxin from puffer fish that selectively blocks voltage-gated sodium channels

Tgf Transforming growth factor

Tie Receptor tyrosine kinase specific for angiopoietin

Tinman The *Drosophila* homolog of *Nkx2.5*

Titin A giant filamentous protein essential for maintaining the structure, development, and elasticity of muscle

Tll1 tolloid-like-1; a metalloprotease similar to Bmp1 expressed in the ventricular septum

Tonic control Producing or restoring normal tone

Torsades de pointes French for "twisting of points"; a form of ventricular tachycardia in which the QRS complexes swing up and down around the baseline in a chaotic fashion

Trabeculae (trabeculations) Protuberances of myocardium into the ventricles of the heart

Transcription factor A protein that increases or decreases expression of a gene by binding to the sequences that control the expression of the gene

Transgenic An animal that is forced to express different genes than it normally would

Transposition of the great arteries Also called TGA; a congenital heart defect in which the aorta arises from the right (pulmonary) ventricle and the pulmonary trunk arises from the left (systemic) ventricle

Transverse tubules (t-tubules) Invaginations of the plasma membrane (sarcolemma) of any striated muscle that lies between two tubular portions of the endoplasmic (sarcoplasmic) reticulum to form a triad of membrane profiles adjacent to the A band/I band junction in some cases, in other cases to the Z disc, of the resting sarcomere. Depolarization of the T tubule membrane triggers the release of calcium from the sarcoplasmic reticulum and eventually muscle contraction

TrkA Receptor tyrosine kinase that binds Ngf

TrkC Receptor tyrosine kinase that binds Nt3

Trophoblast Part of the placenta

Troponin One of the elements of the contractile apparatus in a muscle cell

Truncus (truncus arteriosus) Distalmost part of the outflow tract that is covered by myocardium

Tunic A layer in the wall of a blood vessel

Tunica media The middle layer of the wall of a blood vessel containing smooth muscle

Tyrosine hydroxylase One of the rate-limiting enzymes needed for catecholamine biosynthesis

Umbilical veins Veins that carry arterial blood from the placenta to the sinus venosus in early development and into the right atrium after atrial septation

Urokinase plasminogen activator A proteolytic enzyme important for degrading many proteins. In heart development it is important in altering the subepicardial matrix for epithelial–mesenchymal transformation

Valve leaflets The thin flaps of tissue that together form a valve that allows passage of blood unidirectionally

Varicose nerve fibers Axons with a beaded appearance where synaptic vesicles accumulate and are released

Vasculogenesis Creation of a new vessel de novo

Vasoactive intestinal peptide A small peptide hormone used as a neurotransmitter in the autonomic nervous system

Vcam Vascular cell adhesion molecule; a cytokine-inducible surface protein that mediates cell adhesion to other cells. Expressed by cardiomyocytes and is required for development of the epicardium

Vegf Vascular endothelial growth factor

Velocardiofacial syndrome *See* Sprintzen syndrome

Velopharyngeal insufficiency Improper closure of soft palate during speech, allowing air to escape through the nose instead of the mouth

Venous pole The region of attachment of the sinus venosus and atria to the body

Ventriculoarterial junction Also called arterial pole is the junction of the ventricle with the arterial trunks. During development the ventriculoarterial junction is represented by the junction of the most distal myocardium with non-myocardial cells at the arterial pole

Versican An extracellular matrix chondroitin sulfate glycoprotein associated with development of the right ventricle and outflow tract

Vesicle A spherical, hollow ball of cells

Vestibular spine A condensation of mesenchyme incorporated into the primary atrial septum

Vg1 A signaling factor in the Tgfβ superfamily

Vimentin An intermediate filament protein (58 kDa) found in mesenchymal cells

Visceral endoderm A layer of the mouse embryo before gastrulation that becomes part of the extraembryonic tissue during gastrulation

Visceroatrial heterotaxia Discordance between the left–right placement of the abdominal organs especially the spleen and liver and the right and left atria

Vitelline veins Veins that return the blood from the yolk sac and gut to the sinus venosus

Vitronectin A multifunctional adhesive glycoprotein found in the extracellular matrix. It contains binding sites for integrins, collagen, and heparin among other things

Vmhc1 Chick ventricular myosin heavy chain 1; contractile protein specifically expressed by ventricular myocardium

VSD Ventricular septal defect; one or more holes in the muscular wall that separates the right and left ventricles of the heart. The most common congenital heart defect

Wedging Seating of the aorta between the atrioventricular valves during final adjustments in outflow alignment

Wnt Named for the *Drosophila* gene wingless. A family of signaling factors used widely in embryonic development

Wolff-Parkinson-White syndrome An abnormal conduction pathway between the atria and ventricles that causes excitation of the ventricles that is not coordinated with atrial excitation

Wt1 Wilms Tumor 1 gene; a tumor suppressor that is necessary for epicardial development

Yolk sac Part of the extraembryonic tissue developing with an embryo that provides nourishment to the embryo before circulation is established

Z-disc Region of the sarcomere into which thin filaments are inserted and where α-actinin is located

Zic A family of genes that encode zinc-finger transcription factors, each composed of five Cys2His2 zinc-finger domains. The zinc-finger domains share homology with *Gli1* and *Gli3*, transcription factors in the Shh pathway

This page intentionally left blank

Index

Accretion, 4, 26, 69, 91
Acetylcholine, 179–180, 182, 187, 191–192, 247
  muscarinic receptor, 41, 168, 186, 188, 191–192
Acetylcholinesterase, 162, 181, 186–187, 247
Actin, 62–64
  α-Cardiac, 28, 41–43, 46, 63, 238
  cytoskeleton, 29, 90, 95, 137, 189
  polymerization, 62, 90
  α-Smooth, 40, 43, 105, 136, 150
  γ-Smooth, 137
α-Actinin, 43, 46, 236–238
Action potential (AP), 53–57, 59, 61, 64, 163–164, 167, 173, 188, 190, 234, 236–238, 247
Activation sequence, 164–165, 170, 172, 206
  apex-to-base activation, 162, 164–165, 168–169, 172, 248
  base-to-apex, 164–165, 168–169, 172, 206, 248
Activin, 36–37, 92–94, 97, 123, 247
Activin receptor, 82, 92, 94, 97–98
Activin-like kinase (Alk) receptor, 15–17, 93, 123, 172, 234, 247
Adenomatous polyposis coli (Apc), 123. *See also* Wnt
Adenosine, 189, 247
Adenoviral expression vector, 147, 247
Adherens junctions, 29, 247
Adherons, 122
Adrenal gland, 56, 136, 184–185, 191, 251
Adrenergic
  nerves, 56, 180, 183, 188–189, 191–192, 238, 247
  α-receptors, 168, 188, 191–192
  β-receptors, 61, 188–192
Afferent nerves. *See* Innervation
Aggrecan, 126
Alagille syndrome, 17, 215, 247
Alk receptors. *See* Activin-like kinase receptors
Amnion, 23, 247
Amphibian, 25, 134, 182, 204–205, 219
Angina, 140, 180–181, 241, 247
Angioblasts, 9–10, 12
Angiogenesis, 9–10, 12–13, 15, 112, 138, 190, 237, 240, 247
Angiopoietin (Ang), 13–14, 112, 120, 247
Angiotensin, 169, 247
Annulus fibrosis, 161, 173, 248
Anomalous pulmonary venous return, 72, 78, 97–98, 113, 222, 248, 258
Anterior heart field, 25–27, 30, 105, 248
Anterior intestinal portal, 7, 25, 28, 30, 87, 89, 90–91, 107, 225, 248
Anterior lateral plate mesoderm, 3, 23, 25, 30
Anti-epileptic drugs (phenytoin, valproate, carbamazepine), 223
Antisense, 17, 41, 95–97, 136, 151, 153, 248
Aorta, 73, 75, 77, 105, 134, 139–140, 150, 154, 156, 161, 163, 169, 182, 203, 207, 248
  alignment/wedging, 79–82, 87, 92, 105–106, 205
  arch. *See* Aortic arch
  defects, 16, 79–83, 92, 113, 140, 150, 152, 155–156, 215–216, 220–223
  dorsal, 10, 12, 14, 16–17, 105, 145, 184–185, 187, 252
  formation/patterning, 11–12, 16–17, 75, 144–145, 149
  septation, 87, 105–106, 150, 156
  smooth muscle, 14–15, 74–77, 139, 149, 150
Aortic arch, 17, 81, 113, 146–147, 149, 154–156, 208, 216–218
Aortic arch arteries, 6, 10–12, 17, 91, 105, 144–146, 149, 151, 153, 155, 248
Aortic semilunar valve, 6, 27, 74, 79, 81, 105–106, 119, 125–127, 147–149, 156, 222
Aortic sinus, 8, 71–73, 77–78, 80, 138–140, 163, 171, 200, 203, 209, 220, 236, 248, 261. *See also* Coronary sinus
Aortic stenosis, 81, 113, 216, 221–223
Aortic vestibule, 6, 74, 104–105
Aorticopulmonary septation complex, 147–148, 156, 248
Aorticopulmonary septum (APS), 6, 105, 127, 139, 143–144, 150, 248
Apex, 140, 161–162, 164, 172, 206, 248
Apoptosis. *See* Programmed cell death
Appendages. *See* Atrium
Arrhythmias, 45, 57, 78, 156, 167, 173, 236–237, 241, 248
Arterial pole, 27, 69, 74–77, 79, 82–83, 91, 105, 133, 143, 183, 188, 203, 215, 218, 248
  malformations, 79, 82–83
Arteriovenous malformations, 16–17, 139
Ascending limb, 26, 30, 64, 69, 111, 248
Asplenia syndrome, 97
Asymmetry, 10–12, 82, 87, 89, 90, 92–97, 107, 146, 172, 248
Atrialis, 126
Atrioventricular
  bundle (of His, AV bundle), 43, 95, 105, 107, 161–164, 166–170, 172–173, 188–189, 208–209, 248
  canal, 4–5, 24–26, 29, 31, 38, 40, 42, 69–74, 80, 88, 97, 103–104, 106–109, 111–112, 119, 121–125, 127, 133, 138, 155, 164–168, 172, 201, 205–206, 208, 218, 248
  conduction block, 41, 248
  conduction disease, 172
  cushions, 71, 74, 78–79, 121–122, 126–127, 167, 170, 218, 220, 248. *See also* Atrioventricular cushions
  delay, 161–163, 166, 168, 170–172, 206
  groove, 71, 134–135, 181, 248
  node (AV node), 56, 161–164, 166, 172–173, 181, 188–189, 208, 220, 248
  septal defect, 98, 127, 216, 218–219, 221. *See also* Common atrioventricular canal
  septum, 5–6, 104–105, 121–122, 124, 248
  valves, 6, 79, 80, 82, 87–88, 92, 112, 119, 123, 126, 219
Atrioventricular (AV) cushions, 5–6, 71–72, 74, 78–79, 113, 121–122, 124, 126–127, 136, 167, 170, 218, 220, 248
  cushion mesenchyme, 113, 122, 124, 126, 218
  dorsal (superior), 121, 126
  ventral (inferior), 121, 126, 172
Atrioventricular septum (septum intermedium), 5–6, 104–105, 121–122, 124, 248

Atrium
atrial myosin heavy chain 1 (Amhc1–chick; Mhc1A–mouse), 107–108
appendages, 69, 72–73, 181, 188
chamber-specific gene expression, 107, 110–111, 200
isomerism, 94, 96–98, 248
myocardial lineage, 25, 91, 120, 210
Autonomic ganglia, 179, 186, 248
Autonomic nervous system, 163, 168, 179–198, 249
dysfunction, 192–193
Autophosphorylation, 13, 248
Autoradiography, 22
Autosomal
dominant, 17, 45–46, 64, 79, 96–97, 173, 215–216, 219, 221
recessive, 173, 219, 221
Axon guidance, 153–154
Axons, 12–13, 179–185, 189

Bachmann's bundle, 172, 248
Barx1, 154, 248
Base-to-apex. *See* Activation sequence
Basic helix-loop-helix (bHLH) transcription factor, 9, 15–16, 41–42, 95, 136–137, 249
Bellow, Saul, 3
β-catenin. *See* Catenin
Bilateral superior vena cava, 98
Bilateral symmetry, 10–13, 146
Biomechanical forces, 87
Blastoderm, 22, 249
Blastodisc, 22
Blood islands, 9–10, 135, 249
Body axis, 92, 104, 106, 204
Body turning, 89, 91, 97
Bone morphogenetic protein (Bmp), 10, 37, 39, 125, 137, 185, 209, 249
Bmp antagonists, 208. *See also* Noggin
Bmp type Ia receptor, 172
Bmp type II receptor, 77, 123, 126, 148
Bmp1, 113
Bmp2, 10, 25, 37–38, 42, 76–77, 123, 136, 148, 187, 208–210
Bmp4,10, 24, 37, 76–77, 96–97, 126, 136, 148, 208
Bmp5, 209
Bmp6, 126
Bmp7, 209
signaling, 36, 38, 40–41, 123, 125, 144, 153, 200, 209–210
Bone morphogenetic protein-binding endothelial cell precursor-derived regulator (Bmper), 10, 249
Brachiocephalic
arteries, 11–12, 80, 149
veins, 78, 249
(Brachmann-)Cornelia-de Lange syndrome, 216
Bradycardia, 56, 191–192, 209, 249
Brain, 12, 216, 218, 225
Brain-derived neurotrophic factor (Bdnf), 180, 185, 249
Brainstem, 179, 181, 249
Brugada syndrome, 173, 174, 249
Bulbar plexus, 138
Bulboventricular fold, 103–104, 249
Bulbus arteriosus (bulbus), 104, 206, 249
Bundle (of His). *See* Atrioventricular, bundle
Bundle branches, 107, 161–162, 164, 168–169, 172, 209, 249
Bves, 137, 249

Ca^{++} stores, 58, 191
CADASIL, 17
Calcineurin, 123–124, 126–127, 148, 218, 249
calcineurin A, 218
calcineurin B, 123
Calcitonin-gene-related peptide (Cgrp), 182, 189, 249
Calcium transient, 38, 58, 61, 63, 151, 154, 191, 234, 236–237, 249
Calcium-induced calcium release (CICR), 57–61, 249
Calmodulin, 54, 59–62, 249
Calponin, 137, 249
Calsequestrin, 60–61, 249
cAMP responsive element (Creb), 59, 251
Campomelic dysplasia, 216
Capsulin, 137, 250
Cardia bifida, 30–31, 41, 90, 107, 207, 250
Cardiac crescent, 24–25, 30, 119, 208, 210
Cardiac cushions, 5, 119, 121–122, 124–125
Cardiac ganglia, 139, 179–184, 187–190, 250
Cardiac jelly, 4–5, 69, 90–91, 96, 104, 106, 112, 121–124, 133, 250
Cardiac myosin binding protein C, 163, 169, 250
Cardiac neural crest, 65, 75–76, 91, 143–156, 182–183, 187, 218
ablation, 64, 80, 91, 143–144, 150–156, 186, 218
migration, 144, 149, 205
Cardiac output, 6, 12, 64, 151
Cardinal veins, 11–12, 16–17, 70, 72–73, 163, 203, 250
Cardiocraniofacial field, 7–8, 224–225, 250
Cardiogenic field, 3–4, 21–30, 35, 37–38, 40–43, 69, 74, 77, 95, 103–104, 106–109, 120, 152, 209, 226, 250
Cardiogenic mesoderm, 5, 21, 23–28, 31, 35, 36–37, 39–41, 62, 90, 93, 95–96, 105, 107, 110–111, 119–121, 200, 208–211
Cardiogenic potential, 22–23
Cardiomyopathy, 45–46, 54, 62, 64–65, 151, 233, 250
Cardiosensor mice, 111
Caronte, 95, 250
CATCH22 syndrome, 156, 217. *See also* Syndromes
Catecholamine, 56, 180, 184–185, 188, 190–191, 250
Catenin, 29, 38–39, 123, 156, 210, 250
Caudal pharynx, 76, 143, 145–146, 153
CCS-lacZ, 172, 250
Cell adhesion, 12, 29–30, 82, 136, 218, 239
Cell cycle, 110, 225, 233, 237
Cell division, 23, 210, 216
Cell fate, 15, 17, 21–22, 187, 210, 215, 250
Cell junctions, 29
Cell lineage, 250
autonomic, 185–187
embryonic stem cell, 238
endocardial, 23, 29, 119–120, 137
endothelial, 9–10, 14–15, 122, 136, 233
epicardial, 137–138
hemangioblast, 137
hematopoietic, 235
modules, 204–206, 209–210, 224
myocardial, 21, 23, 25–26, 28–29, 35, 38, 40–42, 62, 91, 111, 120, 133, 136–137, 164, 200, 206, 210, 233–235
neural crest, 74–77, 149, 154, 156, 184
smooth muscle, 15, 42, 136–137
Cell motility, 29
Cell polarity, 12, 30, 144
Cell tracing, 135, 164
Cell–cell interaction, 112, 235
Cell–matrix interaction, 9, 29
Cell–substrate interactions, 112–113
Central conduction system, 168, 172
Cerebrovascular thrombolysis, 127
c-Ets, 136, 250
Chamber myocardium, 70, 107, 109, 111–112, 161, 164–165, 168, 171, 206
Chamber specification, 3, 6, 25, 42, 57, 87–88, 101–113, 208–209
CHAMP, 110, 250
Channelopathy, 54, 250
CHARGE syndrome, 216
Chemoattractant, 13, 250
Chimeras, 22–23, 43, 74, 76, 96, 135–136, 138, 143, 147–150, 234, 250
Chisel, 107, 109, 111, 250
Cholestasis, 215, 250
Cholesterol, 221
Choline acetyltransferase, 183–184, 250
Choline uptake, 187
Cholinergic neurons, 180, 183–184, 186, 191, 250
Chondroitin sulfate, 96, 112–113
Chordae tendineae, 8, 126–127, 250
Chorioallantoic grafts, 22, 250
Chromaffin cells, 184–185, 250
Chromogranin, 185, 250
Chromosomes, 216–217
chromosome Y, 234, 237
chromosome 4, 219
chromosome 6, 221
chromosome 7, 222–223
chromosome 8, 216
chromosome 9, 17, 192
chromosome 11, 45
chromosome 12, 221, 234
chromosome 17, 222
chromosome 18, 222
chromosome 19, 17
chromosome 20, 215
chromosome 21, 127, 218–219
chromosome 22, 80, 156, 217
Chromosome 22q11 microdeletion, 80, 154–156, 217, 218
Cilia, 93–94, 96–98, 202, 250
Ciliary dyskinesia, 97
Ciliary neurotrophic factor (Cntf), 185–186, 251
Circulatory shunts, 16–17, 78, 206, 261
Circumpharyngeal ridge, 144–145, 250
Cited1, 109
Cloche, 120
C-looping, 87, 89–91,103
Clubbing, 156, 216, 222, 251
Coalignment, 23, 25, 251

Coarctation of the aorta, 113, 155, 216, 220–221, 251
Cognitive deficit, 127, 156–157, 223
Collagen, 172, 218, 233, 251
  type I, 126, 134
  type II,124, 126
  type III, 126
  type IV, 134
  type V, 126, 134
  type VI, 134, 218
  type IX, 124
  type XI, 124
Collagen gel, 122
Collateral circulation, 139, 251
Common atrioventricular canal, 97, 127, 167, 251
Common atrium, 79, 104, 219
Common cardinal vein, 163, 251
Common carotid arteries, 12, 146, 149
Common precursor, 28, 120
Compact myocardium, 44–45, 92, 108, 112–113, 136, 138, 205, 251
  noncompaction, 45, 258
Condensed mesenchyme, 147–148
Conductance, 53–55, 166–167, 251
Conduction, 3, 79, 105, 107, 161–174, 181, 206, 238
Conduction disease/abnormalities, 41, 46, 79–80, 167, 172–174, 208, 219–220
Conduction myocardium, 105, 107, 127, 161–165, 167–170, 172, 205–206, 209
Conduction system, 6, 46, 80, 107, 112, 161–173, 206, 208
Connexin (Cx), 42, 92, 127, 164, 166, 167, 169, 238, 251
Connexon, 166
  Cx30.2, 167
  Cx37, 120–121
  Cx40, 42, 107, 109, 111, 121, 127, 166–167, 169–172, 208–209, 220, 238
  Cx42, 169
  Cx43, 82, 94–95, 107, 109, 127, 137, 149, 155, 166–167, 208, 235–238
  Cx45, 123, 166–167, 170, 238
Conotruncal anomaly face syndrome, 217–218
Conotruncal heart defects, 91–92, 150, 156, 216–218, 251
  double outlet right ventricle, 79–82, 92, 96–97, 152, 156, 217, 221–222, 251
  overriding aorta, 79–81, 150, 152, 258
  persistent truncus arteriosus (PTA, common trunk, truncus), 81–82, 144, 150–156, 208, 217–218, 260
  tetralogy of Fallot, 41, 80–81, 92, 173, 215–218, 221–222, 262
  transposition of the great arteries (TGA), 77, 80–83, 95, 97–98, 217, 221, 263
Conotruncal myocardium, 24, 26–27, 91–92, 105, 138
Conotruncus, 4, 25, 26, 74, 77, 113, 133, 154, 156, 205, 251
Conoventricular groove, 134, 251
Contractile apparatus, 5, 35, 45, 61–63, 112, 151, 251
Conus (conus arteriosus), 6, 23, 25–27, 31, 38, 69, 74, 103, 105–106, 147–148, 200–201, 203–204, 210, 251
Convergence of outflow and inflow, 4, 87, 91, 104, 251
Coordinate grid, 25
Coronary arteriovenous fistula, 139
Coronary artery malformations, 80, 82, 113, 139–140, 154, 222
Coronary artery ostia, 139
Coronary sinus, 71–72, 78, 80, 138–139, 251. *See also* Aortic sinus
Coronary vascular plexus, 135, 138
Coronary vessels, 6, 69, 80, 77, 82, 113, 133–140, 150, 163–164, 169, 172, 181, 183, 189, 190, 234, 237, 240–241, 251
Couplons, 58, 251
Coup-tfII, 108, 112, 200, 251
Cranial neural crest, 143–144, 205, 223
Craniocaudal axis, 25, 87, 92, 103, 106, 111, 113, 200, 205
Craniocaudal polarity, 31, 103, 106
Cre recombinase, 122, 149, 251
Crescent, 39, 210, 251
Crista terminalis, 163, 251
Cryptic, 82, 92–93, 95, 97, 110, 251. *See also* Egf–cfc
Cushion mesenchyme, 113, 119, 121–126, 135, 220
Cyclostomes, 182, 252
Cytochalasin B, 90
Cytokeratin, 134, 136–137, 252
Cytotactin, 120

DAPT, 123
Delamination, 120–121, 126, 128, 135–136, 143, 148, 205, 252
Delayed rectifier, 55, 167, 172, 174, 190
Delta, 15–16
Depolarization, 53–61, 64, 164, 173, 190–191, 238, 252
Descending limb, 30, 63–64
Dextral (D-looping), 87
Dextrocardia, 95, 97, 252
Dextroposed aorta, 80, 92, 223
Diabetes (type I), 98
Diastolic (resting) potential, 54–57, 252
Differentiation, 252
  artery/vein, 16
  cardioblast, 200
  chamber, 104–105, 107, 112–113
  conduction system, 164–165, 167–171
  endothelial, 9–10, 12, 38, 120, 136, 236–237, 239
  endocardial, 120–121, 124, 207, 216
  epicardial, 136–138
  hemangioblast, 10
  hematopoietic, 235
  myocardial, 29–30, 35–46, 58, 61, 70, 77, 90, 112, 127, 136, 138, 152, 200, 207, 209–211, 215, 226, 235–240
  neural crest, 144, 183, 187
  neuronal, 185, 187
  renal, 16
  smooth muscle, 15, 136–138, 236
  stem cell, 232, 234–240
DiGeorge syndrome, 155–157, 208, 217–218, 225–226
  phenotype, 150–151, 154, 156, 217–218, 225–226, 252
Dihydropyridine 55, 58–59, 252
DiI, 26, 75
Dimerization, 93
Discordance, 82, 252
Dishevelled (Dsl), 144, 156, 252
Dissecting aorta, 83, 252
Distal-less, 146, 252
  Dlx2, 154
  Dlx3, 154
  Dlx6, 146
Dopamine-β-hydroxylase, 185, 188
Dorsal mesocardium, 4–5, 23, 39, 69–71, 73–74, 87–88, 90–91, 96, 252
Dorsal root ganglia, 153–154, 179–181, 184, 187
Dorsal vagal motor complex, 181, 252
Dorsoventral axis, 39, 110
Dorsoventral polarity, 103
Double inlet left ventricle, 96–97, 252
Double outlet right ventricle (DORV), 79–82, 92, 96–97, 152, 156, 217, 221–222, 252. *See also* Conotruncal heart defects
Down syndrome critical region I (DSCR1), 127, 218
Down syndrome (trisomy 21), 74, 127, 193, 218–219, 224, 252
Dscam (Down syndrome cell adhesion molecule), 218
Ductus arteriosus, 11–12, 80,146–147, 149
  patent ductus, 82, 113, 156, 216, 221–222
Ductus caroticus, 12
Ductus venosus, 78

E-boxes, 137
Ebstein anomaly, 128, 173, 252
Ectoderm, 17, 29, 37–38, 40, 76, 94, 143–144, 146–147, 151–154, 199, 210, 225
Ectomesenchyme, 76, 106, 143–144, 147, 183, 252
Egf–cfc, 82, 92, 93, 95, 97, 110, 252
Ejection fraction, 151, 240–241
Elastin15, 134, 222–223, 253
Electrical activity, 30, 55, 163, 165, 171
Electrocardiogram, 64, 167–168, 171–173
Ellis-van Creveld syndrome (chondroectodermal dysplasia), 219
Embryoid bodies, 38, 238, 253
Embryonic axis, 25
Embryonic stem (ES) cells, 10, 14, 38, 40–41, 57, 146, 233, 238, 240, 253
Endocardial cell lineage. *See* Cell lineage
Endocardial cushions, 6, 73, 112, 121–127, 150, 172, 214, 253
  atrioventricular (AV), 5–6, 71–72, 74, 78–79, 113, 121–122, 124, 126–127, 136, 167, 170, 218, 220, 248
  outflow cushions (conotruncal), 6, 121, 123, 125, 147, 148–149, 155
Endocardial fibroelastosis, 113
Endocardium, 3–6, 21, 23, 29, 35, 41, 44, 69, 73–74, 91, 105–106, 112–113, 119–127, 133, 137, 147, 161, 163, 169, 190, 200–201, 205, 209, 218, 220, 253
Endoderm, 7, 10, 23–25, 28–30, 35–41, 75–76, 94, 119–120, 144, 146, 150, 152–157, 207–210, 218, 225–226, 238, 253
Endoglin, 16–17, 123, 253
Endothelial cell polarity, 12

Endothelial cells, 6, 9–17, 29, 38, 77, 119–125, 127, 135–139, 142, 146, 148, 155, 169, 171, 185, 190, 200, 216, 220, 233–237, 239, 253
Endothelial precursor cells, 9, 12, 119–120, 138
Endothelial strands, 10, 71, 139, 146
Endothelin (Et1), 120, 146, 154, 169–171, 253
  endothelin A receptor (EtA), 146, 154, 169, 171, 253
  endothelin converting enzyme (Ece), 169, 171, 252
Endothelium, 14–17, 69–70, 112, 120, 122, 133, 139, 146–147, 154, 169, 189–190, 201–202, 239
  arterial, 16–17
Engrailed (En) enhance, 172, 253
Enkephalin, 185, 253
EpasI, 121
EPDCs, 122, 133–138, 253. *See also* Epicardially-derived cells
Ephrin, 13, 16, 253
  Eph receptors, 13
  EphB3, 3, 16
  EphB4, 13, 16–17
  EphrinA, 13
  EphrinB, 13, 16–17
Epiblast, 21–23, 35–36, 95, 253
Epicardially-derived cells, 122, 133–138, 253
Epicardin, 120, 136, 253
Epicardium, 5–6, 14, 44–45, 69, 77, 122, 133–138, 170, 200, 205, 208, 253
Epidermal growth factor (Egf), 112, 124–125
Epilepsy, 223
Epithelial-to-mesenchymal transformation, 74, 82, 119, 121–124, 135–136, 155
Epithelium, 28, 122, 134, 136, 143, 253
ErbB, 124, 170, 185, 253
  ErbB1, 124–127
  ErbB2, 44, 112, 124–125, 169, 185
  ErbB3, 120, 124–126, 185, 216
  ErbB4, 44, 112, 124, 169
Erk, 38, 253
Erk5, 110
Ethanol, 223
Excitation-contraction coupling, 5, 53, 57–58, 151, 253
Explant, 21–22, 27, 35, 39, 70, 123, 210, 253
Extracellular matrix, 15, 29, 82, 95–96, 112–113, 124, 126, 134–136, 202
Extracellular matrix bridge, 134. *See also* Proepicardial bridge
Extraembryonic endoderm, 30. *See also* Visceral endoderm
Extraembryonic tissue, 23, 30, 41
  mesenchyme, 9
  yolk sac, 9–10

Facial dysmorphism, 45, 156, 215, 221
Familial dysautonomia, 192, 252
Fast conduction, 162, 164, 166, 168, 206
Fate map, 22, 35, 153, 211, 253
Faust, 120, 207
Fetal alcohol syndrome (FAS), 223, 226
Fibrillin, 96, 120, 134, 253
Fibrillin-related protein (JB3), 95–96, 120, 122, 256
Fibroblast growth factor (Fgf), 37–38, 45, 82, 91, 134, 136–138, 144, 169, 185, 210, 225, 253
  Fgf2, 38, 45, 136, 138, 190
  Fgf4, 37–38, 124, 170, 210
  Fgf8,17, 25, 38, 65, 76, 81–82, 92–93, 146–147, 152–153, 157, 210, 218, 224, 226
  Fgf9, 138
  Fgf10, 26, 208, 224, 225
Fibroblast growth factor receptor (Fgfr), 82, 210
  Fgfr1, 38, 45, 124, 138, 144
  Fgfr2, 124, 138
  Fgfr3, 124
Fibroblasts-interstitial myocardial, 133, 135–137, 233
Fibronectin, 29–30, 113, 126, 134, 135, 253
Fibrosis, 128, 139, 161, 173, 233–234
Fibulin, 15, 126, 134, 253
Filopodia, 12, 13, 122, 254
FKB binding protein, 60, 254
Flectin, 95–96, 134, 254
Flk1 (VEGF receptor 2, VEGFR2), 9–10, 12–14, 16, 92, 146, 236–237, 254
Floating head, 95, 254
Flt1 (VEGFR1), 12, 120, 254
Fluorescence in situ hybridization (FISH), 217–218
Fluorescent Ca^{2+} indicators, 60–61, 162
Fluorescent dye labeling, 22–23, 25, 75, 106
Fog2, 41, 127–128, 136, 254
Foramen ovale, 73–74
  patent foramen ovale, 128, 156, 259
Foregut, 3–4, 23, 25, 27, 30, 72, 74, 87–88, 91, 108, 119, 222, 225. *See also* Anterior intestinal portal
Foregut pocket, 4, 7, 25–26, 30, 89, 226, 254
Fox, 144, 254
  AmphiFoxD1, 205, 254
  Foxc1, 155
  Foxc2, 155
  Foxh1, 110
Frizzled2, 39, 156, 254. *See also* Wnt
Funny current (I_f), 55–57, 64, 190, 255

GABAergic neurons, 185, 254
Galanin, 185, 254
Gap junction, 137, 161–164, 166–167, 171, 208, 236–238. *See also* Connexin, Cx; Connexon
  communication, 94–95, 123, 155
  heteromeric gap junction, 166, 255
  junctional plaque, 162, 166, 256
Gastrulation, 9, 21, 23, 29, 35, 36, 39, 42, 67, 87, 89, 92, 96, 103, 106, 107, 120, 200, 207, 210, 238, 254
Gata, 36, 39–42, 108, 111, 127, 136, 200, 206–207, 210, 254
  Gata4, 25, 27, 30, 35–42, 74–76, 79–80, 107–108, 111, 120, 128, 170, 207, 210, 224, 234–238
  Gata5, 41, 107, 120, 207
  Gata6, 41, 107, 172, 207
Genetic marking, 25–26
Gill arteries, 146
Gills, 3, 150, 202–204
Glial cell line-derived neurotrophic factor (GDNF), 185, 254
Glucocorticoids, 185, 254
Glucuronic acid, 125
Glutaminergic neurons, 180, 254
Glycogen, 163–164, 173, 254
Glycogen synthase kinase 3β (Gsk3β), 39, 254
Glycosaminoglycans, 121
Goosecoid, 154, 254
G-protein coupled receptors, 154, 189–190
Gradients
  electrochemical, 61, 163, 174
  gene expression, 107–108, 111, 204
  morphogen, 39, 93, 106, 107, 138, 144, 257
Great arteries, 9–12, 17, 27, 80–82, 91, 141, 144, 146, 150, 153–154, 156, 217–218, 223, 254
Gridlock (grl), 16–17, 254
Growth cone, 12
Growth factors, 13, 15, 33, 40–41, 58, 65, 76, 82, 96, 124, 134, 170, 185–186, 224–225
GTPase activity, 30, 41, 123, 125
GTPase-activating domain (GAP), 125
Guidance molecules (cues), 13, 153–154, 185
Guillain-Barre syndrome, 192, 254

H^+/K^+ transporters, 92, 254
H^+/K^+-ATPase activity, 94
Hand, 40, 42, 206–207, 254
  hand1, 40–43, 95–97, 109–111, 154
  hand2, 40–43, 95–97, 109–111, 113, 146, 154
Haploinsufficiency, 12, 42, 79, 146, 155, 187, 208, 219, 222, 254
Head mesoderm, 23, 155
Head process, 22, 255
Heart tube
  action potentials/beating, 53, 55–56, 62, 161, 164–166, 168, 170–172, 200
  anterior heart field, 26–27, 75, 110
  chamber specification, 1, 103
  evolution, 200–205, 208–211
  fusion/formation, 4, 7, 21–22, 25–27, 28–31, 69, 90, 107, 119, 200, 208, 225
  gene expression, 29–30, 42–43, 93, 96–97, 106–113, 166, 172, 208, 209–211, 217
  lengthening, 4, 21, 26–27, 28, 69, 80, 90–91
  looping, 4, 23, 26, 87–91, 256
  polarity/patterning of/segmentation of, 4, 5, 23, 25, 30, 43, 103, 106–107, 112–113, 106–113, 204, 205
  primary/primitive, 21, 28, 55, 62, 69, 80, 107, 112, 162, 200–201
  progenitors, 4, 21–23, 25, 44, 69
  remodeling, 3, 70, 73, 104
  secondary heart field, 26–27, 75–76, 91, 106, 110, 180
  venous pole, 69–71, 73
Hemangioblasts, 9–10, 136–137, 255
Hematoblasts, 9–10, 255
Hematopoietic stem cells, 9–10, 137, 235, 236
Hemodynamics, 9, 63–64, 110, 139, 188
Hemorrhage, 17
Hensen's node, 25, 89, 94, 95. *See also* Node (Hensen's organizer)
Heparin sulfate, 112
Heparin-binding epidermal growth factor-like growth factor (Hb–Egf), 125–126
Hereditary hemorrhagic telangiectasia, 16–17, 255

Hes (Hairy/Enhancer of Split), 15, 255
Heterotaxia, 94–98
HF-1b, 170
HIF1α. *See* Hypoxia inducible factor
Hindbrain, 205
HIRA, 151, 153, 218
His bundle. *See* Atrioventricular bundle
His-Purkinje system, 162, 165–167, 172–173, 206
hLAMP1 (Heart-Specific Lectin-Associated Matrix Protein-1), 95–96, 255
HNK1, 75, 163, 255
Holt-Oram syndrome, 74, 79, 208, 209, 219–220, 224, 255
Hox code, 144, 153, 217, 255
Hyaluronic acid, 112, 123, 125
Hyaluronic acid synthetase (Has2), 112, 123, 254
Hyaluronidase, 90
Hyperplasia, 16, 123, 125, 186
Hyperpolarization, 55–56, 60, 163, 255
Hyperproliferation, 127
Hypertension, 64
  pulmonary, 78, 260
Hypochord, 255
Hypomorph, 38, 76, 81–82, 95, 96, 127, 152, 210, 255
Hypoplasia, 16, 42, 44–45, 108, 113, 123, 125, 150, 156, 189, 216, 220, 224, 255
Hypoplastic left ventricle (hypoplasia of the left heart), 108, 113, 221, 222
Hypoxia, 9, 30, 55–56, 92, 124, 136, 168, 191, 205, 239
Hypoxia inducible factor (HIF1α), 30, 92, 239, 255

I_f. *See* Funny current
Inflow limb, 4–5, 25–26, 31, 73, 91, 103–104, 107–108, 111, 161, 205, 209
Inflow tract, 5, 21, 30, 69–70, 80, 89, 92, 106, 108, 138, 164, 171
Infundibulum, 6, 74, 81, 90, 92, 105, 150, 255. *See also* Pulmonary infundibulum
Ingression, 21, 23, 35, 255
Inner curvature, 4, 30, 87–88, 106–107, 111, 121, 138, 172
Innervation
  adrenergic. *See* Adrenergic
  afferent, 179–183, 189, 192, 247
  autonomic, 163, 168, 179–180, 182, 184, 186–188, 189–192
  defects of, 192–193
  efferent, 179, 192, 252
  heart, 4, 142, 162, 179, 180, 191
  insertional mutagenesis, 113
  parasympathetic, 4, 144, 163, 179–184, 186–187, 190–192
  sensory, 179–182, 185–187, 189
  sympathetic, 4, 144, 163, 179–182, 184–186, 187–192
Insulin-like growth factor, 169, 255
Integrin, 12, 29, 113, 135, 255
  α1 integrin, 207
  α4 integrin, 44, 135, 138
  β1 integrin, 113
Intercellular permeability, 12
Interendothelial tight junctions, 12
Intermediolateral cell column, 179, 184, 192, 256
Interrupted aortic arch (IAA), 17, 154–156, 208, 218, 256
Interruption of the inferior vena cava, 98
Intersegmental vessels, 12, 256
Intrinsic ganglia, 6, 190
Inv mouse, 96, 256
Inversion, 30
Inward rectifier (Kir), 46, 55–56, 191, 255
Ion channel, 38, 46, 53–65, 95, 167–169, 171–174, 188–192, 238, 256
  calcium-gated, 54–61. *See also* L-type calcium current, L type calcium channels; T type calcium channel
  chloride (Cl^-), 189
  ligand-gated, 54
  mechanically-gated, 54
  open probability (P_0), 54, 259
  potassium (K^+), 46, 55–56, 64, 167–168, 172, 174, 189, 191
  sodium (Na^+), 56, 64, 172, 174, 189, 191
  voltage-gated, 54–55, 58–59, 61, 64, 167, 174, 256
Iron particles, 22
Irx, 40, 112, 256
  Irx1, 109
  Irx2, 109
  Irx3, 109
  Irx4, 40, 107–110, 112, 170
  Irx5, 111–112
Ischemia,139–140, 180, 189–190, 233–234, 236–239, 241, 256
Isl1 (Islet1), 24–26, 28, 91, 110, 113, 206, 256
Isomerism, 94, 96–98
Isoproterenol, 188–189, 234
Iv mouse, 96, 109, 256
Ivemark syndrome, 97, 256

Jagged, 15–17, 81, 215, 256
JB3, 95–96, 120, 122, 256
Jekyll mutant, 112, 256
Jervell-Lange-Nielsen syndrome, 173, 256

Kabuki syndrome, 220
Kartagener syndrome, 97, 256
Kidney, 12, 137, 215–216
Kif3B, 93, 96 256
Kinesin, 96

Laminin, 13, 134, 256
Lateral plate mesoderm, 3, 23, 25, 28, 30, 41, 93–95, 97, 105, 112, 208–209, 224–225, 256
Lateralization, 97
Left atrial isomerism 97–98. *See also* Polysplenia syndrome
Left cardiogenic field (contribution to heart tube), 90, 96, 106
Left sinus horn, 70–73
Left superior vena cava, 71–72, 78, 156, 221
Left venous valve leaflet, 70, 172
Left ventricle, 5, 24–28, 31, 38, 42–43, 45–46, 69, 72–73, 75, 81–82, 89–91, 96–97, 103–113, 121, 126, 133, 140, 150, 154, 163, 165, 169, 201, 205, 209, 219–220, 234–236, 241, 256
Left–right axis, 11, 13, 82–83, 87, 89, 92–95, 97, 104, 106
Left–right dynein, 96, 256
Left-sided dominance, 90
Lefty, 92–93, 95–98, 256
  LEFTYA, 98
Limb bud, 12, 224
Limk1, 222, 256
Liver 6, 17, 82–83, 94, 96–97, 201, 215, 235, 237
Long QT syndrome, 64–65, 167, 173–174, 192, 256
Looping, 3–5, 22, 26, 29, 38–39, 43, 57, 69, 80–81, 87–98, 103–104, 106, 107–109, 112, 133, 150–152, 168, 205, 207, 209, 220, 256
  bending, 87–90, 95
L-type calcium current, 151, 154, 188, 190–191, 255
  L-type calcium channel, 38, 55–61, 188–191, 249
Lumenization, 4, 9
Lung, 12, 71–72, 78, 82–83, 94, 97, 143, 204–206, 241

MADS, 42, 110, 206, 256
Malalignment, 80, 152–153
Map kinase (mitogen-activated protein kinase, Mapk), 38, 59, 123, 125–127, 257
Mash1 (mouse achaete scute homolog), 185–187, 257
Matrix metalloproteinases, 136, 257
Maximum diastolic (resting) potential, 54–57, 252
Mef2, 36, 40, 42, 110, 200, 206–207, 209, 235, 257
  Mef2a, 42, 110
  Mef2b, 42
  Mef2c, 38–42, 110
  Mef2d, 42
Meis, 144, 257
Mekk3, 110
Membrane potential, 53–55, 167–168, 257
Membrane transport, 30
Membranous septum, 105, 127, 257
Mesenchymal-to-endothelial signaling, 14
Mesenchymal-to-epithelial transformation, 28–29, 257
Mesenchyme Fork Head1 (Mfh1), 17, 257
Mesocardium (dorsal), 4–5, 23, 39, 69–71, 73–74, 87–88, 90–91, 96, 252
Mesoderm, 14, 16–17, 21–30, 35–37, 39–40, 42–43, 62, 71, 89, 93, 96–97, 113, 119–120, 144, 154–155, 184, 199–200, 208, 210, 216, 237
  cardiogenic, 5, 21, 23–28, 31, 35–37, 39–41, 62, 90, 93, 95–96, 105, 107, 110–111, 119–121, 200, 208–211
  lateral plate, 3, 23, 25, 28, 30, 41, 93–95, 97, 105, 112, 204, 208–209, 224–225, 256
  pharyngeal, 26–27, 69, 74–75, 106, 119, 154
  somatic, 28–29, 261
  splanchnic, 3–5, 26, 28–30, 37, 69–72, 74, 119–121, 133–136, 205, 261
Mesoderm splitting, 28
Mesodermal cores, 26, 69, 147
Mesp1, 23, 257
Metabolic requirements, 9, 45, 205
MHC1V. *See* Myosin heavy chain
Microdeletion, 81, 155–156, 215, 217–218, 222, 226
Microtubules, 30, 93–94, 144
Midline
  embryo, 3, 22, 24–25, 29–30, 37, 43, 92, 95, 119, 199–200, 207, 209

Midline (*contd*)
heart tube
dorsal, 4, 87, 91, 106–107
ventral, 20, 87, 91, 103, 106–107
midline heart tube, 4, 7, 31, 85, 117, 119, 225
Migration, 257
angioblasts, 9
cardiac cushion mesenchyme, 121, 123–124
dorsal vessel, 199–200
endocardium, 29, 122, 124
endothelial cells, 9, 12–13, 15, 120, 123, 190, 234, 239
epicardially-derived cells, 6, 14, 135–138
neural crest, 13–14, 65, 82, 143–147, 149–150, 152–156, 183–185, 190, 205
precardiac, 29–30, 113
primitive streak, 22–23, 25
secondary heart field, 76, 151
smooth muscle, 15, 137
MinK, 167, 170, 172, 174, 257
MinK–lacZ, 172–173
Mitochondria, 45, 58
Mitogen activated protein (MAP) kinase, 38, 41, 59, 123, 125–127, 257
Mitral valve, 79–80, 91– 92, 106, 110, 113, 122, 126–127, 201, 257
defects, 139, 216
Module, 7, 110, 199, 201, 204–206, 209, 211, 215, 224–226, 257
Molecular cues, 9
Molecular switch, 29
Morphogen, 12, 35, 89, 93, 209, 257
Morphogenetic field, 7, 204
Morpholino antisense, 17, 38, 96
Msx2, 153, 159
Mural cells, 14–15
Muscarinic receptors, 186
Muscular ventricular septum, 105, 127
Myelination, 180, 257
demyelination, 192
Myocardial angiogenesis, 12
Myocardial fate, 23
Myocardial function, 45, 65, 150–151
Myocardial growth, 38, 42, 44–45, 135, 137–138, 220
Myocardial hypoplasia, 16
Myocardial maturation, 43, 112, 137, 224
Myocardial wall stress, 63, 151, 235
Myocardialization, 71, 147, 257
Myocardin, 15, 42, 257
MyoD, 15, 25, 40, 257
Myoepicardium, 133, 257
Myofibrillogenesis, 29–30, 43, 257
Myofibrils, 62, 162–164, 166, 236–238
Myofibroblast, 136
Myosin, 202–203
Myosin heavy chain (Mhc), 164, 207, 236–238, 258
atrial myosin heavy chain 1 (Mhc1A-mouse; Amhc1-chick), 108, 169, 257
α-myosin heavy chain (αMhc), 108, 236
β-myosin heavy chain (βMhc), 108, 236
myosin light chain (Mlc), 62, 72, 257
myosin light chain 1A (Mlc1A), 24
myosin light chain 1V (Mlc1V), 40, 108
myosin light chain 2V (Mlc2V), 237–238
slow myosin heavy chain (slow MyHC), 169, 203, 261
smooth muscle myosin heavy chain, 137
ventricular myosin heavy chain 1 (Mhc1V-mouse; Vmhc1-chick), 108, 257, 263
Myotendinous junction, 126–127

Na^+ channel, 55–56, 64, 173–174, 189
Na^+/Ca^{++} exchanger (NCX), 54–57, 238, 261
N-acetylglucosamine (GlcNAc), 125
N-cadherin, 28–29, 236
Neonatal lupus syndrome, 173, 257
Nerve cell bodies (Perikarya), 183, 259
Nerve growth factor (Ngf), 180, 185, 258
Neural cell adhesion molecule (N–Cam), 122, 163, 204, 218, 260
Neural crest, 5, 14, 17, 43, 65, 69, 74–79, 83 119, 143, 145–146, 216, 218, 257
ablation, 80, 91, 144–145, 150–152, 154–156, 186
circumpharyngeal ridge, 145
Cx43, 155
ectomesenchyme, 106, 143, 150, 154, 186, 252
endothelin (Et), 146, 154
induction, 144
innervation, 144
lineage tracing, 77
migration, 13, 65, 144–145
mouse, 149, 154
outflow septum, 147, 149–150
retinoic acid, 156
signaling, 152–153
trunk, 144, 184
valve leaflets, 148
zebrafish, 149
Neural tube, 11, 143–145, 153, 205, 210, 223
Neuregulin, 44, 112, 124–125, 169–170, 185, 187, 258
NeuroD, 187
Neuroepithelium, 143
Neurofibromatosis Type 1 (von Recklinghausen neurofibromatosis), 220
Neurofibromin (Nf1), 123, 125, 220
Neurofilament, 145, 169, 185
NF160, 163, 168
Neuron-specific enolase, 185, 258
Neuropathy, 192, 222, 258
Neuropeptide Y, 182–183, 185, 187, 190, 258
Neuropilin (Np), 12, 16, 154, 258
Neurotrophin (Nt), 180, 185–186, 258
neurotrophin-3 (Nt3), 81, 180
neurotrophin-4 (Nt4), 180
Nfat, 41, 45, 120, 122–127, 148, 216, 218, 220, 258
NK element (NKE), 41, 42, 111, 258
Nkx, 36, 40
Nkx2.3, 207
Nkx2.5, 24–25, 27, 35–43, 74–76, 79, 98, 108, 111, 169–170, 173, 200, 206–207, 209–211, 224, 234–238, 258
Nkx3.2, 95, 205
tinman, 40, 207–210
No tail (Brachyury, T), 95, 258
No turning mutant mouse (nt), 97
Nodal, 36, 92–97, 258
Nodal-related 1 (Nr1), 97
Node (atrioventricular, AV), 55, 161–168, 172–173, 181, 188–190, 208, 220, 248
Node (Henson's, organizer), 22–23, 25, 39, 89, 92–95, 144, 258
Node (sinoatrial, SA), 53, 55–56, 64, 161–163, 165, 168, 172, 181, 186, 188–190, 192, 208, 220–221, 236, 238, 260
Nodose ganglia, 179, 180–181, 187, 258
Nodose placodes, 186
Noggin, 37, 40, 77, 208–209, 258
Noonan syndrome, 126–127, 220–221
Norepinephrine, 180, 187–189, 192–193, 258
Notch, 15–17, 39, 81, 94, 123, 210–211, 215, 258
Notochord, 30, 37, 40, 55, 97, 151, 258
Nppa (also called Atrial natriuretic factor, ANF), 40–42, 72, 107, 109, 111, 208–209, 224, 236–238, 247
Nucleus of the solitary tract, 179, 181, 258

Omphalomesenteric veins, 90
Opitz GBBB syndrome, 217
Optical mapping, 162, 164–165, 171, 206
Organizer, 226
Otic placode, 143, 150, 151, 183, 258
Otocyst, 145, 182
Outer curvature, 3–4, 30, 87, 96, 104, 106–107, 109, 111, 121
Outflow cushions, 6, 121, 123, 125, 147, 148–149, 155
Outflow limb, 4–5, 26, 31, 76, 91, 103–104, 107, 110–111, 151, 205, 210
Outflow pole, 2, 39, 74, 87–88, 103–104, 113, 133, 258
Outflow septation, 11, 76, 87, 105–106, 121, 143, 147–151, 153, 155, 164, 205
Outflow septum-spiraling, 5, 6, 79, 82, 105, 113, 147, 156, 258
Outflow tract, 4–6, 26, 28, 38, 69–70, 74–77, 79–83, 87–88, 91–92, 104–113, 119, 121–122, 124, 127–128, 133–134, 138, 143–145, 147, 150–156, 164–165, 168, 172, 183, 205, 208–210, 219
distal, 6, 27, 77, 87, 122, 147, 252. *See also* Truncus arteriosus
proximal, 6, 108, 119, 121, 260. *See also* Conus (conus arteriosus)
shortened, 80–81, 91–92, 151–152, 205
Overriding aorta, 79–81, 150, 152, 258

P0 cre, 149, 258
p38, 41, 110
Pacemaker, 54, 57, 163–165, 171, 188–189, 204, 206, 238, 258
Pacemaker current (If, HCN), 55, 56, 60, 189, 191
Pancreas, 12
Papillary muscles, 8, 126, 258
Parallel circulation, 3, 86
Parasympathetic innervation, 144, 181, 183, 186–187, 191
Parathyroid, 144, 150, 153, 155–156, 217–218
Paravertebral ganglia, 6, 179, 184
Parietal pericardium, 23, 255
Partial anomalous pulmonary venous return (PAPVP), 78, 258
Patch clamp, 54

Patch mutant mouse, 153, 259
Patent ductus arteriosus, 82, 113, 156, 216, 221, 222, 259
Patent foramen ovale, 128, 156, 259
Pathfinding, 12–13
Patterning
  aortic arches (great arteries), 143, 146–147, 151, 153–154, 218, 223
  cardiogenic field, 27
  coronary, 77, 80, 138, 139
  heart, 200–201, 209
  neural crest, 144, 154
  pharyngeal (branchial), 144–145, 150, 155, 208, 226
  vascular, 9–13, 16–17
Pax3, 149, 150, 153, 218. *See also* Splotch mouse
Periarterial conduction fibers, 169
Pericardial cavity, 39, 73, 133–134, 138, 145. *See also* Pericardial coelom
Pericardial coelom, 28, 29, 43, 134, 159, 200
Pericytes, 9, 15
Peritruncal vascular ring, 138–139
Perivascular cells, 9, 15, 239
Persistent truncus arteriosus (truncus, common trunk), 81, 82, 144, 150, 151, 152–156, 208, 217, 218, 260
Pharyngeal arch arteries. *See* Aortic arch arteries
Pharyngeal arches, 7, 10, 17, 26, 41–43, 69, 75–76, 82, 105, 122, 144–146, 149, 150, 152, 183, 205, 218, 223, 225–226, 259
Pharyngeal (branchial) endoderm (foregut endoderm), 7, 10, 37–38, 41, 74–75, 119, 144–146, 150, 152–157, 208, 210, 218, 225–226
Pharyngeal ectoderm, 147, 154
Pharyngeal mesenchyme, 27, 69, 75, 106, 119, 154
Pharyngeal pouch, 143, 145, 153, 156, 226
Pharynx, 4, 9, 23, 26–28, 41, 69, 74, 76–77, 87, 89, 91, 119, 121, 133, 143, 145–147, 149–153, 208, 218. *See also* Foregut
Phenylalkamine, 59, 259
Phenylethanolamine-N-methytranferase, 185, 189
Phospholamban, 46, 61, 191, 234, 238, 259
Phospholipase C, 46, 58, 61, 125, 168, 191, 234, 238, 259
Phospholipase C-dependent signaling, 58, 125, 168, 259
Phox2a, 185, 187
Pigmentation, 153, 216
Pitx2, 71, 73, 93–97, 156, 259
  Pitx2 isoforms, 96
  Pitx2c, 96, 110
Plasminogen activator, 76, 136, 259
Platelet endothelial cell adhesion molecule (Pecam), 122
Platelet-derived growth factor (Pdgf), 15, 136, 137, 169, 259
  Pdgf receptor, 15, 259. *See also* Patch mutant mouse
Plexin, 149, 154, 259
PlexinA2, cre, 149, 154
Polaris, 96
Polycomb, 216–217, 259
Polysplenia syndrome, 97, 98
Postganglionic neurons, 179–184, 187, 189–191, 255
Potency, 21–23, 25, 209, 240, 259
Prechordal plate, 7, 24–25, 119, 225–226, 259
Pre-endocardial cells, 120–121
Preganglionic neurons, 179, 181, 183–184, 187, 259
Pre-myocardial cells, 28, 120, 121
Prepattern, 9, 11
Prepharyngeal mesoderm, 74
Primary atrial septum (septum primum), 5, 70–74, 78–79, 104, 127, 259
Primary capillary plexus, 9, 12–13
Primary dilated cardiomyopathy, 151
Primary sympathetic trunks, 184, 187, 259
Primary vascular plexus, 10
Primary ventricular foramen, 104, 259
Pulmonary pit, 71, 73–74, 256
Primitive streak, 7, 21–25, 30, 35–37, 41, 92, 95, 106, 120, 259
Proepicardial bridge, 134
Proepicardium, 5–6, 44, 133–138, 155, 259
Programmed cell death (apoptosis), 13, 80, 92, 105–106, 108, 125–126, 147, 156, 180, 185, 205, 223, 233–236, 238, 248
Proliferation
  cushion mesenchyme, 124–126, 216
  endothelium, 9–10, 120, 124, 148, 190
  myocardium, 37–38, 42, 44–45, 81, 105, 110, 138, 153, 167, 189, 218, 220, 225, 233–234, 239
  neural crest cells, 146, 156–157, 185
  smooth muscle, 15, 190
Prongs, 6, 147, 259
Protein tyrosine phosphatase (PTP), 127, 221
Proteoglycans, 96, 123–124, 136, 260
Proto-oncogene, 136, 260
Protrusive activity, 12
Psa-ncam, 163, 206, 260
Pseudotruncus, 81, 260
PTPN11, 127, 221. *See also* Noonan syndrome
Pulmonary circulation, 6, 161, 205
Pulmonary infundibulum, 6, 74, 81, 90, 92, 105, 150, 255
Pulmonary semilunar valve, 6, 74, 81, 96, 105–106, 119, 125–127, 147–149, 222
Pulmonary sinuses, 8, 77, 260
Pulmonary stenosis, 80–82, 96, 215–216, 220–221, 223
Pulmonary trunk, 6, 12, 73–77, 80–82, 87, 92, 105–106, 139, 149–150, 154, 169, 182, 205, 215, 260
Purinergic receptors, 189, 260
Purkinje fibers/cells, 56, 62, 161–173, 260

Rabbit, 28, 53, 61–62, 168, 172, 182–183
Rami communicantes, 184, 260
Randomization of heart looping, 92, 96–97
Ras, 59, 123, 125, 127, 220
Ras-GTPase, 30, 123, 125
Ras/mitogen activated protein kinase (Mapk), 59, 123, 125, 127
Rat, 44–45, 53, 60, 62, 74, 137, 149, 163, 181–183, 187–190, 192, 234, 236–237
Rbpjκ, 15, 16, 123, 260
Receptor tyrosine kinase (Rtk), 9, 13, 44, 81, 120, 125, 180, 260
Regeneration
  myocardium, 25, 40, 233–237, 239–240
  neural crest, 143–144
Rendu-Olser-Webber disease, 17
Renin, 193, 260
Replication-incompetent retrovirus, 23, 260
Repolarization, 54–57, 64, 167–168, 172–173, 190, 192, 260
Ret tyrosine kinase, 185, 187, 260
Retinaldehyde dehydrogenase (Raldh), 45, 106–108, 112, 134–135, 260
Retinoic acid (RA), 45, 77, 82, 96, 106–107, 112, 120, 123, 135, 138, 144, 156, 187, 209, 223–224, 238, 260
  retinoic acid-deficient quail, 108
  retinoic acid induced gene 1 (RAI1), 222
  retinoic acid receptor (Rar), 45, 138, 156, 224, 260
  retinoic acid response element (RARE), 76
  retinoid signaling, 82, 106–107, 112, 138, 224
  retinoid X receptor (Rxr), 45, 138, 156, 224, 260
  retinopathy, 223, 226
  vitamin A teratogenesis, 223
Retroviral labeling, 23, 92, 119–120, 136, 138, 147, 164, 260
Rho GTPase, 29, 41, 260
Rhombomeres, 143, 145, 260
Rhythmicity, 30, 53, 56–57, 59–60, 166, 192, 206, 237
Rieger syndrome, 96, 260
Right atrial isomerism, 96, 97. *See also* Asplenia syndrome
Right cardiogenic field (contribution to heart tube), 104, 106–107
Right ventricle, 4–6, 42–43, 69, 73–75, 81–82, 90–91, 103–113, 126–128, 133, 140, 148, 154–156, 163, 165, 169, 219, 221, 260
  anterior heart field, 25–27, 30, 105, 248
  cardiogenic field, 22, 24–27, 38, 69, 90, 104, 107
  double outlet, 79–82, 92, 96–97, 152, 156, 217, 221–222, 252
  evolution, 201, 205, 209–210
  gene expression, 42–43, 111–113, 209
Right-sided dominance, 90
Ritscher-Schinzel syndrome (Cranio-Cerebello-Cardiac, 3C), 221
Romano–Ward syndrome, 173, 260
ROSA26R (R26R), 127, 150
Rostrocaudal order, 22, 23, 25
Rotation
  embryonic, 89
  heart field, 30
  heart tube, 87–90
  outflow, 80, 82, 87–88, 92, 205
Roundabout (Robo), 13, 260
Ryanodine receptor, 58, 60, 260

Sarcolemma, 57–61, 190
Sarcomere, 41, 43–44, 46, 62–64, 234, 236–237, 260
Sarcoplasmic Ca^{++} ATPase (SERCA), 58, 60–61, 191
Sarcoplasmic reticulum (SR), 46, 57–61, 63, 65, 105, 190–191, 237, 260
Satellite cells
  neural, 182–183, 261
  skeletal muscle, 236
Schwann cells, 183, 187, 261

Scl, 9–10, 261
Secondary atrial septum (septum secundum), 5, 71, 73, 78–79, 219, 261
Secondary heart field, 4, 27, 69, 74–83, 91–92, 96, 105, 139, 149, 151, 152, 153, 155–157, 215–216, 218, 226
Secretogranin, 185
Secundum atrial septal defect, 78, 218, 220
Semaphorin 3C (Sema3C), 153, 154, 155, 261
Semilunar valve, 6, 27, 74, 79, 105, 106, 119, 125, 126, 127, 147–149, 156, 203, 222, 261
Septation, 3, 4, 5, 38, 80, 87, 108, 122, 123, 138, 164, 165, 172, 184
  atrial, 5, 71, 77, 78, 104, 220
  atrioventricular, 122, 124, 167
  outflow, 6, 11, 74, 75, 76, 77, 80, 82, 87, 92, 105, 106, 121, 143, 145, 147, 148, 149, 150, 151, 153, 155, 156, 183, 205
  ventricular, 82, 103, 105, 113, 127, 209
Septum intermedium. *See* Atrioventricular septum
Septum transversum, 6, 69, 134, 136, 261
SERCA, 46, 60, 61, 261
Serial circulation, 3, 87
Serrate, 15, 39, 261
Serum response factor (SRF), 15, 40, 41, 42, 110, 111, 136, 262
Shear stress, 147
Short rib-polydactyly syndrome, 219, 221
Short stature, 127, 221–222
Shp2 (src homology region 2, phosphatase 2), 125, 126, 127, 221
SIDS (sudden infant death syndrome), 192–193, 261
SIF (small intensely fluorescent cells), 182–183, 261
Signaling modules, 209
Signaling networks, 12
Signaling pathways, 12, 13, 29, 30, 35, 58, 92, 125, 199, 209, 210
Sinoatrial junction, 70, 261
Sinoatrial (SA, sinus) node, 53, 55, 64, 161, 162, 163–165, 168, 172, 181, 188–189, 192, 208, 220, 236, 238, 260
Sinoatrial valve, 70–71, 73, 261
Sinus horns, 70–73, 104
Sinus venosus, 4, 5, 13, 70–73, 78, 97, 108, 112, 133–134, 163, 200, 202, 209, 220, 261
siRNA, 30
Situs, 82, 95, 261
  situs inversus, 94, 96–98, 109, 219, 221
  situs solitus, 96–97
Skeletal muscle, 15, 25, 58, 60, 62–63, 163, 169, 216, 233, 235, 236–237, 241
Slit, 13, 261
S-looping, 87–88, 90–91
Slow conduction, 105, 107, 162, 164, 166, 168, 206
Slow myosin heavy chain. *See* Myosin heavy chain
Slug, 122–123, 136, 144, 261
Smad, 123, 125, 210, 261
  Smad 1, 96, 97, 123, 125
  Smad 2, 97
  Smad 4, 17, 123
  Smad 5, 125
  Smad 6, 123, 125
  Smad 8, 125
Smith-Lemli-Opitz syndrome, 221
Smith-Magenis syndrome, 221–222
Smooth muscle, 14–16, 27, 42–43, 69, 74–77, 82–83, 105, 133, 135–139, 144, 146, 149, 150, 154, 155, 167, 170, 189–190, 203, 205, 207, 215, 234–236
  smooth muscle gamma actin. *See* Actin
  smooth muscle myosin heavy chain. *See* Myosin heavy chain
Snail, 93, 122–123
Sodium-calcium exchanger (NCX), 30, 41, 55–58, 61, 238, 261
Solitary tract, 179, 181, 261
Somatic mesoderm, 28–29, 261
Somatostatin, 182, 185, 189, 261
Somites, 12, 13, 24, 43, 107, 120–121, 143–145, 150–151, 155, 163, 182–184, 208, 223
Sonic hedgehog (Shh), 36–38, 89, 92–94, 96, 218, 222–223, 261
Sox, 126, 144, 261
  Sox 4, 155
  Sox 8, 126
  Sox 9, 126, 216, 220
  Sox 10, 187–188
Specification, 35, 209, 252
  cardiogenic mesoderm, 35–36, 209, 215
  chamber, 3, 6, 25, 42–43, 57, 87, 89, 103–118, 208–209
  conduction myocardium, 167
  left–right axis, 92, 104
  myocardium, 23, 29, 35–37, 42
  neural crest, 144
Spina bifida, 153, 261
Spina vestibuli, 5, 71, 73–74
Spinal cord, 12, 179, 181, 184, 261
Splanchnic mesoderm, 4–5, 26, 28–30, 37, 70–72, 74–75, 104, 119–121, 133–136, 205, 261
Spleen, 12, 41, 82–83, 94, 96–98, 136
Splotch mouse, 153, 154, 218. *See also* Pax3
Spongiosa 126
Sprintzen (velocardiofacial) syndrome, 150, 156, 217–218, 225–226, 261
SR junctions, 58, 60
SSA/Ro, 173, 262g
SSB/La, 173, 262g
Starling's law (Frank–Starling relationship), 63, 64
Stat3, 186
Stellate ganglia, 180, 262
Stem cells, 10, 14, 57, 133, 163, 171, 187, 233–241
Stenosus, 262
  aortic, 81, 216, 221–223
  aortic valve, 113
  coronary, 139–140
  infundibular, 81, 96
  mitral valve, 113
  pulmonary, 80–82, 215–216, 221, 223
  pulmonary valve, 81–82, 220
  subaortic, 81
Stomach, 12, 82, 83, 96, 98
Su5402, 152, 262
Subclavian arteries, 12, 156, 215
Subepicardial matrix, 134–136, 164, 181
Subepicardial myocardium, 136, 188
Subepicardial plexus, 187
Subepicardial space, 135–136
Substance P, 181–182, 184, 189, 262
Suppressor of Hairless (SuH), 17, 262
Sympathectomy, 188, 192, 262
Sympathetic innervation, 144, 181, 183–184, 186–189, 191
Synaptic vesicles, 181, 262
Synaptophysin, 185, 262
Syncytium, 161, 166, 238, 262
Syndecans, 92, 262
Syndromes, 17, 64, 77–78, 82–83, 97, 150, 215–231
  Alagille, 17, 215
  anticonvulsant, 223
  (Brachmann-)Cornelia-de Lange, 216
  brugata, 173–174
  CATCH22, 156, 217
  CHARGE, 216
  conotruncal anomaly face, 218
  DiGeorge, 155–157, 217–218, 225
  Down (trisomy 21), 74, 127, 193, 208, 218–219, 224, 252
  Edward (trisomy 18), 222
  Ellis-van Creveld (chondroectodermal dysplasia), 219
  Goldenhar, 216
  Guillain-Barré, 192
  Holt-Oram, 208–209, 219–220, 224
  Ivemark, 97, 256
  Jervell-Lange-Nielsen, 173, 256
  Kabuki, 220
  Kartagener, 97, 256
  long QT, 173–174
  neonatal lupus, 173
  Noonan, 221
  polysplenia, 97
  retinopathy (hypervitaminosis A), 223–224
  Rieger, 96, 260
  Riley-Day, 192
  Ritscher-Schinzel (Cranio-Cerebello-Cardiac, 3C), 221
  Romano-Ward, 173
  short rib-polydactyly, 221
  Smith-Lemli-Opitz, 221
  Smith-Magenis, 222
  sudden infant death (SIDS) 192–193
  trisomy 18 (Edward), 222
  trisomy 21 (Down), 74, 127, 193, 208, 218–219, 224, 252
  Turner, 220
  22q11 deletion, 80, 154–156, 208, 217–218
  ulnar-mammary, 208, 219
  VACTERL, 222
  velocardiofacial, 150, 156, 217–218, 225–226, 263
  von Recklinghausen neurofibromatosis, 220
  Williams-Beuren, 220–222
Systemic circulation, 3, 6, 80, 82, 105, 113, 145–147, 150, 160, 203–205
Systemic veins, 69–73, 78, 107
Systole, 57–58, 61–63, 126, 204, 262

Tachyarrhythmia, 167, 173, 262
TASK1, 167–168
T-box transcription factors, 40–42, 111, 207–208, 225
  AmphiTbx1/10 (Amphioxus Tbx1 and 10), 208
  HrT (zebrafish Tbx5), 42, 112
  TBE (also called T-box binding factor element), 41–42, 111, 225, 262
  Tbx1, 41–42, 80, 136–137, 146–147, 154–157, 207–209, 218, 226
  Tbx2, 41–42, 95–97, 109–112, 171, 208–209

Tbx3, 41–42, 111–112, 168, 208–209, 219
Tbx4, 40, 209
Tbx5, 40–42, 79, 95–97, 107–112, 136, 173, 206, 208–209, 219–220, 224–225
Tbx10, 208
Tbx12, 41, 209
Tbx18, 136–137, 208
Tbx20, 42, 95–97, 109–112, 120, 206, 208–209
Tenascin, 126, 148, 262
tenascin C, 29
tenascin X, 120, 134, 148
Tension, 30, 62–64, 90, 190–191, 205, 239
Teratogen, 77, 80, 82, 98, 156, 216, 221, 223–224, 262
Tetralogy of Fallot (TOF), 41, 80–81, 92, 173, 215–218, 221–222, 262
Tetrodotoxin, 55–56, 262
Thorax, 10, 12, 143, 217
Thymic hypoplasia, 150, 156
Thymus, 12, 144, 150, 153, 155–156, 217–218
Thyroid, 44, 144, 150, 153, 156, 222
Tie1, 13
Tie2 (Tek), 13–15, 120
Tie2-cre, 122, 126
Tolloid-like 1 (Tll1), 113, 262
Torsades de pointes, 173, 262
Torsion, 87
Total anomalous pulmonary venous return (TAPVR), 78, 97–98, 222, 262
Trabeculae, 44–45, 81, 104, 107, 111–113, 152, 162, 164–165, 170, 205–206, 219, 262
Trabecular channels, 44, 138
Transcription factor, 9, 15–17, 25, 36–37, 39–42, 79, 92, 95, 110–111, 120–123, 125, 136, 144, 146, 154–155, 169, 184, 186, 200–201, 206–209, 222, 225, 234, 236, 238, 239, 262
Transcriptional activity, 17, 30, 38, 42, 123, 188
Transcriptional repression, 107, 111
Transforming growth factor-α (Tgfα), 187
Transforming growth factor-β (Tgfβ), 16, 36–37, 92–93, 95, 120–121, 123, 136–137, 262
TbrII, 15, 16, 123
TbrIII, 123
Tgfβ receptor I (TbrI), 123
Tgfβ1, 10, 15–16, 123, 137
Tgfβ2, 123
Tgfβ3, 123
Transmembrane potentials, 168
Transmural vascularization, 136, 138
Transplantation
backtransplantation, 151, 153
fate mapping, 23, 25, 30, 171
stem cells, 233, 234, 235, 237–239, 241
Transposition of the great arteries (TGA), 77, 80–83, 95, 97–98, 217, 221, 263
corrected transposition, 82, 97
Transverse (t) tubules, 55, 57–60, 63, 263
Triadin, 60
Tricuspid atresia, 127–128, 217, 221
Tricuspid valve, 80, 88, 91, 104–106, 110, 122, 126–128, 173, 201
posteroinferior leaflet, 122
septal leaflet, 105, 122, 126–127
Trisomy 18 (Edward syndrome), 222
Trisomy 21, 127, 218–219
Tritiated thymidine, 23–24
TrkA, 180, 185, 263
Tropomyosin, 46, 63, 236
Troponin, 38, 46, 61, 63, 236–238, 263
troponin C, 41, 61
troponin complex, 63, 263
troponin I, 41, 46, 62, 111, 236
troponin I–lacZ, 172
troponin T, 38, 46, 237–238
Truncal outflow cushions, 147, 149, 220
Truncus. *See* truncus arteriosus
Truncus arteriosus (truncus), 4, 6, 26–27, 38, 69, 74, 81, 87, 91, 103, 105–106, 138, 144, 147–148, 201, 210, 263
persistent truncus arteriosus (truncus), 38, 81–82, 144, 150–156, 208, 217–218, 260
pseudotruncus, 81, 260
Trunk neural crest. *See* Neural crest
T-type calcium channel ($I_{Ca,T}$), 55, 57, 59–60, 249, 255
Tubular heart, 3–5, 22, 25–26, 28, 105–108, 112–113, 119, 133, 161, 167–169, 206
Tumor necrosis factor alpha converting enzyme (Tace), 125
TUNEL, 92
Tunica media, 27, 75–77, 137, 146, 149, 263
Twist, 120
Tyrosine hydroxylase, 182–185, 188, 190, 263

Uridine 5′-diphosphate (UDP)-glucose dehydrogenase, 112, 256

VACTERL association, 217, 222–223
Valve cusps. *See* Valve leaflets
Valve leaflets (cusps), 6, 75, 126, 263
atrioventricular (AV), 6, 8, 79, 122, 124–128
layers, 126
semilunar (SL), 126, 147–148, 156
sinoatrial (SA), 70, 72, 172
Valvulogenesis,124–125
Vascular branching, 13–15, 82, 138, 169, 215
Vascular cell adhesion molecule (Vcam), 44, 135, 138, 237, 263
Vascular dysplasia, 17
Vascular endothelial growth factor (Vegf), 9–14, 29, 92, 120, 124, 135–137, 148, 169, 236, 263
Vegf isoforms, 12
Vegf receptor 2 (Flk1), 9, 12, 92, 148, 236
Vegf receptor 2 (Flt1), 12
Vascular endothelial (VE) cadherin, 29, 122–123, 240
Vascular fusion, 12–13, 72
Vascular network, 9–10, 13
Vascular remodeling, 13, 15, 112
Vascular smooth muscle, 14–15, 75, 149
vascular smooth muscle-coronary, 135, 136–138
Vascular stabilization, 13–14
Vasculogenesis, 9–10, 12, 119, 138, 263
Vasoactive intestinal peptide (VIP), 182, 189–190, 263
Veins, 9–12, 15–17, 69–73, 77–78, 90, 181, 183, 202–203
Velocardiofacial syndrome, 150, 156, 217–218, 225–226, 263
Velopharyngeal insufficiency, 217, 263
Venous endothelium, 16
Venous pole, 39, 70, 87–88, 91, 103–104, 133–134, 147, 204, 255
Venous system, 11, 13, 71–72, 107, 215
Ventral bending, 87–90
Ventral midline, 3, 22, 30–31, 43, 87, 91, 103, 106–107, 119, 207
Ventral pharynx, 10, 23, 26–28, 69, 76, 87, 89, 119, 133
Ventricular aneurysm, 139
Ventricular hypertrophy, 221
Ventricular hypoplasia, 189
Ventricular (interventricular) septum, 6, 31, 71, 79, 82, 92, 103–105, 107, 109–111, 113, 127–128, 137–138, 150, 161, 164, 169, 172, 188, 219
Ventricular pre-excitation, 128, 172–173
Ventricular septal defect (VSD), 44, 79–82, 96–97, 113, 127–128, 150, 155–156, 173, 216–217, 219–221, 223, 263
Ventriculoarterial junction (arterial pole), 6, 8, 74, 82, 105, 263
Verapamil, 56–57, 59
Versican, 113, 123, 263
Vertebral arteries, 12, 217
Vesicles
angioblast, 9, 12
otic, 218
proepicardial, 134
synaptic, 181–183, 262
Vessel stabilization, 13–14
Vestibular spine (spina vestibuli), 5–6, 69, 74, 263
Vestibule, 6, 74, 104–105
Vg1, 92–93, 263
Vimentin, 136, 263
Visceral endoderm, 35–36, 41, 207, 263
Visceroatrial heterotaxia, 94, 97–98, 263
Vitamins
vitamin A, 156, 223–224, 260. *See also* Retinoic acid
vitamin D receptor, 107–108, 112
vitamin D receptor binding element, 108
Vitronectin, 126, 134, 263

Wedging, 80, 87–88, 91–92, 263
Whole embryo culture, 22, 69
Williams-Beuren syndrome, 222–223
Wilms tumor (WT1), 44, 136–138, 263
Wnt, 29, 37–39, 123, 144, 155–156, 210, 224, 250, 263
Wnt antagonists (inhibitors), 39, 144, 210
Wnt1, 144, 210
Wnt1 cre, 149–150, 156
Wnt3a, 39
Wnt6, 123
Wnt7a, 169
Wnt8, 39
Wnt11, 36, 39, 169, 210
Wolff-Parkinson-White syndrome, 173, 263
Working myocardium, 6, 55, 107, 111, 162, 164, 166, 168–169, 171, 205–206, 209

Yolk sac, 9–10, 23, 263

Zebrafish, 3, 12–13, 16, 30, 38, 42, 53, 56, 76, 92, 95–96, 112, 119–120, 123, 126, 149, 162, 206–210, 233
Zic1, 44, 263
Zic3, 97–98